

Sheffield Hallam University

Biochemical studies on scorpion (Mesobuthus tamulus) and bee (Apis mellifera) venom peptides.

NEWTON, Kirsti A.

Available from the Sheffield Hallam University Research Archive (SHURA) at:

<http://shura.shu.ac.uk/20116/>

A Sheffield Hallam University thesis

This thesis is protected by copyright which belongs to the author.

The content must not be changed in any way or sold commercially in any format or medium without the formal permission of the author.

When referring to this work, full bibliographic details including the author, title, awarding institution and date of the thesis must be given.

Please visit <http://shura.shu.ac.uk/20116/> and <http://shura.shu.ac.uk/information.html> for further details about copyright and re-use permissions.

LEARNING CENTRE
CITY CAMPUS, POND STREET,
SHEFFIELD, S1 1WQ.



Fines are charged at 50p per hour

16 NOV 2006

9pm

REFERENCE

ProQuest Number: 10697423

All rights reserved

INFORMATION TO ALL USERS

The quality of this reproduction is dependent upon the quality of the copy submitted.

In the unlikely event that the author did not send a complete manuscript and there are missing pages, these will be noted. Also, if material had to be removed, a note will indicate the deletion.



ProQuest 10697423

Published by ProQuest LLC (2017). Copyright of the Dissertation is held by the Author.

All rights reserved.

This work is protected against unauthorized copying under Title 17, United States Code
Microform Edition © ProQuest LLC.

ProQuest LLC.
789 East Eisenhower Parkway
P.O. Box 1346
Ann Arbor, MI 48106 – 1346

**Biochemical Studies on Scorpion (*Mesobuthus tamulus*) and
Bee (*Apis mellifera*) Venom Peptides**

Kirsti Amanda Newton

A thesis submitted in partial fulfilment of the requirements of
Sheffield Hallam University
for the degree of Doctor of Philosophy



November 2004

In Memory of
ELSIE and GEORGE BRIDGE
and
ELSIE and WILLIAM NEWTON

Abstract

Animal venoms are essentially diverse libraries of compounds evolved to have both high affinity and high specificity, making them ideal targets for bioprospecting. Despite advances in antivenom therapy, envenomations remain clinically significant, accounting for numerous human fatalities.

The Indian red scorpion (*Mesobuthus tamulus*) is a serious threat to life in India, but its venom is poorly characterised. This study examines antigenic and proteomic variability of *Mesob. tamulus* venoms obtained in two geographical regions with distinct biotopes. In addition to highlighting general venom differences between the two populations, the study identified a peptide of 2947Da that may prove diagnostic between the venom types. As an aid to the future isolation of specific peptides, particularly those initially identified via their DNA sequences, a mass profile of fractionated, commercially available venom was also generated.

Scorpion short insectotoxins may have importance as chloride channel blockers and in cancer therapeutics. Only a few such molecules have been isolated and in general, relatively little is known about their properties. Analysis of a *Mesob. tamulus* telson cDNA library, using probes based upon the signal peptide sequence of a known short insectotoxin (Bm12 from *Buthus martensii*), yielded two novel "short-insectotoxin" sequences, BtCh11 and BtCh12. Mass spectrometry-guided isolation has been used to purify a corresponding peptide from the venom, based upon its calculated mass. Additional studies using the same cDNA revealed evidence supporting the amidation of tamulustoxin (a potassium channel toxin found in the venom of this species), and evidence to suggest the existence of a novel long-chain potassium channel toxin.

Toxins also play an important role as molecular probes for the dissection of ion channel structure. The structure-function relationships of apamin (a calcium-activated potassium channel toxin from the honey bee, *Apis mellifera*) were examined by investigating the effect of addition of a fluorescent label, non-native disulphide pairings, and disruption of the β -turn on the toxin's affinity for its receptor on rat brain membranes.

Table of Contents

Abstract	3
Table of Contents	4
List of Figures	10
List of Tables	13
Abbreviations	14
Relevant Publications	19
Acknowledgements	20
1. Introduction	21
1.1. Significance of Natural Toxins	22
1.2. Ion Channels	23
1.2.1. Voltage-Gated Na ⁺ Channels	32
1.2.2. Voltage-Gated Calcium Channels	33
1.2.3. Chloride Channels	35
1.2.4. Potassium Channels	39
1.2.4.1. Kv	41
1.2.4.2. Calcium-Activated Potassium Channels	42
1.2.5. Clinical Relevance of Ion Channels	45
1.3. Venoms	49
1.3.1. Disulphide-Bond Motifs	50
1.4. Bee Venom	53
1.4.1. Apamin	56
1.5. Scorpion Venom	62
1.5.1. Scorpion Sting	62
1.5.1.1. Symptoms of Scorpion Sting	65
1.5.2. Scorpion Venom Composition	66
1.5.3. Scorpion Venom Ion Channel Neurotoxins	67
1.5.3.1. Sodium Channel Toxins	68
1.5.3.2. Potassium Channel Toxins	71
1.5.3.3. The Short Insectotoxins	76

1.5.3.4. Toxins Active on Ca ²⁺ Channels	77
1.5.4. Other Scorpion Venom Peptides	79
1.5.5. Scorpion Venom cDNA and Genes	80
1.5.6. Significance of Scorpion Venom Components	81
1.6. <i>Mesobuthus tamulus</i>	84
1.7. Aims and Objectives	87
2. Studies on the <i>Mesobuthus tamulus</i> Venome, and Possible Regional Variation Within it	88
2.1. Introduction	89
2.2. Materials and Methods	93
2.2.1. Materials	93
2.2.2. Harvesting and Preparation of Venom Samples	93
2.2.3. Venom Fingerprinting	94
2.2.3.1. Development of an ELISA Using <i>Mesob. tamulus</i> Antivenom, and Assessing its Ability to Recognise Different Venom Extracts	94
2.2.3.2. SDS-PAGE (Sodium Dodecyl Sulphate-Polyacrylamide Gel Electrophoresis) and Western Blotting of Individual Venom Samples	95
2.2.3.3. Analysis of Individual Venom Samples by SELDI-TOF Mass Spectrometry	98
2.2.3.4. LC-Electrospray Ionisation Mass Spectrometry (LC/ESI MS) on Individual Venom Samples	99
2.2.3.5. LC-MS Data Analysis	101
2.2.4. Venom Profiling	101
2.2.4.1. Size Exclusion Chromatography	101
2.2.4.2. Cation Exchange Chromatography	102
2.2.4.3. Reversed Phase HPLC	102
2.2.4.4. Matrix-Assisted Laser Desorption/Ionisation Time-of-Flight Mass Spectrometry (MALDI-TOF MS)	103
2.2.4.5. LC-MS	104
2.2.4.6. Data Analysis	104

2.3. Results	105
2.3.1. Ability of <i>Mesob. tamulus</i> Antivenom to Recognise Venom Extracts by ELISA	105
2.3.2. SDS-PAGE and Western Blotting on Individual Venoms	109
2.3.3. Mass Spectrometry	113
2.3.3.1. SELDI-TOF Fingerprinting	113
2.3.3.2. LC-MS	114
2.3.4. Fractionation of <i>Mesob. tamulus</i> Venom for Venom Profiling	130
2.3.5. Mass Profiling of Venom Fractions by MALDI-TOF and LC-MS	134
2.4. Discussion	141
3. Studies on Peptides from the Venom of the Indian Scorpion	151
<i>Mesobuthus tamulus</i>. (i) Cloning of Chlorotoxin Gene Family Members and Purification of the Corresponding Gene Products. (ii) Structure of the 3' Untranslated Region of Tamulustoxin	
3.1. Introduction	152
3.2. Materials and Methods	155
3.2.1. Materials	155
3.2.2. Identification of Putative Short Insectotoxin cDNA Sequences from <i>Mesob. tamulus</i>	156
3.2.2.1. Scorpions	156
3.2.2.2. Isolation of Total RNA	156
3.2.2.3. Generation of an Adaptor Ligated cDNA Library	156
3.2.2.4. Primer Design	158
3.2.2.5. PCR	158
3.2.2.6. DNA Agarose Gel Electrophoresis and Purification of Fragments / Bands from Agarose Gels	159
3.2.2.7. Preparation of Competent Cells	159
3.2.2.8. Cloning PCR Fragments into pCR [®] 4-TOPO [®] Vector	160
3.2.2.9. Plasmid DNA Isolation (Mini Preps)	160
3.2.2.10. Screening for Inserts by Restriction Digest	161
3.2.2.11. Stock Culture	161
3.2.2.12. Dideoxy Sequencing	162

3.2.2.13. Analysis of Deduced cDNA Sequences	162
3.2.3. Mass Spectrometry-Guided Purification of a Putative Chloride Channel Toxin Identified by cDNA Cloning	163
3.2.3.1. Calculation of Candidate Masses	163
3.2.3.2. Chromatographic Purification of the Peptide	163
3.2.3.3. Screening of Fractionated Venom by Mass Spectrometry	164
3.2.4. Generation of Synthetic BtCh1	164
3.2.4.1. Peptide Synthesis	164
3.2.4.2. Peptide Purification	164
3.2.4.3. MALDI-TOF Mass Spectrometry	165
3.2.4.4. Peptide Folding	165
3.2.4.5. Homology Modelling of BtCh1 and BtCh2	166
3.2.5. Analysis of the 3'UTR of Tamulustoxin cDNA	166
3.2.5.1. Primer Design	167
3.2.5.2. PCR Reaction	167
3.2.6. Identification of a Long-Chain Potassium Channel Toxin-Like Signal Peptide Sequence in <i>Mesob. tamulus</i> cDNA	168
3.2.6.1. Primers	168
3.2.6.2. PCR Reaction	168
3.3. Results	169
3.3.1. Identification of Putative Short Insectotoxin cDNA Sequences from <i>Mesob. tamulus</i>	169
3.3.2. Purification of a Putative BtCh1 Peptide from <i>Mesob. tamulus</i> Venom	175
3.3.3. Synthesis and Purification of a Synthetic BtCh1	180
3.3.4. Homology Modelling of BtCh1 and BtCh2	184
3.3.5. Analysis of the 3'UTR of Tamulustoxin cDNA	188
3.3.6. Identification of a Long-Chain Potassium Channel Toxin-Like Signal Peptide Sequence in <i>Mesob. tamulus</i> cDNA	191
3.4. Discussion	194
3.4.1. Short Insectotoxins	194
3.4.2. Amidation of Tamulustoxin	203
3.4.3. A Putative Long-Chain Potassium Channel Toxin Signal Peptide	205

4. Modification of Apamin, and the Effects on its Binding 208

Affinity for Acceptors on Rat Brain Synaptic Membranes

4.1. Introduction	209
4.2. Materials and Methods	214
4.2.1. Materials	214
4.2.2. Determination of Apamin Binding Parameters	214
4.2.2.1. Radioiodination of Native Apamin	214
4.2.2.2. Preparation of Rat Brain Synaptic Plasma Membranes	215
4.2.2.3. BCA Protein Assay	216
4.2.2.4. Saturation Binding Assays	216
4.2.2.5. Determination of Non-Specific Binding	217
4.2.2.6. Time Course of Apamin Binding to Rat Brain Synaptic Membranes	217
4.2.2.7. Analysis of Binding Data	218
4.2.3. Binding of Apamin-N2A Isoforms	220
4.2.3.1. Synthesis, Refolding and Purification of Apamin Analogues	220
4.2.3.2. Screening of Synthetic Peptides for Inhibition of Monoiodo[¹²⁵ I]apamin Binding	220
4.2.3.3. Competition Binding Assays with Apamin Analogues	220
4.2.3.4. Competition Binding Curves for the Two halves of the HPLC Peak for Apamin N2A-Anti	221
4.2.4. Binding Studies on Alexa Fluor 488 Apamin	222
4.2.4.1. Testing the Ability of Alexa Fluor 488 Apamin to Inhibit Monoiodo[¹²⁵ I]apamin Binding to Rat Brain Synaptic Plasma Membranes	222
4.2.4.2. Competition Binding Curves for Alexa Fluor 488 Apamin	222
4.2.4.3. Competition Binding Curves for Alexa Fluor 488 Apamin Under Physiological Buffer Conditions	222
4.2.4.4. Use of Alexa Fluor 488 Apamin to Visualise Transfected SK Channels in HEK Cells	223
4.2.4.5. Electrophysiology of Block of rSK2 with Alexa Fluor Apamin	223

4.3. Results	224
4.3.1. Radioiodination of Native Apamin	224
4.3.2. Determination of Biological Relevance of Binding	226
4.3.3. Time Course of Apamin Binding	228
4.3.4. Saturation Binding Assays	230
4.3.5. Analysis of Binding Data	232
4.3.6. Synthesis, Refolding and Purification of Apamin and the Apamin N2A Disulphide Analogues	235
4.3.7. Effect of Native Apamin, Synthetic Apamin, and its N2A Analogues on Binding of Radiolabelled Apamin to Rat Brain Membranes	237
4.3.8. Affinity of Alexa Fluor Apamin for Apamin Binding Sites on Rat Brain Membranes	242
4.4. Discussion	250
5. Summary	261
References	264
Appendix	i

List of Figures

Figure 1.1	The Action Potential	26
Figure 1.2	Structure of KscA	28
Figure 1.3	Membrane Topology of Voltage-Gated Na ⁺ , Ca ²⁺ and K ⁺ Channel α -Subunits	29
Figure 1.4	Chloride Channel Topology	37
Figure 1.5	Structure of Apamin	60
Figure 1.6	Apamin Gene Structure	61
Figure 1.7	Scorpion Venom Apparatus	64
Figure 1.8	Models for KTx Interactions	74
Figure 1.9	<i>Mesobuthus tamulus</i>	86
Figure 2.1	Location of the Two <i>Mesobuthus tamulus</i> Populations Studied	92
Figure 2.2	Typical ELISA Profile using <i>Mesob. tamulus</i> Control Venom	107
Figure 2.3	ELISA on Individual <i>Mesob. tamulus</i> Venom from Different Regions	108
Figure 2.4	SDS-PAGE Analysis of Non-Reduced Venom Samples	111
Figure 2.5	Western Blotting of <i>Mesob. tamulus</i> Venom from Different Geographical Regions	112
Figure 2.6	SELDI-TOF Mass Spectrometry on Individual <i>Mesob. tamulus</i> Venom Samples from Scorpions Collected in Different Regions	117
Figure 2.7	TIC (Total Ion Current) Chromatographs of LC-MS on 'Average' A, K and LQ Venom Samples	118
Figure 2.8	Relative Mass Fingerprints of LQ and 'Average' A and K Venoms as Determined by LC-MS	119
Figure 2.9	Venom Components Grouped by Mass	120
Figure 2.10	Differences in Mass Composition of A and K as Determined by LC-MS	121
Figure 2.11	Fractionation of <i>Mesob. tamulus</i> Venom by Size-Exclusion and Cation-Exchange Chromatography	131
Figure 2.12	Reverse Phase HPLC on <i>Mesob. tamulus</i> Venom Ion Exchange Fractions	132
Figure 2.13	Sample Mass Spectrometry Profiles of <i>Mesob. tamulus</i> Venom Fractions	135

Figure 3.1	Homology of Short Insectotoxin Nucleotides	171
Figure 3.2	PCR Products and Products of Restriction Digests Observed in the Cloning of Putative Short Insectotoxin cDNA Sequences	172
Figure 3.3	Sequencing of Putative Short Insectotoxin cDNA	173
Figure 3.4	Alignment of BtCh11 and BtCh12 with the Amino Acid Sequences of Known Members of the Short Insectotoxin Family	174
Figure 3.5	Size Exclusion and Ion Exchange Chromatography of <i>Mesob. tamulus</i> Venom and Mass Spectrometry of Fractions to Detect Masses Corresponding to Putative BtCh11 Gene Products	177
Figure 3.6	Purification of a Venom Component of Approximate Mass 3797 by Mass Spectrometry-Guided Reverse Phase Chromatography	178
Figure 3.7	ESI Mass Spectrometry on 3797 Peak from C8 Reverse Phase Column	179
Figure 3.8	Analysis of Crude and Folded Synthetic BtCh11 by Reverse Phase HPLC and MALDI-TOF Mass Spectrometry	181
Figure 3.9	Fractionation of Crude and Folded BtCh11 on a C8 Reverse Phase HPLC Column	182
Figure 3.10	Optimised HPLC Fractionation of Folded Synthetic BtCh11 Analysed by MALDI-TOF/MS	183
Figure 3.11	Homology Modelling of BtCh11 and BtCh12 and Calculation of their Electrostatic Surfaces	185
Figure 3.12	PCR Products and Products of Restriction Digests Observed in the Cloning of 3' Tamulustoxin cDNA Sequences	189
Figure 3.13	Sequencing of Tamulustoxin cDNA to Identify Cleaved N-Terminal and 3'UTR Sequences	190
Figure 3.14	PCR Products and Products of Restriction Digests Which Yielded a Putative Long-Chain Potassium Channel Toxin Signal Peptide	192
Figure 3.15	TxK β Signal Peptide-Like cDNA Sequence from <i>Mesob. tamulus</i>	193
Figure 3.16	Sequence Alignment of Long-Chain Potassium Channel Toxin Precursors	207
Figure 4.1	Diagrammatic Representation of Apamin-N2A	213
Figure 4.2	Purification of Monoiodo[¹²⁵ I]apamin by Ion Exchange	225

Figure 4.3	Comparison of Binding in the Presence of Cold Apamin or <i>d</i> - Tubocurarine	227
Figure 4.4	Time Course of Apamin Binding to Rat Brain Membranes	229
Figure 4.5	Binding of ¹²⁵ I-Apamin to Rat Brain Membranes	231
Figure 4.6	Scatchard Plot of Saturable Binding of Radiolabelled Apamin to Rat Brain Membranes	233
Figure 4.7	Hill Plot of Saturable Binding of Radiolabelled Apamin to Rat Brain Membranes	234
Figure 4.8	Purification of Apamin N2A-Par and -Anti	236
Figure 4.9	Comparison of Binding in the Presence of Native Apamin, Synthetic Apamin, Apamin N2A (Anti) and Apamin N2A (Par)	239
Figure 4.10	Competition Binding Curves for Apamin and its Synthetic Derivatives	240
Figure 4.11	Competition Binding Curves for the Two Halves of the HPLC Peak Containing Apamin N2A (Anti)	241
Figure 4.12	Radiolabelled Apamin Binding in the Presence and Absence of Alexa Fluor Apamin	245
Figure 4.13	Competition Binding Curves for Alexa Fluor Apamin	246
Figure 4.14	Alexa Fluor Apamin Competition Binding Curves in Physiological Buffer	247
Figure 4.15	Alexa Fluor Apamin Binding to Expressed SK Channels	248
Figure 4.16	Electrophysiological Block of rSK2 Currents by Alexa Fluor Apamin	249
Figure 4.17	Proposed Orientation of Apamin in the Mouth of the SK2 Channel Pore	259
Figure 4.18	Structure of Alexa 488	260

List of Tables

Table 1.1	Human Channelopathies	48
Table 2.1	Major Component Masses in <i>Mesob. tamulus</i> Regional Venoms and in <i>L. quinquestriatus hebraeus</i> Venom	122
Table 2.2	Occurrence of Known <i>Mesobuthus tamulus</i> Peptides in A and K Type Venoms	125
Table 2.3	Occurrence of Known Peptides in <i>L. quinquestriatus hebraeus</i> Venom	127
Table 2.4	Mass Spectrometric Analysis of <i>Mesob. tamulus</i> Venom	138
Table 2.5	Occurrence of Known <i>Mesobuthus tamulus</i> Peptides in Venom Fractions	140
Table 4.1	Published Apamin Binding Parameters	212

Abbreviations

3'RACE	3' Rapid amplification of cDNA ends
3'UTR	3' Untranslated region
5'UTR	5' Untranslated region
α-CHCA	α -cyano-4-hydroxycinnamic acid
<i>A. australis</i>	<i>Androctonus australis</i>
<i>A. mauretanicus</i>	<i>Androctonus mauretanicus mauretanicus</i>
<i>mauretanicus</i>	
<i>A. mellifera</i>	<i>Apis mellifera</i>
ABC transporter	ATP-binding cassette transporter
ACE	Angiotensin-converting enzyme
AChR	Acetylcholine receptor
AHP	After-hyperpolarisation
AP	Action potential
AP1	Adaptor primer
AP2	Nested adaptor primer
β-KTx	Long-chain potassium channel scorpion toxins
<i>B. eupeus</i>	<i>Buthus eupeus</i>
<i>B. martensii</i>	<i>Buthus martensii</i>
<i>B. occitanus</i>	<i>Buthus occitanus</i>
<i>B. indicus</i>	<i>Buthus indicus</i>
BCA	Bicinchoninic acid
Bis-Tris	Bis (2-hydroxy ethyl) imino-tris (hydroxy methyl) methane-HCl
BK	Large (big) conductance calcium-activated potassium channel
B_{max}	Maximal binding capacity (receptor density)
BSA	Bovine serum albumen
<i>C. limpidus</i>	<i>Centruroides limpidus</i>
<i>C. noxius</i>	<i>Centruroides noxius</i>
<i>C. sculpturatus</i>	<i>Centruroides sculpturatus</i>
<i>C. suffuses</i>	<i>Centruroides suffuses</i>
[Ca²⁺]_i	Intracellular free calcium concentration
CaCC	Calcium-activated chloride channel
cAMP	Cyclic-AMP (adenosine-3, 5-monophosphate)

Ca_v	Voltage-gated calcium channel
CD analysis	Circular dichroism analysis
cDNA	Complementary DNA
CFTR	Cystic fibrosis transmembrane conductance regulator
cGMP	Cyclic-GMP (guanosine monophosphate)
ChITx	Chlorotoxin
ClC	Voltage-gated chloride channel
CNG	Cyclic nucleotide-gated cation channel
CNS	Central nervous system
CSH	Cystine-stabilised α -helix
DHPR	Dihydropyridine receptor
dNTP	Deoxynucleotide triphosphate
Ds DNA	Double stranded DNA
DTT	DL-dithiothreitol
<i>eag</i>	<i>Ether-a-go-go</i>
EAG	<i>Ether-a-go-go</i> gene potassium channel
EAM	Energy absorbing molecule
EDTA	Ethylene diamintetraacetic acid
ELISA	Enzyme-linked immunosorbent assay
ELK	<i>Ether-a-go-go</i> -like potassium channel
ERG	<i>Ether-a-go-go</i> -related gene potassium channel
ESI	Electrospray ionisation
ExPASy	Expert protein analysis system (www.expasy.org)
FCS	Foetal calf serum
GABA	γ -aminobutyrate
GABA_A	γ -aminobutyrate receptor A
GABA_C	γ -aminobutyrate receptor C
GCC	Glioma chloride current/channel
GIRK	G Protein-coupled inwardly rectifying potassium channel
GluR	Glutamate receptor
GSP	Gene-specific primer
<i>H. bengalensis</i>	<i>Heterometrus bengalensis</i>
<i>H. fulvipes</i>	<i>Heterometrus fulvipes</i>
<i>H. gravimanus</i>	<i>Heterometrus gravimanus</i>
<i>H. longimans</i>	<i>Heterometrus longimans</i>

<i>H. scaber</i>	<i>Heterometrus scaber</i>
<i>H. spinifer</i>	<i>Heterometrus spinifer</i>
HBPCL	Haffkine Bio-pharmaceutical Corporation Limited, Pimpri, Pune, India
HBSS	HEPES buffered saline solution
HERG	Human <i>ether-a-go-go</i> -related gene
HPLC	High performance liquid chromatography
HRP	Horseradish peroxidase
I5A	Insectotoxin 5A
IK	Intermediate conductance calcium-activated potassium channel
IKC	Inhibitor cystine knot
IPA	Isopropyl alcohol
IPSP	Inhibitory postsynaptic potential
IPTG	Isopropyl β -D-thio-galactoside
IpTxA	Imperatoxin A
IRK	Inwardly rectifying potassium channel
K_{Ach}	Acetylcholine-activated or muscarinic potassium channel
K_{Ca}	Calcium-activated potassium channel
KcsA	<i>A Streptomyces lividans</i> potassium channel
K_d	Equilibrium dissociation constant
K_i	Equilibrium dissociation constant for the inhibitor/competitor
K_{ir}	Inward rectifier potassium channel
K_v	Channel belonging to the <i>Shaker</i> -voltage-gated potassium channel family
<i>L. quinquestriatus</i> <i>hebraeus</i>	<i>Leiurus quinquestriatus hebraeus</i>
<i>L. quinquestriatus</i> <i>quinquestriatus</i>	<i>Leiurus quinquestriatus quinquestriatus</i>
<i>Lqh</i>	<i>Leiurus quinquestriatus hebraeus</i>
LB	Luria-Bertani broth
LC-MS	Liquid chromatography/ Mass spectrometry
LD₅₀	Half maximal lethal dose
LDS	Lithium dodecyl sulphate
m/z	Mass-to-charge ratio
MALDI	Matrix-assisted laser desorption ionisation

MALDI-TOF	Matrix-assisted laser desorption ionisation – time of flight
MCa	Maurocalcine
MCD peptide	Mast cell degranulating peptide or peptide 401
MES	2-(N- (N-morpholino) ethane sulphonic acid)
<i>Mesob. tamulus</i>	<i>Mesobuthus tamulus</i>
MMLV	Murine Moloney leukaemia virus
MMP	Matrix metalloproteinase
mRNA	Messenger RNA
MS	Mass spectrometry
NMR	Nuclear magnetic resonance
NUS	National University of Singapore
<i>P. imperator</i>	<i>Pandinus imperator</i>
PAL	Peptidyl- α -hydroxyglycine α -amidating lysase
PAM	Peptidyl-glycine α -amidating monooxygenase
<i>Parab. granulatus</i>	<i>Parabuthus granulatus</i>
<i>Parab. schlechteri</i>	<i>Parabuthus schlechteri</i>
<i>Parab. transvaalicus</i>	<i>Parabuthus transvaalicus</i>
PBS	Phosphate buffered saline
PBS-T	Phosphate buffered saline containing 0.1% Tween
PCR	Polymerase chain reaction
PHM	Peptidylglycine α -hydroxylating monooxygenase
PLA₂	Phospholipase A ₂
PMSF	Phenylmethanesulphonyl fluoride
PNS	Peripheral nervous system
PVDF	Polyvinylidene difluoride
ROMK	Renal outer medullary potassium channel
RT	Room temperature
RyR	Ryanodine receptor
sAHP	Slow afterhyperpolarisation
SCICS	Irula Snake Catchers Industrial Cooperative Society Ltd.
SDS	Sodium dodecyl sulphate
SDS-PAGE	Sodium dodecyl sulphate – polyacrylamide gel electrophoresis
SEAC	Surface-enhanced affinity capture
SELDI	Surface-enhanced laser desorption ionisation

SELDI-TOF	Surface-enhanced laser desorption ionisation – time of flight
ShK	<i>Stichodactyla helianthus</i> toxin
SK	Small conductance calcium-activated potassium channel
SR	Sarcoplasmic reticulum
<i>T. bahiensis</i>	<i>Tityus bahiensis</i>
<i>T. cambridgei</i>	<i>Tityus cambridgei</i>
<i>T. serrulatus</i>	<i>Tityus serrulatus</i>
<i>T. stigmurus</i>	<i>Tityus stigmurus</i>
TALK	Alkaline-activated background potassium channel
TASK	TWIK-related acid-sensitive potassium channel
TBE buffer	Tris/ boric acid/ EDTA buffer
TEA⁺	Tetraethylammonium cation
TFA	Trifluoroacetic acid
TGE buffer	Tris/ glucose/ EDTA buffer
THIK	Halothene-inhibited 2P domain potassium channel
TIC	Total ion current
TM	Transmembrane domain
TMB	3, 3', 5, 5' Tetramethylbenzidine
TOF	Time-of-flight
TRAAK	TWIK-related arachidonic acid-stimulated potassium channel
TREK	TWIK-related potassium channel
TTX	Tetrodotoxin
TWIK	Tandem of P domains in weak inward rectifier potassium channel
VGCC	Voltage-gated calcium channel
VGSC	Voltage-gated sodium channel
X-gal	5-bromo-4-chloroindol-3-yl β -D-galactopyranoside

Relevant Publications

Newton K.A., Dempsey C.E., Strong P.N. 2003 Apamin: Functional effects of engineered destabilising conformations. *IST 14th world congress on animal, plant and microbial toxins, Adelaide, Australia. 14-19 September 2003*

Newton K.A., Chai S.C., Armugam A., Bhor V., Suji G., Sapatnekar S.M., Gadre S.V., Sivakami S., Strong P.N. and Jeyaseelan K. 2003 Characterisation of individual scorpion venom samples using SELDI-TOF mass spectrometry. *IST 14th world congress on animal, plant and microbial toxins, Adelaide, Australia. 14-19 September 2003*

Newton K.A., Armugam A., Strong P.N. and Jeyaseelan K. 2003. Cloning of putative chloride channel toxin cDNAs from the Indian red scorpion. *British Neurosci. Assoc. Abstr. 17:63.*

Newton K.A., Armugam A., Strong P.N. and Jeyaseelan K. 2002. cDNA sequences encoding putative chloride channel toxins from the Indian red scorpion, *Mesobuthus tamulus*. *Association canaux ioniques 13^{ème} colloque. Presqu'île de Giens, France. 22-25 September 2002.*

Newton K.A., Armugam A., Strong P.N. and Jeyaseelan K. 2002. Cloning of cDNAs encoding short insectotoxins from *Mesobuthus tamulus*. *IST 6th Asia-Pacific congress on animal, plant and microbial toxins & 11th annual scientific meeting of the Australasian College of Tropical Medicine, Cairns, Australia. 8-12 July 2002.*

Newton K.A., Armugam A., Strong P.N. and Jeyaseelan K. 2002. Cloning of cDNAs encoding short insectotoxins from *Mesobuthus tamulus*. *The 1st bilateral symposium on advances in molecular biotechnology and biomedicine between the National University of Singapore and University of Sydney, Singapore. 23-24 May 2002.*

Acknowledgments

I would like to thank my supervisor Professor Peter Strong for his support and guidance throughout the PhD. I am also grateful to Professor K. Jeyaseelan and Dr A. Armugam, National University of Singapore, for their assistance and warm hospitality. Thanks also to Dr M. Clench for his assistance with mass spectrometry.

For the milking of scorpions, I am grateful to past and present directors of the Haffkine Institute, Mumbai, India, Dr V. Yemul and Dr S.M. Sapatnekar, their scientific colleagues Dr R. Kamat, Dr S.V. Gadre, and Dr Mahatjarani, and also Dr S. Sivakami, Dr V. Bhor and Mr G. Suji, Mumbai University, India.

I would like to thank the Biomedical Research Centre, Sheffield Hallam University and the National University of Singapore for providing the financial support for this work.

Thank-you to my colleagues at Sheffield Hallam University, and the National University of Singapore for providing thoughtful discussion and moral support.

I am very grateful to my family for their constant support, and for filling in the missing punctuation. Finally, I would like to thank Kristian, for his love, support and patience, for the taxi service, and for understanding when a few months in Singapore stretched to over a year.

1.1 Significance of Natural Toxins

Plant extracts have been used medicinally for thousands of years and are the origin of many well-known drugs, e.g. cardiac glycosides (from *Digitalis* species) and quinine (from *Cinchona* species). Approximately 50% of the world's best selling pharmaceuticals were originally derived from natural sources (for reviews on the use of natural products in the pharmaceutical and agrochemical industry see Harvey 1993; Clark, 1996; Tulp and Bohlin, 2004). Research has generally focussed in two areas, the study of plant compounds and the study of natural toxins, including bacterial and fungal toxins and animal venoms. In particular, natural toxins make attractive targets for bioprospecting. There are three key features of natural toxins that make them ideal for drug screening. Natural toxins are very diverse and are evolved to recognise specific pharmacological targets. In general, they recognise these targets with high specificity and affinity (Rappuoli and Montecucco, 1997).

Many drugs derived from, or modelled on, natural toxins are in clinical trials or already in use. These include *Clostridium botulinum* toxin (for which novel clinical uses are constantly being proposed), derivatives of epibatidine (an alkaloid from frog skin, which causes analgesia via its action on nicotinic receptors) and a large number of snake-derived compounds, which include the ACE (angiotensin-converting enzyme) inhibitors and anticoagulants such as tirofiban.

These toxins are also important tools in the study of a number of physiological processes and disease states, allowing the study of their receptors at the molecular, biochemical and behavioural level, and providing a means of receptor purification (for a review of the use of toxins in cell biology see Rappuoli and Montecucco, 1997).

This study will focus on a group of naturally derived toxins, specifically ion channel toxins from bee and scorpion venoms.

1.2 Ion Channels

An ion-impermeable extracellular membrane allows cells to maintain differential intra- and extra-cellular ion concentrations. Ions can pass across this membrane by virtue of ATP-driven active transport systems, or passively through ion channels, driven by their electrochemical gradient. Most cells at rest maintain an increased concentration of potassium and organic anions in their cytoplasm, whilst $[\text{Na}^+]$ and $[\text{Cl}^-]$ are higher extracellularly. When open, ion channels provide an aqueous environment through which ions can rapidly cross hydrophobic membranes. This rapid transfer of charged molecules generates membrane currents and also enables rapid changes in concentrations of key ions important for cellular signalling.

Ion channels are ubiquitous and vital for normal cellular function. In animals they form the basis of excitability of nerve and muscle and are also involved in non-neuronal processes. In plants, like animals, ion channels are required for control of membrane potential, cell volume and signal transduction, and play an additional role in large scale transport systems such as in the phloem (Zimmermann and Sentenac, 1999; Schachtman, 2000). Ion channels are also present in viruses (Fischer and Sansom, 2002) and in prokaryotic organisms. Ion channels of bacteria have proved especially important in recent years, providing structural data from which properties of their eukaryotic counterparts can be inferred (Booth et al., 2003).

The importance of ion channels is best demonstrated by the role they play in the nervous system, where they are involved in the entire neuronal process, i.e. maintaining resting potential, sensory signal transduction, synaptic transmission, and muscle contraction. They are crucial to the propagation of impulses via action and inhibitory potentials. Hodgkin and Huxley, 1952, first demonstrated that the action potential (AP) was produced by coordinated opening of K^+ and Na^+ channels (see fig 1.1). Ion channels have numerous roles in non-neuronal systems, for instance cellular regulation and signalling, endocrine, secretory and absorptive processes.

Structurally, ion channels are oligomers containing pore forming α -subunits and accessory modulatory subunits (which have many functions including altering gating kinetics and regulation of channel expression, Trimmer, 1998). Generally, a single pore spans the membrane and often shows selectivity for different ions (for reviews on

selectivity and permeation of ion channels see Imoto, 1993; Sather et al., 1994). The first channel structure to be determined was that of KcsA, a K^+ channel from *Streptomyces lividans*, fig 1.2 (Doyle et al., 1998; Zhou et al., 2001). The data from this and subsequent bacterial channel structures (e.g. Chang et al., 1998; Jiang et al., 2002; Bass et al., 2002; Dutzler et al., 2002) have been used to model the pore-forming regions of a number of voltage-gated channels (Giorgetti and Carloni, 2003).

Opening and closing of a channel is an all or nothing event with spontaneous switching between the states, the overall conductance being determined by the number of channels open at any time. However, in order for a channel to be capable of passing ions, it must first be activated. In a phenomenon known as gating, an electrical, chemical or mechanical stimulus causes a conformational change in the ion channel, allowing the passage of ions through the pore (for a discussion of models for structural changes during gating by different stimuli see Beckstein et al., 2003; Doyle, 2004; Ahern and Horn, 2004). In many channels, after a period of activation, a second structurally-distinct conformational change occurs (deactivation), restricting ion-flow.

α -Subunits of voltage-gated channels contain a region sensitive to membrane potential and responsible for channel gating. The pore forming subunits of most voltage-gated channels form a superfamily of evolutionary related proteins, with similar sequence, structural and functional properties. In sodium and calcium channels the pore region is contained within a single polypeptide, whereas the potassium channel (regarded as the ancestral voltage-gated ion channel) is a tetramer of similar, but not necessarily identical, subunits (see fig 1.3). Voltage-sensitive ion channels have been reviewed by Catterall, 1988; Catterall, 1995; and Conley and Brammer, 1999, and their accessory subunits reviewed by Adelman, 1995. Excitation and signalling in excitable tissues is almost exclusively determined by voltage-gated channels with Na^+ , K^+ , Ca^{2+} or Cl^- permeability and these same channels are the target of a large number of venom neurotoxins.

The ligand- or transmitter-gated channel groups contain a large number of important channels, responsible for coupling chemical and electrical signalling. The ligands themselves may be intracellular, e.g. cAMP, cGMP, G-proteins, or extracellular, e.g. neurotransmitters. In vertebrate skeletal muscle and the peripheral nervous system, nicotinic acetylcholine receptors (AChRs) (Lindstrom, 1995) are the major excitatory

ligand-gated channel. In the CNS, glutamate receptors (Sprengel and Seeburg, 1995) dominate, a distribution that is reversed in insects. The anion selective glycine (Langosch, 1995) and GABA (γ -aminobutyrate) receptors (Tyndale et al., 1995) are the primary channels responsible for receptor-mediated hyperpolarisation, increasing the threshold required to trigger an action potential. Glycine predominates in the brain stem and spine, GABA being utilized in the cerebellum and cortex. For a review on the permeation and selectivity of ligand-gated ion channels, see Sather et al., 1994. The torpedo electric organ AChR was one of the first ion channels studied, due both to the availability of specific toxins (i.e. α -bungarotoxin and cobratoxin) and its high tissue abundance. Ligand-gated ion channels are thought to be the sites of action of a number of drugs, including nicotine (AChRs), barbiturates (GABA receptor type A, GABA_A) and ethanol (GABA_A).

Relatively little is known about mechano-gated channels, which convert membrane deformation into an electrical signal, either directly or via secondary messengers controlled by mechanosensitive enzymes. They have a variety of ion permeabilities and may be selective for K⁺, Cl⁻ or cations, or be non-selective. The mechanical signal may prompt channel activation or inactivation, and sensitivities vary from those found in the hair cells of the inner ear, to those that respond to stimulation above the threshold for cellular damage. See Garcia-Anoveros and Corey, 1997; Patel et al., 2001; Pivetti et al., 2003 for reviews on mechano-gated channels.

Ion channels include a large number of proteins, with approx. 140 members in the voltage-gated family alone. Only those on which apamin, or scorpion venom toxins are active will be discussed further. Data on the genetic, molecular and functional properties of known receptor- and voltage-gated channels can be found on the International Union of Pharmacology website (www.iuphar-db.org/iuphar-rd and www.iuphar-db.org/iuphar-ic respectively).

Fig 1.1 The Action Potential

In a resting neuron, the ionic gradients maintained by the Na^+/K^+ ATPase pump ensure that the interior of the cell has a high potassium ion concentration and a low sodium ion concentration relative to the cell exterior. In this resting state the membrane is more permeable to potassium ions than to sodium ions. The resting membrane potential is therefore largely determined by the electrochemical gradient of K^+ . The generation of a nerve impulse in a neuron is predominantly the result of large changes in the permeability of the axon membrane to sodium and potassium ions.

A) Initiation of the action potential. Localised depolarisation of the membrane leads to opening of voltage-gated Na^+ channels. Since the action potential is an all-or-nothing response, a depolarisation threshold of -55mV must be reached before the action potential is propagated. Below this value, the outward flow of K^+ channels prevents further depolarisation. Above the threshold, sufficient Na^+ channels are open that the inward Na^+ flow exceeds the outward K^+ flow. The resulting depolarisation in turn opens more Na^+ channels and the depolarisation becomes self-propagating.

B) Towards the peak of the action potential, Na^+ channels are beginning to inactivate and the Na^+ conductance starts to fall. At the same time, K^+ channels (also gated by the membrane depolarisation, but which activate more slowly than the sodium channels (delayed rectifiers)) begin to open and K^+ flows out of the cell.

C) At the peak of the action potential, outward K^+ flow begins to exceed inward Na^+ flow and the membrane begins to repolarise.

D) In many cells, elevated K^+ conductance through both voltage- and calcium-gated K^+ channels leads to the after-hyperpolarisation (AHP). This AHP, in conjunction with residual inactivation of the Na^+ channels, accounts for the refractory period. During this time a greater than usual depolarisation is required to reach threshold value, allowing for the spacing of neuronal signals and accounting for desensitisation.

Only a small proportion of the total potassium and sodium ions in the cell participate in action potential generation.

Fig 1.1 The Action Potential (From Aidley, 1989)

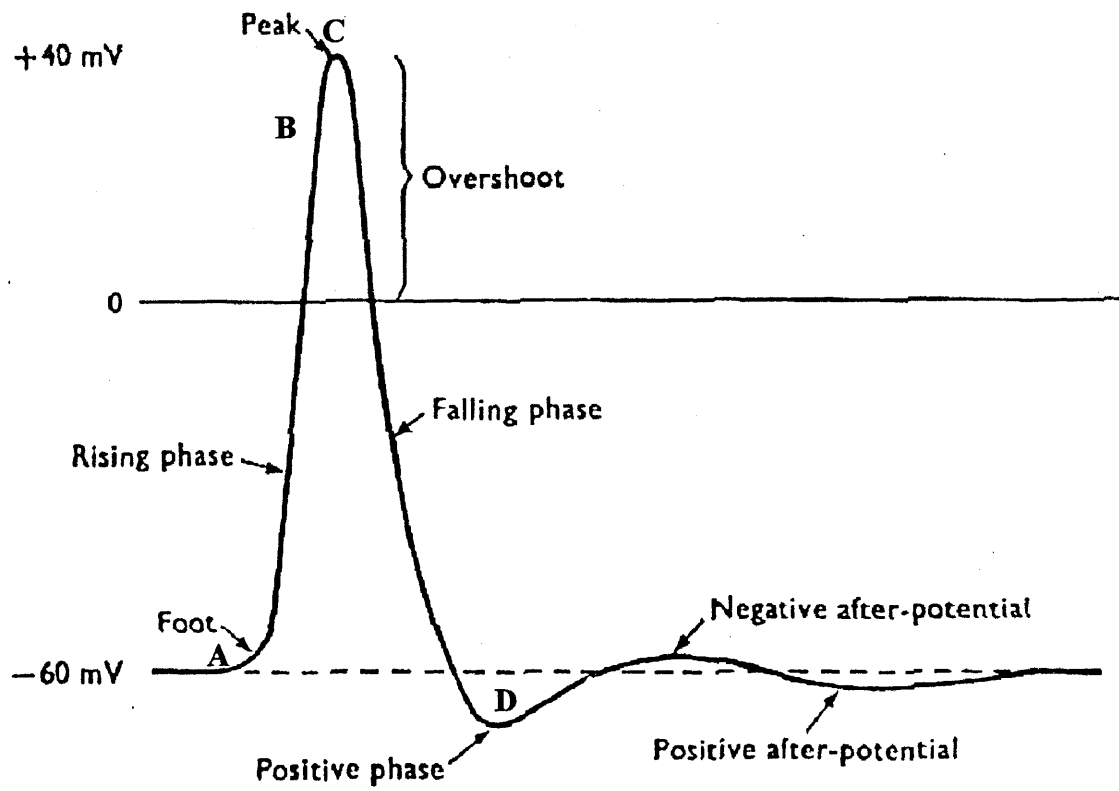


Fig 1.2 Structure of KscA



Intracellular (left) and side-view (right) of the bacterial potassium channel KscA from *Streptomyces lividans*. Each of the four subunits is shown in a different colour. The long helices are the transmembrane segments, the shorter helical regions form the pore loop, and in the centre is the selectivity filter.

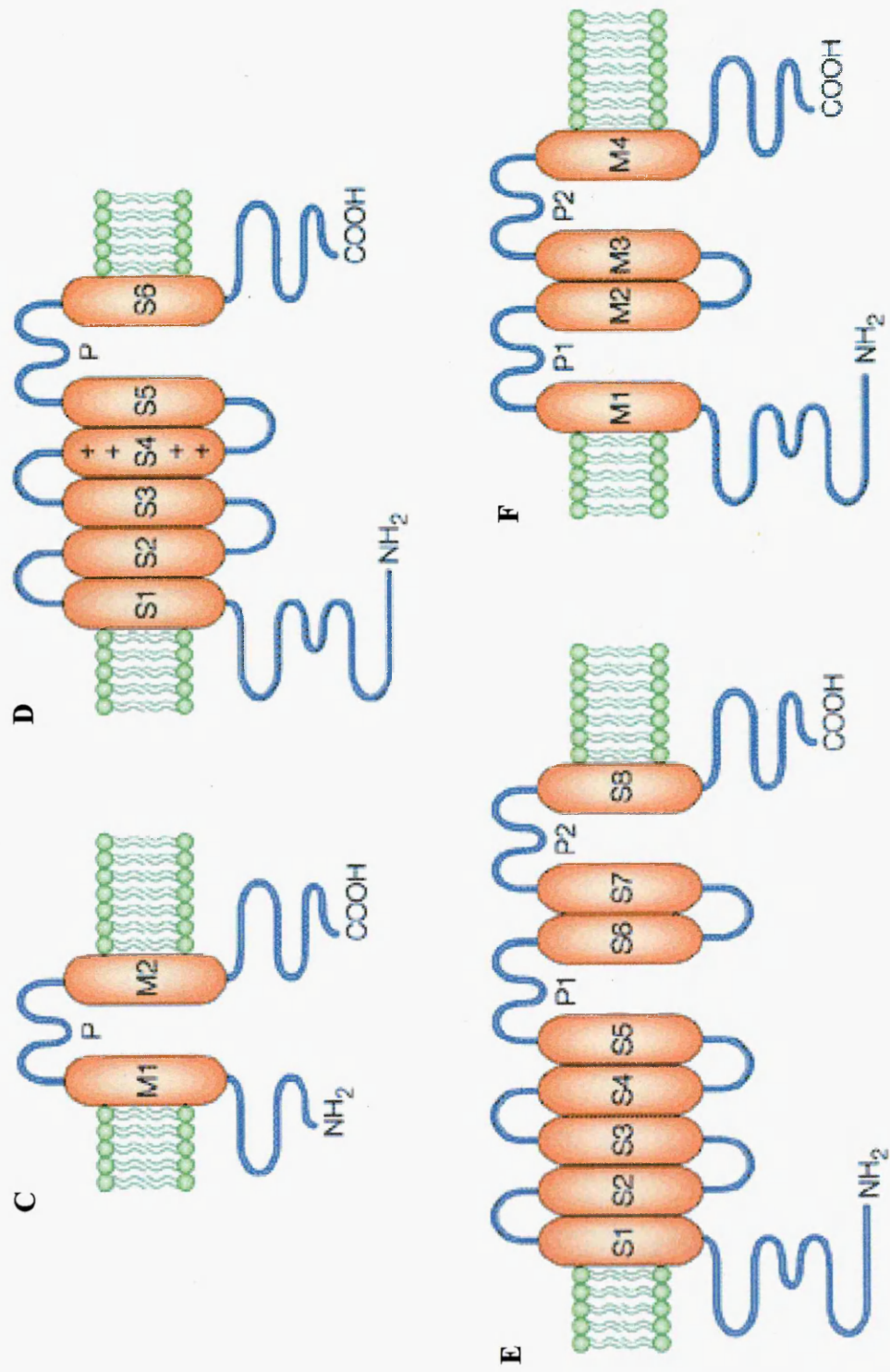
Fig 1.3 Membrane Topology of Voltage-Gated Na⁺, Ca²⁺ and K⁺ channel α -Subunits

- A)** Subunit structure of the voltage-gated sodium channels (see 1.2.1). The extracellular domains of the β 1 and β 2 subunits are shown as immunoglobulin-like folds. Picture taken from Catterall et al., 2003a.
- B)** Subunit structure of Ca_v1 voltage-gated calcium channels (see 1.2.2) purified from skeletal muscle. Picture taken from Catterall et al 2003.
- C–F)** The subunit structure of the four main classes of potassium channel α -subunits. Refer to 1.2.4 for details. Picture taken from Choe, 2002.
- C)** 2TM/P channels e.g. inward rectifiers and KcsA (see 1.2.4). Subunits assemble as tetramers.
- D)** 6TM/P channels e.g. K_v (see 1.2.4.1) and K_{Ca} (see 1.2.4.2) channels. Subunits assemble as tetramers.
- E)** 8TM/2P channels. Found in yeast. Subunits assemble as dimers.
- F)** 4TM/2P channels. E.g. TWIK and TREK (see 1.2.4). Subunits assemble as dimers.

In all cases α -helical segments are represented by cylinders. In **A** and **B**, **P** indicates sites of demonstrated phosphorylation by protein kinase.

Fig 1.3 Membrane Topology of Voltage-Gated Na^+ , Ca^{2+} and K^+ channel α -Subunits

C-F) K^+ channels



1.2.1 Voltage-Gated Sodium Channels (VGSC)

Voltage-gated Na⁺ channels (VGSC) (Goldin, 2001) are present in the membranes of most excitable cells and are responsible for the depolarising phase of action potentials in these tissues (see fig 1.1). They are highly selective for sodium ions and show rapid voltage-dependent activation and inactivation.

Much of the early work on channel structure was carried out on sodium channels (for comprehensive reviews see Catterall, 1992, Catterall, 1995). One of the reasons for the ease of their study was the availability of specific blockers (e.g. tetrodotoxin (TTX) isolated from the puffer fish).

VGSCs were traditionally classified based on tissue and species (e.g. eel electroplax sodium channel [eNa1], Noda et al., 1984), the channels from different tissues having distinct physiological and pharmacological properties. The subunit composition of voltage-gated sodium channels differs from tissue to tissue, e.g. mammalian heart (one α -subunit), skeletal muscle (one α - and one β 1-like subunit) and brain (one α -subunit, one β 1-subunit and one β 2-subunit).

The α -subunit (see fig 1.3) forms the pore itself and is composed of four domains, each with a similar primary sequence and containing six transmembrane (TM) domains. One of these TM domains (S4) is highly charged and has been identified as the voltage sensor. Another important feature of this subunit is the intracellular loop between domains III and IV, which is thought to act as the inactivation gate and produces the refractory period of the channel. The actual pore is lined by the residues between the S5 and S6 segments. The selectivity filter is located at a narrowing of the channel and is thought to contain negatively charged ion binding sites (Imoto, 1993). To date nine mammalian α -subunit genes have been identified and are classified Na_v1.1-Na_v1.9 (Catterall et al., 2003a). Expression of an α -subunit alone is sufficient to produce sodium currents (Noda et al., 1986), but the β -subunits are required for native gating and kinetics (Patton et al., 1994). These β -subunits may also play a role in localising the channels at specific cellular locations (Srinivasan et al., 1998).

A number of sodium channel modulators have been identified. Briefly, these fall into six classes grouped according to their binding site on the channel. Tetrodotoxin and μ -

conotoxins bind to site 1, causing channel block. Toxins binding to site 2 (e.g. veratridine, batrachotoxin) alter the kinetics of activation and inhibit inactivation; site 3 toxins (e.g. sea anemone toxins, α -scorpion toxins) also block inactivation. Other scorpion toxins (β -toxins) bind to site 4, altering either voltage-dependence of activation and inactivation, or that of activation alone. Site 5 toxins (e.g. brevetoxins) and site 6 modulators (e.g. pyrethroid insecticides) also affect kinetics of activation and inactivation, but by interaction with different binding sites.

Some voltage-gated sodium channels play a role in nociception and it is speculated that they play a role in neuropathy, inflammation and acute and chronic pain. Classic local anaesthetics such as lidocaine are sodium channel blockers, and the channels represent viable targets for novel analgesics.

1.2.2 Calcium Channels

Intracellular calcium concentration plays a major role in cellular signalling; therefore calcium channels have a direct effect on membrane excitability and are also involved in signalling pathways. Influx of Ca^{2+} through these channels, together with the release of stored intracellular calcium acts as an important secondary messenger involved in processes such as activation of other ion channels, neurotransmission, synapse formation, exocytosis, cell division and gene activation and a number of Ca^{2+} -dependent enzyme mediated effects.

Voltage-gated Ca^{2+} channels (Brammar, 1999; Yamakage and Naniki, 2002; Catterall et al., 2003) are ubiquitous in excitable membranes. VGCCs open in response to membrane depolarisation and, in general, produce long depolarising pulses since they do not show fast inactivation. This property is important in sustained contractions of heart and smooth muscle, and in maintaining secretion. At high $[\text{Ca}^{2+}]$ they are highly selective ($\text{Ca}^{2+}:\text{Na}^+$ 1000:1), but at low $[\text{Ca}^{2+}]$, this selectivity is lost (McKlesky 1994).

Like voltage gated Na^+ channels, native VGCCs consist of a single pore-forming α -subunit (α_1) in complex with auxiliary subunits (one isoform each of: - $\alpha_2\delta$, β , and γ). As with VGSCs, the α -subunits contain four homologous domains, each with 6TM regions (including an S4 voltage sensor, and a pore forming loop) (see fig 1.3). The α_2

and δ -subunits are expressed as a single polypeptide, the mature forms resulting from posttranslational processing (Dejongh et al., 1990). The mature transmembrane δ -subunit anchors the extracellular α_2 -subunit to the membrane via a disulphide bond (Campbell et al., 1988, Catterall, 1988). The δ/α_2 -subunit influences activation and inactivation. The β -subunits are intracellular and direct membrane trafficking of the α_1 -subunits to specific cellular compartments. They also affect open time, activation and inactivation, and modulation by other proteins. The γ -subunit, initially thought to be specific to skeletal muscle, has four TM segments and seems to have a general role in the regulation of surface expression of a number of receptors and ion channels (Chetkovich et al., 2000). Ten α -subunit genes have been identified and each auxiliary subunit has several gene variants. A number of these subunit genes provide several splice variants, further increasing channel and current diversity. For a discussion of VGCC auxiliary subunits see Adelman, 1995.

There are at least six classes of voltage-gated calcium channels, distinguished by their differential location, pharmacology, structure and electrophysiology. T- type (transient) channels (important in pacemaker activity of cardiac muscle) are the most distinctive, needing only small depolarisations for activation, and showing rapid voltage-dependent deactivation. By lowering the action potential threshold in neurons and cardiac cells during periods of hyperpolarized resting potential, they stimulate repetitive firing. In contrast, much higher depolarising voltages are required for activation of the other channel types (L, N, P, Q and R-types).

Voltage-gated calcium channels are sensitive to a number of venom toxins, N-, P-, and Q-type channels showing sensitivity to spider and/ or molluscan venom peptides. These toxins are being investigated for their neuroprotectant properties, since a high intracellular free calcium concentration is toxic and a primary cause of ischemic brain damage.

Intracellular calcium concentration in a resting eukaryotic cell is maintained at a low concentration by active Ca^{2+} transport both out of the cell and into intracellular stores. Various stimuli provoke release of calcium from the intracellular stores, causing a rapid increase in intracellular free calcium ion concentration ($[\text{Ca}^{2+}]_i$). This stored calcium release is largely modulated by the InsP_3 and the ryanodine receptor (RyR) families.

The ryanodine receptors (Fill and Copello, 2002) are multimeric proteins comprised of four large (approx. 5000 amino acids) and four small (100 amino acids) subunits and are localised on the sarcoplasmic reticulum. They are gated by voltage-induced conformational changes in the dihydropyridine receptors of the T-tubule plasma membrane. RyRs are regulated by a wide variety of intracellular signals, one of the most important of which is Ca^{2+} itself (Ca^{2+} -induced Ca^{2+} release). They show far less Ca^{2+} selectivity than do plasma membrane Ca^{2+} channels. This is permitted by the fact that selective passage of Ca^{2+} into the intracellular stores is provided by the Ca^{2+} pump, making selective release superfluous. Ryanodine, the ligand after which the ryanodine receptor was named, is a plant alkaloid from *Ryania speciosa* that binds with high affinity to the open state of the channel.

1.2.3 Chloride Channels

The Cl^- channels form a large and very diverse group, but we have limited knowledge of their specific functions compared to that of Na^+ , K^+ and Ca^{2+} channels. Although in most cases, intracellular $[\text{Cl}^-]$ is less than extracellular $[\text{Cl}^-]$; intracellular $[\text{Cl}^-]$ is maintained at levels close to electrochemical equilibrium. Cl^- fluxes are rarely involved in electrical excitation; instead, they generally suppress it. Opening of these channels holds the membrane potential at its resting value, or at a hyperpolarized value, making it more difficult to depolarise the membrane and hence excite the cell. They are therefore important in neurons and in muscle, where they contribute to resting conductance and dampen down electrical excitability. Probably present in the plasma membrane of all eukaryotic cells, chloride channels also have roles in cell volume regulation, secretion, and sensory signal transduction.

A large number of genes for functional chloride channels have been cloned (Jentsch et al., 1995; Jentsch, 1996; Frings et al., 2000), but the structure and functional properties of most of these are unclear. There are many different types of chloride channel; these include those gated by extracellular ligands, intracellular calcium, voltage and cell volume.

The first voltage gated Cl^- channel to be cloned was ClC-0 from the electric organ of *Torpedo* (Jentsch et al., 1990). Since then, nine human ClC channels have been

identified (Jentsch et al., 2002; Dutzler, 2004; Dutzler, 2004a). ClC-1 modulates resting potential in skeletal muscle, ClC-2 has a similar function in some neurons, and ClC 3, 4, 6 and 7 are involved in acidification, as is kidney-localised ClC-5. ClCKa and ClCKb are also localised in the kidney and are responsible for trans-epithelial Cl⁻ transport in the renal inner medulla (Matsumara et al., 1999). ClC channels have two pores; one located on each of two homodimeric subunits (see fig 1.4 a-d).

The calcium-activated chloride channels (CaCC, Frings et al., 2000) may be localised to specific regions of the cell where their activity depends upon local Cl⁻ equilibrium potential and Ca²⁺ concentrations. Neuronal CaCCs participate in sensory signal processing of some somatic senses, as well as vision, olfaction and taste, and are also present in non-sensory neurons in the CNS (central nervous system) and PNS (peripheral nervous system). They have a wide non-neuronal distribution including epithelia, muscle, blood and endocrine cells, and a wide range of functions. In striated muscle, for example, they contribute to the initial phase of repolarisation during the action potential.

GABA and glycine are responsible for fast inhibitory transmission in the mammalian central nervous system. GABA_A, GABA_C, and glycine receptors (see Chebib and Johnston, 2000; Whiting, 2003; Colquhoun and Sivilotti, 2004) mediate these inhibitory Cl⁻ currents. One such example is the production of the inhibitory postsynaptic potential (IPSP) in the direct inhibitory pathway of muscles. These channels are members of the ligand-gated ion channel superfamily (see fig 1.4 f).

Expressed in the epithelium and the heart, and of great clinical importance, the cystic fibrosis transmembrane conductance regulator (CFTR, McAuley and Elborn, 2000) gene was identified and cloned by Riordan et al., 1989. It is expressed in the apical membrane in many epithelial tissues e.g. in the airways, pancreas, sweat ducts and the intestine. A variant is also found in cardiac muscle. Although functionally an ion channel responsible for the I_{Cl (cAMP)} current, structurally it belongs to the traffic ATPase superfamily (see fig 1.4 e for membrane topology). It may have a regulatory as well as ion channel function, and interacts with the epithelial sodium channel. Inhibitors of the channel are important in the study of cystic fibrosis and have been proposed as therapeutics for secretory diarrhoeas e.g. cholera.

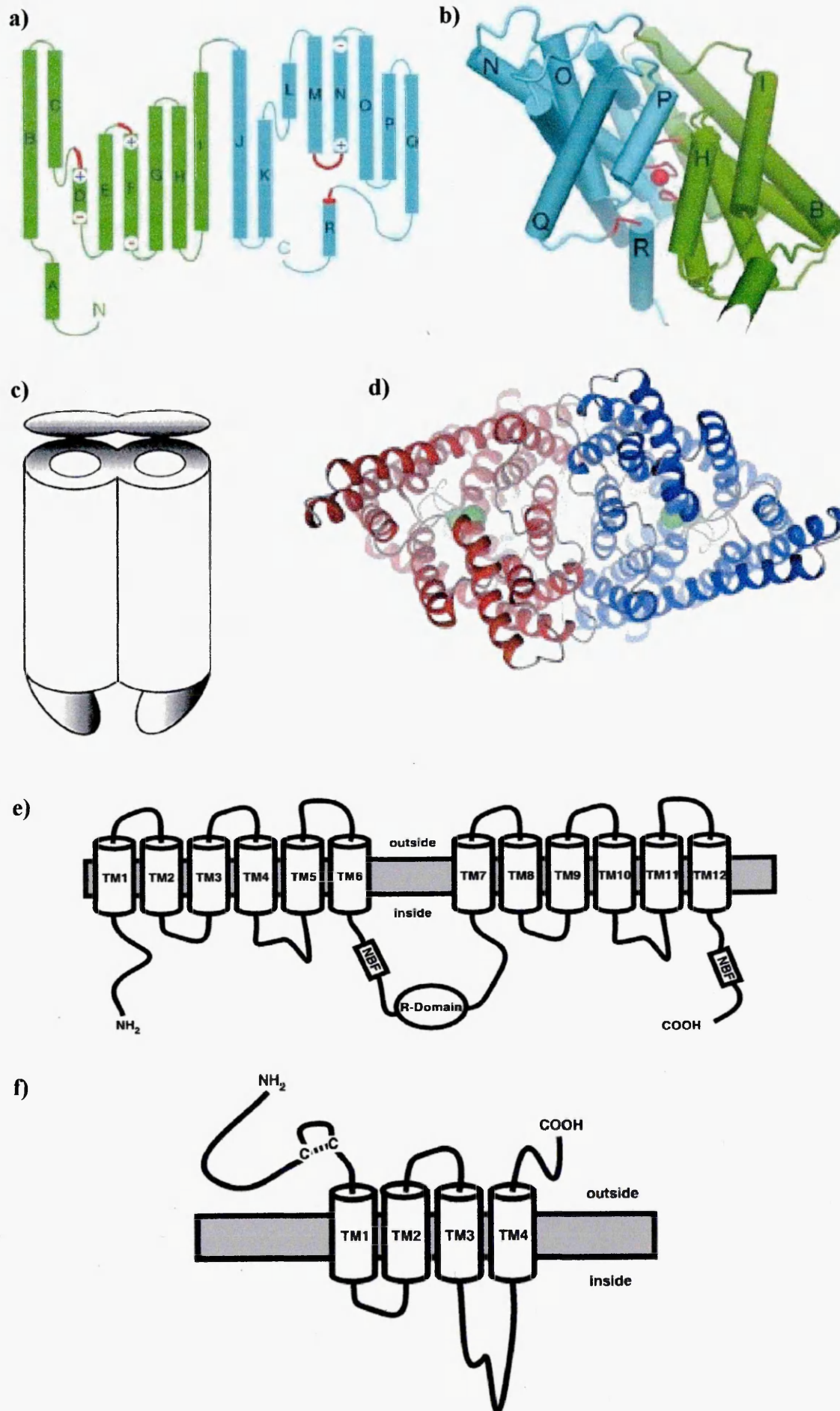
Figure 1.4 Chloride Channel Topology

a-d) ClC channel structure. (Based upon that of the *E. coli* Cl⁻ channel EcClC. See Dutzler, 2004, 2004a for a review of ClC structure). **(a)** The ClC protein is composed of 17 α -helices (A-R) many of which do not fully span the membrane (helix A is not inserted in the membrane). Each subunit consists of two domains (blue and green regions). The helices in each of these domains are tilted in opposite directions, with the pore located between the domains **(b)**. Early electrophysiological data on ClC-0 suggested a 'double-barrelled' structure for ClC channels **(c)**. In this model the channels are dimers, with each subunit contributing a pore. These pores can be gated individually, or both pores closed by a common gate. The structure of EcClC (viewed from the extracellular side) confirmed this dimeric architecture, both of the identical subunits contributing a pore **(d)**. Pictures taken from Jentsch et al., 2002 and Dutzler, 2004.

e) Membrane topology of CFTR. The CFTR protein is divided into two 6TM regions separated by a cytoplasmic region. The regulatory domain (R-domain) and the first of two nucleotide-binding folds (NBF) are located in this intracellular segment. A second NBF is located close to the C-terminus. It is currently unclear if CFTR is a monomer or a dimer. Picture taken from Jentsch et al., 2002.

f) Membrane topology of a ligand-gated anion channel subunit. GABA and Glycine receptors are members of the ligand-gated ion channel superfamily (which also contains the nicotinic acetylcholine receptors). These receptors share sequence and structural homology and are believed to have evolved from a common ancestral receptor subunit. The channels are homo- and hetero-pentamers of 4TM subunits. Picture taken from Jentsch et al., 2002.

Figure 1.4 Chloride Channel Topology



1.2.4 Potassium Channels

Potassium channels are the largest and most diverse family of ion channels. They have a range of functions including: setting resting membrane potential; shaping action potentials and determining their frequency; cell volume control; and secretion of salt, hormones and transmitters. Although they may be voltage-, ligand-, or mechano-gated, only those activated by changes in membrane potential, and their relatives (the voltage-gated potassium channel gene family), are considered in this section. K^+ channels have a near-perfect selectivity for potassium ($K^+ : Na^+ > 1000:1$), which is achieved at conductance rates approaching the diffusion limit. All of these channels contain a highly conserved K^+ channel signature sequence (Heginbotham et al., 1994) that forms the selectivity filter. These channels, their classification and the mechanisms determining their selectivity have been reviewed by a number of authors (Miller, 2000; Choe, 2002; MacKinnon, 2003; Gutman et al., 2003).

Primarily due to lack of specific probes, the early studies of voltage-gated potassium channels lagged behind that of their sodium channel counterparts and it was not until the advent of molecular cloning techniques, and discovery of natural ligands, that detailed study was possible.

A wide variety of functionally and pharmacologically different K^+ currents have been recorded *in vivo*. The last fifteen years have seen a rapidly increasing family of K^+ channels emerge, identified via cloning. These K^+ channels can be classified into four groups according to the membrane topology of their pore-forming subunits (see fig 1.3).

In the first group, a single pore is surrounded by four subunits with two TM domains and a pore loop each (2TM/P, a motif that essentially forms the basic unit of the K^+ channel family). This group includes the inward rectifiers (Kir) and the bacterial channel KcsA. The large family of Kir's tend to open at membrane potentials near to, or more negative than, the resting potential (Reimann and Ashcroft, 1999; Loussouarn et al., 2002). They are homo- or heteromeric and are involved in maintenance of the resting membrane potential and regulation of the action potential. They also have a role in electrolyte processing in the kidney. The KcsA channel from *Streptomyces lividans* is of particular significance as the first ion channel to have its 3D structure determined

(Doyle et al., 1998), providing important information on the structure and function of the K⁺ channel pore.

The largest group is comprised of channels containing four 6TM segment subunits surrounding a single pore (6TM/P). Four TM regions, including an S4 voltage sensor, precede the 2TM/P motif. This topology is shared by the *Shaker* voltage-gated potassium channel family (K_v), calcium-activated potassium channels (although the slopoke subfamily has an extra transmembrane segment close to the extracellular C-terminus), the eag (*ether-a-go-go*)-like gene family (including EAG (*ether-a-go-go* gene potassium channel), ERG (*ether-a-go-go*-related gene potassium channel), and ELK (*ether-a-go-go*-like potassium channel); showing inward rectification and of particular importance in the heart (Cooper and Jan, 1999; Karle and Kiehn, 2002), KCNQ channels (responsible for the M-Type potassium currents, which activate near the threshold for action potential generation and regulate neuronal excitability, Jentsch, 2000; Robbins, 2001) and the CNGs (cyclic nucleotide-gated cation channels).

In 1995 a yeast channel was identified containing two tandemly arranged pore-like domains (Ketchum et al., 1995). The dimeric 8TM/2P subunits have a 6TM/P motif and a 2TM/P region arranged in tandem.

The last group contains proteins with 2x 4TM subunits and two pore domains (4TM/2P, consisting of two 2TM/P repeats). These include the TWIKs (tandem of P domains in weak inward rectifier K⁺ channels), TREKs (TWIK-related K⁺ channels), TRAAKs (TWIK-Related arachidonic acid-stimulated K⁺ channels), TASKs (TWIK-related acid-sensitive K⁺ channels), THIKs (halothene-inhibited 2P domain K⁺ channels) and TALKs (alkaline-activated background K⁺ channels). The two-pore potassium channels include a number of mechano-gated and lipid sensitive channels. They tend to be constitutively active, may mediate background K⁺ currents and are the targets of many anaesthetics (Lesage and Lazdunski, 2000; Patel et al., 2001).

Potassium channels are generally homo- or hetero-multimers of pore-forming α -subunits. Alternative gene splicing creates further diversity (Pongs 1992) and accessory β -subunits may also be present, regulating channel targeting or modulating function (McManus et al., 1995; Fink et al., 1996; Mangubat et al., 2003).

Drugs that alter K^+ channel activity are in development for a variety of conditions (e.g. diabetes, cardiac arrhythmias, hypertension, angina). The great diversity of K^+ channels, however, creates problems in the development of selective drugs. Also, different physiological channels may be structurally related, so a drug often acts on multiple channel types.

1.2.4.1 Kv Channels

The first ion channel to be cloned was the *Shaker* channel α subunit from *Drosophila* (Temple et al., 1987), followed by three related genes (*Shab*, *Shaw*, and *Shal*) (Butler, et al., 1989). Seventeen mammalian homologues have been found and grouped into Kv1-4, related to *Shaker*, *Shab*, *Shaw* and *Shal* respectively. These mammalian counterparts share 50-82% homology with the *Drosophila* genes but, unlike the *Drosophila* channels, are encoded on separate, intronless genes.

Kv subunits and (associated β subunits) are found in neuronal and non-neuronal cells, and form delayed rectifiers (which activate a short while after membrane depolarisation, inactivate slowly, or not at all, and are involved in the falling phase of the action potential) and A-type channels (which activate and inactivate rapidly on initial depolarisation producing a brief outward current thus buffering depolarisations below threshold value and inserting a gap between successive action potentials). Kv α -subunits form homotetramers, or hetrotetramers within and between Kv subfamilies. Functional channels are often dependent on co-expression with β - or γ -subunits (Robertson, 1997).

Kv channels are the most characterised of potassium channels and much of what is now known about K^+ channel structure (from KscA, and more recent structural studies) had previously been postulated, based upon studies on Kv channels. The channels are the targets of a number of naturally-derived inhibitors from scorpion, snake and sea anemone venoms, for example, and from plants (e.g. correolide from *Spachea correa*) (see Kaczorowski and Garcia, 1999 for details). Not only do these inhibitors show potential in the design of therapeutic drugs but they have also been used extensively in channel characterisation. As an example, studies using charybdotoxin led to the

characterisation of the outer vestibule of the *Shaker* channel as a shallow hole approx. 30Å wide (Miller, 1995).

1.2.4.2 Calcium-Activated Potassium Channels (K_{Ca})

Change in intracellular free calcium concentration is a ubiquitous signalling mechanism. This calcium may be released from cytosolic stores or may enter the cell, via voltage-activated calcium channels, during an action potential. This $[Ca^{2+}]_i$ is coupled to membrane potential by a group of potassium channels that are activated by local increases in cytosolic calcium concentration. Opening of these calcium-activated potassium channels leads to potassium ion efflux and membrane hyperpolarisation.

K_{Ca} channels have a number of functions. They generate membrane potential oscillations and are the predominant channel involved in spike frequency adaptation. The prolonged afterhyperpolarisation seen after the action potential is due to the slow inactivation kinetics of a K_{Ca} channel. These channels also play a role in hormone secretion (Montiel et al., 1995).

An intracellular-calcium linked potassium permeability was first noted by Gardos, 1958 in human erythrocytes and later a K_{Ca} current was identified in *Aplysia* neurons (Meech and Strumwasser, 1970). A number of different calcium activated currents have since been distinguished on the basis of pharmacology and kinetics, and at the molecular level several channel proteins have been identified. These have been divided into three groups according to the rate of conductance and are termed SK, IK and BK (small conductance, intermediate conductance and large (big) conductance calcium-activated potassium channels respectively).

K_{Ca} channels represent targets for the development of therapeutics for asthma, hypertension, psychoses, depression, memory disorders, convulsions, ischemic stroke and traumatic brain injury (Kaczorowski and Garcia, 1999; Faber and Sah, 2003).

Large Conductance Calcium-Activated Potassium Channels (BK or maxi-K)

BK channels have a single channel conductance of 100-250pS, open rapidly on increase of $[Ca^{2+}]_i$, and close rapidly when the calcium is removed. The K_d of the channel for calcium is voltage-sensitive. The greater affinity for calcium at more positive potentials translates to a greater open probability under these conditions. The channels are highly expressed in smooth muscle and are also found in the brain, inner ear, kidney, human T-cells (Deutsch et al., 1991) and endocrine and exocrine epithelium. They have a number of functions, including regulation of smooth muscle contraction, the duration of the action potential and quantity of neurotransmitter release. In the chicken cochlea, they adjust the oscillation frequency in individual hair cells (Rosenblatt et al., 1997).

BK channels contain a combination of α - and β -subunits. The alpha subunit is unusual amongst the voltage-activated potassium channel superfamily in having seven transmembrane domains. The extra transmembrane segment (S0) means that the N-terminus has an extracellular location. Despite this, the channel retains sensitivity to TEA^+ (tetraethylammonium cation, 0.5-1mM) and charybdotoxin, suggesting the pore structure is similar to that of voltage gated channels and has the distinctive S4 voltage sensor. The different forms of this subunit are encoded by a single gene (Tseng-Crank et al., 1994; Lagrutta et al., 1994). Splice variants give rise to channels with different voltage and calcium sensitivities.

For recent general reviews on BK channels, see Gribkoff et al., 2001 and Weigner et al., 2002.

Intermediate Conductance Calcium-Activated Potassium Channels (IK)

The intermediate conductance (20-80 pS) IK channels are six transmembrane domain proteins and are often grouped with the SK channels (IK1 is sometimes referred to as SK4). The IK channels are voltage-insensitive, being gated by $[Ca^{2+}]_i$ to which they are more sensitive than are BK channels. This calcium sensitivity is mediated by calmodulin (Fanger, 1999). The channels can also be activated by cell swelling and are pH sensitive.

The channel is expressed in many non-neuronal tissue types. In red blood cells IK forms the Gardos channel (Maher and Kuchel, 2003). This channel is sensitive to clotrimazole, which is in clinical trials for sickle cell anaemia. By blocking potassium loss through erythrocyte IK channels, the drug may help prevent water loss and hence cell sickling (Brugnara et al., 1996). In the colon the IK is essential for acetylcholine-mediated secretion (Warth and Bleich, 2000). They may be responsible for the effects of bradykinin in kidney capillary cells. The channels are generally not considered neuronal, although one group has reported the associated currents in rat supraoptic nuclear neurons (Greffrath et al., 1998).

Small Conductance Calcium-Activated Potassium Channels (SK)

As their name suggests, the small conductance calcium-activated potassium channels have only a small single channel conductance (2-20pS) and are activated by an increase in intracellular calcium, as is seen during an action potential. The potassium current produced causes membrane depolarisation. This hyperpolarisation is long-lasting due to the slow decrease in $[Ca^{2+}]_i$ after the action potential. The current is the slow afterhyperpolarisation, and limits the firing frequency of action potentials. This sAHP can be divided into two pharmacologically distinct currents, which vary according to their sensitivity to apamin, and their activation and inactivation properties.

The gene family responsible for the apamin-sensitive current has been identified (SK1-3, Kohler et al., 1996), although, as discussed by Faber and Sah, 2003, the precise channel responsible for the apamin insensitive current is unclear. All three subtypes are sensitive to apamin, though in the case of SK1 the affinity is much lower. Early reports indicated SK1 was insensitive to the toxin (Kohler et al., 1996), but subsequent studies in a different expression system revealed that this was not the case (Strobaek et al., 2000).

These expressed SK channels seem to be able, in themselves, to produce functional pores, and they are capable of forming functional homo- and heteromers (Kohler et al., 1996; Ishii et al., 1997a). They are voltage insensitive but respond rapidly to small changes in free calcium ($K_d < 1\mu M$) (Hirschberg et al., 1998). The channels co-assemble with calmodulin. Calcium ions do not bind directly to the α -subunit. Instead,

gating is regulated by Ca^{2+} binding to the calmodulin moiety, which in turn produces conformational changes in the channel itself (Xia et al., 1998; Maylie et al., 2004).

SK mRNAs are found throughout the CNS (although the subtypes have differential distributions, Stocker and Pedarzani et al., 2000) and are also found in many non-neuronal cell types. The SK1 gene has eight exons, and over 30 predicted transcripts, of which 20 have been detected in the brain (Shmukler, et al., 2001).

The importance of these channels in the CNS is demonstrated by the effects of apamin (see 1.4.1) and they play important roles in learning and memory (Faber and Sah, 2003). Aside from their neuronal functions, calcium activated potassium channels provide an important link between metabolism and membrane potential. SK channels appear to have roles in endocrine mechanisms and have been implicated in regulating the release of adrenaline from chromaffin cells (Monteil et al., 1995).

1.2.5 Clinical Relevance of Ion Channels

Not surprisingly, disorders of ion channels result in hyper- or hypo-activity of cells. Ion channel defects underlie a number of clinical disorders, of which the channelopathies are the most extensively studied. Channelopathy refers to a disorder caused by mutations in the genes encoding various proteins that together form functional ion channels. Naturally arising channelopathies, together with knockout gene studies, can provide valuable information on the role of specific ion channel proteins. The gene products involved in such genetic disorders and relevant recent reviews are summarised in table 1.1.

Considering the wide diversity of ion channels, it is perhaps surprising that more pathological ion channel mutations have not been recognised. It is thought that most mutations of key ion channels lead to non-viability or early mortality and are, therefore, not maintained within the gene pool. There is, however, a degree of functional redundancy provided by the large number of subtypes of the ion channels and many mutations may produce only mild, or periodic, symptoms. Mutations in a single gene can give rise to different disorders and a single disorder can arise from mutations in genes encoding different ion-channel families.

Several ion channel diseases are caused by defects in trafficking. Spinocerebellar ataxia (SCA6) is a polyglutamine disease caused by the expansion of a CAG repeat in a single splice variant of Ca α -subunit α 1A. It is postulated that this expansion results in the protein forming aggregates in the cytoplasm of Purkinje cells (Ishikawa et al., 1999), although researchers disagree as to whether the pathology seen with this disorder is due to these aggregates or to loss of channel function (Frontali, 2001). The SK3 gene [KCNN3] also contains polymorphic CAG repeats. There has been controversy over the role that this polymorphism may play in schizophrenia (e.g. Bowen et al., 1996; Li et al., 1998; Cardno et al., 1999). The role of trinucleotide repeats in this disorder is discussed by Vaswani and Kapur, 2001.

A large number of ion channel defects are acquired. These include ion channel autoimmune disorders (Vincent et al., 2000), of which myasthenia gravis, affecting the nicotinic AChR in skeletal muscle (Hoedemaekers et al., 1997), is the most common. Other ion channel autoimmune diseases include Rasmussen's encephalitis (affecting the GluR3 glutamate receptor subunit, Granata, 2003), acquired neuromyotonia (voltage-gated potassium channels, Vincent et al., 1998) and Lambert-Eaton myasthenic syndrome (P- and Q-type voltage-gated calcium channels, Takamori et al., 2000). Ion channels may also play a role in certain demyelinating autoimmune diseases. For example, relapses commonly seen in multiple sclerosis have been blamed on endogenous substances reversibly blocking sodium channels (Brinkmeier et al., 2000).

Recently, transcriptional ion channel disorders have been the subject of investigation (Waxman, 2001). One of the most studied of these is peripheral nerve injury, which causes a change in expression levels of sodium channel genes (both up- and down-regulation) leading to hyperexcitability of spinal sensory neurons and to neuropathic pain (Dib-Hajj et al., 1996).

Ion channels are the therapeutic targets for a number of classes of drugs, including local anaesthetics (Na^+ , Ca^{2+}), neuroprotectants (Na^+ , Ca^{2+}), antihypertensives (K^+), immunosuppressants (K^+), analgesics (Ca^{2+}), anticonvulsants (GABA), antiepileptics (glutamate); neuromuscular blockers (ACh), antidepressants (GABA), cardioprotectants (K^+), antidysrhythmias (Ca^{2+} , K^+), hypoglycaemics (K^+) and drugs for treating neurodegeneration (ACh, glutamate). For many of these pharmacological agents, the site of action has only been elucidated relatively recently. Knowledge of the structure

and function of the ion channels involved is leading to a new generation of specific drugs.

Action on ion channels has also been shown to underlie some of the unwanted side effects of many pharmaceuticals. One such example is the production of cataracts by tamoxifen, a potent blocker of volume-activated outwardly rectifying Cl⁻ currents, used in the treatment of breast cancer. Aside from its cancer cell target, the drug also blocks a lens Cl⁻ channel involved in volume and hydration of the lens, and hence its transparency (Zhang et al., 1994). The use of a wide range of drugs (including antihistamines, antimicrobials and antipsychotics) has been associated with increased risk of torsade de pointes, via interactions with the HERG K⁺ channel (Redfern et al., 2003). Polymorphisms in ion channel genes may have important effects on susceptibilities to certain drugs. For example a SCN5A sodium channel variant found in African races, unproblematic under normal conditions, may provoke a long QT syndrome in the presence of I_{Kr} blockers (Splawski et al., 2002). Such unwanted actions of many existing ion channel drugs, and genetic variation in susceptibility, highlight the need for increased knowledge regarding the precise therapeutic targets of these compounds and the development of modulators with a heightened specificity.

Increasing knowledge of the structure and function of ion channels, has highlighted them as targets for novel therapeutics. In sickle cell anaemia, dehydration of erythrocytes leads to polymerisation of haemoglobin, which produces the sickling effect. The calcium activated K⁺ efflux (via the Gardos pathway) is accompanied by further water loss and dehydration, and increased sickling. A number of inhibitors of the IK channel that carries this current have been identified, of which Clotrimazole has undergone clinical trials in humans (Brugnara et al., 1995). Research is now focussing on finding compounds with a higher specificity (Jensen et al., 2001). A number of ion channels may provide targets for anti cancer drugs. ERG1, for example, is expressed in several tumour types and is responsible for the inward rectifier current which maintains the resting potential at a depolarised value necessary for unlimited tumour growth (Bianchi et al., 1998). The much-publicised discovery of the CatSper ion channels in sperm may provide a target for contraceptives (Ren et al., 2001).

Table 1.1 Human Channelopathies

Type of disorder	Disorder	Channel [gene]	Recent reviews
Skeletal muscle	Hyperkalemic Periodic Paralysis	Na α subunit [SCN4A]	Krause and McNamara, 1995; Dworakowska and Dolowy, 2000; Gargus, 2003
	Paramyotonia	Na α subunit [SCN4A]	Krause and McNamara, 1995; Weinreich and Jentsch, 2000; Dworakowska and Dolowy, 2000
	Hypokalemic Periodic Paralysis	L-type Ca channel α 1 subunit (Dihydropyridine Receptor) [CACNA1S]; Na channel α subunit	Weinreich and Jentsch, 2000; Dworakowska and Dolowy, 2000; Gargus, 2003,
	Potassium sensitive myotonia (myotonia fluctuans; myotonia permanens)	Na channel α subunit [SCN4A]	Cannon, 1997; Dworakowska and Dolowy, 2000; Gargus, 2003
	Myotonia (Thomsens; Beckers)	Cl channel [CLCN1]	Dworakowska and Dolowy, 2000; Pusch, 2002; Gargus, 2003
	Malignant hyperthermia (central core disease; King-Denborough syndrome)	Na channel α subunit [SCN4A]; L-type Ca α 1 or α 2 subunits [CACNA1S] [CACNL2A]; ryanodine receptor [RYR1]	Dworakowska and Dolowy, 2000; Wappler, 2001; Gargus, 2003
	Congenital myasthenia	ACh receptor subunits [CHRNA1] [CHRN1] [CHRE]	Dworakowska and Dolowy, 2000; Lindstrom, 2000; Gargus, 2003
Nervous system	Episodic ataxia type 1 (Myokymia)	Potassium α subunit Kv 1.1 [KCNA1]	Krause and McNamara, 1995; Shieh et al., 2000; Dworakowska and Dolowy, 2000
	Episodic ataxia type 2	Ca α subunit [CACNA1A]	Jen, 1999; Weinreich and Jentsch, 2000; Dworakowska and Dolowy, 2000
	Hyperreflexia (familial startle disease)	Glycine receptor α 1 subunit [GLRA1]	Krause and McNamara, 1995; Rajendra et al., 1997; Dworakowska and Dolowy, 2000
	Spinocerebellar ataxia type 6	Ca α subunit [CACNA1A]	Jen, 1999; Weinreich and Jentsch, 2000; Pietrobon, 2002
Heart	Long QT type 3 syndrome	[KCNQ1], cardiac Na channel [SCN5A]	Weinreich and Jentsch, 2000; Jentsch, 2000; Head and Gardiner, 2003,
	Long QT type 2 syndrome	[HERG] heart K ⁺ channel	Weinreich and Jentsch, 2000; Shieh et al., 2000; Dworakowska and Dolowy, 2000
	Long QT type 5 syndrome	[KCNE1] K ⁺ channel β subunit minK (IsK)	Weinreich and Jentsch, 2000; Shieh et al., 2000; Dworakowska and Dolowy, 2000
	Cardiac arrhythmia	[KCNE2] MiRP1 which associates with HERG channels	Weinreich and Jentsch, 2000; Dworakowska and Dolowy, 2000; Gargus, 2003
	Familial idiopathic ventricular fibrillation	[SCN5A] cardiac Na channel	Dworakowska and Dolowy, 2000; Gargus, 2003; Head and Gardiner, 2003
Brain	Benign familial neonatal convulsions	Volt gated K ⁺ α subunits [KCNQ2], [KCNQ3]	Steinlein and Nobel, 2000; Shieh et al., 2000; Steinlein, 2002,
	Generalised epilepsy with febrile seizures 'plus'	Na channel subunits [SCN1B], [SCN1A], [SCN2A]; GABA _A receptor subunit [GABRG2]	Weinreich and Jentsch, 2000; Steinlein, 2002; Gargus, 2003
	Familial hemiplegic migraine	Brian P/Q type Ca α subunit [CACNA1A]	Weinreich and Jentsch, 2000; Dworakowska and Dolowy, 2000; Carrera et al., 2001,
	Familial nocturnal frontal lobe epilepsy (Autosomal dominant nocturnal frontal lobe epilepsy)	Neuronal nicotinic ACh receptor [CHRNA4], [CHRN1], [CHRN2]	Weinreich and Jentsch, 2000; Steinlein, 2002; Gargus, 2003
	Severe myoclonic epilepsy of infancy	[SCN1A] sodium channel	Head and Gardiner, 2003; Gargus, 2003; Mulley et al., 2003
Sensory	DFNA2 (Hereditary hearing loss, nonsyndromic dominant deafness)	[KCNQ4] K ⁺ α subunit	Weinreich and Jentsch, 2000; Shieh et al., 2000; Jentsch, 2000
	Congenital stationary night blindness type 2	Retina-specific Ca channel α subunit Ca 1.4 [CACNA1F]	Dworakowska and Dolowy, 2000; Celesia, 2001; Pietrobon, 2002
	Colour blindness	Cone photoreceptor CNG channels [CNGA3]	Dworakowska and Dolowy, 2000; Kaupp and Seifer, 2002
Renal	Bartters syndrome	Kir 1.1 [KCNJ1] CLC-Kb	Shieh et al., 2000; Dworakowska and Dolowy, 2000; Thakker, 2000
	X-linked recessive nephrolithiasis (Dents disease)	Chloride channel [CLC-5]	Dworakowska and Dolowy, 2000; Thakker, 2000; Yu, 2001
Secretory	Cystic fibrosis	Epithelial chloride channel [CFTR] *	Dworakowska and Dolowy, 2000; Rubin, 2003; Ratjen and Doring, 2003
Metabolic	Familial Persistent Hyperinsulinemic Hypoglycaemia of Infancy	Sulfonylurea receptor 1 of ATP-sensitive potassium channel. [SUR1]	Shieh et al., 2000; Dworakowska and Dolowy, 2000; Fournet and Junien, 2003

This table shows some of the naturally occurring human channelopathies. A large number have also been identified in mice.

*It should be noted that although the CFTR is functionally a chloride channel, structurally it forms part of the ABC (ATP-binding cassette) transporter family and therefore its classification as a true ion channel is controversial

1.3 Venoms

There are over 1000 species of venomous animals from a wide variety of phyla, including arthropods, cnidaria, nematodes, echinoderms, molluscs and chordates, which use their venoms for prey capture, defence from predators and to deter competitors. The distinction between poisonous and venomous species is the possession of specialised delivery apparatus. This distinction becomes blurred when considering some frogs, for example, which have specialised glands under the skin for venom storage (Terreni et al., 2003). Delivery, however, is via nothing more than expulsion of the 'venom' onto the skin as a predator deterrent. Frog 'venom' is therefore better classified as a toxic secretion.

A wide variety of venom delivery systems have evolved. In some fish the venom apparatus is little more than venom secreting cells associated with a modified spine. Venom release is entirely involuntary (the direct result of mechanical pressure on the spine) and is therefore used solely for defensive purposes (Church and Hodgson, 2002). In contrast, scorpions not only control the timing and quantity of venom release, but may also be able to control its composition. Other organisms use modified teeth, the most obvious of these being the snakes. In the gila monster (*Heloderma suspectum*), the venom is not injected via fangs, but venomous saliva is chewed into the victim using grooved teeth (Raufman, 1996). One of the most sophisticated of envenomation devices is that of the cnidaria, and consists of specific organelles, or nematocysts (Tardent, 1997).

Similarly, there is much variation in the venom itself. In some cases this is synthesised *de novo* (e.g. in spiders, Escoubas and Rash, 2004); in other species (e.g. the blue ringed octopus), the toxins are produced by a symbiotic bacteria contained within the venom glands. Venom may be a highly complex mixture of proteins, such as in cone snails (McIntosh and Jones, 2001), or largely comprised of alkaloids, as is the case in some ant venoms. In some cases, e.g. snakes, the lethal components are largely enzymes, whilst in scorpions, for example, the lethal components are small neurotoxic peptides.

Many venoms (e.g. those of fire ants and bees) contain histamine or histamine-releasing factors, producing pain, itching and burning sensations at the site of the sting. Spreading factors such as hyaluronidase are also common components (e.g. in venoms from lizard

and snake), catalysing the breakdown of connective tissue and increasing the diffusion and absorption of the venom. Venoms often contain cytolytic peptides, e.g. lycotoxins in spider venom (Yan and Adams, 1998) and anoplin in wasp venom (Konno et al., 2001a), which may have both offensive and immunodefensive uses.

The bee and scorpion envenomation systems discussed in this study share two features that set them apart from those of snakes. Whereas snakes have an envenomation system modified from existing salivary glands, both scorpions and bees have developed independent highly specialised venom delivery apparatus. Whilst snake venoms contain large numbers of enzymes, again thought to be adapted from those present in the digestive system, the scorpion and hymenoptera venoms have a small number of enzymes, in conjunction with basic, pharmacologically active peptides. It is possible that scorpion toxins are derived from components of the arthropod innate immune system.

In summary, animal venoms contain a cocktail of pharmacologically active components, each highly evolved to a specific target, making them ideal libraries in the screening of novel therapeutics. The venoms are also of great clinical importance in their own right, with a significant number of human fatalities arising from various envenomations.

1.3.1 Disulphide Bond Motifs

Multiple paired cystines are common in venom peptides, particularly those active on ion channels. They are believed to account for the high stability of these molecules and their resistance to proteolytic digestion, and may have a role in directing the folding process. Upon analysis of these peptides, several common patterns of cysteine distribution and disulphide pairing have been noted. Two of these, the cystine-stabilised- α -helix (CSH) and the cystine knot, will be discussed.

The CSH Motif

In finalising the 3D structure of the scorpion potassium channel toxin charybdotoxin, Bontems et al., (1991 and 1991a) noted that there were common structural elements

shared between long- and short-chain scorpion toxins and insect defensins, which showed identical pairings of three disulphide bonds. A similar observation was made by Tamaoki et al., (1991), who proposed the cystine stabilised α -helix motif (CSH) (Kobayashi et al., 1991). The group noted a consensus pattern of Cys-X-X-X-Cys disulphide-bonded to a second conserved motif, Cys-X-Cys in scorpion- and honeybee-ion channel toxins, producing a parallel alignment of the peptide backbones in these regions. These consensus sequences were also conserved in mammalian endothelins and snake sarafotoxin, with the exception that the cystine pairings were reversed, generating antiparallel alignment of the backbones. The Cys-X-X-X-Cys motif was contained within an α -helical segment whilst Cys-X-Cys was located on an extended β -strand. A search of protein databases (Tamaoki et al., 1998) showed that this cysteine framework was present in a number of additional proteins, including serine proteinase inhibitors, insect and plant defensins, and members of the growth factor family. In all proteins containing this cysteine pattern, and which had known 3D structures, the CSH motif was preserved, with the exception of the cystine knot growth factor super family (in which a third disulphide penetrates the cyclic structure formed by the CSH disulphides, disrupting the orientation of an α -helix). In peptides containing different cysteine spacing, no conformational preferences linked with the formation of an α -helix were observed. This disulphide pattern was proposed to be critical for the correct folding of CSH-containing peptides.

It has been noted that plant γ -thionins, human endothelins, snake sarafotoxins, insect and scorpion defensins, short and long chain scorpion neurotoxins, and the bee venom toxins apamin and mast cell degranulating (MCD) peptide are all basic peptides which alter membrane permeability. Despite different mechanisms of action, they share high affinity of binding to their relative receptors (Froy and Gurevitz, 1998). The authors speculate as to the evolutionary origins of the CSH motif, which could have arisen through divergent evolution of a common ancestor, or have arisen independently on one or more occasions.

The CSH motif connecting an α -helix to a double or triple stranded β -sheet, as commonly seen in scorpion toxins, is often referred to as the (cysteine-stabilised) α/β fold.

The Cystine Knot

The conserved cystine framework of the CSH motif is also present in the cystine knot motif. Members of this family possess an additional disulphide bond, which penetrates the ring structure formed by the other four cystines, forming a ten membered cystine knot (McDonald and Hendrickson, 1993). This motif occurs in growth factor cystine knot proteins (Isaacs, 1995 and Sun and Davies 1995), the cycleotides (Craik et al., 1999), and in the small inhibitor cystine knot proteins (Pallaghy et al., 1994). In a growth factor cystine knot, the penetrating disulphide is Cys1-Cys4. In the cases of the inhibitor cystine knot and the cyclic cystine knot, the ring is formed by the first 2 bonds (1-4 and 2-5) and the third disulphide (3-6) passes through this (Pallaghy et al., 1994). The inhibitor cystine knot (IKC) is common in toxic and inhibitory peptides including some conotoxins and spider toxins (Qu et al., 1997) and appears to be able to support various pharmacological activities.

1.4 Bee Venom

Much of the early work on bee venom has been discussed by Habermann, 1972; for a more recent review see Strong and Wadsworth, 2000. Of relatively simple composition when compared to many other venoms, that of the honey bee (*Apis mellifera*) contains approx. 70% protein (dry weight), with lesser quantities of carbohydrates, amino acids (Nelson and O'Connor, 1968) and phospholipids. A number of biogenic amines, predominately histamine, are present and may contribute to the initial pain felt following a bee sting. Dopamine and noradrenaline are also present (Owen, 1971), their concentrations varying according to age and season (Owen and Bridges 1982).

The major enzymatic components are phospholipase A₂ (PLA₂) and hyaluronidase (Habermann, 1972 and references therein), which act as spreading factors. Acid phosphomonoesterase, glycosidase and lysophospholipase activities are also present (Shkenderov and Koburova, 1979) in lower quantities. The PLA₂ acts as an indirect lytic agent, causing the release of lysolecithin from lecithin (Habermann, 1972 and references therein). Interestingly, the phospholipase is found exclusively in worker bee venom, and is almost absent in that of queen bees (Kuchler et al., 1989).

PLA₂ would appear to act in synergy with another cell membrane lytic factor, melittin, which has a direct cytolytic effect. Melittin (Habermann, 1972 and references therein) is the main constituent of bee venom. Its amphipathic nature gives the peptide detergent-like properties. As a result of its general lytic action, melittin brings about a wide range of pharmacological effects. This peptide is an inhibitor of a number protein kinases (Dudkin et al., 1983; Raynor et al., 1991) and is a potent anti-inflammatory agent. To protect the bee from the lytic effects of melittin, the peptide is secreted into the venom sac as a propeptide (Kreil and Bachmayer, 1971; Kindas-Mugge, 1979) before being cleaved to form the mature peptide (Kreil et al., 1980). Two other forms of the peptide are present, a N-terminal formylated variant (Lubke et al., 1971) and a smaller quantity of a partially degraded melittin known as melittin F (Gauldie et al., 1976, 1978).

Aside from melittin, several small, basic, neurotoxic peptides are contained in the venom. Apamin, mast cell degranulating peptide, tertiapin and secapin are disulphide-bridged peptides sharing a similar structure of a β -turn covalently linked to an α -helix by one or two disulphide bonds (Hider and Ragnarsson, 1981). The first of these,

apamin, is an 18 residue highly basic C-terminally amidated neurotoxin, containing two disulphide bonds, and is an inhibitor of small conductance calcium-activated potassium channels. This peptide will be discussed in more detail later.

MCD peptide (mast cell degranulating peptide or peptide 401) (Breithaupt and Habermann, 1968) is even more basic than apamin and was named for its ability to release histamine from mast cells, which occurs without cell lysis (Fredholm, 1966; Jasani et al., 1979). The peptide has also been shown to have potent anti-inflammatory action (Winter et al., 1962; Hanson et al., 1972; Billingham et al., 1973). Of particular note was its anti inflammatory effects in a rat model of arthritis, a condition which apitherapy has long been claimed to alleviate (Newbould, 1963). Like apamin, MCD peptide is a centrally acting neurotoxin (Habermann, 1977; Bidard et al., 1987; Gandolfo et al., 1989). These neurotoxic effects can be attributed to its ability to suppress the activity of Kv1.1 channels (Stuhmer, et al., 1988).

Tertiapin was first isolated 30 years ago (Gauldie et al., 1976). It has been shown to have presynaptic activity (Ovchinnikov et al., 1980), originally suggested to be due to its binding to calmodulin (Dudkin et al., 1983). More recently, the peptide's ability to block inwardly rectifying potassium channels (discriminating between GIRK1/4 /ROMK and IRK1) (Jin and Lu, 1998) and to selectively inhibit muscarinic potassium channels (K_{ACh}) in cardiac monocytes, (Kitamura et al., 2000) have been demonstrated.

Unlike the other bee venom neurotoxins, secapin (Gauldie et al., 1976) contains only a single disulphide bridge and little is known about its pharmacology. Interestingly, the peptide is far more abundant in the venom of queen bees than in that of the workers (Vlasak and Kreil, 1984), raising intriguing questions as to secapin's functional role.

Adolapin, a larger (approx 11100-11500 Da) basic polypeptide with anti-inflammatory and analgesic properties has also been isolated from honey bee venom (Shkenderov and Koburova, 1982; Koburova et al., 1985). Although other peptides, procamine A, procamine B and minimine (named for its ability to produce miniature flies from *Drosophila* larvae) have been reported (Nelson and O'Connor, 1968; Lowy et al., 1971), subsequent studies have failed to repeat these findings (Gauldie et al., 1976).

In humans, the pharmacological effects of envenomation are generally local ones. Histamine acts upon nerve endings and small blood vessels, causing pain and swelling; hyaluronidase permeabilises connective tissue, acting as a spreading factor; MCD peptide releases more histamine; phospholipase increases capillary permeability and produces lytic agents, which in conjunction with melittin, cause general tissue damage and liberate further active substances, e.g. potassium, histamine and serotonin.

Hymenoptera are, however, responsible for more deaths than any other venomous creature (Gueron et al., 2000). This is not a direct effect of the venoms, but due to hyperimmunity leading to anaphylactic shock in hypersensitive individuals. Multiple allergens would appear to be present, IgE from hypersensitive patients recognising several venom proteins. Opinions vary as to which is the major allergen, with patients showing varying reactivity, although PLA₂, hyaluronidase, acid phosphatase and melittin would all appear to play a significant role (Shkenderov, 1974; Hoffman and Shipman, 1976; Light et al., 1976; Sobotka et al., 1976; Hoffman et al., 1977; Paull et al., 1977; Kemney et al., 1984; Kettner et al., 1999). Further components, e.g. Api m 6, allergen B and allergen C (Hoffman, 1977; Kettner et al., 2001), have been isolated on the basis of their immunogenic properties. It has been postulated that some of these allergens are not components of the venom *per se*, but are proteolytic fragments from larger structural and membrane proteins.

Research into bee venom thus has three main foci. As demonstrated by recent progress in identifying ion channel targets of tertiapin, despite 30 years of research the venom is still yielding novel pharmacological tools. Continuing progress is being made in the identification and synthesis of bee venom antigens required for effective venom immunotherapy. Finally, apitherapy has long been associated with alleviation of symptoms of a number of autoimmune conditions. More research is required into the validity of such treatment, and into the components responsible for its effects, in order to provide synthetic and recombinant alternatives, and to reduce the risk of anaphylactic side effects.

1.4.1 Apamin

Apamin is an 18 amino acid toxin and a minor active component of *A. mellifera* venom. Apamin intoxication seems to produce symptoms specific to the central nervous system. When purified apamin was injected into mice, it led to convulsions, followed by respiratory distress and death (mouse $LD_{50} = 2.05 \text{ mg/Kg i.p.}$) within 2-4 hours (Shipolini et al., 1967; Lallement et al., 1995). Sub-lethal doses gave rise to hyperexcitable mice over a 24hr period. Direct injection into the spinal cord gave similar, but local effects. In general, the toxin has an excitatory effect on the CNS and is the only toxin known to be able to pass through the blood-brain barrier.

Nanomolar concentrations of apamin specifically block a potassium current, activated by an increase in free intracellular calcium concentration, in a variety of cell types. This includes currents in neuronal and in non-neuronal cells (Cook et al., 1983). The toxin acts on the external side of the channel carrying these currents, disassociating when internal potassium concentration is high, suggesting the block is via a simple plugging mechanism.

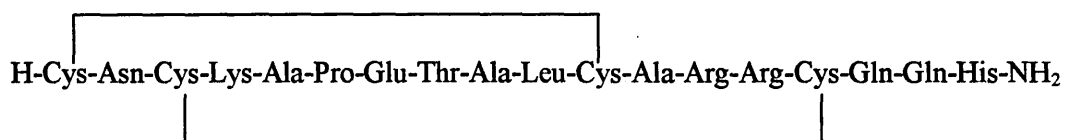
Apamin was successfully radiolabelled by Habermann and Fischer, 1979 and purified mono [^{125}I]apamin was characterised by Hugues et al., 1982c. The radiolabelled toxin was initially used to look at the distribution of acceptors in whole organisms, showing a concentration of acceptors in the spinal cord (Vincent et al., 1975). Later, autoradiographic studies using the toxin showed the acceptor to be heterogeneously distributed in the brain. Areas containing a large proportion of glial cells showed low levels of labelling (Mourre et al., 1986), suggesting that, in the brain, receptors are located primarily on neurons within the cerebellum.

A specific binding site for radiolabelled apamin was identified on rat skeletal muscle cells (Hugues et al., 1982a; Hugues et al., 1982c); and apamin binding sites were identified on membranes, whole cells and cultured cell lines prepared from a wide range of both neuronal and non-neuronal tissues (refer to table 4.1). These studies strongly implied that the apamin acceptor was a component of the SK channel, since binding occurred at a single class of binding sites on tissues expressing these channels.

Apamin was the first specific probe for a potassium channel. It binds specifically to SK1, SK2 and SK3 (although it has far lesser affinity for SK1: - K_d hSK1 = 390pM; K_d hSK2 = 4pM; K_d rSK3 = 11pM, Grunnet et al., 2001; Finlayson et al., 2001) and has no effect on BK or IK. The identification of apamin as a ligand of the SK channel has provided valuable information on the quantity and distribution of these channels and provided a ligand to aid in their purification (Schmid-Antomarchi et al., 1984; Lazdunski et al., 1985; Seagar et al., 1987; Sokol et al., 1994).

Studies using apamin have also provided structural information on the channel. For example, apamin cross-linking studies proved the channel to be a heteroligomer and suggested the presence of SK channel β -subunits. Apamin binding assays, and radioimmunoassays using anti-apamin antibodies were used to suggest the presence of an endogenous apamin-like factor in mammalian (porcine) brain (Fosset et al., 1984). They have helped to identify additional SK channel ligands, e.g. P05 (Sabatier et al., 1993), scyllatoxin (Sabatier et al., 1994), Tsk (Legros et al., 1996), BmP05 (Romi-Lebrun et al., 1997), maurotoxin (Kharrat et al., 1997), Pi1 (Fajloun et al., 2000c) and tamapin (Pedarzani et al., 2002). Strong and Evans, 1987, used internalisation of radiolabelled apamin into liver endosomal membranes to provide evidence for receptor-mediated endocytosis of toxins. Apamin has notable effects on behaviour. It improves cognition, memory and learning in mice (Messier et al., 1991; Deschaux et al., 1997; Deschaux and Bizot, 1997; Ikonen et al., 1998; Van der Staay et al., 1999; Fournier et al., 2001) and decreases their appetite (Ghelardini et al., 1997). The toxin is therefore used as tool in the study of these behaviours and in the understanding of, and development of treatment for, various behavioural, psychiatric and memory disorders.

The sequence of apamin was determined by two independent groups (Shiponlini et al., 1967; Callewaert, 1968 and also Haux et al., 1967). The peptide is highly basic, with only one hydrophobic amino acid and a net charge of three, and the C-terminal carboxyl group is amidated (Gauldie et al., 1976).



Analysis of the primary sequence, circular dichroism (CD) conformational studies and nuclear magnetic resonance (NMR) studies (Busetta, 1980; Bystrov et al., 1980; Freeman et al., 1986; Pease and Wemmer, 1988) predicted a tertiary structure (fig 1.5) containing a CSH motif. This structure, an α -helical core and two β -turn regions linked by Cys1- Cys11 and Cys3 - Cys15 disulphide bonds, is very resistant to changes in solvent polarity, pH, addition of denaturants and even chemical modification of side chains. The compactness and thermodynamic stability of the peptide have led to its use as a model, e.g. to examine structure-antigenicity relationships (Defendini et al., 1990), for analysis of disulphide linkages (Gray, 1993) and in the testing of structural algorithms (Sun 1995).

Two residues, Arg13 and Arg14, seem crucial for activity (Vincent et al., 1975; Albericio et al., 1984). Substitution of one of these residues by lysine maintains 80% of biological activity (Granier et al., 1978). Activity is lost, however, on substitution by ornithine or homoarginine (Cosland and Merrifield, 1977), the distance between the positive charges being critical (Granier et al., 1978). Bisquaternary neuromuscular blocking agents, e.g. tubocurarine, gallamine and decamethonium compete for apamin binding sites. All of these molecules contain two positively charged nitrogens separated by approx 11Å, comparable to Arg13 and Arg14 in apamin (Cook and Haylett, 1985). This motif has been proposed as the SK-channel pharmacophore (Cook and Haylett, 1985; Galanakis et al., 1995, 1996, 2004). These positive residues are thought to interact with complementary negative residues on the apamin receptor, the binding augmented by hydrophobic interactions between the receptor and the side chains of these residues (Demonchaux et al., 1991; Labbe-Jullie et al., 1991). The single negatively charged residue of apamin (Glu7) is located on the opposite side of the molecule. This produces a high dipole moment, which may contribute to the precise positioning of the toxin in the receptor (Ciechanowicz-Rutkowska et al., 2003). The differences in sensitivity of the SK channels to apamin have been shown to be influenced by residues in the pore region (Ishii et al., 1997a).

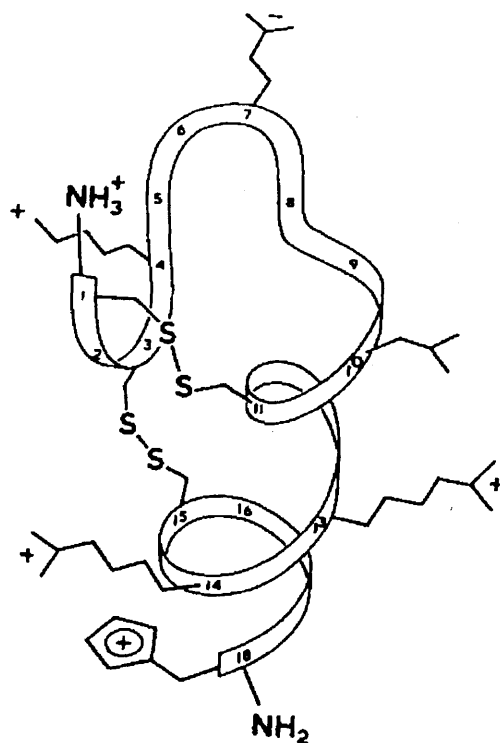
The apamin cDNA precursor has been identified (Gmachl and Kreil 1995). This precursor (preproapamin) has both a signal peptide (19 amino acids) and a propeptide (8 amino acids) preceding the mature peptide sequence. As would be expected from the amidation of the C-terminal His, an additional Gly is present at the C-terminus of the precursor. This signal peptide and propeptide region is identical to that of MCD peptide,

and the cDNA sequences of this region and the 5' untranslated region (UTR) show 85% identity. The 3' ends are completely identical. This is because the two toxins reside in tandem on a single gene. This gene has six exons in the following order: three exons of the MCD precursor, two exons of the apamin precursor and a final exon common to the mRNA for both toxins. This final exon represents the final six residues of apamin and 3'UTRs for both toxins (see fig 1.6).

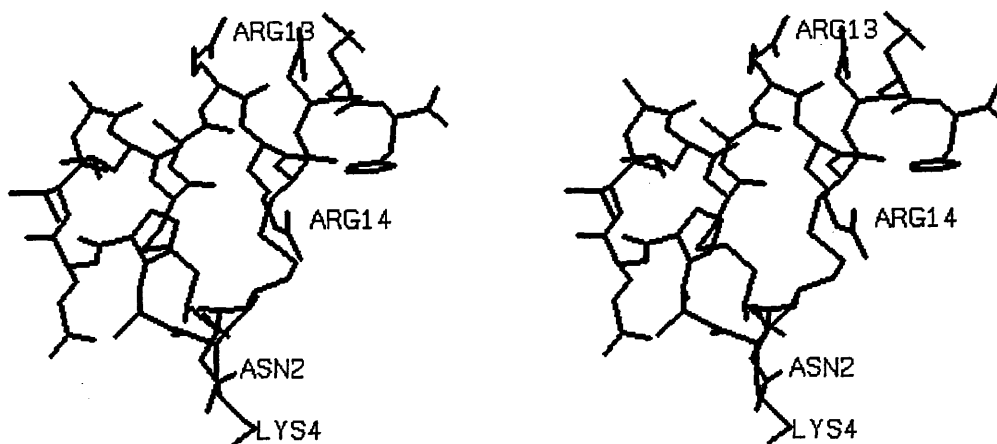
For reviews on apamin and its relationship with SK channels, see Habermann, 1984; Lazdunski et al., 1985; Castle et al., 1989 and Strong, 1990.

Fig 1.5 Structure of Apamin

A)



B)



A) Ribbon structure (Freeman et al., 1986).

B) Stereoview of apamin, showing positions of the two arginines critical for binding. Image was created, using the coordinates of Pease and Wemmer, 1988, in Protein Explorer (<http://molvis.sdsc.edu/protexpl/frntdoor.htm>).

1.5 Scorpion Venom

Scorpions (class arachnida) are the oldest living arthropods, evolved over 400 million years. The largest scorpion species (e.g. genus *Pandinus*) may be 20cm in length, although the majority of scorpions are much smaller. Their bodies are composed of 18 segments terminating in a teardrop shaped telson that contains the venom glands, which produce potent pharmacologically active peptides. Scorpions also possess two anterior pincer-like pedipalps. In general terms, the bigger the pedipalps, the less dangerous the sting.

Scorpions are very robust. They can withstand desert or freezing conditions for weeks and months of starvation. Generally, scorpions are nocturnal opportunistic predators. Their diet is mostly comprised of insects and other arthropods, although they also eat isopods and gastropods, and the larger species may feed on small reptiles and mammals (Keegan, 1998). Cannibalism has been noted in scorpions kept in close confinement under laboratory conditions.

All known scorpion species possess venom, which is used both defensively and to attack and immobilise prey. Of approximately 1500 scorpion species only about 25 (mostly in the Buthidae family) are capable of causing human fatalities. Those scorpions considered to be of medical importance have been described by Keegan, 1998, and include *Androctonus australis* in North Africa, *Leiurus quinquestriatus* in North Africa and West Asia, *Parabuthus* spp in South Africa, *Tityus bahiensis* and *Tityus serrulatus* in South America, *Centruroides limpidus* and *Centruroides suffuses* in Central America, *Centruroides sculpturatus* in North America and *Mesobuthus tamulus* in Asia.

1.5.1 Scorpion Sting

The scorpion telson consists of two portions, the swollen ampulla and the slightly upturned sharp hollow spine or sting. When the scorpion is in defensive/offensive pose, the abdomen is curved back over body, so that the sting points forward. Towards the tip of the spine are two oval openings (aculeus) for venom release. Each opening has its own venom duct leading from one of a pair of venom glands located, either side of the

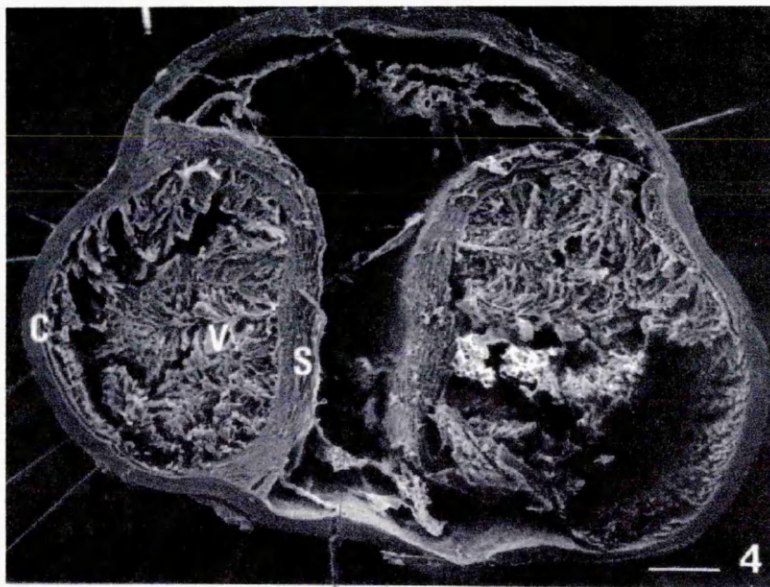
mid-line, in the ampulla. Each gland is covered in a sheet of muscle (the compressor muscle) on its dorsal and medial sides, which squeezes the venom through the ducts and out of the aculeus. This contraction, and the extent of the contraction, is entirely under the voluntary control of the scorpion. The structure of the venom glands of *Heterometrus longimans* has been studied in detail by Gopalakrishnakone, 1995 (see fig 1.7).

Fig 1.7 Scorpion Venom Apparatus. (from Gopalakrishnakone, 1995)

A)



B)



A) Spine with opening of venom duct, scanning electron micrograph x100.

B) Scanning electron micrograph of cross section of telson (x110). The venom glands (V) are surrounded by the cuticle (C) and the skeletal compressor muscle (S). The venom glands are lined with glandular epithelia. Despite great differences in the effect of the sting, the microscopic structure of the telson and venom gland tissue appears almost identical between species. The lumen of the venom gland, however, ranges from smooth to highly folded, depending upon species.

1.5.1.1 Symptoms of Scorpion Sting

Scorpion venoms can be toxic to insects, amphibians, crustaceans and mammals. Scorpion envenomation is a common and life threatening public health problem in many parts of the world, particularly Africa, Asia and South and Central America. In Mexico there are over 200,000 cases of scorpionism annually, and approximately 700 deaths (Dehesa-Davila and Possani, 1994). Brazil records 10,000 cases per annum (Alvarenga et al., 2002) and, in Tunisia, 30,000 to 45,000 incidents are reported annually, of which 1000 are severe and 35-105 fatal (Krifi et al., 1996). Indeed, in some regions more deaths are caused by scorpion sting than by snakebite.

Symptoms of scorpion envenomation vary widely depending on offending species, but can broadly be divided into two categories. The sting of most scorpions is harmless and less painful than a bee sting. In the severest of cases in this category, discolouration, severe pain, oedema and sweating may last for several days. These symptoms remain localised to the site of the sting, however, and severe pain is often an indicator of a good clinical prognosis. Envenomations in the second category also produce initial pain at the site of the sting. These local symptoms are mild and short lived, however, being rapidly replaced by the systemic effects characteristic of severe envenomation and possibly leading to death. There is a broad spectrum of severity within these two categories. The effects of the sting depend upon scorpion species, season of sting, age of scorpion and victim, and size of victim. Children are particularly vulnerable to severe prognosis.

The effect of clinical and experimental envenomation by a wide range of scorpions has been reviewed in detail by Ismail, 1995. The severe symptoms affect many systems and include both hyper- and hypo-tension, increased activity of the secretory glands (sweating, hypersalivation, lacrimation), CNS effects (hyperirritability, focal and generalised seizures, hemiplegia, hyperthermia and hypothermia, shivering, hyperirritability), cardiac arrhythmia, cyanosis and renal failure. Fatality is usually due to cardiac or respiratory failure complicated by pulmonary oedema. These symptoms are characteristic of a generalised stimulation of both the sympathetic and parasympathetic nervous system, with the sympathetic effects dominating. Hassan and Mohammed, 1940, first proposed that the effects of scorpion envenomation were due to powerful stimulation of the autonomic nervous system. This is via a massive rise in circulating catecholamines and acetylcholine in a process termed 'autonomic storm'.

Ismail, 1995 also noted that changes in serum electrolyte concentration (hyponatremia, hyperkalemia, hypocalcaemia and hypomagnesaemia) contributed to the cardiac effects of the venom. This was concluded to be partly due to catecholamines causing release of potassium from the liver (and possibly due to high K^+ levels in pre venom, Inceoglu et al., 2003), but also associated with opening of Na^+ channels and block of K_{Ca} .

In mild but painful stings, localised pain is caused by liberation of serotonin and kinins causing continuous stimulation of C-fibres, and also by direct stimulation of nerves by the venom. The absence of local pain at the site of the sting in severe envenomations is due to peripheral vasoconstriction and hypoxia due to elevated circulating catecholamines.

Antivenoms are available for many scorpion venoms, although their effectiveness is debated. Treatment is often a combination of antivenom therapy and symptomatic treatments, although the recommended treatments vary according to species.

1.5.2 Scorpion Venom Composition

Scorpion venom is a tasteless, odourless, slightly acidic liquid. The initial drops are colourless (pre venom), the subsequent ones translucent (venom) (Caius and Mhaskar, 1932). The venoms are typically a mixture of mucus, inorganic salts, oligopeptides, nucleotides, amino acids, low molecular weight organic molecules and a number of proteins, but as the symptoms of scorpion sting vary widely between scorpion species, so does the composition.

The venoms with high toxicities are the most widely studied. Unlike snake venoms, for example, most of the high-toxicity scorpion venoms lack, or have only low, enzyme activity. A few enzymes have been isolated, however, e.g. hyaluronidases from *T. serrulatus* (Pessini et al., 2001). These scorpion venoms alter neuronal action potentials and cause release of neurotransmitters from cholinergic and adrenergic neurons. This is due to the presence of low molecular weight, basic, neurotoxic peptides that act upon ion channels and have pre-junctional effects on synaptic transmission. Most of the neurotoxins are selective for voltage-activated sodium channels of excitable cells,

prolonging action potentials and causing spontaneous neuronal firing. In addition, minor components act selectively on voltage-gated or calcium-activated potassium channels.

A few studies have been carried out on black scorpions belonging to the scorpionidae. These scorpions are generally formidable looking, with large pincers, but their sting is not fatal, instead producing intense localised pain. Of this type of scorpion, the venoms from *Heterometrus scaber* (Nair and Kurup, 1975), *H. longimans* and *Heterometrus spinifer* (Gwee et al., 1993, 1996, 2003; Nirthanan et al., 2002) are the most studied. These venoms have a direct, post-junctional, agonist effect on muscarinic M3 cholinceptors and α -adrenoceptors. The venoms appear to lack significant sodium or potassium channel blocking activity. Instead, noradrenaline and/or acetylcholine are the major venom components, accounting for the direct noradrenergic and cholinergic agonistic effects of the venoms when applied to rat muscle. It is proposed that the acetylcholine acts as an algescic, and noradrenaline is responsible for the potent vasoconstrictive effects of these venoms, helping to localise and intensify the effects of the algescics. Histamine has been isolated from *Heterometrus gravimamus*, adding to the symptoms of pain, burning and itching (Ismail et al., 1995). Unlike in the more toxic scorpions, these less dangerous species have significant enzyme activities. PLA₂ is a major component of the venom from *Heterometrus fulvipes* (Ramanaiah et al., 1990), and *H. scaber* venom contains significant quantities of acid phosphatase, 5'-nucleotidase, phospholipase A₂, acetylcholine esterase and the spreading factor hyaluronidase.

Sometimes identical peptides may be present in venoms from different, but closely related, species of scorpion, e.g. kurtotoxin from *Parabuthus granulatus* and *Parabuthus transvaalicus* (Olamendi-Portugal et al., 2002); butantoxin from *T. serrulatus*, *T. bahiensis* and *Tityus stigmurus* (Holaday et al., 2000).

1.5.3 Scorpion Venom Ion Channel Neurotoxins

The main pharmacological components, and hence the majority of those identified, are small peptides acting on ion channels, or peptides with sequence homology to known ion channel toxins. The venoms contain multiple classes of ion channel toxins specific for different targets. This specificity is twofold. Most of the toxins are highly specific

for a particular class of ion channel (e.g. sodium channel selective) and often a particular channel subtype. Scorpion toxins also show a large degree of host specificity, with different toxins targeting mammals, insects and crustaceans found in a single venom.

All known scorpion ion channel toxins are single-chain polypeptides, between 23 and 80 residues in length, and bridged by two to four disulphide bonds. Most known examples contain the CSH motif (see 1.3.1). Their primary targets are voltage-gated sodium channels (generally modifying the gating kinetics), and potassium channels, K_v and K_{Ca} in particular (usually by a direct block of the pore). Although abundant in spider and cone snail venoms, calcium channel toxins are rare in scorpions and are of variable size. Toxins affecting chloride currents exist in scorpion venoms, but their mode of action is poorly characterised.

Scorpion neurotoxins are often divided into two groups based on molecular weight. The short-chain toxins contain 23-41 amino acids cross-linked by two, three or four disulphide bridges, and are active on a wide range of channel types (K^+ , Cl^- and some Ca^{2+} channel toxins fall into this category). The sodium channel toxins (and a few recently discovered K^+ channel toxins) are contained within the long-chain scorpion toxins. These peptides are between 60 and 80 residues in length and have four disulphide bonds.

Together, the neurotoxins act to prolong the action potential and cause repetitive firing. They are generally of higher toxicity than snake neurotoxins. Scorpion ion channel toxins have been classified and reviewed by Possani et al., 2000. The authors divided the scorpion ion channel toxins into 26 families, although for the sake of simplicity a less complex classification has been adopted in this work.

1.5.3.1 Sodium Channel Toxins

Much of the toxicity of scorpion venoms has been attributed to their action on sodium channels. For this reason, and due to their often-high abundance in the venom, scorpion sodium channel toxins are well studied (Gurevitz et al., 1998; Possani et al., 1999; and Martin-Eauclaire and Rochat, 2000). These toxins are 60-76 amino acid peptides

containing four disulphide bridges and exert their pharmacological effect by altering the opening or closing of the voltage-gated sodium channel responsible for the depolarising phase of the action potential in nerve, muscle and heart. The scorpion Na⁺ channel toxins have traditionally been grouped according to host specificity: those active on vertebrates (mammalian Na⁺ channel toxins) and those active on invertebrates (insect Na⁺ channel toxins). For a more detailed classification, based upon sequence homology, host specificity and mode of action, refer to Possani et al., 1999.

The 'mammalian' toxins all increase Na⁺ influx into cells. Two groups (α - and β) are distinguished by their site of action on the sodium channel. These toxins share a similar structure of a short α -helical segment and a three-stranded antiparallel β -sheet. Two disulphides link the secondary structure, a third bridge links the N-terminus and the C-terminus, and the final bridge links the loops. It has been proposed that differences in these loop regions determine the differences in α - and β -toxin activities (Fontecilla-Camps et al., 1980), and a hydrophobic region on one face of the toxin has been implicated in the high-affinity binding of the toxins to their targets (Fontecilla-Camps et al., 1980). Although initially characterised as mammalian toxins, some members of the α - and β -toxin families show insect activity.

α -Scorpion toxins were the first to be purified and characterised (Miranda et al., 1970). They are the main toxic components of the venoms of 'Old World' scorpions from Africa and Asia (e.g. *Androctonus*, *Buthus* and *Leiurus* species). Four such toxins (AaHI-AaHIV) together account for 90% of *A. australis* venom mammalian toxicity, but represent only 3% of the composition (Martin and Rochat, 1986). α -Toxins have also been isolated from New World scorpions, e.g. *T. serrulatus* (Barhanin et al., 1982; Vijerberg et al., 1984), though they are present at far lower abundance and have a lower affinity for their receptors. α -Toxins prolong the action potential by slowing sodium channel inactivation (Jover et al., 1980; Catterall, 1988; Kirsch et al., 1989). They exert this action via receptor site 3 of the Na⁺ channel α -subunit, specifically a site formed by the extracellular S3-S4 loops of domains I and IV (Tejedor and Catterall, 1988; Thomsen and Catterall, 1989; Rogers et al., 1996), in a voltage dependent manner (Catterall, 1979; Jover et al., 1980).

Since these early studies, a number of toxins (α -like toxins) have been isolated with α -toxin-like primary sequence and insect toxicity (Gordon et al., 1996; Possani et al.,

1999). They-too slow Na⁺ channel inactivation, characterised by a contractile paralysis in the insect, and bind to similar, but non-identical, sites on Na⁺ channels of insects and mammals (Eitan et al., 1990; Borchani et al., 1996). The selectivity of α- (and α-like) toxins for insect or mammalian receptors, and for distinct mammalian Na⁺ channel subtypes, have been reviewed by Gordon and Gurevitz, 2003.

The main components responsible for mammalian toxicity in the venoms of 'New World scorpions' (e.g. *Centruroides* and *Tityus* species) are also sodium channel toxins, increasing Na⁺ influx. These β-toxins exert their effect by shifting the voltage-dependence of activation to more negative potentials (Cahalan, 1975; Couraud et al., 1982; Yatani, et al., 1988), leading to spontaneous and repetitive firing of action potentials. They bind to a different sodium channel receptor site from that of α-toxins (Couraud et al., 1982) in a voltage-independent manner. This binding region (receptor site 4) is located on the S3-S4 extracellular loop in domain II of the Na⁺ channel α-subunit (Cestele et al., 1998). Like α-toxins, β-toxins do not act exclusively on mammalian channels. The main toxic component of *T. serrulatus* (Tsy or TsVII, Possani et al., 1981; Ceard et al., 1992) additionally binds to the insect sodium channel with high affinity (Pauron et al., 1985; De Lima et al., 1986, 1989), possibly because of its high structural flexibility (Loret et al., 1990). A toxin that is active against crustaceans and has a β-like sequence has been isolated from *Centruroides noxius* (Garcia et al., 1997). The differences between this and an archetypal β-toxin are concentrated on a surface region that is hence proposed to be involved in species specificity.

The potency of scorpion venoms in insects is largely due to Na⁺ channel toxins, which, unlike the 'mammalian' toxins, are exclusively selective for insects. These toxins are structurally distinct from their mammalian-active counterparts and can essentially be classified according to their opposing paralytic effects.

Zlotkin et al., 1972 described the first scorpion insect toxin (AaHIT, *A. australis*), reporting an immediate contractile paralysis caused by repetitive firing of insect motorneurons, and due to a shift in the voltage-dependence of activation and a reduction in deactivation of the Na⁺ channel (Walther et al., 1976; Lester et al., 1982; Pelhate and Zlotkin, 1982). The binding of this 'excitatory insect toxin' is non-voltage dependent and shows high selectivity for insect over mammalian sodium channels (Gordon et al.,

1984). This specificity may be due to the rigid structure of the toxin, imparted by a different disulphide pairing to that seen in the mammalian toxins (Darbon et al., 1982; Loret et al., 1990). Structural studies on excitatory insect toxins have led to the proposal that the C-terminus region forms part of a putative bioactive surface important for insect specificity (Darbon et al., 1991; Froy et al., 1999a).

The depressant insect toxins (e.g. Bj IT2, *Bothotus judaicus*, Lester et al., 1982) share their disulphide pairing with the mammalian Na⁺ channel toxins and are reviewed by Zlotkin et al., 1993. They are specific for insects and block action potentials, causing a slow flaccid paralysis (Zlotkin, 1983; Zlotkin et al., 1985). This paralysis is preceded by a transient contraction, similar to that seen with the excitatory toxins (Zlotkin et al., 1991; Benkhalifa, 1997). The excitatory and depressant toxins bind to distinct binding sites, in close proximity to one another on the extracellular loops of domains I, III, and IV of the insect sodium channel (Goudet et al., 2002).

In 1991, Loret et al., isolated AaHiT4 from *A. australis* Hector. This toxin competes for binding sites with both α - and β -type mammalian scorpion toxins and also insect Na⁺ channel scorpion toxins, and is proposed to be an ancestral scorpion toxin.

1.5.3.2 Scorpion Potassium Channel Toxins (KTx).

The other well-studied group of scorpion venom components is the potassium channel toxins (KTx) (Garcia et al., 1995; Harvey et al., 1995; Rodriguez de la Vega and Possani, 2004). They are minor venom components (each having a far lower abundance than the Na⁺ channel toxins) that increase cell excitability by potassium channel block. These molecules are basic peptides containing three or four disulphide bridges. Although most known scorpion KTx are 30-40 amino acids in length, long-chain scorpion potassium channel toxins (approx 60-65 amino acids) and peptides as small as 22 amino acids (Srinivasan et al., 2002) have been isolated in more recent years.

The first scorpion potassium channel toxin to be purified was noxiustoxin from *C. noxius* venom (Carbone et al., 1982; Possani et al., 1982). This toxin inhibited potassium currents in the squid giant axon, in a voltage-independent manner, without altering the gating kinetics. In the ensuing years, several homologous scorpion venom

peptides were isolated that blocked either voltage-gated (K_v) or calcium-activated (K_{Ca}) potassium channels. Miller, 1995 grouped the known scorpion KTx peptides in a single family (α -KTx) divided into three subfamilies based upon sequence similarity (α -KTx1-3, containing charybdotoxin-like, noxiustoxin-like and kaliotoxin-like sequences respectively). The last decade has seen a dramatic increase in the α -KTx family and the nomenclature was expanded by Tytgat et al., 1999; Goudet et al., 2002 and Batista et al., 2002, to include a total of eighteen subfamilies, currently encompassing about 75 peptides active on K_v, or SK, IK, or BK subtypes of K_{Ca} channels.

Since 1995, three further families have been added to the nomenclature. The β -KTx family consists of the long-chain potassium channel toxins, of which four have been identified (Legros et al., 1998; Zhu, 1999). They contain 60-64 amino acids but only three-disulphide bridges.

The γ -KTx family contains the ergtoxins, active on the *ether-a-go-go*-related gene (ERG) potassium channels (Gurrola, 1999a). Twenty-six such peptides have been identified to date. It is hoped that, in the same way that α -KTx have been beneficial in the study of K_v and K_{Ca} channels, the ergtoxins will prove vital tools in the understanding of their associated channels and in therapeutic drug design.

A potassium channel toxin that became the founding member of the κ -KTX family has recently been identified in *H. fulvipes* (Srinivasan et al., 2002). κ -Hefutoxin differs from previously identified KTx peptides. It does not share the common CSH motif, but has two antiparallel α -helixes joined by a loop region and linked by two disulphide bonds. Regions of β -sheet structure appear to be absent. In common with other KTx, the action of κ -hefutoxin on K_v1.3 and K_v1.2 appears to be via occlusion of the pore. However, unlike other KTx, this toxin is also able to alter the gating of K_v1.3 currents, slowing the kinetics of activation. Since this is the first potassium channel toxin identified in a *Heterometrus* species, it is unclear whether this toxin family is present in all scorpions or if it is characteristic to the venom from this non-lethal scorpion family.

The traditional model of potassium channel toxin binding was based on the interactions of charybdotoxin, iberiotoxin and noxiustoxin with their targets. It predicted the toxins fitting snugly in the rim of the pore and physically plugging the mouth of the selectivity filter. The minimum requirement for functional block of K⁺ channels was proposed to

be a 'functional diad' of a lysine and an aromatic residue 6.6Å apart (Dauplais et al., 1997). Further studies on the interactions of various KTx and their acceptors showed that this model was not applicable in all cases. For a detailed discussion of these studies, and recent proposals on the interactions of KTx with their targets, see Rodriguez de la Vega et al., 2003; Xu et al., 2003; and Rodriguez de la Vega and Possani, 2004. Although all these toxins (aside from κ -hefutoxin) appear to produce functional block by physically occluding the channel pore, the precise nature of this block, and the toxin's orientation in the channel outer vestibule appear to vary (see fig 1.8).

See Rodriguez de la Vega and Possani, 2004, for a list of the known and putative scorpion K⁺ channel scorpion toxins identified to date.

Fig 1.8 Models for KTx-channel Interactions

This figure is adapted from recent models of KTx-channel interactions presented by Rodriguez de la Vega et al, 2003 and Xu et al., 2003. The approximate locations of residues critical for the interaction are marked in red (○), and the position of the toxin β-turn region is marked in blue (X).

A) Pore block. The interaction of residues on the β-hairpin containing surface of toxins in α-KTx 1-3 subfamilies, with residues located close to the selectivity filters of their respective targets (Kv1.x and K_{Ca}1.1), is firmly established (Goldstein et al., 1994). In this model, the toxin sits inside the outer vestibule, with its α-helix facing away from the pore. Surface interactions involve residues in the channel's selectivity filter, pore helix, and in the 'turret' region (the S5-S6 extracellular loop). The interaction between α-KTx 3.2 and the *Shaker* channel is illustrated.

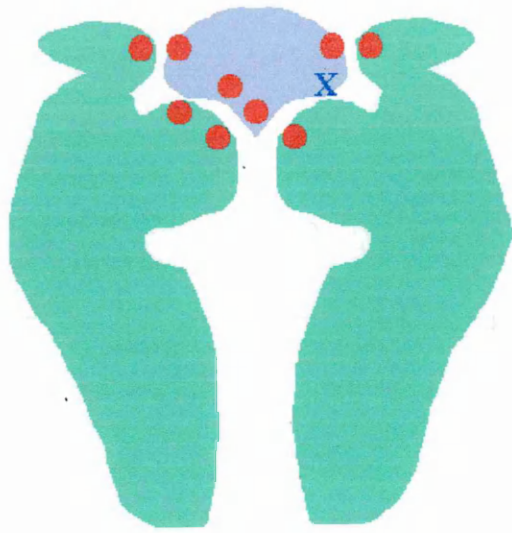
B) Intermediate-type block. In this model, the toxin sits slightly further out of the channel mouth, with its alpha-helix orientated towards the channel. Surface interactions involve residues at the base of the outer vestibule and in the 'turret' region of the channel, and residues in the α-helix of the toxin, (as opposed to the β-turn). This type of interaction is seen in the binding the α-KTx5 subfamily and α-KTx 4.2 to K_{Ca}2.x channels (Auguste et al., 1992; Lecomte, et al, 1999; Shakkottai, 2001; Cui et al., 2002). The interaction between α-KTx5.3 and K_{Ca}2.2 is illustrated.

C) Turret block. The HERG channel appears to contain an extra α-helix in the S5-pore linker (Liu et al., 2002; Pardo-Lopez et al., 2002, 2002a), producing an extended 'turret'. Ergtoxins are thought to interact with a more external region of the channel than seen in the other models. The toxin is proposed to have 'two heads', a hydrophobic and a hydrophilic patch in separate regions of the toxin, which interact with the turret α-helix and the channel vestibule respectively. This block of the outer region of the pore allows the flow of residual current. The illustrated interaction is based upon a docking model of the interaction between ergtoxin (γ-KTx1.1) and HERG (Xu, et al., 2003).

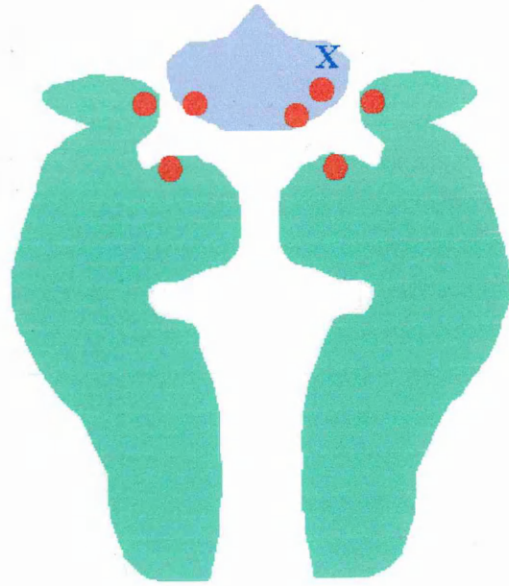
D) The structures of the selectivity filter (∗) and outer vestibule (◊) of two of the pore forming KcsA subunits are illustrated for orientation purposes.

Fig 1.8 Models for KTx-Channel Interactions

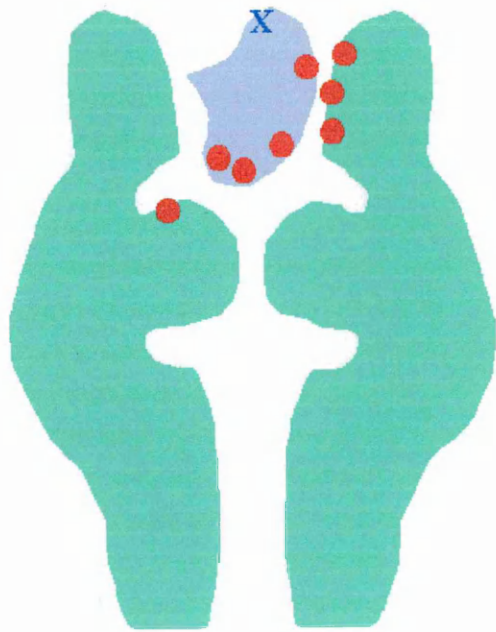
A)



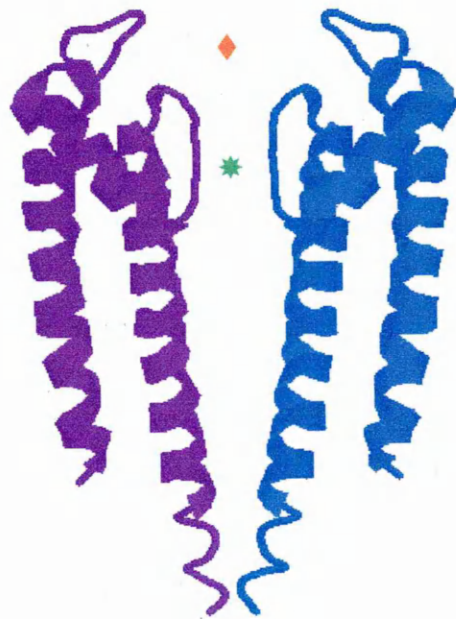
B)



C)



D)



1.5.3.3 The Short Insectotoxins

In the late 1970s and early 1980s, a group of toxins were isolated from the scorpion *Buthus eupeus* that were active on insects, but smaller than the already well-documented long-chain insect sodium channel blockers (Ovchinnikov, 1984 and references therein). The toxins were named 'short' insectotoxins and related protein or cDNA sequences have since been isolated from five other scorpion species. Compared to the long-chain insectotoxins, this group of molecules is poorly characterized. Less than 15 have been identified to date, including toxin variants: chlorotoxin from *Leiurus quinquestriatus quinquestriatus* (Debin and Strichartz, 1991; Debin et al., 1993) (and cDNA sequence variants from *Leiurus quinquestriatus hebraeus*, Froy et al., 1999); Lqh-8/6 from the same venom (Adjadj et al., 1996, 1997); Bs 8, Bs 14 (Ali et al., 1998) and peptide 1 (Fazal et al., 1989) from *Buthus indicus*; Be I5A and BeI1 from *Buthus eupeus* (Grishin, 1978; Lomize et al., 1991); AmmP2 from *Androctonus mauretanicus mauretanicus* (Rochat et al., 1979); PBITx1 from *Parabuthus schlechteri* (Tytgat et al., 1998); and Bm-12 (Wu et al., 2000) and BmKCT (Zeng et al., 2000) from *Buthus martensii* Karsch.

The short insectotoxins are basic polypeptides (net charge +2 to +5) of 34-38 residues, cross-linked by four disulphide bridges. The cysteine positions are highly conserved (consensus sequence ...CX₂CX₁₀CX₂CCX₅₋₇CX₃₋₄CXCX_n) and, as in the excitatory insect toxins, the fourth and fifth cysteine residues are adjacent. NMR structures have been determined for I5A (Arseniev et al., 1984), chlorotoxin (Lippens et al., 1995) and Lqh-8/6 (Adjadje et al., 1997). Disulphide bridges are formed between Cys1-Cys4, Cys2-Cys6, Cys3-Cys7, Cys5-Cys8 and cross-link one α -helix and three β -sheets. The extra disulphide bridge, when compared to K⁺ channel toxins, joins the free N-terminal β -sheet to the rest of the molecule.

The most studied of the short insectotoxins is chlorotoxin, which has been reported to block colonic epithelial and glioma-specific chloride ion channels (Debin and Strichartz, 1991; Debin et al., 1993; Ullrich et al., 1995). Gelatinase A (Matrix metalloproteinase 2, MMP-2) activity has also been demonstrated for this toxin (Deshane, et al., 2003). These epithelial and glioma chloride channels are unlikely to be chlorotoxin's natural target, however. The group of peptides is neurotoxic to crustaceans and insects, although this insecticidal activity is weak when compared to

long-chain counterparts (Rosso and Rochat, 1985). Indeed, only one short insectotoxin has had its natural target investigated; BeIT5A is believed to be active on the insect postsynaptic glutamate receptor (Grishin et al., 1980, 1982).

1.5.3.4 Toxins Active on Ca²⁺ Channels

Although they have been discovered more recently than Na⁺, K⁺, and Cl⁻ toxins, a few scorpion peptides active upon Ca²⁺ channels have been reported. Three types of toxin affect ryanodine receptors, whilst a fourth type is active on voltage-gated calcium channels.

The ryanodine receptor is involved in excitation-contraction coupling in skeletal muscle and forms part of a complex with the L-type voltage-dependent calcium channel (dihydropyridine receptor, DHPR). Ryanodine is a plant alkaloid that binds specifically to the open state of the ryanodine receptor.

Imperatoxin A from *Pandinus imperator* (IpTxA, Valdiva et al., 1992; Zamudio, 1997) and maurocalcine from *Scorpio maurus palmatus* (MCA, Fajloun et al., 2000a), are highly homologous (82%), 33 amino acid, basic peptides which affect ryanodine receptors. Three ryanodine receptors have been identified which differ in their sensitivity to IpTxA. Maximum IpTxA sensitivity is seen for RyR1, with RyR3 being less sensitive. In contrast, RyR2 is not significantly affected by the toxin (Simeoni et al., 2001; Nabhani et al., 2002). Both toxins increase ryanodine binding to the ryanodine receptor (presumably via their ability to stabilise the channel into long lasting, voltage- and concentration dependent, subconductance states, Tripathy et al., 1998; Eteve et al., 2003), increase the rate and amplitude of Ca²⁺ release in developing skeletal muscle and promote Ca²⁺ release from SR vesicles (Valdiva et al., 1992; El-Hayek et al., 1995; Gurrola et al., 1999; Samso et al., 1999; Nabhani et al., 2002; Chen et al., 2003). MCA appears to alter the Ca²⁺ sensitivity of the channel, since the toxin increases the sensitivity of ryanodine binding to low (stimulatory) levels of Ca²⁺ and decreases the sensitivity of binding to high (inhibitory) Ca²⁺ levels.

Single site image analysis revealed that IpTxA binds distal to the channel pore, supporting an allosteric mode of action (Samso et al., 1999). Both IpTxA and MCA

contain a cluster of basic peptides (KKCKRR) also present in domain A (II-III loop) of the voltage-sensor subunit ($\text{Ca}_v\alpha 1.1$) of DHPR. The exact role of this domain is unclear, but it seems to be essential for the physical coupling to RyR1 and also enhances ryanodine binding. Arg24 of maurocalcine, contained within this conserved region, is critical for MCa-RyR interaction (Esteve et al., 2003). Gurrola et al., 1999 showed that domain A and IPTxA activate RyRs in a similar manner and would appear to compete for a common binding site on the channel. It has been proposed that the 3D surface of the two toxins mimics that of DHPR domain A (Green et al., 2003). However, MCa and domain A have different effects on channel gating, suggesting different mechanisms of channel modification (Chen et al., 2003).

MCa is the first scorpion toxin to show the inhibitor cystine knot motif, also present in a number of other non-scorpion toxins active on voltage gated calcium channels (ω -conotoxins and μ -agitoxins) (Mosbah et al., 2000). Projecting from this compact core is a double-stranded antiparallel β -sheet, with an extended strand perpendicular to the β -sheet. Given the high sequence homology of MCa and IpTxA, it is likely that they have similar overall structure. However, despite the sequence homology of the two toxins, they do not produce identical effects, since they have distinct subconductance states (Gurrola et al., 1999; Simeoni et al., 2001). Therefore minor structural differences in the toxins may give rise to them stabilising slightly different channel conformations. Both of these toxins represent useful tools in the study of the ryanodine receptor, and of excitation-contraction coupling.

Imperatoxin I (Zamudio et al., 1997a), also from *Pandinus imperator*, is a heterodimer of ~12kDa and ~3kDa, linked by a disulphide bond. It inhibits ryanodine binding and blocks the RyR channel. The larger subunit has phospholipase A_2 activity and it is likely that the toxin's effect on the Ca^{2+} channel is an indirect effect due to liberation of fatty acid.

BmK-PL from *B. martensii* Karsch also seems to exert its effects on the RyR by an indirect mechanism (Kuniyashi et al., 1999). Stimulation of RyR activity and an increase in ryanodine binding was seen with partially purified, but not with purified, ryanodine receptors. The authors suggest triadine, an associated molecule in the receptor complex, to be the site of BmK-PL action.

Chuang et al., 1998 screened scorpion venom for activity directed against α_1 C-T-type calcium channels expressed in *Xenopus* oocytes and identified kurtoxin from *Parab. transvaalicus*. The primary sequence classified kurtoxin as an α -scorpion toxin and the peptide showed α -toxin activity, binding to sodium channels and slowing their inactivation. Subsequent studies revealed the toxin to modify the gating of native P-type, N-type and L-type Ca^{2+} currents, in addition to T-type currents (Sidach and Mintz, 2002). The nature of these gating modifications was specific to channel type. An identical peptide has been isolated from the related scorpion *Parab. granulatus* (KLII, kurtoxin-like II), together with KLI, which differs by 6 amino acids (Olamendi-Portugal., et al 2002). Both toxins bind to T-type Ca^{2+} -channels and cardiac Na^+ -channels.

1.5.4 Other Scorpion Venom Peptides

Insect defensins are antimicrobial peptides found in the haemolymph, which interact with lipid bilayers or proteins in them, altering the membrane permeability and causing cell death. These peptides share the CSH motif with scorpion toxins. The presence of this structural motif in insect defensins led to the proposal that insect defensins and scorpion toxins could derive from a common ancestor. 4kDa homologues of insect defensins (scorpion defensins), with antibacterial properties, have been found in the haemolymph of *L. quinquestriatus* (Cociancich et al., 1993). Further evidence for an evolutionary relationship between the two classes of compounds was provided by the isolation of a cDNA encoding a scorpion defensin-like peptide from the venom gland of *B. martensii* (Zhu et al., 2000). In terms of primary sequence, cysteine pattern and RNA structure, the scorpion defensins show similarity to the scorpion long-chain potassium channel toxins.

A second group of scorpion venom antimicrobials are the scorpines (Conde et al., 2000; Zhu and Tytgat, 2004). Like the scorpion defensins, they have three disulphide bridges, but are significantly longer (75 amino acids). They appear to be hybrid molecules; the N-terminal segment resembles some cecropins, whilst the C-terminal region resembles some defensins.

A number of scorpion venom antimicrobial and antifungal peptides that do not contain disulphide bridges have been isolated, e.g. pandinin 1 and 2 (*P. imperator*, Corzo et al., 2001), IsCT (*Opisthacanthus madagascariensis*, Dai et al., 2001), parabutopeporin, and opistoporin1 and 2 (*Parab. schlechteri* and *Opistophthalmus carinatus*, Moerman et al., 2002). They are polycationic, α -helical, pore-forming peptides and have been likened to the magainins (antimicrobial peptides from frog skin, Zasloff, 1987). Although they all demonstrate antimicrobial activity, these scorpion peptides vary markedly in their size and primary structures.

Other linear pharmacological peptides isolated from scorpion venoms include the bradykinin-potentiating peptides, e.g. peptide K₁₂ (*Buthus occitanus*, Meki et al., 1995), believed to act via ACE (angiotensin-converting enzyme) inhibition, and peptide T (*T. serrulatus*, Ferreira, et al., 1993), which is only 13 amino acids long. Even smaller are the tetrapandins, tetrapeptides isolated from *P. imperator* venom via their ability to inhibit store-operated Ca²⁺ entry in human embryonic kidney cells (Shalabi et al., 2004).

There are a number of 'orphan' scorpion venom peptides. These are either native peptides with no-known function (e.g. Pi7, *P. imperator*, Delepierre, 1999, and BmKn1, *B. martensii*, Zeng et al., 2001a) or peptides which have been deduced from cDNA sequences, but show little sequence homology to known scorpion venom components (e.g. BmAP1, *B. martensii* Zeng et al., 2002, Zhu and Li, 2002). In the case of the native peptides, these may have an, as yet undefined, function or they may prove to be the degradation products of larger bioactive components (as is the case with IsCTf, *Opisthacanthus madagascariensis*, Dai et al., 2002).

1.5.5 Scorpion Venom cDNA and Genes

Scorpion toxin cDNAs typically encode a single precursor containing the mature peptide and a signal peptide of approx. 18-28 amino acids, which is removed by post-translational processing. This signal peptide is often highly conserved within groups of related toxins. The C-terminal also often undergoes C-terminal modification, involving the removal of one or two residues from the C-terminus with, or without, amidation of the new terminal residue. Scorpion defensins, the long-chain potassium channel toxins

and the bradykinin potentiating peptide BmKbpp all contain a short propeptide between the signal peptide and the mature toxin (Zhu et al., 1999; Zeng et al., 2000a).

The first complete scorpion toxin genomic sequence to be reported was that of *T. serrulatus* toxin gamma (Becerril et al., 1993). The data from this, and the subsequent sequencing of other scorpion toxin genes, led to the proposal of a universal scorpion toxin gene structure (Becerril et al., 1995; Corona et al., 1996). This model describes a gene comprised of one intron and two exons. Exon 1 includes the 5' non-coding region and the region encoding the first two-thirds of the signal peptide. An intron splits a cordon in the signal peptide sequence and the second exon encodes the final third of the signal peptide, the mature toxin and the 3' non-coding region. The size of the intron varies from approx. 80-100bp in the short chain toxins to over 400bp in the long chain toxins.

Although most known scorpion venom peptides conform to this model, a few exceptions have been noted. Scorpion defensin genes and those encoding the ryanodine receptor toxins BmKAs and BmKAS1 are intronless (Zhu et al., 1999; Lan et al., 1999). The scorpine gene family has two large introns, the first in the 5' UTR and the second at the boundary of the mature-peptide coding region (Zhu and Tytgat 2004a). The long-chain potassium channel toxin BmKTx β also contains two large introns. The first is >997bp and is located in the signal peptide sequence, the second (886bp) is located in the mature peptide sequence (Xiao et al., 2003).

1.5.6 Significance of Scorpion Venom Components

There would appear to be much redundancy in scorpion venom toxins. Why do scorpions need both Na⁺ channel and K⁺ channel toxins, when both cause membrane depolarisation? Why are there several examples of toxins having a very similar site and mechanism of action, e.g. several sodium channel α -toxins, in a single scorpion venom? The work of Miller, 1995 and of Inceoglu et al., 2003 presented possible answers to the former question.

It has been postulated (Miller, 1995) that K⁺ and Na⁺ channel toxins work cooperatively to produce a depolarised state. The author proposed that since the K⁺ channel toxins are

non voltage-dependent, initial block of repolarising potassium currents promotes a depolarised state conducive to the voltage-dependent binding of the Na⁺ channel toxins, which are then the primary cause of catastrophic effects of envenomation.

It has long been documented that the first few drops of scorpion venom (prevenom) are different in appearance to the main venom and that this change from a transparent, to an opaque and viscous, secretion occurs in successive stings. Recently Inceoglu et al., 2003 showed this prevenom to have a different composition to the main venom. The study revealed prevenom to be rich in potassium salts and almost totally devoid of the sodium channel toxins that account for the majority of the lethality of the main venom. The authors propose the conservative use of the metabolically expensive venom by scorpions. In this hypothesis the prevenom is used when the scorpion is not in a life-threatening situation, to deter predators or immobilise small prey. It is envisaged that the high extracellular K⁺ causes significant long lasting pain due to localised depolarisation. This effect is potentiated by the block of voltage-gated potassium channels delaying recovery of the membrane potential. Only when necessary does the scorpion inject the metabolically expensive venom, containing the highly toxic sodium channel blockers.

Much of our knowledge of K⁺ channels is the result of a combination of the use of high-affinity probes isolated from animal venoms, particularly those from scorpions, and the molecular cloning and expression of these channels. Scorpion toxins were essential for the determination of the tetrameric nature of voltage-activated potassium channels (MacKinnon, 1991) and charybdotoxin was vital to the identification of the pore region (MacKinnon and Miller, 1989). Pardo-Lopez et al., 2002, used ergotoxin1 and site directed mutagenesis of HERG to deduce the presence of a previously unknown segment of α -helix in the channel. Scorpion toxins are useful in the purification of native ion channels, and in determining subunit composition, molecular structure, and the functional role of ion channels. The role of scorpion toxins in the study of ion channels is discussed by Garcia and colleagues (Garcia et al., 1998, 2001). Due to their compact, well-defined structure, scorpion peptides also make ideal model peptides in the study of peptide folding (e.g. Khandelwal et al., 2000).

Studies using toxin chimeras show that different sequences can be attached to the basic scorpion toxin CSH scaffold, altering functional properties whilst maintaining structural

integrity. There is, therefore, the potential to engineer biologically active sites onto this stable scaffold, with implications for *de novo* drug design. This principle was tested by Vita et al., 1995. The group were able to engineer a functional metal binding site onto a charybdotoxin scaffold. Peptides engineered in this way may be more resistant to degradation than those without the scorpion toxin core.

AaH IT is highly potent and highly specific for insect sodium channels. There has been much interest in the use of this toxin, and other insect-selective scorpion toxins, as biodegradable, selective insecticides that are non-toxic to mammals. Studies on AaIT and similar toxins, and their potential as an aid to pesticide design have been reviewed (Gurevitz et al., 1998; Zlotkin et al., 2000).

Several scorpion sodium channel peptides have been reported to have anti-nociceptive effects in animals. The therapeutic potential of such peptides and their promise as tools for the study of pain have been discussed (Goudet et al., 2002). Traditional Chinese medicine used scorpion stings for relief of paralysis and spasms. Scorpion ion channel toxins therefore have potential use not only in the design of novel therapeutics, but also in the investigation of the underlying causes of ion channel disorders.

Venom components, other than ion channel toxins, may also have therapeutic potential. Bradykinin-potentiating peptides may prove useful models in the design of antihypertensive agents. With increasing antibiotic resistance there is an urgent need for novel antimicrobials. The defensins and the linear antimicrobial peptides present in both the venom and in the haemolymph of scorpions have therefore generated much interest, as templates for the next generation of antibiotics. The antimalarial property of such peptides has also generated interest. Possani et al., 2002, have assessed their potential use in the creation of transgenic, malaria-resistant, mosquitoes.

Less than 1% of the estimated 100,000 peptides believed to be present in the combined venoms of all scorpion species have been identified (Possani et al., 2002). The main focus of studies to date has been the identification and characterisation of the major toxic components and in particular those components active on ion channels. More recently peptides with novel pharmacological properties have been discovered and it is envisaged that these minor, non-ion channel blocking agents will be the focus of a rapidly expanding field of research in the next decade.

1.6 *Mesobuthus tamulus* (formally *Buthus tamulus* or *Buthotus tamulus*)

There are 86 scorpion species in India, of which two are of medical note, the Asian giant forest scorpion *Heterometrus swammerdami* (also found throughout South East Asia) and the Indian red scorpion *Mesobuthus tamulus* (Mahaddevan, 2000). *Mesob. tamulus* (fig 1.9) is a small (65-90mm) scorpion, with insignificant pedipalps and one of the most poisonous venoms known (mouse LD₅₀ = 3.65 mg/kg, Ramachandran et al., 1986). Left untreated, stings from this species are often lethal and there is no effective anti-venom (Kankonkar et al., 1998).

There are approximately 12 reported cases of red scorpion envenomation per month in India, with reports of 1-5% fatality, increasing to 15% in children (Bawaskar, 1982, 1999; Bawaskar and Bawaskar, 2003). The fatalities occur predominately in the state of Maharashtra. Most stings are reported at night and incidence of stings is seasonal, dramatically increasing in summer months.

Like that of all dangerous scorpions, the venom of *Mesob. tamulus* is a potent stimulator of the autonomic nervous system causing a rise in circulating catecholamines. It slows down the inactivation of sodium currents and induces repetitive firing of action potentials (Siemen and Vogel, 1983; Rowan and Harvey, 1996). A number of studies have investigated specific physiological effects of the venom in animal models (Murthy and Hossein, 1986; Murthy et al., 1988; Murthy and Medh, 1989; Murthy et al., 1991; Deshpande et al., 1999).

The currently recommended treatment of scorpion sting in India is nifedipine (a slow calcium-channel blocker which uncouples excitation-contraction, causing smooth muscle relaxation, and relieving the pressure on the heart and lungs) plus prazosin (a selective inhibitor of post-synaptic α -adrenergic receptors, blocking the action of catecholamines), a treatment that is readily available, cheap and effective (Bawaskar, 1999; Bawaskar and Bawaskar, 2003). Sodium nitroprusside, hydralazine, captopril, and digoxin are also administered as vasodilators. Since most victims are stung in rural locations, by the time medical treatment is obtained, symptoms have often progressed past the stage where antiserum treatment, if available, would be effective. Bawaskar, 1999, has reported a decrease in scorpion sting fatality from 30% (1977) to 1% (1993)

with advances in treatment and provided an extensive review of clinical and pharmacological aspects of the venom of this scorpion.

Scorpion venom has already been shown to contain large numbers of specific toxins acting on a wide range of sodium and potassium channels. Compared to those of American and African species, the toxins produced by Asian scorpions are poorly investigated (with the exception of *B. martensii* from which over 80 peptides have been isolated Goudet et al., 2002). Chhatwal and Habermann, (1981) identified the presence of three distinct neurotoxic components of MW ~ 4400Da, ~7500Da and ~8000Da in *Mesob. tamulus* venom and in 1994, Lala and Narayanan partially sequenced a sodium channel toxin, neurotoxin Bt-II.

A few potassium channel toxins have been identified in this species. The most notable *Mesob. tamulus* toxin characterised is iberitoxin (Galvez et al., 1990), a highly specific blocker of high-conductance calcium-activated potassium channels, which binds to the channel's outer vestibule. It belongs to the α KTx 1.x subfamily, and is structurally related to charybdotoxin. Tamapin (Pedarzani et al., 2002) targets SK channels, and demonstrates high selectivity for SK2 over SK1 and SK3. Indeed, it is the most potent inhibitor of SK2 identified to date, and was the founding member of subfamily 16 of α KTx. A toxin isoform (tamapin-2) differing in a single C-terminal residue has also been isolated from *Mesob. tamulus* venom. Tamulustoxin (Strong et al., 2001) and BTK-2 (Dhawan et al., 2003) are both Kv channel blockers. Tamulustoxin inhibits currents through Kv1.6 channels expressed in HEK293 cells. Although members of the α KTx family, tamulustoxin and its isoform tamulustoxin-2 (which differs by a single amino acid) are yet to be assigned a Ktx subfamily or a systematic number (Rodriguez de la Vega and Possani, 2004). BTK-2 falls into α KTx subfamily nine but, unlike other members of this subfamily (which are either non-toxic, or show weak SK channel activity), it is a weak blocker of Kv1.1.

In addition, a number of enzyme activities are present the venom, including phospholipase and hyaluronidase, although these activities are considerably lower than seen in *Heterometrus bengalensis* (Achyuthan et al., 1982). Indian red scorpion venom also contains at least four histamine releasing factors and one protease inhibitor (Chhatwal and Habermann, 1981).

Fig 1.9 *Mesobuthus tamulus*



Photograph taken by Prof. P. Strong.

1.7 Aims and Objectives

There were three main aims of the work presented.

a) Characterisation of the *Mesob. tamulus* venom, particularly with reference to small peptide components. The objective was twofold: -firstly to utilise immunological and mass spectrometric techniques to investigate possible regional differences in the venom composition of this scorpion species; and secondly to construct a mass profile of commercially available *Mesob tamulus* venom as a tool to aid in future isolation of specific venom components.

b) Use of molecular biology to identify short insectotoxin cDNA sequences derived from the telson of *Mesobuthus tamulus*. Mass spectrometry-guided purification would then be used to isolate one of the corresponding gene products from the venom itself. It was also envisaged that a similar molecular biology protocol would be used to provide evidence of the amidation status of the known *Mesob tamulus* venom peptide tamulustoxin.

c) Study of the functional implications of modifications to the well-characterised bee venom peptide apamin. Radioligand binding assays would be used to study the effects of an Asp2Ala substitution, and a consequential non-native disulphide bridged isoform on the interaction of the toxin with its acceptors on rat brain membranes. The same techniques would be used to examine the effects of labelling apamin with Alexa Fluor 488.

Chapter 2

Studies on the *Mesobuthus tamulus* Venome, and Possible Regional Variation Within it.

2.1 Introduction

The proteomic analysis of venoms is increasingly seen as a useful tool in taxonomic analysis and has been proposed as a complementary method to morphology and behavioural characteristics for species and ultimately sub-species discrimination. The concept of the venome was described by Pimenta et al., 2003. Since venom contains a mixture of peptides and proteins secreted by a specific gland, analysis of venom components can produce a fingerprint that can be used as a reference for identification and classification of related specimens. Conversely, it can also be used to identify specimens that do not conform to this fingerprint and study the factors that affect venom variability.

Composition of animal venoms has previously been studied by a variety of methods including electrofocussing, gel electrophoresis, and liquid chromatography (Meier, 1986; Williams, et al., 1988; Mendoza et al., 1992; Otero et al., 1998; Francischetti et al., 2000; Binford, 2001). Development of sensitive mass spectrometry techniques and advances in data processing capabilities (enabling the characterisation of complex mixtures of biomolecules) has, however, revolutionised the study of animal venoms and toxins. Mass spectrometry is now the tool of choice for venom profiling (e.g. Sweetman et al., 1992; Stocklin and Savoy, 1994; Jones et al., 1996; Roda et al., 1997; Escoubas et al., 2002; Dyason et al., 2002; Pimenta et al., 2003), having the advantages of increased accuracy, sensitivity and speed. The techniques require only small samples and, unlike some traditional taxonomic methods allow the use of live specimens.

In this study, we have chosen to investigate the venom fingerprint and composition of the Indian red scorpion *Mesobuthus tamulus*. *Mesob. tamulus* is present in West Bengal (Dasgupta et al., 1989), parts of Karnataka, Andhara Pradesh, and Tamil Nadu (Mahadevan, 2000; Bawaskar and Bawaskar 2003). This scorpion is also common in the state of Maharashtra. Kankonkar et al., 1998, showed differences in toxicity and neutralisation by antisera of commercial *Mesob. tamulus* venom obtained from HITRT (Haffkine Institute for Training, Research and Testing, Mumbai) and that obtained from ISCICS, (Irula Snake Catchers Industrial Co-operative Society Ltd., Madras), suggesting geographical variation. There is also evidence to suggest that Indian red scorpions found in different regions of the state of Maharashtra (fig 2.1) differ in respect to their venom (Kulkarni, D.G.; Haffkine Bio-pharmaceutical Corporation Limited

(HBPCL), Pimpri, Pune, India. *Personal communication*). Antiserum raised against scorpions from Aurangabad does not effectively neutralise venom from scorpions of the Konkan coastal region. This Konkan venom is of considerably higher toxicity and antigenicity than the venom of Aurangabad individuals. This is reflected clinically with Bawaskar, 1999, reporting that, within the state of Maharashtra, fatal scorpion envenomations occur only in the Konkan region.

Geographical and individual variability in venom composition is important on a number of levels. Clinically it is crucial in the production of antivenom, in ascertaining a suitable dose and in understanding variation in clinical symptoms. There are obvious implications in taxonomy and venom research. With increasing numbers of studies on venom components, it is becoming increasingly important to accurately identify the venom of origin. Work presented in this chapter examines both the immunological- and protein- fingerprints of venom from individual scorpions collected from the two regions as an initial study on possible compositional differences.

Mesob. tamulus venom is not one of the most studied scorpion venoms, and no mass spectrometric studies have been carried out (although the masses of some purified toxins have been determined). A combination of chromatography and mass spectrometry was also used to examine the peptide mass profile of commercially available *Mesob. tamulus* venom. Identification of the masses present will aid in the detection of components with novel pharmacology and in the purification of existing toxins. Toxin-like molecules are increasingly being identified by cloning techniques; without the native protein, however, these molecules remain putative venom toxin components and cleavage sites from precursor peptides remain theoretical. A venom mass profile can provide evidence suggesting expression of the component, support proposed cleavage site locations and, by pinpointing appropriate masses to specific venom fractions, aid in the purification of the active molecule. The latter is of particular use in the absence of a suitable functional assay.

The aim of the work presented in this chapter was thus twofold. Firstly, it was intended as a preliminary study investigating possible differences in the immunology and composition of *Mesob. tamulus* venom collected from two geographical regions. Secondly, it was intended to use chromatographic and mass spectrometric techniques to construct a profile of the mass composition of *Mesob. tamulus* venom and the

chromatographic distribution of the components. For ease of understanding, the studies on the different venoms will be referred to as mass fingerprinting, whilst the more thorough dissection of pooled venom will be referred to as venom profiling.

Fig 2.1 Location of the Two *Mesobuthus tamulus* Populations Studied



Map of India showing location of Maharashtra state and (expanded view) Aurangabad district and the Konkan coastal region (incorporating Thane, Raigad, Ratnagiri and Sindhugurg districts). The Konkan region is a narrow strip just above sea level. It is hilly, with a tropical climate, and is separated from the semi-arid and rocky Deccan plateau (300-600m), on which Aurangabad is located, by the Sahyadri mountains (Western Ghats).

2.2 Materials and Methods

2.2.1 Materials

Commercial pooled *Mesob. tamulus* venom was supplied by Haffkine Institute, Mumbai, India; antiserum was supplied by Haffkine Bio-pharmaceutical Corporation Limited (HBPCL), Pimpri, Pune, India. *Leiurus quinquestriatus hebraeus* (*Lqh*) and *Pandinus imperator* venoms were obtained from Latoxan, Paris, France. Solvents used for high performance liquid chromatography and mass spectrometry (acetonitrile, trifluoroacetic acid (TFA) and formic acid) were all of analytical grade or better and were filtered (0.45µm membrane filter) and degassed prior to use. For LC-MS, solvents were degassed on-line using helium. Water for HPLC was purified on an Elga system and, for LC-MS, HPLC grade water (Sigma-Aldrich, UK) was used. Standard peptide solution was a partially purified synthetic peptide supplied by Hallam Biotech, Sheffield Hallam University.

2.2.2 Harvesting and Preparation of Venom Samples

Red scorpions were collected from Ratnagiri and Chiplun (Konkan coastal region) and Aurangabad, in the state of Maharashtra, India. They were electrically milked and individual venom samples collected and freeze-dried. Single specimens of another Indian species (*Heterometrus fulvipes*) were obtained in a similar fashion.

Samples were extracted for 1hr with 100µl de-ionised water (acidified to pH3.0 with acetic acid), centrifuged at 12,500 xg for 30min to remove insoluble material and the supernatant retained. A further three extractions were performed on the pellet in further aliquots of 100µl sterile acidified water, stored overnight at 4°C, and centrifuged as above. Extracts showing absorbance at 280nm were pooled for each individual. The final protein concentration was determined by the BCA assay, using BSA as standard, as described 4.2.2.3. Pooled freeze-dried venoms from *Mesobuthus tamulus* and the African species *Pandinus imperator* and *Leiurus quinquestriatus hebraeus* were also used. These venoms were extracted as above, using 20µl acidified water per mg venom in the initial extraction, aliquotted and stored at -20°C prior to use.

2.2.3 Venom Fingerprinting

2.2.3.1 Development of an ELISA (Enzyme-Linked Immunosorbent Assay) Using *Mesob. tamulus* Antivenom and Assessing its Ability to Recognize Different Venom Extracts

Mesob. tamulus antivenom raised in horse, against a mixture of Aurangabad and Konkan scorpion venom, was used to perform a direct ELISA on *Mesob. tamulus* venom.

Initial experiments optimised the ELISA in terms of primary and secondary antibody concentrations using a range of pooled control venom concentrations. The final assay was carried out as follows: Venom was diluted to the appropriate concentration in carbonate/bicarbonate buffer (15mM NaCO₃/ 35mM NaHCO₂, pH9.6) and 100µl diluted venom per well was adsorbed onto a 96-well polystyrene microtitre plate (Falcon, Becton Dickinson, USA) overnight at 4°C. After washing once in phosphate buffered saline (Sigma-Aldrich, Poole) containing 0.1% Tween-20 (PBS-T), each well was blocked with 200µl PBS-T/ 5% foetal calf serum (FCS) for 2hr at 37°C and washed again with PBS-T. A 1:50 dilution (in PBS-T/ 5% FCS) of the antivenom was added (100µl per well), and incubated for 1hr at 37°C before washing x3 in PBS-T. A HRP (horseradish peroxidase)-conjugated secondary antibody (rabbit α-horse whole molecule IgG affinity isolated peroxidase conjugate (Sigma)) was diluted 1:3000 in PBS-T/ 5% FCS and applied at 100µl per well. After 1hr at 37°C the plate was again washed 3 times in PBS-T. 3,3', 5,5'-tetramethyl benzidine (TMB, Sigma) (50µl) was added to each well and allowed to develop in the dark (25min), before addition of stop reagent (Sigma) according to manufacturer's instructions. The absorbance was read at 450nm on a microtitre plate reader.

A standard curve was created using pooled control venom between 50ng/ml-10mg/ml in triplicate. A non-venom control was used as a blank, and this absorbance reading was subtracted from the other values before plotting. From this curve, a concentration of individual venom samples suitable for use in the assay could be determined.

In order to compare the ability of the antiserum to recognise the different individual scorpion venom extracts, 1µg (100µl of 10µg/ml) of individual samples were adsorbed

to an ELISA plate and probed as above. For comparison, the venom of a single individual of *H. fulvipes*, and commercially available *L. quinquestriatus hebraeus* venom, were also tested. As above, samples were tested in triplicate and a non-venom blank used, its absorbance value subtracted from that of the samples. The results were normalized against a *Mesob. tamulus* pooled venom control and plotted both individually, and pooled by scorpion type.

2.2.3.2 SDS-PAGE (Sodium Dodecyl Sulphate – Polyacrylamide Gel Electrophoresis) and Western Blotting of Individual Venom Samples

SDS-PAGE and Western blotting (using the HBPCCL antiserum) were performed on venom extracts from individual scorpions. A representative Konkan scorpion (K), Aurangabad scorpion (A), and a single individual of *H. fulvipes* (H) were used, as well as pooled commercially available *L. quinquestriatus hebraeus* (LQ) venom. Samples were run on both 4-20% Bis-Tris and 16% Tricine non-reducing gels, and the proteins visualized by Coomassie staining, silver staining and by Western blotting using the *Mesob. tamulus* antiserum used for the ELISA. Test gels were run in order to determine suitable quantities of sample required for each method (Bis-Tris silver: 0.2µg, 0.5µg, 1µg K and A; 0.5µg LQ. Bis-Tris Coomassie: 5µg, 15µg, 30µg K and A; 4µg, 15µg LQ. Bis-Tris Western blotting: 0.5µg, 2µg, 5µg K and A; 2µg LQ; 2µg H. Tricine silver: 1µg, 5µg, 10µg K and A; 5µg, 10µg LQ. Tricine Coomassie: 5µg, 10µg, 20µg K, A and LQ. Tricine blotting: 1µg, 5µg, 10µg K and A; 5µg, 10µg LQ; 1µg H). Due to limited venom quantity, not all gels contained a *H. fulvipes* sample.

Bis-Tris [Bis (2-hydroxy ethyl) imino-tris (hydroxy methyl) methane-HCl] NuPAGE®

The NuPAGE® Bis-Tris discontinuous buffer system runs at neutral pH (c.f. pH8.8 for Laemmli system, Laemmli, 1970) which provides better stability of gel matrix and proteins resulting in a longer shelf life and better band resolution (Moos et al., 1988). Samples were prepared by heating in NuPAGE® LDS (Lithium dodecyl sulphate) sample buffer (106mM Tris-HCl, 141mM Tris Base/ 2% LDS/ 10% glycerol/ 0.51mM EDTA/ 0.22mM SERVA® blue G250/ 0.175mM Phenol Red/ pH 8.5) at 70°C for

10mins prior to loading on a pre-cast Novex NuPAGE[®] 1 x 80 x 80mm Bis-Tris 4-12% acrylamide gel (Invitrogen, CA, USA). The gel was run in MES [2-(N-(N-morpholino) ethane sulphonic acid)] SDS running buffer (50mM MES/ 50mM Tris-Base/ 0.1% SDS/ 1mM EDTA/ pH7.3) using an Xcell SureLock mini-cell system (Invitrogen) at 200V constant for 35min.

To allow molecular weight estimation, Mark12 unstained molecular weight standards (Invitrogen) were used. The components and apparent molecular weights were as follows: myosin (apparent MW 200 kDa), β -galactosidase (116.3 kDa), phosphorylase B (97.4 kDa), bovine serum albumin (66.3 kDa), glutamic dehydrogenase (55.4 kDa), lactate dehydrogenase (36.5 kDa), carbonic anhydrase (31 kDa), trypsin inhibitor (21.5 kDa), lysozyme (14.4 kDa), aprotinin (6 kDa), insulin B chain (3.5 kDa) and insulin A chain (2.5 kDa).

Tricine SDS-PAGE

To allow for better separation of the small molecular weight peptides, venom samples were run using a modification of the Tris-glycine discontinuous buffer system (Laemmli, 1970) which substitutes Tricine for glycine in the running buffer (Schaegger and Von Jagow, 1987). Samples were heated for 2min at 85°C in Tricine SDS sample buffer (450mM Tris-HCl/ 12% glycerol/ 4% SDS/ 0.0025% Coomassie[®] blue G/ 0.0025% phenol red/ pH8.45). These samples and a Mark-12 molecular weight standard (see above) were then run using Tricine SDS running buffer (100mM Tris Base/ 100mM Tricine/ 0.1% SDS/ pH8.3) on a pre-cast Novex 1 x 80 x 80mm, 16% acrylamide Tricine gel (Invitrogen) at 125V (constant) for 90min.

Staining Gels for Protein

Following separation by SDS-PAGE, venom proteins were stained using either a colloidal Coomassie blue stain (Gelcode colloidal blue stain reagent, Pierce, IL, USA) or a Silver staining kit (silver xpress staining kit, Invitrogen).

Western Blotting of Venom Proteins

Venom proteins were separated by Bis-Tris or by Tricine SDS-PAGE as described above, and for each gel format the blotting protocol was optimised with regards to protein concentration, transfer time, and concentrations of both primary and secondary antibodies. The final optimised protocols are described. When running gels to be visualised by Western blotting procedures, SeeBlue[®]Plus2 pre-stained standards (Invitrogen) were used. The components and their apparent molecular weights in NuPAGE MES/ and Tricine buffer systems were as follows: myosin (188/ 210 kDa); phosphorylase B (98/ 105 kDa); bovine serum albumin (62/ 78 kDa); glutamic dehydrogenase (49/ 55 kDa); alcohol dehydrogenase (38/ 45 kDa); carbonic anhydrase (28/ 34 kDa); myoglobin (17/ 17 kDa); lysozyme (14/ 16 kDa); aprotinin (6/ 7 kDa); insulin (3/ 4 kDa).

For NuPAGE Bis-Tris gels: 0.45µm PVDF (polyvinylidene difluoride) membranes (Invitrogen) were pre-wetted for 30secs in methanol and rinsed in deionised water prior to equilibration in Bis-Tris transfer buffer (25mM bicine/ 25mM Bis-Tris free base/ 1mM EDTA/ pH7.2) containing 10% methanol per gel. Proteins were transferred using an Xblot mini-cell system (Invitrogen) for 1hr at 30V constant in the above transfer buffer. Transfer conditions for Tricine gels were 25V constant for 1½hr, using a Tris-glycine transfer buffer (12mM Tris base/ 96mM glycine/ pH8.3) containing 20% methanol.

Transferred membranes were blocked in 2% fat-free dried milk in PBS-T (50ml blocking solution per membrane) for 30-40mins with agitation. Primary antiserum (*Mesob. tamulus* antivenom from HBPCCL, Pune, India) diluted in blocking solution (1:2500 dilution for blots from NuPAGE gels, 1:1500 for Tricine gel blots) was added to the membranes for 1hr with agitation. After washing x4 in PBS-T (10min per wash) secondary antibody (rabbit α-horse whole molecule IgG affinity isolated peroxidase conjugate, Sigma-Aldrich) diluted 1:2000 (Bis-Tris) or 1:2500 (Tricine) in blocking buffer was added and the membranes agitated for 1hr at RT. Excess antibody was removed by washing in PBS-T (four 10min washes) and an enzyme chemoluminescent substrate (ECL⁺ plus Western blotting detection system, Amersham-Pharmacia, UK) added as per manufacturer's protocol. Light emission was visualised using a UVP imager (UVP, UK) and the image captured using Labworks software (UVP, UK).

2.2.3.3 Analysis of Individual Venom Samples by SELDI-TOF Mass Spectrometry

SELDI-TOF (surface-enhanced laser desorption ionisation–time of flight) mass spectrometry is a variation on the MALDI-TOF (matrix-assisted laser desorption ionisation - time of flight) technique. In its most common form (surface-enhanced affinity capture, SEAC), SELDI utilises chemically engineered chips to differentially capture proteins, prior to MALDI analysis. A variety of surfaces (e.g. hydrophilic, hydrophobic, metal affinity, cationic, anionic, antibody, DNA, enzyme, receptor) are available. The H50 protein chip binds proteins through a reverse phase or hydrophobic interaction mechanism and has binding properties similar to C6-C12 reverse phase resins. The NP20 chip has properties similar to normal phase chromatographic media i.e. it primarily retains hydrophilic compounds. The sample is directly applied to this surface, and after a short incubation period, unbound sample washed away. A matrix solution (or EAM, Energy Absorbing Molecule) is applied and the sample analysed by the traditional MALDI-TOF technique.

Mass spectrometry is a three-step process which generally takes place under high vacuum. Sample molecules are ionised (in an ion source) to form ions, which are repelled out of the ion source and accelerated into the mass analyser, where they separate based on their mass-to-charge ratios (m/z). The path of the ions through the analyser is bent by a magnetic field, focussing ions of interest onto the detector. The ions strike the detector, where they are converted to an electrical signal.

Many types of ion source and mass analyser are available. Dependent upon the mode of ionisation, sample is applied in the gas phase, or converted either before, or during, the ionisation process. In the case of MALDI, desorption (conversion to the gas phase) and ionisation occur simultaneously. Sample and matrix are combined on the target and as the solvent evaporates, the matrix co-crystallises with the analyte. The matrix has two important properties. The first is its ability to form these composite crystals and the second is its ability to absorb energy at the wavelength of the laser. Upon laser illumination, analyte molecules are both vaporised and ionised (usually by protonation or deprotonation). The exact process by which this occurs remains unknown.

With a TOF (Time-of-Flight) mass analyser, the ions are accelerated by a pulsed potential into a field-free tube (drift region) where they move towards the detector. The

ion's velocity through this drift region is determined by its m/z value. Ions of a lower m/z ratio will have a higher velocity and reach the detector first. Thus, m/z can be determined by calculating the 'time-of-flight'.

In collaboration with Dr Arun Armugam, National University of Singapore (NUS), SELDI-TOF protein profiling samples were run by a service facility at NUS. Briefly, venom extracts from individual Konkan (K) and Aurangabad (A) *Mesob. tamulus* specimens were examined by protein profiling on SELDI-TOF Proteinchip System II (Ciphergen, USA) using both a H50 hydrophobic chip and a NP20 hydrophilic chip (Ciphergen, USA). Single specimens of another Indian species (*H. fulvipes*) and of the African species *P. imperator* (P) were used as comparisons.

Samples (5 μ g) and standards (Protein MW Standards Kit, Ciphergen, USA) were spotted onto proteinchips, and incubated in a humid chamber for 30-40min before washing with PBS. Spots were air dried prior to addition of 1 μ l matrix (saturated solution of sinapinic acid in 50% acetonitrile/ 0.1% TFA). This was air-dried, and the chips inserted into the instrument for analysis. Instrument parameters were as follows: NP20 chips- focus mass 10500Da; calibration set 100ppm; intensity 185V; sensitivity 9V. H20 chips- focus mass 16000Da; calibration set 100ppm; intensity 195V; sensitivity 9V.

Mass fingerprints were determined using the software supplied by the manufacturers.

2.2.3.4 LC- Electrospray Ionisation Mass Spectrometry (LC/ESI MS) on Individual Venom Samples

ESI (Electrospray Ionisation) is another desorption/ionisation technique. The ionisation is produced by spraying a sample solution through a conducting capillary tube at a high potential. The spray results from the high voltage potential between the electrospray needle and the counter-electrode in the ion source housing, and is composed of multiply-charged droplets containing the sample. In 'ion spray' this spray is enhanced by nitrogen gas forced over the outer surface of the needle. Unlike in MALDI the ionisation occurs at atmospheric pressure and the ions pass through a series of reduced pressure chambers before entering the analyser. The ions generated are often multiply-

charged, bringing larger proteins well within the m/z detection range. It is also a very gentle ionisation technique, producing little fragmentation of molecules. However, compared to MALDI, ESI is much more sensitive to salts, detergents, etc. Unlike MALDI, the ionisation is continuous, allowing ESI to be coupled to separation techniques such as capillary electrophoresis and HPLC.

LC/MS (Liquid Chromatography/Mass Spectrometry) links the effluent from a liquid chromatographic system (usually HPLC) to a mass spectrometer (normally with an ESI ion source). The technique allows on-line separation of complex mixtures prior to mass spectrometry. The chromatographic process can also allow for pre-concentration and removal of salts that would otherwise interfere with ESI. LC/MS can be used to look at a wide variety of biologically important compounds including peptides, proteins, oligonucleotides and lipids.

In order to minimise sample variation, 'average' Aurangabad (A) and Konkan (K) regional *Mesob. tamulus* venom samples were created. Resulting A and K venom samples were comprised of equal quantities of all available individual venoms for each type (n=10, (K); n =6, (A)) made to a final protein concentration of 0.1mgml⁻¹. *Lqh* venom was also diluted to 0.1mgml⁻¹. To enable relative quantitative analysis, venoms were spiked with 0.01mgml⁻¹ of a standard peptide solution. To identify masses arising from this standard and from possible solvent contamination, 0.01mgml⁻¹ peptide standard and a sample-blank were analysed.

Direct on-line analysis of venom LC samples using an electrospray ion source and a quadrupole time-of-flight hybrid mass analyser was carried out. An Ultimate LC system (LC packings, Amsterdam) controlled by Chromeleon client software (Dionex) coupled on-line to an API QSTAR pulsar1 (Applied biosystems) LCMS/MS system controlled by Analyst QS software (Applied biosystems) was used. 6µl samples were separated on a Dionex C18, 3µm, 100Å 1mm x 15cm Pepmap column (LC packings) at a flow rate of 30µl min⁻¹ using a 5-42% gradient of acetonitrile in 0.1% formic acid over 80min. Separation was followed using uv detection at 280nm and eluate introduced directly into the electrospray ion source. The mass spectrometer was operated in positive ionisation mode at 5000V, scanning over a mass range of 500-4000m/z. The ion source and curtain gas were at 40 and 25 respectively. The instrument was calibrated on

service, and the calibration checked prior to sample run using a test solution of apamin (>0.01% accuracy).

2.2.3.5 LC-MS Data Analysis

All analysis was carried out using Analyst-QS software. Total ion current (TIC) chromatograms were produced for the sample run over m/z range 500-4000. The LC-MS peak reconstruct program, which uses isotopic and charge series from each scan to calculate component masses and their elution window, was applied to the data. A mass tolerance of 0.01% and a final mass range of 2000-10000 was used. The signal-to-noise ratio was set to 10, an intermediate value enabling the detection of nearly all chemical species in MS data, with virtually no false positives.

Data for components with a mass and elution time corresponding to those contained within the peptide standard sample were removed, and the remaining peak areas standardised against that of the main peptide standard component ($[M+H]^+ = 2463.7$). Masses differing by -1Da were assumed to be products of either amidation or oxidation and, as such, their relative areas combined with that of the higher mass. Masses possibly representing adducts were noted, but retained. Relative areas of calculated masses were plotted to give mass fingerprints. Differences in A and K venoms were plotted by subtracting the relative area in K from the relative area in A for each mass.

2.2.4 Venom Profiling

Commercially available *Mesob. tamulus* venom was extracted, and fractionated by size-exclusion, ion exchange and reverse-phase chromatography. At each stage venom samples were tested by MALDI-TOF and/or LC-ESI mass spectrometry.

2.2.4.1 Size Exclusion Chromatography

2ml venom extract was loaded onto a 75ml Sephadex G50 column equilibrated in 50mM ammonium formate, and run at $\sim 40\text{ml hr}^{-1}$. 1ml fractions were collected,

absorbance measured at 215 and 280nm, dried in a rotary evaporator and stored at -20°C . Prior to use, samples were reconstituted and pooled in the following groups: - lead peak (fractions 11-18), main peak (19-38), and trailing peak (39-55). 'Main peak' samples to be analysed by mass spectrometry were desalted using a C18-ziptip (Millipore) as per manufacturer's instructions.

2.2.4.2 Cation Exchange Chromatography

The reconstituted, pooled, main peak from the size exclusion column was diluted until it had a conductivity approximating that of 100mM ammonium acetate pH4.8. Ion exchange chromatography was performed at 1ml min^{-1} using a Pharmacia FPLC system. 20mg protein was filtered and loaded onto a Hiload 16/10 SP-sepharose fast flow 10cm x 1.6cm cation exchange column (Pharmacia) pre-equilibrated in the above buffer. A segmented gradient of 0-1M NaCl in 100mM NaAc, pH4.8, was run as follows: 0-0.5M over 300ml, 0.5-0.7M over 40ml and 0.7-1M over 30 ml. The absorbance was followed at 280nm, and 2ml fractions collected. The profile was divided into eight sections, the fractions pooled within each section and stored frozen.

For illustrative purposes a 2mg sample was run on an AKTA HPLC system (Amersham-Pharmacia) using the column and conditions described above.

Samples to be analysed by mass spectrometry were desalted using Sep-Pak cartridges (Waters, Millipore), pre-conditioned as per manufacturer's instructions and eluted with 75% acetonitrile/ 0.1% TFA.

2.2.4.3 Reversed Phase HPLC

Ion exchange samples were fractionated by reverse-phase HPLC prior to mass spectrometric analysis. Separation was carried out on an AKTA system (Amersham-Pharmacia) using a Dynamax C18, 300A, 250 x 4.6mm, $5\mu\text{m}$ column at a flow rate of 0.5ml min^{-1} . 0.5mg non-desalted ion exchange samples were filtered through a $0.45\mu\text{m}$ membrane filter and injected onto the column, which was pre-equilibrated in solvent A (0.1% TFA). The column was washed until absorbance returned to baseline, and flow

through and column wash pooled and retained for subsequent analysis. Samples were eluted using a linear gradient of solvent B (90% acetonitrile/ 0.1% TFA) i.e. 0-50% over 12 column volumes. Effluent was monitored at 218 and 280nm and 1ml fractions collected and stored at 4°C. After testing by MALDI-TOF MS, remaining sample was frozen at -20°C to allow for possible future analysis.

2.2.4.4 Matrix-Assisted Laser Desorption/Ionisation Time-of-Flight Mass Spectrometry (MALDI-TOF MS)

Several sample preparation techniques and matrix solutions were tested. The best results were obtained using a saturated (10mgml⁻¹) solution of α CHCA (α -cyano-4-hydroxycinnamic acid) in 60% acetonitrile/ 0.3% TFA and the preparation techniques described below.

For size exclusion and ion exchange samples: 1 μ l desalted fraction was diluted in 10 μ l matrix solution, 0.5 μ l spotted onto target and air-dried. Insulin and apamin standard solutions were prepared in an identical fashion using an initial concentration of 1mgml⁻¹.

For reverse phase samples: 50-200 μ l fractions were evaporated to dryness in a rotary evaporator (volume required was estimated from UV signal, and adjusted if poor ionisation obtained with MALDI). The sample was redissolved in 10 μ l matrix solution, 0.5 μ l spotted onto target and air-dried.

For all samples, triplicate spots were analysed.

MALDI-MS analysis was carried out on a SAI LaserTOF LT1500 mass spectrometer (Scientific Analysis Instruments Ltd, Manchester, UK) with a 337nm nitrogen laser operated in the positive-ionisation mode under the control of LaserTOF (SAI Ltd.) software. Optimal results were obtained using a 20KV accelerating voltage, time delayed pulse extraction, a focus mass of 8500 and a data transfer rate of 1-0.8 sec. To obtain good spectra the laser power was automatically adjusted to near threshold for ionisation. The instrument was calibrated using porcine insulin ($[M+H]^+=5773.6$), data was collected in the range 2000-10000Da and the spectra averaged over 25 laser shots

to overcome shot-shot variability. 5 spectra were collected for each sample. Since apamin has a similar structure to scorpion toxins and known mass within the range studied, a control apamin sample was run, which produced an accurate mass ($\pm 0.1\%$).

MALDI peaks were assigned by eye with a clear inflection point on curve used as indication of a separate peak. The software calculated the mass at maximum peak height and these masses were noted. Masses from different spectra and samples were deemed to represent the same component if the variation was $<0.1\%$ and a mean mass was taken. Masses observed in less than three spectra from two different sample spots were discarded.

2.2.4.5 LC-MS

Samples were diluted to 0.1mgml^{-1} protein and LC-MS was carried out as described previously (2.2.3.4), but without the addition of peptide standard solution. TIC spectra were created and peak reconstruction carried out as described (2.2.3.5). Masses differing by -1Da were assumed to be products of amidation and as such their relative areas combined with that of the higher mass.

2.2.4.6 Data Analysis

Some isomasses were observed eluting at different times or in different fractions. Where there was fraction separation (off-line MALDI-TOF analysis) or elution window separation (LC-MS), these masses were considered separate components. Where masses were collected in successive fractions the masses were averaged and pooled. In MALDI and LC-MS data a large number of putative adducts were observed i.e. representing addition of Na (+22), K (+38), Na+K (+60), loss of CO_2 (-44), NH_3 (-17), H_2O (-16), mono and di oxidation (+16, +32), matrix adduct (+188). These masses, along with ones corresponding to +74 and +104 (unknown adducts observed in scorpion venoms by Pimenta et al., 2001), were removed from the final dataset.

2.3 Results

2.3.1 Ability of *Mesob. tamulus* Antivenom to Recognise Venom Extracts by ELISA

The ability of the antiserum to recognise venom extracts was assessed by direct ELISA. Venom extracts were adsorbed to a microtitre plate and probed using *Mesob. tamulus* antivenom. A typical curve using pooled control *Mesob. tamulus* venom is shown (fig 2.2), the data fitted to a sigmoidal curve using *Prism* (graphpad software, San Diego USA). 10µg venom with no primary-, and another with no secondary- antibody were used as controls and produced signals less than that of a venom negative sample. The standard curve showed that there was a concentration-dependent sigmoidal relationship between venom concentration and ELISA signal. Although further optimisation would probably increase the sensitivity, 10µgml⁻¹ venom corresponded to the most sensitive region of the curve and allowed a 1µg sample to be utilised, sufficient for the purpose required.

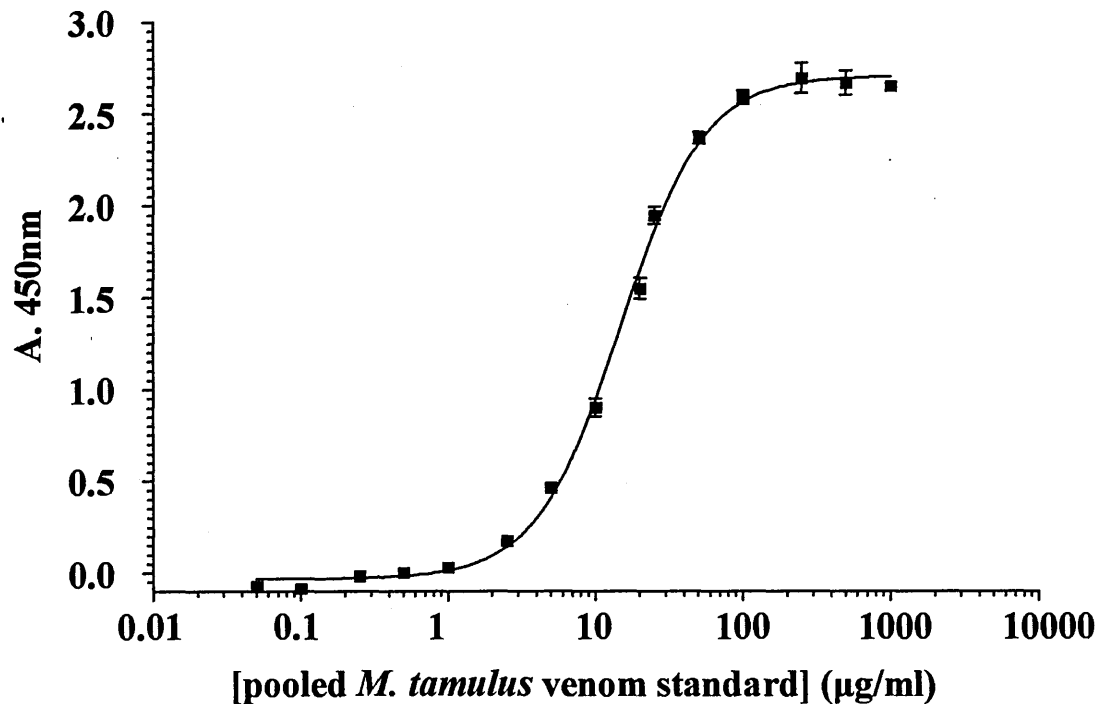
1µg of individual venom extracts from regional *Mesob. tamulus* specimens, and a single individual of *H. fulvipes* were tested alongside a sample of commercially available *L. quinquestriatus hebraeus* venom using the ELISA described. Resulting absorbances are shown standardised against commercial control *Mesob. tamulus* venom in fig 2.3a. The data suggests considerable venom variability between individuals and between species.

Fig 2.3b illustrates the same data grouped according to geographical region, statistical analysis shows significant differences in the ability of the antiserum to recognise *Mesob. tamulus* venom from the Konkan and Aurangabad regions (2-tailed student t-test, $\alpha=0.05$), likely to reflect differences in the venom composition in individuals from the two regions. The two reference venoms showed opposing results. There is slight recognition and therefore cross reactivity with *Heterometrus* venom. *Lqh* venom gave a high signal, suggesting more cross reactivity with this venom than with that of some individuals of the species against which the antiserum was raised.

The differences above do not necessarily reflect the neutralisation abilities of the venom, since the ELISA gives no indication of the types of molecules responsible for the antigenicity. In order to further analyse the venom components responsible for the differences, the venoms were separated electrophoretically. A1 and K3 individuals

appeared to be suitable representatives for further investigation of antigenicity by Western blotting.

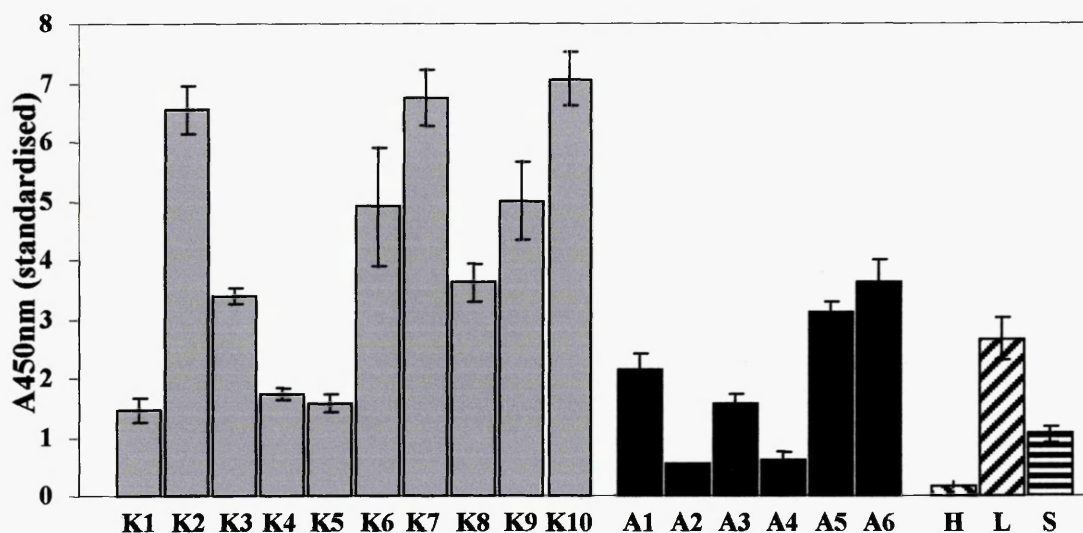
Fig 2.2 Typical ELISA Profile using *Mesob. tamulus* Control Venom



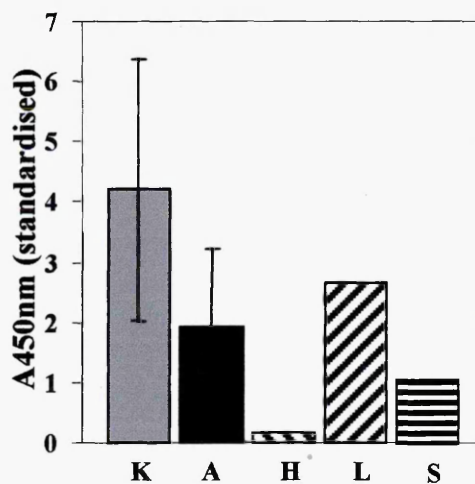
The ability of *Mesob. tamulus* venom antiserum to recognise venom extracts was assessed by direct ELISA. Venom extracts were adsorbed to a microtitre plate and probed using 1:50 dilution of Haffkine antiserum, followed by an anti-horse HRP conjugate. A typical profile using varying concentrations (as determined by protein concentration) of pooled control venom is shown. Data shown is mean \pm SD of triplicate samples, corrected for blank (no venom). In the above figure *Prism* (graphpad software, San Diego USA) has been used to fit a sigmoidal curve to the data.

Fig 2.3 ELISA on Individual *Mesob. tamulus* Venom from Different Regions

a)



b)



1µg of individual Konkan (K1-10) and Aurangabad (A1-10) venom extracts were adsorbed to an ELISA plate and probed with 1:50 dilution of *Mesob. tamulus* venom antiserum (Haffkine institute), followed by an anti-horse HRP-conjugated secondary antibody. Antibody complexes were visualised by the addition of a TMB substrate solution and quantified by A450nm. Resulting absorbances (mean +/- SD from triplicate samples) are shown standardised against that of pooled control *Mesob. tamulus* venom (S) (a). Values for a single individual of *H. fulvipes* (H) and for commercially available *Leiurus quinquestriatus hebraeus* (L) venom (Latoxan, France) are also shown. (b) Illustrates the same data pooled by scorpion type.

2.3.2 SDS PAGE and Western Blotting on Individual Venoms

SDS-PAGE and Western blotting were carried out on venom from a single Konkan scorpion (K3) and from an Aurangabad scorpion (A1). For comparison, venom from a single individual of *H. fulvipes* and commercially available *Leiurus quinquestriatus hebraeus* venom were also used. In order to achieve good resolution for both high and low molecular-weight proteins, samples were run on both 4-20% Bis-Tris, and 16% Tricine gels under non-reducing conditions (fig 2.4). Western blotting was carried out on both gel types using *Mesob. tamulus* antiserum (fig 2.5). Although the majority of peptide toxins are thought to be single chain, a recent report has identified disulphide-linked oligomers in *Mesobuthus gibbosus* venom (Ucar et al., 2004). Non-reducing conditions were therefore chosen in order to ensure bands corresponded to intact proteins.

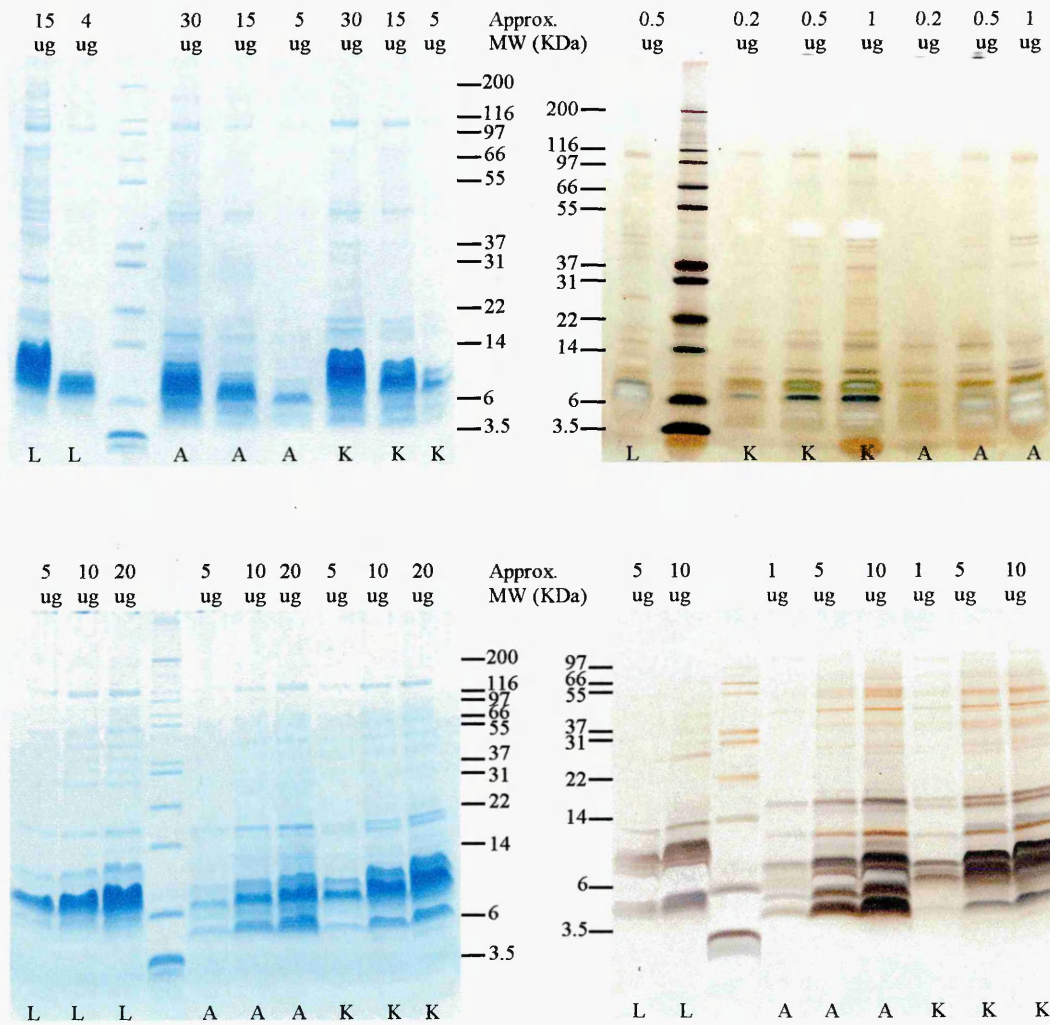
SDS-PAGE page shows the presence of both high and low molecular weight components in all venom types tested. Groups of proteins ~7kDa and ~4kDa may correspond to long and short chain neurotoxins known to be present in scorpion venoms. Larger proteins may include enzymes and cellular derived components. Although there appear to be common, or similar components between the species in the 97-116 kDa range, *Mesob. tamulus* venom would appear to have more low weight components (<14kDa) than that of *Lqh*. Differences are also apparent between *Mesob. tamulus* venoms from the different regions. Konkan venom may contain an extra protein in the 55kDa region. There is a clear difference between the venoms at around 14kDa, and a number of differing bands occur in the 3-7 kDa region.

Antigenic differences were assessed by Western blotting. As seen in ELISA, the antisera had a strong overall reaction with the *Mesob. tamulus* and *Lqh* venoms, whilst there was only slight cross reactivity with *Heterometrus* venom. Antigens would appear to fall into three groups: the high MW components (>34kDa), and two groups ~7kDa and ~4kDa, possibly the long and short chain toxins respectively. Results do show, perhaps unsurprisingly, that the higher MW (possibly enzymic components) are generally more antigenic than the lower (possibly neurotoxic) ones. The antivenom does not react with any low MW *Heterometrus* components that may be present, all of the cross reactivity occurring towards the higher mass proteins. High MW components (>34kDa) also account for much of the cross-reactivity seen with *Lqh* venom. Similar

bands are seen in venoms from both buthoid species, perhaps suggesting shared, or similar, components, possibly enzymes. There is some reaction in the 4 and 7kDa regions, believed to represent the neurotoxins, but far less than seen with *Mesob. tamulus* venoms. It is thus likely that the high signal seen with the ELISA was due to reaction with non-toxic components and therefore unlikely that the antisera would afford much neutralization of *Lqh* toxicity. No significant differences were seen in *Mesob. tamulus* regional venoms in the >34kDa components. Antigenic differences do appear, however, in the mass ranges corresponding to the neurotoxic components.

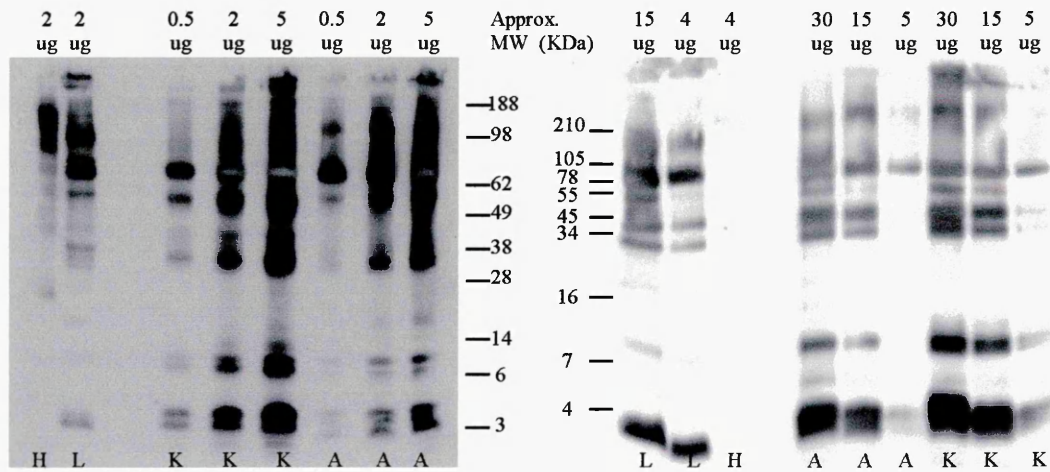
These experiments relate to venoms from single individuals from each region. From ELISA it is apparent that there is much inter-specimen variability, which should be noted when considering the results presented. There is no indication whether the venom differences are qualitative or quantitative, nor the molecular identities of the proteins involved. To further understand the venom variability samples were analysed by mass spectrometry.

Fig 2.4 SDS-PAGE Analysis of Non-Reduced Venom Samples



SDS-PAGE was performed on non-reduced regional *Mesobuthus tamulus* venom samples. Varying quantities (as determined by BCA protein assay) of venom from a single Konkan scorpion K3 (K) and from an Aurangabad scorpion A1 (A) were run on both 4-20% Bis-Tris (top) and 16% Tricine gels (bottom). Lanes containing venom from a commercially available *L. quinquestriatus hebraeus* venom (L) are shown for comparison. Gels were stained using a colloidal Coomassie blue protein stain (left) and silver staining (right).

Fig 2.5 Western Blotting of *Mesob. tamulus* Venom from Different Geographical Regions



Western blotting was carried out on venom from a single Konkan scorpion K3 (K) and from an Aurangabad scorpion A1 (A). Various quantities of venom protein were run on both 4-20% Bis-Tris (left) and 16% Tricine gels (right). *Mesob. tamulus* antivenom was used at a 1:2500 (Bis-Tris) or 1:1500 (Tricine) dilution, followed by a 1:2000 (Bis-Tris) or 1:2500 (Tricine) dilution of anti-horse-HRP. Lanes containing venom from a single individual of *H. fulvipes* (H) and commercially available *L. quinquestriatus hebraeus* (L) venom are also shown.

2.3.3 Mass Spectrometry

Having established that there are antigenic and possibly compositional differences between *Mesob. tamulus* venoms harvested from different geographical regions, mass spectrometry was utilised to investigate further. Analysis was restricted to the 2000-10000Da mass range in order to exclude small peptide fragments, the larger enzymes and matrix interference. Although intact peptides <2kDa and enzymic components may play an important role in scorpion venom, the focus of this study is on the peptide toxins, which occur predominately in the 3000-8000Da mass range, believed to account for the main pharmacological properties.

2.3.3.1 SELDI –TOF Fingerprinting

Venom extracts from individual Konkan (K) and Aurangabad (A) *Mesob. tamulus* specimens, single *H. fulvipes* specimens and from *P. imperator* were examined by SELDI-TOF protein profiling using both hydrophobic and hydrophilic chips (fig 2.6).

Both chip types bind venom components, but it would appear that either more peptides bind to the hydrophobic chip or the resolution is worse with this chip. Differences in venom fingerprints are apparent with both chips.

The different species show clear differences in venom peptides. Masses for *Mesob. tamulus* are predominately clustered in two regions: - ~3000-4500Da and ~6500-8000Da, perhaps corresponding to long- and short-chain toxins respectively. *Heterometrus* has some masses within these ranges but most are between 4500-5500Da, a distribution possibly reflecting a lower proportion of ion channel toxins, sodium channel toxins in particular. The masses in the *Pandinus* sample are of low intensity with less distinct mass grouping.

Despite having similar fingerprints, there are apparent differences between *Mesob. tamulus* venoms from the two regions. There would appear to be variation in the type of peptides represented; on the hydrophobic chips, the Aurangabad venoms have higher overall intensity than Konkan venoms, whereas on the hydrophilic chips the situation is reversed. There are several clear differences in components' masses between the

regions, perhaps the most obvious of which is seen in the 6500-8000Da range on the hydrophobic chip. There is a prominent peptide ~3000Da in the Konkan venom (hydrophilic chip), apparently much reduced or absent in Aurangabad venom. Although the SELDI profiles suggest a distinct mass fingerprint for regional *Mesob. tamulus* venoms, fingerprints of individuals within a region are not identical, showing qualitative, if not quantitative differences.

Since the preliminary data obtained by SELDI-TOF in Singapore showed distinct regional venoms for *Mesob. tamulus*, further experiments were carried out by LC-MS in Sheffield to determine more precise masses for the peptides involved.

2.3.3.2 LC-MS

SELDI-TOF data showed variation in the venom from individual scorpions. Due to limited mass spectrometry resources, LC-MS on several individuals was not possible. Individual venoms were thus pooled for each region, reducing intraregional variations. Different peptides ionise differently in mass spectrometry. The observed abundance of different ions does not therefore represent abundance in the original sample. It is, however, possible to compare abundances of the same ion between samples, since it ionises to the same extent. To eliminate run-to-run variation, absolute intensity was not used. Instead, data was standardised to a single reference ion species. Since venom protein expression may vary between regions, LC-MS samples were spiked with equal amounts of the peptide standard solution.

Aurangabad (A), Konkan (K) and *Lqh* samples were run, and differing TIC profiles obtained for each sample (fig 2.7). Abundances were standardised against the main standard-mass peak and masses present in blank and standard-only samples were removed. In all samples, the relative proportions of standard-peptide solution masses were approximately the same, validating standardisation. Masses corresponding to possible adducts were noted. (See appendix A-C for complete list of component masses). The total number of peptides identified was far greater in K (296) than in A (170), although this could be an experimental artefact or due to greater interindividual variation in the Konkan region. However, total relative area of K (8.77) was similar to that of A (7.311) which, despite differences in ionisation properties, suggests similar

peptide concentrations in the mass range, comprised of differing numbers of components.

Differences in dominant masses determined by LC-MS are readily visible in standardised mass fingerprints (fig 2.8). However, species grouping is not obvious using this technique, possibly due to the technique itself, venom pooling or the use of a different reference species (*Mesob. tamulus* and *Lqh* are both dangerous buthoid species, whereas *Heterometrus* and *Pandinus* are more distantly related, with less potent venom). In contrast to SELDI-TOF, there is far more data in the lower than higher mass range for all three species, possibly be due to inherent differences between ionisation methods or to LC-MS being optimised for data in the lower range. Concentrating on the 2500-5000Da range, the LC-MS data shows good correlation to that seen with the SELDI hydrophilic chip. Prominent peaks, possibly relating to 2947 (for Konkan) and 3448 (for Aurangabad) LC-MS masses are visible in SELDI-TOF fingerprints.

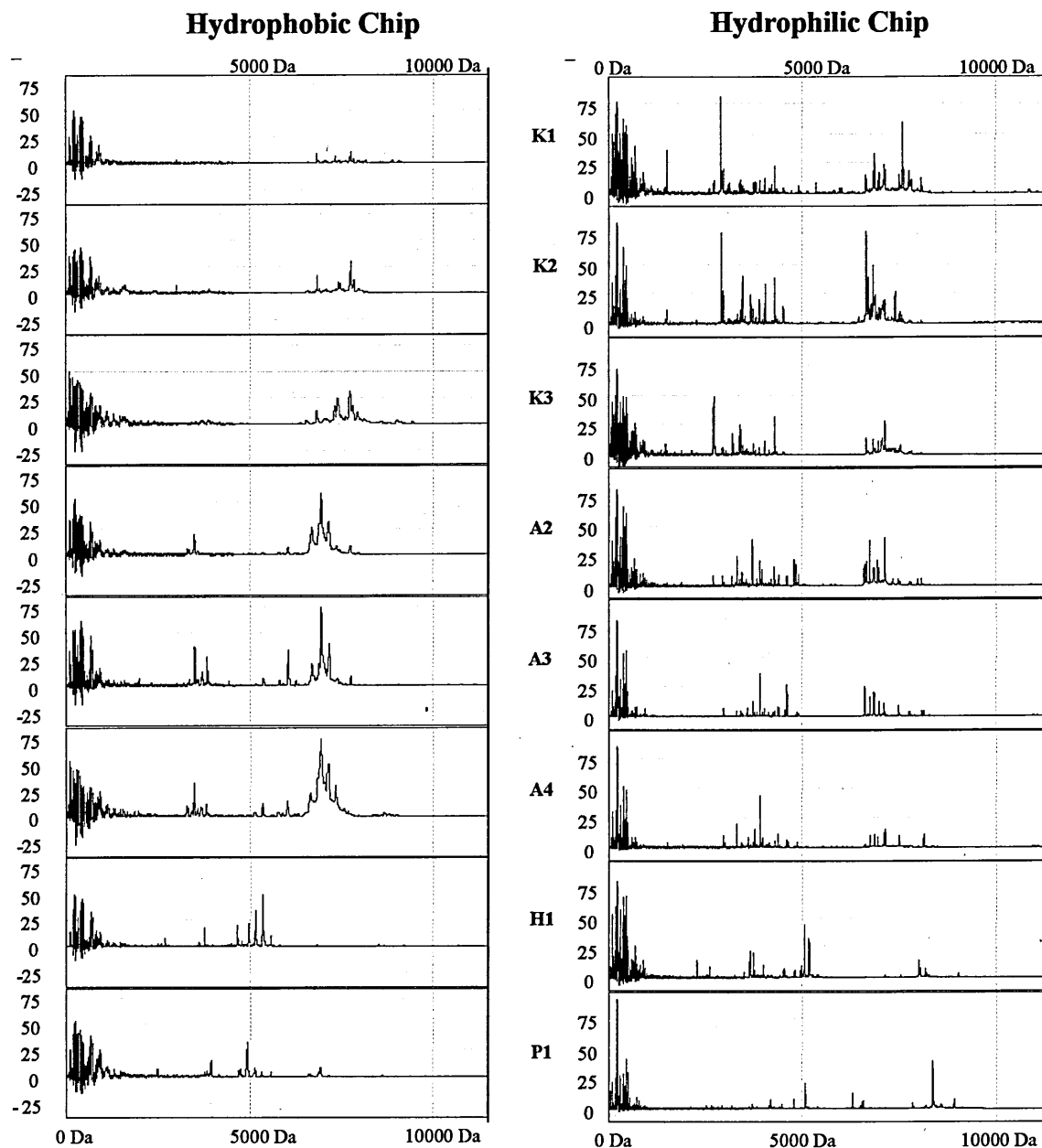
Differences are also apparent in the mass distribution of components (fig 2.9). *Lqh* venom has a large proportion of lower mass peptides compared with the Indian species' venom. Whether this effect is real or due to degradation is unclear, since different species' venoms were derived from different sources. Again, comparison of regional venoms shows some similarities with the SELDI-TOF 2500-5000Da range. Using both techniques there is a shift towards the top of this range in the Aurangabad venom.

Standardised peak areas for each mass in Konkan venom were deducted from the equivalent mass in Aurangabad venom (fig 2.10), highlighting differences in expression levels. Table 2.1 summarises the dominant masses for each venom type. There are considerable regional differences in expression of the prominent masses seen in the venom fingerprints. Although the majority of these masses are shared, a number of major masses, particularly in Konkan venom, are not expressed or not detected in the other venom type. It would appear on initial inspection that the majority of masses are unique to a single region. It should be noted, however, that a large number of these are detected only at low levels and small differences in relative concentration may push them below the detection threshold.

A number of masses seen in this study appear to correspond to known venom components (tables 2.2 and 2.3). Two known *Mesob. tamulus* peptides (BTK-2, BtITx3)

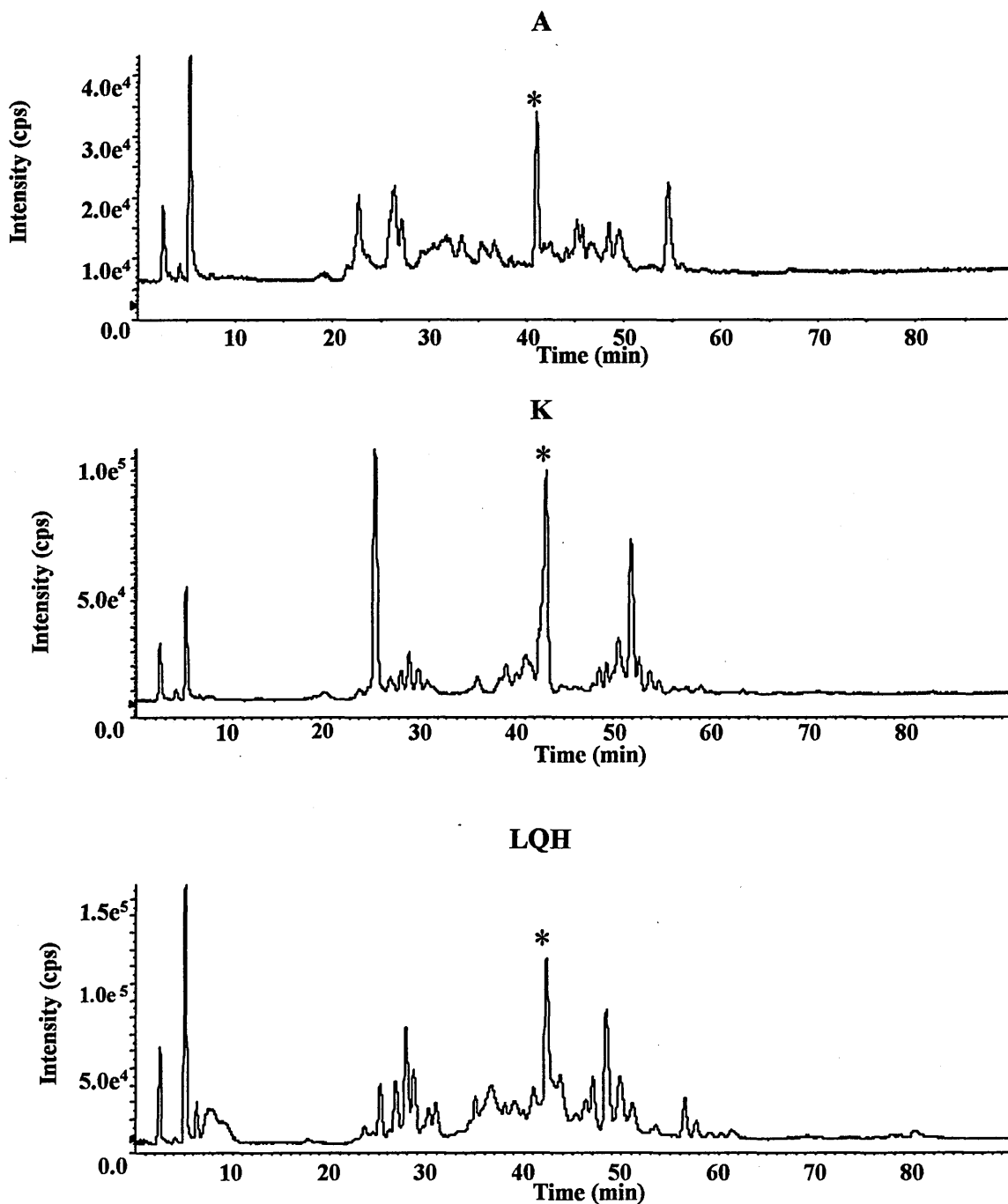
and four known *Lqh* peptides (LQH-IT2-44, LQHIT2-53, LQHIT5, LQH8/6) are represented in the top 20 detected masses. Their abundance probably accounts for their isolation. Importantly, the two major known *Mesob. tamulus* peptides are present in both types of venom. Masses corresponding to Tamapin, Tamapin-2 and ButaIT were only detected in venom from a single region, however. The masses corresponding to a number of known peptides of both species were not found by LC-MS.

Fig 2.6 SELDI-TOF Mass Spectrometry on Individual *Mesob. tamulus* Venom Samples from Scorpions Collected in Different Regions



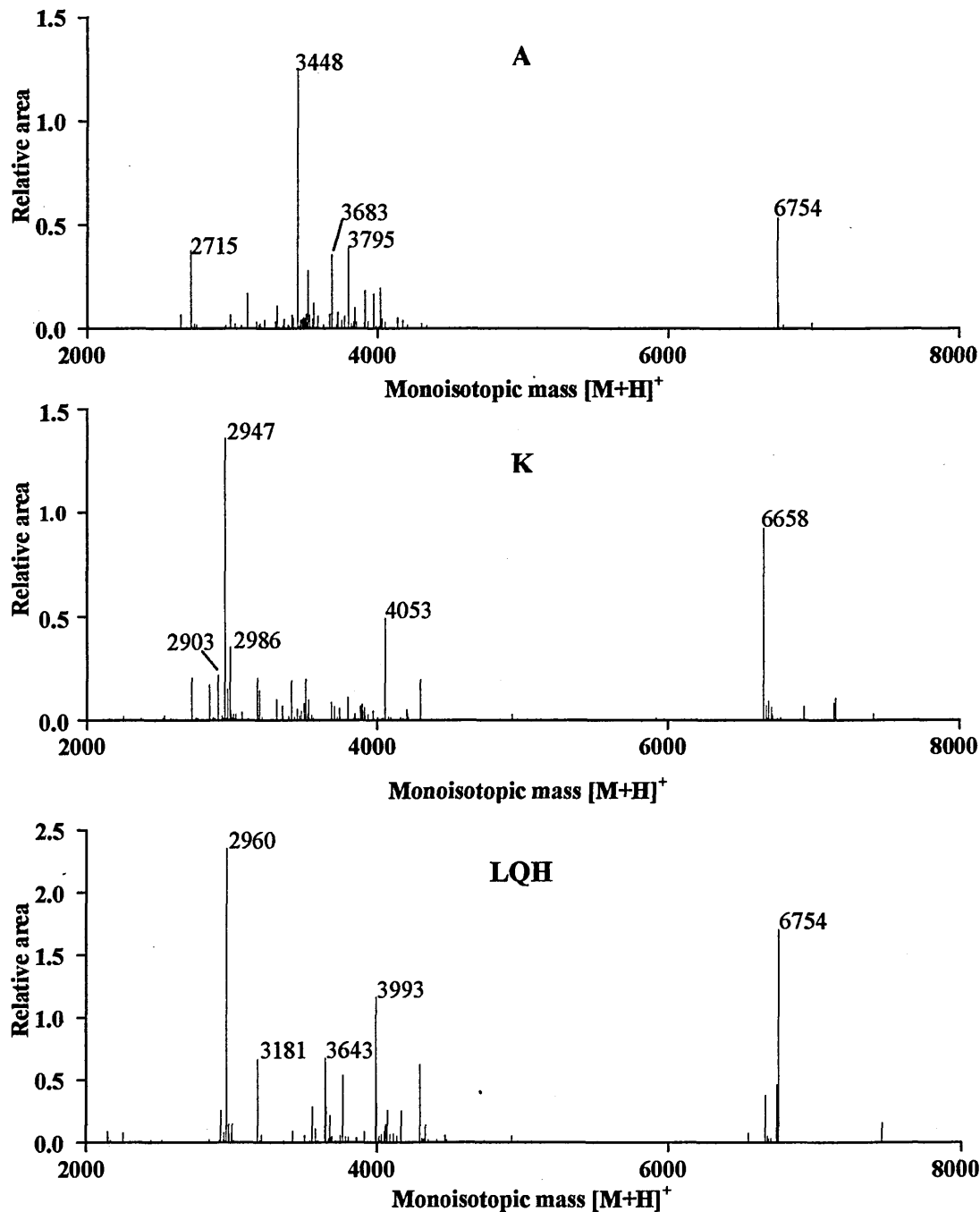
Venom extracts from individual Konkan (K) and Aurangabad (A) *Mesob. tamulus* specimens were examined by protein profiling on SELDI-TOF Proteinchip System II (Ciphergen, USA) using H50 hydrophobic (left) and NP 20 hydrophilic chips (right) (Ciphergen, USA) and a sinapinic acid matrix. Samples and standards (Protein MW Standards Kit, Ciphergen Biosystem Inc.) were spotted onto chips before washing with PBS and loading into the instrument. Single specimens of another Indian species (*H. fulvipes*) (H) and the African species *P. imperator* (P) were also used, as comparisons.

Fig 2.7 TIC (Total Ion Current) Chromatographs of LC-MS on ‘Average’ A, K and LQ Venom Samples



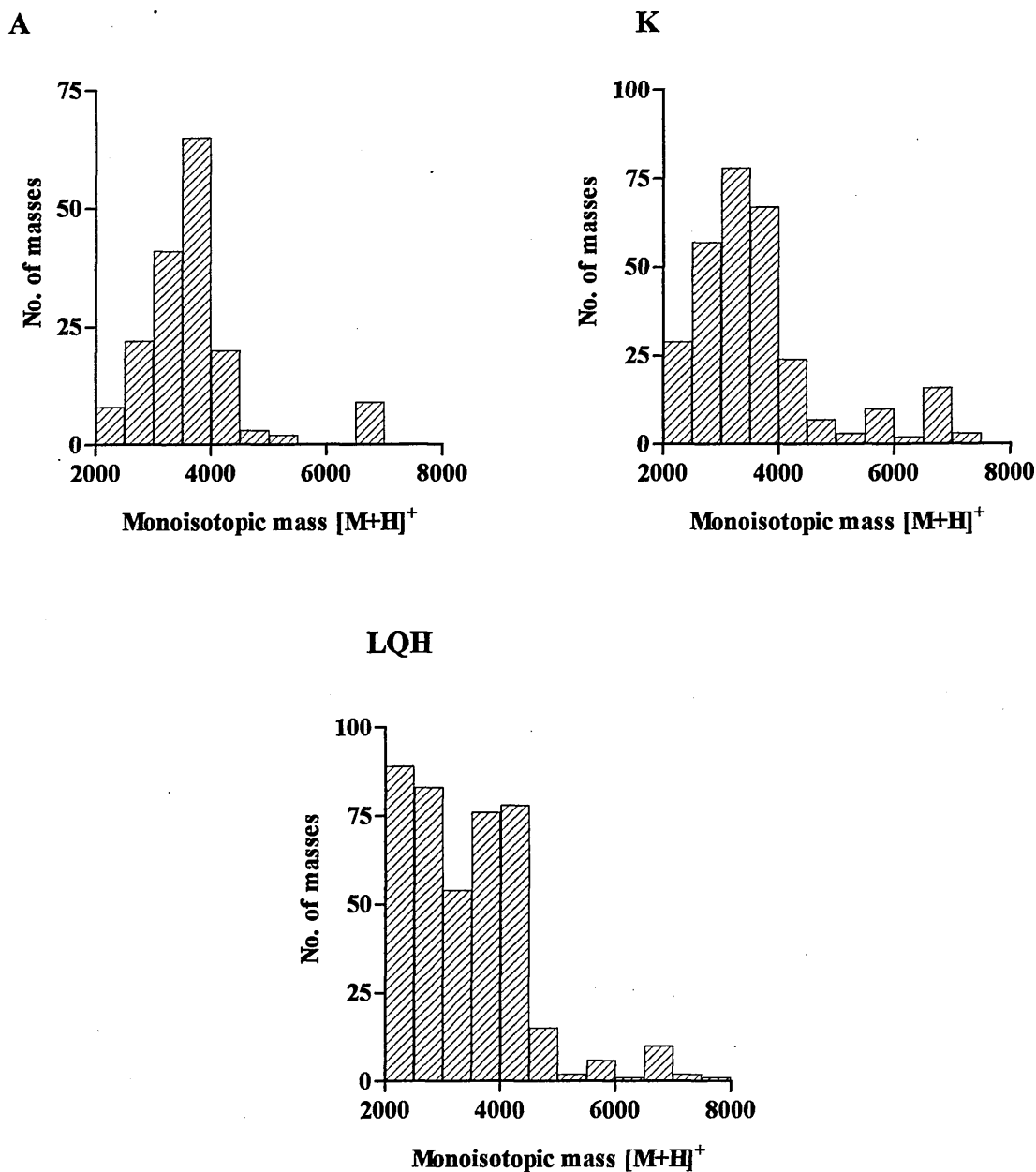
‘Average’ Aurangabad (A) and Konkan (K) regional *Mesob. tamulus* venom samples were created by mixing equal quantities (by protein) of individual venom samples. 6 μ l of a 0.1mgml⁻¹ A, K and LQH (*Leiurus quinquestriatus hebraeus*) venoms (spiked with 0.01mgml⁻¹ standard peptide solution) were fractionated by reverse phase HPLC and analysed by in-line LC-MS. Total ion current produced over time is shown above. Peak containing standard peptide is shown (*).

Fig 2.8 Relative Mass Fingerprints of LQ and ‘Average’ A and K Venoms as Determined by LC-MS



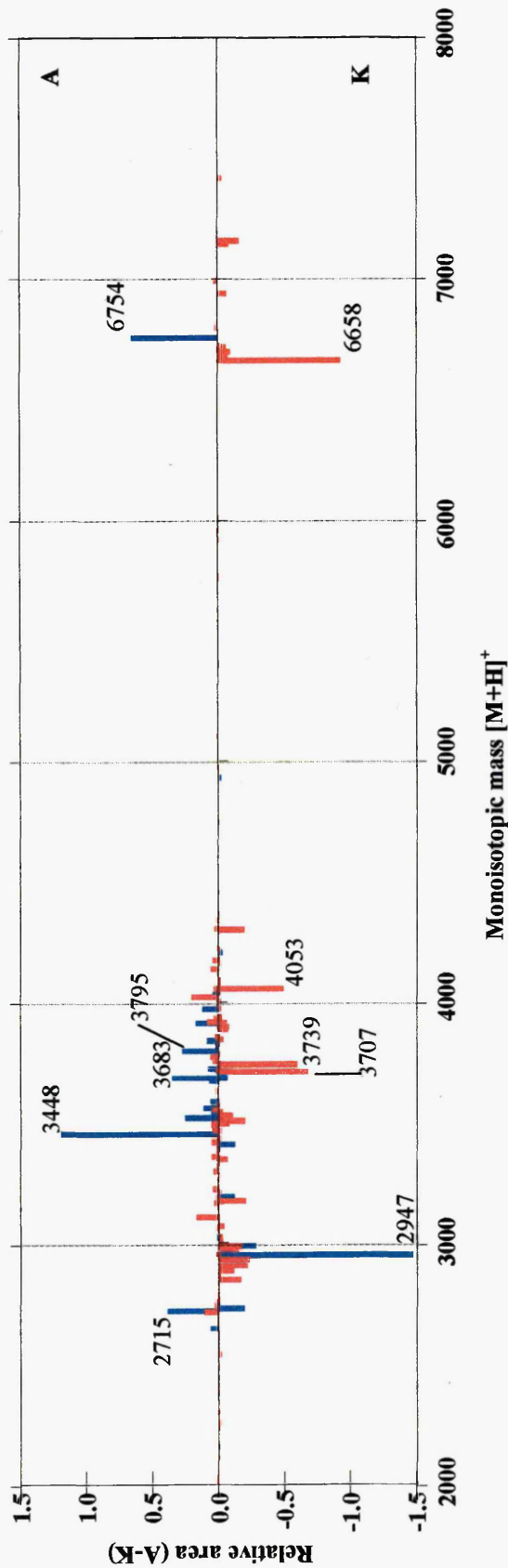
LC-MS data was analysed using LC-MS peak reconstruct software for masses 2-10kDa. Components occurring in a peptide standard-only run were removed from venom data. Peak areas (ion intensity x peak volume) were standardised against that of the major peptide standard component to produce a relative mass fingerprint for the three venom types: - ‘average’ Aurangabad (A) and Konkan (K) regional *Mesob. tamulus* venoms, and *L. quinquestriatus hebraeus* venom (LQH). The 5 most prominent masses (by peak area) are labelled for each venom type.

Fig 2.9 Venom Components Grouped by Mass.



Masses contained within Aurangabad (top left) and Konkan (top right) regional *Mesob. tamulus* venoms, and *L. quinquestriatus hebraeus* venom (LQH), as detected by LC-MS, were grouped into 500Da classes in order to give an overall picture of venom-component mass distribution. Masses are plotted against the number of mass components contained within the class.

Fig 2.10 Differences in Mass Composition of A and K as Determined by LC-MS



Peak areas (peak volume x intensity) for each mass detected by LC-MS analysis of *Mesob. tamulus* regional venoms were standardised against that of spiked peptide standard. Relative peak area in venom from scorpions of Konkan coastal region (**K**) was subtracted from that in Aurangabad regional venom (**A**) in order to visualise difference in expression levels. Masses illustrated in blue are common to both venoms, whilst those in red were only detected in venom from that region. Labelled masses are those showing the largest apparent difference in expression in the two venom types.

Table 2.1 Major Component Masses in *Mesob. tamulus* Regional Venoms and in *L. quinquestriatus hebraeus* Venom

Samples of *L. quinquestriatus hebraeus* venom, and venom from *Mesob. tamulus* collected in Aurangabad and Konkan coastal regions were analysed by LC-MS. Peak area (peak volume x intensity) data was standardised against that for a control peptide spiked into each venom sample to allow comparative analysis. The top twenty mass components (by relative peak area) for each venom type are shown. *Mesob. tamulus* masses are assessed for quantitative differences between the two regions.

Mesob. tamulus Aurangabad regional venom

Rank	Monoisotopic mass [M+H] ⁺	Relative area	Unique to A?	Relative area in K	Rank in K	Notably different quantities in A and K? †
1	3448.1 *	1.25	-	0.055	34	+/-
2	6752.9	0.54	-	0.096	104	+
3	3795.0 *	0.39	-	0.11	17	-
4	2714.6	0.38	-	0.0011	251	+
5	3683.1	0.36	-	0.086	21	-
6	3517.1	0.28	-	0.031	47	+/-
7	4017.3	0.20	+			+
8	4017.3	0.19	+			+
9	3910.3	0.18	-	0.060	32	-
10	3103.7	0.17	+			+
11	3969.3	0.17	-	0.043	41	-
12	6755.9	0.12	-	0.0081	118	+
13	3558.1	0.12	-	0.011	98	+
14	3306.8	0.11	-	0.10	18	-
15	2712.6	0.11	+			+
16	3838.1	0.10	-	0.015	76	+
17	3912.1	0.091	-	0.0036	168	+
18	3720.1	0.080	-	0.0024	202	+
19	3509.1	0.073	-	0.033	44	-
20	3670.1	0.072	-	0.0033	176	+

Mesob. tamulus Konkan regional venom

Rank	Monoisotopic mass [M+H] ⁺	Relative area	Unique to K?	Relative area in A	Rank in A	Notably different quantities in A and K? †
1	2947.5	1.36	-	0.011	81	+
2	6657.7	0.93	+			+
3	4053.1	0.49	+			+
4	2986.7	0.35	-	0.068	23	+/-
5	2903.7	0.22	+			+
6	2725.6	0.21	-	0.0080	93	+
7	3172.9	0.21	+			+
8	3504.9	0.20	+			+
9	4297.5	0.20	+			+
10	3408.8	0.19	-	0.066	25	-
11	2985.4	0.18	+			+
12	2843.6	0.17	+			+
13	7155.1	0.16	+			+
14	2970.4	0.15	+			+
15	3189.6	0.14	-	0.024	55	+
16	2947.5	0.12	+			+
17	3794.9 *	0.11	-	0.39	4	-
18	3306.7	0.10	-	0.11	15	-
19	3527.0	0.10	+			+
20	6694.6	0.090	+			+

* Mass corresponds to that of known component (see table 2.2).

† + Ranked below 50 in other venom, and more than x5 difference in relative area. - Ranked top 50 in both venoms, and less than x5 difference in peak area. +/- Ranked in top 50 in both venoms, but >x5 difference in relative area.

L. quinquestriatus hebraeus venom.

Rank	Monoisotopic mass [M+H] ⁺	Relative area	Rank	Monoisotopic mass [M+H] ⁺	Relative area
1	2960.7	2.36	11	3643.9	0.29
2	6754.0 *	1.71	12	3556.0	0.29
3	3993.1	1.17	13	2922.6	0.26
4	3643.0	0.68	14	4068.4	0.26
5	3180.8	0.67	15	4163.2 *	0.26
6	4293.5	0.63	16	3673.9	0.22
7	3764.3	0.54	17	2964.6	0.21
8	6740.9 *	0.47	18	7461.4	0.16
9	6664.7 *	0.39	19	2977.6	0.15
10	3994.1	0.32	20	2999.6	0.15

*Mass corresponds to that of known components (see table 2.3)

Table 2.2 Occurrence of Known *Mesobuthus tamulus* Peptides in A and K Type Venoms

SCORPION (Srinivasan et al., 2001) and SwissProt (Bairoch and Apweiler, 1996) databases were searched for known *Mesob. tamulus* venom components. Peptide masses of these components were obtained by submitting the sequences (after removal of any signal peptides) to ExPASy PeptideMass software, and adjusting the resulting masses to allow for disulphide bonding. Any experimentally-derived masses were also noted. Samples of venom from *Mesob. tamulus* collected in Aurangabad and Konkan coastal regions were analysed by LC-MS and component masses calculated using LC-MS peak reconstruction software. Resulting data was searched for masses potentially representing known venom components.

For the experimental data described in this chapter, the monoisotopic mass is based upon the lowest detected peak in the isotope series, and the average mass is based on the average mass of the neutral species. For the calculation of theoretical peptide masses, the monoisotopic mass was determined as the sum of the exact masses of the lightest stable isotope for each component atom. For calculation of the average mass, the average of the masses for each component atom was used.

Table 2.2 Occurrence of Known *Mesobuthus tamulus* Peptides in A and K Type Venoms

Toxin name(s)	Average mass [M+H] ⁺	Mono-isotopic mass [M+H] ⁺	Published experimental mass	Corresponding average mass (this work)		Corresponding monoisotopic mass (this work)	
				A	K	A	K
Iberiotoxin ^a IBTX	4248.0	4244.9	-	-	-	-	-
Lepidopteran-selective toxin ^b ButaIT BTCh2	3856.5	3853.7	MW=3856.7 Method=ESI _b	3855.0	-	3853.1	-
Neurotoxin ^c	7032.9	7028.0	-	-	-	-	-
BtITx3 ^d BTCh1	3798.4	3795.5	MW=3796.5 Method= MALDI ^e	3797.8	3797.7	3795.0	3794.9
Potassium channel inhibiting toxin ^f	5233.2	5229.4	-	-	-	-	-
Tamapin ^g	3459.1	3456.7	MW=3457.9 Method=ESI _g	3460.1	-	3457.8	-
Tamapin-2 ^g	3433.1	3430.7	MW=3431.4 Method=ESI _g	-	3432.1 3433.4	-	3430.7 3431.1
Tamulotoxin ^h	4206.9	4204.0	-	4205.2	4205.3	4203.6	4203.5
Tamulustoxin 1 ⁱ TmTX Alpha-KTx 16.1	3946.7	3943.8	MW=3945.7 Method=ESI _i	-	-	-	-
Tamulustoxin 2 ⁱ	3960.6	3957.9	-	-	-	-	-
Toxin BTK-2 ^j	3450.1	3447.5	MW=3452; Method=ESI _j	3450.4 3451.9	3450.5 3454.6	3448.0 3450.0	3447.9 3450.7

a Galvez et al., 1990

b Wudayagiri et al., 2001

c Sharma, M. 2001, direct submission to PDB database.

d Newton, K. A. 2002, direct submission to EMBL database.

e Dhawan et al., 2002

f Jeyaseelan, K. 1998, direct submission to EMBL database.

g Pedarzani et al., 2002

h Escoubas et al., 1991

i Strong et al., 2001

j Dhawan et al., 2003

Table 2.3 Occurrence of Known Peptides in *L. quinquestriatus hebraeus* Venom

SCORPION (Srinivasan et al., 2001) and SwissProt (Bairoch and Apweiler, 1996) databases were searched for known *L. quinquestriatus hebraeus* venom components. Peptide masses of these components were obtained by submitting the sequences (after removal of any signal peptides) to ExPASy PeptideMass software, and adjusting the resulting masses to allow for disulphide bonding. Any experimentally derived masses were also noted. A sample of the venom was analysed by LC-MS, and component masses calculated using LC-MS peak reconstruction software. Resulting data was searched for masses potentially representing known venom components.

For the experimental data described in this chapter, the monoisotopic mass is based upon the lowest detected peak in the isotope series, and the average mass is based on the average mass of the neutral species. For the calculation of theoretic peptide masses, the monoisotopic mass was determined as the sum of the exact masses of the lightest stable isotope for each component atom. For calculation of the average mass, the average of the masses for each component atom was used.

Table 2.3 Occurrence of Known Peptides in *L. quinquestriatus hebraeus* Venom

Toxin name(s)	Average mass [M+H] ⁺	Mono-isotopic mass [M+H] ⁺	Published experimental mass	Corresponding mass (this work)	
				average	Mono-isotopic
Leurotoxin I^a LeTx I LTX1 Scyllatoxin ScyTx SCTX Alpha-KTx 5.1	3424.2	3421.6	-	3423.5	3421.1
Agitoxin 1^b Leurotoxin II AGTX1 LeTx II	4022.9	4012.0	-	-	-
Agitoxin 2^b AGTX2	4090.9	4087.9	-	4090.5	4088.5
Agitoxin 3^b AGTX 3	4101.0	4097.9	-	-	-
LQHII^c	7277.2	7272.3	-	-	-
Alpha-like toxin LQH III^c LqhIII Lqh3	7049.0	7044.2	-	-	-
Neurotoxin Lqh IV^d LqhIV Lqh4	7212.2	7207.3	MW=7211.3 METHOD= MALDI ^d	-	-
Alpha-like neurotoxin Lqh VI^e Lqh6	6794.8	6790.1	-	-	-
Charybdotoxin^f ChTX ChTX-Lq1 ChTx-a Alpha-KTx 1.1	4313.0	4309.9	-	4312.5	4309.5
Charybdotoxin^g ChTx-b	4270.9	4267.9	-	4268.7	4267.5
Charybdotoxin^g ChTx-c	43112.0	4309.0	-	4309.7	4309.5
LQH 18-2^h ChTx-LQ2 Toxin 18-2, Charybdotoxin 2 ChTx-d	4353.0	4350.0	-	4352.7	4349.6
Chlorotoxin^g ClTx-a	4053.8	4050.63	-	4053.2	4050.4
Chlorotoxin^g ClTx-b	3591.1	3587.4	-	-	-
Chlorotoxin^g ClTx-c	3639.3	3636.5	-	-	-
Chlorotoxin^g ClTx-d	3704.2	3701.5	-	3705.2	3702.8
Insect neurotoxin^g LQH IT1-A	7873.0	7867.7	-	-	-
Insect neurotoxin^g LQH IT1-B	7931.0	7925.7	-	-	-
Insect neurotoxin^g LQH IT1-C	7908.1	7902.7	-	-	-

Insect neurotoxin^g LQH IT1-D	7965.0	7959.6	-	-	-
Depressant insect neurotoxin^g LQH IT2-13	6637.3	6632.8	-	-	-
Depressant insect neurotoxinⁱ LQH IT2 LqhIT2-44	6758.6	6753.9	-	6758.0	6754.0
Depressant insect neurotoxin^g LQH IT2-53	6744.6	6739.9	-	6744.1	6741.0
Insect toxin 5^j LqhIT5	6669.4	6664.8	-	6668.1	6664.7
Insect toxin alpha 6A alpha-IT ^g LQH ALPHA 6A	7338.3	7333.3	-	-	-
Insect toxin alpha 6C ALPHA-I ^g LQH alpha 6C	7431.4	7426.3	-	-	-
Leuropeptide I^k LpI	2948.4	2946.2	-	2948.5	2946.6
Leuropeptide II^k LpII	3192.6	3190.3	-	-	-
Leuropeptide III^k LpIII	3207.6	3205.3	-	3207.0	3204.7
Potassium channel blocking toxin 15-1^l Lqh 15-1	4137.8	4134.9	-	4138.1	4136.4
Probable toxin Lqh 8/6^m	4165.9	4162.7	MW=4165	4166.1	4163.2

a Chicci et al., 1988
b Garcia et al., 1994
c Sautiere et al., 1998
d Corzo et al., 2001a
e Hamon et al., 2002
f Gimenez-Gallego et al., 1988
g Froy et al., 1999

h Lucchesi et al., 1989
i Zlotkin et al., 1991
j Moskowicz et al., 1998
k Buisine et al., 1997
l Marshall et al., 1994
m Adjadj et al., 1997

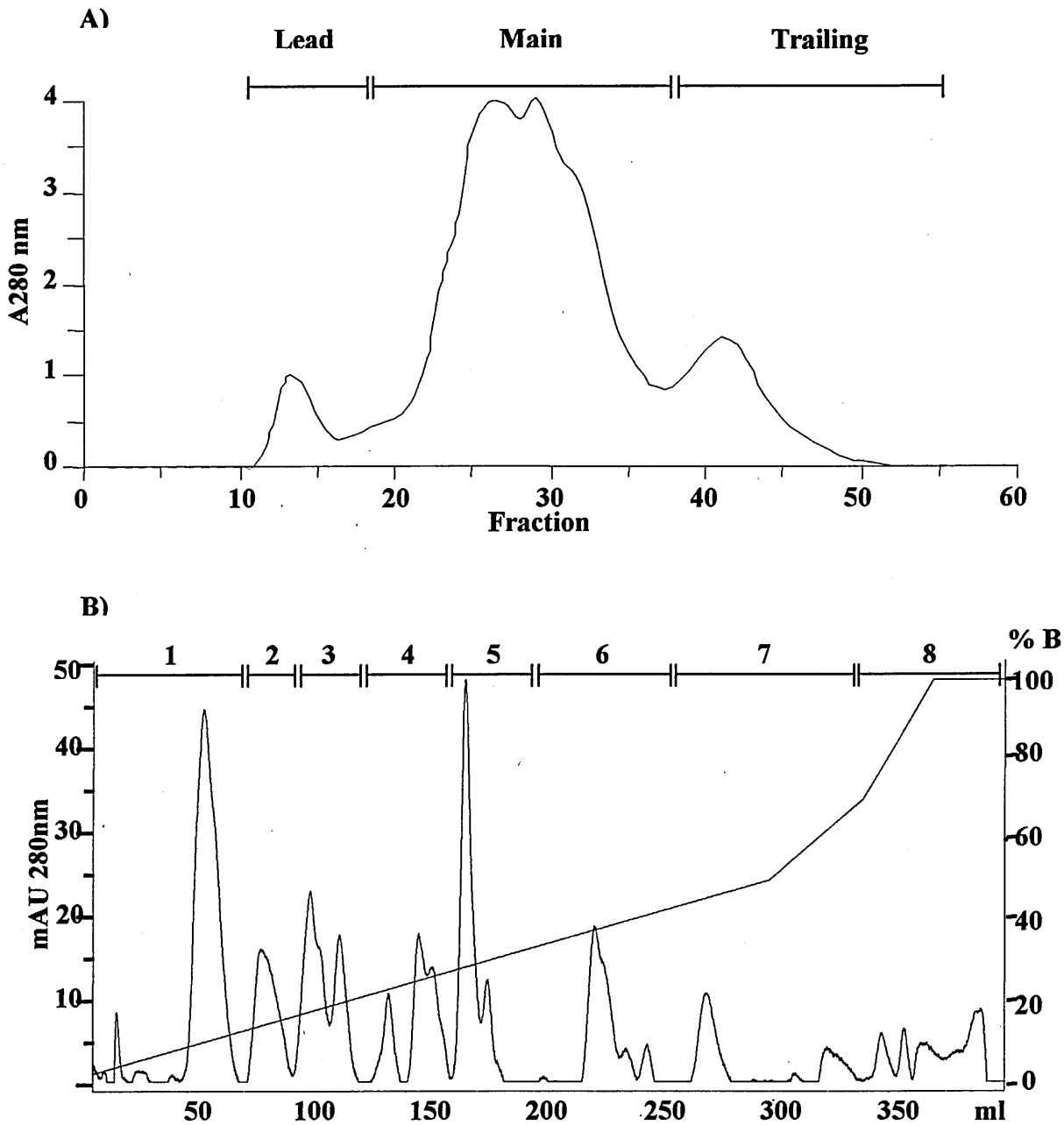
2.3.4 Fractionation of *Mesob. tamulus* Venom for Venom Profiling

Extracted commercial *Mesob. tamulus* venom was fractionated by size exclusion (fig 2.11a), ion exchange (fig 2.11b) and reverse phase (fig 2.12) chromatography. The size exclusion profile was similar to that seen in the same venom by Pedarzani et al., 2002, and was crudely divided into three peaks: lead-fractions 11-18, main-fractions 19-38, and trailing-fractions 39-55. The lead peak, which also showed absorbance at 218nm, is proposed to contain high molecular weight enzymes and cellular components. The trailing peak had no absorbance at 218nm, is therefore non-proteinaceous, and most likely comprised of nucleic acids. Since neither fraction is likely to contain the pharmacological peptides, they were not examined further. The main peak appears to be comprised of at least two separate subpeaks, and is likely to contain the pharmacological peptides. Main peak fractions were pooled and further fractionated.

Ion exchange conditions were selected to favour fractionation of basic peptides and hence the ion channel toxins, to which the majority of venom pharmacology has been attributed. 36% of protein (by A280) was recovered in fractions, and the remainder in the flow through. The ion exchange profile was divided into 8 sections and the fractions within each section pooled. These groups and the flow through were both directly submitted for mass spectrometry, and further fractionated.

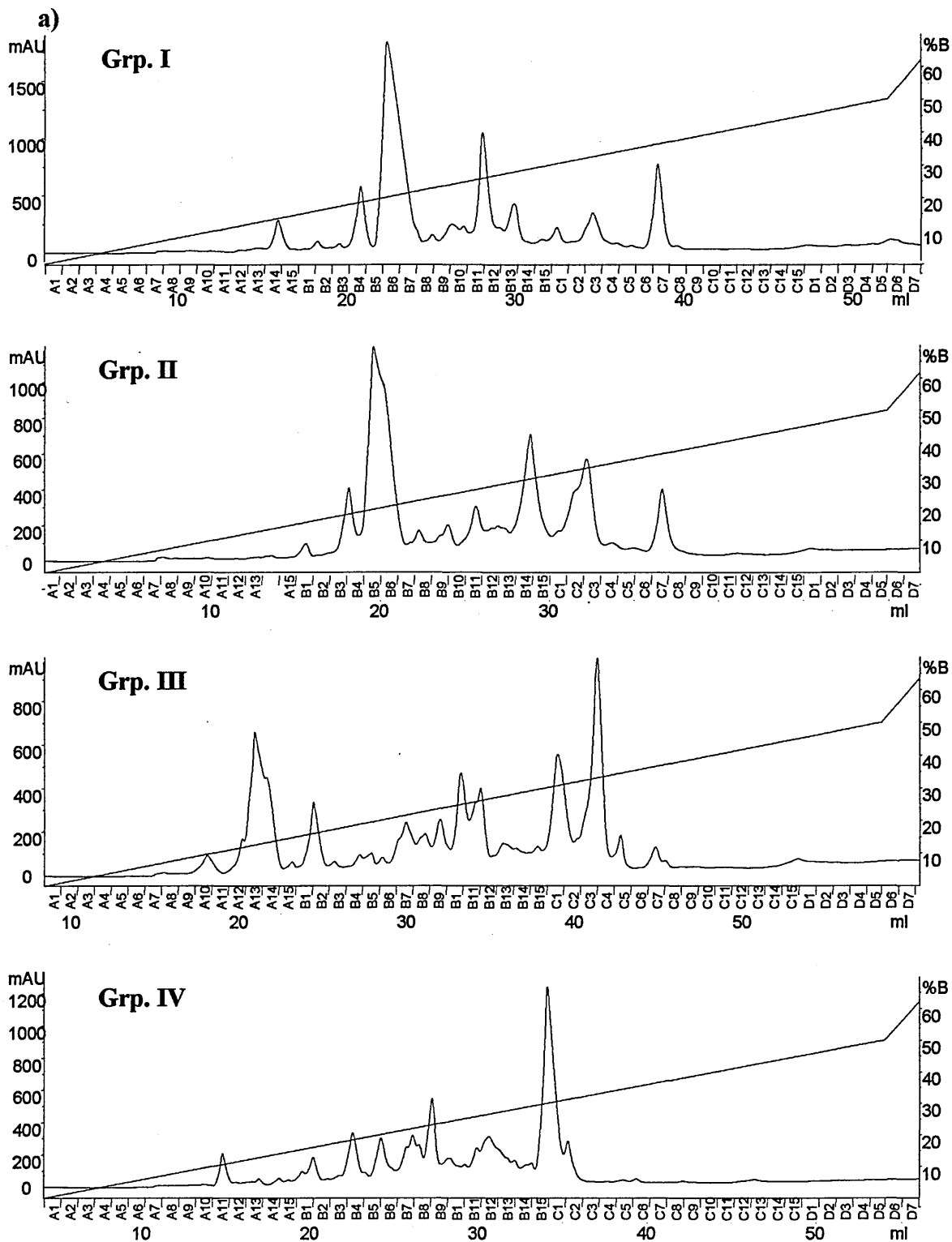
Offline reverse-phase fractionation of ion exchange pools was carried out prior to SELDI-TOF analysis. The profiles clearly demonstrate that each ion exchange pool was comprised of many components, as were the majority of the reverse phase fractions.

Fig 2.11 Fractionation of *Mesob. tamulus* Venom by Size-Exclusion and Cation-Exchange Chromatography



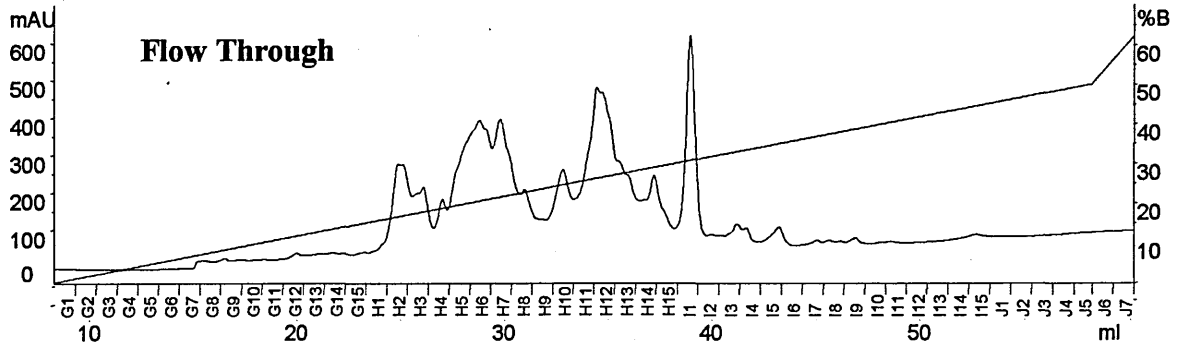
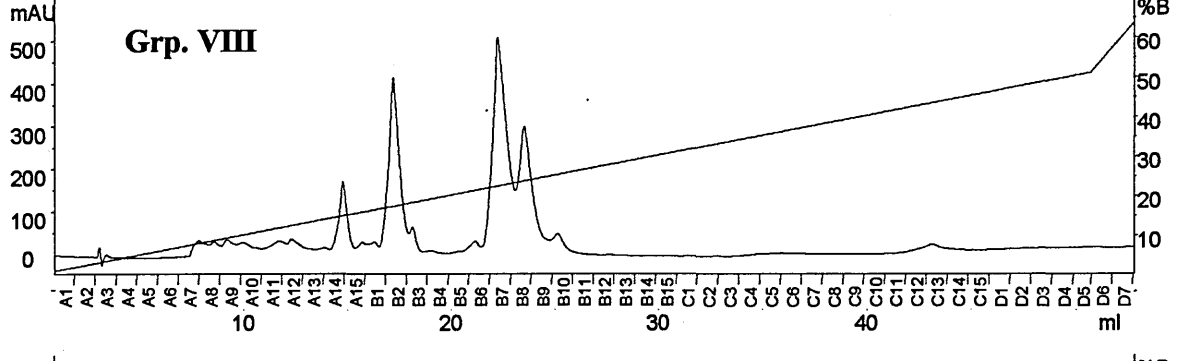
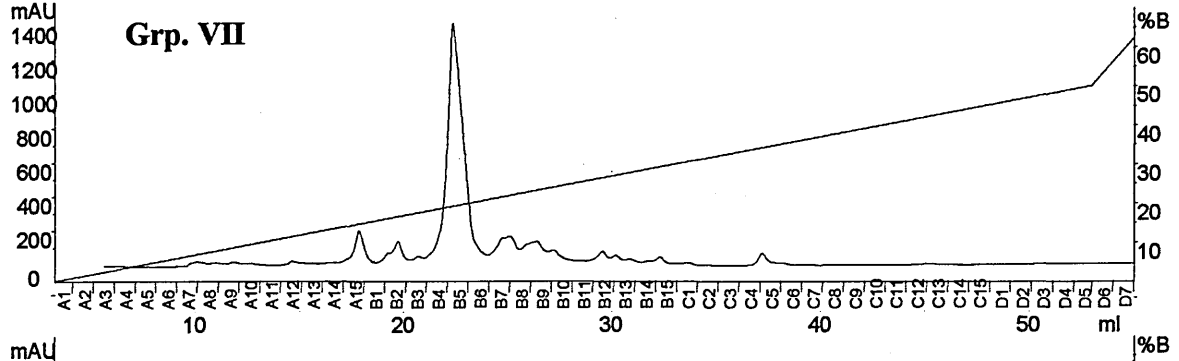
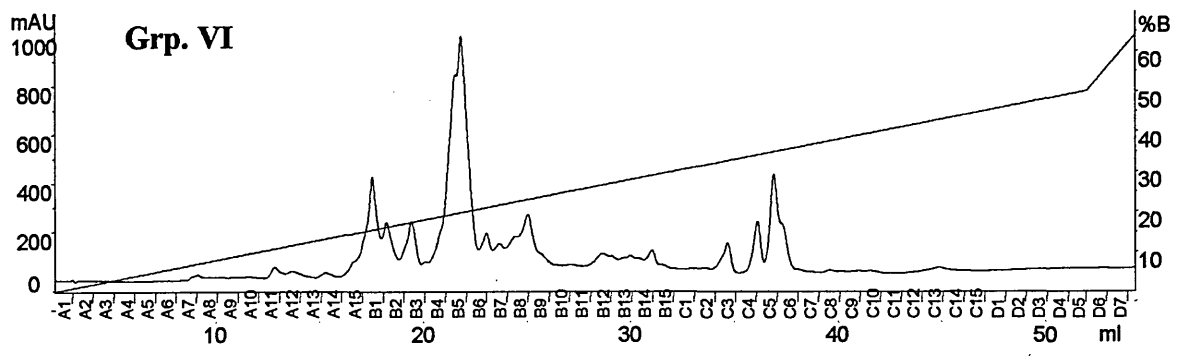
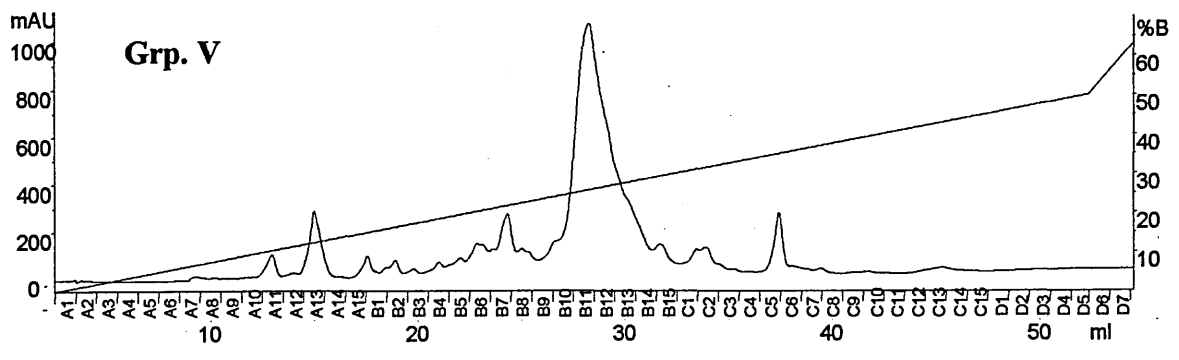
2ml venom extracts were initially run on a 75ml Sephadex G50 size exclusion column in 50mM ammonium formate at a flow rate of $\sim 40\text{ml hr}^{-1}$, and the absorbance of the fractions measured at 280nm (A). Fractions were pooled into 'lead', 'main' and 'trailing' peaks. The 'main' peak was further fractionated on a Hiload 16/10 SP-sepharose cation exchange column, using a gradient of 0.1M NaCl in 100mM NaAc (B). The absorbance was followed at 280nm and the profile divided into eight sections as shown. Fractions within each section were pooled prior to further analysis.

Fig 2.12 Reverse Phase HPLC on *Mesob. tamulus* Venom Ion Exchange Fractions



Separation of a) groups I-IV, and b) groups V-VIII and flow through, from the ion exchange column, by reversed phase HPLC. 0.5mg venom protein was run on a Dynamax C18, 300Å, 250 x 4.6mm, 5µm column equilibrated in 0.1% TFA at 0.5ml min⁻¹. Samples were eluted with a 0-50% gradient of solvent B (90% acetonitrile/ 0.1% TFA), and the eluent monitored at 218nm. Eluted sample was collected in 1ml fractions.

Fig 2.12b)



2.3.5 Mass profiling of venom fractions by MALDI-TOF and LC-MS

Venom fractions from the size exclusion, reverse phase and ion exchange columns were individually analysed by MALDI-TOF/MS. Size exclusion and ion exchange fractions were also separated and analysed online by LC-MS. As with venom fingerprinting, analysis was restricted to the 2000 to 10000Da mass range, both in order to focus on peptide toxins and to remove matrix interference. Sample MALDI-TOF, and LC-MS TIC and mass profiles are shown (fig 2.13). With the less fractionated samples (e.g. 'main' size exclusion fraction) MALDI analysis gave poor peak resolution making mass analysis impossible. Reverse phase samples however, gave good resolution, and reproducible masses were obtained for the majority of peaks. The mass measurement achieved in the LC-MS experiment was more accurate but detected fewer masses in the >5000Da mass range. MALDI-TOF detected more masses in this higher mass range, but resolution was poor and few masses were able to be determined accurately.

In MALDI and LC-MS data a large number of putative adducts were observed all of which were removed from the final dataset. Isomasses eluting in successive fractions were averaged and pooled. After analysis, 665 masses were determined in total (352 by MALDI-TOF and 524 by LC-MS), with a large number detected by both methods. These masses ranged from 2005.5, close to the lower detection threshold, to 8515.4. The greater separation seen in this study led to far more masses being detected than with the venom fingerprinting. A summary of masses of *Mesob. tamulus* venom components is given (table 2.4); full details of data from which this table was derived are given in appendix D. Masses similar to those of all known venom components were detected (table 2.5), although it should be noted that this does not confirm their identity.

Fig 2.13 Sample Mass Spectrometry Profiles of *Mesob. tamulus* Venom Fractions

(A) MALDI-TOF mass spectrum of a typical venom fraction (ion exchange group 1). Venom fractions were analysed on a SAI LaserTOF LT1500 mass spectrometer with a 337nm nitrogen laser. The instrument was operated in the positive-ionisation mode with 20KV accelerating voltage and an α CHCA matrix was used.

(B) Total ion current of the same fraction, analysed by LC-MS. 0.1mgml^{-1} protein was separated by reverse phase (5-42% gradient of acetonitrile in 0.1% formic acid over 80 min) and eluate introduced directly into the electrospray ion source of an API QSTAR pulsar I LCMS/MS system. (+5000V, ion source gas 40V, curtain gas 25V, mass range 500-4000m/z).

(C) Reconstructed mass profile of sample shown in (B). Data was processed using LC-MS peak reconstruct software (API) within the 2000-10000 mass range to calculate component masses.

Fig 2.13 Sample Mass Spectrometry Profiles of *Mesob. tamulus* Venom Fractions

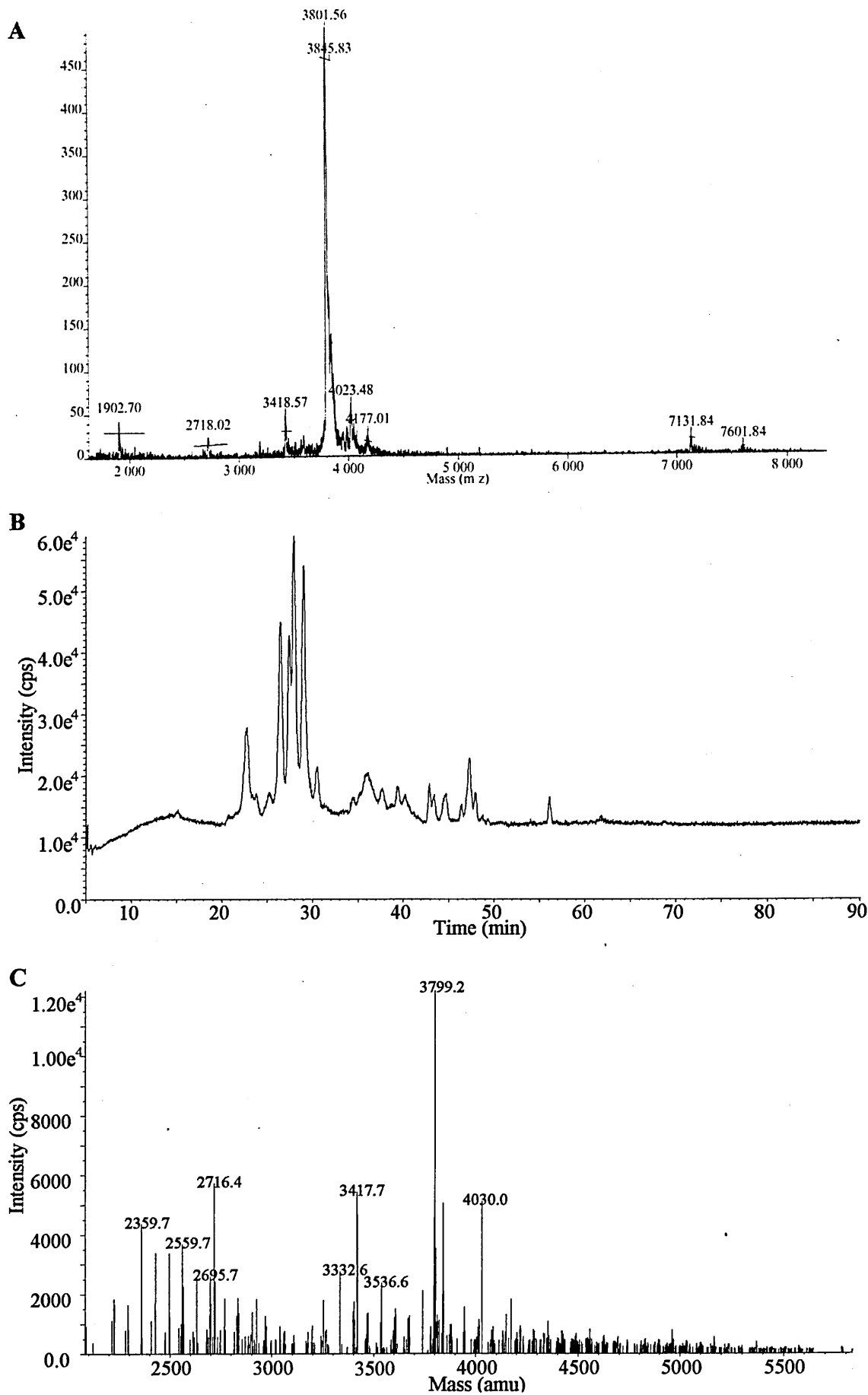


Table 2.4 Mass Spectrometric Analysis of *Mesob. tamulus* Venom

Mass data was obtained by MALDI-TOF and LC-ESI mass spectrometry for the 'main' size exclusion peak fractionated by ion exchange and reverse phase chromatography as described. LC-MS masses were calculated from component ions using commercial LC-MS mass reconstruction software. Within an ion exchange group (or the data corresponding to direct analysis of the 'main' size exclusion peak) MALDI-TOF data was assumed to represent a single mass if data was within 0.1% variation and was detected in continuous consecutive fractions, and as such were averaged. Mean MALDI-derived masses with $>0.1\%$ SD and those derived from <3 separate masses from <2 sample spots were discarded. Resulting LC-MS and MALDI-TOF data is shown in appendix D. Within a single group, all possible adduct masses for addition of matrix, Na, K and Na+K, loss of CO_2 , NH_3 and H_2O , mono- and di-oxidation, along with those corresponding to +74 and +104, were calculated, and any corresponding masses ($\pm 0.1\%$ for MALDI-TOF, $\pm 0.01\%$ for LC-MS) removed from the dataset. MALDI and LC-MS data was combined within a group (0.1% mass tolerance) and any masses only eluting in LC-MS flow-through removed. Data from all groups was combined (mass tolerance $\pm 0.1\%$ for MALDI-TOF, $\pm 0.01\%$ for LC-MS); assuming identical masses found in consecutive ion exchange fractions represented a single molecular species. Masses close to those of recorded venom components were noted. The resulting summary of the mass spectrometry data is shown. Masses detected by LC-MS analysis are in **bold**, whilst those detected by MALDI-TOF are underlined. Shaded masses represent those observed by direct MALDI or LC-MS analysis of the 'main' size exclusion peak. Masses similar to those expected for known venom components (refer to table 2.5) are noted (*).

Table 2.4 Mass Spectrometric Analysis of *Mesob. tamulus* Venom

<u>2005.5</u>	<u>2628.8</u>	<u>2940.4</u>	<u>3141.6</u>	<u>3345.3</u>	<u>3466.8</u>	<u>3573.0</u>	<u>3696.8</u>	<u>3823.6</u>
<u>2007.6</u>	<u>2646.7</u>	<u>2941.1</u>	<u>3150.5</u>	<u>3349.2</u>	<u>3467.4</u>	<u>3578.0</u>	<u>3698.3</u>	<u>3824.6</u>
<u>2014.8</u>	<u>2657.0</u>	<u>2941.5</u>	<u>3155.1</u>	<u>3351.5</u>	<u>3468.7</u>	<u>3579.1</u>	<u>3701.5</u>	<u>3825.3</u>
<u>2016.6</u>	<u>2669.0</u>	<u>2941.8</u>	<u>3163.9</u>	<u>3354.1</u>	<u>3469.3</u>	<u>3581.7</u>	<u>3703.0</u>	<u>3827.8</u>
<u>2018.5</u>	<u>2683.8</u>	<u>2951.3</u>	<u>3164.7</u>	<u>3365.3</u>	<u>3480.4</u>	<u>3591.1</u>	<u>3704.3</u>	<u>3829.3</u>
<u>2027.3</u>	<u>2687.3</u>	<u>2963.6</u>	<u>3166.2</u>	<u>3365.3</u>	<u>3482.6</u>	<u>3592.2</u>	<u>3706.5</u>	<u>3829.9</u>
<u>2043.5</u>	<u>2687.6</u>	<u>2969.2</u>	<u>3169.6</u>	<u>3366.2</u>	<u>3482.8</u>	<u>3596.9</u>	<u>3708.9</u>	<u>3834.0</u>
<u>2046.3</u>	<u>2690.1</u>	<u>2969.2</u>	<u>3176.6</u>	<u>3367.3</u>	<u>3483.0</u>	<u>3597.6</u>	<u>3709.7</u>	<u>3834.9</u>
<u>2051.6</u>	<u>2690.9</u>	<u>2969.7</u>	<u>3176.7</u>	<u>3369.8</u>	<u>3484.6</u>	<u>3601.9</u>	<u>3710.0</u>	<u>3835.6</u>
<u>2055.6</u>	<u>2701.4</u>	<u>2986.5</u>	<u>3176.8</u>	<u>3375.9</u>	<u>3488.9</u>	<u>3604.7</u>	<u>3710.3</u>	<u>3836.9</u>
<u>2065.8</u>	<u>2708.3</u>	<u>2988.5</u>	<u>3182.6</u>	<u>3376.9</u>	<u>3497.0</u>	<u>3607.3</u>	<u>3711.4</u>	<u>3840.2</u>
<u>2075.4</u>	<u>2710.5</u>	<u>2988.6</u>	<u>3183.9</u>	<u>3380.7</u>	<u>3501.9</u>	<u>3608.4</u>	<u>3712.0</u>	<u>3840.7</u>
<u>2079.4</u>	<u>2710.6</u>	<u>2990.4</u>	<u>3184.7</u>	<u>3381.0</u>	<u>3502.3</u>	<u>3608.8</u>	<u>3714.6</u>	<u>3848.2</u>
<u>2084.8</u>	<u>2711.8</u>	<u>2990.6</u>	<u>3193.9</u>	<u>3382.2</u>	<u>3502.6</u>	<u>3609.1</u>	<u>3716.2</u>	<u>3854.3</u>
<u>2085.4</u>	<u>2711.9</u>	<u>3006.5</u>	<u>3202.3</u>	<u>3383.6</u>	<u>3503.2</u>	<u>3609.2</u>	<u>3720.3</u>	<u>3856.8*</u>
<u>2089.4</u>	<u>2712.1</u>	<u>3012.2</u>	<u>3205.5</u>	<u>3394.0</u>	<u>3510.3</u>	<u>3615.3</u>	<u>3722.4</u>	<u>3860.2</u>
<u>2105.0</u>	<u>2715.1</u>	<u>3012.7</u>	<u>3207.9</u>	<u>3394.4</u>	<u>3510.6</u>	<u>3617.4</u>	<u>3723.5</u>	<u>3863.1</u>
<u>2109.2</u>	<u>2716.1</u>	<u>3021.1</u>	<u>3208.2</u>	<u>3396.9</u>	<u>3512.0</u>	<u>3620.6</u>	<u>3724.0</u>	<u>3866.2</u>
<u>2112.7</u>	<u>2716.6</u>	<u>3021.6</u>	<u>3216.3</u>	<u>3397.9</u>	<u>3514.2</u>	<u>3621.8</u>	<u>3724.3</u>	<u>3869.5</u>
<u>2143.5</u>	<u>2716.7</u>	<u>3021.9</u>	<u>3222.2</u>	<u>3400.5</u>	<u>3515.6</u>	<u>3631.8</u>	<u>3724.4</u>	<u>3872.6</u>
<u>2144.2</u>	<u>2717.1</u>	<u>3033.4</u>	<u>3225.2</u>	<u>3401.7</u>	<u>3517.3</u>	<u>3635.3</u>	<u>3725.5</u>	<u>3874.5</u>
<u>2169.5</u>	<u>2718.0</u>	<u>3038.4</u>	<u>3226.1</u>	<u>3402.1</u>	<u>3519.0</u>	<u>3635.3</u>	<u>3737.3</u>	<u>3878.3</u>
<u>2181.3</u>	<u>2719.3</u>	<u>3038.9</u>	<u>3226.2</u>	<u>3402.6</u>	<u>3519.5</u>	<u>3637.4</u>	<u>3740.3</u>	<u>3878.8</u>
<u>2183.4</u>	<u>2734.5</u>	<u>3043.9</u>	<u>3228.3</u>	<u>3404.4</u>	<u>3520.0</u>	<u>3638.4</u>	<u>3740.6</u>	<u>3881.0</u>
<u>2191.7</u>	<u>2738.9</u>	<u>3045.7</u>	<u>3229.6</u>	<u>3406.0</u>	<u>3521.2</u>	<u>3639.5</u>	<u>3740.7</u>	<u>3892.3</u>
<u>2201.7</u>	<u>2754.4</u>	<u>3060.5</u>	<u>3237.0</u>	<u>3411.3</u>	<u>3522.2</u>	<u>3647.5</u>	<u>3742.7</u>	<u>3892.3</u>
<u>2216.2</u>	<u>2756.8</u>	<u>3071.6</u>	<u>3237.5</u>	<u>3412.5</u>	<u>3522.4</u>	<u>3650.5</u>	<u>3745.5</u>	<u>3895.9</u>
<u>2265.8</u>	<u>2764.9</u>	<u>3078.0</u>	<u>3251.3</u>	<u>3417.9</u>	<u>3528.2</u>	<u>3652.5</u>	<u>3755.1</u>	<u>3898.9</u>
<u>2279.6</u>	<u>2767.3</u>	<u>3078.8</u>	<u>3254.3</u>	<u>3418.7</u>	<u>3528.7</u>	<u>3658.2</u>	<u>3755.3</u>	<u>3902.1</u>
<u>2286.2</u>	<u>2773.4</u>	<u>3081.6</u>	<u>3286.1</u>	<u>3420.4</u>	<u>3538.7</u>	<u>3665.7</u>	<u>3756.1</u>	<u>3908.3</u>
<u>2326.1</u>	<u>2783.7</u>	<u>3087.8</u>	<u>3287.3</u>	<u>3430.5</u>	<u>3539.8</u>	<u>3673.0</u>	<u>3756.5</u>	<u>3909.2</u>
<u>2332.3</u>	<u>2789.8</u>	<u>3092.9</u>	<u>3288.5</u>	<u>3430.6</u>	<u>3541.8</u>	<u>3675.6</u>	<u>3759.6</u>	<u>3909.2</u>
<u>2335.4</u>	<u>2794.8</u>	<u>3092.9</u>	<u>3297.0</u>	<u>3431.8</u>	<u>3544.9</u>	<u>3677.8</u>	<u>3762.1</u>	<u>3909.6</u>
<u>2336.7</u>	<u>2795.1</u>	<u>3094.3</u>	<u>3297.6</u>	<u>3432.3</u>	<u>3547.3</u>	<u>3679.4</u>	<u>3770.2</u>	<u>3912.8</u>
<u>2340.3</u>	<u>2812.5</u>	<u>3096.6</u>	<u>3298.1</u>	<u>3433.2*</u>	<u>3552.9</u>	<u>3680.3</u>	<u>3770.5</u>	<u>3913.0</u>
<u>2366.2</u>	<u>2814.8</u>	<u>3097.8</u>	<u>3306.3</u>	<u>3434.2</u>	<u>3553.0</u>	<u>3684.4</u>	<u>3774.4</u>	<u>3913.7</u>
<u>2374.8</u>	<u>2825.4</u>	<u>3098.6</u>	<u>3310.7</u>	<u>3437.8</u>	<u>3555.0</u>	<u>3685.3</u>	<u>3776.2</u>	<u>3913.7</u>
<u>2411.2</u>	<u>2828.8</u>	<u>3102.0</u>	<u>3312.9</u>	<u>3440.3</u>	<u>3556.4</u>	<u>3685.8</u>	<u>3777.1</u>	<u>3914.7</u>
<u>2415.6</u>	<u>2836.6</u>	<u>3105.1</u>	<u>3313.5</u>	<u>3450.2*</u>	<u>3557.3</u>	<u>3685.9</u>	<u>3780.7</u>	<u>3915.2</u>
<u>2442.3</u>	<u>2889.5</u>	<u>3105.8</u>	<u>3314.0</u>	<u>3456.9</u>	<u>3560.8</u>	<u>3686.1</u>	<u>3781.0</u>	<u>3932.3</u>
<u>2462.0</u>	<u>2889.6</u>	<u>3105.9</u>	<u>3316.8</u>	<u>3458.3*</u>	<u>3561.8</u>	<u>3686.6</u>	<u>3782.7</u>	<u>3937.6</u>
<u>2468.5</u>	<u>2890.9</u>	<u>3106.5</u>	<u>3319.2</u>	<u>3459.9</u>	<u>3562.9</u>	<u>3686.9</u>	<u>3794.8</u>	<u>3944.8</u>
<u>2551.6</u>	<u>2904.6</u>	<u>3112.5</u>	<u>3321.2</u>	<u>3460.0</u>	<u>3563.9</u>	<u>3688.2</u>	<u>3798.4*</u>	<u>3945.5*</u>
<u>2554.1</u>	<u>2909.5</u>	<u>3114.7</u>	<u>3325.7</u>	<u>3460.5*</u>	<u>3564.7</u>	<u>3691.3</u>	<u>3799.2*</u>	<u>3946.9*</u>
<u>2557.1</u>	<u>2922.8</u>	<u>3115.7</u>	<u>3328.8</u>	<u>3464.2</u>	<u>3565.5</u>	<u>3692.7</u>	<u>3819.7</u>	<u>3954.2</u>
<u>2584.0</u>	<u>2925.2</u>	<u>3127.6</u>	<u>3336.4</u>	<u>3465.9</u>	<u>3567.8</u>	<u>3693.1</u>	<u>3821.9</u>	<u>3955.5</u>
<u>2618.2</u>	<u>2927.0</u>	<u>3138.3</u>	<u>3339.4</u>	<u>3466.4</u>	<u>3572.3</u>	<u>3695.2</u>	<u>3822.9</u>	<u>3958.0</u>

<u>3960.0*</u>	<u>3989.1</u>	<u>4031.0</u>	<u>4148.9</u>	<u>4268.1</u>	<u>4544.8</u>	<u>4939.0</u>	<u>7004.9</u>	<u>7500.3</u>
<u>3963.4</u>	<u>3990.8</u>	<u>4031.6</u>	<u>4150.2</u>	<u>4276.3</u>	<u>4548.8</u>	<u>4951.1</u>	<u>7006.0</u>	<u>7588.6</u>
<u>3965.8</u>	<u>3992.5</u>	<u>4040.9</u>	<u>4153.9</u>	<u>4286.0</u>	<u>4565.3</u>	<u>5133.6</u>	<u>7007.8</u>	<u>7653.7</u>
<u>3970.8</u>	<u>3992.6</u>	<u>4041.1</u>	<u>4158.9</u>	<u>4287.3</u>	<u>4569.4</u>	<u>5233.4*</u>	<u>7017.9</u>	<u>7743.7</u>
<u>3972.2</u>	<u>3993.9</u>	<u>4041.3</u>	<u>4172.2</u>	<u>4287.4</u>	<u>4584.7</u>	<u>5277.7</u>	<u>7026.8</u>	<u>7814.6</u>
<u>3972.4</u>	<u>3996.2</u>	<u>4042.0</u>	<u>4178.8</u>	<u>4292.0</u>	<u>4597.8</u>	<u>5319.6</u>	<u>7032.8*</u>	<u>7815.2</u>
<u>3972.9</u>	<u>3996.9</u>	<u>4052.0</u>	<u>4189.8</u>	<u>4298.9</u>	<u>4605.4</u>	<u>5469.1</u>	<u>7036.8</u>	<u>7823.5</u>
<u>3973.2</u>	<u>3998.7</u>	<u>4053.7</u>	<u>4196.6</u>	<u>4300.8</u>	<u>4611.6</u>	<u>5522.2</u>	<u>7048.9</u>	<u>7840.8</u>
<u>3973.5</u>	<u>4000.9</u>	<u>4058.6</u>	<u>4200.0</u>	<u>4302.4</u>	<u>4637.6</u>	<u>5553.7</u>	<u>7055.7</u>	<u>7850.7</u>
<u>3973.6</u>	<u>4001.4</u>	<u>4061.1</u>	<u>4201.0</u>	<u>4319.2</u>	<u>4665.3</u>	<u>5564.2</u>	<u>7065.3</u>	<u>7918.1</u>
<u>3974.0</u>	<u>4002.4</u>	<u>4070.3</u>	<u>4201.5</u>	<u>4323.1</u>	<u>4667.4</u>	<u>5778.0</u>	<u>7125.4</u>	<u>8045.6</u>
<u>3975.8</u>	<u>4003.2</u>	<u>4078.5</u>	<u>4205.9</u>	<u>4329.3</u>	<u>4673.0</u>	<u>6181.5</u>	<u>7125.7</u>	<u>8103.0</u>
<u>3978.3</u>	<u>4005.1</u>	<u>4078.8</u>	<u>4206.5</u>	<u>4337.5</u>	<u>4682.1</u>	<u>6304.5</u>	<u>7139.2</u>	<u>8144.0</u>
<u>3978.7</u>	<u>4006.8</u>	<u>4081.0</u>	<u>4207.0</u>	<u>4338.0</u>	<u>4684.7</u>	<u>6408.7</u>	<u>7143.3</u>	<u>8210.1</u>
<u>3979.1</u>	<u>4009.6</u>	<u>4082.5</u>	<u>4207.5</u>	<u>4339.2</u>	<u>4727.6</u>	<u>6624.0</u>	<u>7159.6</u>	<u>8213.2</u>
<u>3979.9</u>	<u>4010.4</u>	<u>4083.7</u>	<u>4209.5*</u>	<u>4345.3</u>	<u>4752.9</u>	<u>6652.8</u>	<u>7170.5</u>	<u>8226.0</u>
<u>3981.6</u>	<u>4011.2</u>	<u>4092.3</u>	<u>4210.0</u>	<u>4355.6</u>	<u>4753.1</u>	<u>6658.4</u>	<u>7224.6</u>	<u>8290.3</u>
<u>3981.7</u>	<u>4012.5</u>	<u>4097.9</u>	<u>4214.5</u>	<u>4366.1</u>	<u>4780.0</u>	<u>6678.6</u>	<u>7234.0</u>	<u>8317.2</u>
<u>3982.1</u>	<u>4013.7</u>	<u>4098.2</u>	<u>4218.8</u>	<u>4401.5</u>	<u>4796.6</u>	<u>6712.0</u>	<u>7255.3</u>	<u>8327.1</u>
<u>3982.7</u>	<u>4016.7</u>	<u>4100.7</u>	<u>4224.1</u>	<u>4463.4</u>	<u>4808.8</u>	<u>6760.6</u>	<u>7269.1</u>	<u>8357.7</u>
<u>3983.0</u>	<u>4016.9</u>	<u>4103.2</u>	<u>4225.6</u>	<u>4464.4</u>	<u>4825.2</u>	<u>6829.7</u>	<u>7331.0</u>	<u>8515.4</u>
<u>3984.3</u>	<u>4020.2</u>	<u>4106.6</u>	<u>4228.8</u>	<u>4466.1</u>	<u>4876.1</u>	<u>6850.4</u>	<u>7356.3</u>	
<u>3985.1</u>	<u>4021.0</u>	<u>4113.0</u>	<u>4232.3</u>	<u>4468.5</u>	<u>4880.4</u>	<u>6910.0</u>	<u>7365.5</u>	
<u>3985.6</u>	<u>4022.3</u>	<u>4123.7</u>	<u>4236.1</u>	<u>4491.5</u>	<u>4881.1</u>	<u>6919.6</u>	<u>7393.2</u>	
<u>3988.1</u>	<u>4022.5</u>	<u>4132.6</u>	<u>4246.7</u>	<u>4493.7</u>	<u>4882.2</u>	<u>6929.2</u>	<u>7403.4</u>	
<u>3988.1</u>	<u>4024.3</u>	<u>4133.8</u>	<u>4247.7*</u>	<u>4543.7</u>	<u>4900.4</u>	<u>6988.4</u>	<u>7449.8</u>	
<u>3989.0</u>	<u>4026.2</u>	<u>4142.6</u>	<u>4262.7</u>	<u>4544.1</u>	<u>4919.5</u>	<u>6988.4</u>	<u>7467.9</u>	

Table 2.5 Occurrence of Known *Mesobuthus tamulus* Peptides in Venom Fractions

Toxin name(s)	Average mass [M+H] ⁺	Mono-isotopic mass [M+H] ⁺	Published experimental mass	Closest mass match (this work)		Ion exchange fraction
				Average	Mono-isotopic	
Iberiotoxin ^a IBTX	4248.0	4244.9	-	4247.6	4245.3	Group 3
Lepidopteran-selective toxin ^b ButaIT BTCh12	3856.5	3853.7	MW=3856.7 Method=ESI ^b	3856.8	3854.1	Group 7
Neurotoxin ^c	7032.9	7028.0	-	7032.8	7031.2	Group 7
BtITx3 ^d BTCh11	3798.4	3795.5	MW=3796.5 Method= MALDI ^e	3798.4 3799.2	3798.7 3797.7	Group 1 Group 1
Potassium channel inhibiting toxin ^f	5233.2	5229.4	-	5233.4	5230.4	Group 1
Tamapin ^g	3459.1	3456.7	MW=3457.9 Method=ESI ^g	3460.5 3458.3	3457.8 3457.7	Group 6 Group 7
Tamapin-2 ^g	3433.1	3430.7	MW=3431.4 Method=ESI ^g	3433.2 3433.2	3431.9 3431.9	Group 6 Group 7
Tamulotoxin ^h	4206.9	4204.0	-	4205.9	4204.5	Group 1
Tamulustoxin 1 ⁱ TmTX Alpha-KTx 16.1	3946.7	3943.8	MW=3945.7 Method=ESI ⁱ	3945.4 3946.9	3942.7 3944.2	Group 5 Group 7
Tamulustoxin 2 ⁱ	3960.6	3957.9	-	3960.0 3960.0	3958.2 3958.2	Group 7 Group 8
Toxin BTK-2 ^j	3450.1	3447.5	MW=3452; Method=ESI ^j	3450.2	3447.8	Group 4

a Galvez et al., 1990

b Wudayagiri et al., 2001

c Sharma, M. 2001, direct submission to PDB database.

d Newton, K. A. 2002, direct submission to EMBL database.

e Dhawan et al., 2002

f Jeyaseelan, K. 1998, direct submission to EMBL database.

g Pedarzani et al., 2002

h Escoubas et al., 1991

i Strong et al., 2001

j Dhawan et al., 2003

SCORPION (Srinivasan et al., 2001) and SwissProt (Bairoch and Apweiler, 1996) databases were searched for known *Mesob. tamulus* venom components. Peptide masses of these components were obtained by submitting the sequences (after removal of any signal peptides) to ExPASy PeptideMass software, and adjusting the resulting masses to allow for disulphide bonding. Any experimentally derived masses were also noted. Data obtained in the mass profiling study (this work, see appendix D) was searched for masses potentially representing known venom components.

For the experimental data described in this chapter, the monoisotopic mass is based upon the lowest detected peak in the isotope series, and the average mass is based on the average mass of the neutral species. For the calculation of theoretic peptide masses, the monoisotopic mass was determined as the sum of the exact masses of the lightest stable isotope for each component atom. For calculation of the average mass, the average of the masses for each component atom was used.

2.4 Discussion

The work presented represents the first detailed dissection of *Mesob. tamulus* venom composition. The chapter is concerned with both regional venom variation and the fractionation of venom components, with the identification of a large number of component masses.

Variation in venom composition relating to geographical region has been previously reported in other animals e.g. spiders (Binford, 2001), snakes (Prasad et al., 1999; Fry et al., 2002) and cone snails (Jones et al., 1996) but, to our knowledge, this is the first study in scorpions. Symptomatic and antigenic differences have been observed in *Mesob. tamulus* venom (Kankonkar et al., 1998; and Kulkarni, D.G.-unpublished observations). The symptomatic variation could be explained by differences in behaviour. The two populations may inject different quantities of venom, or one population may be more aggressive, more readily injecting venom as opposed to pre-venom. On the other hand, the venom itself may be more concentrated or there may be qualitative or quantitative differences in composition. For other scorpions, the protein content of venom does not appear to correlate with toxicity (Kalapothakis and Chavez-Olortegui, 1997; El Hafney et al., 2002,), the latter being more closely related to levels of individual toxins. This study therefore set out to examine antigenic and peptide variability between *Mesob. tamulus* venoms found in two geographical regions with distinct biotopes.

Intra- and interspecific venom variation has been studied using various techniques in other venomous species e.g. bees (Owen and Sloley, 1988), spiders (De Oliveira et al., 1999; Goncalves de Andrade et al., 1999; Rash et al., 2000; Binford, 2001; Escoubas et al., 2002), snakes (Daltry et al., 1996; Prasad et al., 1999; Fry et al., 2002), cone snails (Jones et al., 1996) and scorpions (El Ayeub and Rochat, 1985; Kalapothakis and Chavez-Olortegui, 1997; Martin-Eauclaire, et al., 1987; Tare et al., 1992; Inceoglu et al., 2003). ELISA has been used previously to study scorpion venom variability (Kalapothakis and Chavez-Olortegui, 1997). In this chapter, analysis by ELISA suggested general variability between venoms from *Mesob. tamulus* individuals, but clearly showed these differences to be greater between the two geographical regions. However, the large degree of overlap between the two groups makes ELISA an ineffective identification tool. Indeed, the apparent cross-reactivity of the *Mesobuthus*

antiserum with the venom from *Leiurus quinquestriatus hebraeus* (*Lqh*) shows that this assay is not even diagnostic for venom derived from *Mesob. tamulus* species. Subtle differences in both protein and antigenic composition of regional venoms were also evident by SDS page and Western blotting.

The immunological studies described also examined cross reactivity between *Mesob. tamulus* antivenom and venom from *H. fulvipes* (another Indian scorpion) and from *Lqh* (another Buthidae species). The results show the two regional *Mesob. tamulus* venoms to share common antigenic determinants with *Lqh* venom, but show very little antigenic cross reactivity between the Indian scorpion species. A number of previous studies have demonstrated antigenic similarities between venoms of related scorpion species (for example, Das Gupta et al., 1989 (also for references to earlier studies dating back to the 1930s); Nishikawa et al., 1994; and Becerril et al., 1996). Antigenic cross-reactivity of snake, toad, bee and scorpion venoms has also been reported (Lipps and Khan, 2000), with scorpion venom most closely related to bee venom. Although the authors did not speculate, this result was likely due to similarities in the enzymic components.

Although *Leiurus quinquestriatus hebraeus* is a North African species of scorpion, it shares high venom toxicity with other Buthidae (most clinically significant species belong to this family) and homologous neurotoxic venom components. Conversely, the Asian forest black scorpion (*H. fulvipes*) is widely distributed in South India (and in Malaysia and Indonesia) but belongs to the Scorpionidae family of scorpions, which, although morphologically impressive, have reportedly lower toxicity than the Buthidae. This is likely to be due, in part, to differences in the number and levels of neurotoxins in the venom and a lower cross-reactivity with *Mesob. tamulus* antiserum would be expected. Indeed, immuno-gel diffusion experiments between venom of *Mesob. tamulus* and that of another *Heterometrus* species (*H. bengalensis*) also failed to show cross-reactivity (Das Gupta et al., 1989). Although unlikely, it is also possible that the lower cross-reactivity produced with *H. fulvipes* venom was due to intraspecies variation, since venom from a single individual was used in the study.

The cross-reactivity between the venoms of the Buthidae seen in ELISA may suggest therapeutic applications. Western blotting, however, revealed that this activity was primarily directed against larger, probably enzymatic, components and, as such,

unlikely to equate to neutralizing capability. Indeed Borges et al., 1999, showed cross-reactivity of *Tityus* antivenoms to be non-neutralising.

Toxin fingerprinting is based on the idea that, within any species, individuals will express peptides from their venom glands which have the same sequence and hence molecular weight, and that these toxin sequences will differ between species. A number of studies have used venom mass spectrometry to aid in classification and species identification, (e.g. scorpions (Dyason et al., 2002), spiders (Escoubas et al., 1997, 1998, 1999), snakes (Stocklin et al., 2000), amphibians (Steinborner et al., 1996), and cone snails (Jones et al., 1996)). The SELDI-TOF and LC-MS analysis described here determined venom fingerprints for the two regional venoms and highlighted differences between them. One mass (2947 Da) in particular stands out as a potential diagnostic tool in distinguishing between the regional venoms. Although clear regional differences in this peptide's expression are evident in all samples tested by SELDI, far more samples are needed before any firm conclusion can be made. A large-scale study would also aid in selection of other diagnostic masses, since analysis based upon a single component might prove unreliable.

When looking for taxonomic differences in the venom it is important to consider other sources of venom variability. The venom fingerprint and toxicity of a given species can vary between different individuals and also from the same specimen over time, although it is generally assumed that any intraspecific variation will predominantly manifest in quantitative rather than qualitative differences. The protein content and lethality of scorpion venoms have been shown to vary between individuals of the same species (El Ayeub and Rochat, 1985; Martin et al., 1987; Kalapothakis and Chavez-Olortegui, 1997; El Hafney et al., 2002). Kalapothakis and Chavez-Olortegui, 1997, also demonstrated antigenic variability of *T. serrulatus* in a paper that seems to show a direct correlation between individual variation in expression levels of the main α and β sodium channel toxins and variation in venom toxicity. Previous studies have indicated variation in *Mesob. tamulus* venom. Achyuthan et al., 1982, reported batch-to-batch variation in enzymic activity in the venom, and there are clear differences between individuals in the quantity of venom produced and the protein concentration within it (K. Newton and P. Strong unpublished observations). The SELDI-TOF data presented shows this variation is also evident at the level of toxin expression.

A number of factors may be responsible for this variation. Variation in the composition of animal venoms have been previously reported relating to age (Owen and Sloley, 1988; Goncalves de Andrade et al., 1999; Escoubas et al., 2002), gender (Sheumack et al., 1984; Rash et al., 2000; Escoubas et al., 2002), and diet (Daltry et al., 1996). Observed expression levels of toxin components may also be affected by genetic variations, environmental conditions, season, captivity, and the venom extraction method.

Even within an individual, the venom composition may vary. Pimenta et al., 2003, used MALDI-TOF MS to examine venom variability within *T. serrulatus* individuals after a period of starvation (fully mature venom gland production) and at subsequent repeat extractions. The authors reported variations due to the stage of venom maturation to be greater than those between individuals, particularly in the mass regions corresponding to the ion channel toxins. The interval between previous use of the venom gland and extraction of the venom used in this study is not known, and thus could be the source of some of the variation observed. However, since scorpions from the two regions were treated identically, this is unlikely to account for the observed geographical variation. Inceoglu et al., 2003, used mass spectrometry to look at differences between venom and pre-venom, another source of intra-individual variation. However, the differences were observed using manual venom extraction techniques. Venoms used in this study were extracted using electrical milking techniques, which are not under the neuronal control of the scorpion, and produce a more complete emptying of the venom gland. This extraction technique was important for the study of geographical variation, since it proved that these regional differences were not simply due to differences in scorpion aggression leading to preferences for pre-venom or venom production.

In order to minimise the effects of the observed variation between individuals, LC-MS data was obtained using venom pooled from a number of individuals from each geographical region. The *Lqh* venom used as a comparison was one that is commercially available, and hence represents pooled extractions from a number of individuals. Variation in venom concentration was eliminated by the standardisation of venom samples by protein concentration, focusing the study on differences in protein composition.

Further examination of individual *Mesob. tamulus* venoms will afford a clearer picture of their variation and how this relates to the variation seen in the different regions. In particular, any putative diagnostic process for identifying the different venoms will need to be assessed in a large number of individuals and the effect of variation within the region assessed. If non-specific variation is to be reduced in the future, ideally scorpions should be starved prior to milking, ensuring expression of mature venom peptides with fewer precursor products, and ensuring that the venom gland is full. Scorpions should also be standardised with respect to body length, minimising possible differences related to maturity. It should be noted, however, that these measures may not necessarily be practical.

Previous studies have analysed scorpion venom mass components to one degree or another in a number of species, but this is the first such report on an Asian scorpion. Indeed, with around 1500 scorpion species, it is likely that venom analysis is just in its infancy. Pimenta et al., 2001, identified 380 different mass components in the venom of *Tityus serrulatus* and stated that to their knowledge this was the largest number of masses detected in venom of a single species. The profiling of *Mesob. tamulus* (this study) identified 667 venom mass components and produced a profile to aid in the location and purification of peptides corresponding to a specific mass of interest. Such data may be of particular use in verifying that sequences derived from molecular cloning (such as those described in chapter 3) are expressed in venom, and as an aid to mass-spectrometric assisted peptide purification.

Pooled commercial venom was used for the venom profiling, to get a good overall picture of venom composition, reducing both extraction-related and individual-related variation. Since ion channel toxins are the components of scorpion venom that have generated the most scientific interest, the profiling method described was skewed towards finding such peptides. This was evident both in the mass range analysed, and in the bias towards basic peptides seen in the fractionation (most ion channel toxins are basic in nature). Generally, K^+ toxins have masses in the 3-4.5 KDa range, and Na^+ channel toxins are 6.5-8 KDa. There are exceptions to this rule (the smallest K^+ channel toxin identified is Tc1 (from *T. cambridgei*) with a mass of 2446 (Batista et al., 2000), and not all masses within these ranges are ion channel toxins (defensins will occur in the K^+ channel toxin mass range, for example). A few pore forming scorpion toxins of around 5 KDa have also been noted. One would therefore expect to see the masses

largely in two clusters representing toxins for the two monovalent cation channels, which is generally the pattern observed. Sodium channel toxin masses may be under-represented however, a phenomenon discussed later.

An obvious progression from the venom profiling described would be to obtain sequence data for the peptides. In a recent study by Batista et al., 2004, mass-spectrometric venom fingerprinting of *T. cambridgei* was followed by Edman degradation of 26 peptide components producing partial sequences. In the future we hope to apply mass spectrometry for these purposes as a continuation of the profiling described. Initial speculative attempts at MS-MS analysis of the venom samples used in this study were unsuccessful. It is anticipated, however, that optimisation of the experimental protocol, probably including the reduction and alkylation of samples prior to analysis, will enable amino-acid sequencing of a large number of *Mesob. tamulus* venom peptides without the need for a proteolytic digest. This will have implications in the discovery of novel component types and in knowledge of structure and functional properties of existing toxin classes. MALDI-TOF MS with collision induced dissociation/post-source decay has already been used to sequence peptides from the venom of solitary wasps (Hisada et al., 2000). Although these wasp peptides are considerably shorter than their scorpion counterparts, it is envisaged that future studies will produce MS-MS sequences of at least the smaller-mass scorpion venom peptides.

Although a large number of masses were identified in the venom fingerprinting and venom profiling described, a number of venom components may remain undetected - a fact that is supported by the lack of detection of some known venom components. Components outside the mass range will obviously be excluded, as will any contained within other size exclusion fractions in the profiling data. Positive ionisation was used for MALDI-TOF and LC-MS, selecting for basic peptide toxins. Negatively charged components may not ionise sufficiently in this mode. The reverse phase conditions used are not necessarily suitable for all peptides (some may not bind, some may bind irreversibly). Other components may represent too low a proportion of venom protein to be detected. In MALDI and LC-MS data a large number of putative adducts were observed. These masses were removed from the profiling data. It is possible, however, that some of these removed masses represented real venom components. Co-eluting venom components and, in the case of mass fingerprinting, peptide-standard masses may cause suppression effects. With MALDI-TOF analysis, above 5000Da in

particular, poor resolution and mass reproducibility caused many observed mass peaks to be rejected. In addition, the missing known toxin masses may be due to errors in sequencing of peptides or cDNA, errors in estimation of cleavage sites from signal peptides in cDNA derived sequences, differences between calculated and actual mass due to post translational modifications, or low relative expression levels.

Conversely, it is likely that a number of the observed masses are artefactual. Electrical venom extraction is particularly prone to contamination with cellular debris, which may account for some of the observed masses. The more sensitive the detection method, the more prone it is to contamination, which may have occurred at the sample preparation and/or fractionation stage (although at the MS stage itself, matrix or buffer interference was eliminated by running sample-negative controls).

Many masses may relate to same original peptide. This study assumed different retention times to equate to different molecular species. It should be noted that cis/trans isomerisation and alternative disulphide-bond pairings, for example, can result in differing chromatographic behaviour of the same peptide. As demonstrated by Pimenta et al., 2001, in *T. serrulatus* venom, peptides present may be incompletely cleaved from the precursor, or the mature peptides cleaved by proteolytic enzymes. These may be released from cells disrupted during venom extraction, or could contaminate the sample during its preparation. The mass spectrometry conditions themselves may lead to peptide degradation. Collision thermal degradation is a well-known phenomenon, which has recently been demonstrated in the analysis of scorpion toxins (Batista et al., 2004). A 'proline effect' has been seen, both by ESI and by MALDI-TOF/MS using an α CHCA matrix. This results from artefactual cleavage at the N-terminal of a proline residue in non-disulphide bonded N-terminal segments. At the data analysis stage, although many putative adduct masses were identified, others may be present, further increasing the number of artificial masses seen in this study.

MALDI-TOF and LC-MS techniques for the analysis of venoms have been compared previously (Escoubas et al., 1999, Pimenta et al., 2001) and the relative merits will not be discussed in detail here. In this particular study, the LC-ESI/MS instrument has the advantage of better mass resolution than the MALDI instrument. The LC-ESI/MS instrument will simultaneously fraction the sample and, if required, allow for the monitoring and fragmentation of a single ion species. However, offline separation of

venom allowed for enrichment of less concentrated protein fractions and hence better sensitivity for minor components. The high sample throughput of MALDI-TOF meant it was the ideal instrument for analysis of the large number of samples produced by offline separation. It should also be stressed that, although the particular MALDI-TOF instrument used in this study was of relatively low resolution, advances in the technology (for example coupling with a quadrupole device) mean that far more sensitive instruments utilising MALDI technology are now available. Importantly, different components have different ionisation efficiencies with the different technologies, hence the use of both methods for mass profiling in this study maximised the number of components observed.

Although LC-MS proved an ideal technique for detailed analysis of the regional venom samples, the length of time taken to run and the complexity of the data produced may limit its use as a diagnostic tool. In contrast, although costly, the SELDI technique may prove far more suitable for this task.

One major difference between the mass spectrometric methods was that seen in the higher mass range. SELDI-TOF data appears to reveal far more masses above 6KDa than do the other two methods. This relatively low apparent abundance of Na⁺ channel toxins is surprising considering that these toxins are usually the most important components in terms of relative concentration (Batista et al., 2002). In MALDI-TOF MS peaks were often observed in the sodium channel toxin mass region but were generally eliminated at the data processing stage due to poor reproducibility, poor peak resolution, and high standard errors in mass determination. Parallel analysis using an alternative matrix (e.g. sinapinic acid) may result in better resolution in the higher MW range. Although the LC-MS parameters used gave good results in the K⁺ channel toxin range, they not have been optimal for the higher end of the mass spectrum. Ideally, the studies should be repeated under optimal conditions for the higher end of the 2-10KDa range.

To conclude, having established antigenic differences in the venoms of *Mesob. tamulus* found in two distinct biotopes, this study set out to investigate the possibility that differences in the type and relative concentration of peptide toxins were responsible for the reported clinical differences. However, as noted earlier, many other factors may contribute to the clinical picture. It should be noted that venoms contain a wide range of

enzymes and non-protein components, and that the venoms may also vary with respect to these, perhaps a candidate for future study. Protein and venom standardisation was necessary for the purposes of the study described. However, the results do not necessarily correlate to the clinical picture, where differences in venom concentration and quantity may also be factors. Future studies may investigate these factors, perhaps utilising manual extraction techniques to give a more 'natural' venom sample if practically possible. Behaviour of the regional scorpions themselves could also be observed. The cause of the variation remains unclear. It is possible that there are underlying genetic differences between individuals in the different regions, as is often seen with discrete isolated populations. It is equally feasible, however, that toxin expression levels are influenced by external factors, e.g. environmental conditions and feeding behaviour (prey available in the region), which may be more significant than genetic variability. Indeed Bawaskar, 1999, postulated that the mortality associated with *Mesob. tamulus* sting in the Konkan region is due to differing venom characteristics brought about by the differing climatic and environmental conditions.

Mesob. tamulus is present in other regions of India, than the state of Maharashtra. It is likely that they too will show regional differences to their venome, which would be interesting to investigate for a clearer picture of variation in the species. What components are common to all geographical regions? Is there a generic *Mesob. tamulus* venom fingerprint diagnostic to the species as a whole? And if so, how does it compare with those of other Buthidae species? This is also the first recorded mass spectrometric study on *Lqh* venom, and although a number of toxins and putative toxins have been identified, very few of them have had their native mass confirmed. Further analysis of the data contained within this study may yield information on posttranslational modifications, point mutations, sequencing errors, etc.

It is now theoretically feasible to sequence the entire venome of an organism using modern proteomic techniques. If the techniques are perfected, this proteomic approach could replace that of gene cloning in the identification of novel toxins. Not only would it have the advantage of speed, but it would also identify only expressed sequences. Biological activity would still need to be examined in order to confirm pharmacology, however. In terms of the study presented in this chapter, it is envisaged that the focus of such techniques will be those masses which are unique, or upregulated, in the venom of

Indian red scorpions found in one particular region, and that the fractionated venom profile may prove an aid in purifying these components.

Chapter 3

Studies on Peptides from the Venom of the Indian Scorpion *Mesobuthus tamulus.*

- (i) Cloning of Chlorotoxin Gene Family Members and the Purification of the Corresponding Gene Products**
- (ii) Structure of the 3' Untranslated Region of Tamulustoxin**

3.1 Introduction

Chloride channels are ubiquitous and are involved in a wide range of physiological processes, including muscle contraction, regulation of electrical excitability, sensory signal transduction, volume regulation, secretion and absorption. Inherited chloride channel disorders include those leading to kidney stones, myotonia and cystic fibrosis. Chloride channels are far less well studied than their cation channel counterparts. One reason for this has been the lack of suitable ligands with high affinity and selectivity.

Pharmacological modulators of chloride channels included small organic molecules such as TEA⁺ (tetraethylammonium cation), and the xanthine derivatives. These chemical modulators are all of low affinity and have poor chloride channel specificity. Natural toxins active upon Cl⁻ channels include polyamine spider toxins, e.g. argiotoxin-636 (Herlitzes et al., 1993), and ochratoxin A (Gekle et al., 1993). Like the chemical modulators, these toxins have poor affinity and selectivity for chloride channels.

Scorpion venom contains a family of four disulphide bridge toxins, shorter than the known sodium channel toxins, which are active on the nervous system of insects (see 1.5.3.1). One of these short insectotoxins has proved to be a chloride channel inhibitor with significant pharmacological potential.

Chlorotoxin (ChlTx) was originally isolated from *Leiurus quinquestriatus quinquestriatus* venom via its action upon mammalian chloride channels (Debin and Strichartz, 1991; Debin et al., 1993). It was later found to bind to glioma membranes and block an outwardly-rectifying calcium-dependent chloride current expressed in glioma cells (glioma chloride current/ channel-GCC) and absent in normal glial cells (Ulrich et al., 1995, Ullrich and Sontheimer, 1996, 1997; Ullrich et al., 1998). Gliomas account for 40% of all brain cancers, and are highly invasive with most sufferers dying in the year of diagnosis. Prior to the discovery of chlorotoxin, there was no antigen or marker in use to selectively label these cells, and treatment options were limited and largely unsuccessful. Not only does chlorotoxin have the potential to aid in the identification and diagnosis of glioma (Ullrich et al., 1998; Ullrich and Sontheimer, 1999), but it is also reported to reduce the glioma's ability to invade surrounding tissue (Soroceanu et al., 1999). The specific binding to neoplastic glial cells provides the

opportunity to use ChITx for drug targeting (Ullrich and Sontheimer, 1999). Clinical trials of the toxin are underway. Chlorotoxin has more recently been shown to bind to other tumours derived from the neuroectoderm, including medulloblastomas, neuroblastomas, ganglionomas, melanomas and small cell lung carcinomas, thus widening its therapeutic potential (Lyons et al., 2002).

Despite the therapeutic potential, compared with the binding of other ion channel toxins to their targets, the chlorotoxin-GCC interaction is of relatively low affinity. There would appear to be two classes of binding sites on glioma cells ($K_d=4.2\text{nM}$ and $K_d=660\text{nM}$ for binding to D-54 MG human glioma cells) and radiolabelled-chlorotoxin has been shown to bind a 72kDa protein, consistent with members of the ClC ion channel family (Soroceanu et al., 1998).

It is unlikely that the GCC is chlorotoxin's natural target and its biological purpose in envenomation remains to be determined. New clues can be obtained from a recent report by Salbaum et al., 2004. When chlorotoxin was injected into LC (locus coeruleus) neurons, it had no effect upon the induction of action potentials. These action potentials persisted, however, when GABA was bath-applied, suggesting a reduction, but not total block of GABA_A-induced chloride conductance. Chlorotoxin is thus able to reduce GABAergic local synaptic inhibition in these neurons. This study also demonstrated the potential of chlorotoxin as a neurological research tool. Total block of GABA- and glycine- mediated chloride currents leads to neuronal cell death. Conversely, chlorotoxin reduces, but does not abolish, these currents. The authors were able to express chlorotoxin in mouse brain and study the behavioural effects of disinhibition.

Thus chlorotoxin would appear to be a direct or indirect modulator of specific ion channels, but its natural target is still undetermined. Similarly, the site of action of other short insectotoxins remains unknown. Do they have Cl⁻ channel modulating activities? And if so, is this activity directed against alternative channel types? As mentioned previously, the affinity of chlorotoxin for its binding site is not as great as the affinity of other scorpion peptides for their targets. Other members of the short insectotoxin family may thus have equal, or even greater pharmacological potential.

As the first step in a study to screen scorpion venom for peptides with chloride channel activity and to investigate the structure/function relationships of the short insectotoxins, one of the aims of the work described in this chapter was to identify short insectotoxins from the Indian red scorpion. The classical approach to the study of venom toxins is chromatographic separation and isolation based upon biological activity, followed by Edman sequencing of the purified peptide. In this chapter, a different approach was taken. Based upon the signal peptide sequence of Bm-12 from *Buthus martensii*, the first short insectotoxin cDNAs from *Mesob. tamulus* were cloned. One of these sequences, BtCh11, was selected for further study. Based on the predicted molecular mass of BtCh11 from the cDNA sequence, a putative BtCh11 mature toxin was purified, guided by MALDI-TOFF mass spectrometry. A synthetic analogue was also produced and purified. These peptides will form the basis of continuing studies on short insectotoxins from *Mesob. tamulus*.

The same adaptor-ligated *Mesob. tamulus* cDNA library used to identify short insectotoxin sequences was utilized to determine the 3'UTR of tamulustoxin, a voltage gated potassium channel toxin. Strong et al., 2001, reported a difference between the observed and calculated masses of tamulustoxin of approx 1Da. The same author has noted a resistance to carboxypeptidase digestion (P. Strong unpublished observations). Both of these factors suggest C-terminal amidation. Experiments were performed to extend the 3' end of the known cDNA sequence to include any processed C-terminal residues and the 3'UTR. The results reveal additional translated residues consistent with amidation of the precursor peptide, and also slight conservative differences between the published cDNA sequence and that determined in this work.

During the course of investigations on the cDNA sequence of tamulustoxin, a sequence having homology to a long-chain potassium channel toxin signal peptide was identified in *Mesob. tamulus*. Since, within scorpion toxins, related signal peptide sequences generally indicate related mature peptides, and given the lack of examples of long chain potassium channels, this sequence may warrant further investigation.

3.2 Materials and Methods

3.2.1 Materials

Murine Moloney leukaemia virus (MMLV) reverse transcriptase was obtained from Amersham Pharmacia Biotech (Amersham, UK). DNA sequencing reagents were obtained from Applied Biosystems (Foster City, CA). All PCR (polymerase chain reaction) reagents were from Perkin-Elmer, USA and all PCR reactions were carried out using a Perkin-Elmer Cetus thermal cycler (model 480). Oligonucleotide primers were produced by National University Medical Institutes Synthesis Service, National University of Singapore (Singapore), Oswel DNA Service (Southampton, UK) and Alpha DNA (Quebec, Canada). EcoR1 and buffer H were supplied by Promega, and agarose (ultra pure grade) was obtained from BRL.

Standard PCR mix comprised: - 10x PCR buffer (500mM KCl/ 100mM Tris-HCl pH8.3/ 3mM MgCl₂/ 1mgml⁻¹ gelatin) (2.5µl), dNTPs (2.5µl) (175µmol each) and DNazyme 0.5µl (0.5 unit), for a 25µl total reaction volume. For PCR reactions, negative controls were carried out in absence of template DNA.

The *E.coli* strain used was DH5α [*supE44 ΔlacU169 (Φ80lacZΔm15) hsdR17 recA1 endA1 gyrA96 thi-1 relA1*]. *RecA1* mutation reduces the frequency of homologous recombination that may rearrange the structure of cloned DNA inserts. The strain has α complementation of the β galactosidase gene (i.e. contains a deletion eliminating the chromosomal lacZ gene, but carries the C-terminal coding domain of the gene on an episome), so that recombinants appear colourless and non-insert bearing colonies appear blue when grown on IPTG (isopropyl β-D-thio-galactoside) and X-gal (5-bromo-4-chloroindol-3-yl β-D-galactopyranoside).

All centrifugation steps were carried out at 13000rpm in a Beckman microcentrifuge unless stated otherwise.

All reagents used in the purification of synthetic and native BtCh11 were of analytical grade or better. Pooled *Mesob. tamulus* venom was supplied by the Haffkine Institute, Mumbai, India. BtCh11 peptide was synthesised by Hallam Biotech, Sheffield, UK. Zip-tips were obtained from Millipore, UK.

3.2.2 Identification of Putative Short Insectotoxin cDNA Sequences from *Mesob. tamulus*

3.2.2.1 Scorpions

Mesobuthus tamulus (Indian red scorpions) were collected at the end of the rainy season (Sept-Dec) in the state of Maharashtra, India. The scorpions were kept at the Haffkine Institute, Mumbai, where the telsons were removed and snap-frozen in liquid nitrogen. These were shipped on dry ice to Singapore and stored at -80°C until use.

3.2.2.2 Isolation of Total RNA

Three whole frozen (-80°C) telsons were pulverised under liquid nitrogen using a pestle and mortar. Total RNA was extracted using 1ml TRIZOL[®] reagent (Gibco Life Technologies, CA, USA) per 100mg tissue, incubated for 5min at room temperature. TRIZOL is a mono-phasic solution of phenol and guanidine isothiocyanate. The RNA was then chloroform extracted, adding 0.2ml chloroform per 100mg telson, shaking vigorously and incubating for 3min before centrifugation (15min) to separate the phases. The upper aqueous phase was incubated with RNase-free DNase 1 (Boehringer Mannheim, Germany) for 30mins at 37°C . RNA was precipitated by: adding 0.5ml isopropyl alcohol per 100mg tissue, incubating 10min at room temperature and centrifuging for 10mins. The pellet was washed in 1ml 75% ethanol, and air-dried at 37°C . Purified total RNA was redissolved in 100 μl sterile H_2O , heated at 60°C for 10min to denature secondary structure, and stored at -70°C .

3.2.2.3 Generation of an Adaptor Ligated cDNA Library

First Strand Synthesis

1 μg (1-4 μl) purified total RNA from scorpion telson and 1 μl (10 μM) cDNA synthesis primer (5'-TTCTAGAATTCAGCGGCCGC(T)₃₀VN-3' where V \equiv A, C or G and N \equiv A, T, C or G) were made up to final volume of 5 μl with sterile H_2O and mixed. After heating for 2min at 70°C the mixture was cooled on ice for 2min. 2 μl 5x first strand

buffer (250mM Tris pH8.3/ 30mM MgCl₂/ 375mM KCl), 1µl dNTP mix (10mM each), 1µl MMLV reverse transcriptase (100unit µl⁻¹) and 1µl sterile H₂O were added. After incubating for 1hr at 37°C, first strand synthesis was terminated by cooling rapidly on ice.

Second Strand Synthesis

The second strand synthesis reaction was made up as follows: 10µl first stand synthesis from above, 16µl 5x second-strand buffer (500mM KCl/ 50mM ammonium sulphate/ 25mM MgCl₂/ 0.75mM β-NAD/ 100mM Tris pH7.5/ 0.25mgml⁻¹ BSA), 1.6µl dNTP mix (each at 10mM), 4µl 20x second-strand enzyme cocktail (*E.coli* DNA polymerase I (6 units µl⁻¹)/ *E.coli* DNA ligase (1.2 units µl⁻¹) and *E.coli* RNase H (0.25 units µl⁻¹) and 48.8µl sterile H₂O. The reaction was incubated for 1.5hr at 16°C before addition of 2µl (10 units) T4 DNA polymerase and incubation for a further 45min at 16°C.

100µl phenol:chloroform:isoamyl alcohol (25:24:1) was added and mixed to an emulsion before being spun (10min) to separate phases. The aqueous layer was removed and extracted with 100µl chloroform:IPA (24:1), vortexing and centrifuging (10min) as above. The aqueous layer was retained and DNA precipitated by addition of ½ volume 4M ammonium acetate and 2.5 volumes 95% ethanol, followed by centrifugation (10min). The pellet was recovered, washed with 300µl ethanol and air dried at 37°C for 10min. The double stranded (ds) cDNA pellet was dissolved in 10µl sterile H₂O and stored at -20°C.

Adaptor Ligation

5µl ds cDNA, 2µl Marathon cDNA adaptor (10µM, Clontech, see below for sequence), 2µl 5x ligation buffer (250mM Tris-HCl pH7.8/ 50mM MgCl₂/ 5mM DTT/ 5mM ATP/ 25% w/v polyethylene glycol MW 8000) and 1µl T4 DNA ligase (1 unit ul⁻¹) were incubated overnight at 16°C. The ligase was inactivated by heating for 5min at 70°C, and stocks of adaptor-ligated ds cDNA were stored undiluted at -20°C. Prior to use 1/50 and 1/250 dilutions of adaptor ligated ds cDNA were made in TBE (90mM Tris-borate/

2mM EDTA) buffer, heated at 94°C for 2mins to denature ds cDNA, cooled on ice 2mins, and either used immediately or stored at -20°C.

Marathon cDNA adaptor: -

5' -CTAATACGACTCACTATAGGGCTTCGAGCGGCCGCCCGGGCAGGT-3'
3' - H₂N-CCCGTCCA-PO₄-5'

3.2.2.4 Primer Design

Degenerate gene specific primers corresponding to the 5' UTR and signal peptide nucleotide sequence of *Buthus martensii* Karsch short insectotoxin Bm-12 were designed as follows: - mBtCF1 5'-CCAAAACCTCTATTTAAAATG-3' and mBtCF2 5'-TTAAAATGAARTTYCTNTAYGG-3' (where R= G or A, Y= T or C, N= A or T or C or G). These primers were tested for suitability using DNASTar (Madison, USA), and BLAST (NCBI public database), the latter not highlighting any other potential binding sites for the primers amongst other known scorpion sequences.

Adaptor primers with sequences identical to those supplied with the Marathon cDNA amplification kit (Clontech, USA) were used: - adaptor primer 1 (AP1; 27-mer) 5'-CCATCCTAATACGACTCACTATAGGGC-3' and nested adaptor primer 2 (AP2; 23-mer) 5'-ACTCACTATAGGGCTCGAGCGGC-3'.

3.2.2.5 PCR

The enzyme used for the PCR reactions (i.e. DNazyme) produces products with A overhangs, making them suitable for TA cloning. A number of PCR cycle conditions were tried using both GSP mBtCF1 and mBtCF2 (sequences as above) in conjunction with adaptor primers AP1 and AP2 (sequences as above) in primary and secondary PCR. Final PCR conditions were as follows. Standard PCR mix (see 3.2.1) was used with the addition of 1µl adaptor ligated mBt-telson cDNA library, 2.5µl (5µmol) AP1, 2.5µl (5µmol) GSP mBtCF2 and sterile H₂O to a 25µl total reaction volume. Cycle conditions were: 30sec at 94°C/ 1min at 45°C/ 2min at 60°C for 10 cycles, then 10

cycles of 94°C for 30sec/ 50°C for 1min/ 72°C for 2min, followed by a 7min final extension at 72°C.

The PCR products (5µl reaction mix) were visualised by agarose gel electrophoresis.

3.2.2.6 DNA Agarose Gel Electrophoresis and Purification of Fragments/ Bands from Agarose Gels

Flatbed agarose gel electrophoresis was routinely performed using 1% agarose in TBE (90mM Tris-base/ 90mM boric acid / 2mM EDTA) buffer. 0.2ugml⁻¹ ethidium bromide solution was routinely included in the gel to enable visualisation of bands on a UV transilluminator. Gels were run in the TBE buffer for 45min at 95V. 123 base pair or 100 base pair ladder markers were used to aid size estimation.

Fragments of interest were excised from agarose gels and immediately purified with QIAquick gel extraction kit (Qiagen, USA) as per manufacturer's protocol.

3.2.2.7 Preparation of Competent Cells

Competent *E. coli* were produced by the calcium chloride method of Cohen et al., 1972. *E. coli* strain DH5α [*supE44 ΔlacU169 (Φ80lacZΔm15) hsdR17 recA1 endA1 gyrA96 thi-1 relA1*] was streaked onto a LB (Luria-Bertani broth) agar plate and grown overnight. A 10ml LB overnight culture was generated from a single colony and used to inoculate 100ml LB. The culture was grown approx 3hrs at 37°C to an OD₆₀₀ of 0.5-0.7. The media was transferred to 2x 50ml sterile centrifuge tubes and cooled on ice for 10mins prior to centrifugation (Sorvall GS3 4000rpm 10mins 4°C). The liquid was discarded and the pellets drained and resuspended in 20ml ice-cold 0.1M CaCl₂. Bacteria were harvested as above and the CaCl₂ wash repeated. The drained pellets were resuspended in 2ml ice-cold 0.1M CaCl₂/ 40% glycerol solution, 200µl aliquots were dispensed into pre-chilled sterile eppendorfs and stored at -70°C. Prepared competent cells were checked for growth, antibiotic sensitivity and competence by plating onto LB plates (+/- 50ugml⁻¹ ampicillin) or transformation with empty plasmid respectively.

3.2.2.8 Cloning PCR Fragments into pCR[®]4-TOPO[®] Vector

Purified PCR fragments were ligated into a TA cloning vector by virtue of the A overhang produced by DNazyme. The TOPO TA Cloning[®] Kit for sequencing (Invitrogen, CA, USA), which uses the pCR[®]4-TOPO[®] vector, was used. This vector is supplied linearised with 3' T overhangs and is covalently bound to topoisomerase.

Transformations were performed by combining 4µl purified PCR product with 1µl pCR[®]4-TOPO vector (10ngµl⁻¹ plasmid DNA in 50% glycerol/ 50mM Tris-HCL pH7.4/ 1mM EDTA/ 2mM DTT/ 0.1% Triton X-100/ 100µgml⁻¹ BSA/ 30µM phenol red). After 5min at room temperature, 1µl salt solution (1.2M NaCl/ 0.06M MgCl₂) was added and the mixture chilled on ice. 50µl chemically competent cells (either DH5α [supE44 ΔlacU169 (Φ80lacZΔm15) hsdR17 recA1 endA1 gyrA96 thi-1 relA1] prepared as in 3.2.2.7 above, or DH5α-tT1 One Shot[®], Invitrogen, CA, USA) were added. Transformation mixture was stored on ice for 20mins before heat shock for 120secs at 42°C and rapid chilling in ice for 1-2 mins. The bacteria were then allowed to recover and express ampicillin resistance in 250µl S.O.C medium (2% tryptone/ 0.5% yeast extract/ 10mM NaCl/ 2.5mM KCl/ 10mM MgCl₂/ 10mM MgSO₄/ 20mM glucose) for 1hour at 37°C on an orbital shaker.

Transformed *E.coli* were selected by growing overnight at 37°C on 1.3% LB agar plates containing 50µgml⁻¹ ampicillin. To allow for selection of recombinant colonies by α-complementation of the β-galactosidase gene, plates were coated with 5µl 1M IPTG (isopropyl β-D-thio-galactoside)/ 20µl 40mgml⁻¹ X-gal (5-bromo-4-chloroindol-3-yl β-D-galactopyranoside)/ 75µl sterile H₂O prior to use.

Recombinant white (or light blue) colonies were selected at random and grown overnight in 1.5ml LB medium containing 50µgml⁻¹ ampicillin.

3.2.2.9 Plasmid DNA Isolation (Mini Preps)

Plasmid DNA was isolated and purified from 1ml overnight bacterial culture samples by the alkaline lysis method (Sambrook *et. al.*, 1989). Briefly, the cells were isolated by centrifugation (1min) and resuspended in 100µl TGE buffer (50mM glucose/ 25mM

Tris-Cl pH8.0/ 10mM EDTA). 200µl lysis solution (0.2M NaOH/ 1% (w/v) SDS) was added, and the solution mixed by inversion until the cells were fully lysed. 150µl ice-cold potassium acetate solution (60ml 5M potassium acetate/ 11.5ml glacial acetic acid/ 28.5ml sterile H₂O) was added, mixed vigorously to yield a white precipitate, and then left on ice for 10min to precipitate further. The solution was spun (10min) to pellet the high molecular weight DNA and cell debris, and the cleared supernatant (containing plasmid and RNA) was transferred to a fresh microcentrifuge tube. RNA was removed by incubating with 3µl 10µgml⁻¹ RNase A (heat treated to inactivate any DNase) for 20min at 60°C. Samples were cooled and the plasmid DNA precipitated with isopropanol (450µl for 15mins at -70°C) and recovered by centrifugation (20mins). The plasmid DNA pellet was washed in 100µl 70% ethanol, vacuum dried in a speed vac and resuspended in 20µl sterile H₂O.

3.2.2.10 Screening for Inserts by Restriction Digest

Samples of plasmid DNA were tested for recombination with appropriately sized PCR fragments by digestion with the restriction endonuclease EcoR1. Restriction digests, containing 0.2µl (10units µl⁻¹) EcoR1, 1µl x10 buffer H (Promega) and approx. 1µg (1-4µl) DNA in a total volume of 20µl, were performed overnight at 37°C. Linearised plasmids and any excised cDNA fragments were visualised by agarose gel electrophoresis as described (3.2.2.6). Plasmid DNA containing appropriately sized inserts was prepared for sequencing.

3.2.2.11 Stock Culture

Stock cultures of colonies of interest were prepared as follows. 1ml overnight culture was spun to pellet cells (1min), the supernatant discarded and the cells gently resuspended in 500µl LB broth: 80% glycerol (1:1). Stocks were stored at -70°C.

3.2.2.12 Dideoxy Sequencing

The multiple cloning site of pCR[®]4-TOPO contains both M13 forward and reverse priming sites as well as T3/ T7 priming sites. Sanger dideoxy sequencing (Sanger et al., 1977) was carried out using the Taq DyeDeoxy[™] Terminator Cycle Sequencing Kit (Applied Biosystems) and either T3 (5'-ATTAACCCTCACTAAAGGGA-3') or T7 5'-TAATACGACTCACTATAGGG-3' primers. 4-6µl plasmid DNA, 4µl primer (1.0 OD), 8µl sequencing pre-mix and sterile H₂O (to 20µl total reaction volume) were subjected to 25 cycles (96°C 30sec/ 50°C 15sec/ 60°C 1min) PCR.

Chloroform extraction was performed on the PCR reaction (80µl sterile water was added, followed by 100µl chloroform, and the mixture was vortexed. The suspension was spun briefly to separate the aqueous and organic phases and the aqueous phase retained. The DNA was precipitated by addition of 15µl 3M sodium acetate pH4.5 and 300µl cold 100% ethanol and the solution incubated on ice 10min. The precipitate was recovered by centrifugation (10min) and the pellet washed in 200µl 70% ethanol before being vacuum dried for 10min. The DNA was redissolved in 4µl EDTA/ formamide buffer, denatured for 2mins at 100°C and immediately cooled on ice.

Samples were loaded onto a 6% acrylamide/ 50% (w/v) urea sequencing gel in TBE buffer (90mM Tris-borate/ 2mM EDTA) and run on an automated DNA sequencer (Applied Biosystems USA, model 373A).

3.2.2.13 Analysis of Deduced cDNA Sequences

Sequences were translated and examined visually for consensus sequences, and also matched against known sequences via BLAST (NCBI public database).

3.2.3 Mass Spectrometry-Guided Purification of a Putative Chloride Channel Toxin Identified by cDNA Cloning

Mass spectrometry was used to identify masses corresponding to putative BtCh11 gene products in *Mesob. tamulus* venom. A candidate mass was isolated by mass spectrometry-guided purification.

3.2.3.1 Calculation of Candidate Masses

Masses of peptides corresponding to a BtCh11 gene product:- having no C-terminal modification; and with removal of a single; and double C-terminal glycine residue were calculated using ExPASy PeptideMass software, and the resulting masses were adjusted to allow for disulphide bonding.

3.2.3.2 Chromatographic Purification of the Peptide

Mesob. tamulus venom was extracted as described in 2.2.2 and fractionated by size exclusion and ion exchange chromatography as described previously (see 2.2.4.1 and 2.2.4.2). Samples from all size exclusion fractions, and desalted samples from all ion exchange groups, were analysed by mass spectrometry (see below). The mass of interest was isolated from ion exchange group 1 by a combination of C18 and C8 reverse phase HPLC using an AKTA system (Amersham-Pharmacia) and progress followed by mass spectrometry. Optimal reverse phase conditions are described. 1mg non-desalted ion exchange samples were filtered (0.45µm membrane filter) and applied to a Dynamax C18, 300A, 250 x 4.6mm, 5µm column at a flow rate of 0.5ml min⁻¹ in 0.1% TFA. The sample was eluted using a linear gradient of 0-45% acetonitrile in 0.1% TFA over 12 column volumes. Fractions shown by mass spectrometry to contain the mass of interest were pooled and dried in a rotary evaporator. The sample was reconstituted in 0.1% TFA and applied to a Vydac 208TP C8, 300A, 250 x 3.2mm, 5µm column at 0.5ml min⁻¹. The sample was eluted using a 4.5-27% gradient of acetonitrile in 0.1% TFA over 12 column volumes. Fractions were again analysed by mass spectrometry to detect the mass of interest. Purification was monitored throughout by absorbance at 280nm.

3.2.3.3 Screening of Fractionated Venom by Mass Spectrometry

The different chromatography samples were analysed separately. Size exclusion samples were analysed, using MALDI-TOF mass spectrometry, by the Mass Spectrometry Service, National University of Singapore.

1µl desalted ion exchange fractions were diluted in 10µl matrix solution (10mg αCHCA in 1ml 60% acetonitrile/ 0.3% TFA) and 0.5ml was spotted onto a MALDI-TOF target and air-dried. Reverse-phase samples were prepared by evaporating 10µl to near-dryness in a rotary evaporator, re-suspending in the matrix solution and applying to the target as above. Analysis of these samples was carried out on a SAI LaserTOF LT1500 mass spectrometer as described 2.2.4.4, but with a 4500Da focus mass.

The purified peptide was analysed by quadrupole mass spectrometry, using an API QSTAR pulsar1 (Applied biosystems) quadrupole mass analyser with an electrospray ion source (Analytical Services, Sheffield Hallam University). Mass data was analysed using Analyst QS software (Applied Biosystems).

3.2.4 Generation of Synthetic BtCh11

3.2.4.1 Peptide Synthesis

The peptide RCPPCFTTNPMEADCRKCCGGRGYCSYQCICPG-COOH was synthesised using standard Fmoc chemistry by Hallam Biotech, Sheffield, UK. Product was supplied lyophilised and was stored at -20°C.

3.2.4.2 Peptide Purification

1mgml⁻¹ crude peptide was resuspended in 0.1% TFA for 24hrs under nitrogen. The resulting suspension was clarified by centrifugation and passing through a 0.45µm syringe filter. The solution was subjected to MALDI-TOF mass spectrometry (see below) and reverse phase HPLC. 1ml samples were run on a Dynamax C18, 300A, 250 x 4.6mm, 5µm column at a flow rate of 0.5ml min⁻¹ using an AKTA system

(Amersham-Pharmacia). Samples were eluted using a 0-100% linear gradient of 90% acetonitrile in 0.1% TFA. The eluent was monitored at 280nm and 1ml fractions collected, which were analysed by mass spectrometry. The folded peptide (see below) was fractionated and analysed in the same way.

1ml crude, and folded, peptide solutions were separated on a Vydac 208TP C8, 300A, 250 x 3.2mm, 5 μ m column run at 0.5ml min⁻¹. Samples were eluted with a 0-100% linear gradient of 90% acetonitrile in 0.1% TFA over 10 column volumes, monitored by absorbance at 280nm. 1ml fractions were collected and analysed as above.

Final purification conditions used the C18 column described, but a shallower gradient of 4.5-22.5% acetonitrile in 0.1% TFA was employed over 10 column volumes.

3.2.4.3 MALDI-TOF Mass Spectrometry

For HPLC fractions, 100 μ l was evaporated to near-dryness in a rotary evaporator and redissolved in 10 μ l matrix solution (10mg α CHCA in 1ml 60% acetonitrile/ 0.3% TFA). 0.5ml was spotted onto the target and air-dried. For analysis of the crude peptide, a number of sample preparation techniques were used. 1, 10 and 100 μ l samples were evaporated and dried as above. Identical samples were prepared, desalting on a C18 zip-tip according to manufacturer's instructions. For all samples, triplicate spots were analysed. Crude sample preparation was repeated three times.

MALDI-TOF/ MS analysis was carried out on a SAI LaserTOF LT1500 mass spectrometer as described in 2.2.4.4, but with a 4500Da focus mass.

3.2.4.4 Peptide Folding

The peptide was allowed to fold according to the method of Di Luccio et al., 2002. 1mg lyophilised crude peptide was resuspended in 1ml 20mM sodium phosphate, pH8.2, in a 15ml falcon tube. The solution was agitated and allowed to oxidise under air for 94hrs. The resulting suspension was centrifuged and passed through a 0.42 μ m syringe filter.

3.2.3.5 Homology Modelling of BtChl1 and BtChl2

Automated comparative modelling was carried out using Swiss-Model (ExPASy, Expert protein analysis system, www.expasy.org) in the 'first approach' mode. Two suitable template structures were located in the RCSB Protein Databank (PDB, www.rcsb.org/pdb): that for chlorotoxin (1CHL, Lippens et al., 1995) and that for insectotoxin I5A (1SIS, Lomize et al., 1991). BtChl1 and BtChl2 were each modelled using 1CHL, 1SIS, and 1CHL + 1SIS as templates. The templates, and the resulting structures, were submitted to the protein structure verification program WHAT IF (Vriend, 1990) via the Swiss-Model server.

PDB files were displayed using DeepView/ Swiss-PDB Viewer (www.expasy.org) or using Protein Explorer (<http://molvis.sdsc.edu/protexpl/frntdoor.htm>). Molecular surfaces were calculated and electrostatic potentials computed and mapped to these surfaces using DeepView. For the calculation of electrostatic potentials, atomic partial charges were utilised using the coulomb computation method and illustrated with the following cut-offs (Lippens et al., 1995): - red=-1.6kT/e; white=0.0kT/e; blue=1.6kT/e (k is the Boltzmann constant, T is temperature in Kelvin and e is the charge of the electron. At 298K kT/e=25.6 mV).

The charybdotoxin structure used for comparison was 2CRD (PDB, Bontems et al., 1992).

3.2.5 Analysis of the 3' UTR of Tamulustoxin cDNA

An adaptor ligated cDNA library from Indian red scorpion telson, and a gene specific primer based upon the known protein sequence of tamulustoxin were used in 3'RACE. Purified products were cloned into *E. coli* using a commercial sequencing vector and the recombinant plasmid DNA sequenced. Methods used were identical to those used in short insectotoxin cloning (see 3.2.2), with the exception of primer design, PCR conditions and PCR fragment purification, which were as described below. Clones originating from two separate ligations were sequenced. All clones were sequenced using T7 primer and sequencing was repeated on three clones using T3 primer.

3.2.5.1 Primer Design

The gene specific primer used for 3'RACE of tamulustoxin cDNA was one of those used to derive the cDNA sequence of the coding region. This primer (TmTx F) 5' – CGYTG YCAYTTYGTYGTYTGYAC-3' (where Y= T or C) is a degenerate primer based on the known protein sequence for the toxin (Strong et al., 2001). The adaptor primer AP1 and the nested adaptor primer AP2 had sequences as described earlier (3.2.2.4).

3.2.5.2 PCR reaction

A number of PCR cycle conditions were tried using TmTx F primer (see above) in conjunction with adaptor primers AP1 and AP2 (sequences as described 3.2.2.4) in primary and secondary PCR. The PCR conditions that produced the final sequences were as follows. For primary PCR, standard PCR mix (see 3.2.1) was used with the addition of 1µl adaptor ligated mBt-telson cDNA library, 2.5µl (5µmol) Adapter primer 1, 2.5µl (5µmol) GSP TmTx F, and sterile H₂O to a 25µl total reaction volume. Cycle conditions were: 1min at 94°C/ 2min at 50°C/ 2min at 72°C for 30 cycles, followed by 10min final extension at 68°C.

5µl primary PCR reaction, 2.5µl (5µmol) Adapter primer 2, and 2.5µl (5µmol) GSP TmTx F were added to standard PCR mix and made up to 25µl total reaction volume with sterile H₂O. For secondary PCR, the annealing temperature was raised to 55°C with the remainder of the cycling conditions as per primary PCR.

The PCR products (5µl reaction mix) were visualised by agarose gel electrophoresis. The PCR products were directly purified with QIAquick gel extraction kit (Qiagen, USA) as per manufacturer's protocol.

3.2.6 Identification of a Long-Chain Potassium Channel Toxin-Like Signal Peptide Sequence in *Mesob. tamulus* cDNA

In the course of studies on tamulustoxin cDNA, a sequence encoding a putative signal peptide was deduced. Experimental conditions were as per 3.2.5 except as detailed below.

3.2.6.1 Primers

The primer used to obtain the signal peptide-like sequence was a degenerate reverse primer (TmTx R) 5' – YTCYTTRCCYTTYTCYTTYTT-3' (where Y =C or T, R= G or A), based upon the C-terminal sequence of tamulustoxin. The adaptor primer AP1, and nested adaptor primer AP2 had sequences as described earlier (3.2.2.4).

3.2.6.2 PCR Reaction

Primary and secondary PCR conditions were identical to those described for the tamulustoxin 3' sequence (3.2.6.2), with the exchange of TmTx F primer for TmTx R.

The PCR products (10µl reaction mix) were visualised by agarose gel electrophoresis, producing a lower band at approx 200bp and a higher band of approx 250bp. The lower bands from two identical PCR reactions were excised, combined, and purified with QIAquick gel extraction kit (QIAGEN, USA) as per manufacturer's protocol.

3.3 Results

3.3.1 Identification of Putative Short Insectotoxin cDNA Sequences from *Mesob. tamulus*

An adaptor-ligated *Mesob. tamulus* telson cDNA library was probed for sequences that may represent short insectotoxins and hence have potential chloride channel modulating activity.

The 5'UTRs and signal peptides of scorpion ion channel toxins displaying similar pharmacological properties are often well conserved between species (Bougis et al., 1989; Zeng et al., 2001, Corona et al., 2001), showing greater homology than the mature toxin sequences. Very little has been published on short insectotoxin nucleotide sequences. The 3'UTR and signal peptide nucleotide sequence is available for Bm-12 (Zeng et al., 2000) and its variant Bm-12b (Xu et al 2000 – direct submission to Entrez database) and the signal peptide nucleotide sequence for chlorotoxin variant CITx-c has been published (Froy et al., 1999). These nucleotide sequences were aligned using ClustalW (www.ch.embnet.org) (fig 3.1). As expected, there is high homology between Bm-12 and Bm-12b. There is also high homology between Bm-12 and CITx1 at the nucleotide level. This homology is slightly higher at the end of the 5'UTR and the signal peptide (88.9%) than in the sequence encoding mature toxins (81.9%). If one considers the peptide sequences (all known isoforms of all known short insectotoxins), which are slightly more extensive; 58.3% signal peptide residues are conserved in all sequences, c.f. 30.8% mature peptide residues (see fig 3.4). Primers were designed based upon the 5'UTR and signal peptide of Bm-12 (a putative short insectotoxin from *Buthus martensii* Karsch).

Primary- and secondary-PCR was carried out using nested adaptor-primers and one of two degenerate gene-specific primers based upon the 5'UTR or signal peptide sequence using various PCR conditions. One such experiment yielded primary PCR products of approx. 370 base pairs (fig 3.2a). 20µl PCR reaction was run on an agarose gel, the bands excised and purified on a QIAquick column (Qiagen). The DNA was ligated into pCR®4-TOPO® vector via its A overhangs, and transformed into competent *E. coli*. After ampicillin resistance and *lac z* screening, a number of colonies were selected and

plasmid DNA purified by miniprep. Restriction digests on minipreps from a number of colonies revealed inserts of approx. 370 base pairs (examples shown in fig 3.2b).

Seven clones containing inserts of interest were selected for sequencing. Sequence analysis and comparison with those of known short insectotoxins revealed two novel cDNA sequences capable of encoding scorpion short insectotoxins (fig 3.3) which were named BtChl1 and BtChl2. BtChl1 was encoded by four clones, whilst BtChl2 was isolated from a single colony. Both sequences were submitted to the Entrez database (BtChl1 = AF481880, BtChl2 = AF481881) and were the first short insectotoxin sequences determined in this species.

In order to determine the mature sequence, the position of cleavage of the signal peptide was determined by a combination of von Heijne's rules (von Heijne, 1986) and comparison with known short insectotoxin sequences (see fig 3.4). Both mature toxins appear to have an N-terminal arginine. The locations of the C-terminals of the mature toxins are less clear. BtChl1 amino acid sequence ends with a proline followed by two glycine residues. It is not uncommon for scorpion toxins to be amidated via removal of a C-terminal glycine, although not all scorpion toxins are processed in this manner. Therefore, BtChl1 may encode a mature peptide of 34, 35 or 36 residues, with or without C-terminal amidation. Using known rules for scorpion toxin C-terminal processing, one would expect BtChl2 to be unprocessed at this end, since it does not terminate in a basic residue. The validity of this assumption will be addressed later.

Fig 3.1 Homology of Short Insectotoxin Nucleotides

```

Bm-12      -----GC AAAACTCTAT TAAAAATGAA
Bm-12b    TGATATTGCA ATAATATACC AAAACTCTAT TAAAAATGAA
ClTx1     -----ATGAA

GTTCCCTCTAC GGAATCGTTT TCATTGCACT TTTTCTAACT GTAATGTTCC
GTTCCCTCTAC GGAATCGTTT TCATTGCACT TTTTCTAACT GTAATGTTCC
GTTCCCTCTAT GGAATCGCTT TTATTGCCGT TTTTTTAACA GTAATGATCG

CAACTCAAAC TGATGGATGT GGGCCTTGCT TTACAACGGA TGCTAATATG
CAACTCAAAC TGATGGATGT GGGCCTTGCT TTACAACGGA TGCTAATATG
CAACTCATAT TGAAGCATGT GGACCTTGCT TTACAACGGA TCGTCAAATG

GCAAGGAAAT GTAGGGAATG TTGCGGAGGT ATTGGAAAAT GCTTTGGCCC
GCAAGGAAAT GTAGGGAATG TTGCGGAGGT AATGGAAAAT GCTTTGGCCC
GAACAGAAGT GTGCAGAATG TTGCGGAGGC ATTGGAAAAT GCTATGGTCC

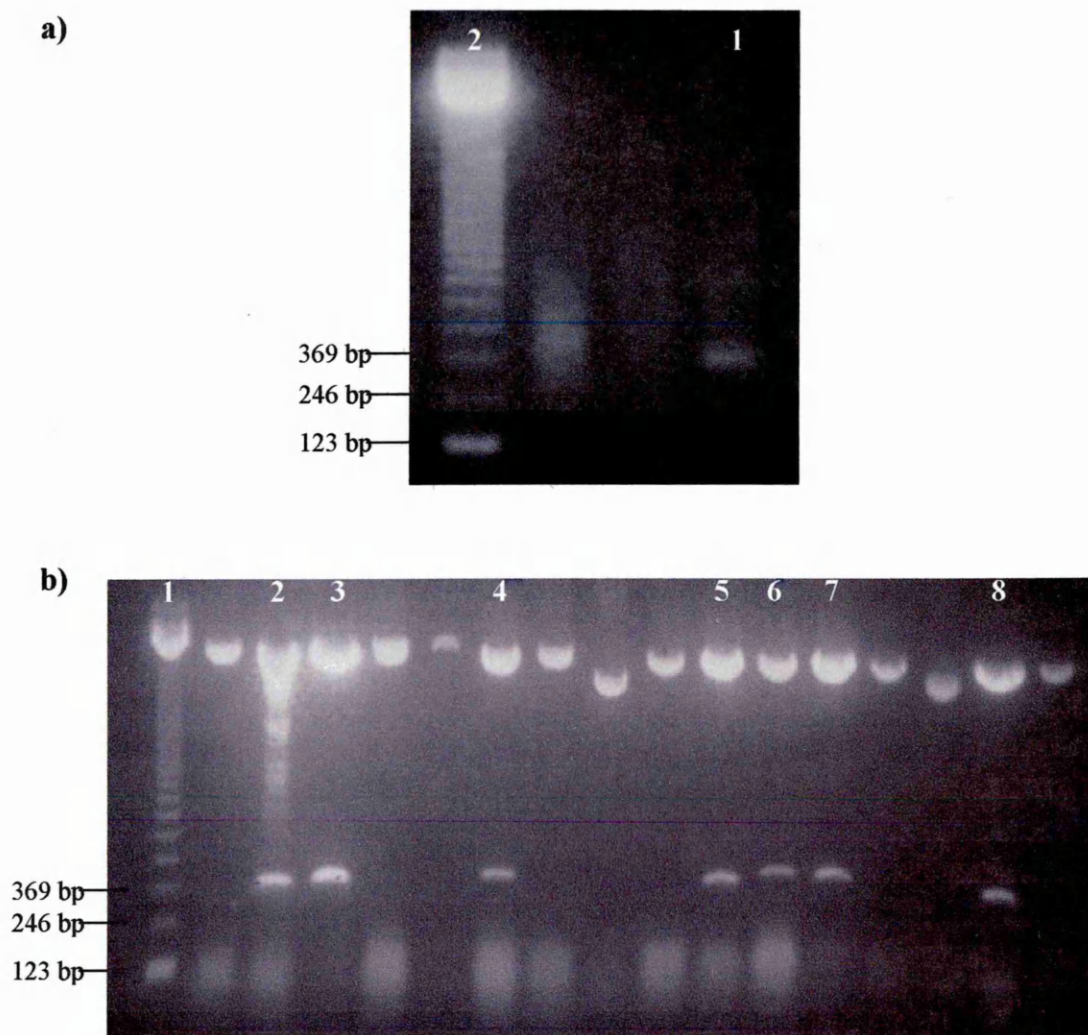
ACAATGTCTG TGTAACCGTA TATGAATAAT TAAAAATGTA CACCTGAACA
ACAATGTCTG TGTAACCGTG AATGAATAAT TAAAAATGTA CACCTGAACA
ACAATGTTTG TGT---CGTG GTTGA----- -----

GATCATTTAA TGAATAATAA ATATTAATAA GCATTAAAAA AAAAAAAAAA
GATCATTTAA TGAATAATAA ATATTAATAA GCATTAAAGAA AAAAAAAAAA
-----

```

The three published short insectotoxin nucleotide sequences were aligned using ClustalW. Bm12 (Zeng et al., 2000) and Bm12-b (Xu et al., 2000 – direct submission to Entrez database) are variants of the same toxin from *Buthus martensii* Karsch. ClTx1 is a chlorotoxin variant from *Leiurus quinquestriatus hebraeus* (Froy et al., 1999). Regions encoding signal peptides are underlined, whilst regions encoding the mature peptide are shown in **bold**. Areas of homology are in **red**.

Fig 3.2 PCR Products and Products of Restriction Digests Observed in the Cloning of Putative Short Insectotoxin cDNA Sequences



(a) Primary PCR was performed using a degenerate Bm-12 signal peptide gene-specific forward-primer, and a universal adaptor-specific reverse-primer on an adaptor-ligated *Mesob. tamulus* cDNA library template. PCR products are shown (lane 1) run on a 1% agarose gel alongside a 123bp ladder (lane2). 20 μ l PCR products were run on a separate agarose gel, excised, purified using a QIAquick column (QIAGEN, USA), ligated into pCR[®]4-TOPO[®] cloning vector (Invitrogen, USA) and transformed into competent *E. coli*. *Lac Z* screening was used to select recombinant colonies for plasmid DNA purification. (b) Plasmids were digested using EcoR1, products visualised by agarose gel electrophoresis using 123bp marker (lane 1), and a number of colonies containing inserts of approx 370bp (lanes 2-8) selected for sequencing.

Fig 3.3 Sequencing of Putative Short Insectotoxin cDNA

a) BtChl1

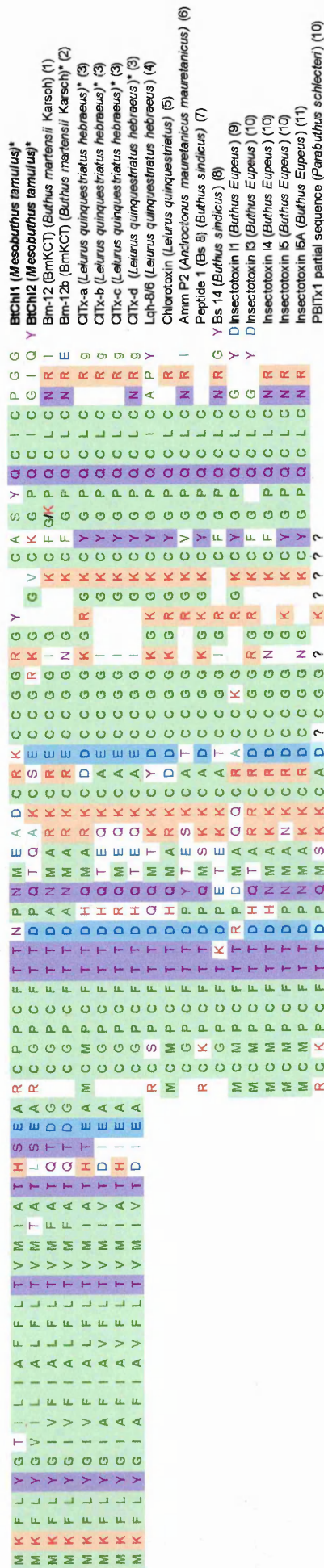
<u>ttaaaa</u>	ATG	AAR	TTY	CTN	TAY	GG						
ttaaaa	ATG	AAG	TTT	CTT	TAT	GGA	ACC	ATT	TTG	ATT	GCT	
	M	K	F	L	Y	G	T	I	L	I	A	
TTT	TTC	TTA	ACT	GTA	ATG	ATT	GCA	ACT	CAT	TCT	GAA	
	F	F	L	T	V	M	I	A	T	H	S	E
GCT	CGT	TGT	CCT	CCT	TGC	TTT	ACA	ACA	AAT	CCG	AAT	
	A	R	C	P	P	C	F	T	T	N	P	N
ATG	GAA	GCC	GAT	TGT	AGG	AAA	TGT	TGC	GGG	GGT	AGG	
	M	E	A	D	C	R	K	C	C	G	G	R
GGA	TAC	TGC	GCT	AGT	TAT	CAA	TGT	ATA	TGT	CCT	GGA	
	G	Y	C	A	S	Y	Q	C	I	C	P	G
GGA	TAA	tatgaatgacccttgaactgcagcgatcattaatg aataaaa aaatattatgacactgtataaaaaaa										
G	STOP											

b) BtChl2

<u>ttaaaa</u>	ATG	AAR	TTY	CTN	TAY	GG						
ttaaaa	ATG	AAG	TTC	CTG	TAT	GGA	GTT	ATT	TTG	ATT	GCT	
	M	K	F	L	Y	G	V	I	L	I	A	
CTT	TTC	TTA	ACT	GTG	ATG	ACT	GCT	ACT	CTG	TCG	GAA	
	L	F	L	T	V	M	T	A	T	L	S	E
GCA	AGG	TGT	GGT	CCT	TGC	TTT	ACA	ACT	GAT	CCT	CAA	
	A	R	C	G	P	C	F	T	T	D	P	Q
ACA	CAA	GCC	AAG	TGT	AGT	GAG	TGT	TGT	GGG	CGA	AAG	
	T	Q	A	K	C	S	E	C	C	G	R	K
GGT	GGA	GTA	TGC	AAG	GGC	CCA	CAA	TGT	ATC	TGT	GGT	
	G	G	V	C	K	G	P	Q	C	I	C	G
ATA	CAA	TAC	TGA	gatgtacacgtgaacattaaggaa aataaaa tattaatataagcactactataaaaaa								
I	Q	Y	STOP									

Seven putative short insectotoxin clones were sequenced using the Sanger dideoxy method (Sanger et al., 1977) on an automated sequencer (model 373A, Applied Biosystems, USA). Five clones produced sequences, which on comparison to known sequences, seemed to belong to the short insectotoxin family. Four of the sequences were as shown in (a). This sequence was named BtChl1. A fifth clone produced the sequence shown in (b), which was named BtChl2. The translation of the nucleotide sequence is shown in **bold**. Primer sequence is also shown (underlined). Potential polyadenylation sites are shown in **red**.

Fig 3-4 Alignment of BtCh11 and BtCh12 with the Amino Acid Sequences of Known Members of the Short Insectotoxin Family



Sequences were aligned manually and coloured by residue type. The consensus sequence is shown in bold and conserved residues are shaded. Sequences marked * were determined from cDNA sequences.

References are in parentheses.

- ¹ Zeng et al., 2000/ Wu et al., 2000
- ³ Froy et al., 1999
- ⁵ Debin et al., 1993
- ⁷ Fazal et al., 1989
- ⁹ Adamovich et al., 1977
- ¹¹ Grishin et al., 1982

²Xu et al., 2000. Entrez database direct submission.

⁴Adjadj et al., 1997

⁶Rosso and Rochat, 1985

⁸Ali et al., 1998

¹⁰Tytgat et al., 1998

3.3.2 Purification of a Putative BtCh11 Peptide from *Mesob. tamulus* Venom

Since the presence of an mRNA sequence in the telson does not prove expression of the gene product in the venom, mass spectrometry was used to screen the venom for masses of a size corresponding to the proposed mature peptide sequences. Since there was uncertainty about C-terminal processing of the BtCh11 peptide, efforts were focussed upon this molecule.

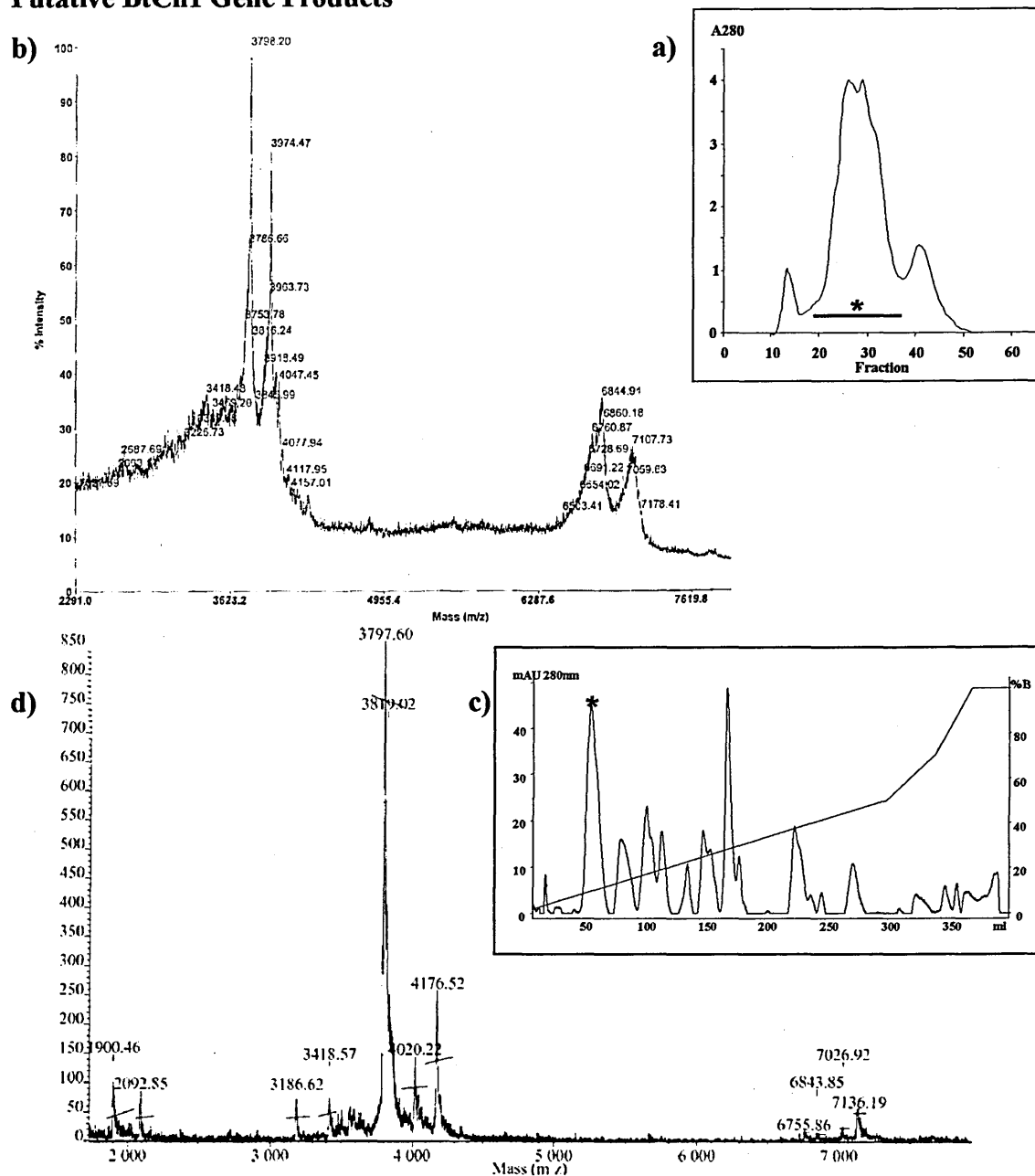
Protein was extracted from crude venom, and the extract fractionated by size exclusion chromatography with the aim of separating low and high molecular weight molecules from the neurotoxic components. Particularly problematic were the mucopolysaccharides, which afforded high viscosity and hydroscopicity to the venom extract, and which it was anticipated that the size exclusion column would remove. Size exclusion chromatography produced three peaks as seen by A280 (fig 3.5a). Mass analysis of the 'main' central peak fractions revealed a significant component of $m/z \sim 3798$ that corresponded to a BtCh11 expression product terminating in a single glycine (fig 3.5b). This initial analysis did not reveal masses relating to any of the other putative BtCh11 mature peptides. It was decided to purify this component further. Since the biological activity of the component was unknown, a mass-spectrometry guided purification approach was employed.

Fractions from the 'main' size exclusion peak were pooled and re-fractionated by ion exchange chromatography (fig 3.5c). Fractions were pooled into eight eluted groups and column flow through. Upon desalting and analysis by mass spectrometry (fig 3.5d), the mass of interest was revealed in ion exchange group 1. This fraction elutes much earlier than potassium channel toxins elute. This is consistent with a less basic molecule such as that encoded by BtCh11. Group 1 was further separated by reverse phase chromatography (fig 3.6a), screened by mass spectrometry and fractions containing the mass of interest pooled. Optimisation of this step, and of a C8 reverse phase clean up stage (fig 3.6b), yielded a product which appeared as two peaks in MALDI-TOF mass spectrometry, one of $m/z 3797 \pm 0.1\%$ and another with a m/z , approximately half of this (fig 3.6c). In order to confirm that these two peaks were indeed related to a single molecular entity and to get a more precise mass, the sample was analysed on a more accurate and sensitive ESI/mass spectrometer. Mass reconstruction of m/z values (fig 3.7) revealed two dominant masses (average masses 3797.2 and 3798.2 Da) exactly one

mass unit apart, possibly representing a single peptide in both amidated and non-amidated forms. The analysis also revealed a number of minor contaminants, or possibly variants of a single component, of masses 3800-3900.

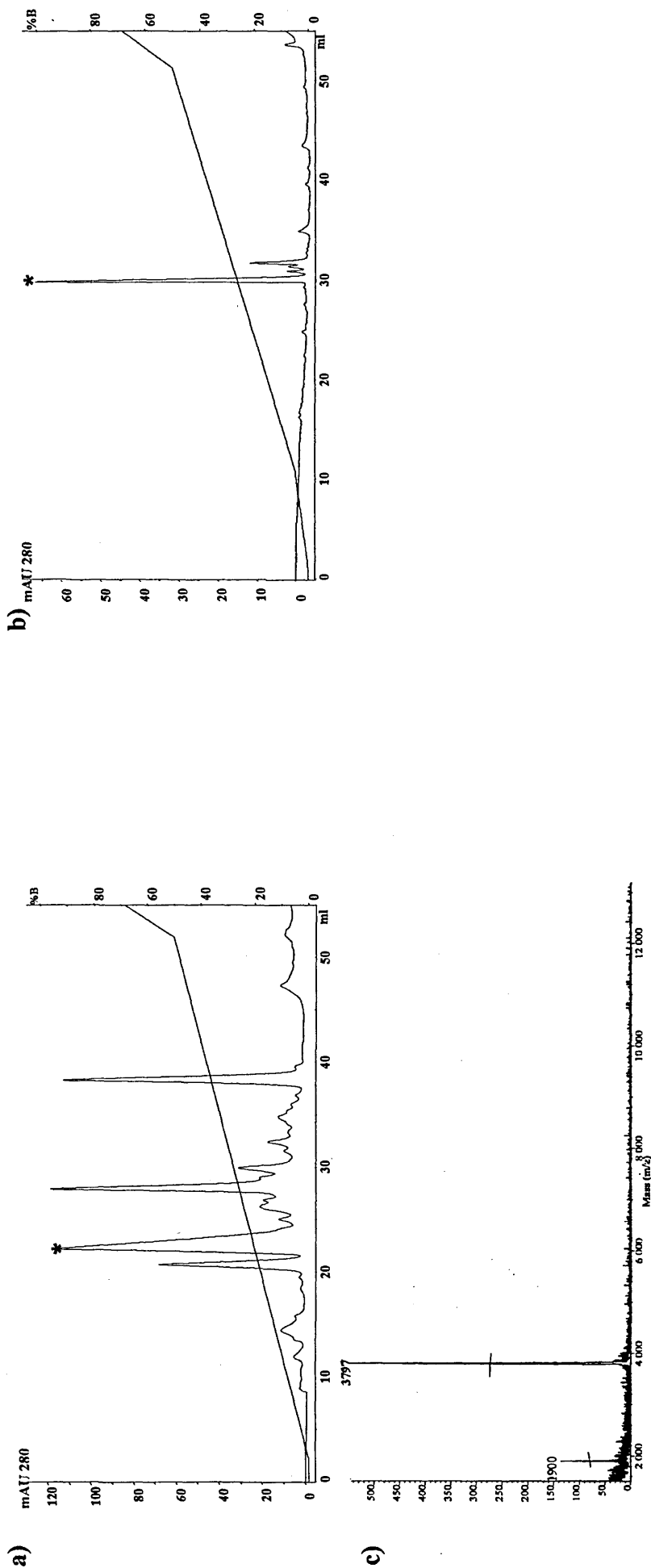
←

Fig 3.5 Size Exclusion and Ion Exchange Chromatography of *Mesob. tamulus* Venom, and Mass Spectrometry of Fractions to Detect Masses Corresponding to Putative BtCh1 Gene Products



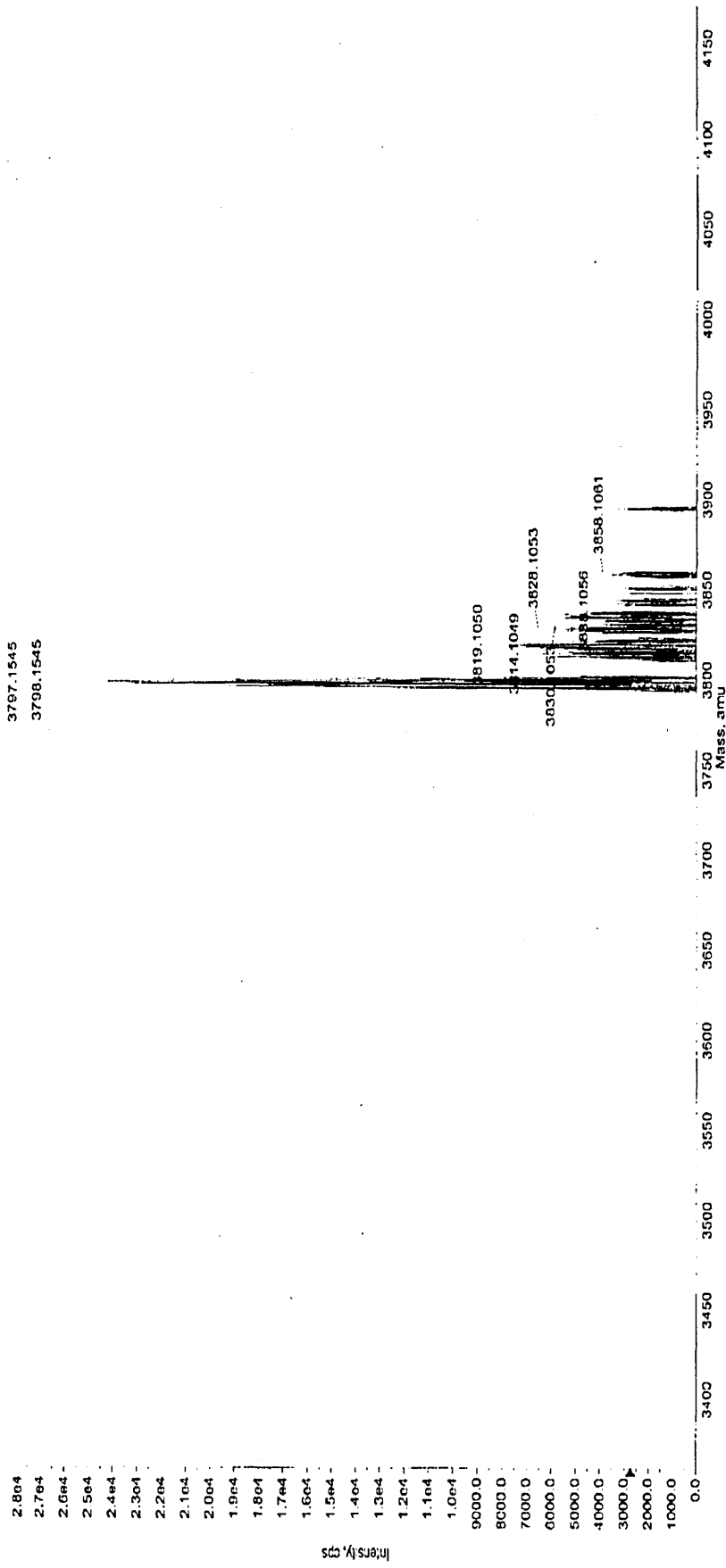
Mesob. tamulus venom was extracted in acidified water and 2ml fractionated by size exclusion chromatography in 50mM ammonium formate on a 75ml Sephadex G50 column. 1ml fractions were collected and the absorbance measured at 280nm (a). Upon analysis by mass spectrometry, a number of fractions from the central 'main' peak were shown to contain a mass of approx 3797 (e.g. b). Fractions in this 'main' peak (19-38 *) were pooled. This pool was applied to an ion exchange column in 100mM NaAc, pH4.8 and eluted by a segmented gradient of 0-1M NaCl in the same buffer (c). Fractions comprising the first peak (*) were pooled to form 'group 1' which was shown by mass spectrometry to contain the mass of interest (d).

Fig 3.6 Purification of a Venom Component of Approximate Mass 3797 by Mass Spectrometry-Guided Reverse Phase Chromatography



Ion exchange group 1 was run on a C18 reverse phase HPLC column, and eluted with a linear gradient of 0-45% acetonitrile in 0.1% TFA over 12 column volumes (a). Fractions were screened by MALDI-TOF/MS and those containing the mass of interest (peak *) were pooled and applied to a C8 reverse phase column. Sample was eluted using a 4.5-27% gradient of acetonitrile in 0.1% TFA over 12 column volumes (b). The marked peak (*) contained a mass of 3797 +/- 0.1% (c).

Fig 3.7 ESI Mass Spectrometry on 3797 Peak from C8 Reverse Phase Column



The purified product shown in figure 3.6c was subjected to ESI mass spectrometry on a more sensitive and accurate instrument in order to gain a better measure of peptide purity and to get an accurate mass. As can be seen above the peptide is not totally pure and is predominately a mixture of 3797.2 and 3798.2 (average mass) masses.

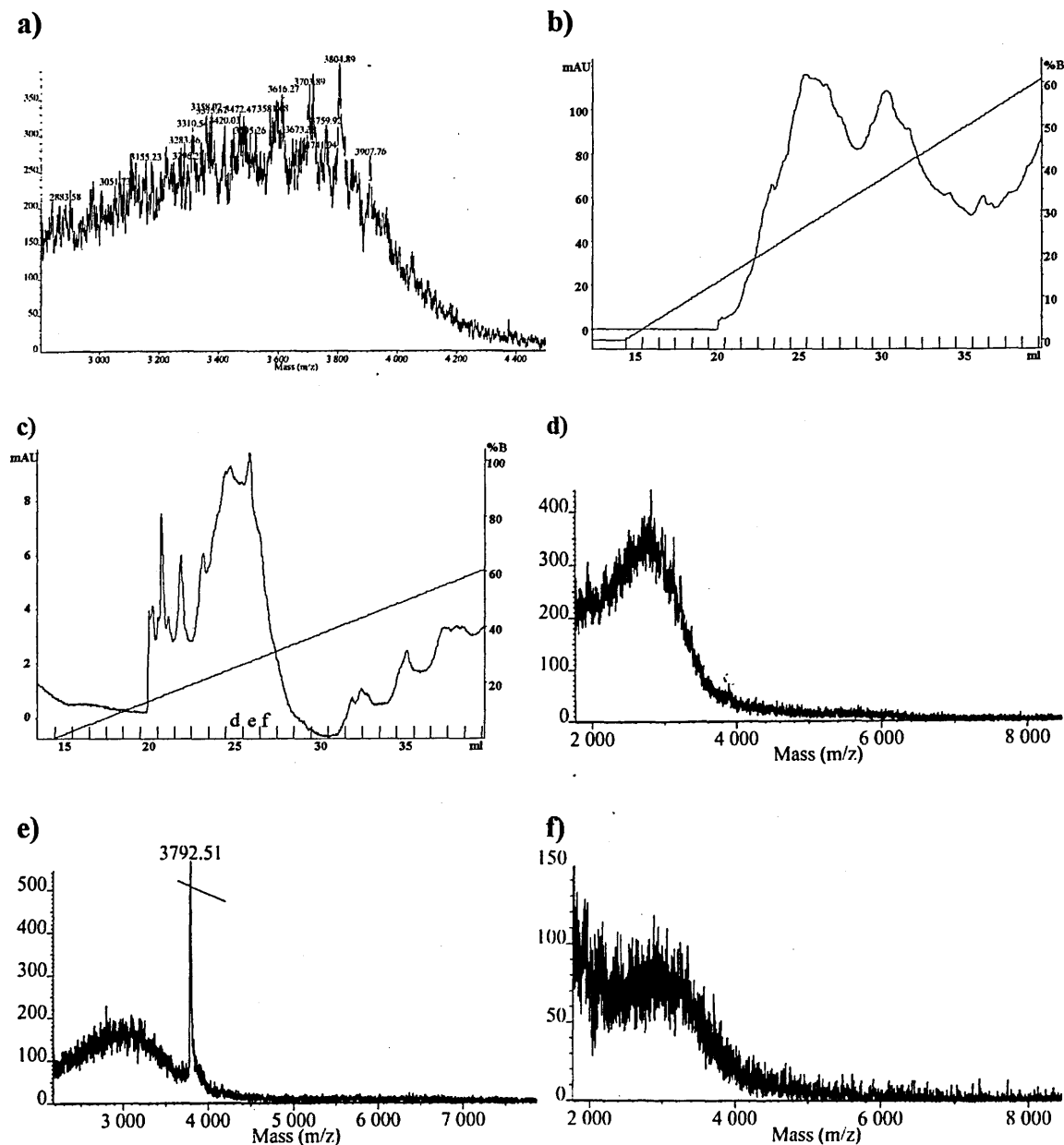
3.3.3 Synthesis and Purification of a Synthetic BtChl1

A non-amidated version of the putative mature BtChl1 peptide (terminating in a single C-terminal glycine) was synthesised 'in house'. Two previous synthesis attempts by alternative commercial peptide synthesis services had failed. It was initially intended that the mature peptide be purified by HPLC, as followed by mass spectrometry, prior to folding. Initial experiments suggested, however, that the synthesis had been unsuccessful. Mass spectrometry on a solution of the crude peptide (fig 3.8a) failed to show the presence of any dominant mass. Reverse phase chromatography failed to indicate the presence of discrete synthesis products (fig 3.8b), and mass spectrometry on the resultant fractions failed to detect an appropriate discrete mass.

It was decided to attempt to fold any peptide present prior to purification. A simple folding procedure was undertaken, in which the crude synthetic peptide was allowed to gently oxidise in buffer solution. After 94hrs, a considerable amount of material was present as a precipitate, but some material was in solution. Separation of this folded solution by C18 reverse phase chromatography produced far greater peak resolution than obtained previously (fig 3.8c), and mass spectrometry of the fractions indicated the presence of a mass of interest (fig 3.8d-f).

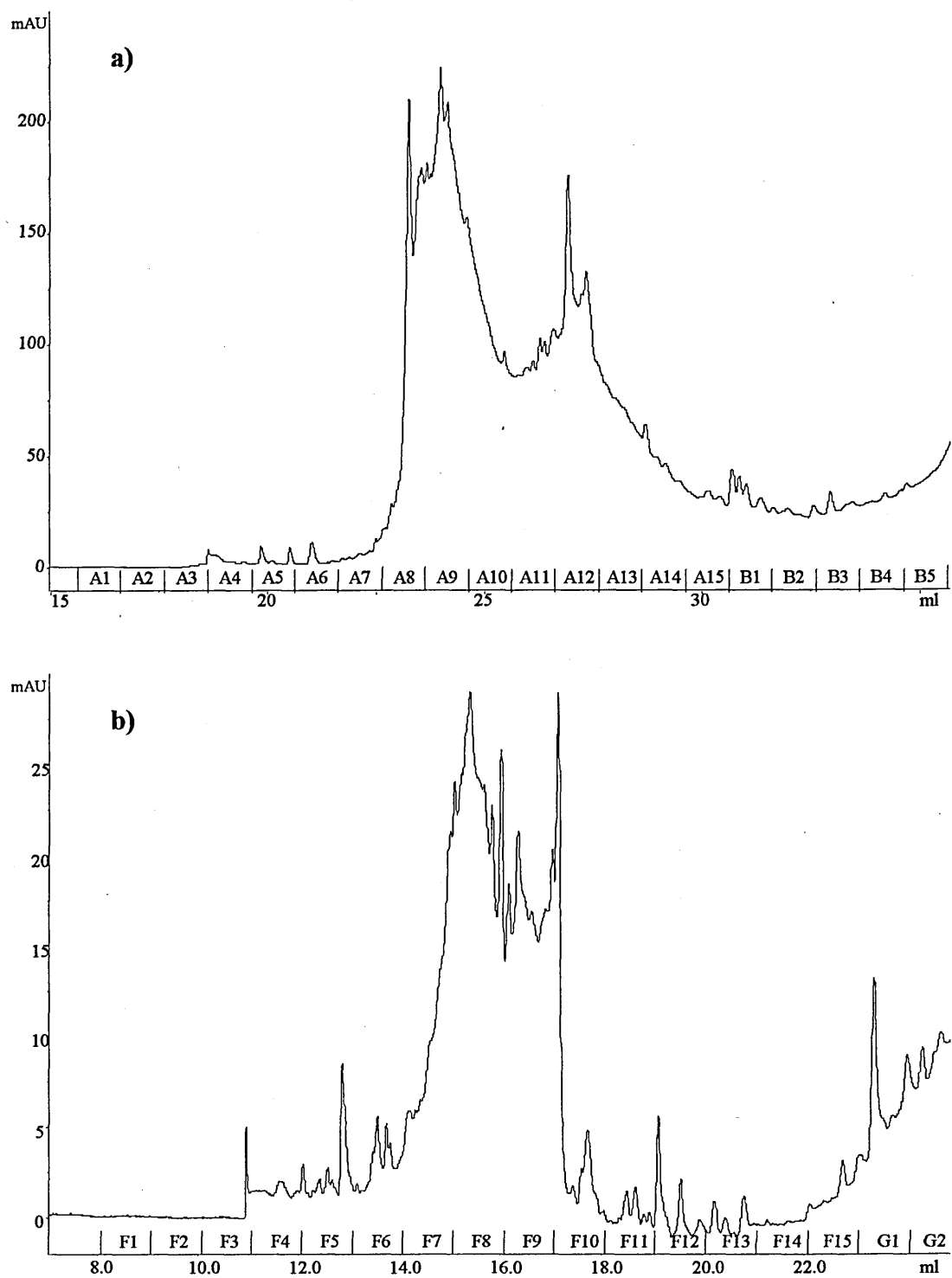
Although the yield was low, since this was the only material of the correct mass isolated from any synthesis, it was decided to purify this material in order for its biological activity to be assessed. Attempts to utilise a C8 column failed; neither the unfolded nor folded crude solutions yielded fractions containing peaks of interest (fig 3.9). Peptide-containing fractions from the C18 column also gave a disappointing result when applied to a C8 column. Purification of the folded peptide was instead improved by further optimisation of the solvent gradient on the C18 column. Final conditions yielded a single fraction containing an appropriate mass at acceptable purity, and additional, more complex, fractions also containing the mass of interest (fig 3.10). The purified fractions from a number of experiments were pooled and stored at -20°C . Remaining fractions containing the peak of interest were pooled, concentrated and re-purified under identical conditions.

Fig 3.8 Analysis of Crude and Folded Synthetic BtCh11 by Reverse Phase HPLC and MALDI-TOF Mass Spectrometry



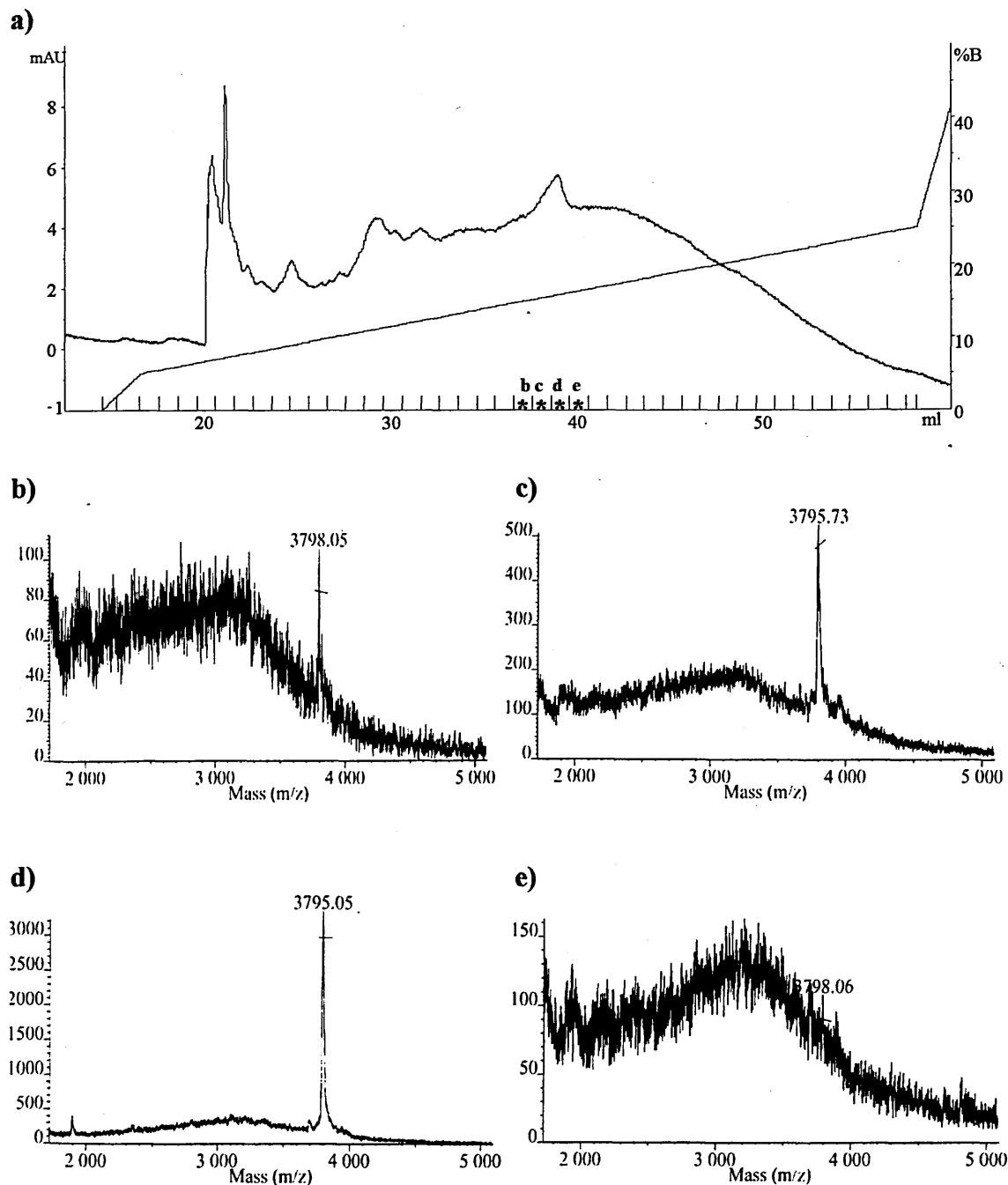
A solution of crude synthetic BtCh11 was analysed by MALDI-TOF/ MS (a) and 1mg fractionated by reverse phase HPLC on a C18 column at 0.5ml min^{-1} (b). Samples were eluted with a 0-100% linear gradient of 90% acetonitrile in 0.1% TFA. The eluent was monitored at 280nm and 1ml fractions collected. All fractions were analysed by MALDI-TOF/ MS but none contained the mass of interest. The crude peptide was allowed to fold (1mgml^{-1} in 20mM NaPO_4 pH8.2, agitated under air for 94hrs), and 1ml fractionated as above (c). All fractions were analysed by MALDI-TOF/MS. One fraction showed evidence of a mass potentially representing BtCh11 (d-f).

Fig 3.9 Fractionation of Crude and Folded BtChl1 on a C8 Reverse Phase HPLC Column



Crude (a) and folded (b) solutions of synthetic BtChl1, identical to those previously run on a C18 column, were fractionated by C8 reverse phase HPLC. Samples were eluted with a 0-100% linear gradient of 90% acetonitrile in 0.1% TFA. The eluent was monitored at 280nm and 1ml fractions collected. All fractions were analysed by MALDI-TOF/ MS but none contained the mass of interest.

Fig 3.10 Optimised HPLC Fractionation of Folded Synthetic BtCh11 Analysed by MALDI-TOF/ MS



1ml folded synthetic BtCh11 solution was fractionated on a C18 reverse phase column (a). The sample was eluted at 1ml min^{-1} with a 4.5-22.5% gradient of acetonitrile in 0.1% TFA. 1ml fractions were collected and analysed by mass spectrometry. MALDI-TOF profiles of four fractions (*) are shown. Fraction d contained a molecule of the predicted mass with relatively little contamination. Fractions (b, c and e) also contained the molecule of interest but at low purity.

3.3.4 Homology Modelling of BtChl1 and BtChl2

Automated comparative modelling was carried out using Swiss-Model. BtChl1 and BtChl2 were each modelled using 1CHL (chlorotoxin), 1SIS (I5A) and 1CHL + 1SIS as templates. Analysis of the parent structures by WHAT IF suggested 1SIS to be the more reliable of the template structures. Similarly, modelling on 1SIS produced apparently better structures than modelling on 1CHL alone or 1CHL in conjunction with 1SIS. The structures produced with 1SIS as a template were no less reliable than the parent structures, and it was these 1SIS-derived models that were used for analysis. Structures obtained for BtChl1 and BtChl2 are shown (fig 3.11a), together with the published structures of insectotoxin I5A and chlorotoxin. The new molecules share the same basic structure as chlorotoxin, of an α -helical region (purple) and three stretches of β -sheet (green) cross-linked by four disulphide bridges (yellow). The C-terminal stretch of β -sheet is divided into two fragments in BtChl2.

The electrostatic surfaces of the four insectotoxins were calculated, and are illustrated alongside that of the potassium channel blocker charybdotoxin (fig 3.11b). The surface charge differences between the two groups of molecules are obvious, the insectotoxins having far more neutral (white) and negative surfaces (red) than the potassium channel toxin, which has predominately positive surfaces (blue). The negative charges at the C-terminus (top-right) should be viewed with caution, however, since the amidation status of BtChl1 and chlorotoxin is unknown. Interestingly, the highly conserved negative charge at position 9 has surface effects only in chlorotoxin (bottom centre, red region in chlorotoxin).

Fig 3.11 Homology Modelling of BtChl1 and BtChl2 and Calculation of their Electrostatic Surfaces

a) Automated comparative modelling of the putative mature toxins encoded by BtChl1 and BtChl2 was carried out using Swiss-Model in the 'first approach' mode. The template structure (insectotoxin I5A, 1SIS, Lomize et al., 1991) was obtained from the RCSB Protein Databank. The structure of chlorotoxin (1CHL, Lippens et al., 1995) is shown for comparison. Stereoscopic images were produced from the PDB data using Protein Explorer.

b) Molecular surfaces were calculated, and electrostatic potentials computed and mapped to these surfaces using DeepView. Potentials were calculated using the coulomb computation method and atomic partial charges. Cut-offs: - red=-1.6kT/e; white=0.0kT/e; blue=1.6kT/e (k is the Boltzmann constant, T is temperature in Kelvin, and e is the charge of the electron. At 298K $kT/e=25.6$ mV). Non-amidated forms of the short insectotoxins were used. Charybdotoxin (2CRD, Bontems et al., 1992) is shown for comparison. Orientation is as for (a), with the α -helix to the left and the C-terminus pointing to the top right.

Fig 3.11a Stereoscopic Images of BtCh1 and BtCh2 Obtained by Homology Modelling.

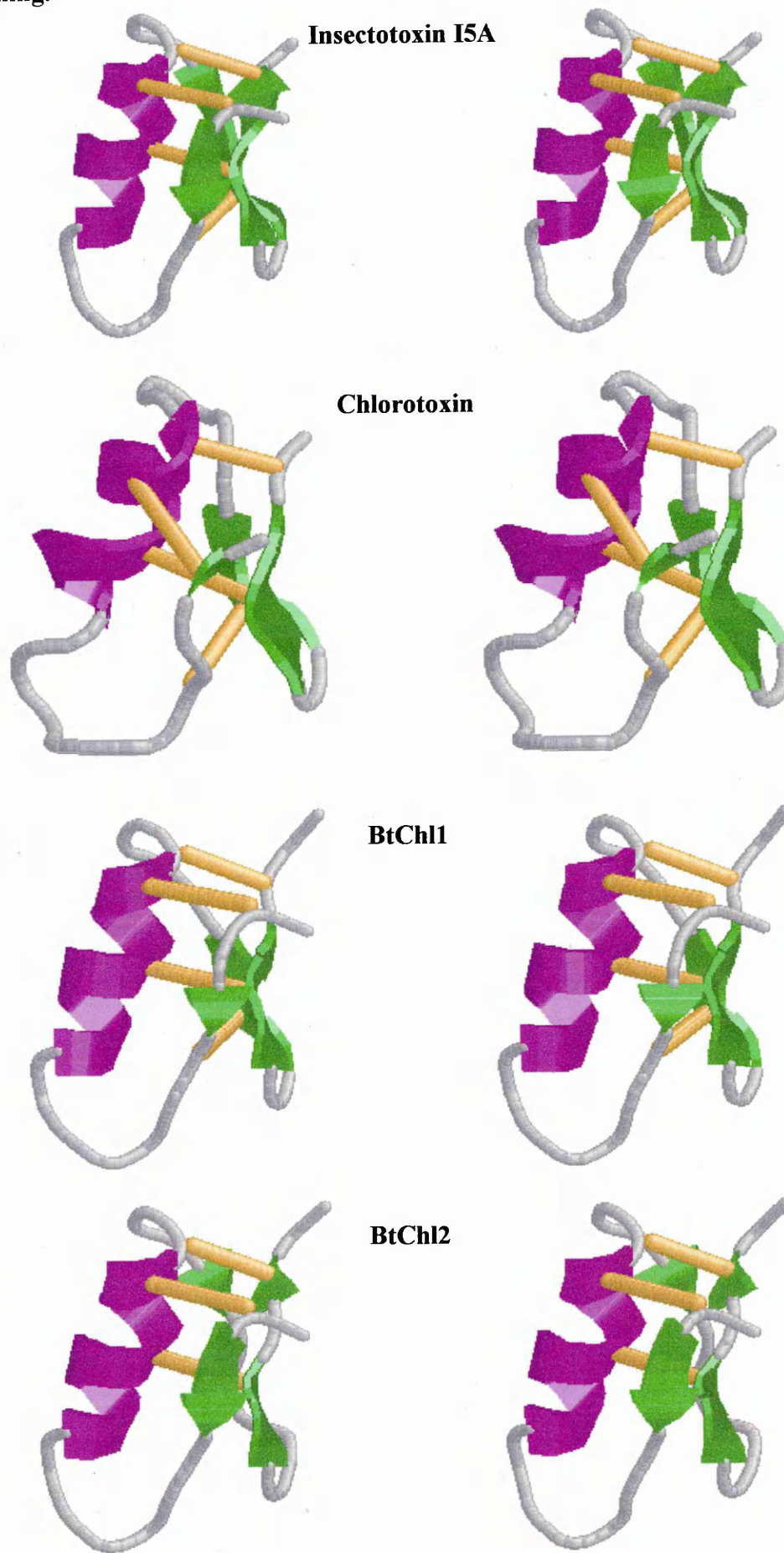
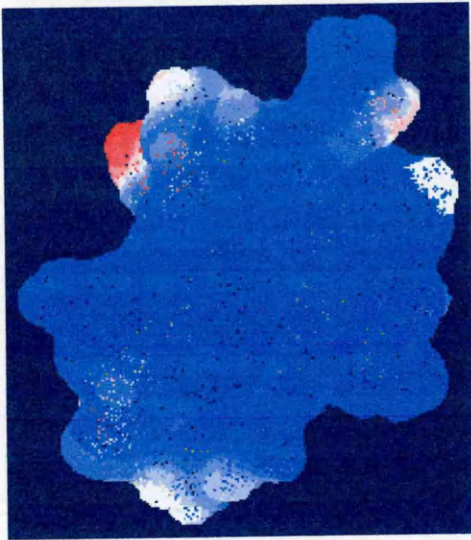
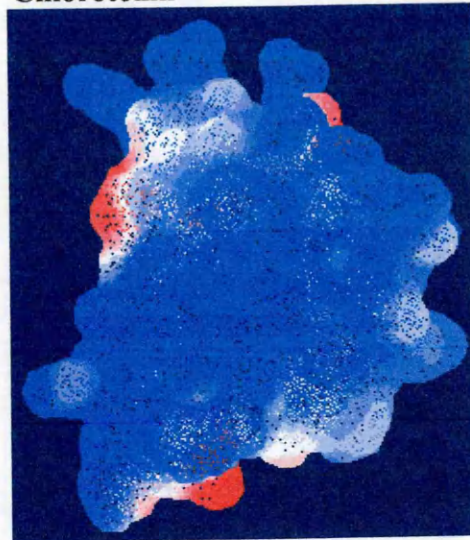


Fig 3.11b Electrostatic Surfaces of Short Insectotoxins and Charybdotoxin

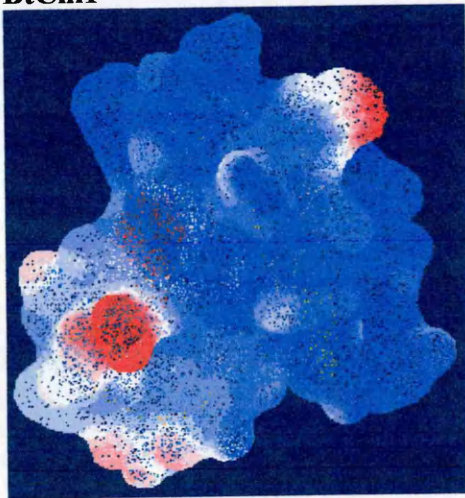
Insectotoxin I5A



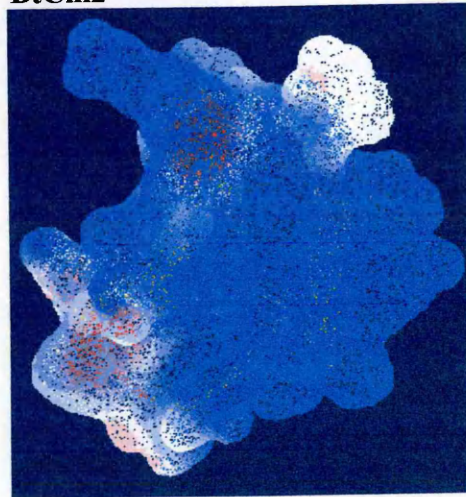
Chlorotoxin



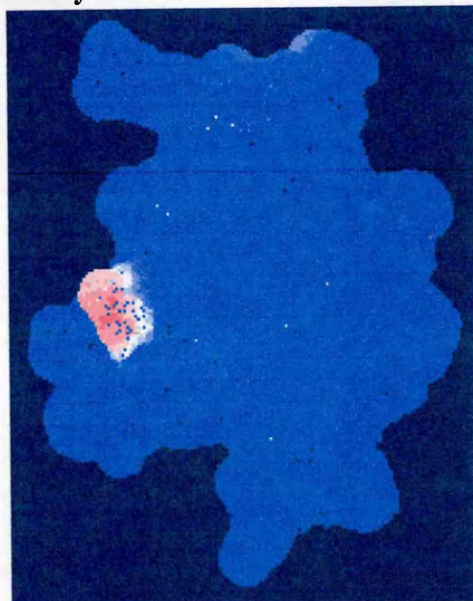
BtCh1



BtCh2



Charybdotoxin



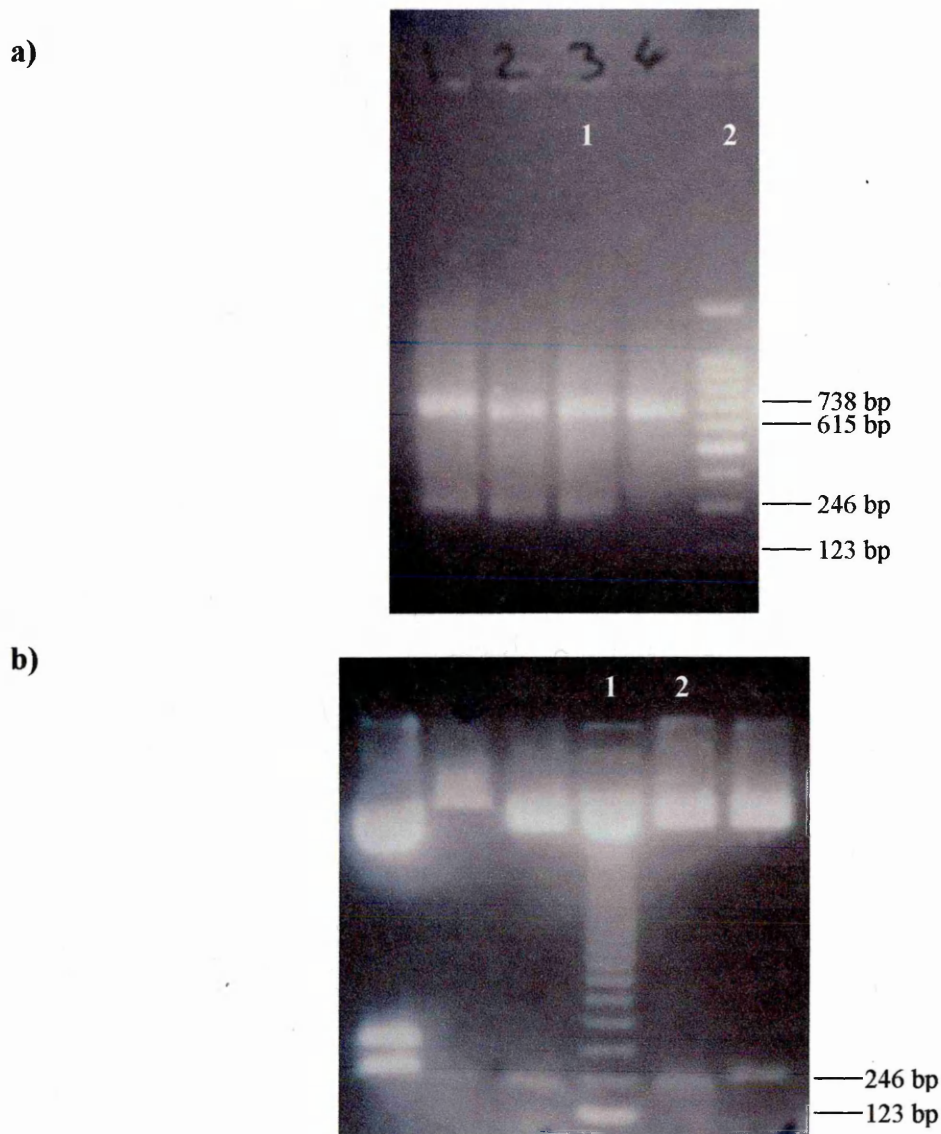
3.3.5 Analysis of the 3' UTR of Tamulustoxin cDNA

There is circumstantial evidence to suggest amidation of the tamulustoxin C-terminus (discussed in 3.1). The same adaptor-ligated cDNA library used to generate the chlorotoxin-like sequences was used to examine the 3'UTR and C-terminal precursor-peptide sequence of tamulustoxin, with the aim of providing further evidence for C-terminal amidation of the toxin.

Primary- and secondary-PCR was carried out using nested adaptor-primers and a degenerate gene-specific primer based upon the N-terminal peptide sequence of tamulustoxin. After optimisation of conditions, secondary PCR yielded two bands of approx. 245 and 730 base pairs (fig 3.12a) as visualised by agarose gel electrophoresis. The PCR mixture was directly purified on a QIAquick column (Qiagen), ligated into pCR[®]4-TOPO[®] vector, and transformed into competent *E. coli*. After blue/white screening a number of colonies were selected and plasmid DNA purified by miniprep. Restriction digests on minipreps from a number of colonies revealed inserts of approx. 245 base pairs, a size similar to the lower PCR band (examples shown in fig 3.12b).

Several positive clones were selected for sequencing. In total 12 clones were identified with sequences corresponding to tamulustoxin. Three clones were re-sequenced using an alternative sequencing primer, yielding identical results. The consensus sequence is shown (fig 3.13a). Some sequence discrepancies did occur between the clones, although, in the majority of cases, the difference occurred in a single clone. There were more serious discrepancies, however, but these were primarily located in the region of primer binding and were, in all cases, conservative. As can be seen (fig 3.13b), there is also slight variation between this sequence and that previously reported (Strong et al., 2001). This would not appear to be restricted to ambiguities in the new sequence but is, in all cases, conservative. The translated sequence of the peptide precursor reveals a potential amidation site (GK) at the C-terminus.

Fig 3.12 PCR Products and Products of Restriction Digests Observed in the Cloning of 3' Tamulustoxin cDNA Sequences



(a) Primary and secondary PCR reactions were performed using degenerate tamulustoxin gene-specific forward-, and universal adaptor-specific reverse-primers on an adaptor-ligated *Mesob. tamulus* cDNA library template. Secondary PCR products are shown (lane 1) run on a 1% agarose gel alongside a 123bp ladder (lane2). Products were purified directly from the PCR reaction mixture using a QIAquick column (Qiagen, USA), ligated into pCR[®]4-TOPO[®] cloning vector (Invitrogen, USA) and transformed into competent *E. coli*. Lac Z screening was used to select recombinant colonies for plasmid DNA purification.

(b) Plasmids were digested using EcoR1, products visualised by agarose gel electrophoresis using 123bp marker (lane 1), and a number of colonies containing inserts of approx 250bp (e.g. lane 2) selected for sequencing.

Fig 3.13 Sequencing of Tamulustoxin cDNA to Identify Cleaved N-Terminal and 3'UTR Sequences

a)

<u>CGY</u>	<u>TGY</u>	<u>CAY</u>	<u>TTY</u>	<u>GTY</u>	<u>GTY</u>	<u>TGY</u>	<u>AC</u>					
CGT	TGT	CAT	TTT	GTT	GTT	TGC	ACT	ACT	GAC	TGT	CGT	
R	C	H	F	V	V	C	T	T	D	C	R	
CGG	AAT	TCT	CCT	GGT	ACA	TAC	GGA	GAA	TGC	GTA	AAG	
R	N	S	P	G	T	Y	G	E	C	V	K	
AAA	GAA	AAG	GGT	AAA	GAA	TGC	GTT	TGT	AAA	AGT	GGA	
K	E	K	G	K	E	C	V	C	K	S	G	
AAA	TAA	aattcgacgtc tcctttctt gagaataaa aatcaatctt gatttatg tcatggttt tcaagtgaat										
K	stop											
aaagaaaatt aaaattgaa aaaaaaaaa												

b)

CGT	TGT	CAT	TTT	GTT	GTT	TGC	ACT	ACT	GAC	TGT	CGT	
R	C	H	F	V	V	C	T	T	D	C	R	
<i>CGC</i>	<i>TGT</i>	<i>CAT</i>	<i>TTC</i>	<i>GTT</i>	<i>GTT</i>	<i>TGT</i>	<i>ACT</i>	<i>ACT</i>	<i>GAC</i>	<i>TGT</i>	<i>CGT</i>	
CGG	AAT	TCT	CCT	GGT	ACA	TAC	GGA	GAA	TGC	GTA	AAG	
R	N	S	P	G	T	Y	G	E	C	V	K	
<i>CGG</i>	<i>AAT</i>	<i>TCT</i>	<i>CCT</i>	<i>GGT</i>	<i>ACA</i>	<i>TAC</i>	<i>GGA</i>	<i>GAA</i>	<i>TGC</i>	<i>GTA</i>	<i>AAA</i>	
AAA	GAA	AAG	GGT	AAA	GAA	TGC	GTT	TGT	AAA	AGT	GGA	
K	E	K	G	K	E	C	V	C	K	S	G/stop	
<i>AAA</i>	<i>GAA</i>	<i>AAA</i>	<i>GGC</i>	<i>AAG</i>	<i>GAA</i>	<i>TGT</i>	<i>GTT</i>	<i>TGT</i>	<i>AAA</i>	<i>TCT</i>	<i>TGA</i>	
AAA	TAA											
K/-	stop/-											
----	----											

Putative tamulustoxin clones were sequenced using the Sanger dideoxy method (Sanger et al., 1977) on an automated sequencer (model 373A, Applied Biosystems, USA). Twelve sequences corresponding to tamulustoxin were obtained. Three of these were also sequenced on the second strand, confirming previous results. The consensus cDNA sequence is shown, together with the deduced amino acid sequence (a). Bases conserved in all clones sequenced are shown in black. Those in blue differed in a single clone, whilst those in red showed deviation from the consensus in more than one clone. All observed deviations were conservative. Non-translated regions are in lower case; putative polyadenylation signals are in green. For the amino acid sequence, residues present in the mature toxin are in bold. Primer sequence is underlined. (b) Shows the consensus cDNA sequence (top) aligned against that previously published (below, italics) (Strong et al., 2001). Sequence discrepancies are highlighted.

3.3.6 Identification of a Long-Chain Potassium Channel Toxin-Like Signal Peptide Sequence in *Mesob. tamulus* cDNA

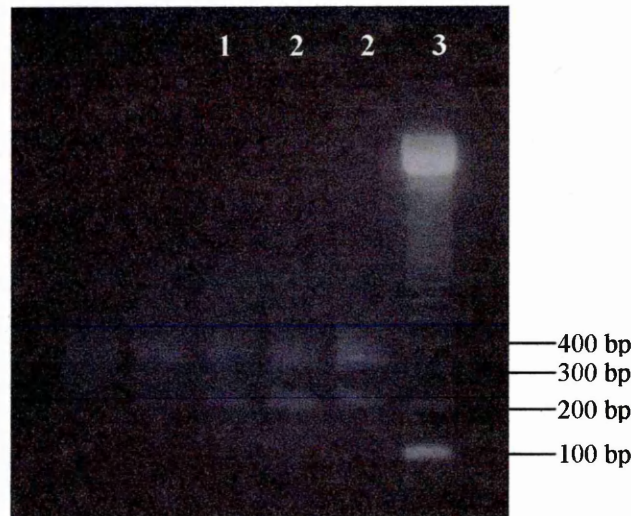
During the course of experiments utilising tamulustoxin cDNA, a sequence was identified which has similarity to a signal peptide for a long-chain potassium channel toxin.

The same adaptor-ligated cDNA library used to generate the chlorotoxin-like sequences was probed with primers based upon the published C-terminal amino acid sequence of tamulustoxin. Primary- and secondary-PCR was carried out using nested adaptor-primers and a degenerate tamulustoxin-specific reverse primer. Secondary PCR yielded two bands of approx. 200 and 350 base pairs (fig 3.14a), as visualised by agarose gel electrophoresis. The lower molecular weight bands from two PCR reactions were excised, the DNA purified on a QIAquick column (Qiagen), ligated into pCR[®]4-TOPO[®] vector and transformed into competent *E. coli*. After blue/white screening a number of colonies were selected, the DNA purified by miniprep and restriction digests performed. A single clone contained an insert of just under 200bp (fig 3.14b), which was then sequenced (fig 3.15).

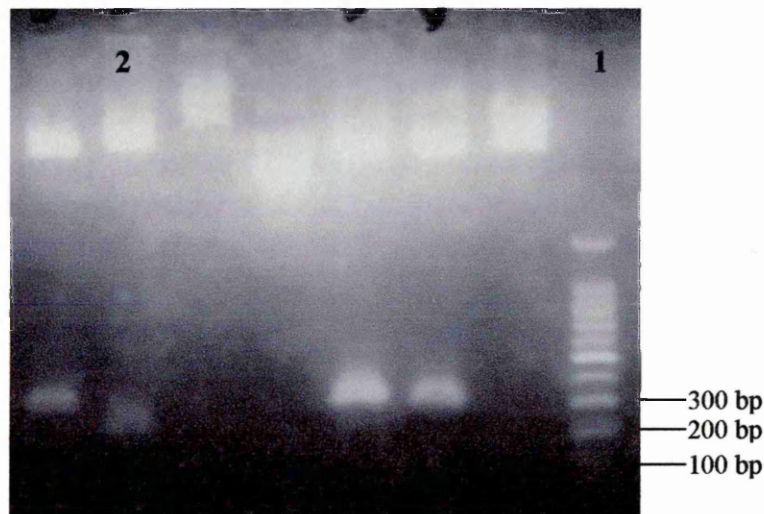
Upon analysis by BLAST (NCBI public database) the sequence proved to be homologous to the 5'UTR and part of the signal peptide of BmTxK β , a putative long-chain potassium channel inhibitor from *Buthus martensii* (Zhu et al., 1999).

Fig 3.14 PCR Products and Products of Restriction Digests Which Yielded a Putative Long Chain Potassium Channel Toxin Signal Peptide

(a)



(b)



(a) Primary and secondary PCR reactions were performed using degenerate tamulustoxin-specific reverse-primers and universal adaptor-specific forward-primers on an adaptor-ligated *Mesob. tamulus* cDNA library template. Primary (lane 1) and secondary (lanes 2) PCR products are shown run on a 1% agarose gel alongside 100bp ladder (lane 3). The smaller bands from secondary PCR were excised, purified using a QIAquick column (Qiagen, USA), ligated into pCR[®]4-TOPO[®] cloning vector (Invitrogen, USA) and transformed into competent *E. coli*. Lac Z screening was used to select recombinant colonies for plasmid DNA purification.

(b) Plasmids were digested using EcoR1 and the products visualised by agarose gel electrophoresis using a 100bp marker (lane 1). The colony that contained the small (approx 200 bp) insert (lane 2) was selected for sequencing.

Fig 3.15 TxK β Signal Peptide-Like cDNA Sequence from *Mesob. tamulus*

```

attttacatagcccgaagattatcaaataaacg ATG AAA CAA CAA TTC TTC TTG
      M   K   Q   Q   F   F   L
      M   M   K   Q   Q   F   F   L
caattttacatagcccgaagattatcggtaaattg ATG AAA CAA CAG TTC TTC TTG

TTC TTA GCA GTG ATT GTG ATG CAN NCT TCT GTC ATT
  F  L  A  V  I  V  M  ?  ?  S  V  I
  F  L  A  V  I  V  M  I  S  S  V  I
TTC TTA GCG GTG ATT GTG ATG ATT TCT TCT GTC ATT

GAA AAA AGA AAA GGG CAA GGA A
  E  K  R  K  G  Q  G
  E  A  G  R  G  K  E  M
GAG GCG GGA AGA GGC AAG GAA ATG.....

```

Mesob. tamulus telson cDNA clones were sequenced using the Sanger dideoxy method (Sanger et al., 1977) on an automated sequencer (model 373A, Applied Biosystems, USA). Upon submission to BLAST (NCBI public database) the insert of a single clone had high homology to TxK β signal peptide (Zhu et al., 1999). The cloned sequence, together with the amino-acid translation, is shown in black above. The published TxK β signal peptide sequence is shown in *blue italics*. The region of binding of the tamulustoxin reverse primer is underlined. Differences between the observed and published sequences are **highlighted**.

3.4 Discussion

3.4.1 Short Insectotoxins

This chapter identifies the first short insectotoxin cDNA sequences to be isolated from *Mesob. tamulus*, and the most complete cDNA sequences from this scorpion to date. Prior to this study, only three short insectotoxin nucleotide sequences had been published, and two of these were isotoxins. BtCh11, identified here, encodes a 60aa precursor consisting of a putative 24aa signal peptide and a C-terminally processed mature peptide. The 62aa protein encoded by BtCh12 was assumed to be a precursor for a 38aa mature peptide.

The site of cleavage of the signal peptide was predicted according to the method of von Heijne (von Heijne, 1986). This is a modification of the (-3, -1) rule which looks at the properties of residues in two positions, N-terminal to the possible cleavage site. The method uses a weighted matrix to assess the probability of a particular residue occurring at each position from -13 to +2 from the cleavage site. The peptide is scored using each of the proposed cleavage sites, the site with the highest score having the greatest probability of cleavage. Both of the sequences deduced from this study were subjected to this analysis, the results being consistent with those that would be predicted from a comparison with known mature insectotoxin sequences.

Although the C-terminus of BtCh12 was assumed to be a tyrosine, the C-terminus of BtCh11 was less clear. C-terminal glycine residues in unprocessed peptides are often utilised to produce an amidated mature protein. In scorpion toxins, however, this is usually only the case if the glycine is followed by one or two positive residues. If there are three positive residues, cleavage alone generally occurs. (See section 3.4.2 for a more detailed discussion of scorpion toxin amidation.) In the case of BtCh11, there are no basic C-terminal residues and two glycines. Investigation of venom components by mass spectrometry, however, revealed a significant mass corresponding to the version terminating in a single glycine.

Since the deposition of these cDNA sequences in the database, both native toxins have been isolated by different groups. In the case of BtCh11, the amino acid sequence confirms this study's prediction as to the location of the N-terminus, and reveals that the

precursor undergoes C-terminal processing. Dhawan et al., 2002, reported a 35mer, toxic to insects, which is consistent with that encoded by BtChl1, with the removal of a single C-terminal glycine. The amidation status of the carboxylate residue is unclear.

Wudayagiri et al, 2001, reported the purification of a short insectotoxin from *Mesob. tamulus* that had lepidopteran toxicity. This native amino acid sequence (validated by mass spectrometry data) is identical to that predicted by BtChl2 cDNA, but with the omission of the C-terminal tyrosine. Since the cDNA sequence, described here, was derived from a single clone, there is the possibility of a sequencing error. However, the occurrence of an error that inserts a single amino acid, leaving the remaining sequence intact, is highly unlikely. We therefore assume this to be a real phenomenon. The additional tyrosine may thus either be the result of a polymorphism, or indicative of C-terminal processing of the insectotoxin precursor. If the observed nucleotide sequence was indeed the result of polymorphism, it would be interesting to examine the effect of this extra residue on activity. If the native peptide is the result of C-terminal processing of the precursor molecule, this processing again differs from that traditionally seen with scorpion toxins.

All of the chlorotoxin homologues found in *L. quinquestratus hebraeus* that have had their precursor sequences reported (ClTx-a to ClTx-d) have a C-terminal glycine (Froy et al., 1999) and no subsequent basic residues. On comparison with native chlorotoxin, one would predict post-translational cleavage of this glycine residue. Bm-12 however, shows no C-terminal processing (Wu et al., 2000, Zeng et al., 2000). Some other short insectotoxins are reported to be amidated (e.g. I5, I5A, Ovchinnikov, 1984), whilst others have been shown to have a free C-terminus (e.g. AmmP2, Rosso and Rochat, 1985). The short insectotoxins may therefore demonstrate a different pattern of C-terminal processing from that seen in sodium channel scorpion toxins (see Possani et al., 1999 for details on sodium channel toxin processing).

Alignment of the short insectotoxins shows this group of peptides to be highly homologous. Aside from chlorotoxin, which has been reasonably well studied, very little is known about their physiological effects. Consequently, nothing is known about structural requirements for blocking chloride channels or inhibiting MMP-2 activity. It would therefore be interesting to assess the functional properties of BtChl1 and 2, and to assess their potential as chloride channel specific probes. This requires either the

purification of the native molecule, the synthesis of the peptide by solid-state methods or the generation of a recombinant analogue.

The presence in the venom of a component of molecular mass ~3797Da (one of those which would be predicted from analysis of the BtCh11 cDNA sequence) supported the case for peptide BtCh11 being an expressed venom protein terminating in a single glycine residue. In the absence of a functional assay for short insectotoxins (the use of insect neurotoxicity as a bioassay would be hampered by the presence of more potent and abundant long-chain insectotoxins in the venom), it was decided to purify the venom peptide that had the appropriate mass. Konno et al., 2001 utilised MALDI-TOF/MS guided fractionation to purify peptides from wasp venom. This type of approach enables characterisation of the native peptide with little loss of sample, therefore maximising output from the purification.

ESI analysis of the purified component showed average masses of 3797.2 and 3798.2 Da plus minor contaminants. Calculated masses for the amidated and non-amidated forms of BtCh11 (assuming peptide termination after Gly35) were 3797.4 and 3798.4 Da respectively. Mass spectrometry analysis did not reveal the presence of masses corresponding to any other putative BtCh11 expression products (see chapter 2). This peptide is thus the most likely venom candidate for the expression product of BtCh11 cDNA. After confirmation of the primary sequence, this peptide will be used for studies on biological activity.

As previously mentioned, the native peptide sequence has since been reported (Dhawan, et al., 2002), confirming the proposed C-terminal processing. The native toxin has a similar mass to the peptide purified in this study (3796.5Da, by MALDI-TOF/MS), but would appear to elute from a C18 reverse phase column at a far higher acetonitrile concentration. It is hoped that sequence analysis of the purified peptide will reveal its molecular identity, either as a short insectotoxin or as a new venom component from *Mesob. tamulus*.

The crude synthetic peptide was not of good quality or yield. However, since two previous synthesis attempts by outside commercial services had failed, it was decided to persist with purification of the peptide despite the bad quality. This poor quality meant that HPLC traces were of little use and the extensive use of mass spectrometry was

crucial. Initial folding attempts yielded a peptide of the correct mass, identifiable by mass spectrometry, which was purified by reverse-phase HPLC. The current yield of purified, folded, peptide is very low. If this peptide proves biologically active, attempts will be made to improve yields, concentrating on optimisation of the folding process. The concentration of peptide used in the folding reaction is rather high, and the reaction yields a considerable quantity of insoluble material. Significant improvements in yield may be achieved by simply decreasing this concentration, therefore reducing intermolecular disulphide bonding. Folding of the synthetic peptide may also be improved by the addition of the cellular enzymes peptidylprolyl *cis-trans* isomerase (PPIase, or FK binding protein) and/or protein disulphide isomerase (PDI) to the reduced peptide, as recommended in the refolding of maurotoxin (Di Luccio et al., 2001).

The synthetic and native molecules purified in this study have similar elution times on a C18 column; however, they appear to show different behaviours on a C8 column. Future work will sequence these peptides and look for chlorotoxin-like biological activity.

A number of approaches were initially considered when deciding upon the methodology for identification of putative chloride channel blockers in this venom, including biological assays based upon known properties of chlorotoxin. A molecular biology approach was decided upon, since, even if the venom did not contain chloride channel or chlorotoxin-like activity, it was likely to contain short-insectotoxin homologues. With so little known about such molecules, further examples of short insectotoxins would prove valuable, even in the absence of Cl⁻ channel activity. Now that *Mesob. tamulus* short insectotoxins have been identified, the alternative approaches may provide useful information on the functional properties of BtCh11 and BtCh12. Once established, these assays could also be used for further screening of venom fractions for components of pharmacological interest.

Based on the ability of chlorotoxin to bind to membrane receptors on glioma cells (Soroceanu et al., 1998) and rat colonic enterocytes (Debin and Strichartz, 1991), it should be possible to develop binding assays for the screening of potential chlorotoxin-like molecules, of venom and of venom fractions. Colonic epithelial cell membranes would be prepared from epithelial cell scrapings of dissected rat colons in a

modification of the method described by Reinhardt et al., 1987 and Debin et al., 1993. Use of this cell preparation would also provide details of chlorotoxin binding to these cells. Cultured glioma cells could also be used. Binding could either be assessed directly, using Biacore (or similar technology), or through competition binding assays using radiolabelled toxin, similar to those described using radiolabelled apamin (chapter 4). Such assays do have limitations, however, with cell binding not necessarily correlating with pharmacological activity.

Recently, Deshane et al., 2003 have shown chlorotoxin to be an inhibitor of MMP-2 activity. Matrix metalloproteinases (MMPs, reviewed by Visse and Nagase, 2003) are involved with extracellular matrix remodelling in a number of physiological processes, e.g. embryogenesis, wound healing, ovulation and menstruation, as well as general maintenance of the matrix. MMP activity has also been associated with a number of pathological states, for example, atherosclerosis, and multiple sclerosis. MMP-2 (or gelatinase A) is primarily active against basement membrane components and has been implicated as a therapeutic target in obesity (Chavey et al., 2003), prevention of airway remodelling in asthma (Suzuki et al., 2004), rheumatoid arthritis (Jackson et al., 2001) and a number of cancers (John and Tuszynski, 2001) including pancreatic (Bloomston et al., 2002), cervical (Mittra et al., 2003), breast (Duffy et al., 2000) and skin cancers (Hofmann et al., 2000), and glioma (Chintala et al., 1999). (In such cancers MMP2 contributes to angiogenesis, providing a blood supply to solid tumours, and also breaks down the natural barriers to cell migration and metastasis). Commercial assays are available for MMP-2 enzyme activity, which could easily be applied to screen venom components for MMP-2 inhibition.

The two assays, described above, screen for chlorotoxin-like activities and are not a screen for chloride channel toxins in general. A more general assay would look for block of chloride ion flux. Electrophysiological methods have been utilised for such purposes by Fuller et al., 2004. Electrophysiological studies of Cl⁻ channels are not as straight forward as equivalent studies on cation channels and, without good indications of a positive result, are impractical. More practical would be the use of Cl⁻ sensitive fluorescent dyes to visualise, or quantitate, block of Cl⁻ flux. Such assays have been used, for example, to examine chloride ion movement in epithelial cells, fibroblasts (Woll et al., 1996), synaptosomes and brain slices (Yu and Schwartz, 1995). They have

also been utilised by Soroceanu et al., 1999 to examine the effect of chlorotoxin on glioma cells.

Finally, although not suitable for use with non-purified venom components, the insect neurotoxicity of the purified peptides could be explored. Chlorotoxin produces reversible paralysis in crayfish and in cockroaches (Debin et al., 1993) and Ammp2 has been reported as toxic to both insects and crustaceans (blowfly, beetle, and isopod) but not to mice (Rosso and Rochat, 1985). Native BtChl1 (BtITx3, Dhawan, et al., 2002) and BtChl2 (ButaIT, Wudagagiri et al., 2001) were both isolated through their lepidopteran toxicities. Locust and cockroach insect synaptosomes have been used previously to study insect sodium channels (Gordon et al., 1990, 1992). Similar preparations could be used to study native binding of the short insectotoxins.

Short insectotoxins show high sequence homology. This is concentrated in three regions of the primary sequence. Structural analysis enables the location of these regions in a 3D model of the protein to be predicted. There is a highly conserved region stretching from residue 2 of chlorotoxin through the β -sheet to Asp9 at the base of the N-terminal loop. In contrast, the α -helix is a region of high variability between short insectotoxins, although there are a few largely conserved residues (e.g. Lys15 and a negative residue at position18). At the top turn of the molecule (see fig 3.11a) there is a conserved CCGG motif. The final conserved region is located around the C-terminal β -sheet ending at the final Cys residue. These conserved regions are therefore concentrated on the face opposite the α -helix.

Given the importance of charge in ion-channel toxin binding, the electrostatic properties of the short insectotoxins were investigated. The net charge of the known short insectotoxins varies between +1 (e.g. ChITx-b) and +5 (e.g. Bs8). BtChl1 and BtChl2 both have a net charge of +2; however, the distribution of charges differs markedly in these two peptides. Whilst the charged residues of BtChl2 generally conform to the consensus, the charge positions of BtChl1 vary markedly. More importantly, in terms of proposed function, the positions of four charges are conserved between BtChl2 and chlorotoxin (D9, K15, E18, and K23) and three between BtChl2 and I5A (D9, K15, and E18). BtChl1 shares only a single charged residue with chlorotoxin (R23) or with I5A (R17). It has been noted (Lippens et al., 1995) that residue Lys27 is conserved between chlorotoxin and the K⁺ channel blocker charybdotoxin, but its effect is negated by the

close proximity of the negatively charged Asp residues. This lysine residue is critical for the interaction of charybdotoxin with the potassium channel pore, a K27R mutant destabilises the *Shaker*-charybdotoxin interaction by 1000-fold (see Miller, 1985). The residue is also present in all short insectotoxins, with the exception of Bs14 and the two sequences described in this chapter. Nothing is known about the structural requirements for the recognition of chloride channels, but, given the importance of charge distribution in binding of ion channel toxins, and the fact that no single charged residue is conserved in all short insectotoxins, it would appear likely that there is considerable variation in pharmacological targets between members of this family.

To get a clearer picture of the extent to which these charged residues might be involved in toxin-receptor interactions, the electrostatic surfaces of four short insectotoxins were calculated. These four short insectotoxins have very different surface charge distributions. The positive surface seen in the solvent-exposed side of the C-terminal β -sheet in potassium channel toxins is important in charybdotoxin binding (Park and Miller, 1992). This basic surface is maintained in I5A and BtChl2 but not in chlorotoxin or in BtChl1. Differing patterns of surface charge between short insectotoxins are also seen on the opposite side of the molecule. Although charged residues on the solvent-exposed face of the α -helix are critical for the binding of SK channel toxins to their target, in contrast, the charge distribution in this region varies widely within the ChlTx-like molecules. Thus the differing overall charge distributions seen in the primary structures of ChlTx-like molecules produce differing surface charge distributions, suggesting either that the short insectotoxins are binding to differing targets, or that electrostatic interactions are not critical determinants in the short insectotoxins' mode of action.

The long-chain toxins active on sodium channels show marked variation in their species selectivities. Mammalian versus invertebrate selectivity of the sodium channel toxins and the structural basis of these species specificities is discussed by Gordon and Gurevitz, 2003. Examination of the limited functional data on the chlorotoxin family does suggest at least minor variations in the natural targets for short insectotoxins, revealed by their differing toxicity profiles. Chlorotoxin and I5A are both active on crustaceans, with chlorotoxin also acting on cockroaches (Debin et al., 1993) and I5A also acting on blowfly (Ovchinnikov, 1984). AmmP2 shows blowfly and beetle toxicity (Rosso and Rochat, 1985). As stated previously, both of the short insectotoxins isolated

from *Mesob. tamulus* are active on lepidoptera (Wudayagiri et al., 2001; Dhawan et al., 2002). In the case of BtChl2, this toxicity is selective and the toxin has no effect on blowflies. None of the other toxins have been reported to be tested against lepidoptera. There are two regions where ChlTx and I5A are similar and BtChl1 and BtChl2 also show electrostatic similarities. The first is at the C-terminal end of the α -helix where chlorotoxin and I5A show areas of negative surface charge. The second is in the N-terminal loop spreading to the N-terminal region of the α -helix. Arseniev et al., 1984 notes general structural homology between the α - β fold of the long- and short-chain insectotoxins. By this analogy, the second region of electrostatic similarity is structurally comparable to part of the region of long chain insectotoxins that determines their specificity for insects (Froy et al., 1999a). This area is far less basic in BtChl1 and BtChl2 than in ChlTx and I5A. Could this be the region that determines the *Mesob. tamulus* toxins' selectivity for lepidoptera? Is the fact that both short insectotoxins found in this species are active against lepidoptera a reflection of an evolutionary adaptation for a specific prey type?

Finally, in the last few years, a series of papers has raised intriguing questions as to the status of chlorotoxin as a chloride channel blocker. Maertens et al., 2000 report no action of peptide containing fractions of *Leiurus quinquestriatus quinquestriatus*, nor of chlorotoxin itself, upon volume-regulated anion channels (VRAC), nor calcium-activated chloride channels when applied externally or cytoplasmically. The group was unable to repeat the observed block of GCC by chlorotoxin reported by Ullrich et al., 1996, and dispute GCC being a chloride current, concluding that the current is through a K^+ channel with non-exclusive K^+ permeability. The 72 kDa protein that Soroceanu et al., 1998 reported to be the chlorotoxin acceptor was similar in size to predicted gene products of the ClC family (Jentsch et al., 1995). Recently this protein was identified as MMP-2 (Deshane et al., 2003), throwing further confusion into the issue. Chlorotoxin was shown to bind to surface-expressed MMP-2 on glioma cells, inhibiting its enzymic activity and increasing its endocytosis by caveolae. This enzyme inhibition and reduction of surface expression can account for the anti-invasive action of chlorotoxin on these cells. Taken together, these findings would appear to discount any chloride channel activity of chlorotoxin.

There have, however, been three recent reports documenting electrophysiological block of chloride channels upon intracellular application of scorpion venom components.

Dalton et al., 2003, report a block of a Ca^{2+} activated Cl^- channel which modulates the resting potential in a specific subpopulation of reactive astrocytes, by chlorotoxin itself. Fuller et al., 2004, have recently reported that intracellular application of a peptide component of *Leiurus quinquestriatus hebraeus* venom inhibits CFTR Cl^- currents. This inhibition was not due to alteration of binding kinetics, but by block of the channel pore. The same group has also reported block of ClC-2 (but not ClC-0 or ClC-1) currents by components of the same venom (Thomposon et al., 2003). Since the venom peptides only act intracellularly on these channels, it is unlikely that they are the natural target for short insectotoxins.

Thus chlorotoxin *does* affect certain ion channels, although it is unclear if this action is a direct one. Is the action on MMP-2 responsible for these ion channel effects? Or does chlorotoxin have a second site of action? Soroceanu et al., 1998 detected binding of chlorotoxin to two distinct classes of receptor on glioma cells. Are the venom components that are responsible for the block of CLC-2 and CFTR ion channels members of the short insectotoxin family? Do other members of the short insectotoxins bind MMP-2? If this molecule is their natural target what is its usefulness to the scorpion? How do the short insectotoxins produce their neurotoxic effects in insects? What is the nature of their natural target, and what structural features of the toxins are responsible for their activity?

From a pharmacological viewpoint, if BtChl1 and BtChl2 are found to inhibit chloride currents when applied intracellularly, this may not have direct therapeutic applications, but will provide tools for the investigation of chloride channels. Like chlorotoxin, they may prove active upon MMPs, with diverse therapeutic potential. To conclude, recent studies on chlorotoxin have served to highlight what little we know about the short insectotoxins, their targets, and mode of action. The identification of novel members of this toxin family, as described in this chapter, can only aid in the dissection of the mechanism of action of these little-studied molecules, irrespective of the pharmacological targets of such peptides.

3.4.2 Amidation of Tamulustoxin

C-terminal amidation is a post-translational modification common in peptides found in the nervous system. Approximately half of nervous and endocrine system bioactive peptides possess a C-terminal α -amide group, critical for correct biological activity. The mechanism of amidation has been reviewed by Martinez and Treston, 1996. In the unprocessed molecule, the amino acid to be modified (which will form the carboxy terminus in the mature peptide) is followed by a glycine, which provides the amide group. This modification is a two-step process of hydrolysis and lysis, which, in mammals and amphibians, is carried out by a bifunctional peptidyl-glycine α -amidating monooxygenase enzyme (PAM). In the first reaction step, the glycine is oxidized to form alpha-hydroxy-glycine via the peptidylglycine α -hydroxylating monooxygenase activity (PHM). The peptidyl- α -hydroxyglycine α -amidating lysase (PAL) then cleaves the hydroxyglycine releasing the amidated peptide and glycoxylate. In *Drosophila*, however, these PHM and PAL activities are encoded by separate genes (Kolhekar et al., 1997), although it is not known if this is the pattern in invertebrates in general. Although all amino acids can be amidated, in principal, neutral hydrophobic residues such as Val or Phe are preferred substrates, whilst charged residues such as Asp or Arg are much less reactive. Amidation is believed to take place throughout the secretory pathway, particularly in the secretory granules. In virtually all cases, removal of the amide group significantly reduces, or destroys, the peptide's biological activity. The addition of an amide group at the C-terminus may enhance stability and biological activity of peptides that are not naturally amidated.

C-terminal processing of scorpion toxins often occurs during maturation. Several rules for this processing have been deduced through examination of sodium channel toxin sequences (as summarised by Possani et al., 1999). In the simplest case (as is seen with excitatory insect toxins), the nucleotides encoding the C-terminal residue of the mature peptide are followed directly by a stop codon and no C-terminal processing takes place. In other toxins, additional basic residues are processed, and in general, if the last two residues of the precursor peptide are basic, they are cleaved during processing. If the precursor has a glycine followed by one or two basic residues at the C-terminus, the amino group of the glycine is used for amidation of the previous amino acid, which forms the new terminus. If the glycine is followed by three basic residues, however, the

amino-acids are removed, but no amidation occurs. As more toxins types are examined, exceptions to these rules may become evident.

The majority of scorpion toxins active on voltage-gated potassium channels appear to be amidated. In potassium channel toxins, amidation would appear to determine affinity for the acceptor. Leiurotoxin, for example, is an SK channel toxin that is present in the venom in both amidated and non-amidated forms. The most abundant of these is the amidated form, which has an increased affinity for its receptor (Sabatier et al., 1994). P05, another SK channel toxin, has a C-terminal carboxylate. Amidation of this toxin strengthens the toxin-acceptor interaction to the extent that the binding to rat brain synaptosomes becomes, in effect, irreversible (Sabatier et al., 1993). Interestingly, in both molecules, the α -amidation status had no apparent effect on mouse toxicity.

With synthetic versions (both recombinant and produced by solid state methods) of scorpion toxins increasingly being used in experiments as a substitute for native ones, there is obviously a need to confirm the amidation status of the toxin prior to synthesis. Our group already had circumstantial evidence of C-terminal amidation of tamulustoxin, and the cDNA analysis carried out in this chapter has demonstrated that an additional C-terminal Gly and Lys are encoded by the cDNA. Following the current consensus for scorpion toxin processing, one would predict amidation to occur. Taken with the approximately 1Da discrepancy in mass of the native molecule (Strong et al., 2001), and its resistance to carboxypeptidase (P. Strong, unpublished observation), the cDNA evidence strongly supports amidation of the C-terminal serine in the mature toxin.

Analysis of the cDNA sequences of tamulustoxin clones revealed variation between the deduced and the published sequences, and also between the sequences of the clones themselves. In all cases, the deviations are conservative, not affecting the amino-acid sequence, but the cause of these differences should still be addressed. Slight conservative deviation from native cDNA sequence is often associated with the use of degenerate peptide sequence-based primers, and care should be taken when analysing such sequences in the region of primer binding. Degenerate primers were used for forward amplification in the current and published studies, and for reverse amplification in determination of the published sequence (Strong et al., 2001). Differences between individual clones, and between the consensus and published sequences in the 5' region,

correspond to those expected from the primer sequence, and a definitive identification of native sequence is impossible. At the 3' end, the primers used in this study bound outside the range of the published sequences. Discrepancies are therefore most likely due to primer-related artefacts in the original sequence. However, four sequence differences cannot be attributed to the use of degenerate primers. They are all conservative, and occurred in all clones sequenced in this study. The reason for the discrepancy is unclear, although since all the clones sequenced in this study were derived from a single PCR reaction, an error during an early round of PCR cannot be ruled out.

All clones sequenced corresponded to tamulustoxin-1, and therefore no inferences on the amidation status of the tamulustoxin-2 variant can be made.

3.4.3 A Putative Long-Chain Potassium Channel Toxin Signal Peptide

Most scorpion potassium channel toxins are short peptides of 30-40 amino acids. The long-chain potassium channel toxins (β -KTx) have 61-64 amino acids cross-linked by only three disulphide bonds and are non-amidated. To date only four members of the β -KTx family have been identified from three scorpion species: TsTxK β from *Tityus serrulatus* (Rogowski et al., 1994; Legros et al., 1998), AaTxK β from *Androctonus australis* (Legros et al., 1998), and BmTxK β and BmTxK β 2 from *Buthus martensii* (Zhu et al., 1999). TsKxK β is active against a delayed rectifier voltage-gated potassium channel (Rogowski 1994). Recombinant BmTXXK β reversibly inhibits the transient outward potassium current in rabbit atrial monocytes and significantly prolongs the duration of the action potential in these cells (Cao et al., 2003). Aside from this data, very little is known about the function, three-dimensional structure or mode of action of these toxins.

All β -KTx have a similar RNA structure (Zhu et al., 1999) that encodes a signal peptide, propeptide and mature toxin (fig 3.16). Legros et al., 1998 suggest that these toxins may be related to scorpion defensins. Defensins and β -KTx both have a propeptide in their precursor and a phylogenetic analysis groups them both together. The same authors also suggested that these toxins represent an evolutionary link between sodium and potassium channel toxins, speculating that the increased length paved the way for an

increase from three to four disulphides. With so few examples of these molecules, however, there is little in the way of evidence to support any theory as to their evolutionary relationships.

During the course of studies on tamulustoxin, a cDNA fragment showing high homology to the signal peptide of BmTxK β was isolated. In general, signal peptide sequences show high homology within a scorpion toxin group. However, only four putative long-chain potassium channel toxin sequences have been identified and the signal peptides of these do not appear conserved. BmTxK β is of low nucleotide and amino acid sequence similarity to the other three peptides in this family, but shows the same cysteine pattern (C...CXXC...C...CXC), suggesting a similar cysteine pairing (see fig 3.16). It is therefore possible that BmTxK β , and the putative long-chain toxin represented by the signal-peptide identified, represent a subfamily of β -KTx, explaining the signal peptide homology. It should be borne in mind, however, that the sequence was produced from a single clone, and that a fragment of homologous sequence, although warranting further investigation, does not provide conclusive evidence for a β -KTx in this scorpion venom.

Fig 3.16 Sequence Alignment of Long-Chain Potassium Channel Toxin Precursors

	SIGNAL PEPTIDE	PROPEPTIDE
BmTxKB	M MKQQFF LFLAVI VMI SSVIEA	G RGKEIM
BmTxKB2	M QRNLVVLFLGM VALSSC	GLREKHFQ
AaTxKB	M QRNLVVLFLGM VALSSC	GLREKHVQ
TsTxKB	RKALLLI LGM VTLASC	GLREKHVQ
MATURE TOXIN		
BmTxKβ	KNIKEKLT EVKDKMKHS WNKLTSM SEYACPVI EKWCEDHCA A KKAIGKCEDTECKCLKLRK	
BmTxkβ2	KLVKYAVPEGLRTI IQTAVHKL GKTQFGCP AYQGYCDDHCQDI KKEEGFCHGFKCKCGIPMGF	
AaTxKβ	KLVKYAVPVGTLRTI LQT VVHKVGTQFGCP AYQGYCDDHCQDI KKEEGFCHGFKCKCGIPMGF	
TsTxKβ	KLVAL IPNDQLRSILKAVVHKVAKTQFGC AYEGYCNDHCNDIERKD GECHGFKCKCAKD	

The figure (adapted from Zhu et al., 1999) illustrates the precursor structure and homology of the four known members of the β-KTx family. Residues are aligned against the conserved cysteines. Residues in red are conserved in all peptides, whilst those in blue are present in two or more peptides.

**Modification of Apamin, and the Effects on its Binding Affinity for
Acceptors on Rat Brain Synaptic Membranes**

4.1 Introduction

Monoiodoapamin has previously been used to identify apamin binding sites, and hence SK channels to which it binds selectively and with high specificity, on membranes, whole cells and cultured cell lines prepared from a wide range of both neuronal and non-neuronal tissues. The results of these studies, which show binding to single classes of molecules, are summarized in table 4.1. In general, the values for B_{\max} are low, reflecting the low abundance of the acceptor, and therefore SK_{Ca} channels, in mammalian tissues (1-50 fmol mg⁻¹ protein), an abundance generally one fifth that of the sodium channel (Hugues et al., 1982d). Affinity of apamin for its acceptor is very high, being in the picomolar range.

The binding of radiolabelled apamin to rat brain synaptic membranes has been well characterised (Hugues et al., 1982c). This chapter describes the radiolabelling of apamin, and preparation of rat brain synaptic plasma membranes for use in filtration binding studies. The binding parameters of these components were determined in order to confirm assay performance prior to their use in competition binding studies. Once characterised, the assay was used to look at the apamin-acceptor binding properties of a number of test substances.

Information on protein conformation can be of great importance when elucidating function. Dempsey et al., 2000, used apamin as a model peptide for the study of β -turn structures, which are poorly characterised in relation to α -helices and β -sheets. Apamin contains an asparagine as the first β -turn residue, which is characteristic of Asn-stabilised type 1 β -turns. In this toxin, the β -turn is connected to a C-terminal α -helix by two disulphide bridges, resulting in a highly stable, well-defined structure (see fig 1.5).

Asn2 is thought to be involved in hydrogen bonding and hence the stability of a local β -turn (involving Asn2, Cys3, Lys4, and Ala5) as well as the peptide in general. Dempsey's group have generated synthetic apamin analogues with an Asn2 to Ala2 substitution, which produces peptides with two different disulphide bond patterns (as shown in fig 4.1).

In molecular modelling of the structures, replacing Asn2 with an alanine residue (which has a non-polar side chain unable to contribute to hydrogen bonding) did not retain the

β -turn conformation. This destabilized the C-terminal helix region (connected to the β -turn by two disulphide bonds), and subsequently the whole peptide. This prediction was confirmed by NMR spectroscopy studies on the analogues themselves.

These observations confirmed previous studies linking the stability of C-terminal α -helices with that of N-terminal β -turns, and also showed that the hydrogen bonds involving the Asn2 side chain were important for stability of the entire structure. The experiments allowed quantification of the contribution of the β -turn structure to total protein stability. This motif, in combination with the disulphide bonds and electrostatic interactions between the glutamate and the N-terminal primary α -amine group, account for almost all of the thermodynamic stability of the molecule.

As a complementary study to the structural studies described above, the work described in this chapter looks at the functional effects of this amino acid substitution, and of the wrongly-paired disulphide bridge analogue (see fig 4.1), on binding of apamin to its acceptor on rat brain membranes.

The effective and specific labelling of ion channel proteins is critical for their visualisation in cell biology studies and is achieved by a variety of direct and indirect methods. Immunostaining is often utilised, but finding suitable antibodies to ion channel subtypes may be hampered by high sequence conservation, such as that seen in many K^+ channel subfamilies (Chandy and Gutman, 1993). Antibodies to ion-channels tend to recognise intracellular epitopes, and sample preparation often requires permeabilisation and fixation of samples, making them unsuitable for real-time studies. Direct labelling of channels, for example by expression with a green fluorescent protein tag, overcomes this problem, but the channels produced are non-native.

Ion channel toxins are able to interact with native ion channels in living cells, and most ion channels toxins bind extracellularly. To facilitate their use in cell biology, fluorescently labelled toxins have been made. For example Massensini et al., 2002, used fluorescently labelled scorpion toxins to visualise the distribution of voltage-dependent sodium channels in living GH3 cells via laser scanning confocal microscopy. Fluorescent toxin probes have a number of potential uses, for example in flow cytometry or studying up-regulation of specific channel types, as often occurs in tumour cells. Use of differently coloured fluorophores allows for simultaneous labelling of

different receptors in the same cell, thus providing greater flexibility than radioactive counterparts.

Alexa Fluor 488 is a commercially available fluorescently-labelled apamin. It has been used to study transfection of HEK cells with SK2 (Cingolani et al, 2002). However, the binding properties of Alexa Fluor apamin to SK channels has, to our knowledge, not been reported. Experiments were carried out to validate the use of fluorescent apamin as a cell biology tool.

Table 4.1 Published Apamin Binding Parameters

Tissue	Kd (pM)	B _{max} * ¹	Hypo-/ Iso-osmotic?	Author
Rat synaptic membranes	2.7	42	Hypo-osmotic	Wadsworth et al., 1994
Rat brain synaptic plasma membranes	3.3	47	Hypo-osmotic	Wadsworth et al., 1996
Rat synaptic membranes	15-25	12.5	Hypo-osmotic	Hugues et al., 1982c
Rat brain synaptic membranes	35	22	Hypo-osmotic	Hugues et al., 1982b
Solubilized rat brain synaptosomes	40	17	Hypo-osmotic	Seagar et al., 1987
Rat forebrain homogenate	10-25	1-3	Hypo-osmotic	Habermann and Fischer, 1979
Canine cerebral cortex synaptic membranes	33	17.3	Hypo-osmotic	Wu et al., 1985
Neuroblastoma (Clone NIE 115)	15-22	12	Hypo-osmotic	Hugues et al., 1982d
Cultured rat neonatal skeletal muscle membranes	36-60	3.5	Hypo-osmotic	Hugues et al., 1982
Guinea pig colon smooth muscle membranes	36	30	Hypo-osmotic	Hugues et al., 1982a
Guinea pig ileum smooth muscle	67	42	Hypo-osmotic	Marqueze et al., 1987
Rat heart membranes	59	24	Hypo-osmotic	Marqueze et al., 1987
Guinea pig liver membranes	15	43	Hypo-osmotic	Marqueze et al., 1987
Guinea pig liver plasma membranes	12.6	4.2	Hypo-osmotic	Strong and Evans, 1987
Rat liver plasma membranes	-	<0.2	Hypo-osmotic	Strong and Evans, 1987
Guinea pig plasma membranes	12.6	4.2	Hypo-osmotic	Strong and Evans, 1987a
PC12 cell membranes	5.8	23	Hypo-osmotic	Wadsworth et al., 1997
Solubilized rat cortex synaptic membranes	40-150	-	Iso-osmotic	Schmid-Antomarchi et al., 1984
Cultured rat embryonic neurons	60-120	3-8	Iso-osmotic	Seagar et al., 1984
Cultured rat brain astrocytes	90	3	Iso-osmotic	Seagar et al., 1987a
PC12 cell membranes	350	600	Iso-osmotic	Schmid-Antomarchi et al., 1986
Bovine adrenal medulla chromaffin cells	132	0.72* ³	Iso-osmotic	Lara et al., 1995
Guinea pig hepatocytes (whole cells)	390	1.1* ²	Iso-osmotic	Cook and Haylett, 1985
Rat hepatocytes	-	0 [†]	Iso-osmotic	Cook et al., 1983; Cook and Haylett, 1985
Liver (guinea pig hepatocytes)	390	0.99* ²	Iso-osmotic	Cook et al., 1983
Human erythrocytes	-	0 [†]	Iso-osmotic	Cook et al., 1983; Cook and Haylett, 1985
Rat heart cultured cells (primary cardiac cells)	69	2.8	Iso-osmotic	Marqueze et al., 1987

*¹ fmol/mg membrane or cell protein

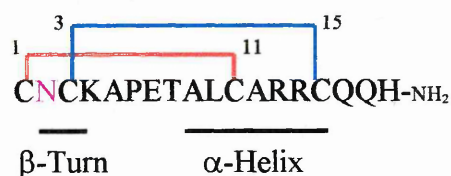
*² fmol/mg dry weight cells

*³ fmol/10⁶ cells

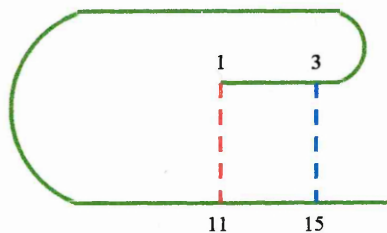
† No inhibitable binding at concentrations up to 500pM toxin.

Fig 4.1 Diagrammatic Representation of Apamin-N2A.

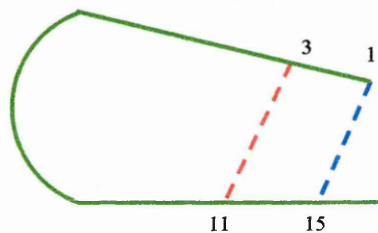
a)



b)



c)



Synthetic apamin-N2A is an 18 amino acid apamin homologue (a) with an Asn2 to Ala2 substitution. The diagram illustrates the Cys1-Cys11 and Cys3-Cys15 native disulphide bond pairings and the positions of the β -turn and α -helix. Apamin N2A-par (b) has wild-type disulphide bond pairing, with the participating cysteine residues arranged in a parallel fashion adopting the 'globule' formation. In the apamin N2A -anti isomer (c), these cysteines are antiparallel with Cys1-Cys15 and Cys3-Cys11 disulphide bond pairings resulting in a structure known as the 'ribbon' formation in the notation of Pegoraro et al., 1999.

4.2 Materials and Methods

4.2.1 Materials

Sodium ^{125}I -Iodide was purchased from Amersham-Pharmacia. The BCA protein assay kit and Iodogen were purchased from Pierce. Whole frozen rat brains were purchased from Charles River Laboratories. Native and synthetic apamin, and the synthetic apamin derivatives N2A-par and N2A-anti, were supplied by Dr Chris Dempsey (University of Bristol). Alexa Fluor 488 apamin was purchased from Molecular Probes. All other chemicals were obtained from Sigma or BDH and were AR quality or equivalent where available.

4.2.2 Determination of Apamin Binding Parameters

4.2.2.1 Radioiodination of Native Apamin

Radiolabelled apamin was prepared by a modification of the procedure described by Strong and Brewster, 1992, which uses the Iodogen method to label His₁₈. 1.5ml microcentrifuge tubes were coated with iodogen as follows: 10mg iodogen (Pierce) was dissolved in 25ml dichloromethane and 80 μl of this solution was transferred to a microcentrifuge tube. The solution was evaporated to dryness under a gentle stream of nitrogen.

To this tube 100 μg apamin (100 μl , 1 mgml^{-1}), 2mCi Na^{125}I (20 μl , 100mCi ml^{-1}) and 60 μl 30mM Tris-HCl (pH8.6) were added, and incubated for 20min at room temperature, shaking intermittently. The contents of the vial were transferred to a fresh microcentrifuge tube for 10min to allow unincorporated $^{125}\text{I}^+$ to revert to I_2 .

The reaction mixture was purified on a SP-Sepharose (Pharmacia) cation exchange column (14 x 1cm) equilibrated with 50mM sodium phosphate pH6.0/ 160mM NaCl (8ml hr^{-1}). Elution with the same buffer (1ml fractions) yielded three radioactive peaks when measured in a calibrated γ -counter. The initial peak containing unincorporated Na^{125}I , was followed by a minor di-iodo [$^{125}\text{I}_2$] apamin peak, after which mono-iodo [^{125}I] apamin eluted. Non-radiolabelled apamin remained on the column and could be eluted

with 50mM sodium phosphate pH6.0/ 300mM NaCl if required. Mono-iodo[¹²⁵I] apamin (specific activity 2200Ci mmol⁻¹) was stored at 4°C in the presence of 2mgml⁻¹ BSA.

4.2.2.2 Preparation of Rat Brain Synaptic Plasma Membranes

Rat brain membranes were prepared, essentially according to the method of Dodd et al., 1981, from whole frozen (-70°C) rat brains. Sucrose solutions were buffered with 10mM HEPES/ 2mM Na EDTA pH7.5. All solutions were ice cold and contained the following protease inhibitors: - 25µgml⁻¹ bacitracin, 10µgml⁻¹ soybean trypsin inhibitor, 0.2mM benzamidine and 0.1mM PMSF (dissolved in ethanol). All manipulations were performed on ice. Centrifugations were performed at 4°C using a Sorval SS34 rotor in a Sorval RC5B centrifuge or a Beckman 45Ti rotor in a Sorval Pro 80 ultracentrifuge.

Six rat brains were homogenized using five up and down strokes of a Wheaton glass-perspex homogeniser (0.1- 0.15mm radial clearance) in 2 x 35ml 0.32M sucrose. The homogenate was spun 3700rpm (1000 x g) in a SS34 rotor for 10min and the supernatant collected on ice. The pellets were resuspended, spun, and the supernatants collected, as above. The supernatants were pooled to give the S1 fraction, which was spun in a 45Ti rotor for 20min at 20500rpm (33000 x g). The crude mitochondrial pellet (P2) was retained and the supernatant discarded. The pellet was resuspended in 130ml 0.32M sucrose and homogenized with eight up and down strokes of the homogeniser above. This homogenate was layered onto 4 x 30ml cushions of 1.2M sucrose in 45Ti centrifuge tubes and spun for 45min at 45000rpm (150000 x g). The membrane material suspended at the interface of the two solutions was collected, leaving the fat behind. This material was diluted to 140ml final volume with the HEPES/ EDTA buffer described above and layered onto 4 x 30ml 0.8M sucrose solutions in 45Ti tubes. These tubes were centrifuged 45min at 45000rpm (150000 x g). Myelin at the sucrose interface was removed, as was any disturbed fat. The remaining liquid was then removed and discarded, leaving a synaptosome pellet. This pellet was resuspended in 10ml 10mM KCl/ 25mM Tris, pH8.4, snap-frozen in liquid nitrogen, and stored at -70°C.

4.2.2.3 BCA Protein Assay

Proteins were quantified using a BCA (bicinchoninic acid) protein assay kit (Pierce) by a method based on that described by Smith et al., 1985. This assay method is highly sensitive, shows little protein-to-protein variation and is compatible for use with a wide range of substances (e.g. nonionic detergents and Tris) that normally interfere in the Lowry assay. BSA was used as a standard.

4.2.2.4 Saturation Binding Assays

The binding of radiolabelled apamin to rat brain membranes was performed using a filtration binding assay based on that described in Wadsworth et al., 1994. All incubations were on ice and all solutions kept ice-cold. Three such experiments were performed, each with triplicate samples.

Radiolabelled toxin was diluted to concentrations in the range 0.1–100pM in 950µl ice cold binding buffer (10mM KCl/ 25mM Tris pH8.4 containing 0.1% BSA). Tubes were counted individually in a calibrated Packard Cobra γ -counter (approx. 85% efficiency) until a 1% sigma confidence was reached (or for a maximum of 20min), to obtain accurate values for calculation of total toxin concentration. 50µl membrane solution (diluted in above buffer) was added to give a final concentration of 100µg membrane protein per tube. Tubes were vortexed, and incubated on ice for 90min.

Bound ligand was separated from free using Whatman GF/B glass-fibre filters pre-soaked for 1hr at 4°C in 0.5% w/v polyethyleneimine. With this technique, introduced by Bruns et al., 1983, acidic membrane proteins are electrostatically retained by the polycation, whereas neutral or basic ligands, e.g. apamin, are not. This helps to dramatically reduce non-specific binding of free (basic) apamin to filters. Excess liquid was drained from the filter, which was placed in a Brandell cell harvester. Samples were rapidly filtered and washed with 5ml ice cold binding buffer. Filters were placed in the bottom of tubes and read in the γ -counter as above.

Non-inhibitable binding was determined by parallel incubations in the presence of 0.1 μ M native apamin and subtracted from total binding to give the inhibitable component.

4.2.2.5 Determination of Non-Specific Binding

d-Tubocurarine, another blocker of SK_{Ca} channels, was used to ensure that the inhibitable binding determined by competition with excess cold apamin described above was due to specific and biologically relevant binding to the apamin acceptor. 100pM radiolabelled apamin was incubated with the membranes in the presence and absence of 0.1 μ M unlabelled apamin or 1mM *d*-tubocurarine chloride and filtered as described above. Results were determined in triplicate experiments, each carried out with triplicate samples.

4.2.2.6 Time Course of Apamin Binding to Rat Brain Synaptic Membranes

50 μ l membrane solution was added to 900 μ l binding buffer (described above) to give 100 μ g membrane protein per tube, and incubated on ice. At appropriate time intervals, 50 μ l radiolabelled apamin solution was added to give a final concentration of 15pM, which is close to the K_d (equilibrium dissociation constant) for this reaction. Total incubation times with labelled toxin varied between 120min and 1.5min, which was the lowest practical incubation time. After incubating with radiolabelled apamin, membrane samples were filtered and counted in a γ -counter as described (4.2.2.4).

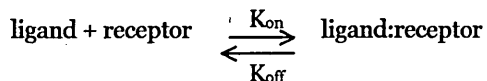
Diluted membrane samples for assessing non-specific binding were pre-incubated with 0.1 μ M unlabelled apamin for 1hr on ice, prior to the addition of labelled apamin and then processed as above.

For the time course experiments triplicate tubes were prepared for each sample. The time points used were interspaced over three individual experiments and the data combined to produce a single time course.

4.2.2.7 Analysis of Binding Data †

Data from three experiments on the time course of binding using different incubation times were combined and plotted using *Prism* (Graphpad software, San Diego USA), and an exponential association rate curve was fitted to the data using the same software. Results from saturation binding experiments were analysed using *Radlig* (Biosoft, Cambridge, UK). Site modelling and non-linear curve fitting allowed for Scatchard analysis of the saturation binding data, and estimations of K_d , B_{max} (maximum binding site density) and Hill coefficients were determined using the same software. Plots shown in the results section were produced from appropriate curve fitting algorithms using *Prism* and show typical results from three separate experiments, each with three replicate samples.

† The analysis of the binding data (Hulme and Birdsall, 1990; and Haylett, 1996) assumed a simple bimolecular interaction, and was based upon the law of mass action:



Free ligand (L) and receptor (R) collide due to diffusion. If this collision is in the correct orientation and is of sufficient energy, binding occurs to form a receptor-ligand complex (LR). The rate of association (number of binding events in a period of time) is determined by: $[L] \times [R] \times K_{on}$, where K_{on} is the on rate constant ($M^{-1} \text{ min}^{-1}$). Similarly, the rate of dissociation (number of dissociation events in a given period of time) is determined by: $[LR] \times K_{off}$, where K_{off} is the off rate constant (min^{-1}).

At equilibrium, the rate of dissociation is equal to the rate of formation of new complexes, thus

$$[L] \times [R] \times K_{on} = [LR] \times K_{off}$$

The relationship between the on rate and the off rate constants at equilibrium is defined by the equilibrium dissociation constant K_d (M).

$$K_d = \frac{[L][R]}{[LR]} = \frac{K_{off}}{K_{on}}$$

Note that when half of the receptors are occupied, the concentration of occupied is equal to the concentration of unoccupied receptors: $[R] = [LR]$ therefore $K_d = [L]$. Thus K_d is the concentration of ligand that will occupy half of the receptors at equilibrium.

In the equilibrium binding studies B denotes the amount of radioligand bound, whilst B_{max} denotes the maximum capacity.

$$[RL] = [R]_{tot} \times \frac{[L]}{K_d + [L]} \text{ where } [R]_{tot} \text{ is the concentration of bound and free receptor.}$$

Therefore $B = B_{max} \times \frac{[L]}{K_d + [L]}$ and a plot of B against $[L]$ should produce a rectangular hyperbola.

The top of this curve can give an estimation of B_{max} , and K_d can be estimated by reading the ligand concentration that produces half maximal binding.

In practice, the observed binding is the result of both specific radioligand binding to the receptor and non-specific binding. Since under ideal conditions, non-specific and specific binding are independent, for a given ligand concentration specific binding can be calculated by subtraction of non-specific binding from total binding. In the case of the apamin binding studies described in this chapter, non-specific binding is determined by repeating radioligand binding in the presence of excess unlabelled apamin.

In order to obtain a linear representation of the relationship, saturation binding data is often subjected to linear transformation. A number of transformations may be used, the most common of which is the Scatchard plot:

From the previous equation, $\frac{B}{[L]} = \frac{B_{max}}{K_d} - \frac{B}{K_d}$, and bound/free ($\frac{B}{[L]}$) is plotted against bound (B).

If the data is from a first order reaction, a straight line will be obtained with an x intercept of B_{max} and a slope of $-\frac{1}{K_d}$. Non-linear data may indicate the presence of multiple binding sites of different affinities or cooperativity of binding.

A more common method for the determination of multiple binding sites or cooperativity of binding is transformation of data to a Hill plot. The above equation can be further rearranged:

$$\frac{B}{B_{max} - B} = \frac{[L]}{K_d} \text{ therefore } \log\left(\frac{B}{B_{max} - B}\right) = \log[L] - \log K_d$$

If data is derived from non-cooperative binding to a single class of binding sites, plotting $\log\left(\frac{B}{B_{max} - B}\right)$ against $\log [L]$ should yield a straight line of slope = 1.

4.2.3 Binding of Apamin-N2A Isoforms

4.2.3.1 Synthesis, Refolding and Purification of Apamin Analogues

The synthesis, purification and refolding of the apamin analogues was carried out by Dr Chris Dempsey, (University of Bristol).

Synthetic apamin and synthetic apamin-N2A (both with C-terminal carboxamide) were synthesised using standard Fmoc chemistry 5-10mg of the crude synthetic peptides were purified by reverse phase HPLC using a linear gradient (0-30% acetonitrile/ 0.1% TFA over 35mins) on a Vydac C4 semi-preparative column with a flow rate of 2-3ml min⁻¹. Correct synthesis was confirmed by a) mass spectrometry and b) 2-D NMR.

Disulphides were allowed to form by air oxidation of the synthetic apamins in aerated 10mM sodium phosphate pH7.0, in the presence of 0.1mM EDTA (to remove trace metals which may bind to cysteine side chains and prevent disulphide formation). Disulphide formation was followed by reverse phase HPLC, which was also used to separate and purify the various disulphide-bonded isoforms.

4.2.3.2 Screening of Synthetic Peptides for Inhibition of Monoiodo[¹²⁵I]apamin Binding

The various apamin-based peptides were assessed for their ability to inhibit the binding of radiolabelled apamin to its acceptor on rat brain membranes using a variation of the filtration binding assay described in 4.2.2.5. A single concentration of radiolabelled toxin (100pM) was incubated in the presence or absence of a ten-fold excess of the test substance.

4.2.3.3 Competition Binding Assays with Apamin Analogues

Filtration binding studies, in the presence of increasing concentrations of the peptides were used to construct competition binding curves. 10pM radiolabelled apamin solutions containing varying concentrations of putative competitor were assayed in

triplicate for binding to rat brain synaptic membranes using the filtration binding assay described. The non-specific component was determined by inclusion of 100nM cold native apamin in parallel incubations. As with the screening experiment above, the experiment was carried out in triplicate, with triplicate samples used for each experiment.

Competition binding data was analysed[†] using sigmoidal curve-fitting and Hofstee analysis (*Radlig*). K_i values were estimated for the competitors of radiolabelled native apamin binding.

4.2.3.4 Competition Binding Curves for the Two Halves of HPLC Peak for Apamin N2A-Anti

In order to determine whether or not the competitive binding shown by apamin N2A-anti was due to contamination with the native disulphide bridges isoform, leading and trailing halves of the N2A-anti isoform peak, as purified by HPLC, were collected separately. Competition binding studies were carried out against ¹²⁵I-apamin as before.

[†]In general, assuming non-cooperative binding to single class of receptors, if a range of unlabelled competitor concentrations ([i]) are incubated with the receptor in the presence of fixed amount of radioligand ($<[K_d]$) the resulting concentration of bound radioligand can be plotted against log [i] to produce a sigmoid curve. Inhibitors/competitors are often defined in terms of IC_{50} ([I] which produces 50% reduction in radioligand binding). The $\log IC_{50}$ can be determined directly from this plot. The Hofstee plot linearises this relationship. If the % reduction of ligand binding is plotted against % reduction/competitor concentration, a straight line with a slope of $[IC_{50}]$ is produced.

The relationship between inhibitor concentration [i] and specific binding in the presence of inhibitor (B_i) is given by the equation

$$B_i = B_{max} \times \frac{[L]}{K_d \left(1 + \frac{[I]}{K_i}\right) + [L]}$$

Provided K_d is known for the labelled ligand, non-linear least squares analysis can be used to derive K_i (the equilibrium dissociation constant for the inhibitor/competitor) from the competition binding curves using this equation.

The equations above were taken from Haylett, 1996 and Hulme and Birdsall, 1990. For further information on the subject, refer to these references.

4.2.4 Binding Studies on Alexa Fluor 488 Apamin

4.2.4.1 Testing the Ability of Alexa Fluor 488 Apamin to Inhibit Monoiodo[¹²⁵I]apamin Binding to Rat Brain Synaptic Plasma Membranes

A single concentration of radiolabelled toxin (100pM) was incubated with rat brain membranes membranes, in the presence or absence of 1nM Alexa Fluor 488 apamin in the filtration binding assay described in 4.2.2.5.

4.2.4.2 Competition Binding Curves for Alexa Fluor 488 Apamin

Competition binding curves were created as described for the synthetic apamin analogues (4.2.3.3) using 10pM radiolabelled toxin and concentrations of Alexa Fluor apamin in the range 1pM-100nM. Control curves were created in parallel using 10fM-100pM native apamin.

4.2.4.3 Competition Binding Curves for Alexa Fluor 488 Apamin Under Physiological Buffer Conditions

Competition binding curves for native and Alexa Fluor apamin were performed in physiological HEPES buffered saline solution (HBSS: 124mM NaCl/ 4mM KCl/ 2mM CaCl₂/ 1.2mM MgCl₂/ 10mM glucose/ 25mM HEPES, pH7.4 in the presence of 0.1% BSA) (Massensini et al., 2002). In order to ascertain a suitable concentration of radiolabelled apamin for use in the assay an approximate saturation binding curve was constructed. 40pM proved to be a suitable concentration of radiolabelled apamin and was therefore used. The concentration ranges of the native, and fluorescently labelled toxins used to construct competition binding curves in HBSS were 100fM-10nM and 100fM-100nM respectively.

4.2.4.4 Use of Alexa Fluor 488 Apamin to Visualise Transfected SK Channels in HEK Cells

Alexa Fluor apamin was used to label HEK-293 transfected with the SK2 gene (Cingolani et al., 2002). The same group also used the fluorescent apamin probe to visualise transfected SK3 in these cells (Dr Martin Stocker, University College London - unpublished data). Briefly, cells were incubated with 50nM Alexa Fluor apamin on a coverslip for 10mins. Slide was washed by three dips in PBS and embedded in 20% glycerol in PBS. Binding was visualised with a fluorescent microscope and images recorded with a CCD camera.

4.2.4.5 Electrophysiology of block of rSK2 with Alexa Fluor Apamin

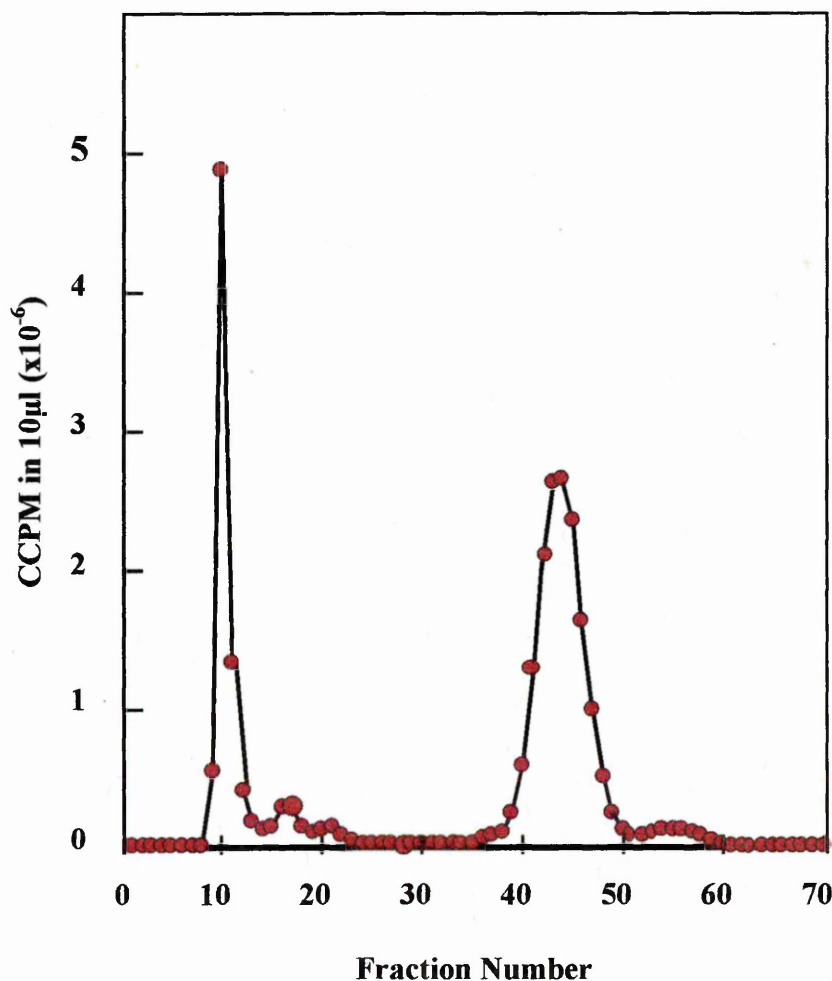
Electrophysiological recordings were performed for the Alexa Fluor apamin block of rSK2 by Mr Dieter D'Hoedt (University College London). The recording conditions were as described for whole cell patch clamp on HEK293 expressing chimeric rSK1 channels in D'Hoedt et al., 2004.

4.3 Results

4.3.1 Radioiodination of Native Apamin

Native apamin was labelled with ^{125}I at His 18 by the Iodogen method, and monoiodo[^{125}I]apamin was purified from the reaction mixture by isocratic ion exchange chromatography (fig 4.2). The first peak represents unincorporated Na^{125}I . The second peak contains monoiodo[^{125}I]apamin free from unlabelled apamin, which remained on the column. The approximate recovery after purification was 50%, and the purity of the final product was >98%. Monoiodo[^{125}I]apamin had a specific activity of 2200Ci /mmol and was stable stored in the presence of 2mgml^{-1} BSA at 4°C for two months.

Figure 4.2 Purification of Monoiodo[¹²⁵I]apamin by Ion Exchange

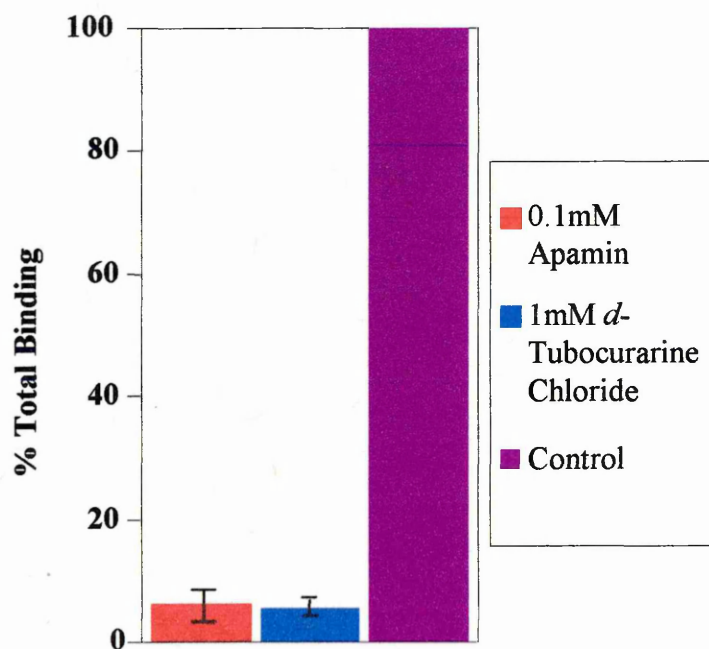


Native apamin was radiolabelled at His18 by the Iodogen method. Monoiodo[¹²⁵I]apamin was purified from the reaction mixture under isocratic conditions (50mM sodium phosphate pH6.0/ 160mM NaCl) on an SP sepharose ion exchange column as described (4.2.2). Fractions were quantified by reading 10µl samples in a γ -counter. The elution profile above is typical of that obtained from three separate iodinations and purifications. The first peak (fractions 9-12) contains unincorporated Na¹²⁵I, and the second major peak (fractions 39-49) contains purified monoiodo[¹²⁵I]apamin with a specific activity of 2200 Ci/mmol. Unlabelled apamin was retained on the column, which was later discarded.

4.3.2 Determination of Biological Relevance of Binding

Unlabelled apamin is obviously very similar in structure to the radiolabelled toxin, and it is therefore possible that it could displace non-biologically relevant saturable binding of the radiolabelled variant. *d*-Tubocurarine differs in basic structure to apamin, but contains the SK channel 'pharmacophore' of two positive charges 11Å apart. These positive charges interact with SK channels providing an additional method of displacing radiolabelled apamin bound specifically to its acceptor. Figure 4.3 shows the percentage displacement of radiolabelled apamin by *d*-tubocurarine chloride to be comparable to that displaced by native apamin and there is no significant difference between the two treatments (2-tail student t-test, $\alpha=0.05$). The binding of the radiolabelled toxin to these membranes is thus both specific and biologically relevant. Displacement by native apamin is a suitable method for determination of non-specific binding as used in the experiments presented in this chapter.

Fig 4.3 Comparison of Binding in the Presence of Cold Apamin or *d*-Tubocurarine



Equilibrium binding assays were performed, incubating 100 μ g rat brain membranes with 100pM radiolabelled apamin. Parallel incubations were carried in the presence of either 0.1 μ M unlabelled apamin or 1mM *d*-tubocurarine chloride, as described in 4.2.2.5. Both treatments are effective at displacing the specific component of 125 I-apamin binding. Data shown is the mean (\pm SD) of that obtained from triplicate incubations and is typical of results obtained in three separate experiments.

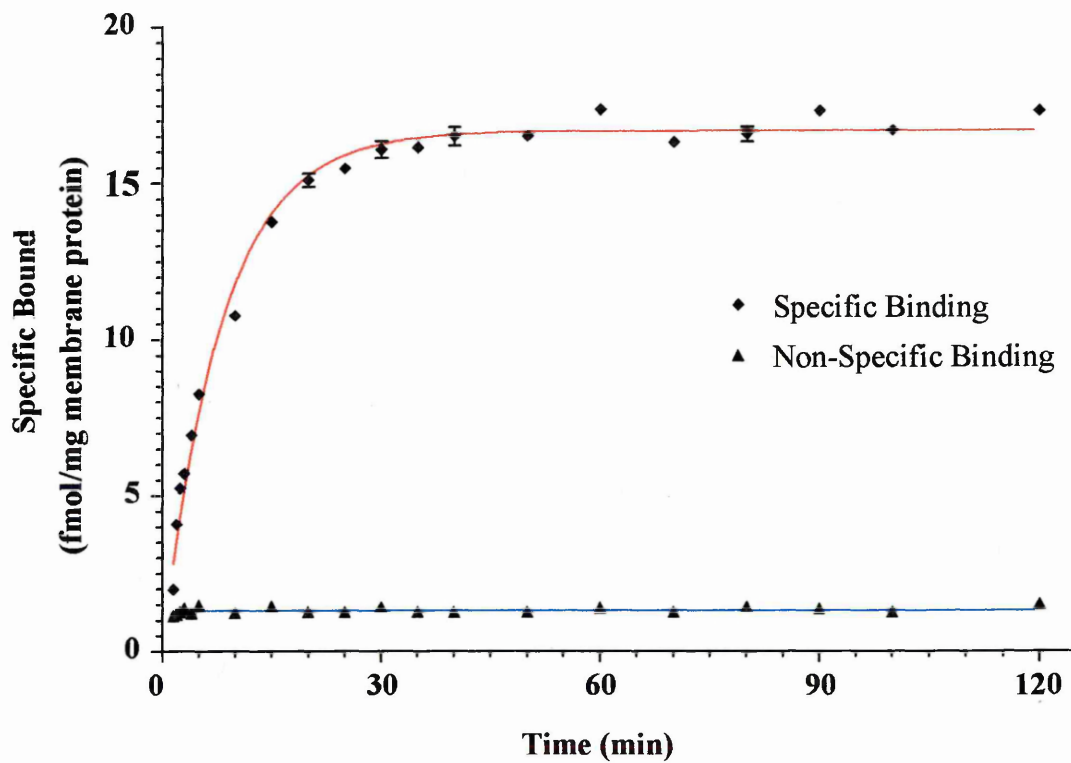
4.3.3 Time Course of Apamin Binding

Rat brain membranes were prepared, and purified by sucrose density gradient centrifugation. A number of experiments were then performed to validate the methodology used and to confirm the quality of the membranes and radiolabelled toxin prior to use in competition binding studies.

In order to confirm that equilibrium was being reached during the incubation of the radiolabelled toxin and the rat brain membranes, a time course was plotted (fig 4.4). The results show that binding of a 15pM radiolabelled apamin solution on ice in the hyposmotic binding buffer used for the majority of the binding experiments is complete in less than 60min. No decay of binding was seen during the course of the experiment, and the data confirms 90min to be a suitable incubation time for binding studies. It is recommended for binding analysis that the concentration of bound radioligand accounts for no more than 10% of that added. Specific maximum binding was less than 10% in this experiment, and indeed throughout the studies, eliminating the need to adjust calculations for ligand depletion[†].

[†]If used in conjunction with data from either dissociation curves, or additional curves showing time course of binding at differing concentrations of radiolabelled toxin, the data from the time course could be used to calculate the association rate constant. Since this has previously been determined for apamin binding to rat brain synaptic membranes (Hugues et al., 1982c), and the purpose of the above experiment was purely validation of assay methodology, these further experiments were not undertaken.

Figure 4.4 Time Course of Apamin Binding to Rat Brain Synaptic Membranes

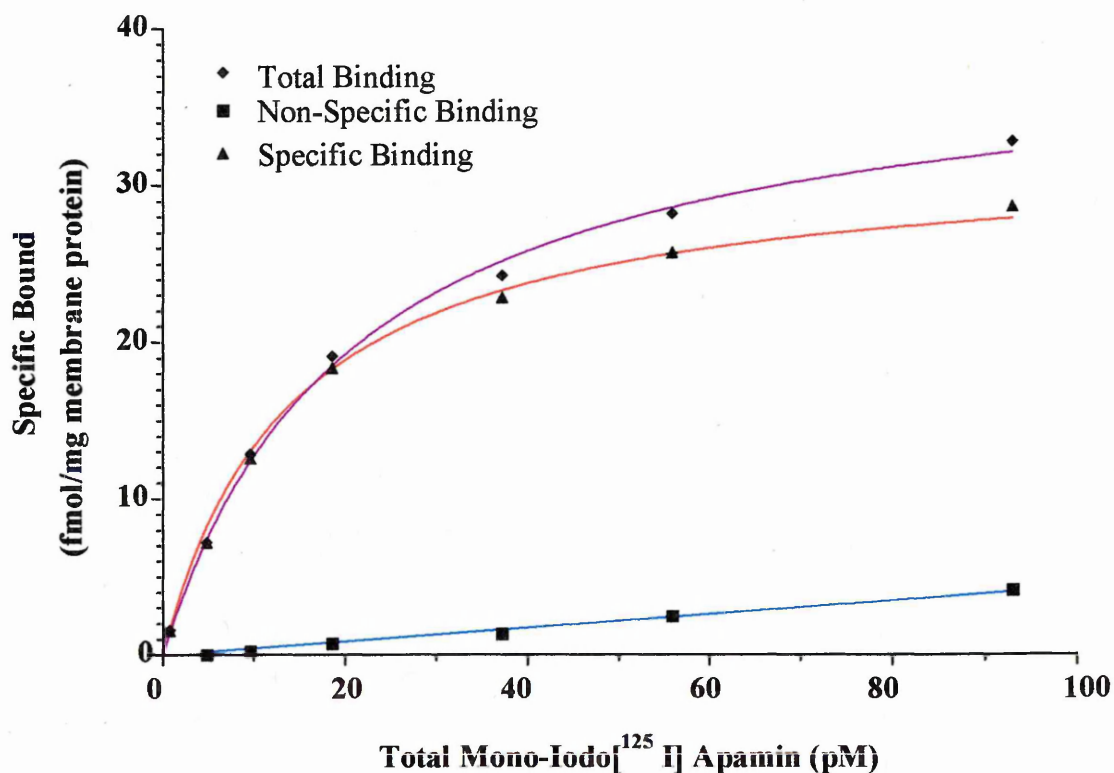


15pM radiolabelled apamin was incubated on ice in the presence of $100\mu\text{gml}^{-1}$ rat brain membranes (\blacklozenge) or $100\mu\text{gml}^{-1}$ membranes pre-incubated with $0.1\mu\text{M}$ native apamin (\blacktriangle) for times ranging between 1.5 and 120min as described 4.2.2.6. All incubations were carried out in triplicate. Points shown are mean \pm SD. Binding curves are the result of fitting combined data from three separate experiments utilizing different incubation times to a one phase exponential association equation using *Prism*.

4.3.4 Saturation Binding Assays

In order to examine the effects of potential competitors on ^{125}I -apamin binding to rat brain membranes, it was necessary to first characterize the binding of the radiolabelled native toxin itself. This was effected by saturation binding analysis, measuring equilibrium binding of increasing concentrations of monoiodo[^{125}I]apamin to prepared membranes. Bound ligand was separated from free on a cell harvester and total binding was quantified using a gamma counter (fig 4.5). Non-specific binding was determined by parallel incubations with unlabelled native toxin. There was no significant saturable binding of ^{125}I -apamin to the filters themselves, and non-specific binding increased linearly with increasing concentrations of labelled apamin. Specific binding was determined by subtracting the non-specific binding from total binding. This specific binding is saturable, at approximately 30pM, proving that the radiolabelled apamin is binding to a limited number of binding sites and is therefore likely to be biologically relevant.

Figure 4.5 Binding of ^{125}I -Apamin to Rat Brain Membranes

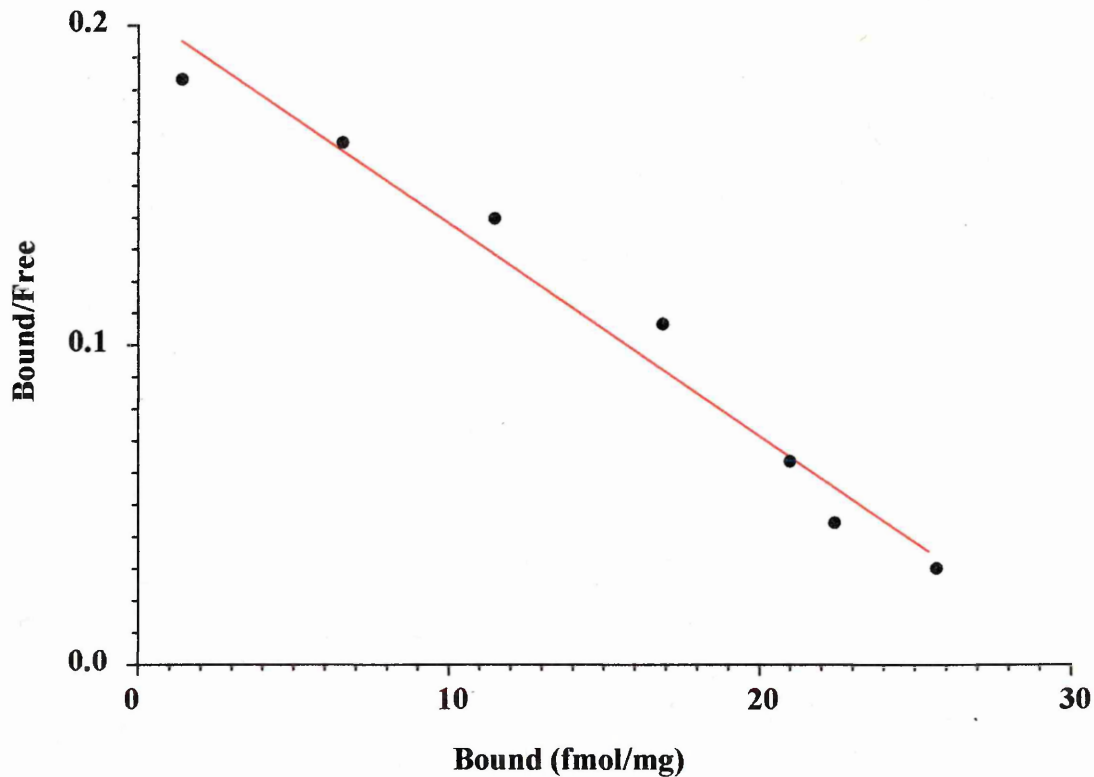


Equilibrium binding studies were performed as described in 4.2.2.4. Rat brain membranes ($100\mu\text{g}$) were incubated with increasing concentrations (0.1 - 100pM) of ^{125}I -apamin in the presence (\blacksquare) and absence (\blacklozenge) of $0.1\mu\text{M}$ unlabelled native apamin for 90min on ice. After rapid filtration, the membrane bound activity was quantified. Saturable specific binding of radiolabelled apamin to its acceptor was calculated as the difference between total and non-specific binding (as determined in the presence of $0.1\mu\text{M}$ unlabelled apamin) (\blacktriangle). Data in the figure above is typical of three separate experiments, each performed with triplicate incubations. In the above figure, *Prism* has been used to fit curves (— and —) to the measured data and a single-site binding curve (—) to the data for specific binding.

4.3.5 Analysis of Binding Data

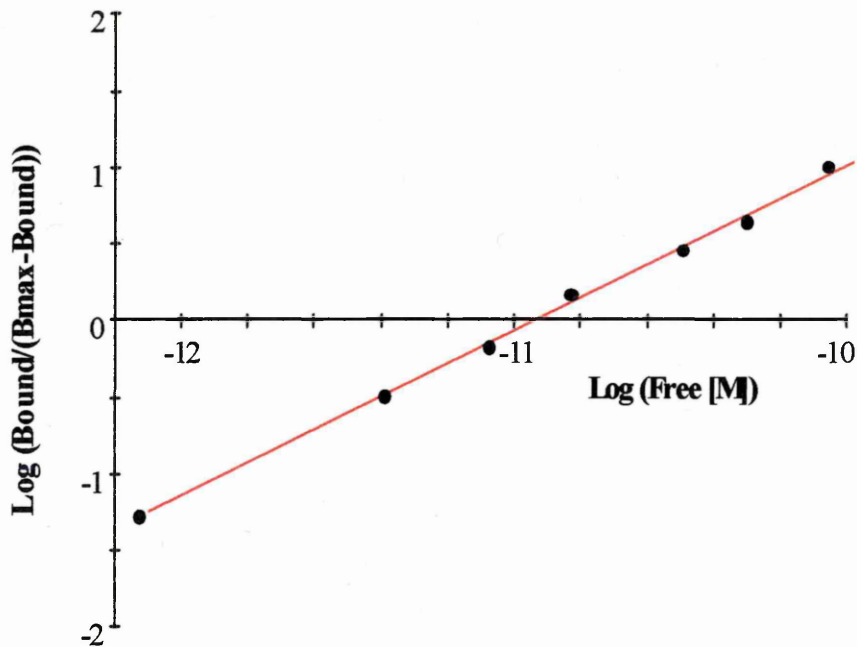
The ratio of bound to free radiolabelled toxin was plotted against the amount bound to give a linear Scatchard plot (fig 4.6). Multi-site modelling using *Ligand* suggests binding to a single class of non-interacting binding sites (correlation coefficient=0.998 +/- 0.001) with K_d 14.8 +/- 4.1 pM and B_{max} 33.8 +/- 3.5 fmol mg⁻¹ membrane protein. Log₁₀ occupancy was plotted against log₁₀ unbound in a Hill plot (fig 4.7). This plot was linear (correlation coefficient=0.998 +/- 0.002), with a Hill coefficient nH=0.98 +/- 0.09 thus showing no evidence for cooperativity, i.e. increasing occupancy of binding sites does not alter affinity of binding. The binding constants are comparable to previous studies suggesting both membranes and radiolabelled apamin are of high quality.

Figure 4.6 Scatchard Plot of Saturable Binding of Radiolabelled Apamin to Rat Brain Membranes



Equilibrium binding studies were performed as described in 4.2.2.4. Rat brain membranes (100 μ g) were incubated with increasing concentrations (0.1-100pM) of 125 I-apamin in the presence and absence of 0.1 μ M unlabelled native apamin for 90min on ice. After rapid filtration the membrane bound activity was quantified. Saturable specific binding of radiolabelled apamin to its acceptor was calculated as the difference between total and non-specific binding. This data (●) was transformed to give a Scatchard plot. *Radlig* used multi-site modelling and non-linear curve fitting to estimate the binding parameters. In all cases the data best fitted a single class of non-interacting binding sites (—). The figure presented is typical of Scatchard plots obtained from three separate experiments each performed with triplicate incubations. The mean observed $K_d=14.8 \pm 4.1$ pM and $B_{max}=33.8 \pm 3.5$ fmol mg^{-1} membrane protein.

Figure 4.7 Hill Plot of Saturable Binding of Radiolabelled Apamin to Rat Brain Membranes



Equilibrium binding studies were performed as described in 4.2.2.4. Rat brain membranes (100 μ g) were incubated with increasing concentrations (0.1-100pM) of 125 I-apamin in the presence and absence of 0.1 μ M unlabelled native apamin for 90min on ice. After rapid filtration the membrane bound activity was quantified. Saturable specific binding of radiolabelled apamin to its acceptor was calculated as the difference between total and non-specific binding. This data was transformed in *Radlig* to give a Hill plot (\bullet) and non-linear curve fitting (---) produced an estimate of the Hill coefficient. In all cases a straight line was obtained with a slope of approximately one ($nH=0.98 \pm 0.09$), indicating non-cooperative binding. The figure presented is typical of Hill plots produced from three separate experiments each performed with triplicate incubations.

4.3.6 Synthesis, Refolding and Purification of Apamin and the Apamin N2A Disulphide Analogues

Apamin and apamin-N2A (a synthetic apamin analogue with Asn-2 replaced by Ala-2) were synthesized using standard Fmoc chemistry, and the crude synthetic peptides purified by reverse phase HPLC. The resulting trace for apamin N2A is shown in figure 4.8(a). The largest peak (for each synthetic peptide) was assumed to be the reduced peptide having the correct sequence. This assumption was verified by analysis of the peptides via mass spectrometry and 2-D NMR.

Disulphides were allowed to form by air oxidation and the reaction followed by analytical HPLC. Oxidation of apamin resulted in formation of a single peptide with native disulphide bridge pairings. In contrast, apamin-N2A underwent oxidation to give two disulphide isomers. Figure 4.8(b) shows an analytical reverse-phase HPLC of the products of apamin N2A oxidation, the peaks being apamin N2A-par, which eluted first, followed by apamin N2A-anti. Apamin N2A-par (parallel cys residues) has the same disulphide bond pairing as native apamin. Apamin N2A-anti (antiparallel cys residues) has an incorrect disulphide bond pairing (Cys1–Cys15 and Cys3–Cys11). Both oxidation reactions were complete after approx. 24hrs.

The oxidation products for synthetic apamin and the N2A analogue were purified by preparative reverse phase HPLC, lyophilized and stored frozen ready for use in the binding assays.

Fig 4.8 Purification of Apamin N2A-Par and -Anti

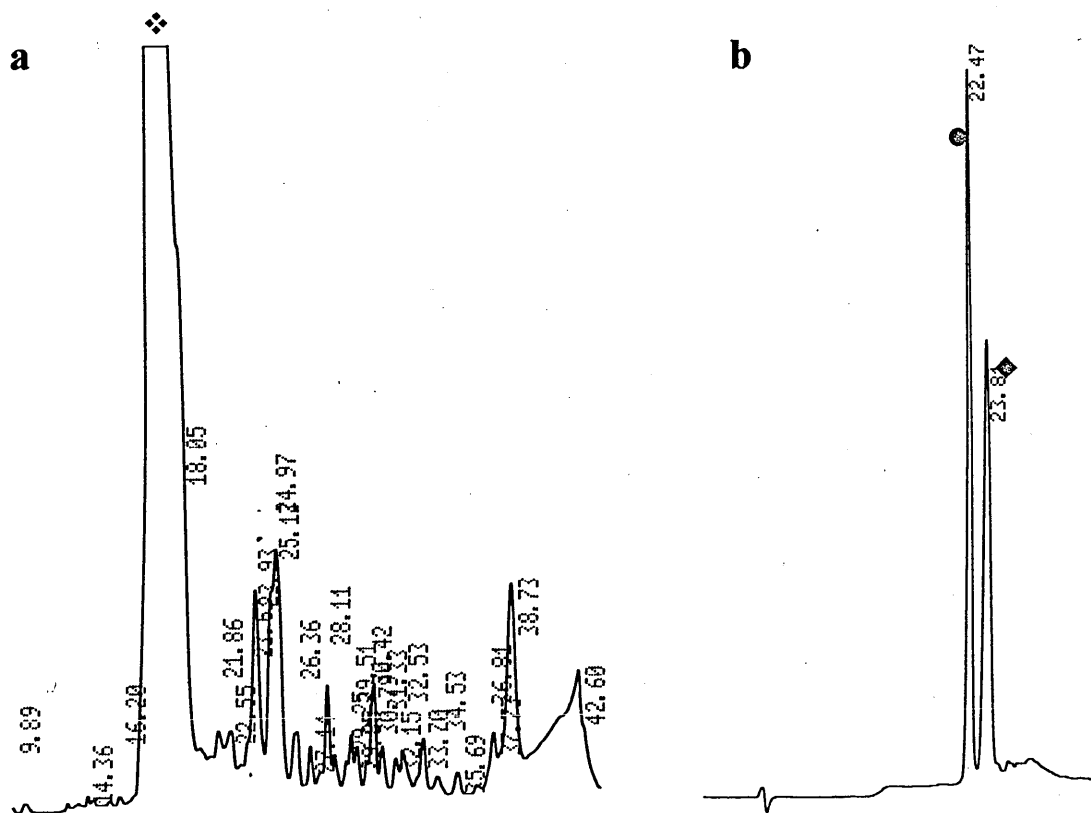


Figure a shows the purification of crude synthetic apamin-N2A by reversed phase HPLC with a gradient of 0-30% acetonitrile over 35min. The largest peak ❖ is the reduced peptide with the correct sequence.

The purified apamin N2A peptide underwent air-oxidation to give two isomers that are seen as two separate peaks after air oxidation is complete. Figure b shows an analytical reverse phase HPLC on the products of apamin N2A oxidation. ○ Apamin N2A-Par (disulphides in native conformation). ❖ apamin N2A-anti (non-native disulphide conformation).

4.3.7 Effect of Native Apamin, Synthetic Apamin, and its N2A Analogues on Binding of Radiolabelled Apamin to Rat Brain Membranes

In preliminary experiments the native and synthetic peptides were assessed for their ability to compete with iodinated apamin for binding to the rat brain membranes. Equilibrium binding assays were performed as previously, incubating a single concentration of radiolabelled apamin with the membranes. Parallel incubations were performed containing a ten-fold excess of the test ligands. Non-specific binding was taken as the binding in the presence of 1nM unlabelled native toxin. Fig 4.9 shows that all ligands significantly compete (1-tailed t-test, $\alpha=0.05$), to various degrees, with the radiolabelled toxin for binding to the apamin acceptor. Although the inhibition of binding seen on addition of apamin N2A-anti was considerably less than that seen with the other peptides, there was no significant difference between the % total binding seen in the presence of native, synthetic, or N2A-par apamin.

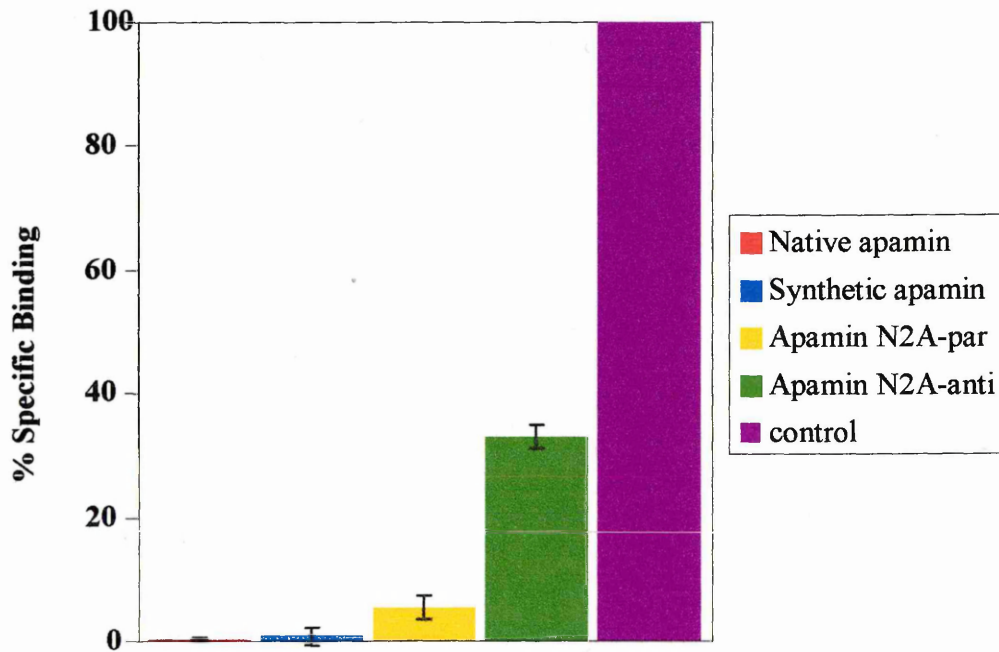
The inhibition of ^{125}I - apamin binding was further examined using 10pM unlabelled toxin in the presence of increasing concentrations of the peptides (100nM-0.01pM). The data was corrected for non-specific binding as determined in the presence of excess (0.1mM) native apamin, and used to construct competition binding curves (fig 4.10). Site modeling using *Radlig* suggested competitive inhibition at a single class of binding sites for all ligands tested and Hofstee analysis provided estimates of K_i for each ligand. Synthetic apamin and apamin N2A-par showed competitive binding of the same order as the native molecule, there being no significant difference (1-way ANOVA, $\alpha=0.05$) between the K_i for native apamin (6.32 +/- 1.55pM), synthetic apamin (9.38 +/- 5.42pM) and apamin N2A-par (5.38 +/- 1.17pM). Apamin-N2A anti was also found to competitively inhibit binding to ^{125}I -apamin binding sites ($K_i = 0.203$ +/- 0.038nM) but with significantly less affinity than the native toxin (1-tailed t-test, $\alpha=0.05$). The affinity constants quoted above are the mean +/- SD of K_i estimates obtained from three separate experiments, each containing triplicate samples.

It should be noted that there was a significant difference (2-tailed t-test, $\alpha=0.05$) between the affinity constant for the native toxin as determined by competition binding, and the

figure obtained using Scatchard analysis. Although some variation is expected due to the different methodology used to generate the data, this is not the cause of the approximately two-fold difference in affinity. The difference is in fact due to the fact that different molecules are being studied. The affinity constant produced by the Scatchard analysis was for the radiolabelled toxin, whilst the figure produced by competition binding was equivalent to the affinity constant for the native unmodified toxin.

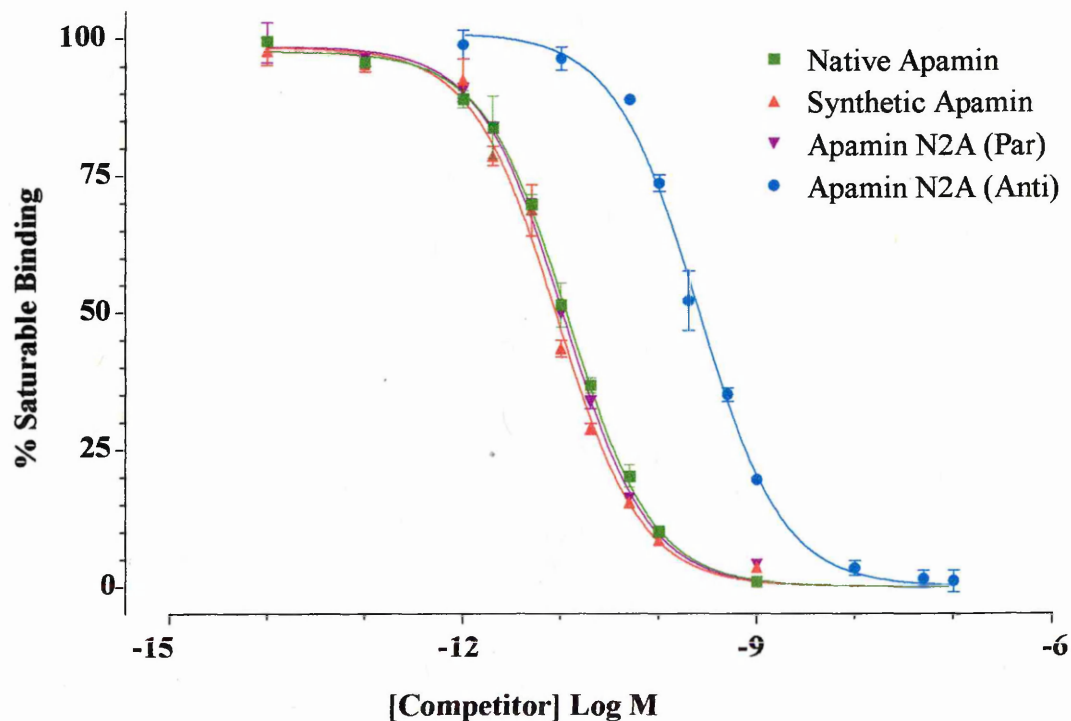
The two isoforms of apamin N2A had been purified by HPLC and showed baseline separation, meaning that contamination of the non-wild type disulphide-paired molecule with its wild-type disulphide-bonded isoform was negligible. In order to confirm that the apamin-acceptor binding seen in the N2-anti isotype was not due to such a contamination, the leading and trailing halves of the HPLC peak were assayed separately. Competition binding studies were performed against ^{125}I -apamin, the data processed, and competition binding curves plotted as for the intact peak above (see fig 4.11). Again, the data fitted a model of competitive inhibitable binding to a single class of binding sites. There was no significant difference (2 tailed t-test, $\alpha=0.05$) between the K_i for the two halves of the peak (leading sample $K_i = 0.201 \pm 0.076\text{nM}$, trailing sample $K_i = 0.208 \pm 0.054\text{nM}$), or between these samples and the whole peak. This suggests that the inhibition of ^{125}I -apamin seen with this ligand was not due to contamination.

Fig 4.9 Comparison of Binding in the Presence of Native Apamin, Synthetic Apamin, Apamin N2A-Anti and Apamin N2A-Par



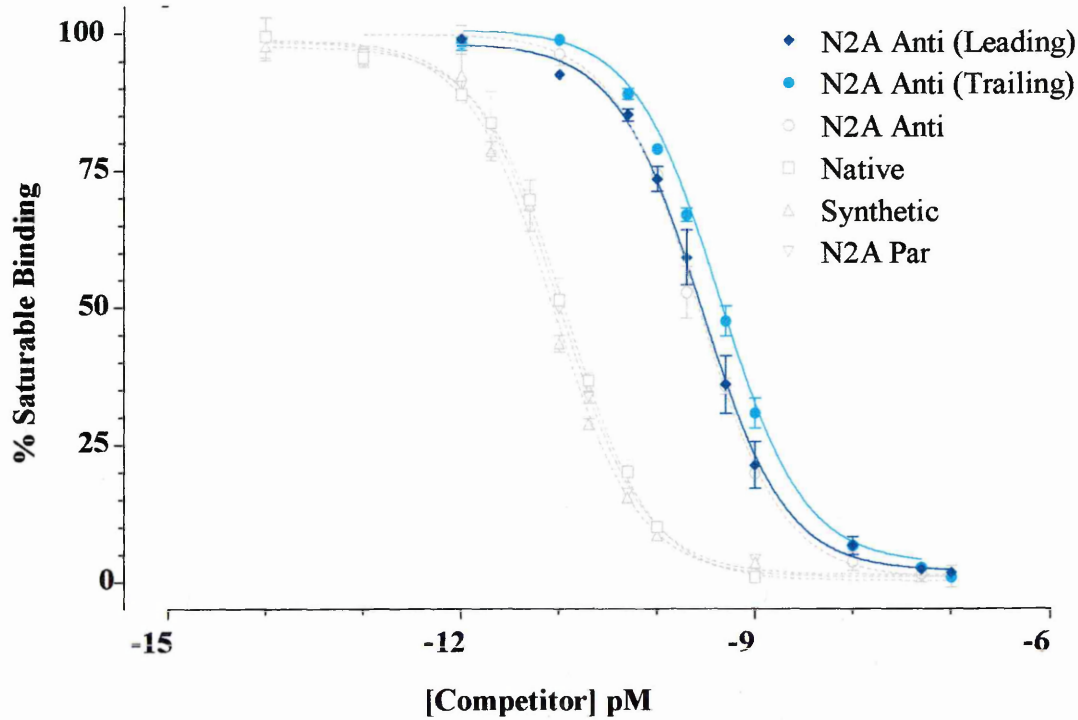
Equilibrium binding assays were performed, incubating 100 μ g rat brain membranes with 100pM radiolabelled apamin. Parallel incubations were carried out in the presence of 1nM unlabelled native apamin; 1nM synthetic apamin; 1nM apamin N2A-par or 1nM apamin N2A-anti as described in 4.2.3.2. All the substances tested inhibited total binding of radiolabelled apamin. Data shown is the mean (+/- SD) of that obtained from triplicate incubations and is typical of results obtained in three separate experiments.

Figure 4.10 Competition Binding Curves for Apamin and its Synthetic Derivatives



The figure shows the inhibition of binding of ^{125}I -apamin to rat brain membranes by native apamin and by the synthetic analogues. Rat brain membranes ($100\mu\text{g}$) were incubated for 90min on ice in the presence of ^{125}I -apamin (10pM) together with increasing concentrations of (■) native apamin, (▲) synthetic apamin, (▼) apamin N2A-par, or (●) apamin N2A-anti. Membranes were harvested by rapid filtration, and ^{125}I -apamin binding calculated as percentage of total binding determined in the absence of competitors. Data was corrected for non-specific binding as determined in the presence of excess ($0.1\mu\text{M}$) native apamin. The data presented is the mean (\pm SEM) of that obtained from triplicate incubations and is typical of results obtained in three separate experiments. The curves displayed are the result of fitting the data points to a one-site competition model using non-linear regression analysis (*Prism*).

Figure 4.11 Competition Binding Curves for the Two Halves of the HPLC Peak Containing Apamin N2A -anti



The figure shows the inhibition of ^{125}I -apamin binding to rat brain membranes by the two halves of the HPLC peak containing apamin N2A-anti. As in figure 4.10, rat brain membranes (100 μg) were incubated for 90min on ice in the presence of ^{125}I -apamin (10pM) together with increasing concentrations of the leading (\blacklozenge) and trailing (\blacklozenge) halves of the apamin N2A-anti peak. Membranes were harvested by rapid filtration, and ^{125}I -apamin binding calculated as percentage of total binding determined in the absence of competitors. Data was corrected for non-specific binding as determined in the presence of excess (0.1 μM) native apamin. The data presented is the mean (\pm SEM) of that obtained from three separate experiments each performed with triplicate incubations. Data obtained previously (fig 4.10) is shown for comparison. The curves displayed are the result of fitting the data points to a one-site competition model using non-linear regression analysis (*Prism*).

4.3.8 Affinity of Alexa Fluor Apamin for Apamin Binding Sites on Rat Brain Membranes

The effectiveness of Alexa Fluor 488 apamin binding to rat brain synaptic membranes was tested. As an initial experiment the ability of the fluorescent derivative to competitively inhibit 100pM radiolabelled apamin binding to its rat brain acceptor was examined as described previously. As can be seen in fig 4.12 the percentage total binding was significantly reduced (one-tailed t-test, $\alpha=0.05$) in the presence of Alexa Fluor apamin. The degree of this reduction was somewhat surprising, however, when compared with that seen previously using a comparable concentration of apamin N2A-anti (see fig 4.9). This initial experiment appears to indicate Alexa Fluor apamin to have a considerably lower affinity than the non-wild type disulphide bonded N2A-anti apamin analogue. Full competition binding curves carried out with the fluorescent toxin confirmed these results (fig 4.13). As would be expected, site modelling using *Radlig* showed the data to fit a model for competitive inhibition at a single class of binding sites. The calculated K_i was 0.47 ± 0.07 nM, which represents an approximately 70-fold drop in affinity when compared to native apamin ($K_i=6.32$ pM).

From these results it appears that Alexa Fluor apamin has a considerably lower binding affinity than native apamin, yet immunocytochemistry experiments carried out with the probe (Cingolani et al., 2002) give good results. The immunocytochemistry was carried out under physiological buffer conditions. Both native and radioiodinated apamin show lower binding affinity in isosmotic buffers than under the low ionic strength conditions used above (as can be seen in the summary of published apamin binding parameters, table 4.1). Since the majority of experiments requiring the use of Alexa Fluor apamin would be carried out under physiological buffer conditions, binding studies were repeated using such buffers.

Since the change in buffer was expected to reduce the affinity of 125 I-apamin binding, it was anticipated that the 10pM radiolabelled apamin concentration, used under low-salt conditions, would not produce sufficient binding to allow for the construction of accurate competition binding curves. In order to ensure that the physiological buffer experiments were carried out using a suitable concentration of radiolabelled apamin, a single experiment was carried out (triplicate incubations, $n=1$) to construct a saturation binding curve and give an rough approximation of $K_d=40$ pM under these conditions

(data not shown), which is at the lower end of the range reported in the literature (see table 4.1). Since estimates for apamin affinity constants obtained by our research group (Wadsworth et al., 1994; Wadsworth et al., 1996) in low ionic strength buffer have been consistently at the lower end of the spectrum, this 40pM value would seem to be feasible, and thus 40pM radiolabelled apamin was used experimentally to determine the effects of higher salt on Alexa Fluor Apamin binding.

As can be seen (fig 4.14), under isosmotic conditions, there is still a significant (one tailed t-test, $\alpha=0.05$) reduction in Alexa Fluor apamin binding ($EC_{50}=156 \pm 6$ pM) compared to that of the native toxin ($EC_{50} 25.7 \pm 0.8$ pM), but the difference between the two toxins would appear to be reduced. Again, site modelling using *Radlig* showed the data to fit a model for competitive inhibition at a single class of binding sites. It is not possible to calculate K_d values from the existing data, and hence compare the binding in the two buffers directly[†], but without knowledge of the mechanism leading to the reduction of binding seen with the Alexa Fluor apamin derivative, such quantification would be of little practical use.

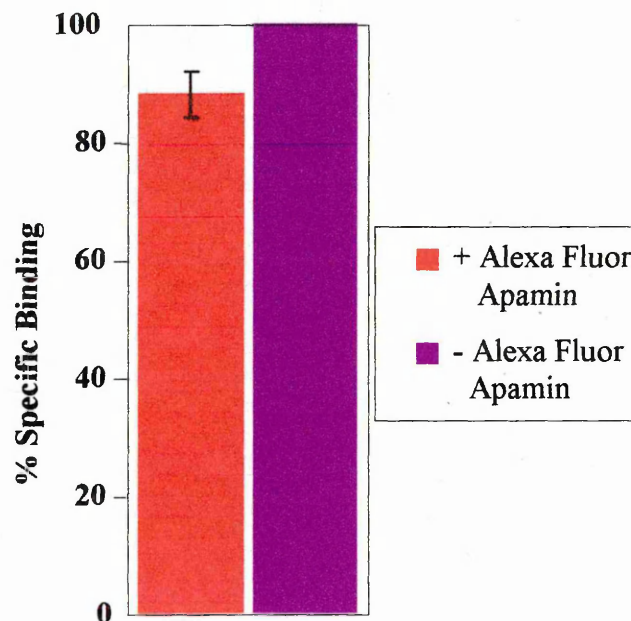
Parallel observations on the effectiveness of Alexa Fluor apamin binding were noted by our collaborators at University College London. The fluorescent toxin was used to visualise apamin receptors on SK2 (Cingonali et al., 2002) and SK3 cell lines (Dr Martin Stocker) (see fig 4.15). The UCL group noted experimental difficulties due to a very fast off rate associated with SK2 binding. Alexa Fluor apamin binding to SK2 was further studied electrophysiologically (fig 4.16). There was no difference in the association and dissociation kinetics. The observed IC_{50} was 324 ± 42 pM, indicating an approximately 6-fold reduction in affinity compared to the native toxin (Mr Deiter D'Hoedt and Dr Martin Stocker unpublished data). The UCL data is comparable to our data showing a reduction in membrane binding for the fluorescent versus native toxin under physiological salt conditions (fig 4.15).

[†]Ideally, in order to be able to directly compare binding affinities in the two buffers, the two sets of experiments should have been carried out using identical 10pM quantities of radiolabelled toxin. The differences in binding seen under the two conditions was such that 10pM radiolabelled apamin did not produce adequate inhibitable binding under high-salt conditions to allow for the construction of accurate competition binding curves. A single experiment was carried out to determine a suitable ¹²⁵I-apamin

concentration for use under these conditions, the figure of 40pM being a rough estimate of binding affinity, produced for this purpose.

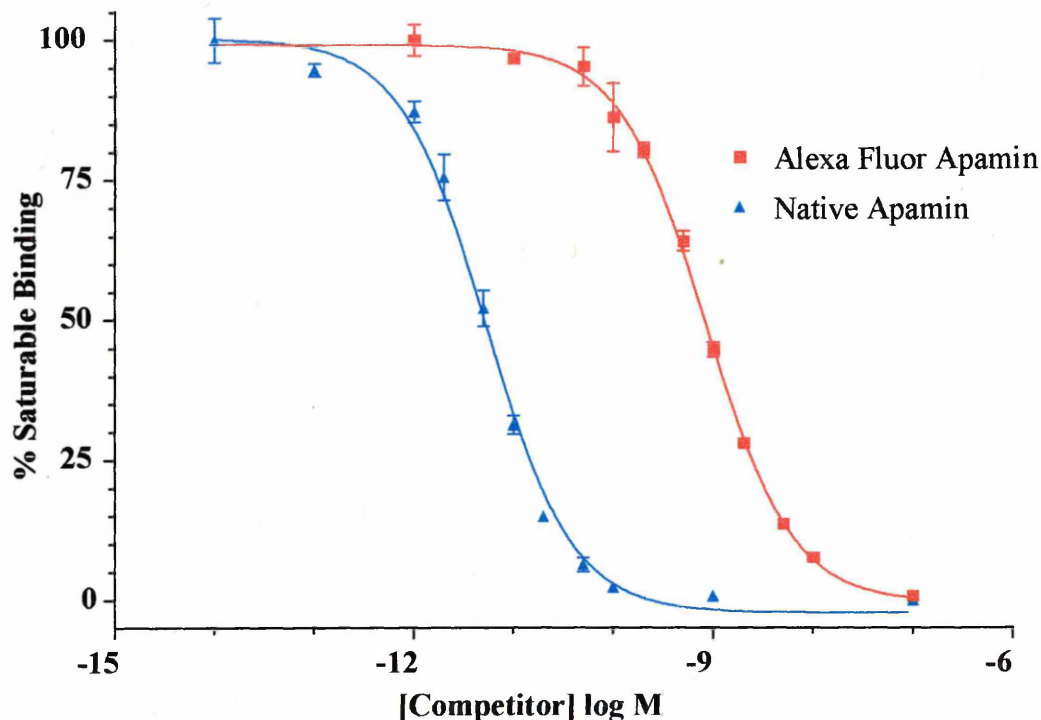
For this reason, this value was not used to determine K_d for native and fluorescent apamin in the competition assay described in isosmotic buffer. Determination of an accurate K_d for these compounds, and thus direct comparison between binding in high- and low-salt would have required construction of full binding curves in triplicate. Since quantitative analysis would be unlikely to shed light on the mechanism of this salt effect, these experiments were not undertaken.

Fig 4.12 Radiolabelled Apamin Binding in the Presence and Absence of Alexa Fluor Apamin



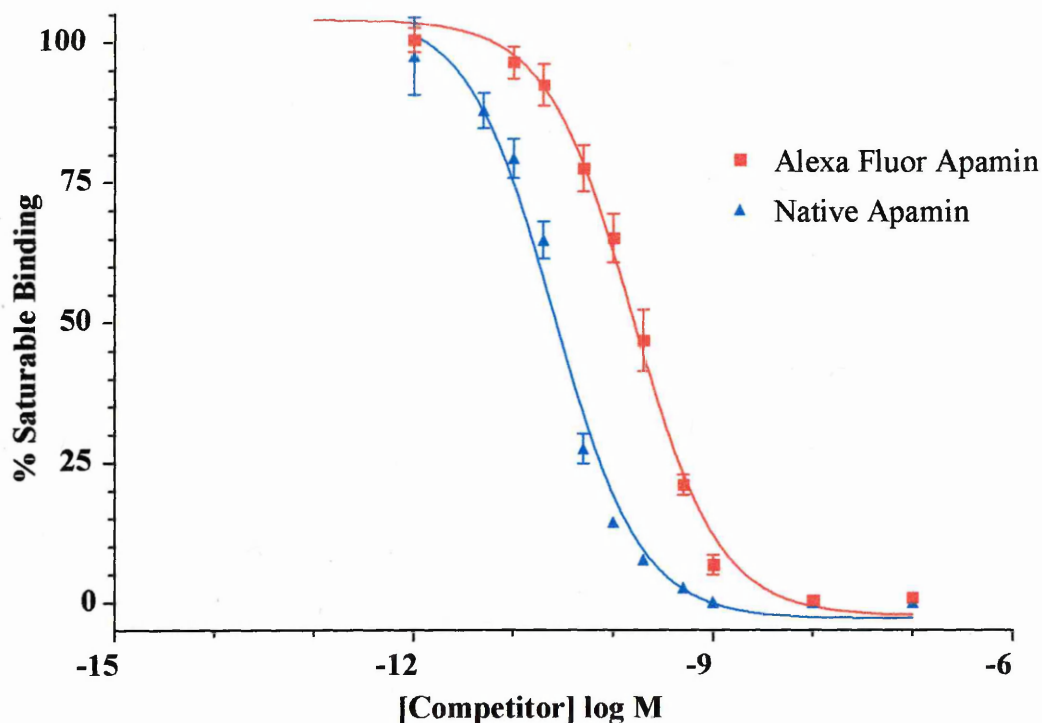
Equilibrium binding assays were carried out, incubating 100 μ g rat brain membranes with 100pM radiolabelled apamin. Parallel incubations were carried out in the presence of 1nM Alexa Fluor apamin as described in 4.2.4.1. Binding of radiolabelled apamin was reduced in the presence of the fluorescently labeled toxin. Data shown is the mean (\pm -SD) of that obtained from triplicate incubations and is typical of results obtained in three separate experiments.

Fig 4.13 Competition Binding Curves for Alexa Fluor Apamin



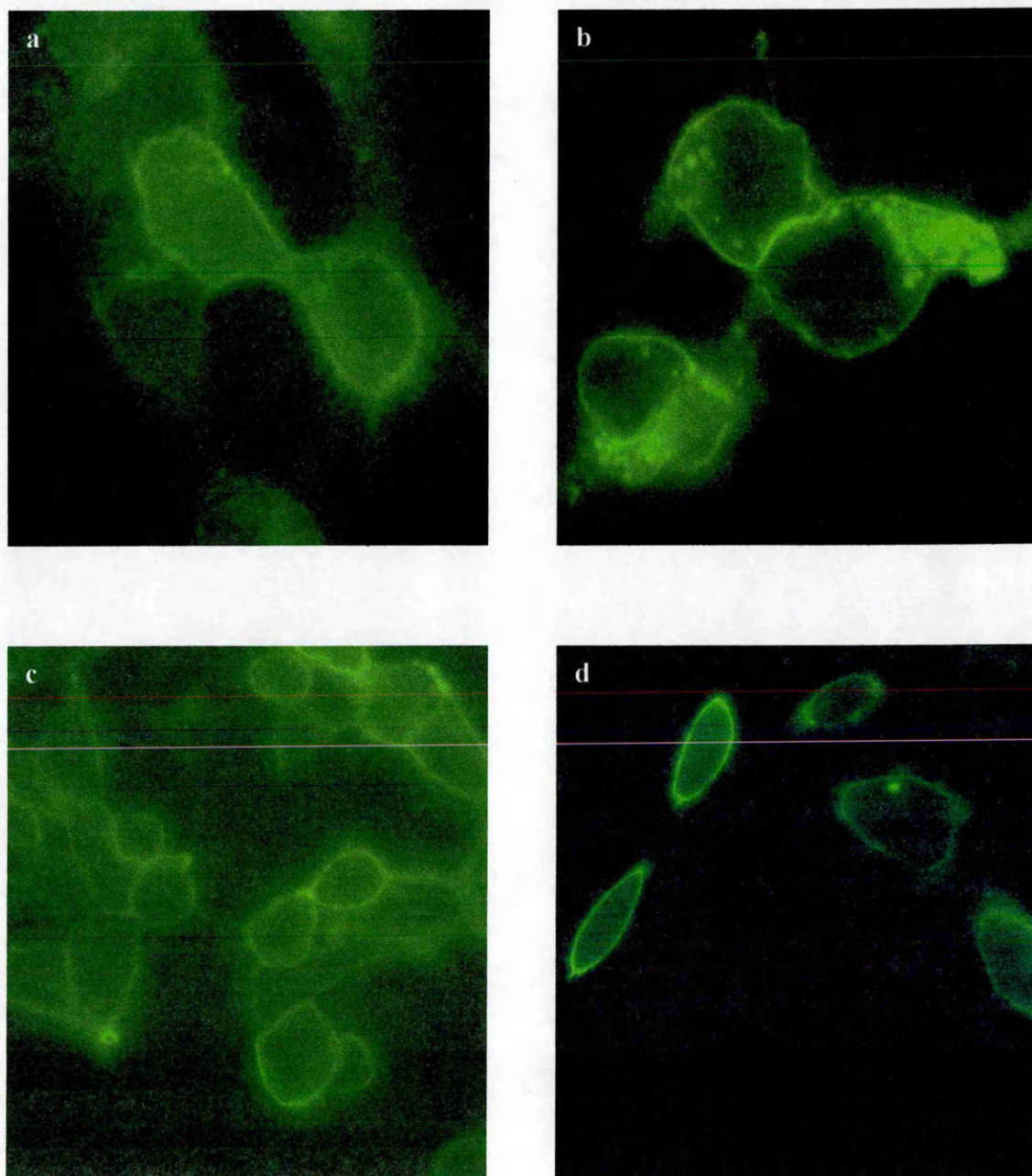
The figure shows the inhibition of binding of ^{125}I -apamin to rat brain membranes by native apamin and by the fluorescently labelled Alexa Fluor toxin. Rat brain membranes (100 μg) were incubated for 90min on ice in the presence of ^{125}I -apamin (10pM) together with increasing concentrations of (\blacktriangle) native apamin or Alexa Fluor apamin, (\blacksquare). Membranes were harvested by rapid filtration, and ^{125}I -apamin binding calculated as percentage of total binding determined in the absence of competitors. Data was corrected for non-specific binding as determined in the presence of excess (0.1 μM) native apamin. The data presented is the mean (\pm SEM) of that obtained from triplicate incubations and is typical of results obtained in three separate experiments. The curves displayed are the result of fitting the data points to a one-site competition model using non-linear regression analysis (*Prism*, GraphPad software, San Diego USA).

Fig 4.14 Alexa Fluor Apamin Competition Binding Curves in Physiological Buffer



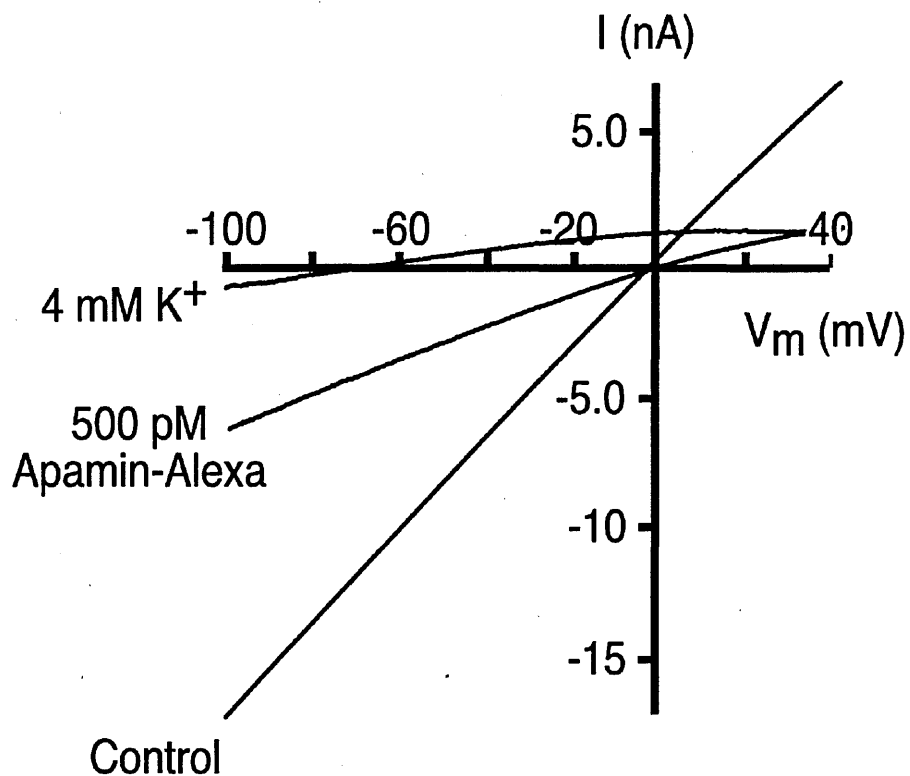
The figure shows the inhibition of binding of ¹²⁵I-apamin to rat brain membranes by native apamin and by the fluorescently labelled Alexa Fluor toxin in physiological strength buffer. Rat brain membranes (100µg) were incubated for 90min on ice in the presence of ¹²⁵I-apamin (10pM) together with increasing concentrations of (▲) native apamin or Alexa Fluor apamin, (■). Membranes were harvested by rapid filtration, and ¹²⁵I-apamin binding calculated as percentage of total binding determined in the absence of competitors. Data was corrected for non-specific binding as determined in the presence of excess (0.1µM) native apamin. The data presented is the mean (+/- SEM) of that obtained from triplicate incubations and is typical of results obtained in three separate experiments. The curves displayed are the result of fitting the data points to a one-site competition model using non-linear regression analysis (*Prism*, GraphPad software, San Diego USA).

Fig 4.15 Alexa Fluor Apamin Binding to Expressed SK Channels



HEK-293 cells expressing SK2 (a and b) and SK3 (c and d) cell lines were incubated for 10mins with 50nM Alexa Fluor apamin on coverslips. Cells were washed by dipping x3 in PBS and embedded in PBS/ 20% glycerol. Images were recorded using a CCD camera. Images were supplied by Dr Martin Stocker, UCL.

Fig 4.16 Electrophysiological Block of rSK2 Currents by Alexa Fluor Apamin



Whole-cell patch clamp recordings were made in the presence of $1\mu\text{M}$ $[\text{Ca}^{2+}]_i$ on HEK-293 cells expressing rSK2 channels. Voltage ramps of -100 to $+40\text{mV}$ were applied (ramp duration 400ms) in the presence, and absence, of Alexa Fluor apamin. A representative experiment is shown above. ($\text{IC}_{50}=324 \pm 42\text{pM}$, $n=4$). Data was provided by Mr Dieter D'hoedt and Dr Martin Stocker (UCL).

4.4 Discussion

Prior to its use in the characterisation of potential competitors of apamin binding, various parameters of the apamin-binding assay were tested. The saturation binding studies reported in this chapter show binding of monoiodo[¹²⁵I]apamin to a single class of acceptors on rat brain membranes with $K_d=14.8 \pm 4.1$ pM and $B_{max}=33.8 \pm 3.5$ fmol mg⁻¹. These values are comparable to those seen in previous studies (table 4.1). Binding was shown to be specific and biologically relevant by carrying out assays in the presence of excess unlabelled apamin and also in the presence of tubocurarine (as described by Cook and Haylett, 1985). These results proved both membranes and radiolabelled apamin were of high quality and that the binding assay was functioning correctly.

The structure of apamin has been investigated by a number of authors, and the main residues critical for binding to SK channels and for toxicity have been identified. The compactness and high stability of apamin have led to its use as a model peptide, for instance in structure-antigenicity relationships (Defendini et al., 1990), testing of structural algorithms (Sun, 1995), analysis of disulphide linkages (Gray, 1993) and, as in this study, functional determination of secondary structure.

The experiments using synthetic apamin analogues described in this chapter examine the functional importance of the β -turn motif and the Asn 2 residue. Native apamin had a K_d of approximately half that for the radiolabelled toxin. This two-fold decrease in activity on radioiodination at His18 is in agreement with the observations of Hugues et al., 1982a. Synthetic apamin has been shown to have full biological activity (Sandberg and Ragnarsson, 1978) and as would be expected the synthetic apamin peptide used in this study showed the same level of binding as the native, thus proving the effectiveness of synthesis and the validity of its use.

Apamin has a well-characterized β -turn motif that helps to stabilize the structure. NMR studies show that replacement of Asn2 with Ala2 destabilizes the peptide, and it was envisaged that this would lead to a reduction of binding activity. The data for the competition binding curves with apamin N2A-par show the Asn-2 amino acid and the β -fold to be non-critical for binding. The structural studies performed on this peptide (Dempsey et al., 2000, Dempsey personal communication) showed apamin N2A-par is

only transiently unfolded, this state accounting for approx 10% of its conformation at any given time. Therefore 90% of the toxin would show full binding affinity, with the remaining 10% binding with reduced affinity. Taking into account errors in peptide quantification and the inherent error in the binding studies, it is likely that such a small decrease in affinity would not be statistically significant. It is also possible that the native state is stabilized on binding; thus the loss of the β -turn region would have a greater effect on the kinetics of binding than on the overall affinity. A third possibility is that despite structural changes in the molecule as a whole, spatial relationships between residues critical for apamin binding are maintained. Future studies using Biacore technology will explore the effects of the N2A substitution on binding kinetics.

Since apamin contains four cysteines, there are three possible ways that disulphides can form. The globule and ribbon formations (illustrated in fig 4.1) are produced by Cys1-Cys11, Cys3-Cys15 and Cys1-Cys15, Cys3-Cys11 respectively. A third 'bead' conformation would be produced by Cys1-Cys3, Cys11-Cys15 pairing, producing two small loops in the structure. This is thought to be highly unfavourable due to steric interactions. Callewaert et al., 1968, determined the disulphide pairing of apamin to be Cys3-Cys15, Cys1-Cys11 and upon air oxidation fully reduced native apamin folds spontaneously to give this native disulphide bond pairing (Huyghues-Despointes and Nelson, 1992). The apamin N2A analogue used in here, however, produces an additional ribbon conformer under these conditions.

Surprisingly, the molecule containing mispaired disulphide bonds showed only a 30-fold reduction in its ability to displace apamin from SK channels. Further experiments ruled out the possibility of contamination with the native disulphide bridged isoform, and it seems that despite the incorrect disulphide bond pairing apamin N2A-anti retains a significant, if low, affinity for the apamin acceptor.

One disulphide-bridged intermediates are rare in the formation of apamin, but at least three of these intermediates are found at very low concentrations in an equilibrium folding mixture (Chau and Nelson, 1992). By substitution of specific cysteines with alanines, the properties of two of these single disulphide structures have been examined, namely those containing each of the native disulphide bonds (Chau and Nelson, 1992; Huyghues-Despointes and Nelson, 1992; Xu and Nelson, 1994). The Cys3-Cys15 bond is the most stable and forms first, its formation promoting that of the second disulphide.

CD analysis of molecules containing only this Cys3-Cys15 linkage showed the presence of significantly less α -helix than those with both bonds. NMR, however, showed an overall structure similar to that of the native toxin with similar relative positioning of the α -helix and β -turn. Thus this Cys3-Cys15 linked peptide would appear to have multiple conformations similar to the native and, as one might expect, the absence of one disulphide allows for greater flexibility. Peptides containing only the Cys1-Cys11 disulphide show far less secondary structure; the N-terminal of the α -helix is present along with some secondary structure in the reverse turn region. Although Cys3-Cys15 appears structurally more important, the functional effects of removing this bond have not been investigated.

Reduced apamin and homologs equivalent to the fully-reduced peptide have been synthesised and studied. Reduced and alkylated apamin had been reported to have no neurotoxicity (Habermann, 1972; Vincent et al., 1975). These studies, however, used only a single dose 10 times that of the lethal dose of apamin. A later study (Labbe-Jullie et al., 1991) using higher concentrations of an open-chain apamin analogue, showed apamin-like symptoms followed by complete recovery, when 1-10 μ g (i.e. 100-1000 times the lethal dose of native apamin) was injected into mice. Binding studies with the same open-chain analogue showed that it could completely displace radiolabelled apamin with a $K_{0.5}$ of 79nM (c.f. 0.012nM for the native toxin), suggesting that even without the disulphide bridges a small fraction of the molecules are in a conformation that allows for residual specific binding to the apamin acceptor.

Although removal of disulphide bridges may maintain some secondary structure and allow for greater malleability of the molecule, one would expect, however, alterations of the cysteine partners within the pairings to distort the molecule, preventing formation of a native like structure. Prior to the study by Dempsey et al., 2000, the N-terminal sequence had been shown to play a role in directing disulphide pairing. Deletion of the Lys4 produced a similar disulphide pairing to that seen with apamin N2A-anti (Volkman and Wemmer, 1997) and with endothelin (a powerful vasoconstrictor peptide which, like apamin contains a CSH motif and four cysteine residues at identical positions, but which naturally adopts a ribbon formation). NMR experiments, however, showed the 3D structure of the Lys4-deleted molecule to more strongly resemble apamin than endothelin, implying that the folding, and consequently the structure, is due more to the primary sequence than to the disulphide pairing.

Substitution of selenocysteine for specific cysteine residues encourages apamin to fold with distinct disulphide bridge pairings as a consequence of differences in redox potential between disulphide and diselenocide bonds. In this way apamin analogues have been created in each of the three disulphide conformations (Pegoraro et al., 1999; Fiori et al., 2000) and the structures examined by CD and NMR. The different structures showed far more similar spatial conformations than would have been expected, with the α -helical region left largely intact. There was found to be a *cis-trans* isomerisation of the Ala5-Pro6 peptide bond in all of the selenocysteine-induced structures, with the trans-Pro-6 isomers showing greatest structural similarity to the wild type. The proportions of this isomer varied however, the proportion of the *cis*-isomer being reduced in the bead formation and increased in the ribbon formation. Incidentally, *cis* isomers are increased in the apamin N2A-anti and to a small extent in the apamin N2A-par molecules used in this study (Dempsey et al., 2000). In this ribbon conformation the β -turn is partially and totally disrupted in the *trans* and *cis* isomers respectively but the C-terminal α -helix is only slightly distorted. Surprisingly, the structural conformation of the bead analogue was closer to that of native apamin than that of the ribbon formation, although it demonstrated greater flexibility. Importantly, there was little perturbation of the α -helix, which also maintained its relative position to the N-terminal portion.

Similar experiments with truncated apamin, using selective deprotection of the cysteines to promote the different disulphide pairings, showed only the globule formation to have significant α -helical content (Ramalingam and Snyder, 1993). The apparent difference between the two groups' findings may be due to the ribbon and bead formations being more flexible and having more than one structure, which would show as disorder on a CD spectrum.

Although several authors have looked at the effects of different disulphide pairing on structure, the experiments presented in this chapter would appear to be the first analysis of their effects on function. It would be interesting to test the binding ability of the conformational isomers described above. Of particular interest would be those in the bead formation, which show unexpectedly similar structure to the native toxin, the main differences lying in the β -turn, which has proved non-essential for binding.

Since scorpion toxins share both the ion channel blocking properties and the structural CSH motif of apamin, studies carried out on scorpion toxins may also be relevant to the

bee venom toxin. For example, maurotoxin is a four disulphide-bridged peptide from the scorpion *Scorpio maurus palmatus* with a broad selectivity, blocking SK and Kv1.2 and Kv1.3 channels (Kharrat et al., 1996, 1997; Carlier et al., 2000; and Avdonin et al., 2000). It has a different disulphide pattern to that of other scorpion toxins (C1-C5, C2-C6, C3-C4, C7-C8), but maintains a similar 3D structure (Blanc et al., 1997) and the ability to bind to and interact with potassium channels. For this reason, the effect of maurotoxin's disulphide bridges on folding, structure and function have been well studied (Fajloun et al., 2000, 2000b; Lectome et al., 2000; Carlier et al., 2001; Di Luccio et al., 2002). It has been shown that differential pairing of these disulphide bridges alters the 3D structure and hence spatial distribution of key residues, which in turn alters the selectivity of the toxin (Fajloun et al., 2000; Fajloun et al., 2000b; Lectome et al., 2000; Carlier et al., 2001). These structural alterations still tend to maintain the general α/β scaffold and do not necessarily destroy maurotoxin's binding ability, nor significantly decrease its affinity for potassium channels. Therefore the disulphide arrangement has important roles and these bonds have been proposed to not just stabilize pre-folded structures, but to subtly determine the final 3D structure and hence selectivity of the toxin (Fajloun et al., 2000). Studies on other scorpion toxins have looked at the effects of removing single disulphide bonds and report differing effects on binding activity (Sabatier et al., 1996; Calabro et al. 1997; Drakopoulou et al., 1998; Zhu et al., 2002).

One would expect the sturdy CSH backbone, which is highly conserved in ion channel toxins, to play an important role in stabilizing structure and hence activity. There is, however, increasing evidence that the basic 3D structure of the molecule is not as reliant on this bonding pattern as one might expect and that the α/β fold can be maintained in some toxins in the absence of one or more disulphide bridges. Indeed, it has been suggested by Tamaoki et al., 1998, that the positions of the cysteines are more important in the formation of the CSH motif than the pairing of the disulphides. In the case of apamin N2A, a non-wild-type disulphide-bond pairing imparts less stability, and therefore greater flexibility upon the molecule. Although this peptide spends less time in a conformation compatible for binding, it may still be free to transiently form such a structure. The consequential loss of effective concentration of the ligand would be expected to decrease the K_d through a reduction in the on-rate of the peptide. The off-rate would be unaffected. It is hoped to study the kinetics of apamin binding in future, using real-time measurements on a *Biacore* system. It is thus proposed that in apamin

(and possibly also scorpion toxins) the bridge pattern is not critical for the recognition of potassium channels, as long as structural constraints allow for the formation of the α/β fold and maintain a correct spatial distribution of critical residues. More subtle changes in structure (probably within the α -helical region) are likely to alter binding affinities, and also the selectivity of the molecule. The latter has not been investigated for the apamin analogues used in this study, but would prove interesting for future examination.

The resistance of native apamin to proteolytic digestion results from its tightly folded structure. Fully reduced apamin is readily digested by proteolytic enzymes (K. Newton, unpublished observations). Mice injected with a non-disulphide bridged variant of apamin initially showed symptoms characteristic of apamin poisoning, but subsequently completely recovered (Labbe-Jullie et al., 1991). It was proposed that the toxin was binding to its acceptor (albeit with a lower affinity) but was losing toxicity over time by enzymatic degradation as a consequence of the unfolded state of the molecule. It would be interesting to examine the resistance of the apamin analogues studied in this chapter to proteolytic digestion. Does the increase in flexibility of the molecule leave it more exposed to proteolytic attack? And therefore does the β -sheet serve to stabilize the molecule and impart resistance to degradation? It would also be useful to study the vulnerability of an apamin molecule in the 'bead' conformation, to fully understand the role that correctly formed disulphide bridges play in the proteolytic resistance of the native toxin.

Despite a number of potential applications (as discussed earlier), the use of fluorescently-labelled ion-channel toxins has not often been reported, and only a few ion-channel toxins appear to have been successfully labelled with fluorescent moieties, including toxins active on sodium (Joe and Angelides, 1993; Darbon and Angelides, 1984), calcium (Jones et al., 1989), and NMDA receptor (Benke et al., 1993) channels. As an example, a variety of fluorescent derivatives of *Leiurus quinquestriatus quinquestriatus* toxin V have been reported to retain high specificity for the voltage sensitive sodium channel (Angelides and Nutter, 1983) and show only 2-3 fold loss of activity compared to the native toxin. The technique used by a number of groups (Darbon and Angelides, 1984; Angelides, 1986; Jones et al., 1989; Cohen et al., 1991) was to incorporate fluorescent moieties via reaction with primary amines. This is not ideal, since we know that potassium channel toxins tend to rely on the interaction of

positively charged amino acids with the channel for binding, and modification would thus be expected to lead to a loss of affinity. Experiments were designed to determine if this was a potential problem with the use of Alexa Fluor 488 apamin (specifically labelled at Lys4). The results presented indicate a greatly reduced affinity of Alexa Fluor 488 apamin for the rat brain membrane apamin acceptor when compared to native-apamin and to the radiolabelled counterpart used in the majority of experiments in this chapter.

At first sight it may appear that the results described here contradict those of Vincent et al., 1975, who saw a much smaller effect on toxicity of labelling apamin, via primary amines, with a fluorescein derivative. It should be noted, however, that binding does not necessarily directly correlate with toxicity, the former being highly dependent on ionic strength. The work of Albericio et al., 1984 corroborates this; modification of one of the two arginine residues in apamin produced a 100-fold loss of toxicity and a corresponding 1000-fold loss of binding.

The Lys4 residue, which is modified in Alexa Fluor apamin, is located on the opposite side of the toxin to the face believed to interact with the channel pore (Vergara et al., 1998), and would appear unlikely to be involved directly with any toxin-channel interaction (see fig 4.17).

Although the two arginine residues have been shown to be essential for the binding and toxicity of apamin (Vincent et al., 1975), the affinity of apamin for its acceptor is such that other factors also seem to play a role. The same authors reported a 2.6-2.8 fold loss of activity on modification of either the ϵ -amino group of Lys4 or the imidazole side chain of His18. Combined modification of both residues, however, caused a drastic (>10 fold) loss of toxicity. These results could be interpreted such that these amino acids do not play a large role in activity individually, but rather contribute to generalised charge effects. The pH of the low ionic strength buffer used for the binding experiments described in this chapter was such that the histidine would be predominantly uncharged, which may mean that the electrostatic effect of altering the lysine would become more important. Although the modification of the lysine group of apamin will result in a small loss of positive charge, the effect on binding seen with the addition of the Alexa Fluor moiety is probably due more to the presence of the Alexa molecule itself, rather than lysine modification. The structure of Alexa 488 can be seen in fig 4.18. It is a large

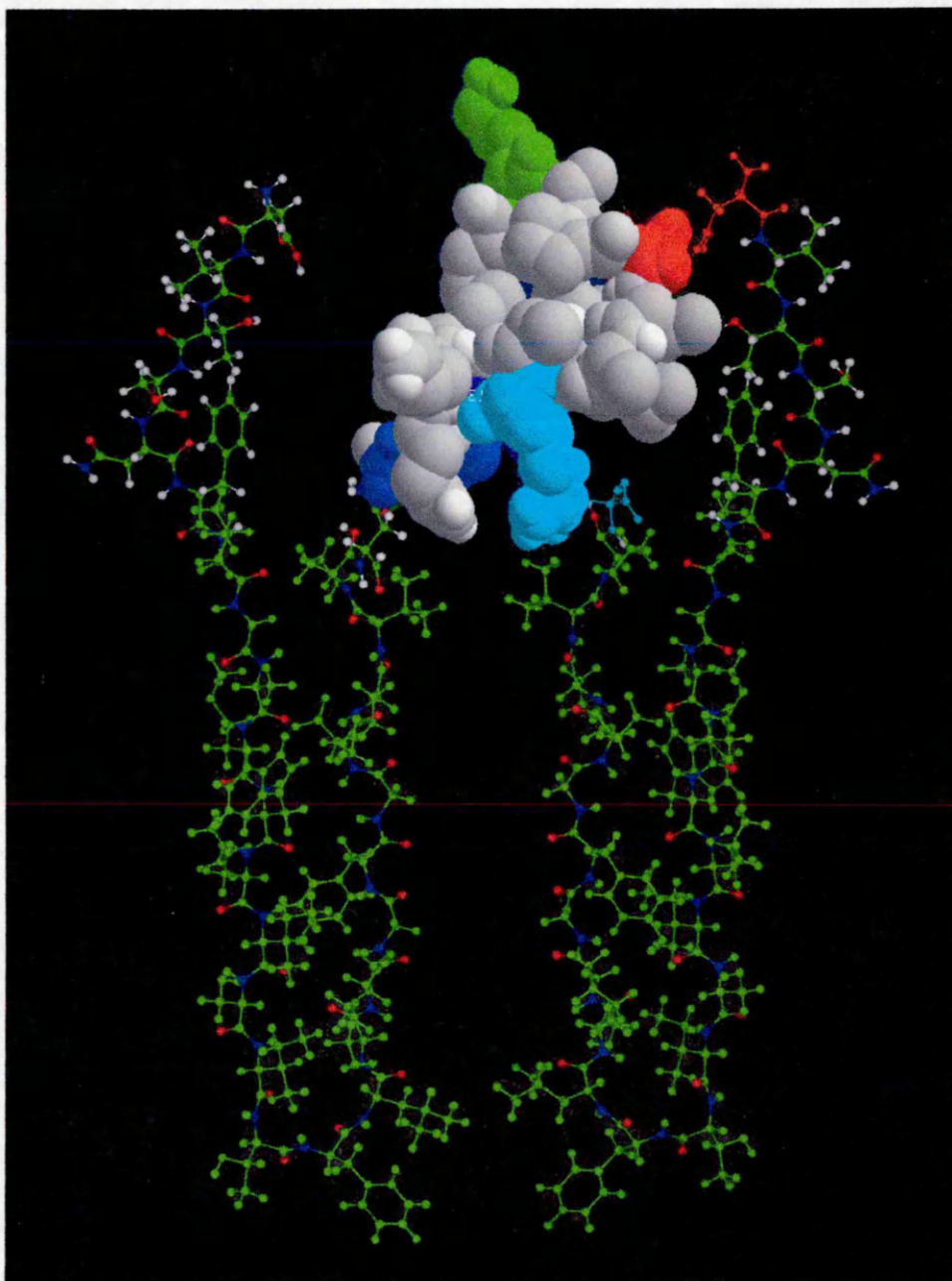
molecule with respect to the lysine it is modifying, with a large overall negative charge (-3). Modification of apamin with Alexa Fluor 488 succinimidyl ester reduces the overall positive charge on apamin by two, hence reducing the electrostatic interaction between apamin and acceptor. The positioning of the charges in native apamin creates a dipole moment. It has previously been suggested that the nature of this dipole moment contributes to the alignment of the toxin with the membrane and the precise positioning of the toxin in its acceptor (Ciechanowicz-Rutkowska et al., 2003). The addition of a highly negatively charged moiety to the molecule is likely to disrupt this charge distribution. The exact orientation of the Alexa Fluor substituent is unknown, but the increased bulk of the modified toxin may also prevent apamin from sitting tightly at the mouth of the pore of the SK channel, thus weakening the charge interactions between channel and toxin.

Cell-labelling experiments are generally carried out in physiological media (i.e. at high ionic strength), conditions at which apamin binding to its receptor is reduced (Hugues et al., 1982c). For this reason, Alexa Fluor apamin binding was also studied in high salt buffer. One would expect any electrostatic effects of the Alexa Fluor label to be reduced under such conditions, and any steric effects to remain unchanged. The results show that, under physiological conditions, the binding affinity of the fluorescent toxin for its receptor is lower than that of the native toxin. This shift in affinity appears to be less than that seen in low salt buffer. These results indicate that electrostatic interactions play a role in the loss of binding affinity seen with the fluorescently labelled toxin, but also suggest the involvement of additional, possibly steric factors.

Beeton et al., 2003, attached a fluorescein probe to the α -amino group of the N-terminal Arg residue of ShK (*Stichodactyla helianthus*) toxin. This residue is located on the opposite face of the toxin to that believed to interact with the channel pore, and the modification produced a 4-fold drop in the affinity of the toxin for Kv1.3 channels. In contrast, the fluorescent toxin showed a 160-fold less affinity for the Kv1.1 subtype than did the native toxin, presumably due to a change in the overall electrostatic properties of the molecule, drastically altering the toxin's selectivity. The work on ShK again demonstrates that generalised charge alterations can have profound effects on the affinities of modified toxins for their ion channel targets.

Since the binding affinity of apamin to its acceptors is so high, the reduced affinity of Alexa Fluor apamin may be insignificant for many applications. The majority of applications requiring a fluorescent SK-channel probe use physiological conditions, where the adverse effects of Alexa Fluor labelling are less pronounced. However, this reduced affinity should be taken in to account when designing experiments and in subsequent analysis of results, since it may have significance both for quantification purposes and for suitable toxin concentrations required for detection of SK-channels.

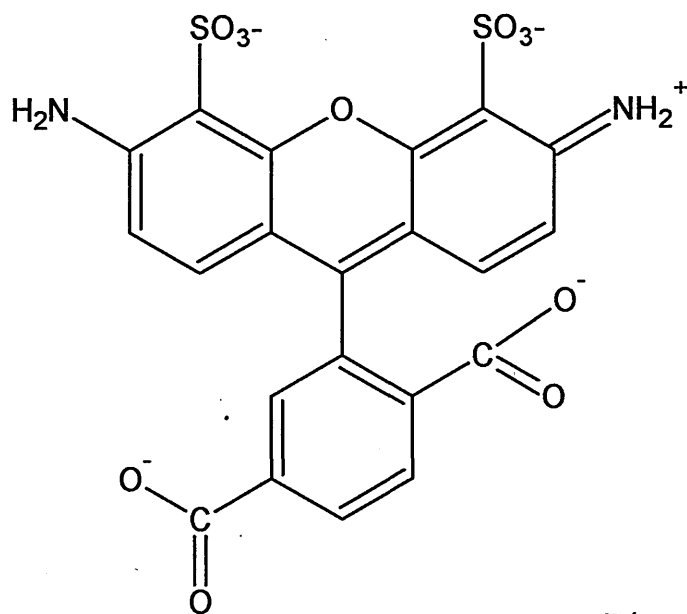
Fig 4.17 Proposed Orientation of Apamin in the Mouth of the SK2 Channel Pore



Two of the four SK2 subunits are shown in a cross section through the membrane. The charged residues of apamin are illustrated: Lys4-green, Glu7-red, Arg13-cyan, Arg14-purple, and His18-blue. Note the location of Lys-4 to which the Alexa Fluor moiety of Alexa Fluor apamin is attached.

SK channel structure and the position of apamin binding are taken from Vergara et al., 1998. The structure of apamin was kindly provided by Dr Chris Dempsey (University of Bristol) and is based upon the co-ordinates of Pease and Wemmer, 1988.

Fig 4.18 Structure of Alexa 488 (adapted from Panchuk-Voloshina, et al., 1999)



Animal venoms are a rich source of pharmacological molecules useful as research tools or as clinical drugs. Scorpion venoms have yielded a number of ion channel toxins, principally those active upon sodium or potassium ion channels. Although many current studies focus on the toxins, scorpion envenomation still causes fatalities, and the venoms themselves still warrant investigation. This work investigates a range of aspects of scorpion and bee venom neurotoxins, from the level of the crude venom to structure/function studies on a well-defined bee venom peptide.

The Indian red scorpion (*Mesobuthus tamulus*) is a serious threat to life in many regions of India. However, the venom of the species is less well studied than that of many other clinically relevant scorpion species. There is anecdotal evidence for regional variation in the severity of Indian red scorpion envenomation. Immunological and proteomic analysis of *Mesob. tamulus* venoms from two regions of the state of Maharashtra, each with differing biotopes, suggests quantitative and qualitative regional variation in the *Mesob. tamulus* venom. A peptide of 2947Da was identified that may prove diagnostic between the two venom types. The different distribution of peptides in regional scorpions has implications for toxin research. It highlights the need to specify the region from which scorpions were collected when identifying new molecules, and considerably increases the potential number of novel pharmaceutical components in the venoms of this scorpion. In addition, a mass profile of fractionated *Mesob. tamulus* venom was generated as an aid to future isolation of specific peptides from the venom of this species.

Scorpion short insectotoxins may be prove to be of clinical importance as chloride channel blockers and cancer-therapeutics. Little is known about these molecules and relatively few have been isolated. Analysis of *Mesob. tamulus* cDNA, using RACE (rapid amplification of cDNA ends), and oligonucleotide primers based upon the signal peptide sequence of the *Buthus martensii* short insectotoxin Bm12, yielded two novel putative short insectotoxin sequences, BtCh1 and BtCh2. A putative BtCh1 expression product has been purified from the venom of this species based upon its calculated mass. Additional experiments on the *Mesob. tamulus* telson cDNA library revealed evidence for the amidation of the K⁺-channel toxin tamulustoxin, and of the existence of a novel long-chain potassium channel toxin in this species.

In contrast to the short insectotoxins, apamin, a calcium-activated potassium channel toxin from the honey bee *Apis mellifera*, has been extensively studied. The toxin has a well-defined structure and mode of action. The specific binding of the toxin to an acceptor on rat brain membranes was utilised to further study specific aspects of its structure and function.

Three reasons have been proposed for the existence of the Asn-stabilised β -turn motif in apamin. The suggestion that the presence of this structure (or at least the Asn residue contained within it) promotes wild-type disulphide-bond pairings was confirmed by structural studies (Dempsey et al., 2000). The second possibility is that the β -turn is required for binding. There was no reduction in binding of a synthetic apamin peptide upon substitution of asparagine-2 for alanine (which has previously been shown to disrupt the β -turn of the toxin, Dempsey et al., 2000), provided the peptide retained the correct disulphide pairing. An Asn2Ala-apamin isoform, which contained non-native disulphide bridges causing the molecule to adopt the ribbon conformation, maintained its ability to bind these receptors, but with a 30 fold decrease in affinity. Thus, promotion of correct disulphide pairing does in turn increase the affinity of apamin for its acceptor. The β -turn itself, however, has little effect on binding affinity, although the structure may yet prove to play some role in the functional block of SK channels. (When considering results from binding experiments, it should be borne in mind that binding does not necessarily constitute functional block and future studies may show differing effects of the Asn-substitution and non-native disulphide pairings on block of SK currents). The third hypothesis suggests that the presence of the β -turn imparts resistance to proteolytic enzymes, and will be the subject of future investigation.

Addition of a large negatively charged fluorescent moiety (Alexa 488) to Lys-4 of synthetic apamin, decreased the binding affinity by seventy-fold compared to the native toxin. This effect was considerably reduced, but not abolished, in low salt buffer, suggesting that most, but not all, of the decrease in affinity could be attributed to electrostatic effects. The results show that overall charge distribution is more important for binding of this toxin to rat brain membranes than the β -turn or disulphide pairings.

ACHYUTHAN,K.E., AGARWAL,O.P. & RAMACHANDRAN,L.K. (1982) Enzymes in the venoms of two species of Indian scorpion - *Heterometrus Bengalensis* & *Buthus tamulus*. *Indian Journal of Biochemistry & Biophysics* **19**, 356-358.

ADAMOVICH,T.B., NASIMOV,I.V., GRISHIN,E.V. & OVCHINNIKOV,Y.A. (1977) Amino acid sequence of insectotoxin I1 from the venom of middle-asian scorpion *Buthus epeus*. *Bioorgan. Khim.* **3**, 485-493.

ADELMAN,J.P. (1995) Proteins that interact with the pore-forming subunits of voltage-gated ion channels. *Current Opinion in Neurobiology* **5**, 286-295.

ADJADJ,E., NAUDAT,V., MISPELTER,J., QUINIOU,E., TARTAR,A. & CRAESCU,C.T. (1996) Conformational properties of the toxin LQH8 isolated from the scorpion venom *Leirus quinquestriatus hebraeus* as studied by 2D ¹H NMR. *Toxicon* **34**, 1082.

ADJADJ,E., NAUDAT,V., QUINIOU,E., WOUTERS,D., SAUTIERE,P. & CRAESCU,C.T. (1997) Solution structure of Lqh-8/6, a toxin-like peptide from a scorpion venom. Structural heterogeneity induced by proline *cis/trans* isomerization. *European Journal of Biochemistry* **246**, 218-227.

AHERN,C.A. & HORN,R. (2004) Stirring up controversy with a voltage sensor paddle. *Trends in Neuroscience* **27**, 303-307.

AIDLEY,D.J. (1989) *The Physiology of Excitable Cells*. Cambridge University Press.

ALBERICIO,F., GRANIER,C., LABBE-JULLIE,C., SEAGAR,M., COURAUD,F. & VAN RIETSCHOTEN,J. (1984) Solid phase synthesis and HPLC purification of the protected 1-12 sequence of apamin for rapid synthesis of apamin analogs differing in the C-terminal region. *Tetrahedron* **40**, 4313-4326.

ALIS,A., STOEVA,S., SCHUTZ,J., KAYED,R., ABASSIA., ZAIDI,Z.H. & VOELTER,W. (1998) Purification and primary structure of low molecular mass peptides from scorpion (*Buthus indicus*) venom. *Comparative Biochemistry and Physiology Part A* **121**, 323-332.

ALVARENGA,L.M., DINIZ,C.R., GRANIER,C. & CHAVEZ-OLORTEGUI,C. (2002) Induction of neutralizing antibodies against *Tityus serrulatus* scorpion toxins by immunization with a mixture of defined synthetic epitopes. *Toxicon* **40**, 89-95.

ANGELIDES,K.J. & NUTTER,T.J. (1983) Preparation and characterization of fluorescent scorpion toxin from *Leirus quinquestriatus quinquestriatus* as probes of the sodium channel of excitable cells. *Journal of Biological Chemistry* **258**, 11948-11957.

ANGELIDES,K.J. (1986) Fluorescently labeled Na⁺ channels are localized and immobilized to synapses of innervated muscle fibres. *Nature* **321**, 63-66.

ARSENIEV,A., KONDAKOV,V.I., MAIOROV,V.N. & BYSTROV,V.F. (1984) NMR solution spatial structure of 'short' insectotoxin I5A. *FEBS Lett.* **165**, 57-61.

AUGUSTE,P., HUGUES,M., MOURRE,C., MOINIER,D., TARTAR,A. & LAZDUNSKI,M. (1992) Scyllatoxin, a block of Ca²⁺-activated K⁺ channels: structure-function relationships and brain localization of the binding sites. *Biochemistry (Mosc)*. **31**, 648-654.

AVDONIN,V., NOLAN,B., SABATIER,J.-M., DE WAARD,M. & HOSHI,T. (2000) Mechanisms of maurotoxin action on Shaker potassium channels. *Biophysical Journal* **79**, 776-787.

BAIROCH,A. & APWEILER,R. (1996) The SWISS-PROT protein sequence data bank and its new supplement TREMBL. *Nucleic Acids Research* **24**, 21-25.

BARHANIN,J., GIGLIO,J.R., LEOPOLD,P., SAMPAIO,S., V & LAZDUNSKI,M. (1982) *Tityus serrulatus* venom contains two classes of toxins. *Tityus gamma* toxin is a new tool with a very high affinity for studying the Na⁺ channel. *J. Biol. Chem.* **257**, 12553-12558.

BASS,R.B., STROP,P., BARCLAY,M. & REES,D.C. (2002) Crystal structure of *Escherichia coli* MscS a voltage-gated and mechanosensitive channel. *Science* **298**, 1582-1587.

BATISTA,C., GOMEZ-LAGUNAS,F., LUCAS,S. & POSSANI,L.D. (2000) Tc1, from *Tityus cambridgei*, is the first member of a new subfamily of scorpion toxin that blocks K⁺-channels. *FEBS Lett.* **468**, 117-120.

BATISTA,C., GOMEZ-LAGUNAS,F., RODRIGUEZ DE LA VEGA,R.C., HADJU,P., PANYI,G., GASPARR,R. & POSSANI,L.D. (2002) Two novel toxins from the Amazonian scorpion *Tityus cambridgei* that block Kv1.3 and Shaker K⁺ channels with distinctly different affinities. *Biochim. Biophys. Acta* **1601**, 123-131.

BATISTA,C.V.F., ZAMUDIO,F., LUCAS,S., FOX,J.W., FRAU,A., PRESTIPINO,G. & POSSANI,L.D. (2002a) Scorpion toxins from *Tityus cambridgei* that affect Na⁺-channels. *Toxicon* **40**, 557-562.

BATISTA,C.V.F., DEL POZO,L., ZAMUDIO,F.Z., CONTRERAS,S., BECERRIL,B., WANKE,E. & POSSANI,L.D. (2004) Proteomics of the venom from the Amazonian scorpion *Tityus cambridgei* and the role of prolines on mass spectrometry analysis of toxins. *Journal of Chromatography B: Biomedical Applications* **803**, 55-66.

BAWASKAR,H.S. (1982) Cardiac premonitory signs and symptoms of red scorpion sting. *Lancet* **1**, 552-554.

BAWASKAR,H.S. (1999) *Scorpion Sting*. Popular Prokashan, Mumbai.

BAWASKAR,H.S. & BAWASKAR,P.H. (2003) Clinical profile of severe scorpion envenomation in children at rural setting. *Indian Pediatrics* **40**, 1072-1075.

BECERRIL,B., CORONA,M., MEJIA,M.C., MARTIN,B.M., LUCAS,S., BOLIVAR,F. & POSSANI,L.D. (1993) The genomic region encoding toxin gamma from the scorpion *Tityus serrulatus* contains an intron. *FEBS* **335**, 6-8.

BECERRIL,B., CORONA,M., GARCIA,C., BOLIVAR,F. & POSSANI,L.D. (1995) Cloning of genes encoding scorpion toxins: an interpretative review. *J. Toxicol. Toxin Reviews* **14**, 339-357.

BECERRIL,B., CORONA,M., CORONAS,F.V., ZAMUDIO,F., CALDERON-ARANDA,E.S., FLETCHER,P.I., MARTIN,B.M. & POSSANI,L.D. (1996) Toxic peptides and genes encoding toxin gamma of the brazilian scorpions *Tityus bahiensis* and *Tityus stigmurus*. *Biochem. J.* **313**, 753-760.

BECKSTEIN,O., BIGGIN,P.C., BOND,P., BRIGHT,J.N., DOMENE,C., GROTTESLA., HOLYOAKE,J. & SANSOM,M.S.P. (2003) Ion channel gating: insights via molecular simulations. *FEBS Lett.* **555**, 85-90.

BEETON,C., WULFF,H., SINGH,S., BOTSKO,S., CROSSLEY,G., GUTMAN,G.A., CAHALAN,M.D., PENNINGTON,M.W. & CHANDY,K.G. (2003) A novel fluorescent toxin to detect and investigate Kv1.3 channel up-regulation in chronically activated T lymphocytes. *Journal of Biological Chemistry* **278**, 9928-9937.

BENKE,T.A., JONES,O.T., GOLLINGGRIDGE,G.L. & ANGELIDES,K.J. (1993) N-methyl-D-aspartate receptors are clustered and immobilized on the dendrites of living cortical neurons. *Proc. Natl. Acad. Sci. USA* **90**, 7819-7823.

BENKHALIFA,R., STANKIEWICZ,M., LAPIED,B., TURKOV,M., ZILBERBERG,N., GUREVITZ,M. & PELHATE,M. (1997) Refined electrophysiological analysis suggests that scorpion insect depressant neurotoxins are sodium channel openers rather than blockers. *Life Sciences* **61**, 819-830.

BIANCHI,L., WIBLE,B., ARCANGELIA., TAGLIALATELA,M., MORRA,F., CASTALDO,P., CROCIANO,O., ROSATI,B., FARAVELLI,L., OLIVOTTO,M. & WANKE,E. (1998) HERG encodes a K⁺ current highly conserved in tumors of different histogenesis: a selective advantage for cancer cells? *Cancer Research* **58**, 815-822.

BIDARD,J.N., GANDOLFO,G., MOURRE,C., GOTTESMANN,C. & LAZDUNSKI,M. (1987) The brain response to the bee venom peptide MCD. Activation and desensitization of a hippocampal target. *Brain Res.* **418**, 235-244.

BILLINGHAM,M.E.J., MORLEY,J., HANSON,J.M., SHIPOLINI,R. & VERNON,C.A. (1973) An anti-inflammatory peptide from bee venom. *Nature* **245**, 163-164.

BINFORD,G.J. (2001) An analysis of geographic and intersexual chemical variation in venoms of the spider *Tegenaria agrestis* (Agelenidae). *Toxicon* **39**, 955-968.

BLANC,E., SABATIER,J.-M., KHARRAT,R., MEUNIER,S., EL AYEB,M., VAN RIETSCHOTEN,J. & DARBON,H. (1997) Solution structure of maurotoxin, a scorpion toxin from *Scorpio maurus*, with high affinity for voltage-gated potassium channels. *Proteins* **29**, 321-333.

BLOOMSTON,M., ZERVOS,E.E. & ROSEMURGY,A.S. (2002) Matrix metalloproteinases and their role in pancreatic cancer: a review of preclinical studies and clinical trials. *Annals of Surgical Oncology* **9**, 668-674.

BONTEMS,F., ROUMESTAND,C., GILQUIN,B., MENEZ,A. & TOMA,F. (1991) Refined structure of charybdotoxin: common motifs in scorpion toxins and insect defensins. *Science* **254**, 1521-1523.

BONTEMS,F., ROUMESTAND,C., BOYOT,P., GILQUIN,B., DOLJANSKY,Y., MENEZ,A. & TOMA,F. (1991a) Three-dimensional structure of natural charybdotoxin in aqueous solution by ¹H-NMR. *European Journal of Biochemistry* **196**, 19-28.

BONTEMS,F., GILQUIN,B., ROUMESTAND,C., MENEZ,A. & TOMA,F. (1992) Analysis of side-chain organization on a refined model of charybdotoxin: structural and functional implications. *Biochemistry (Mosc)*. **31**, 7756-7764.

BOOTH,I.R., EDWARDS,M.D. & MILLER,S. (2003) Bacterial ion channels. *Biochemistry (Mosc)*. **42**, 10045-10053.

BORCHANI,L., MANSUELLE,P., STANKIEWICZ,M., GROLLEAU,F., CESTELE,S., KAROUI,H., LAPIED,B., ROCHAT,H., PELHATE,M. & EL AYEB,M. (1996) A new scorpion venom toxin paralytic to insects that affects Na⁺ channel activation. *Eur. J. Biochem.* **241**, 525-532.

BORGES,A., TSUSHIMA,R.G. & BACKX,P.H. (1999) Antibodies against *Tityus discrepans* venom do not abolish the effect of *Tityus serrulatus* venom on the rat sodium and potassium channels. *Toxicon* **37**, 867-881.

BOUGIS,P.E., ROCHAT,H. & SMITH,L.A. (1989) Precursors of *Androctonus australis* scorpion neurotoxins. Structures of precursors processing outcomes, and expression of a functional toxin II. *Journal of Biological Chemistry* **264**, 19259-19265.

BOWEN,T., GUY,C., SPEIGHT,G., JONES,I., CARDNO,A., MURPHY,K., MCGUFFIN,P., OWEN,M.J. & O'DONOVAN,M.C. (1996) Expansion of 50 CAG/CTG repeats excluded in schizophrenia by application of a highly efficient approach using repeat expansion detection and a PCR screening set. *Am. J. Hum. Genet.* **59**, 912-917.

BRAMMAR,W.J. (1999) Voltage-gated calcium channels. In: *Voltage-Gated Channels* (Ed. E.C.Conley & W.J.Brammar). Academic press, London.

BREITHAUPT,H. & HABERMANN,E. (1968) [MCD-peptide from bee venom: isolation, biochemical and pharmacological properties]. *Naunyn Schmiedebergs Arch. Exp. Pathol Pharmacol.* **261**, 252-270.

BRINKMEIER,H., AULKEMEYER,P., WOLLINSKY,K.H. & RUDEL,R. (2000) An endogenous pentapeptide acting as a sodium channel blocker in inflammatory autoimmune disorders of the central nervous system. *Nature Medicine* **6**, 808-811.

BRUGNARA,C., DE FRANCESCHI,L., ARMSBY,C.C., SAADANE,N., TRUDEL,M., BEUZARD,Y., RITTENHOUSE,A., RIFAI,N., PLATT,O. & ALPER,S.L. (1995) A new therapeutic approach for sickle cell disease. Blockade of the red cell Ca^{2+} -activated K^{+} channel by clotrimazole. *Ann. N Y Acad. Sci.* **763**, 262-271.

BRUGNARA,C., GEE,B., ARMSBY,C.C., KURTH,S., SAKAMOTO,M., RIFAI,N., ALPER,S.L. & PLATT,O.S. (1996) Therapy with oral clotrimazol induces inhibition of the Gardos channel and reduction of erythrocyte dehydration in patients with sickle cell disease. *J. Clin. Invest.* **97**, 1227-1234.

BRUNS,R.F., LAWSON-WENDLING,K. & PUGSLEY,T.A. (1983) A rapid filtration assay for soluble receptors using polyethyleneimine treated filters. *Analytical Biochemistry* **132**, 74-81.

BUISINE,E., WIERUSZESKI,J.-M., LIPPENS,G., WOUTERS,D., TERTAR,A. & SAUTIERE,P. (1997) Characterization of a new family of toxin-like peptides from the venom of the scorpion *Leiurus quinquestriatus hebraeus*. 1H-NMR structure of leuropeptide II. *J. Peptide Res* **49**, 545-555.

BUSETTA,B. (1980) Conformational analysis of apamin using the residual representation. *FEBS Lett.* **112**, 138-142.

BUTLER,A., WEI,A., BAKER,K. & SALKOFF,L. (1989) A family of putative potassium channel genes in *Drosophila*. *Science* **243**, 943-947.

BYSTROV,V.F., ARSENIIEV,A.S. & GAVRILOV,Y.D. (1978) NMR spectroscopy of large peptides and small proteins. *J. Magn. Reson.* **30**, 151-184

BYSTROV,V.F., OKHANOV,V.V., MIROSHNIKOV,A.I. & OVCHINNIKOV,Y.A. (1980) Solution spatial structure of apamin as derived from NMR study. *FEBS Lett.* **119**, 113-117.

CAHALAN,M.D. (1975) Modification of sodium channel gating in frog myelinated nerve fibres by *Centruroides sculpturatus* scorpion venom. *J. Physiol. (Lond.)* **244**, 511-534.

CAIUS,J.F. & MHASKAR,K.S. (1932) *Notes on Indian Scorpions*. Thacker, Spink and Co, Calcutta.

CALABRO,V., SABATIER,J.-M., BLANC,E., LECOMTE,C., VAN RIETSCHOTEN,J. & DARBON,H. (1997) Differential involvement of disulphide bridges on the folding of a scorpion toxin. *Journal of Peptide Research* **50**, 39-47.

CALLEWAERT,G.L., SHIPOLINI,R. & VERNON,C.A. (1968) The disulphide bridges of apamin. *FEBS Lett.* **1**, 111-113.

CAMPBELL,K.P., LEUNG,A.T. & SHARP,A.H. (1988) The biochemistry and molecular biology of the dihydropyridine-sensitive calcium channel. *Trends in Neuroscience* **11**, 425-430.

CANNON,S.C. (1997) From mutation to myotonia in sodium channel disorders. *Neuromuscul. Disord.* **7**, 241-249.

CAO,Y.J., DREIXLER,J.C., ROIZEN,J.D., ROBERTS,M.T. & HOUAMED,K.M. (2001) Modulation of recombinant small-conductance Ca^{2+} -activated K^{+} channels by the muscle relaxant chlorzoxazone and structurally related compounds. *Journal of Pharmacology and Experimental Therapeutics* **296**, 683-689.

CAO,Z., XIAO,F., PENG,F., JIANG,D., MAO,X., LIU,H., LI,W., HU,D. & WANG,T. (2003) Expression, purification and functional characterization of a recombinant scorpion venom peptide BmTXK β . *Peptides* **24**, 187-192.

CARBONE,E., WANKE,E., PRESTIPINO,G., POSSANI,L.D. & MAELICKE,A. (1982) Selective blockage of voltage-dependent K^{+} channels by a novel scorpion toxin. *Nature* **296**, 90-91.

CARDNO,A., BOWEN,T., GUY,C., JONES,L.A., MCCARTHY,G., WILLIAMS,N.M., MURPHY,K., SPURLOCK,G., GRAY,M., SANDERS,R.D., CRADDOCK,N., MCGUFFIN,P., OWEN,M.J. & O'DONOVAN,M.C. (1999) CAG repeat length in the hKCa3 gene and symptom dimensions in schizophrenia. *Biol. Psychiatry* **45**, 1592-1596.

CARLIER,E., AVDONIN,V., GEIB,S., FAJLOUN,Z., KHARRAT,H., ROCHAT,H., SABATIER,J.-M., HOSHI,T. & DE WAARD,M. (2000) Effect of maurotoxin, a four disulphide-bridged toxin from the chactoid scorpion *Scorpio maurus*, on Shaker K^{+} channels. *J. Peptide Res* **55**, 419-427.

CARLIER,E., FAJLOUN,Z., MANSUELLE,P., FATHALLAH,M., MOSBAH,A., OUGHIDENI,R., SANDOZ,G., DI LUCCIO,E., GEIB,S., REGAYA,I., BROCARD,J., ROCHAT,H., DARBON,H., DEVAUX,C., SABATIER,J.-M. & DE WAARD,M. (2001) Disulphide bridge reorganization induced by proline mutations in maurotoxin. *FEBS Lett.* **489**, 202-207.

CARRERRA,P., STENIRRI,S., FERRARI,M. & BATTISTINI,S. (2001) Familial hemiplegic migraine: a ion channel disorder. *Brain Research Bulletin* **56**, 329-241.

CASTLE,N.A., HAYLETT,D.G. & JENKINSON,D.H. (1989) Toxins in the characterization of potassium channels. *Trends in Neuroscience* **12**, 59-65.

CATTERALL,W.A. (1979) Binding of scorpion toxin to receptor sites associated with sodium channels in frog muscle. Correlation of voltage-dependent binding with activation. *J. Gen. Physiol* **74**, 375-391.

CATTERALL,W.A. (1988) Structure and Function of Voltage-Sensitive Ion Channels. *Science* **242**, 50-60.

CATTERALL,W.A. (1992) Cellular and molecular biology of voltage gated sodium channels. *Physiological Reviews* **72**, S15-S48.

CATTERALL,W.A. (1995) Structure and function of voltage-gated ion channels. *Annu. Rev. Biochem.* **64**, 493-531.

CATTERALL,W.A., STRIESSNIG,J., SNUTCH,T.P. & PEREZ-REYES,E. (2003) International union of pharmacology. XL. Compendium of voltage-gated ion channels: calcium channels. *Pharmacological Reviews* **55**, 579-581.

CATTERALL,W.A., GOLDIN,A.L. & WAXMAN,S.G. (2003a) International union of pharmacology. XXXIX. Compendium of voltage-gated ion channels: sodium channels. *Pharmacological Reviews* **55**, 575-578.

CEARD,B., DE LIMA,M.E., BOUGIS,P.E. & MARTIN-EAUCLAIRE,M.-F. (1992) Purification of the main β -toxin from *Tityus serrulatus* venom using HPLC. *Toxicon* **30**, 105-110.

CELESIA,G.G. (2001) Disorders of membrane channels or channelopathies. *Clin. Neurophysiol.* **112**, 2-18.

CESTELE,S., QU,Y., ROGERS,J.C., ROCHAT,H., SCHEUER,T. & CATTERALL,W.A. (1998) Voltage sensor-trapping: enhanced activation of sodium channels by beta-scorpion toxin bound to the S3-S4 loop in domain II. *Neuron* **21**, 919-931.

CHANDY,K.G. & GUTMAN,G.A. (1993) Nomenclature for mammalian potassium channel genes. *Trends in Pharmacological Sciences* **14**, 434.

CHANG,G., SPENCER,R.H., LEE,A.T., BARCLEY,M.T. & REES,D.C. (1998) Structure of the MscL homolog from *Mycobacterium tuberculosis*: a gated mechanosensitive ion channel. *Science* **282**, 2220-2226.

CHAU,M.H. & NELSON,J.W. (1992) Cooperative disulfide bond formation in apamin. *Biochemistry (Mosc)*. **31**, 4445-4450.

CHAVEY,C., MARI,B., MONTHOUEL,M.N., BONNAFOUS,S., ANGLARD,P., VAN OBBERGHEN,E. & TARTARE-DECKERT,S. (2003) Matrix metalloproteinases are differentially expressed in adipose tissue during obesity and modulate adipocyte differentiation. *Journal of Biological Chemistry* **278**, 11888-11896.

CHEBIB,M. & JOHNSTON,G.A. (2000) GABA- activated ligand-gated ion channels: medicinal chemistry and molecular biology. *J. Med. Chem.* **43**, 1427-1447.

CHEN,L., ESTEVE,E., SABATIER,J.-M., RONJAT,M., DE WAARD,M., ALLEN,P.D. & PESSAH,I.N. (2003) Maurocalcine and peptide A stabilize distinct subconductance states of ryanodine receptor type 1, revealing a proportional gating mechanism. *Journal of Biological Chemistry* **278**, 16095-16106.

CHETKOVICH,D.M., CHEN,L., BUNN,R.C., SWEENEY,N.T., AUGUILERA-MORENO,A., NICOLL,R.A. & BRETT,D.S. (2000) Clustering of stargazin by PSD-95. *Soc. Neurosci. Abstracts* **26**, 717.5.

CHHATWAL,G.S. & HABERMANN,E. (1981) Neurotoxins, protease inhibitors and histamine releasers in the venom of the Indian red scorpion (*Buthus tamulus*): isolation and partial characterization. *Toxicon* **19**, 807-823.

CHICCI,G.G., GIMENEZ-GALLEGO,G., BER,E., GARCIA,M.L., WINQUIST,R. & CASCIERI,M.A. (1988) Purification and characterization of a unique, potent inhibitor of apamin binding from *Leiurus quinquestriatus hebraeus* venom. *Journal of Biological Chemistry* **263**, 10192-10197.

CHINTALA,S.K., TONN,J.C. & RAO,J.S. (1999) Matrix metalloproteinases and their biological function in human gliomas. *Int. J. Dev. Neurosci.* **17**, 495-502.

CHOE,S. (2002) Potassium channel structures. *Nature Reviews : Neuroscience* **31**, 115-121.

CHUANG,R.S.I., JAFFE,H., CRIBBS,L., PEREZ-REYES,E. & SWARTZ,K. (1998) Inhibition of T-type voltage-gated calcium channels by a new scorpion toxin. *Nature Neuroscience* **1**, 668-674.

CHURCH,J.E. & HODGSON,W.C. (2002) The pharmacological activity of fish venoms. *Toxicon* **40**, 1083-1093.

CIECHANOWICZ-RUTKOWSKA,M., LEWINSKI,K., OLEKSYN,B. & STEC,B. (2003) Model studies of the function of blockers on the small conductance potassium ion channel. *Journal of Peptide Research* **62**, 125-133.

CINGOLANI,L.A., GYMNOPOULOS,M., BOCCACCIO,A., STOCKER,M. & PEDARZANI,P. (2002) Developmental regulation of small-conductance Ca^{2+} - activated K^{+} channel expression and function in rat purkinje neurons. *Journal of Neuroscience* **22**, 4456-4467.

CLARK,A.M. (1996) Natural products as a resource for new drugs. *Pharm Res* **13**, 1133-1144.

COCIANCICH,S., GOYFFON,M., BONTEMS,F., BULET,P., BOUET,F., MENEZ,A. & HOFFMANN,J.A. (1993) Purification and characterization of a scorpion defensin, a 4kDa antibacterial peptide presenting structural similarities with insect defensins and scorpion toxins. *Biochemical and Biophysical Research Communications.* **194**, 17-22.

COHEN,M.W., JONES,O.T. & ANGELIDES,K.J. (1991) Distribution of Ca^{2+} channels on frog motor nerve terminals revealed by fluorescent omega-conotoxin. *Journal of Neuroscience* **11**, 1032-1039.

COHEN,S.N., CHANG,A.C.Y. & HSU,L. (1972) Non chromosomal antibiotic resistance in bacteria: Genetic transformation of *Escherichia coli* by R-factor DNA. *Proc. Natl. Acad. Sci* **69**, 2110.

COLQUHOUN,D. & SIVILOTTI,L.G. (2004) Function and structure in glycine receptors and some of their relatives. *Trends Neurosci.* **27**, 337-344.

CONDE,R., ZAMUDIO,F.Z., RODRIGUEZ,M.H. & POSSANI,L.D. (2000) Scorpine, an anti-malaria and anti-bacterial agent purified from scorpion venom. *FEBS Lett.* **471**, 165-168.

- CONLEY,E.C. & BRAMMAR,W.J. (1999) *Voltage-Gated Channels*. Academic Press, London.
- COOK,N.S., HAYLETT,D.G. & STRONG,P.N. (1983) High affinity binding of ^{125}I -monoiodoapamin to isolated guinea-pig hepatocytes. *FEBS Lett.* **152**, 265-269.
- COOK,N.S. & HAYLETT,D.G. (1985) Effects of apamin, quinine and neuromuscular blockers on calcium-activated potassium channels in guinea-pig hepatocytes. *Journal of Physiology* **358**, 373-394.
- COOPER,E.C. & JAN,L.Y. (1999) Ion channel genes and human neurological disease: recent progress, prospects, and challenges. *Proc. Natl. Acad. Sci. USA* **96**, 4759-4766.
- CORONA,M., ZURITA,M., POSSANI,L.D. & BECERRIL,B. (1996) Cloning and characterization of the genomic region encoding toxin IV-5 from the scorpion *Tityus serrulatus* Lutz and Mello. *Toxicon* **34**, 251-256.
- CORONA,M., VALDEZ-CRUZ,N.A., MERINO,E., ZURITA,M. & POSSANI,L.D. (2001) Genes and peptides from the scorpion *Centruroides sculpturatus* Ewing, that recognize Na^+ channels. *Toxicon* **39**, 1893-1898.
- CORZO,G., ESCOUBAS,P., VILLEGAS,E., BARNHAM,K.J., HE,W., NOERTON,R.S. & NAKAJIMA,T. (2001) Characterization of unique amphipathic antimicrobial peptides from venom of the scorpion *Pandinus imperator*. *Biochem. J.* **359**, 35-45.
- CORZO,G., VILLEGAS,E. & NAKAJIMA,T. (2001a) Isolation and structural characterization of a peptide from the venom of scorpion with toxicity towards invertebrates and vertebrates. *Protein Pept. Lett.* **8**, 385-393.
- COSLAND,W.L. & MERRIFIELD,R.B. (1977) Concept of internal structural controls for evaluation of inactive synthetic peptide analogues: synthesis of [orn 13,14] apamin and its guanidination to an apamin derivative with full neurotoxic activity. *Proc. Natl. Acad. Sci. USA* **74**, 2771-2775.
- COURAUD,F., JOVER,E., DUBOIS,J.M. & ROCHAT,H. (1982) Two types of scorpion receptor sites, one related to the activation, the other to the inactivation of the action potential sodium channel. *Toxicon* **20**, 9-16.
- CRAIK,D.J., DALY,N.L., BOND,T. & WAINE,C. (1999) Plant cyclotides: A unique family of cyclic and knotted proteins that defines the cyclic cystine knot structural motif. *J. Mol. Biol.* **294**, 1327-1336.
- CUI,M., SHEN,J., BRIGGS,J.M., FU,W., WU,J., ZHANG,Y., LUO,X., CHI,Z., JI,R., JIANG,H. & CHEN,K. (2002) Brownian dynamics simulations of the recognition of the scorpion toxin P05 with the small-conductance calcium-activated potassium channels. *Journal of Molecular Biology* **318**, 417-428.
- D'HOEDT,D., HIRZEL,K., PEDARZANI,P. & STOCKER,M. (2004) Domain analysis of the calcium-activated potassium channel SK1 from rat brain. *Journal of Biological Chemistry* **279**, 12088-12092.

DAL,L., YASUDA,A., NAOKI,H., CORZO,G., ANDRIANTSIFERANA,M. & NAKAJIMA,T. (2001) IsCT, a novel cytotoxic linear peptide from scorpion *Opisthacanthus madagascariensis*. *Biochemical and Biophysical Research Communications*. **286**, 820-825.

DAL,L., CORZO,G., NAOKI,H., ANDRIANTSIFERANA,M. & NAKAJIMA,T. (2002) Purification, structure-function analysis, and molecular characterization of novel linear peptides from scorpion *Opisthacanthus madagascariensis*. *Biochemical and Biophysical Research Communications*. **293**, 1514-1522.

DALTON,S., GERZANICH,V., CHEN,M., DONG,Y., SHUBA,Y. & SIMARD,J.M. (2003) Chlorotoxin -sensitive Ca^{2+} -activated Cl^{-} channel in type R2 reactive astrocytes from adult rat brain. *Glia* **42**, 325-339.

DALTRY,J.C., WUSTER,W. & THORPE,R.S. (1996) Diet and snake venom evolution. *Nature* **379**, 537-540.

DARBON,H., ZLOTKIN,E., KOPEYAN,C., VAN RIETSCHOTEN,J. & ROCHAT,H. (1982) Covalent structure of the insect toxin of the North African scorpion *Androctonus australis Hector*. *Int. J. Peptide. Protein. Res.* **20**, 320-330.

DARBON,H. & ANGELIDES,K.J. (1984) Structural mapping of the voltage-dependent sodium channel. distance between the tetrodotoxin and *Centruroides suffusus suffusus* II beta-scorpion toxin receptors. *Journal of Biological Chemistry* **259**, 6074-6084.

DARBON,H., WEBER,C. & BRAUN,W. (1991) Covalent structure of the insect toxin of the North African scorpion *Androctonus australis Hector*. *Biochemistry (Mosc)*. **30**, 1836-1844.

DAS GUPTA,S.C., GOMES,A., GOMES,A., BASU,A. & LAHIRI,S.C. (1989) Immunological cross reactivity & paraspecificity of the scorpion *Heterometrus bengalensis* antivenom. *Indian Journal of Medical Research* **90**, 140-146.

DAUPLAIS,M., LECOQ,A., SONG,J., COTTON,J., JAMIN,N., GILQUIN,B., ROUMESTAND,C., VITA,C., DE MEDEIROS,C.L.C., ROWAN,E.G., HARVEY,A.L. & MENEZ,A. (1997) On the convergent evolution of animal toxins. Conservation of a diad of functional residues in potassium channel-blocking toxins. *Journal of Biological Chemistry* **272**, 4302-4309.

DE LIMA,M.E., MARTIN-EAUCCLAIRE,M.-F., DINIZ,C.R. & ROCHAT,H. (1986) *Tityus serrulatus* toxin VII bears pharmacological properties of both β -toxins and insect toxin from scorpion venoms. *Biochem. Biophys. Res. Commun.* **139**, 296-302.

DE LIMA,M.E., MARTIN-EAUCCLAIRE,M.-F., HUE,B., LORET,E., DINIZ,C.R. & ROCHAT,H. (1989) On the binding of two scorpion toxins to the central nervous system of the cockroach *Periplaneta americana*. *Insect Biochem.* **19**, 413-422.

- DE OLIVEIRA,K.C., GONCALVES DE ANDRADE,R.M., GIUSTI,A.L., DIAS DA SILVA,W. & TAMBOURGI,D.V. (1999) Sex-linked variation of *Loxosceles intermedia* spider venoms. *Toxicon* **37**, 217-221.
- DEBIN,J.A. & STRICHARTZ,G.R. (1991) Chloride channel inhibition by the venom of the scorpion *Leiurus quinquestriatus*. *Toxicon* **29**, 1403-1408.
- DEBIN,J.A., MAGGIO,J.E. & STRICHARTZ,G.R. (1993) Purification and characterization of chlorotoxin, a chloride channel ligand from the venom of the scorpion *Leiurus quinquestriatus*. *American Journal of Physiology* **264**, C361-C369.
- DEFENDINI,M.L., PIERRES,M., REGNIER-VIGOUROUX,A., ROCHAT,H. & GRANIER,C. (1990) Epitope mapping of apamin by means of monoclonal antibodies raised against free or carrier-coupled peptide. *Molecular Immunology* **27**, 551-558.
- DEHESA-DAVILA,M. & POSSANI,L.D. (1994) Scorpionism and serotherapy in Mexico. *Toxicon* **32**, 1015-1018.
- DEJONGH,K.S., WARNER,C. & CATTERALL,W.A. (1990) Subunits of purified calcium channels α_2 and δ are encoded by the same gene. *J. Biol. Chem.* **265**, 14738-14741.
- DELEPIERRE,M., PROCHNICKA-CHALUFOUR,A., BOISBOUVIER,J. & POS (1999) Pi7, an orphan peptide from the scorpion *Pandinus imperator*: A $^1\text{H-NMR}$ analysis using a nano-NMR probe. *Biochemistry (Mosc)*. **38**, 16756-16765.
- DEMONCHAUX,P., GANELLIN,C.R., DUNN,P.M., HAYLETT,D.G. & JENKINSON,D.H. (1991) Search for the pharmacophore of the K^+ channel blocker apamin. *European Journal of Medicinal Chemistry* **26**, 915-920.
- DEMPSEY,C.E., SESSIONS,R.B., LAMBLE,N.V. & CAMPBELL,S.J. (2000) The asparagine-stabilized β -turn of apamin: Contribution to structural stability from dynamics simulation and amide hydrogen exchange analysis. *Biochemistry (Mosc)*. **39**, 15944-15952.
- DESCHAUX,O., BIZOT,J.C. & GOYFFON,M. (1997) Apamin improves learning in an object recognition task in rats. *Neuroscience Letters* **222**, 159-162.
- DESCHAUX,O. & BIZOT,J.C. (1997) Effect of apamin, a selective blocker of Ca^{2+} -activated K^+ channels, on habituation and passive avoidance responses in rats. *Neuroscience Letters* **227**, 57-60.
- DESHANE,J., GARNER,C.C. & SONTHEIMER,H. (2003) Chlorotoxin inhibits glioma cell invasion via matrix metalloproteinase-2. *Journal of Biological Chemistry* **278**, 4135-4144.
- DESHPANDE,J.M., BAGCHI,S., RAI,O.P. & ARRYA,N.C. (1999) Pulmonary oedema produced by scorpion venom augments a phenyldiguanide-induced reflex response in anaesthetized rats. *Journal of Physiology* **521**, 537-544.

- DEUTSCH,C., PRICE,M., LEE,S., KING,V.F. & GARCIA,M.L. (1991) Characterisation of high affinity binding sites for charybdotoxin in human T-lymphocytes. *Journal of Biological Chemistry* **266**, 3668-3674.
- DHAWAN,R., JOSEPH,J.S., SETHI,A. & LALA,A.K. (2002) Purification and characterisation of a short insect toxin from the venom of the scorpion *Buthus tamulus*. *FEBS Lett.* **528**, 261-266.
- DHAWAN,R., VARSHNEY,A., MATHEW,M.K. & LALA,A.K. (2003) BTK-2, a new inhibitor of the Kv1.1 potassium channel purified from Indian scorpion *Buthus tamulus*. *FEBS Lett.* **539**, 7-13.
- DI LUCCIO,E., AZULAY,D.O., REGAYA,I., FAJLOUN,Z., SANDOZ,G., MANSUELLE,P., KHARRAT,R., FATHALLAH,M., CARREGA,L., ESTEVE,E., ROCHAT,H. & DE WAARD,M. (2001) Parameters affecting *in vitro* oxidation/folding of maurotoxin, a four- disulphide-bridged scorpion toxin. *Biochem. J.* **358**, 681-692.
- DI LUCCIO,E., MATAVEL,A., OPI,S., REGAYA,I., SANDOZ,G., MBAREK,S., CARLIER,E., ESTEVE,E., CARREGA,L., FAJLOUN,Z., ROCHAT,H., LORET,E., DE WAARD,M. & SABATIER,J.-M. (2002) Evolution of maurotoxin conformation and blocking efficacy towards shaker B channels during the course of folding and oxidation *in vitro*. *Biochem. J.* **361**, 409-416.
- DIB-HAJJ,S., BLACK,J.A., FELTS,P. & WAXMAN,S.G. (1996) Down-regulation of transcripts for Na channel alpha-SNS in spinal sensory neurons following axotomy. *Proc. Natl. Acad. Sci. USA* **93**, 14950-14954.
- DODD,P.R., HARDY,J.A., OAKLEY,A.E., EDWARDS,J.A., PERRY,E.K. & DELANEY,J.P. (1981) A rapid method for preparing synaptosomes: comparison with alternative procedures. *Brain Res.* **226**, 107-118.
- DOYLE,D.A., CABRAL,J.M., PFUETZNER,R.A., KUO,A., GULBIS,J.M., COHEN,S.L., CHAIT,B.T. & MACKINNON,R. (1998) The structure of the potassium channel: molecular basis of K⁺ conduction and selectivity. *Science* **280**, 69-76.
- DOYLE,D.A. (2004) Structural changes during ion channel gating. *Trends in Neuroscience* **27**, 298-302.
- DRAKOPOULOU,E., VIZZAVONA,J., NEYTON,J., ANIORT,V., BOUET,F., VIRELIZIER,H., MENEZ,A. & VITA,C. (1998) Consequence of the removal of evolutionary conserved disulphide bridges on the structure and function of charybdotoxin and evidence that particular cysteine spacings govern specific disulphide bond formation. *Biochemistry (Mosc)*. **37**, 1292-1301.
- DUDKIN,S.M., MIKCHAYLOVA,L.I. & SEVERIN,E.S., Jr. (1983) Mechanisms of cyclic AMP phosphodiesterase regulation. *Adv. Enzyme Regul.* **21**, 333-352.
- DUFFY,M.J., MAGUIRE,T.M., HILL,A., MCDERMOTT,E. & O'HIGGINS,N. (2000) Metalloproteinases: role in breast carcinogenesis, invasion and metastasis. *Breast Cancer Research* **2**, 252-257.

DUTZLER,R., CAMPBELL,E.B., CADENE,M., CHART,B.T. & MACKINNON,R. (2002) X-ray structure of a ClC chloride channel at 3.0Å reveals the molecular basis of anion selectivity. *Nature* **415**, 287-294.

DUTZLER,R. (2004) Structural basis for ion conduction and gating in ClC chloride channels. *FEBS Lett.* **564**, 229-233.

DUTZLER,R. (2004a) The structural basis of ClC chloride channel function. *Trends in Neuroscience* **27**, 315-320.

DWORAKOWSKA,B. & DOLOWY,K. (2000) Ion channels-related diseases. *Acta Biochimica Polonica* **47**, 685-703.

DYASON,K., BRANDT,W., PRENDINIL., VERDONCK,F., TYTGAT,J., DU PLESSIS,J., MULLER,G. & VAN DER WALT,J. (2002) Determination of species-specific components in the venom of *Parabuthus* scorpions from southern Africa using matrix-assisted laser desorption time-of-flight mass spectrometry. *Rapid communications in mass spectrometry* **16**, 768-773.

EITAN,M., FOWLER,E., HERRMANN,R., DUVAL,D., PELHATE,M. & ZLOTKIN,E. (1990) A scorpion venom neurotoxin paralytic to insects that affects sodium current inactivation: purification, primary structure, and mode of action. *Biochemistry (Mosc)*. **29**, 5941-5947.

EL-HAYEK,R., LOKUTA,A.J., AREVALO,C. & VALDIVIA,H.H. (1995) Peptide probe of ryanodine receptor function. Imperatoxin A, a peptide from the venom of the scorpion *Pandinus imperator*, selectively activates skeletal-type ryanodine receptor isoforms. *Journal of Biological Chemistry* **270**, 28696-28704.

EL AYEB,M. & ROCHAT,H. (1985) Polymorphism and quantitative variations of toxins in the venom of the scorpion *Androctonus australis hector*. *Toxicon* **23**, 755-760.

EL HAFNEY,B., CHGOURY,F., ADIL,N., COHEN,N. & HASSAR,M. (2002) Intraspecific variability and pharmacokinetic characteristics of *Androctonus mauretanicus mauretanicus* scorpion venom. *Toxicon* **40**, 1609-1616.

ESCOUBAS,P., ROMI-LEBRUN,R., LEBRUN,B., HERRMANN,R., MOSKOWITZ,H., RAJENDRA,W., HAMMOCK,B. & NAKAJIMA,T. (1991) Tamulotoxin, a novel member of the potassium channel active short toxins from the venom of the Indian red scorpion *Buthus tamulus*. *Toxicon* **35**, 806.

ESCOUBAS,P., CELERIER,M.-L. & NAKAJIMA,T. (1997) High performance liquid chromatography matrix-assisted laser desorption/ionization time-of-flight mass spectrometry peptide fingerprinting of tarantula venoms in the genus *Brachypelma*: chemotaxic and biochemical applications. *Rapid communications in mass spectrometry* **11**, 1891-1899.

ESCOUBAS,P., WHITELEY,B.J., KRISTENSEN,C.P., CELERIER,M.-L., CORZO,G. & NAKAJIMA,T. (1998) Multidimensional peptide fingerprinting by high performance liquid chromatography, capillary zone electrophoresis and matrix- assisted laser desorption/ ionization time-of-flight mass spectrometry for the identification of tarantula venom samples. *Rapid communications in mass spectrometry* **12**, 1075-1084.

ESCOUBAS,P., CHAMOT-ROOKE,J., STOCKLIN,R., WHITELEY,B.J., CORZO,G., GENET,R. & NAKAJIMA,T. (1999) A comparison of matrix-assisted laser desorption/ionization time-of-flight and liquid chromatography electrospray ionization mass spectrometry methods for the analysis of crude tarantula venoms in the *Pterinochilus* group. *Rapid communications in mass spectrometry* **13**, 1861-1868.

ESCOUBAS,P., CORZO,G., WHITELEY,B.J., CELERIER,M.-L. & NAKAJIMA,T. (2002) Matrix-assisted laser desorption/ionization time-of-flight mass spectrometry and high-performance liquid chromatography study of quantitative and qualitative variation in tarantula spider venoms. *Rapid communications in mass spectrometry* **16**, 403-413.

ESCOUBAS,P. & RASH,L. (2004) Tarantulas: eight-legged pharmacists and combinatorial chemists. *Toxicon* **43**, 555-574.

ESTEVE,E., SMIDA-REZGUI,S., SARKOZI,S., SZEGEDI,C., REGAYA,I., CHEN,L., ALTAF AJ,X., ROCHAT,H., ALLEN,P., PESSAH,I.N., MARTY,I., SABATIER,J.-M., JONA,I., DE WAARD,M. & RONJAT,M. (2003) Critical amino acid residues determine the binding affinity and the Ca²⁺ release efficacy of maurocalcine in skeletal muscle cells. *Journal of Biological Chemistry* **278**, 37822-37831.

FABER,E.S.L. & SAH,P. (2003) Calcium-activated potassium channels: multiple contributions to neuronal function. *Neuroscientist* **9**, 181-194.

FAJLOUN,Z., FERRAT,G., CARLIER,E., FATHALLAH,M., LECOMTE,C., SANDOZ,G., DI LUCCIO,E., MABROUK,K., LEGROS,C., DARBON,H., ROCHAT,H., SABATIER,J.-M. & DE WAARD,M. (2000) Synthesis, ¹H NMR structure, and activity of a three-disulphide-bridged maurotoxin analog designed to restore the consensus motif of scorpion toxins. *Journal of Biological Chemistry* **275**, 13605-13612.

FAJLOUN,Z., KHARRAT,R., CHEN,L., LECOMTE,C., DI LUCCIO,E., BICHET,D., EL AYEB,M., ROCHAT,H., ALLEN,P.D., PESSAH,I.N., DE WAARD,M. & SABATIER,J.-M. (2000a) Chemical synthesis and characterization of maurocalcine, a scorpion toxin that activates Ca²⁺ release channel/ryanodine receptors. *FEBS Lett.* **469**, 179-185.

FAJLOUN,Z., MOSBAH,A., CARLIER,E., MANSUELLE,P., SANDOZ,G., FATHALLAH,M., DI LUCCIO,E., DEVAUX,C., ROCHAT,H., DARBON,H., DE WAARD,M. & SABATIER,J.-M. (2000b) Maurotoxin versus P1/HsTx1 scorpion toxins. Toward new insights in the understanding of their distinct disulfide bridge patterns. *Journal of Biological Chemistry* **275**, 39394-39402.

- FAJLOUN,Z., CARLIER,E., LECOMTE,C., GEIB,S., DI LUCCIO,E., BICHET,D., MABROUK,K., ROCHAT,H., DE WAARD,M. & SABATIER,J.-M. (2000c) Chemical synthesis and characterization of P11, a scorpion toxin from *Pandinus imperator* active on K⁺ channels. *Eur. J. Biochem.* **267**, 5149-5155.
- FANGER,C.M., GHANSHANI,S., LOGSDON,N.J., RAUER,H., KALMAN,K., ZHOU,J., BECKINGHAM,K., CHANDY,K.G., CAHALAN,M.D. & AIYER,J. (1999) Calmodulin mediates calcium-dependent activation of the intermediate conductance KCa channel, IKCa1. *Journal of Biological Chemistry* **274**, 5746-5754.
- FAZAL,A., BEG,O.U., SHAFQAT,J., ZAIDI,Z.H. & JORNVALL,H. (1989) Characterization of two different peptides from the venom of the scorpion *Buthus indicus*. *FEBS Lett.* **257**, 260-262.
- FERREIRA,L.A., ALVES,E.W. & HENRIQUES,O.B. (1993) Peptide T a novel bradykinin potentiator isolated from *Tityus serrulatus* scorpion venom. *Toxicon* **31**, 941-947.
- FILL,M. & COPELLO,J.A. (2002) Ryanodine receptor calcium release channels. *Physiol. Rev.* **82**, 893-982.
- FINK,M., DUPRAT,F., LESAGE,F., HEURTEAUX,C., ROMEY,G., BARHANIN,J. & LAZDUNSKI,M. (1996) A new K⁺ channel β subunit to specifically enhance Kv2.2 (CDRK) expression. *Journal of Biological Chemistry* **271**, 26341-26348.
- FINLAYSON,K., MCLUCKIE,J., HERN,J., ARAMORI,I., OLVERMAN,H.J. & KELLY,J.S. (2001) Characterisation of [¹²⁵I]-apamin binding sites in rat brain membranes and HEK293 cells transfected with SK channel subtypes. *Neuropharmacology* **41**, 341-350.
- FIORIS,S., PEGORARO,S., RUDOLPH-BOHNER,S., CRAMER,J. & MORODER,L. (2000) Synthesis and conformational analysis of apamin analogues with natural and non-natural cystine/ selenocystine connectives. *Biopolymers* **53**, 550-564.
- FISCHER,W.B. & SANSOM,M.S.P. (2002) Viral ion channels: structure and function. *Biochim. Biophys. Acta* **1591**, 27-45.
- FONTECILLA-CAMPS,J.C., ALMASSY,R.J., SUDDATH,F.L., WATT,D.D. & BUGG,C.E. (1980) Three dimensional structure of a protein from scorpion venom. A new structural class of neurotoxins. *Proc. Natl. Acad. Sci. USA* **77**, 6496-6500.
- FOSSET,M., SCHMID-ANTOMARCHI,H., HUGUES,M., ROMEY,G. & LAZDUNSKI,M. (1984) The presence in pig brain of an endogenous equivalent of apamin, the bee venom peptide that specifically blocks Ca²⁺-dependent K⁺ channels. *Proc. Natl. Acad. Sci. USA* **81**, 7228-7232.
- FOURNET,J.C. & JUNIEN,C. (2003) The genetics of neonatal hyperinsulinism. *Horm. Res.* **59**, 30-34.
- FOURNIER,C., KOURRICH,S., SOUMIREU-MOURAT,B. & MOURRE,C. (2001) Apamin improves reference memory but not procedural memory in rats by blocking small-conductance Ca²⁺-activated K⁺ channels in an olfactory discrimination task. *Behavioural Brain Research* **121**, 81-93.

- FRANCISCHETTI,I.M., GOMBAROVITS,M.E., VALENZUELA,J.C., CARLINI,C.R. & GUIMARAES,J.A. (2000) Intraspecific variation in the venoms of the South American rattlesnake (*Crotalus durissus terrificus*). *Comparative Biochemistry and Physiology Part C* **127**, 23-36.
- FREDHOLM,B. (1966) Studies on a mast cell degranulating factor in bee venom. *Biochem. Pharmacol.* **15**, 2037-2043.
- FREEMAN,C.M., CATLOW,C.R.A., HEMMING,S.A.M. & HIDER,R.C. (1986) The conformation of apamin. *FEBS Lett.* **197**, 289-296.
- FRINGS,S., REUTER,D. & KLEENE,S.J. (2000) Neuronal Ca²⁺-activated Cl⁻ channels - homing in on an elusive channel species. *Progress in Neurobiology* **60**, 247-289.
- FRONTALI,M. (2001) Spinocerebellar ataxia type 6: Channelopathy or glutamine repeat disorder? *Brain Research Bulletin* **56**, 227-231.
- FROY,O. & GUREVITZ,M. (1998) Membrane potential modulators: a thread of scarlet from plants to humans. *FASEB J.* **12**, 1793-1796.
- FROY,O., SAGIV,T., POREH,M., URBACH,D., ZILBERBERG,D. & GUREVITZ,M. (1999) Dynamic diversification from a putative common ancestor of scorpion toxins affecting sodium, potassium, and chloride channels. *Journal of Molecular Evolution* **48**, 187-196.
- FROY,O., ZILBERBERG,D., GORDON,D., TURKOV,M., GILLES,N., STANKIEWICZ,M., PELHATE,M., LORET,E., OREN,D.A., SHAANAN,B. & GUREVITZ,M. (1999a) The putative bioactive surface of insect-selective scorpion excitatory neurotoxins. *Journal of Biological Chemistry* **274**, 5769-5776.
- FRY,B.G., WICKRAMARATNA,J.C., HODGSON,W.C., ALEWOOD,P.F., KINI,R.M., HO,H. & WUSTER,W. (2002) Electrospray liquid chromatography/ mass spectrometry fingerprinting of *Acanthopis* (death adder) venoms: taxonomic and toxinological implications. *Rapid communications in mass spectrometry* **16**, 600-608.
- FULLER,M.D., ZHANG,Z.R., CUI,G., KUBANEK,J. & MCCARTY,N.A. (2004) Inhibition of CFTR channels by a peptide toxin of scorpion venom. *Am. J. Physiol. Cell Physiol.* **in press**.
- GALANAKIS,D., DAVIS,C.A., HERRERO,B.D.R., GANELLIN,C.R., DUNN,P.M. & JENKINSON,D.H. (1995) Synthesis and structure-activity relationships of dequalinium analogues as K⁺ channel blockers. Investigations on the role of the charged heterocycle. *J. Med. Chem.* **38**, 595-606.
- GALANAKIS,D., GANELLIN,C.R., DUNN,P.M. & JENKINSON,D.H. (1996) On the concept of a bivalent pharmacophore for SK_{Ca} channel blockers: synthesis, pharmacological testing, and radioligand binding studies on mono-, bis-, and tris-quinolinium compounds. *Archiv der Pharmazie Pharmaceutical and Medicinal Chemistry* **329**, 524-528.

- GALANAKIS,D., GANELLIN,C.R., CHEN,J.Q., GUNASEKERA,D. & DUNN,P.M. (2004) Bis-Quinolinium cyclophanes: toward a pharmacophore model for blockade of apamin-sensitive SK (Ca) channels in sympathetic neurons. *Bioorg. Med. Chem. Lett.* **14**, 4231-4235.
- GALVEZ,A., GIMENEZ-GALLEGO,G., REUBEN,J.P., ROY-CONTANCIN,L., FEIGENBAUM,P., KACZOROWSKI,G.J. & GARCIA,M.L. (1990) Purification and characterisation of a unique, potent, peptidyl probe for the high conductance calcium-activated potassium channel from the venom of the scorpion *Buthus tamulus*. *Journal of Biological Chemistry* **265**, 11083-11090.
- GANDOLFO,G., GOTTESMANN,C., BIDARD,J.N. & LAZDUNSKI,M. (1989) K⁺ channel openers prevent epilepsy induced by the bee venom peptide MCD. *European Journal of Pharmacology* **159**, 329-330.
- GARCIA-ANOVEROS,J. & COREY,D.P. (1997) The molecules of mechanosensation. *Annu. Rev. Neurosci.* **20**, 567-594.
- GARCIA,C., BECERRIL,B., SELISKO,B., DELEPIERRE,M. & POSSANI,L.D. (1997) Isolation, characterization and comparison of a novel crustacean toxin with a mammalian toxin from the venom of the scorpion *Centruroides noxius* Hoffmann. *Comp. Biochem. Physiol.* **116**, 315-322.
- GARCIA,M.L., GARCIA-CALVO,M., HIDALGO,P., LEE,A. & MACKINNON,R. (1994) Purification and characterization of three inhibitors of voltage-dependent K⁺ channels from *Leiurus quinquestriatus* var. *hebraeus* venom. *Biochemistry (Mosc)*. **33**, 6834-6839.
- GARCIA,M.L., KNAUS,H.H., MUNUJOS,P., SLAUGHTER,R.S. & KACZOROWSKI,G.J. (1995) Charybdotoxin and its effects on potassium channels. *Am. J. Physiol. Cell Physiol.* **269**, C1-C10.
- GARCIA,M.L., HANNER,M. & KACZOROWSKI,G.J. (1998) Scorpion toxins: tools for studying K⁺ channels. *Toxicon* **36**, 1641-1650.
- GARCIA,M.L., GAO,Y.-D., MCMANUS,O.B. & KACZOROWSKI,G.J. (2001) Potassium channels: From scorpion venoms to high-resolution structure. *Toxicon* **39**, 739-748.
- GARDOS,G. (1958) The function of calcium in the potassium permeability of human erythrocytes. *Biochim. Biophys. Acta* **30**, 653-654.
- GARGUS,J.J. (2003) Unraveling monogenic channelopathies and their implications for complex polygenic disease. *Am. J. Hum. Genet.* **72**, 785-803.
- GAULDIE,J., HANSON,J.M., RUMJANEK,F.D., SHIPOLINI,R.A. & VERNON,C.A. (1976) The peptide components of bee venom. *European Journal of Biochemistry* **61**, 369-376.
- GAULDIE,J., HANSON,J.M., SHIPOLINI,R.A. & VERNON,C.A. (1978) The structures of some peptides from bee venom. *Eur. J. Biochem.* **83**, 405-410.

GEKLE,M., OBERLEITHNER,H. & SILBERNAGL,S. (1993) Ochratoxin A impairs "postproximal" nephron function *in vivo* and blocks plasma membrane anion conductance in Madin-Darby canine kidney cells *in vitro*. *Pflugers Archiv: European Journal of Physiology* **425**, 401-408.

GHELARDINI,C., GALEOTTI,N., VETTORI,A.P., CAPACCIOLIS., QUATTRONE,A. & BARTOLINI,A. (1997) Effect of K⁺ channel modulation on mouse feeding behaviour. *European Journal of Pharmacology* **39**, 1-8.

GIMENEZ-GALLEGO,G., NAVIA,M.A., REUBEN,J.P., KATZ,J.P., KACZOROWSKI,G.L. & GARCIA,M.L. (1988) Purification, sequence, and model structure of charybdotoxin, a potent inhibitor of calcium-activated potassium channels. *Proc. Natl. Acad. Sci. USA* **85**, 3329-3333.

GIORGETTI,A. & CARLONI,P. (2003) Molecular modeling of ion channels: structural predictions. *Current Opinion in Chemical Biology* **7**, 150-156.

GMACHL,M. & KREIL,G. (1995) The precursors of the bee venom constituents apamin and MCD peptide are encoded by two genes in tandem which share the same 3'-exon. *Journal of Biological Chemistry* **270**, 12704-12708.

GOLDIN,A.L. (2001) Resurgence of sodium channel research. *Annu. Rev. Physiol.* **63**, 871-894.

GOLDSTEIN,S.A.N., PHEASANT,D.J. & MILLER,C. (1994) The charybdotoxin receptor of a shaker K⁺ channel; peptide and channel residues mediating molecular recognition. *Neuron* **12**, 1377-1388.

GONCALVES DE ANDRADE,R.M., DE OLIVEIRA,K.C., GIUSTI,A.L., DIAS DA SILVA,W. & TAMBOURGI,D.V. (1999) Ontogenetic development of *Loxosceles intermedia* spider venom. *Toxicon* **37**, 627-632.

GOPALAKRISHNAKONE,P. (1995) The black scorpion *Heterometrus longimans*: structure of the venom secreting apparatus. *Journal of Natural Toxins* **4**, 1-18.

GORDON,D., JOVER,E., COURAUD,F. & ZLOTKIN,E. (1984) The binding of the insect selective neurotoxin (AaIT) from scorpion venom to locust synaptosomal membranes. *Biochim. Biophys. Acta* **778**, 349-358.

GORDON,D., MOSKOWITZ,H. & ZLOTKIN,E. (1990) Sodium channel polypeptides in central nervous systems of various insects identified with site directed antibodies. *Biochim. Biophys. Acta* **1026**, 80-86.

GORDON,D., MOSKOWITZ,H., EITAN,M., WARNER,C., CATTERALL,W.A. & ZLOTKIN,E. (1992) Localization of receptor sites for insect-selective toxins on sodium channels by site-directed antibodies. *Biochemistry (Mosc)*. **31**, 7622-7628.

GORDON,D., MARTIN-EAUCLAIRE,M.-F., CESTELE,S., KOPEYAN,C., KALIFA,R.B., PELHATE,M. & ROCHAT,H. (1996) Scorpion toxins affecting sodium current inactivation bind to distinct homologous receptor sites on rat brain and insect sodium channels. *J. Biol. Chem.* **271**, 8034-8045.

- GORDON,D. & GUREVITZ,M. (2003) The selectivity of scorpion α -toxins for sodium channel subtypes is determined by subtle variations at the interacting surface. *Toxicon* **41**, 125-128.
- GOUDET,C., CHI,C.-W. & TYTGAT,J. (2002) An overview of toxins and genes from the venom of the Asian scorpion *Buthus martensi* Karsch. *Toxicon* **40**, 1239-1258.
- GRANATA,T. (2003) Rasmussen's syndrome. *Neurol Sci* **24**, S239-243.
- GRANIER,C., PEDROSO,E. & VAN RIETSCHOTEN,J. (1978) Use of synthetic analogs for a study on the structure-activity relationship of apamin. *European Journal of Biochemistry* **82**, 293-299.
- GRAY,W.R. (1993) Disulfide structures of highly bridged peptides: a new strategy for analysis. *Protein Science* **2**, 1732-1748.
- GREEN,D., PACE,S., CURTIS,S.M., SAKOWSKA,M., LAMB,G.D., DULHUNTY,A.F. & CASAROTTO,M.G. (2003) The three-dimensional structural surface of two beta-sheet scorpion toxins mimics that of an alpha-helical dihydropyridine receptor segment. *Biochem. J.* **370**, 517-527.
- GREFFRATH,W., MARTIN,E., REUSS,S. & BOEHMER,G. (1998) Component of after-hyperpolarisation in magnocellular neurons of the rat supraoptic nucleus *in vitro*. *Journal of Physiology* **513**, 493-506.
- GRIKOFF,V.K., STARRET,J.E. & DWORETZKY,S.I. (2001) Maxi-K potassium channels: form, function, and modulation of a class of endogenous regulators of intracellular calcium. *Neuroscientist* **7**, 166-177.
- GRISHIN,E.V. (1978) Isolation, properties and amino acid composition of toxins from the venom of the central Asiatic scorpion *Buthus eupeus*. *Bioorg. Chem.* **4**, 450-461.
- GRISHIN,E.V., SOLDATOVA,L.N., OVCHINNIKOV,Y.A. & YU,A. (1980) Nature of the membrane receptors for scorpion venom neurotoxin. *Bioorg. Chem.* **6**, 473-480.
- GRISHIN,E.V., VOLKOVA,T.M. & SOLDATOVA,L.N. (1982) Study of toxic components from the venom of caucasus subspecies of scorpion *Buthus eupeus*. *Bioorgan. Khim.* **8**, 155-164.
- GRUNNET,M., JENSEN,B.S., OLESON,S.P. & KLAERKE,D.A. (2001) Apamin interacts with all subtypes of cloned small-conductance Ca^{2+} -activated K^{+} channels. *Pflugers Archiv: European Journal of Physiology* **441**, 544-550.
- GUERON,M., ILIA,R. & MARGULIS,G. (2000) Arthropod poisons and the cardiovascular system. *American Journal of Emergency Medicine* **18**, 708-714.

GUREVITZ,M., FROY,O., ZILBERBERG,N., TURKOV,M., STRUGATSKY,D., GERSHBURG,E., LEE,D., ADAMS,M.E., TUGARINOV,V., ANGLISTER,J., SHAANAN,B., LORET,E., STANKIEWICZ,M., PELHATE,M., GORDON,D. & CHEJANOVSKY,N. (1998) Sodium channel modifiers from scorpion venom: structure-activity relationship, mode of action and application. *Toxicon* **36**, 1671-1682.

GURROLA,G.B., AREVALO,C., SREEKUMAR,R., LOKUTA,A.J., WALKER,J.W. & VALDIVIA,H.H. (1999) Activation of ryanodine receptors by Imperatoxin A and a peptide segment of the II-III loop of the dihydropyridine receptor. *Journal of Biological Chemistry* **274**, 7879-7886.

GURROLA,G.B., ROSATI,B., ROCCHETTI,M., PIMIENTA,G., ZAZA,A., ARCANGELLA, OLIVOTTO,M., POSSANI,L.D. & WANKE,E. (1999a) A toxin to nervous, cardiac, and endocrine ERG K⁺ channels isolated from *Centruroides noxius* scorpion venom. *FASEB J.* **13**, 953-962.

GUTMAN,G.A., CHANDY,K.G., ADELMAN,J.P., AIYER,J., BAYLISS,D.A., CLAPHAM,D., COVARRUBIAS,M., DESIR,G., V, FURUICHI,K., GANETZKY,B., GARCIA,M.L., GRISSMER,S., JAN,L.Y., KARSCHIN,A., KIM,D., KUPERSCHMIDT,S., KURACHI,Y., LAZDUNSKI,M., LESAGE,F., LESTER,H.A., MCKINNON,D., NICHOLS,C.G., O'KELLY,I., ROBBINS,J., ROBERTSON,G.A., RUDY,B., SANGUINETTI,M., SEINO,S., STUHMER,W., TAMKUN,M.M., VANDENBERG,C.A., WEI,A., WULFF,H. & WYMORE,R.S. (2003) International union of pharmacology. XLI. Compendium of voltage-gated ion channels: potassium channels. *Pharmacological Reviews* **55**, 583-586.

GWEE,M.C.E., WONG,P.T.H., GOPALAKRISHNAKONE,P., CHEAH,L.S. & LOW,K.S.Y. (1993) The black scorpion *Heterometrus longimanus*: Pharmacological and biochemical investigation of the venom. *Toxicon* **31**, 1305-1314.

GWEE,M.C.E., CHEAH,L.S., GOPALAKRISHNAKONE,P., WONG,P.T.H., GONG,J.P. & KINI,R.M. (1996) Studies on venoms from the black scorpion *Heterometrus longimanus* and some other scorpion species. *J. Toxicol. Toxin Reviews* **15**, 37-57.

GWEE,M.C.E., NIRTHANAN,S., KHOO,H.E., GOPALAKRISHNAKONE,P., KINI,R.M. & CHEAH,L.S. (2002) Autonomic effects of some scorpion venoms and toxins. *Clinical and Experimental Pharmacology and Physiology* **29**, 795-801.

HABERMANN,E. (1972) Bee and wasp venoms. *Science* **177**, 314-322.

HABERMANN,E. (1977) Neurotoxicity of apamin and MCD peptide upon central application. *Naunyn Schmiedeberg's Archives of Pharmacology* **300**, 189-191.

HABERMANN,E. & FISCHER,K. (1979) Bee venom neurotoxin (apamin): Iodine labelling and characterization of binding sites. *European Journal of Biochemistry* **94**, 355-364.

HABERMANN,E. (1984) Apamin. *Pharmacology and Therapeutics* **25**, 255-270.

- HAMON,A., GILLES,N., SAUTIERE,P., MARTINAGE,A., KOPEYAN,C., ULENS,C., TYTGAT,J., LANCELIN,J.M. & GORDON,D. (2002) Characterization of scorpion alpha-like toxin group using two new toxins from the scorpion *Leiurus quinquestriatus hebraeus*. *Eur. J. Biochem.* **269**, 3920-3933.
- HANSON,J.M., MORLEY,J. & SORIA,C. (1972) Anti-inflammatory property of 401, a peptide from the venom of the bee (*Apis mellifica* L). *Br. J. Pharmacol.* **46**, 537P-538P.
- HARVEY,A.L. (1993) *Drugs From Natural Products*. Ellis Horwood, New York.
- HARVEY,A.L., VANTANPOUR,H., ROWAN,E.G., PINKASFELD,S., VITA,C., MENEZ,A. & MARTIN-EAUCLAIRE,M.-F. (1995) Structure-activity studies on scorpion toxins that block potassium channels. *Toxicon* **33**, 425-436.
- HASSAN,A. & MOHAMMED,A.H. (1940) Atropine and ergotoxin as antidotes to scorpion toxin. *Lancet* **1**, 1001-1002.
- HAUX,P., SAWERTHAL,H. & HABERMANN,E. (1967) Sequence analysis of bee venom neurotoxin (apamin) from its tryptic and chymotryptic cleavage products. *Hoppe-Seyler's Zeitschrift fur Physiologische Chemie* **348**, 737-738.
- HAYLETT,D.G. (1996) Direct measurement of drug binding to receptors. In: *Textbook of Receptor Pharmacology* (Ed. J.C.Foreman & T.Johansen). CRC Press, London.
- HEAD,C. & GARDINER,M. (2003) Paroxysms of excitement: sodium heart channel dysfunction in heart and brain. *Bioessays* **25**, 981-993.
- HEGINBOTHAM,L., LU,Z., ABRAMSON,T. & MACKINNON,R. (1994) Mutations in the K⁺ channel signature sequence. *Biophysical Journal* **66**, 1061-1067.
- HERLITZE,S., RADITSCH,M., RUPPERSBERG,J.P., JAHN,W., MONYER,H., SCHOEPFER,R. & WITZEMANN,V. (1993) Argiotoxin detects molecular differences in AMPA receptor channels. *Neuron* **10**, 1131-1140.
- HIDER,R.C. & RAGNARSSON,U. (1980) A proposal for the structure of apamin. *FEBS Lett.* **111**, 189-193.
- HIDER,R.C. & RAGNARSSON,U. (1981) A comparative structural study of apamin and related bee venom peptides. *Biochim. Biophys. Acta* **667**, 197-208.
- HIRSCHBERG,B., MAYLIE,J., ADELMAN,J.P. & MARRION,N.V. (1998) Gating of recombinant small-conductance Ca-activated K⁺ channels by calcium. *Journal of General Physiology* **111**, 565-581.
- HISADA,M., KONNO,K., ITAGAKI,Y., NOAKI,H. & NAKAJIMA,T. (2000) Advantages of using nested collision induced dissociation/post-source decay with matrix-assisted laser desorption/ionization time of flight mass spectrometry: sequencing of novel peptides from wasp venom. *Rapid communications in mass spectrometry* **14**, 1828-1834.

- HODGKIN,A.L. & HUXLEY,A.F. (1952) A quantitative description of membrane current and its application to conduction and excitation in nerve. *J. Physiol. (Lond.)* **117**, 500-544.
- HOEDEMAEKERS,A.C., VAN BREDA VRIESMAN,P.J. & DE BAETS,M.H. (1997) Myasthenia gravis as a prototype autoimmune receptor disease. *Immunol. Res.* **16**, 341-354.
- HOFFMAN,D.R. & SHIPMAN,W.H. (1976) Allergens in bee venom. I. Separation and identification of the major allergens. *J Allergy Clin. Immunol* **58**, 551-562.
- HOFFMAN,D.R. (1977) Allergens in bee venom. III. Identification of allergen B of bee venom as an acid phosphatase. *J Allergy Clin. Immunol* **59**, 364-366.
- HOFFMAN,D.R., SHIPMAN,W.H. & BABIN,D. (1977) Allergens in bee venom II. Two new high molecular weight allergenic specificities. *J Allergy Clin. Immunol* **59**, 147-153.
- HOFMANN,U.F., WESTPHAL,J.R., VAN MUIJEN,G.N. & RUITER,D.J. (2000) Matrix metalloproteinases in human melanoma. *J. Invest. Dermatol.* **115**, 337-344.
- HOLADAY,S.K., MARTIN,B.M., FLETCHER,P.I. & KRISHNA,N.R. (2000) NMR solution structure of butantoxin. *Arch. Biochem. Biophys.* **379**, 18-27.
- HUGUES,M., SCHMID,H., ROMÉY,G., DUVAL,D., FRELIN,L. & LAZDUNSKI,M. (1982) The Ca²⁺-dependant slow K⁺ conductance in cultured rat muscle cells:- characterised with apamin. *EMBO J.* **1**, 1039-1042.
- HUGUES,M., DUVAL,D., SCHMID,H., KATABGI,P., LAZDUNSKI,M. & VINCENT,J.P. (1982a) Specific binding and pharmacological interactions of apamin, the neurotoxin from bee venom, with guinea pig colon. *Life Sciences* **31**, 437-443.
- HUGUES,M., SCHMID,H. & LAZDUNSKI,M. (1982b) Identification of a protein component of the Ca²⁺-dependent K⁺ channel by affinity labelling with apamin. *Biochemical and Biophysical Research Communications.* **107**, 1577-1582.
- HUGUES,M., DUVAL,D., KITABGI,P., LAZDUNSKI,M. & VINCENT,J.P. (1982c) Preparation of a pure monoiodo derivative of the bee venom neurotoxin apamin and its binding properties to rat brain synaptosomes. *Journal of Biological Chemistry* **257**, 2762-2769.
- HUGUES,M., ROMÉY,G., DUVAL,D., VINCENT,J.P. & LAZDUNSKI,M. (1982d) Apamin as a selective blocker of the calcium-dependent potassium channel in neuroblastoma cells: Voltage-clamp and biochemical characterisation of the toxin receptor. *Proc. Natl. Acad. Sci* **79**, 1308-1312.
- HULME,E.C. & BIRDSALL,N. (1990) *Receptor-Effector Coupling: a Practical Approach*. Oxford Univsity Press, Oxford.
- HUYGHUES-DESPOINTES,B.M.P. & NELSON,J.W. (1992) Stabilities of disulphide bond intermediates in the folding of apamin. *Biochemistry (Mosc).* **31**, 1476-1483.

- IKONEN,S., SCHMIDT,B. & RIEKKINEN,P.J. (1998) Apamin improves spatial navigation in medical septal-lesioned mice. *European Journal of Pharmacology* **347**, 13-21.
- IMOTO,K. (1993) Ion channels: molecular basis of ion selectivity. *FEBS Lett.* **325**, 100-103.
- INCEOGLU,B., LANGO,J., JING,J., CHEN,L., DOYMAZ,F., PESSAH,I.N. & HAMMOCK,B. (2003) One scorpion, two venoms: Prevenom of *Parabuthus transvaalicus* acts as an alternative type of venom with distinct mechanism of action. *PNAS* **100**, 922-927.
- ISAACS,N.W. (1995) Cystine knots. *Curr. Opin. Struct. Biol.* **5**, 391-395.
- ISHII,T.M., SILVIA,C., HIRSCHBERG,B., BOND,C.T. & ADELMAN,J.P. (1997) A human intermediate conductance calcium-activated potassium channel. *Proc. Natl. Acad. Sci. USA* **94**, 11651-11656.
- ISHII,T.M., MAYLIE,J. & ADELMAN,J.P. (1997a) Determinants of apamin and *d*-tubocurarine block in SK potassium channels. *Journal of Biological Chemistry* **272**, 23195-23200.
- ISHIKAWA,K., FUJIGASAKI,H., SAEGUSA,H., OHWADA,K., FUGITA,T., IWAMOTO,H., KOMATSUZAKI,Y., TORU,S., TORIYAMA,H., WATANABE,M., OHKOSHI,N., SHOJI,S., KANAZAWA,I., TANABE,T. & MIZUSAWA,H. (1999) Abundant expression and cytoplasmic aggregations of $[\alpha]1A$ voltage-dependent calcium channel protein associated with neurodegeneration in spinocerebellar ataxia type 6. *Human Molecular Genetics* **8**, 1185-1193.
- ISMAIL,M., EL-ASMAR,M.F. & OSMAN,O.H. (1975) Pharmacological studies with scorpion (*Palamneus gravimanus*) venom: evidence for the presence of histamine. *Toxicon* **13**, 49.
- ISMAIL,M. (1995) The scorpion envenoming syndrome. *Toxicon* **33**, 825-858.
- JACKSON,C., NGUYEN,M., ARKELL,J. & SAMBROOK,P. (2001) Selective matrix metalloproteinase (MMP) inhibition in rheumatoid arthritis-targetting gelatinase A activation. *Inflamm Res* **50**, 183-186.
- JASANI,B., KREIL,G., MACKLER,B.F. & STANWORTH,D.R. (1979) Further studies on the structural requirements for polypeptide-mediated histamine release from rat mast cells. *Biochem. J.* **181**, 623-632.
- JEN,J. (1999) Calcium channelopathies in the central nervous system. *Current Opinion in Neurobiology* **9**, 274-280.
- JENSEN,B.S., STROBAEK,D., OLESEN,S.-P. & CHRISTOPHERSEN,P. (2001) The Ca^{2+} -activated K^{+} channel of intermediate conductance: a molecular target for novel treatments? *Curr. Drug Targets* **2**, 401-422.
- JENTSCH,T.J., STEINMEYER,K. & SCHWARZ,G. (1990) Primary structure of *Torpedo marmorata* chloride channel isolated by expression cloning in *Xenopus* oocytes. *Nature* **348**, 510-514.

- JENTSCH,T.J., GUNTHER,W., PUSCH,M. & SCHWAPPACH,B. (1995) Properties of voltage-gated chloride channels of the ClC gene family. *Journal of Physiology* **482**,P, 19S-25S.
- JENTSCH,T.J. (1996) Chloride channels: a molecular perspective. *Current Opinion in Neurobiology* **6**, 303-310.
- JENTSCH,T.J. (2000) Neuronal KCNQ potassium channels: physiology and role in disease. *Nature Reviews : Neuroscience* **1**, 21-30.
- JENTSCH,J., STEIN,V., WEINREICH,F. & ZDEBIK,A.A. (2002) Molecular structure and physiological function of chloride channels. *Physiol. Rev.* **82**, 503-568.
- JIANG,Y., LEE,A., CHEN,J., CADENE,M., CHAIT,B.T. & MACKINNON,R. (2002) The open-pore conformation of potassium channels. *Nature* **417**, 523-526.
- JIN,W. & LU,Z. (1998) A novel high-affinity inhibitor for inward-rectifier K⁺ channels. *Biochemistry (Mosc)*. **37**, 13291-13299.
- JOE,E.H. & ANGELIDES,K.J. (1993) Clustering and mobility of voltage-dependent sodium channels during myelination. *Journal of Neuroscience* **13**, 2993-3005.
- JOHN,A. & TUSZYNSKI,G. (2001) The role of matrix metalloproteinases in tumor angiogenesis and tumor metastasis. *Pathology Oncology Research* **7**, 14-23.
- JONES,A., BINGHAM,J.-P., GEHRMANN,J., BOND,T., LOUGHNAN,M., ATKINS,A., LEWIS,R.J. & ALEWOOD,P.F. (1996) Isolation and characterisation of conopeptides by high-performance liquid chromatography combined with mass spectrometry and tandem mass spectrometry. *Rapid communications in mass spectrometry* **10**, 138-143.
- JONES,O.T., KUNZE,D.L. & ANGELIDES,K.J. (1989) Localization and mobility of omega-conotoxin-sensitive Ca²⁺ channels in hippocampal CA1 neurons. *Science* **244**, 1189-1193.
- JOVER,E., MARTIN-MOUTOT,N., COURAUD,F. & ROCHAT,H. (1980) Binding of scorpion toxins to rat brain synaptosomal fraction. Effects of membrane potential, ions and other neurotoxins. *Biochemistry (Mosc)*. **19**, 463-467.
- KACZOROWSKI,G.J. & GARCIA,M.L. (1999) Pharmacology of voltage-gated and calcium-activated potassium channels. *Current Opinion in Chemical Biology* **3**, 448-458.
- KALAPOTHAKIS,E. & CHAVEZ-OLORTEGUI,C. (1997) Venom variability among several *Tityus serrulatus* specimens. *Toxicon* **35**, 1523-1529.
- KANKONKAR,R.C., KULKURNI,D.G. & HULIKAVI,C.B. (1998) Preparation of a potent anti-scorpion-venom-serum against the venom of red scorpion (*Buthus tamalus*). *Journal of Postgraduate Medicine* **44**, 85-92.

KARLE,C.A. & KIEHN,J. (2002) An ion channel 'addicted' to ether, alcohol and cocaine: the HETG potassium channel. *Cardiovascular research* **53**, 6-8.

KAUPP,U.B. & SEIFERT,R. (2002) Cyclic nucleotide-gated ion channels. *Physiological Reviews* **82**, 769-824.

KEEGAN,H.L. (1998) *Scorpions of Medical Importance*. Fitzgerald, London.

KEMNEY,D.M., DALTON,N., LAWRENCE,A.J., PEARCE,F.L. & VERNON,C.A. (1984) The purification and characterisation of hyaluronidase from the venom of the honey bee, *Apis mellifera*. *Eur. J. Biochem.* **139**, 217-223.

KETCHUM,K.A., JOINER,W.J., SELLERS,A.J., KACZMAREK,L.K. & GOLDSTEIN,S.A. (1995) A new family of outwardly rectifying potassium channel proteins with two pore domains in tandem. *Nature* **376**, 690-695.

KETTNER,A., HENRY,H., HUGHES,G.J., CORRADIN,G. & SPERTINI,F. (1999) IgE and T-cell responses to high-molecular weight allergens from bee venom. *Clin. Exp. Allergy* **29**, 394-401.

KETTNER,A., HUGHES,G.J., FRUTIGER,S., ASTORI,M., ROGGERO,M., SPERTINI,F. & CORRADIN,G. (2001) Api m 6: a new bee venom allergen. *J. Allergy Clin. Immunol* **107**, 914-920.

KHANDELWAL,P., SETH,S. & HOSUR,R.V. (2000) Step-wise formation of helical structure and side-chain packing in a peptide from scorpion neurotoxin support hierarchic model of protein folding. *Biophysical Chemistry* **87**, 139-148.

KHARRAT,H., MABROUK,K., CREST,M., DARBON,H., OUGHIDENI,R., MARTIN-EAUCLAIRE,M-F., JACQUET,G., EL AYEB,M., VAN RIETSCHOTEN,J., ROCHAT,H. & SABATIER,J.-M. (1996) Chemical synthesis and characterisation of maurotoxin, a short scorpion toxin with four disulphide bridges that acts on K⁺ channels. *Eur. J. Biochem.* **242**, 491-498.

KHARRAT,H., MANSUELLE,P., SAMPIERI,F., CREST,M., OUGHIDENI,R., VAN RIETSCHOTEN,J., ROCHAT,H. & EL AYEB,M. (1997) Maurotoxin, a four disulphide bridge toxin from *Scorpio maurus* venom: purification, structure and action on potassium channels. *FEBS Lett.* **406**, 284-290.

KINDAS-MUGGE,I. (1979) Isolation and translation of melittin mRNA. *Trends in Biochemical Science* **4**, 135-137.

KIRSCH,G.E., SKATTEBOL,A., POSSANI,L.D. & BROWN,A.M. (1989) Modification of Na channel gating by an alpha scorpion toxin from *Tityus serrulatus*. *J. Gen. Physiol* **93**, 67-83.

KITAMURA,H., YOKOYAMA,M., AKITA,H., MATSUSHITA,K., KURACHI,Y. & YAMADA,M. (2000) Tertiapin potently and selectively blocks muscarinic K⁺ channels in rabbit cardiac myocytes. *J Pharmacol. Exp. Ther.* **293**, 196-205.

- KOBAYASHI,Y., TAKASHIMA,H., TAMAOKI,H., KYOGOKU,Y., LAMBERT,P., KURODA,H., CHINO,N., WATANABE,T.X., KIMURA,T., SAKAKIBARA,S. & MORODER,L. (1991) The cystine-stabilized α -helix: a common structural motif of ion-channel blocking neurotoxic peptides. *Biopolymers* **31**, 1213-1220.
- KOBUROVA,K.L., MICHAILOVA,S.G. & SHKENDEROV,S. (1985) Further investigation on the antiinflammatory properties of adolapin-bee venom polypeptide. *Acta Physiol Pharmacol. Bulg.* **11**, 50-55.
- KOHLER,M., HIERSCHBERG,B., BOND,C.T., KINZIE,J.M., MARRION,N.V., MAYLIE,J. & ADELMAN,J.P. (1996) Small-conductance, calcium-activated potassium channels from mammalian brain. *Science* **273**, 1709-1714.
- KOLHEKAR,A.S., ROBERTS,M.S., JIANG,N., JOHNSON,R.C., MAINS,R.E., EIPPER,B.A. & TAGHERT,P.H. (1997) Neuropeptide amidation in *Drosophila*: separate genes encode the two enzymes catalyzing amidation. *Journal of Neuroscience* **17**, 1363-1376.
- KONNO,K., HISADA,M., NAOKI,H., ITAGAKI,Y., YASUHARA,T., JULIANO,M.A., JULIANO,L., PALMA,M.S., YAMANE,T. & NAKAJIMA,T. (2001) Isolation and sequence determination of peptides in the venom of the spider wasp (*Cyphonyx dorsalis*) guided by matrix-assisted laser desorption/ionization time of flight (MALDI-TOF) mass spectrometry. *Toxicon* **39**, 1257-1260.
- KONNO,K., HISADA,M., NAOKI,H., ITAGAKI,Y., KAWAI,N., MIWA,A., NAKATA,Y., YASHARA,T., FONTANA,R., PALMA,M.S. & NAKAJIMA,K. (2001a) Anoplin, a novel antimicrobial peptide from the venom of the solitary wasp *Anoplius samariensis*. *Biochim. Biophys. Acta* **1550**, 70-80.
- KRAUSE,J.E. & MCNAMARA,J.O. (1995) Clinical relevance of defects in signalling pathways. *Curr. Opin. Neurobiol.* **5**, 358-366.
- KREIL,G. & BACHMAYER,H. (1971) Biosynthesis of melittin, a toxic peptide from bee venom. Detection of a possible precursor. *Eur. J. Biochem.* **20**, 344-350.
- KREIL,G., HAIML,L. & SUCHANEK,G. (1980) Step-wise cleavage of the pro part of promelittin by dipeptidylpeptidase IV. *Eur. J. Biochem.* **111**, 49-58.
- KRIFI,M.N., EL AYEB,M. & DELLAGI,K. (1996) New procedures and parameters for better evaluation of *Androctonus australis garzonii* (Aag) and *Buthus occitanus tunetanus* (Bot) scorpion envenomations and specific serotherapy treatment. *Toxicon* **34**, 257-266.
- KUCHLER,K., GMACHL,M., SIPPL,M.J. & KREIL,G. (1989) Analysis of the cDNA for phospholipase A2 from honeybee venom glands. The deduced amino acid sequence reveals homology to the corresponding vertebrate enzymes. *Eur. J. Biochem.* **184**, 249-254.

KUNIYASHI,A., KAWANO,S., HIRAYAMA,Y., JI,Y.-H., XU,K., OHKURA,M., FURUKAWA,K.-I., OHIZUMI,Y., HIRAOKA,M. & NAKAYAMA,H. (1999) A new scorpion toxin (BmK-PL) stimulates Ca^{2+} -release channel activity of the skeletal-muscle ryanodine receptor by an indirect mechanism. *Biochem. J.* **339**, 343-350.

LABBE-JULLIE,C., GRANIER,C., ALBERICIO,F., DEFENDINI,ML., CEARD,B., ROCHAT,H. & VAN RIETSCHOTEN,J. (1991) Binding and toxicity of apamin. Characterisation of the active site. *European Journal of Biochemistry* **196**, 639-645.

LAEMMLI,U.K. (1970) Cleavage of structural proteins during the assembly of the head of bacteriophage 4. *Nature* **227**, 680-685.

LAGRUTTA,A., SHEN,K.-Z., NORTH,R.A. & ADELMAN,J.P. (1994) Functional differences among alternatively spliced variants of Slowpoke, a *Drosophila* calcium-activated potassium channel. *Journal of Biological Chemistry* **269**, 347-351.

LALA,K. & NARAYANAN,P. (1994) Purification, N-terminal sequence and structural characterization of a toxic protein from the Indian scorpion venom *Buthus tamulus*. *Toxicon* **32**, 325-338.

LALLEMENT,G., FOSBRAEY,P., BAILLE-LE-CROM,V., TATTERSALL,J.E.H., BLANCHET,G., WETHERELL,J.R., RICE,P., PASSINGHAM,S.L. & SENTENAC-ROUMANOU,H. (1995) Compared toxicity of the potassium channel blockers, apamin and dendrotoxin. *Toxicology* **104**, 47-52.

LAN,Z.-D., DAIL,L., ZHUO,X.L., FENG,J.C., XU,K. & CHI,C.W. (1999) Gene cloning and sequencing of Bm K AS and Bm K AS-1, two novel neurotoxins from the scorpion *Buthus martensii* Karsch. *Toxicon* **37**, 823.

LANGOSCH,D. (1995) Inhibitory glycine receptors. In: *Ligand and Voltage-Gated Ion Channels* (Ed. R.A.North). CRC press, Florida.

LARA,B., ZAPTER,P., MONTIEL,C., DE LA FUENTE,M.T., MARTINEZ-SIERRA,R., BALLESTA,J.J., GANDIA,L. & GARCIA,A.G. (1995) Density of apamin-sensitive Ca^{2+} -dependent K^+ channels in bovine chromaffin cells: relevance to secretion. *Biochem. Pharmacol.* **49**, 1459-1468.

LAZDUNSKI,M., FOSSET,M., HUGUES,M., MOURRE,C., ROMEY,G. & SCHMID-ANTOMARCHI,H. (1985) The apamin-sensitive Ca^{2+} -dependent K^+ channel. Molecular properties, differentiation and endogenous ligands in mammalian brain. *Biochemical Society Symposia* **50**, 31-42.

LECOMTE,C., FERRAT,G., FAJLOUN,Z., VAN RIETSCHOTEN,J., ROCHAT,H., MARTINEAUCLAIRE,M.-F., DARBON,H. & SABATIER,J.-M. (1999) Chemical synthesis and structure-activity relationships of Ts κ a novel scorpion toxin acting on apamin-sensitive SK channel. *J. Peptide Res.* **54**, 369-376.

LECOMTE,C., BEN KHALIFA,R., MARTIN-EAUCLAIRE,M.-F., KHARRAT,R., EL AYEB,M., DARBON,H., ROCHAT,H., CREST,M. & SABATIER,J.-M. (2000) Maurotoxin and the Kv1.1 channel: voltage-dependent binding upon enantiomerization of the scorpion toxin disulphide bridge Cys³¹-Cys³⁴. *Journal of Peptide Research* **55**, 246-254.

LEGROS,C., OUGHIDENI,R., DARBON,H., ROCHAT,H., BOUGIS,P.E. & MARTIN-EAUCLAIRE,M.-F. (1996) Characterization of a new peptide from *Tityus serrulatus* scorpion venom which is a ligand of the apamin-binding site. *FEBS Lett.* **390**, 81-84.

LEGROS,C., CEARD,B., BOUGIS,P.E. & MARTIN-EAUCLAIRE,M.-F. (1998) Evidence for a new class of scorpion toxins active against K⁺ channels. *FEBS Lett.* **431**, 375-380.

LESAGE,F. & LAZDUNSKI,M. (2000) Molecular and functional properties of two-pore-domain potassium channels. *Am. J. Physiol. Renal Physiol.* **279**, F793-F801.

LESTER,D., LAZAROVICI,P., PELHATE,M. & ZLOTKIN,E. (1982) Two insect toxins from the venom of the scorpion *Buthotus judacicus* : purification, characterisation and action. *Biochim. Biophys. Acta* **701**, 370-381.

LI,H.L., SUI,H.X., GHANSHANI,S., LEE,S., WALIAN,P.J., WU,C.L., CHANDY,K.G. & JAP,B.K. (1998) Two-dimensional crystallization and projection structure of KcsA potassium channel. *Journal of Molecular Biology* **282**, 211-216.

LIGHT,W.C., REISMAN,R.E., ILEA,V.S., WYPYCH,J.I., OKAZAKI,T. & ARBESMAN,C.E. (1976) Studies of the antigenicity and allergenicity of phospholipase A2 of bee venom. *J Allergy Clin. Immunol* **58**, 322-329.

LINDSTROM,J.M. (1995) Nicotinic acetylcholine receptors. In: *Ligand and Voltage-Gated Ion Channels* (Ed. R.A.North). CRC press, Florida.

LINDSTROM,J.M. (2000) Acetylcholine receptors and myasthenia. *Muscle & Nerve* **23**, 453-477.

LIPPENS,G., NAJIB,J., WODAK,S.J. & TARTAR,A. (1995) NMR sequential assignments and solution structure of chlorotoxin, a small scorpion toxin that blocks chloride channels. *Biochemistry (Mosc)*. **34**, 13-21.

LIPPS,B.V. & KHAN,A.A. (2000) Antigenic cross reactivity among the venoms and toxins from unrelated diverse sources. *Toxicon* **38**, 973-980.

LIU,J., ZHANG,M., JIANG,M. & TSENG,G.-N. (2002) Structural and functional role of the extracellular s5-p linker in the HERG potassium channel. *J. Gen. Physiol* **120**, 723-737.

LOMIZE,A.L., MAIOROV,V.N. & ARSENIIEV,A.S. (1991) Determination of the spatial structure of insectotoxin 15A from *Buthus eupeus* by ¹H-NMR spectroscopy data. *Bioorgan. Khim.* **17**, 1613-1632.

LORET,E., SAMPIERI,F., ROUSSEL,A., GRANIER,C. & ROCHAT,H. (1990) Conformational flexibility of a scorpion toxin active on mammals and insects: a circular dichromism study. *J. Biol. Chem.* **263**, 1542-1548.

LORET,E.P., MARTIN-EAUCLAIRE,M.-F., MANSUELLE,P., SAMPIERI,F., GRANIER,C. & ROCHAT,H. (1991) An anti-insect toxin purified from the scorpion *Androctonus australis Hector* also acts on the alpha- and beta-sites of the mammalian sodium channel: sequence and circular dichroism study. *Biochemistry (Mosc)*. **30**, 633-640.

LOUSSOUARN,G., ROSE,T. & NICHOLS,C.G. (2002) Structural basis of inward rectifying potassium channel gating. *Trends Cardiovasc. Med.* **12**, 253-258.

LOWY,P.H., SARMIENTO,L. & MITCHELL,H.K. (1971) Polypeptides minimine and melittin from bee venom: effects on *Drosophila*. *Arch. Biochem. Biophys.* **145**, 338-343.

LUBKE,K., MATTHES,S. & KLOSS,G. (1971) Isolation and structure of N 1 -formyl melittin. *Experientia* **27**, 765-767.

LUCCHESI,K., RAVINDRAN,A., YOUNG,H. & MOCZYDLOWSKI,E. (1989) Analysis of the blocking activity of charybdotoxin homologs and iodinated derivatives against Ca^{2+} -activated K^{+} channels. *Journal of Membrane Biology* **109**, 269-281.

LYONS,S.A., O'NEAL,J. & SONTHEIMER,H. (2002) Chlorotoxin, a scorpion-derived peptide, specifically binds to gliomas and tumors of neuroectodermal origin. *Glia* **39**, 162-173.

MACKINNON,R. & MILLER,C. (1989) Mutant potassium channels with altered binding of charybdotoxin, a pore-blocking potassium channel inhibitor. *Science* **245**, 1382-1385.

MACKINNON,R. (1991) Determination of the subunit stoichiometry of a voltage-activated potassium channel. *Nature* **350**, 232-235.

MACKINNON,R. (2003) Potassium channels. *FEBS Lett.* **555**, 62-65.

MAERTENS,C., WELL., TYTGAT,J., DROOGMANS,G. & NILIUS,B. (2000) Chlorotoxin does not inhibit volume-regulated, calcium-activated and cyclic AMP-activated chloride channels. *British Journal of Pharmacology* **129**, 791-801.

MAHADEVAN,S. (2000) Scorpion sting. *Indian Pediatrics* **2000**, 504-514.

MAHER,A.D. & KUCHEL,P.W. (2003) The Gardos channel: a review of the Ca^{2+} -activated K^{+} channel in human erythrocytes. *International Journal of Biochemistry & Cell Biology* **35**, 1182-1197.

MANGUBAT,E.Z., TSENG,T.T. & JACOBSSON,E. (2003) Phylogenetic analyses of potassium channel auxiliary subunits. *J. Mol. Microbiol. Biotechnol.* **5**, 216-224.

- MARQUEZE,B., SEAGAR,M.J. & COURAUD,F. (1987) Photoaffinity labelling of the K⁺ -channel - associated apamin-binding molecule in smooth muscle, liver and heart membranes. *European Journal of Biochemistry* **209**, 295-298.
- MARSHALL,D.L., VATANPOUR,H., HARVEY,A.L., BOYOT,P., PINKASFELD,S., DOLJANSKY,Y., BOUET,F. & MENEZ,A. (1994) Neuromuscular effects of some potassium channel blocking toxins from the venom of the scorpion *Leiurus quinquestriatus hebreus*. *Toxicon* **32**, 1433-1443.
- MARTIN-EAUCLAIRE,M.-F., ROCHAT,H., MARCHOT,P. & BOUGIS,P.E. (1987) Use of high performance liquid chromatography to demonstrate quantitative variation in components of venom from the scorpion *Androctonus australis* Hector. *Toxicon* **25**, 569-573.
- MARTIN-EAUCLAIRE,M.-F. & ROCHAT,H. (2000) Purification and characterisation of scorpion toxins acting on voltage-sensitive Na⁺ channels. In: *Methods and Tools in Biosciences and Medicine. Animal Toxins*. (Ed. H.Rochat & M.-F.Martin-Eauclaire). Birkhauser, Basel.
- MARTIN,M.F. & ROCHAT,C. (1986) Large scale purification of the venom from the scorpion *Androctonus australis* Hector. *Toxicon* **24**, 1131-1139.
- MARTIN,M.F., ROCHAT,H., MARCHOT,P. & BOUGIS,P.E. (1987) Use of high performance liquid chromatography to demonstrate quantitative variation in components of venom from the scorpion *Androctonus australis* hector. *Toxicon* **25**, 569-573.
- MARTINEZ,A. & TRESTON,A.M. (1996) Where does amidation take place? *Molecular and Cellular Endocrinology* **123**, 117.
- MASSENSINI,A.R., SUCKLING,J., BRAMMER,M.J., MORAES-SANTOS,T., GOMEZ,M.V. & ROMANO-SILVA,M.A. (2002) Tracking sodium channels in live cells: confocal imaging using fluorescently labeled toxins. *Journal of Neuroscience Methods* **116**, 189-196.
- MATSUMARA,Y., UCHIDA,S., KONDO,Y., MIYAZAKI,H., KO,S.B.H., HAYAMA,A., MORIMOTO,T., LIU,W., ARISAWA,M., SASAKI,S. & MARUMO,F. (1999) Overt nephrogenic diabetes insipidus in mice lacking the CLC-K1 chloride channel. *Nature Genetics* **21**, 95-98.
- MAYLIE,J., BOND,C.T., HERSON,P.S., LEE,W.S. & ADELMAN,J.P. (2004) Small conductance Ca²⁺ - activated K⁺ channels and calmodulin. *J. Physiol.* **554**, 255-261.
- MCAULEY,D.F. & ELBORN,J.S. (2000) Cystic fibrosis: basic science. *Paediatric Respiratory Reviews* **1**, 93-100.
- MCDONALD,N.Q. & HENDRICKSON,W.A. (1993) A structural superfamily of growth factors containing a cystine knot motif. *Cell* **73**, 421-424.
- MCINTOSH,J.M. & JONES,R.M. (2001) Cone venom - from accidental stings to deliberate injection. *Toxicon* **39**, 1447-1451.

MCKLESKEY,E.W. (1994) Calcium channels: cellular roles and molecular mechanisms. *Current Opinion in Neurobiology* 4, 304-312.

MCMANUS,O.B., HELMS,L.M.H., PALLANCK,L., GANETZKY,B., SWANSON,R. & LOENARD,R.J. (1995) Functional role of the β subunit of high conductance calcium-activated potassium channels. *Neuron* 14, 645-650.

MEECH,R.W. & STRUMWASSER,F. (1970) Intracellular calcium injection activates potassium conductance in *Aplysia* nerve cells. *Federation Proceedings* 29, 834-836.

MEIER,J. (1986) Individual and age-dependent variations in the venom of the fer-de-lance *Bothrops atrox*. *Toxicon* 24, 41-46.

MEKIA,A., NASSAR,A.Y. & ROCHAT,H. (1995) A bradykinin-potentiating peptide (peptide K₁₂) isolated from the venom of Egyptian scorpion *Buthus occitanus*. *Peptides* 16, 1359-1365.

MENDOZA,C.E., BHATTI,T. & BHATTI,A.R. (1992) Electrophoretic analysis of snake venoms. *Journal of Chromatography* 580, 355-363.

MESSIER,C., MOURRE,C., BONTEMPI,B., SIF,J., LAZDUNSKI,M. & DESTRADE,C. (1991) Effect of apamin, a toxin that inhibits Ca²⁺-dependent K⁺ channels, on learning and memory processes. *Brain Res.* 551, 322-326.

MILLER,C. (1995) The charybdotoxin family of K⁺ channel-blocking peptides. *Neuron* 15, 5-10.

MILLER,C. (2000) Ion channels: doing hard chemistry with hard ions. *Current Opinion in Chemical Biology* 4, 148-151.

MIRANDA,F., KOPEYAN,C., ROCHAT,H., ROCHAT,C. & LISSITZKY,S. (1970) Purification of animal neurotoxins. Isolation and characterisation of 11 neurotoxins from the venoms of the scorpion *Androctonus australis* Hector, *Buthus occitanus tunetanus* and *Leiurus quinquestriatus quinquestriatus*. *European Journal of Biochemistry* 16, 514-523.

MITRA,A., CHAKRABARTI,J., CHATTOPADHYAY,N. & CHATTERJEE,A. (2003) Membrane-associated MMP-2 in human cervical cancer. *J. Environ. Pathol. Toxicol. Oncol.* 22, 93-100.

MOERMAN,L., BOSTEELS,S., NOPPE,W., WILLEMS,J., CLYNEN,E., SCHOOF,S., L., THEVISSSEN,K., TYTGAT,J., VAN ELDERE,J., VAN DER WALT,J. & VERDONCK,F. (2002) Antibacterial and antifungal properties of α -helical, cationic peptides in the venom of scorpions from southern Africa. *European Journal of Biochemistry* 269, 4799-4810.

MONTIEL,C., LOPEZ,M.G., SANCHEZ-GARCIA,P., MAROTO,R., ZAPATER,P. & GARCIA,A.G. (1995) Contribution of SK and BK channels in the control of catecholamine release by electrical stimulation of the cat adrenal gland. *Journal of Physiology (London)* 486, 427-437.

- MOOS,M.J., NGUYEN,N.Y. & LIU,T.Y. (1988) Reproducible high yield sequencing of proteins electrophoretically separated and transferred to an inert support. *Journal of Biological Chemistry* **263**, 6005-6008.
- MOSBAH,A., KHARRAT,R., FAJLOUN,Z., RENISIO,J.-G., BLANC,E., SABATIER,J.-M., EL AYEB,M. & DARBON,H. (2000) A new fold in the scorpion toxin family, associated with an activity on a ryanodine-sensitive calcium channel. *Proteins* **40**, 436-442.
- MOSKOWITZ,H., HERRMANN,R., JONES,A.D. & HAMMOCK,B.D. (1998) A depressant insect-selective toxin analog from the venom of the scorpion *Leiurus quinquestriatus hebraeus* - purification and structure/function characterization. *Eur. J. Biochem.* **254**, 44-49.
- MOURRE,C., HUGUES,M. & LAZDUNSKI,M. (1986) Quantitative autoradiographic mapping in rat brain of the receptor of apamin, a polypeptide toxin specific for one class of Ca²⁺-dependant K⁺ channels. *Brain Res.* **382**, 239-249.
- MULLEY,J.C., SCHEFFER,I.E., PETROU,S. & BERKOVIC,S.F. (2003) Channelopathies as a genetic cause of epilepsy. *Current Opinion in Neurobiology* **16**, 171-176.
- MURTHY,K.R.K. & HOSSEIN,Z. (1986) Increased osmotic fragility of red cells after incubation at 37 degrees C for 24 hr in dogs with acute myocarditis produced by scorpion (*Buthus tamulus*) venom. *Indian Journal of Experimental Biology* **24**, 464-467.
- MURTHY,K.R.K., HOSSEIN,Z. & MEDH,J.D. (1988) Disseminated intravascular coagulation and disturbances in carbohydrate and fat metabolism in acute myocarditis produced by Indian red scorpion (*Buthus tamulus*) venom. *Indian Journal of Medical Research* **87**, 318-325.
- MURTHY,K.R.K. & MEDH,J.D. (1989) Acute pancreatitis and reduction of H⁺ ion concentration in gastric secretions in experimental acute myocarditis produced by Indian red scorpion, *Buthus tamulus*, venom. *Indian Journal of Experimental Biology* **27**, 242-244.
- MURTHY,K.R.K., SHENOI,R. & VAIDYNATHAN,P. (1991) Insulin reverses haemodynamic changes and pulmonary oedema in children stung by Indian red scorpion *Mesobuthus tamulus*, tamulus concanesis, Pocock. *Ann. Trop. Med. Parasitol.* **85**, 651-657.
- NABHANI,T., ZHU,X., SIMEONI,I., SORRENTINO,V., VALDIVIA,H.H. & GARCIA,J. (2002) Imperatoxin A enhances Ca²⁺ release in developing skeletal muscle containing ryanodine receptor type 3. *Biophysical Journal* **82**, 1319-1328.
- NAIR,R.B. & KURUP,P.A. (1975) Investigations on the venom of the South Indian scorpion *Heterometrus scaber*. *Biochim. Biophys. Acta* **381**, 165-174.
- NELSON,D.A. & O'CONNOR,R. (1968) The venom of the honeybee (*Apis mellifera*): free amino acids and peptides. *Can. J. Biochem.* **46**, 1221-1226.

- NEWBOULD,B.B. (1963) Chemotherapy of arthritis induced in rats by mycobacterial adjuvant. *British Journal of Pharmacology* **21**, 127-136.
- NIRTHANAN,S., JOSEPH,J.S., GOPALAKRISHNAKONE,P., KHOO,H.E., CHEAH,L.S. & GWEE,M.C.E. (2002) Biochemical and pharmacological characterization of the venom of the black scorpion *Heterometrus spinifer*. *Biochemical pharmacology* **63**, 49-55.
- NISHIKAWA,A.K., CARICATI,C.P., LIMA,M.L.S.R., DOS SANTOS,M.C., KIPNIS,T.I., EICKSTEDT,V.R., KNYSAK,I., DA SILVA,M.H., HIGASHI,H.O. & DIAS DA SILVA,W. (1994) Antigenic cross-reactivity among the venoms from several species of Brazilian scorpions. *Toxicon* **32**, 989-998.
- NODA,M., SHIMIZU,S., TANABE,T., TAKAI,T., KAYANO,T., IKEDA,T., TAKAHASHI,H., NAKAYAMA,H., KANAOKA,Y., MINAMINO,N., KANGAWA,K., MATSUO,H., RAFTERY,M.A., HIROSE,T., INAYAMA,S., HAYAHIDA,H., MIYATA,T. & NUMA,S. (1984) Primary structure of *Electrophorus electricus* sodium channel deduced from cDNA sequence. *Nature* **312**, 121-127.
- NODA,M., IKEDA,T., SUZUKI,H., TAKESHIMA,H., TAKAHASHI,H., KUNO,M. & NUMA,S. (1986) Expression of functional sodium channels from cloned cDNA. *Nature* **322**, 826-828.
- OLAMENDI-PORTUGAL,T., GARCIA,B.I., LOPEZ-GONZALEZ,I., VAN DER WALT,J., DYASON,K., ULENS,C., TYTGAT,J., FELIX,R., DARSZON,A. & POSSANI,L.D. (2002) Two new scorpion toxins that target voltage-gated Ca²⁺ and Na²⁺ channels. *Biochemical and Biophysical Research Communications*. **299**, 562-568.
- OTERO,R., FURTADO,M.F., GONCALVES,C., NUNEZ,V., GARCIA,M.E., OSORIO,R.G., ROMERO,M. & GUTIERREZ,J.M. (1998) Comparative study of the venoms of three subspecies of *Lachesis muta* (bushmaster) from Brazil, Colombia and Costa Rica. *Toxicon* **36**, 2021-2027.
- OVCHINNIKOV,Y.A., MIROSHNIKOV,A.I., KUDELIN,I.A., KOSTINA,M.B., BOIKOV,V.A., MAGAZANIK,L.G. & GOTGILF,I.M. (1980) Structure and presynaptic activity of tertiapin-neurotoxin from bee venom *Apis mellifera*. *Bioorgan. Khim.* **6**, 359-365.
- OVCHINNIKOV,Y.A. (1984) Bioorganic chemistry of polypeptide neurotoxins. *Pure and Appl. Chem.* **56**, 1049-1068.
- OWEN,D.G. (1971) Insect venoms: identification of dopamine and noradrenaline in wasp and bee stings. *Experientia* **27**, 544-545.
- OWEN,D.G. & BRIDGES,A.R. (1982) Catecholamines in honey bee (*Apis mellifera* L.) and various vespid (Hymenoptera) venoms. *Toxicon* **20**, 1075-1084.
- OWEN,M.D. & SLOLEY,B.D. (1988) 5-Hydroxytryptamine in the venom of the honey bee (*Apis mellifera*): variation with season and with insect age. *Toxicon* **26**, 577-581.

- PALLAGHY,P.K., NIELSEN,K.J., CRAIK,D.J. & NORTON,R.S. (1994) A common structural motif incorporating a cystine knot and a triple-stranded beta-sheet in toxic and inhibitory polypeptides. *Protein Sci.* **3**, 1833-1839.
- PANCHUK-VOLOSHINA,N., HAUGLAND,R.P., BISHOP-STEWART,J., BHALGAT,M.K., MILLARD,P.J., MAO,F., LEUNG,W.-Y. & HAUGHLAND,R.P. (1999) Alexa dyes, a series of new fluorescent dyes that yield exceptionally bright, photostable conjugates. *Journal of Histochemistry and Cytochemistry* **47**, 1179-1188.
- PARDO-LOPEZ,L., ZHANG,M., LIU,J., JIANG,M., POSSANI,L.D. & TSENG,G.-N. (2002) Mapping the binding site of a Human *ether-a-go-go*-related gene-specific peptide toxin (ErgTx) to the channel's outer vestibule. *Journal of Biological Chemistry* **277**, 16403-16411.
- PARDO-LOPEZ,L., GARCIA-VALDES,J., GURROLA,G.B., ROBERTSON,G.A. & POSSANI,L.D. (2002a) Mapping the receptor site for ergtoxin, a specific blocker of ERG channels. *FEBS Lett.* **510**, 45-49.
- PARK,C.S. & MILLER,C. (1992) Interaction of charybdotoxin with permeant ions inside the pore of a K⁺ channel. *Neuron* **9**, 307-313.
- PATEL,A.J., LAZDUNSKI,M. & HONORE,E. (2001) Lipid and mechano-gated 2P domain K⁺ channels. *Current Opinion in Cell Biology* **13**, 422-427.
- PATTON,D.E., ISOM,L., CATTERALL,W.A. & GOLDIN,A.L. (1994) The adult rat brain β_1 subunit modifies activation and inactivation gating of multiple sodium channel α subunits. *Journal of Biological Chemistry* **269**, 17649-17655.
- PAULL,B.R., YUNGINGER,J.W. & GLEICH,G.J. (1977) Melittin: an allergen of honeybee venom. *J Allergy Clin. Immunol* **59**, 334-338.
- PAURON,D., BARHANIN,J. & LAZDUNSKI,M. (1985) The voltage-dependent sodium channel of insect nervous system identified by receptor sites for tetrodotoxin and scorpion and sea anemone toxins. *Biochem. Biophys. Res. Commun.* **131**, 1226-1233.
- PEASE,J.H.B. & WEMMER,D. (1988) Solution structure of apamin determined by nuclear magnetic resonance and distance geometry. *Biochemistry (Mosc).* **27**, 8491-8498.
- PEDARZANI,P., D'HOEDT,D., DOORTY,K.B., WADSWORTH,J.D.F., JOSEPH,J.S., JEYASEELAN,K., KINIR,M., GADRE,S.V., SAPATNEKAR,S.M., STOCKER,M. & STRONG,P.N. (2002) Tamapin, a venom peptide from the Indian red scorpion (*Mesobuthus tamulus*) that targets small conductance Ca²⁺-activated K⁺ channels and afterhyperpolarization currents in central neurons. *Journal of Biological Chemistry* **277**, 46101-46109.

- PEGORARO,S., FIORI,S., CRAMER,J., RUDOLPH-BOHNER,S. & MORODER,L. (1999) The disulphide-coupled folding pathway of apamin as derived from diselenide-quenched analogs and intermediates. *Protein Science* **8**, 1605-1613.
- PELHATE,M. & ZLOTKIN,E. (1982) Voltage dependent slowing of the turn off of Na⁺ current in the cockroach giant axon induced by the scorpion venom 'insect toxin'. *J. Physiol. (Lond.)* **535**, 100-109.
- PESSINI,A.C., TAKAO,T.T., CAVALHEIRO,E.C., VICHNEWSKI,W., SAMPAIO,S., V, GIGLIO,J.R. & ARANTES,E.C. (2001) A hyaluronidase from *Tityus serrulatus* scorpion venom: isolation, characterization and inhibition by flavonoids. *Toxicon* **39**, 1495-1504.
- PIETROBON,D. (2002) Calcium channels and channelopathies of the central nervous system. *Mol. Neurobiol.* **25**, 31-50.
- PIMENTA,A.M., STOCKLIN,R., FAVREAU,P., BOUGIS,P.E. & MARTIN-EAUCCLAIRE,M.-F. (2001) Moving pieces in a proteomic puzzle: mass fingerprinting of toxic fractions from the venom of *Tityus serrulatus* (scorpiones, Buthiod). *Rapid communications in mass spectrometry* **15**, 1562-1572.
- PIMENTA,A.M., ALMEIDA,F.M., DE LIMA,M.E., MARTIN-EAUCCLAIRE,M.-F. & BOUGIS,P.E. (2003) Individual variability in *Tityus serrulatus* (Scorpiones, Buthidae) venom elicited by matrix-assisted laser desorption/ ionization time-of-flight mass spectrometry. *Rapid communications in mass spectrometry* **17**, 413-418.
- PIVETTI,C.D., YEN,M.R., MILLER,S., BUSCH,W., TSENG,Y.H., BOOTH,I.R. & SAIER,M.H. (2003) Two families of mechanosensitive channel proteins. *Microbiology and molecular biology reviews* **67**, 66-85.
- PONGS,O. (1992) Molecular biology of voltage-dependent potassium channels. *Physiological Reviews* **72**, S69-S88.
- POSSANI,L.D., MARTIN,B.M., MOCHEA-MORALES,J. & SVENDENSEN,I. (1981) Purification and chemical characterization of the major toxins in the venom of the Brazilian scorpion *Tityus serrulatus* Lutz and Mello. *Carlsberg Res. Commun.* **46**, 195-205.
- POSSANI,L.D., MARTIN,B.M. & SVENDENSEN,I. (1982) The primary structure of noxiustoxin: a K⁺ channel blocking peptide, purified from the venom of the scorpion *Centruroides noxius hoffmann*. *Carlsberg Res. Commun.* **47**, 285-289.
- POSSANI,L.D., BECERRIL,B., DELEPIERRE,M. & TYTGAT,J. (1999) Scorpion toxins specific for Na⁺ channels. *European Journal of Biochemistry* **264**, 287-300.
- POSSANI,L.D., MERINO,E., CORONA,M., BOLIVAR,F. & BECERRIL,B. (2000) Peptides and genes coding for scorpion toxins that effect ion-channels. *Biochimie* **82**, 861-868.
- POSSANI,L.D., CORONA,M., ZURITA,M. & RODRIGUEZ,M.H. (2002) From noxiustoxin to scorpione and possible transgenic mosquitoes resistant to malaria. *Archives of Medical Research* **33**, 398-404.

PRAGL,B., KOSCHAK,A., TRIEB,M., OBERMAIR,G., KAUFMANN,W.A., GERSTER,U., BLANC,E., HAHN,C., PRINZ,H., SCHUTZ,G., DARBON,H., GRUBER,H.J. & KNAUS,H.G. (2002) Synthesis, characterization, and application of Cy-dye- and Alexa-dye-labeled Hongotoxin₁ analogues. The first high affinity fluorescence probes for voltage-gated K⁺ channels. *Bioconjugate Chem.* **13**, 416-425.

PRASAD,N.B., UMA,B., BHATT,S.K., GOWDA,V.T. & GOWDA,V.T. (1999) Comparative characterisation of Russell's viper (*Daboia/Vipera russelli*) venoms from different regions of the Indian peninsula. *Biochim. Biophys. Acta* **1428**, 121-136.

PUSCH,M. (2002) Myotonia caused by mutations in the muscle chloride channel gene CLCN1. *Hum. Mutat.* **19**, 423-434.

QU,Y., LIANG,S., DING,J., LIU,X., ZHANG,R. & GU,X. (1997) Proton nuclear magnetic resonance studies on huwentoxin-I from the venom of the spider *Selenocosmia huwena*: 2. Three-dimensional structure in solution. *J. Protein Chem.* **16**, 565-574.

RAJENDRA,S., LYNCH,J.W. & SCHOFIELD,P.R. (1997) The glycine receptor. *Pharmac. Ther.* **73**, 121-146.

RAMACHANDRAN,L.K., AGARWAL,O.P., ACHYUTHAN,K.E., CHAUDHURY,L., VEDASIROMANI,J.R. & GANGULY,D.K. (1986) Fractionation and biological activities of venoms of the Indian scorpions *Buthus tamulus* and *Heterometrus bengalensis*. *Indian Journal of Biochemistry & Biophysics* **23**, 355-358.

RAMALINGAM,K. & SNYDER,G.H. (1993) Selective disulphide formation in truncated apamin and sarafotoxin. *Biochemistry (Mosc)*. **32**, 11155-11161.

RAMANAIAH,M., PARTHASARATHY,P.R. & VENKAIAH,B. (1990) Purification and properties of phospholipase A₂ from the venom of scorpion, (*Heterometrus fulvipes*). *Biochemistry International* **20**, 931-940.

RAMANAIAH,M., PARTHASARATHY,P.R. & VENKAIAH,B. (1990a) Isolation and characterisation of hyaluronidase from scorpion (*Heterometrus fulvipes*) venom. *Biochemistry International* **20**, 301-310.

RAPPUOLI,R. & MONTECUCCO,C. (1997) *Guidebook to Protein Toxins and Their Use in Cell Biology*. Sambrook and Tooze, Oxford.

RASH,L.D., KING,R.G. & HODGSON,W.C. (2000) Sex differences in the pharmacological activity of venom from the white-tailed spider (*Lampona cylindrata*). *Toxicon* **38**, 1111-1127.

RATJEN,F. & DORING,G. (2003) Cystic fibrosis. *Lancet* **361**, 681-689.

RAUFMAN,J.P. (1996) Bioactive peptides from lizard venoms. *Regulatory Peptides* **61**, 1-18.

- RAYNOR,R.L., ZHENG,B. & KUO,J.F. (1991) Membrane interactions of amphiphilic polypeptides mastoparan, melittin, polymyxin B, and cardiotoxin. Differential inhibition of protein kinase C, Ca²⁺/calmodulin-dependent protein kinase II and synaptosomal membrane Na,K-ATPase, and Na⁺ pump and differentiation of HL60 cells. *J. Biol. Chem.* **266**, 2753-2758.
- REDFERN,W.S., CARLSSON,L., DAVIES,A.S., LYNCH,W.G., MACKENZIE,I., PALETHORPE,S., SIEGL,P.K.S., STRANG,I., SULLIVAN,A.T., WALLIS,R., CAMM,A.J. & HAMMOND,T.G. (2003) Relationships between preclinical cardiac electrophysiology, clinical Qt interval prolongation and torsade de pointes for a broad range of drugs: evidence for a provisional safety margin in drug development. *Cardiovascular research* **58**, 32-45.
- REIMANN,F. & ASHCROFT,F.M. (1999) Inwardly rectifying potassium channels. *Current Opinion in Cell Biology* **11**, 503-508.
- REINHARDT,R., BRIDGES,R.J., RUMMEL,W. & LINDEMANN,B. (1987) Properties of an anion-selective channel from rat colonic enterocyte plasma membranes reconstituted into planer phospholipid bilayers. *Journal of Membrane Biology* **95**, 47-54.
- REN,D., NAVARRO,B., PEREZ,G., JACKSON,A.C., HSU,S., SHI,Q., TILLY,J.L. & CLAPHAM,D.E. (2001) A sperm ion channel required for sperm motility and male fertility. *Nature* **413**, 603-609.
- RIORDAN,J.R., ROMMENS,J.M., KEREM,B., ALON,N., ROZMAHEL,R., GRZELCZAK,Z., ZIELENSKI,J., LOK,S., PLAUSIC,N. & CHOU,J. (1989) Identification of the cystic fibrosis gene: cloning and characterization of complementary DNA. *Science* **245**, 1066-1073.
- ROBBINS,J. (2001) KCNQ potassium channels: physiology, pathophysiology, and pharmacology. *Pharmacol. Ther.* **90**, 1-19.
- ROBERTSON,B. (1997) The real life of voltage-gated K⁺ channels: more than model behaviour. *Trends in Pharmacological Sciences* **18**, 474-482.
- ROCHAT,H., BERNARD,P. & COURAUD,F. (1979) Scorpion toxins: chemistry and mode of action. *Advances in Cytopharmacology* **3**, 325-334.
- RODA,A., GIOACCHINI,A.M., SERAGLIA,R., MONTAGNANI,M., BARALDINI,M., PEDRAZZINI,S., PURICALLI,M. & TRALDI,P. (1997) A comparison of the analytical performance of sodium dodecyl sulfate-polyacrylamide gel electrophoresis, electrospray and matrix-assisted laser desorption/ionization mass spectrometry in the study of the protein extract from *Bothrops jaraca* snake venom. *Rapid communications in mass spectrometry* **11**, 1297-1302.
- RODRIGUEZ DE LA VEGA,R.C., MERINO,E., BECERRIL,B. & POSSANI,L.D. (2003) Novel interactions between K⁺ channels and scorpion toxins. *Trends in Pharmacological Sciences* **24**, 222-227.
- RODRIGUEZ DE LA VEGA,R.C. & POSSANI,L.D. (2004) Current views on scorpion toxins specific for K⁺-channels. *Toxicon* **43**, 865-875.

- ROGERS,J.C., QU,Y., TANADA,T.N., SCHEUER,T. & CATTERALL,W.A. (1996) Molecular determinants of high affinity binding of alpha-scorpion toxin and sea anemone toxin in the S3-S4 extracellular loop in domain IV of the Na⁺ channel alpha subunit. *Journal of Biological Chemistry* **1996**, 15950-15962.
- ROGOWSKI,R.S., KRUEGER,B.K., COLLINS,J.H. & BLAUSTEIN,M.P. (1994) Tityustoxin K alpha blocks voltage-gated noninactivating K⁺ channels and unblocks inactivating K⁺ channels blocked by alpha-dendrotoxin in synaptosomes. *Proc. Natl. Acad. Sci* **91**, 1475-1479.
- ROMI-LEBRUN,R., MARTIN-EAUCCLAIRE,M.-F., ESCOUBAS,P., WU,F.Q., LEBRUN,B., HISADA,M. & NAKAJIMA,T. (1997) Characterization of four toxins from *Buthus martensi* scorpion venom, which act on apamin-sensitive Ca²⁺-activated K⁺ channels. *European Journal of Biochemistry* **245**, 457-464.
- ROSENBLATT,K.P., SUN,Z.-P., HELLER,S. & HUDSPETH,A.J. (1997) Distribution of Ca²⁺-activated K⁺ channel isoforms along the tonographic gradient of the chickens cochlea. *Neuron* **19**, 1061-1075.
- ROSSO,J.P. & ROCHAT,H. (1985) Characterization of ten proteins from the venom of the Moroccan scorpion *Androctonus mauretanicus mauretanicus*, six of which are toxic to the mouse. *Toxicon* **23**, 113-125.
- ROWAN,E.G. & HARVEY,A.L. (1996) Toxins affecting K⁺ channels. *Braz. J. Med. Biol. Res.* **29**, 1765-1780.
- RUBIN,B.K. (2003) Cystic fibrosis: bench to bedside 2003. *Can. Respir. J.* **10**, 161-164.
- SABATIER,J.-M., ZERROUK,H., DARBON,H., MABROUK,K., BENSLIMANE,A., ROCHAT,H. & MARTIN-EAUCCLAIRE,M.-F. (1993) P05, a new Leiurotoxin I-like scorpion toxin: synthesis and structure-activity relationships of the α -amidated analog, a ligand of Ca²⁺ - activated K⁺ channels with increased affinity. *Biochemistry (Mosc)*. **32**, 2763-2770.
- SABATIER,J.-M., FREMONT,V., MABROUK,K., CREST,M., DARBON,H., ROCHAT,H., VAN RIETSCHOTEN,J. & MARTIN-EAUCCLAIRE,M.-F. (1994) Leiurotoxin I, a scorpion toxin specific for Ca²⁺-activated K⁺ channels. *Int. J. Peptide. Protein. Res.* **43**, 486-495.
- SABATIER,J.-M., LECOMTE,C., MABROUK,K., DARBON,H., OUGHIDENI,R., CANARELLI,S., ROCHAT,H. & MARTIN-EAUCCLAIRE,M.-F. (1996) Synthesis and characterization of Leiurotoxin I analogs lacking one disulphide bridge: Evidence that disulphide pairing 3-21 is not required for full toxin activity. *Biochemistry (Mosc)*. **35**, 10641-10647.
- SALBAUM,J.M., CIRELLI,C., WALCOTT,E., KRUSHEL,L.A., EDELMAN,G.M. & TONONI,G. (2004) Chlorotoxin-mediated disinhibition of noradrenergic locus coeruleus neurons using a conditional transgenic approach. *Brain Res.* **1016**, 20-32.

- SAMSO,M., TRUJILLO,R., GURROLA,G.B. & VALDIVIA,H.H. (1999) Three-dimensional location of the imperatoxin A binding site on the ryanodine receptor. *Journal of Cell Biology* **146**, 493-499.
- SANDBERG,B.E.B. & RAGNARSSON,U. (1978) Solid phase synthesis of apamin, the principal neurotoxin in bee venom. Isolation and characterization of acetamidomethyl apamin. *Int. J. Peptide. Protein. Res.* **11**, 238-245.
- SANGER,F., NICKLEN,S. & COULSON,A.R. (1977) DNA sequencing with chain-terminating inhibitors. *Proc. Natl. Acad. Sci* **74**, 5463-5467.
- SATHER,W.A., YANG,J. & TSIEN,R.W. (1994) Structural basis of ion channel permeation. *Current Opinion in Neurobiology* **4**, 313-323.
- SAUTIERE,P., CESTELES,S., KOPEYAN,C., MARTINAGE,A., DROBECQ,H., DOLJANSKY,Y. & GORDON,D. (1998) New toxins acting on sodium channels from the scorpion *Leiurus quinquestriatus hebraeus* suggest a clue to mammalian vs insect selectivity. *Toxicon* **36**, 1141-1154.
- SCHACHTMAN,D.P. (2000) Molecular insights into the structure and function of plant K⁺ transport mechanisms. *Biochim. Biophys. Acta* **1465**, 127-139.
- SCHAEGER,H. & VON JAGOW,G. (1987) Tricine-sodium dodecyl sulphate-polyacrylamide gel electrophoresis for the separation of proteins in the range from 1-100 KDa. *Analytical Biochemistry* **166**, 368-379.
- SCHMID-ANTOMARCHI,H., HUGUES,M., NORMAN,R., ELLORY,C., BORSOTTO,M. & LAZDUNSKI,M. (1984) Molecular properties of the apamin-binding component of the Ca²⁺-dependent K⁺ channel: Radiation-inactivation, affinity labelling and solubilisation. *European Journal of Biochemistry* **142**, 1-6.
- SCHMID-ANTOMARCHI,H., HUGUES,M. & LAZDUNSKI,M. (1986) Properties of the apamin-sensitive Ca²⁺-activated K⁺ channel in PC12 pheochromocytoma cells which hyper-produce the apamin receptor. *Journal of Biological Chemistry* **261**, 8633-8637.
- SEAGAR,M.J., GRANIER,C. & COURAUD,F. (1984) Interactions of the neurotoxin apamin with a Ca²⁺-activated K⁺ channel in primary neuronal cultures. *Journal of Biological Chemistry* **259**, 1491-1495.
- SEAGAR,M.J., MARQUEZE,B. & COURAUD,F. (1987) Solubilisation of apamin receptor associated with a calcium-activated potassium channel from rat brain. *Journal of Neuroscience* **7**, 565-570.
- SEAGAR,M.J., DREPRESZ,P., MARTIN-MOUTOT,N. & COURAUD,F. (1987a) Detection and photoaffinity labelling of the Ca²⁺-activated K⁺ channel associated apamin receptor in cultured astrocytes from rat brain. *Brain Res.* **411**, 226-230.

- SHAKKOTTAI,V.G., REGAYA,I., WULFF,H., FAJLOUN,Z., TOMITA,H., FATHALLAH,M., CAHALAN,M.D., GARGUS,J.J. & SABATIER,J.-M. (2001) Design and characterization of a highly selective peptide inhibitor of the small conductance calcium-activated K⁺ channel, SkCa2. *Journal of Biological Chemistry* **276**, 43145-43151.
- SHALABI,A., ZAMUDIO,F., WU,X., SCALONIA,A., POSSANI,L.D. & VILLERREAL,M.L. (2004) Tetrapandins, a new class of scorpion toxins that specifically inhibit store-operated calcium entry in human embryonic kidney-293 cells. *J. Biol. Chem.* **297**, 1040-1049.
- SHEUMACK,D.D., BALDO,B.A., CARROLL,P.R., HAMPSON,F., HOWDEN,M.E. & SKORULIS,A. (1984) A comparative study of properties and toxic constituents of funnel web spider (*Atrax*) venoms. *Comparative Biochemistry and Physiology Part C* **78**, 55-68.
- SHIEH,C.C., COGHLAN,M., SULLIVAN,J.P. & GOPALAKRISHNAKONE,P. (2000) Potassium channels: Molecular defects,diseases, and therapeutic opportunities. *Pharmacological Reviews* **52**, 557-593.
- SHIPOLINI,R., BRADBURY,A.F., CALLEWAERT,G.L. & VERNON,C.A. (1967) The structure of apamin. *Chem. Commun.* 679-680.
- SHKENDEROV,S. (1974) Anaphylactogenic properties of bee venom and its fractions. *Toxicon* **12**, 529-534.
- SHKENDEROV,S. & KOBUROVA,K. (1979) Changes of noradrenaline, dopamine and serotonin in rat brain following treatment with apamin or melittin. *Toxicon* **17**, 517-519.
- SHKENDEROV,S. & KOBUROVA,K. (1982) Adolapin-a newly isolated analgetic and anti-inflammatory polypeptide from bee venom. *Toxicon* **20**, 317-321.
- SHMUKLER,B.E., BOND,C.T., WILLHELM,S., BRUENING-WRIGHT,A., MAYLIE,J. & ADELMAN,J.P. (2001) Structure and complex transcription pattern of the mouse SK1 K_{Ca} channel gene KCNN1. *Biochim. Biophys. Acta* **1518**, 36-46.
- SIDACH,S. & MINTZ,I.M. (2002) Kurtoxin, a gating modifier of neuronal high- and low- threshold Ca channels. *Journal of Neuroscience* **22**, 2023-2034.
- SIEMEN,D. & VOGEL,W. (1983) Tetrodotoxin interferes with the reaction of scorpion toxin (*Buthus tamulus*) at the sodium channel of the excitable membrane. *Pflugers Archiv: European Journal of Physiology* **397**, 306-311.
- SIMEONI,I., ROSSI,D., ZHU,X., GARCIA,J., VALDIVIA,H.H. & SORRENTINO,V. (2001) Imperatoxin A (IpTx_a) from *Pandinus imperator* stimulates [³H]ryanodine binding to RyR3 channels. *FEBS Lett.* **508**, 5-10.

SMITH,P.K., KROHN,R.I., HERMANSON,G.T., MALLIA,A.K., GARTNER,F.H., PROVENZANO,M.D., FUJIMOTO,E.K., GOEKE,N.M., OLSON,B.J. & KLENK,D.C. (1985) Measurement of protein using bicinchoninic acid. *Analytical Biochemistry* **150**, 76-85.

SOBOTKA,A.K., FRANKLIN,R.M., ADKINSON,N.F., Jr., VALENTINE,M., BAER,H. & LICHTENSTEIN,L.M. (1976) Allergy to insect stings. II. Phospholipase A: the major allergen in honeybee venom. *J Allergy Clin. Immunol* **57**, 29-40.

SOKOL,P.T., ZIAI,M.R. & CHANDRA,M. (1994) Composition for isolating apamin receptors, apamin binding protein, and uses thereof. [Patent 2,101,468]. Canada.

SOROCEANU,L., GILLESPIE,Y., KHAZAEI,M.B. & SONTHEIMER,H. (1998) Use of chlorotoxin for targeting of primary brain tumors. *Cancer Research* **58**, 4871-4879.

SOROCEANU,L., MANNING,T.J.J. & SONTHEIMER,H. (1999) Modulation of glioma cell migration and invasion using Cl⁻ and K⁺ ion channel blockers. *Journal of Neuroscience* **19**, 5942-5954.

SPLAWSKI,I., TIMOTHY,K.W., TATEYAMA,M., CLANCY,C.E., MALHOTRA,A., BEGGS,A.H., CAPPUCIO,F.P., SAGNELLA,G.A., KASS,R.S. & KEATING,M.T. (2002) Variant of SCN5A sodium channel implicated in risk of cardiac arrhythmia. *Science* **297**, 1333-1336.

SPRENGEL,R. & SEEBURG,P.H. (1995) Ionotropic glutamate receptors. In: *Ligand and Voltage*.

SRINIVASAN,J., SCHACHNER,M. & CATTERALL,W.A. (1998) Interaction of voltage-gated sodium channels with the extracellular matrix molecules tenascin-C and tenascin-R. *Proc. Natl. Acad. Sci U. S. A* **95**, 15753-15757.

SRINIVASAN,K.N., GOPALAKRISHNAKONE,P., TAN,P.T., CHEW,K.C., CHENG,B., KINI,R.M., KOH,J.L.Y., SEAH,S.H. & BRUSIC,V. (2001) SCORPION, a molecular database of scorpion toxins. *Toxicon* **40**, 23-31.

SRINIVASAN,K.N., SIVARAJA,V., HUYS,I., SASAKI,T., CHENG,B., KUMAR,T.K.S., SATO,K., TYTGAT,J., YU,C., SAN,B.C.C., RANGANATHAN,S., BOWIE,H.J., KINI,R.M. & GOPALAKRISHNAKONE,P. (2002) κ -Hefutoxin1, a novel toxin from the scorpion *Heterometrus fulvipes* with unique structure and function. *Journal of Biological Chemistry* **277**, 30040-30047.

STEINBORNER,S.T., WABNITZ,P.A., BOWIE,H.J. & TYLER,M.J. (1996) The application of mass spectrometry to the study of evolutionary trends in amphibians. *Rapid communications in mass spectrometry* **10**, 92-95.

STEINLEIN,O.K. & NOEBELS,J.L. (2000) Ion channels and epilepsy in man and mouse. *Current Opinion in Genetics & Development* **10**, 286-291.

STEINLEIN,O.K. (2002) Channelopathies can cause epilepsy in man. *European Journal of Pain* **6**, 27-34.

STOCKER,M. & PEDARZANI,P. (2000) Differential distribution of three Ca²⁺-activated K⁺ subunits, SK1, SK2 and SK3, in the adult rat central nervous system. *Mol. Cell. Neurosci.* **15**, 476-493.

STOCKLIN,R. & SAVOY,L.-A. (1994) On-line LC-ES-MS: a new method for direct analysis of crude venom. *Toxicon* **32**, 408.

STOCKLIN,R., MEBS,D., BOULIAN,J.C., PANCHARD,P.A., VIRELIZIER,H. & GILLARD-FACTOR,C. (2000) Identification of snake species by toxin mass fingerprinting of their venoms. In: *Mass Spectrometry of Proteins and Peptides* (Ed. J.R.Chapman). Humana Press, Totowa, NJ.

STROBAEK,D., JORGENSEN,T.D., CHRISTOPHERSEN,P., AHRING,P.K. & OLESEN,S.-P. (2000) Pharmacological characterisation of small-conductance Ca²⁺-activated K⁺ channels stably expressed in HEK 293 cells. *Br. J. Pharmacol.* **129**, 991-999.

STRONG,P.N. & EVANS,W.H. (1987) Receptor-mediated uptake of a toxin which binds to plasma-membrane ion channels. In: *Cells, Membranes, and Disease, Including Renal* (Ed. E.Reid, G.M.W.Cook & J.P.Luzio). Plenum publishing corporation.

STRONG,P.N. & EVANS,W.H. (1987a) Receptor-mediated endocytosis of apamin by liver-cells. *European Journal of Biochemistry* **163**, 267-273.

STRONG,P.N. (1990) Potassium channel toxins. *Pharmac. Ther.* **46**, 137-162.

STRONG,P.N. & BREWSTER,B.S. (1992) Apamin: A probe for small-conductance, calcium-activated potassium channels. *Methods in Neurosciences* **8**, 15-24.

STRONG,P.N. & WADSWORTH,J.D.F. (2000) Pharmacologically active peptides and proteins from bee venom. In: *Animal Toxins* (Ed. H.Rochat & M.-F.Martin-Eauclaire). Birkhauser Verlag, Basel/Switzerland.

STRONG,P.N., CLARK,G.S., ARMUGAM,A., DE-ALLIE,F.A., JOSEPH,J.S., YEMUL,V., DESHPANDE,J.M., KAMUT,R., GADRE,S.V., GOPALAKRISHNAKONE,P., KINI,R.M., OWEN,D.G. & JEYASEELAN,K. (2001) Tamulustoxin: a novel potassium channel blocker from the venom of the Indian red scorpion *Mesobuthus tamulus*. *Archives of Biochemistry and Biophysics* **385**, 138-144.

STUHMER,W., STOCKER,M., SAKMANN,B., SEEBURG,P., BAUMANN,A., GRUPE,A. & PONGS,O. (1988) Potassium channels expressed from rat brain cDNA have delayed rectifier properties. *FEBS Lett.* **242**, 199-206.

SUN,P.D. & DAVIES,D.R. (1995) The cystine-knot growth-factor superfamily. *Annu. Rev. Biophys. Biomol. Struct.* **24**, 269-291.

SUN,S. (1995) A genetic algorithm that seeks native states of peptides and proteins. *Biophysical Journal* **69**, 340-355.

- SUZUKI,R., MIYAZAKI,Y., TAGAKI,K., TORII,K. & TANIGUCHI,H. (2004) Matrix metalloproteinases in the pathogenesis of asthma and COPD: implications for therapy. *Treat. Respir. Med.* **3**, 17-27.
- SWEETMAN,G.M.A., GARNER,G.V. & GORDON,D.B. (1992) Electrospray mass spectrometry of Malayan pit viper (*Calloselasma rhodostoma*) venom. *Rapid communications in mass spectrometry* **6**, 724-726.
- TAKAMORI,M., MARUTA,T. & KOMAI,K. (2000) Lambert-Eaton myasthenic syndrome as an autoimmune calcium-channelopathy. *Neurosci. Res.* **36**, 183-191.
- TAMAOKI,H., KOBAYASHI,M., NISHIMURA,S., OHKUBO,T., KYOGOKU,Y., NAKAJIMA,K., KUMAGAYE,S., KIMURA,S. & SAKAKIBARA,S. (1991) Solution conformation of endothelin determined by means of ¹H-NMR spectroscopy and distance geometry calculations. *Protein Eng* **4**, 509-518.
- TAMAOKI,H., MIURA,R., KUSUNOKI,M., KYOGOKU,Y., KOBAYASHI,Y. & MORODER,L. (1998) Folding motifs induced and stabilized by cystine frameworks. *Protein Eng* **11**, 649-659.
- TARDENT,P. (1997) How do Cnidaria make use of their venomous stinging cells? *Toxicon* **35**, 818.
- TARE,T.G., VAD,N.E. & RENAPURKAR,D.M. (1992) Circadian variation in venom yield by the scorpion *Heterometrus indus* (De Geer). *Med. Vet Entomol.* **6**, 307-308.
- TEJEDOR,F.G. & CATTERALL,W.A. (1988) Site of covalent attachment of α -scorpion toxin derivatives in domain I of the sodium channel α -subunit. *Proc. Natl. Acad. Sci. USA* **85**, 8742-8746.
- TEMPEL,B.L., PAPAZIAN,D.M., SCHWARZ,T.L., JAN,Y.N. & JAN,L.Y. (1987) Sequence of a probable potassium channel component at *Shaker* locus of *Drosophila*. *Science* **237**, 770-775.
- THAKKER,R.V. (2000) Molecular pathology of renal chloride channels in Dent's disease and Bartter's syndrome. *Exp. Nephrol.* **8**, 351-360.
- THOMPOSON,C.H., FIELDS,D.M., HUBBARD,K., ZHANG,Z.R. & MCCARTY,N.A. (2003) Inhibition of ClC-2 by a component of scorpion venom. *J. Gen. Physiol.* **122**, 29a.
- THOMSEN,W.J. & CATTERALL,W.A. (1989) Localization of the receptor site for α -scorpion toxins by antibody mapping: implications for sodium channel topology. *Proc. Natl. Acad. Sci. USA* **86**, 10161-10165.
- TRIMMER,J.S. (1998) Regulation of ion channel expression by cytoplasmic subunits. *Current Opinion in Neurobiology* **8**, 370-374.
- TRIPATHY,A., RESCH,W., XU,L., VALDIVIA,H.H. & MEISSNER,G. (1998) Imperatoxin A induces subconductance states in Ca²⁺ release channels (ryanodine receptors) of cardiac and skeletal muscle. *J. Gen. Physiol* **111**, 679-690.

- TSENG-CRANK,J., FOSTER,C.D. & KRAUSE,J.D. (1994) Cloning, expression, and distribution of functionally distinct Ca²⁺-activated K⁺ channels isoforms from human brain. *Neuron* **13**, 1315-1330.
- TULP,M. & BOHLIN,L. (2004) Unconventional natural sources for future drug discovery. *Drug Discovery Today* **9**, 450-458.
- TYNDALE,R.F., OLSEN,R.W. & TOBIN,A.J. (1995) GABA_A receptors. In: *Ligand and Voltage-Gated Ion Channels* (Ed. R.A.North). CRC press, Florida.
- TYTGAT,J., DEBONT,T., ROSTOLL,K., MULLER,G.J., VERDONCK,F., DAENENS,P., VAN DER WALT,J.J. & POSSANI,L.D. (1998) Purification and partial characterization of a 'short' insectotoxin-like peptide from the venom of the scorpion *Parabuthus schlechteri*. *FEBS Lett.* **441**, 387-391.
- TYTGAT,J., CHANDY,K.G., GARCIA,M.L., GUTMAN,G.A., MARTIN-EAUCLAIRE,M.-F., VAN DER WALT,J.J. & POSSANI,L.D. (1999) A unified nomenclature for short-chain peptides isolated from scorpion venoms: KTx molecular subfamilies. *Trends in Pharmacological Sciences* **20**, 444-447.
- ULLRICH,N., GILLESPIE,G.Y. & SONTHEIMER,H. (1995) Human astrocytoma cells express a unique chloride current. *Neuroreport* **7**, 343-347.
- ULLRICH,N., GILLESPIE,G.Y. & SONTHEIMER,H. (1996) Human astrocytoma cells express a unique chloride current. *Neuroreport* **7**, 1020-1024.
- ULLRICH,N. & SONTHEIMER,H. (1996) Biophysical and pharmacological characterization of chloride currents in human astrocytoma cells. *American Journal of Physiology* **270**, C1511-C1521.
- ULLRICH,N. & SONTHEIMER,H. (1997) Cell cycle-dependent expression of a glioma-specific chloride current: proposed link to cytoskeletal changes. *American Journal of Physiology* **273**, C1290-C1297.
- ULLRICH,N., BORDEY,A., GILLESPIE,G.Y. & SONTHEIMER,H. (1998) Expression of voltage-activated chloride currents in acute slices of human gliomas. *Neuroscience* **83**, 1161-1173.
- ULLRICH,N. & SONTHEIMER,H. (1999) Method of diagnosing and treating gliomas. US1996000774154[Patent US5905027].
- VALDIVIA,H.H., KIRBY,M.S., LEDERER,W.J. & CORANADO,R. (1992) Scorpion toxins targeted against the sarcoplasmic reticulum Ca²⁺-release channel of skeletal and cardiac muscle. *Proc. Natl. Acad. Sci* **89**, 12185-12189.
- VAN DER STAAY,F.J., FANELLI,R.J., BLOKLAND,A. & SCHMIDT,B.H. (1999) Behavioral effects of apamin, a selective inhibitor of the SK_{Ca}-channel, in mice and rats. *Neuroscience and Biobehavioral Reviews* **23**, 1087-1110.
- VASWANI,M. & KAPUR,S. (2001) Genetic basis of schizophrenia: trinucleotide repeats, an update. *Prog. Neuro-Pharmacol. & Biol. Psychiat.* **25**, 1187-1201.

- VERGARA,C., LATORRE,R., MARRION,N.V. & ADELMAN,J.P. (1998) Calcium-activated potassium channels. *Current Opinion in Neurobiology* **8**, 321-329.
- VIJERBERG,H.P.M., PUARON,O. & LAZDUNSKI,M. (1984) The effects of *Tityus serrulatus* scorpion toxin on Na channels in neuroblastoma cells. *Pflugers. Arch.* **401**, 297-303.
- VINCENT,A., JACOBSON,I., PLESTED,P., POLIZZIA,A., TANG,T., RIEMERSMA,S., NEWLAND,C., GHORAZIAN,S., FARRAR,J., MACLENNAN,C., WILLCOX,N., BEESON,D. & NEWSOM-DAVIS,J. (1998) Antibodies affecting ion channel function in acquired neuromyotonia, in seropositive and seronegative myasthenia gravis, and in antibody-mediated arthrogryposis multiplex congenita. *Ann. N Y Acad. Sci.* **841**, 482-496.
- VINCENT,A., BEESON,D. & LANG,B. (2000) Molecular targets for autoimmune and genetic disorders of neuromuscular transmission. *European Journal of Biochemistry* **267**, 6717-6728.
- VINCENT,J.P., SCHWEITZ,H. & LAZDUNSKI,M. (1975) Structure-function relationships and site of action of apamin, a neurotoxic polypeptide of bee venom with an action on the central nervous system. *Biochemistry (Mosc).* **14**, 2521-2525.
- VISSE,R. & NAGASE,H. (2003) Matrix metalloproteinases and tissue inhibitors of metalloproteinases: structure, function, and biochemistry. *Circ. Res.* **92**, 827-839.
- VITA,C., ROUMESTAND,C., TOMA,F. & MENEZ,A. (1995) Scorpion toxins as natural scaffolds for protein engineering. *Proceedings of the National Academy of Sciences USA* **92**, 6404-6408.
- VLASAK,R. & KREIL,G. (1984) Nucleotide sequence of cloned cDNAs coding for preprosecapin, a major product of queen-bee venom glands. *Eur. J. Biochem.* **145**, 279-282.
- VOLKMAN,B.F. & WEMMER,D.E. (1997) Deletion of a single amino acid changes the folding of an apamin hybrid sequence peptide to that of endothelin. *Biopolymers* **5**, 451-460.
- VON HEIJNE,G. (1986) A new method for predicting signal sequence cleavage sites. *Nucleic Acids Research* **14**, 4683-4690.
- VRIEND,G. (1990) WHAT IF: a molecular modelling and drug design program. *J. Mol. Graph.* **8**, 52-56.
- WADSWORTH,J.D.F., DOORTY,K.B. & STRONG,P.N. (1994) Comparable 30-kDa apamin binding polypeptides may fulfill equivalent roles within putative subtypes of small conductance Ca²⁺-activated K⁺ channels. *Journal of Biological Chemistry* **269**, 18053-18061.
- WADSWORTH,J.D.F., DOORTY,K.B., GANELLIN,C.R. & STRONG,P.N. (1996) Photolabile derivatives of ¹²⁵I-Apamin: defining the structural criteria required for labelling high and low molecular mass polypeptides associated with small conductance Ca²⁺-activated K⁺ channels. *Biochemistry (Mosc).* **35**, 7917-7927.

- WADSWORTH, J.D.F., TORELLI, S., DOORTY, K.B. & STRONG, P.N. (1997) Structural diversity among subtypes of small-conductance Ca^{2+} -activated potassium channels. *Archives of Biochemistry and Biophysics* **346**, 151-160.
- WALTHER, C., ZLOTKIN, E. & RATHMAYER, W. (1976) Actions of different toxins from the scorpion *Androctonus australis* on a locust nerve-muscle preparation. *J. Insect Physiol.* **22**, 1187-1194.
- WAPPLER, F. (2001) Malignant hyperthermia. *Eur. J. Anaesthesiol.* **18**, 632-652.
- WARTH, R. & BLEICH, M. (2000) K^+ channels and colonic function. *Rev. Physiol. Biochem. Pharmacol.* **140**, 1-62.
- WAXMAN, S.G. (2001) Transcriptional channelopathies: an emerging class of disorders. *Nature Reviews: Neuroscience* **2**, 652-659.
- WEIGNER, T.M., HERMANN, A. & LEVITAN, I.B. (2002) Modulation of calcium-activated potassium channels. *J. Comp. Physiol. A* **188**, 79-87.
- WEINREICH, F. & JENTSCH, T.J. (2000) Neurological diseases caused by ion-channel mutations. *Current Opinion in Neurobiology* **10**, 409-415.
- WEMMER, D. & KALLENBACH, N.R. (1983) Structure of apamin in solution. A two-dimensional nuclear magnetic resonance study. *Biochemistry (Mosc.)* **22**, 1901-1906.
- WHITING, P.J. (2003) The GABA_A receptor gene family: new opportunities for drug development. *Curr. Opin. Drug Discov. Devel.* **6**, 648-657.
- WILLIAMS, V., WHITE, J., SCHWANER, T.D. & SPARROW, A. (1988) Variation in venom proteins from isolated populations of tiger snakes (*Notechis ater niger*, *N. scutatus*) in South Australia. *Toxicon* **26**, 1067-1075.
- WINTER, C.A., RISLEY, E. & NUSS, G.W. (1962) Carrageenin-induced edema in hind paw of the rat as an assay for antiinflammatory drugs. *Proc. Soc. Exp. Biol. Med.* **111**, 544-547.
- WOLL, E. (1996) Fluorescence optical measurements of chloride movements in cells using the membrane permeable dye diH-MEQ. *Pflugers Archiv: European Journal of Physiology* **432**, 486-493.
- WU, J.-J., DAI, L., LAN, Z.-D. & CHI, C.-W. (2000) The gene cloning and sequencing of Bm-12, a chlorotoxin-like peptide from the scorpion *Buthus Martensi* Karsch. *Toxicon* **38**, 661-668.
- WU, K., CARLIN, R., SACHS, L. & SIEKEVITZ, P. (1985) Existence of a Ca^{2+} -dependent K^+ channel in synaptic membrane and postsynaptic density fractions isolated from canine cerebral cortex and cerebellum, as determined by apamin binding. *Brain Res.* **360**, 183-194.

- WUDAYAGIRI,R., INCEOGLU,B., HERRMANN,R., DERBEL,M., CHOUDARY,P.V. & HAMMOCK,B.D. (2001) Isolation and characterization of a novel lepidopteran-selective toxin from the venom of South Indian red scorpion, *Mesobuthus tamulus*. *BMC Biochem.* **2**, 16.
- XIA,X.-M., FALKER,B. & RIVARD,A. (1998) Mechanism of calcium gating in small-conductance calcium-activated potassium channels. *Nature* **395**, 503-507.
- XIAO,F., CAO,Z.J., LU,M., JIANG,D.H., MAO,X., LUI,H. & LI,W.X. (2003) [Analysis of the genomic organization of a novel scorpion toxin BmTXK beta]. *Yi Chuan Xue Bao* **30**, 663-667.
- XU,C.-Q., ZHU,S.-Y., CHI,C.-W. & TYTGAT,J. (2003) Turret and pore block of K⁺ channels: what is the difference? *Trends in Pharmacological Sciences* **24**, 446-448.
- XU,X. & NELSON,J.W. (1994) One-disulfide intermediates of apamin exhibit native-like structure. *Biochemistry (Mosc)*. **33**, 5253-5261.
- YAMAKAGE,M. & NAMIKI,A. (2002) Calcium channels- basic aspects of their structure, function and gene encoding: anesthetic action on the channels- a review. *General Anesthesia* **49**, 151-164.
- YAN,L. & ADAMS,M.E. (1998) Lycotoxins, antimicrobial peptides from the venom of the wolf spider *Lycosa carolinensis*. *J. Biol. Chem.* **273**, 2059-2066.
- YATANI,A., KIRSCH,G.E., POSSANI,L.D. & BROWN,A.M. (1988) Effects of New World scorpion toxins on single-channel and whole cell cardiac sodium currents. *Am. J. Physiol.* **254**, H443-H451.
- YU,A.S. (2001) Role of CIC-5 in the pathogenesis of hypercalciuria: recent insights from transgenic mouse models. *Curr. Opin. Nephrol. Hypertens.* **10**, 415-420.
- YU,X. & SCHWARTZ,R.D. (1995) Optical imaging of intracellular chloride in living brain slices. *Journal of Neuroscience Methods* **62**, 185-192.
- ZAMUDIO,F.Z., GURROLA,G.B., AREVALO,C., SREEKUMAR,R., WALKER,J.W., VALDIVIA,H.H. & POSSANI,L.D. (1997) Primary structure and synthesis of Imperatoxin A (IpTx_a), a peptide activator of Ca²⁺ release channels/ ryanodine receptors. *FEBS Lett.* **405**, 385-389.
- ZAMUDIO,F.Z., CONDE,R., AREVALO,C., BECERRIL,B., MARTIN,B.M., VALDIVIA,H.H. & POSSANI,L.D. (1997a) The mechanism of inhibition of ryanodine receptor channels by Imperatoxin 1, a heterodimeric protein from the scorpion *Pandinus imperator*. *Journal of Biological Chemistry* **272**, 11886-11894.
- ZASLOFF,M. (1987) Magainins, a class of antimicrobial peptides from *Xenopus* skin: isolation, characterization of two active forms, and partial cDNA sequence of a precursor. *Proc. Natl. Acad. Sci. USA* **84**, 5449-5453.

ZENG,X.-C., LI,W.-X., ZHU,S.-Y., PENG,F., ZHU,Z.-H., WU,K.-L. & YIANG,F.-H. (2000) Cloning and characterization of a cDNA sequence encoding the precursor of a chlorotoxin-like peptide from the Chinese scorpion *Buthus martensii* Karsch. *Toxicon* **38**, 1009-1014.

ZENG,X.-C., LI,W.-X., PENG,F. & ZHU,Z.-H. (2000a) Cloning and characterization of a novel cDNA sequence encoding the precursor of a novel venom peptide (BmKbpb) related to a bradykinin-potentiating peptide from the Chinese scorpion *Buthus martensii* Karsch. *IUBMB life* **49**, 207-210.

ZENG,X.-C., LI,W.-X., ZHU,S.-Y., PENG,F., ZHU,Z.-H., LIU,H. & MAO,X. (2001) Molecular cloning and sequence analysis of cDNAs encoding a β -toxin-like peptide and two Mktx1 homologues from scorpion *Buthus martensii* Karsch. *IUBMB life* **51**, 117-120.

ZENG,X.-C., LI,W.-X., WANG,S.-X., ZHU,S.-Y. & LUO,F. (2001a) Precursor of a novel scorpion venom peptide (BmKn1) with no disulphide bridge from *Buthus martensii* Karsch. *IUBMB life* **51**, 117-120.

ZENG,X.-C., WANG,S.-X. & LI,W.-X. (2002) Identification of BmKAPi, a novel type of scorpion venom peptide with peculiar disulphide bridge pattern from *Buthus Martensii* Karsch. *Toxicon* **40**, 1719-1722.

ZHANG,J.J., JACOB,T.J., VALVERDE,M.A., HARDY,S.P., MINTENIG,G.M., SEPELVEDA,F.V., GILL,D.R., HYDE,S.C., TREZISE,A.E. & HIGGINS,C.F. (1994) Tamoxifen blocks chloride channels. A possible mechanism for cataract formation. *J. Clin. Invest.* **94**, 1690-1697.

ZHOU,Y., MORAIS-CABRAL,J.H., KAUFMAN,A. & MACKINNON,R. (2001) Chemistry of ion coordination and hydration revealed by a K^+ channel-Fab complex at 2.0Å resolution. *Nature* **414**, 43-48.

ZHU,Q., LIANG,S., MARTIN,L., GASPARINI,S., MENEZ,A. & VITA,C. (2002) Role of disulfide bonds in folding and activity of leurotoxin just two disulfides suffice. *Biochemistry (Mosc)*. **41**, 11488-11494.

ZHU,S., LI,W., ZENG,X., JIANG,D., MAO,X. & LIU,H. (1999) Molecular cloning and sequencing of two 'short chain' and two 'long chain' K^+ channel-blocking peptides from the Chinese scorpion *Buthus martensii* Karsch. *FEBS Lett.* **457**, 509-514.

ZHU,S., LI,W., JIANG,D. & ZENG,X. (2000) Evidence for the existence of insect defensin-like peptide in scorpion venom. *IUBMB life* **50**, 57-61.

ZHU,S. & LI,W. (2002) Precursors of three unique cysteine-rich peptides from the scorpion *Buthus martensii* Karsch. *Comparative Biochemistry and Physiology Part B* **131**, 749-756.

ZHU,S., HUYS,I., DYASON,K., VERDONCK,F. & TYTGAT,J. (2004) Evolutionary trace analysis of scorpion toxins specific for K^+ -channels. *Proteins* **54**, 361-370.

ZHU,S. & TYTGAT,J. (2004) The scorpine family of defensins: gene structure, alternative polyadenylation and fold recognition. *Cell Mol. Life Sci.* **61**, 1751-1763.

ZIMMERMANN,S. & SENTENAC,H. (1999) Plant ion channels: from molecular structures to physiological functions. *Current Opinion in Plant Biology* **2**, 477-482.

ZLOTKIN,E., MIRANDA,F. & ROCHAT,H. (1972) Proteins in scorpion venoms toxic on mammals and insects. *Toxicon* **10**, 211-216.

ZLOTKIN,E. (1983) Insect selective toxins derived from scorpion venoms: an approach to insect neuropharmacology. *Insect Biochem.* **13**, 219-236.

ZLOTKIN,E., KADOURI,D., GORDON,D., PELHATE,M., MARTIN,M.F. & ROCHAT,H. (1985) An excitatory and a depressant insect toxin from scorpion venom both affect sodium conductance and possess a common binding site. *Arch. Biochem. Biophys.* **240**, 877-887.

ZLOTKIN,E., EITAN,M., BINDOKAS,V.P., ADAMS,M.E., MOYER,M., BURKHART,W. & FOWLER,E. (1991) Functional duality and structural uniqueness of depressant insect-selective neurotoxins. *Biochemistry (Mosc)*. **30**, 4814-4821.

ZLOTKIN,E., GUREVITZ,M., FOWLER,E., MOYER,M. & ADAMS,M.E. (1993) Depressant insect selective neurotoxins from scorpion venom: chemistry, action and gene cloning. *Arch. Insect Biochem. Physiol.* **22**, 55-73.

ZLOTKIN,E., FISHMAN,Y. & ELAZAR,M. (2000) AaIT: From neurotoxin to insecticide. *Biochimie* **82**, 869-881.

Appendices

Biochemical Studies on Scorpion (*Mesobuthus tamulus*) and Bee (*Apis mellifera*) Venom Peptides

Kirsti Amanda Newton

A thesis submitted in partial fulfilment of the requirements of
Sheffield Hallam University
for the degree of Doctor of Philosophy

November 2004

Contents

Appendix A	LC-MS Data for <i>Mesobuthus tamulus</i> venom from Aurangabad region	ii
Appendix B	LC-MS Data for <i>Mesobuthus tamulus</i> venom from Konkan region	vii
Appendix C	LC-MS Data for <i>Leiurus quinquestriatus hebraeus</i> venom	xv
Appendix D	Mass Profiling Data for <i>Mesobuthus tamulus</i> venom	xxv

Appendix A. LC-MS Data for *Mesobuthus tamulus* venom from Aurangabad region.

LC-MS was performed on *Mesob. tamulus* venom (Aurangabad region) and data analysed as described (2.2.3.4 and 2.2.3.5). Component masses and their elution windows were calculated using LC-MS peak reconstruction software (Applied biosystems) with a mass tolerance of 0.01%, signal-to-noise ratio of 10 and 2000-10000Da final mass range. Peak areas were standardised against that of a peptide standard and the masses corresponding to those in a standard-only sample removed. Masses differing by 1Da were assumed products of peptide oxidation or amidation and their relative areas pooled. Masses occurring in venoms from both regions (same isotopic and average mass +/- 0.02%, same retention time +/- 1min) were averaged and noted. Masses suspected of representing adducted peptides were noted.

Mass (Avg) Average mass of the neutral species.

Mass (Mono) Monoisotopic mass ($[M+H]^+$). Based upon the lowest detected peak in the isotope series.

Apex Mass Mass of isotope distribution at maximum intensity.

Area Integrated total intensity (counts sec⁻¹) over the m/z range of the contributing ions.

Relative area Area standardised against that of peptide standard.

Score Least squares correlation coefficient for fit of observed values to calculated masses.

Evidence Type of series used for mass determination. I = isotope series, C = charge series, IC = isotope series that is also part of a charge series.

Time Elution window of ions contributing to mass information. Time is shown to nearest 0.5 min from initiation of data collection.

Shared Mass ✓ indicates mass eluting at similar time is also detected in venom of *Mesob. tamulus* from Konkan region.

Adduct * indicates possible adduct mass. Data was examined for potential masses relating to +Na, +K, +Na+K, -CO₂, -NH₃, -H₂O, mono- and di-oxidation, in addition to +74, +104 (adducts previously observed in scorpion venom mass data (Pimenta et al., 2001)).

Mass (Avg.)	Mass (Mono)	Apex Mass	Area	Relative Area	Score	Series	Time (min)	Shared Mass?	Adduct?
2006.4	2005.6	2005.6	572	0.003	1.00	I	45.0 - 45.5		
2009.3	2008.6	2009.6	3155	0.016	1.00	I	27.0 - 27.5		
2025.8	2025.3	2026.3	406	0.002	1.00	I	28.5 - 29.0		
2150.9	2150.0	2151.1	300	0.002	1.00	I	50.0 - 50.5	✓	
2163.5	2162.5	2163.5	517	0.003	1.00	I	35.0 - 35.5	✓	
2374.6	2373.5	2374.5	358	0.002	0.89	I	46.5 - 47.0	✓	
2393.9	2392.7	2393.7	798	0.004	1.00	I	41.5 - 42.0		
2436.7	2435.7	2437.2	454	0.002	1.00	I	37.0 - 37.5	✓	
2521.2	2519.8	2520.8	1140	0.006	1.00	I	51.0 - 52.0	✓	
2577.9	2576.8	2577.8	768	0.004	1.00	I	45.5 - 46.5	✓	
2592.9	2591.7	2592.7	489	0.003	1.00	I	40.5 - 41.5	✓	
2645.0	2643.5	2645.0	12965	0.068	1.00	IC	47.5 - 48.5	✓	
2667.3	2666.5	2666.5	296	0.002	1.00	I	47.5 - 48.0		
2683.2	2682.4	2682.4	1535	0.008	1.00	I	44.5 - 45.5		*
2714.8	2712.6	2713.6	20916	0.109	1.00	IC	44.0 - 44.5		
2717.0	2715.4	2716.1	72369	0.378	1.00	IC	48.0 - 49.0	✓	
2718.0	2716.2	2717.2	1710	0.009	0.94	I	54.0 - 55.0		
2727.4	2725.6	2727.1	1590	0.008	1.00	IC	45.5 - 46.0	✓	
2736.4	2734.6	2736.6	499	0.003	1.00	I	44.0 - 44.5		*
2738.3	2736.5	2738.6	4840	0.025	1.00	IC	48.0 - 49.0		*
2751.8	2749.8	2750.8	603	0.003	1.00	I	44.0 - 44.5	✓	*
2754.3	2752.5	2753.5	3699	0.019	1.00	IC	48.0 - 49.0		*
2759.9	2758.5	2759.5	1182	0.006	1.00	I	48.0 - 49.0		
2775.6	2774.5	2775.5	317	0.002	1.00	I	48.0 - 49.0		*
2782.9	2781.6	2782.6	827	0.004	1.00	I	36.0 - 37.0		
2949.5	2947.5	2948.5	2144	0.011	1.00	I	22.5 - 23.5	✓	
2953.2	2951.4	2953.4	3352	0.018	1.00	IC	46.5 - 47.0		
2974.9	2973.4	2975.4	1481	0.008	1.00	I	46.5 - 47.0		*
2988.9	2986.7	2988.7	13052	0.068	1.00	IC	5.0 - 5.5	✓	
3021.2	3019.6	3021.1	4437	0.023	1.00	IC	5.0 - 5.5	✓	*
3060.7	3058.8	3059.7	3007	0.016	1.00	IC	41.5 - 42.0		
3105.9	3103.7	3104.7	32162	0.168	1.00	IC	32.0 - 32.5		
3110.5	3108.7	3110.7	802	0.004	1.00	I	30.0 - 31.0	✓	
3145.7	3144.7	3145.7	732	0.004	1.00	I	31.5 - 32.5		
3166.7	3164.7	3165.7	6235	0.033	1.00	IC	43.0 - 43.5		*
3168.5	3166.7	3168.2	1137	0.006	1.00	I	27.0 - 27.5	✓	
3183.6	3182.0	3184.0	4052	0.021	1.00	IC	43.0 - 44.0		
3188.8	3186.7	3188.7	2606	0.014	1.00	I	43.0 - 43.5		*
3191.8	3189.7	3191.7	4689	0.024	1.00	IC	5.0 - 5.5	✓	
3204.3	3202.7	3204.7	1507	0.008	1.00	IC	43.0 - 43.5		*
3223.9	3221.8	3222.8	7982	0.042	1.00	IC	22.5 - 23.0		*
3251.4	3250.9	3250.9	403	0.002	1.00	I	33.5 - 34.0		
3251.7	3249.9	3251.9	822	0.004	1.00	I	33.5 - 34.0		
3261.8	3260.8	3261.8	255	0.001	1.00	I	22.5 - 23.0		*
3296.2	3293.9	3295.9	7009	0.037	1.00	IC	32.5 - 33.5		
3309.0	3306.8	3308.8	20937	0.109	1.00	IC	33.0 - 34.0	✓	
3321.2	3318.9	3319.9	2101	0.011	1.00	IC	23.5 - 24.0		

Mass (Avg.)	Mass (Mono)	Apex Mass	Area	Relative Area	Score	Series	Time (min)	Shared Mass?	Adduct?
3346.9	3345.4	3346.1	2251	0.012	1.00	IC	33.0 - 34.0	✓	
3351.0	3349.0	3350.0	2905	0.015	1.00	I	31.5 - 32.5		
3357.5	3355.9	3356.8	9023	0.047	1.00	IC	33.0 - 33.5	✓	
3380.0	3379.5	3379.5	3251	0.017	0.77	I	54.5 - 55.0		
3389.9	3388.1	3389.6	2183	0.011	1.00	I	54.0 - 55.0	✓	
3391.2	3389.0	3391.0	3096	0.016	1.00	IC	35.0 - 36.0		
3392.8	3391.9	3391.9	290	0.002	1.00	I	27.0 - 27.5		
3392.7	3390.7	3392.7	1087	0.006	1.00	I	49.5 - 50.0	✓	
3397.5	3395.3	3397.5	930	0.005	0.72	I	54.0 - 55.0		
3411.2	3408.8	3410.8	12732	0.066	1.00	IC	46.0 - 46.5	✓	*
3411.8	3410.3	3411.8	931	0.005	1.00	I	48.0 - 48.5	✓	
3418.3	3415.9	3417.9	9745	0.051	1.00	IC	26.0 - 26.5		*
3418.9	3417.9	3418.9	1023	0.005	1.00	I	29.5 - 30.0		*
3430.6	3429.0	3429.9	1723	0.009	0.95	I	22.5 - 23.0		
3435.1	3433.0	3435.0	559	0.003	1.00	I	5.0 - 5.5		*
3449.8	3448.4	3449.4	239426	1.250	1.00	IC	40.0 - 46.5	✓	*
3460.1	3457.8	3459.8	2603	0.014	1.00	IC	27.0 - 27.5		
3467.0	3465.0	3467.0	8718	0.046	1.00	IC	5.0 - 5.5		*
3472.9	3470.0	3472.0	6450	0.034	1.00	IC	5.0 - 5.5		*
3478.3	3476.4	3477.9	9189	0.048	1.00	IC	35.0 - 36.0	✓	
3484.3	3482.0	3484.1	6688	0.035	1.00	IC	5.0 - 5.5		
3487.9	3486.0	3488.0	10494	0.055	1.00	IC	5.0 - 5.5		*
3493.3	3492.0	3492.0	3020	0.016	1.00	IC	5.0 - 5.5		
3494.3	3492.0	3493.0	9101	0.048	1.00	IC	23.0 - 23.5		*
3500.4	3498.0	3500.1	1743	0.009	1.00	IC	5.0 - 5.5		*
3500.6	3498.6	3500.1	9782	0.051	1.00	IC	23.5 - 24.0	✓	
3502.4	3501.0	3502.1	1299	0.007	1.00	IC	5.0 - 5.5		
3511.3	3509.1	3511.6	14005	0.073	1.00	IC	5.0 - 5.5	✓	
3514.0	3512.0	3512.0	672	0.004	1.00	IC	5.0 - 5.5		
3517.2	3514.9	3516.9	5075	0.027	1.00	IC	32.0 - 32.5	✓	*
3519.2	3517.0	3519.0	53972	0.282	1.00	IC	26.0 - 26.5	✓	
3525.4	3523.9	3525.0	1110	0.006	1.00	IC	5.0 - 5.5		*
3535.4	3532.9	3534.9	860	0.004	1.00	I	22.5 - 23.0	✓	
3535.5	3533.0	3535.0	13309	0.070	1.00	IC	35.0 - 35.5	✓	
3540.7	3539.0	3541.0	389	0.002	1.00	I	26.0 - 26.5		
3541.0	3539.0	3541.1	1982	0.010	1.00	I	23.0 - 24.0		*
3546.9	3545.6	3547.5	938	0.005	1.00	I	5.0 - 5.5	✓	
3553.5	3551.1	3553.0	9470	0.049	1.00	IC	30.0 - 31.0		
3557.1	3556.0	3557.0	429	0.002	1.00	I	26.0 - 26.5		
3560.4	3558.1	3560.1	23683	0.124	1.00	IC	5.0 - 5.5	✓	*
3571.9	3570.0	3572.0	1845	0.010	1.00	IC	5.0 - 5.5		
3576.4	3574.0	3576.1	2080	0.011	1.00	IC	5.0 - 5.5		*
3588.3	3586.5	3588.0	12250	0.064	1.00	IC	36.5 - 37.0	✓	
3593.3	3591.5	3593.0	1819	0.010	1.00	IC	5.0 - 5.5	✓	*
3595.2	3594.1	3594.1	768	0.004	1.00	IC	5.0 - 5.5		*
3596.8	3596.1	3596.1	397	0.002	1.00	I	5.0 - 5.5		*
3611.9	3611.0	3612.1	367.2	0.002	1.00	I	5.0 - 5.5		*
3629.3	3627.0	3629.1	3981	0.021	1.00	IC	30.0 - 30.5		

Mass (Avg.)	Mass (Mono)	Apex Mass	Area	Relative Area	Score	Series	Time (min)	Shared Mass?	Adduct?
3672.5	3670.6	3672.1	13768	0.072	1.00	IC	21.0 - 22.0	✓	
3684.9	3682.5	3684.5	3231	0.017	1.00	I	27.5 - 28.5	✓	
3685.5	3683.1	3685.1	68391	0.357	1.00	IC	22.5 - 23.0	✓	
3707.6	3706.1	3707.1	1277	0.007	1.00	IC	22.4 - 23.0		
3715.0	3713.2	3715.2	3439	0.018	1.00	IC	22.0 - 22.5		
3722.4	3720.5	3722.0	15350	0.080	1.00	IC	46.0 - 47.0	✓	*
3723.4	3721.5	3723.5	2787	0.015	1.00	IC	22.5 - 23.0	✓	*
3744.3	3743.0	3744.0	663	0.003	1.00	I	46.0 - 47.0		
3754.8	3752.3	3754.3	7689	0.040	1.00	IC	23.0 - 23.5		*
3756.3	3755.4	3755.4	1219	0.006	1.00	I	23.0 - 23.5		
3760.8	3760.0	3760.0	709	0.004	1.00	IC	46.0 - 47.0		
3769.8	3769.1	3769.1	356	0.002	1.00	I	25.5 - 26.5		
3770.9	3769.0	3770.0	11742	0.061	1.00	IC	49.0 - 49.5	✓	
3792.7	3791.1	3792.0	747	0.004	1.00	I	49.0 - 49.5		*
3797.7	3795.0	3797.5	74055	0.387	1.00	IC	26.0 - 27.0	✓	
3819.6	3816.9	3818.9	46670	0.024	1.00	IC	26.0 - 27.0	✓	*
3821.8	3821.0	3820.5	335	0.002	1.00	I	22.5 - 23.0	✓	
3830.4	3828.2	3830.2	2329	0.012	1.00	IC	26.0 - 27.0		
3835.3	3833.0	3834.5	5969	0.031	1.00	IC	26.0 - 27.0	✓	*
3840.5	3838.1	3840.1	19555	0.102	1.00	IC	22.5 - 23.0	✓	
3841.3	3839.0	3841.0	1387	0.007	1.00	I	26.0 - 27.0	✓	*
3854.7	3852.1	3854.1	5976	0.031	1.00	IC	22.0 - 23.0		
3854.9	3854.1	3854.1	5230	0.027	1.00	IC	22.0 - 23.0		
3895.7	3895.2	3896.3	930	0.005	1.00	I	34.0 - 35.0		*
3896.5	3895.1	3897.1	491	0.003	1.00	I	30.5 - 31.5		*
3910.6	3908.7	3910.2	5541	0.029	1.00	IC	36.5 - 37.0	✓	
3912.5	3911.1	3912.2	34795	0.182	1.00	IC	5.0 - 5.5	✓	
3913.0	3910.2	3912.2	776	0.004	0.88	I	5.0 - 5.5	✓	
3914.6	3912.0	3914.0	17392	0.091	1.00	IC	29.0 - 29.5	✓	*
3929.0	3928.2	3929.3	378	0.002	0.99	I	31.5 - 32.5		*
3932.0	3930.3	3932.2	1310	0.007	1.00	I	31.5 - 32.5		
3932.1	3930.2	3931.2	6858	0.036	0.98	I	42.0 - 43.0		
3934.2	3933.2	3934.2	160	0.001	1.00	I	5.0 - 5.5		*
3950.2	3948.3	3949.3	801	0.004	1.00	I	5.0 - 5.5		*
3951.9	3951.0	3951.0	358	0.002	1.00	I	29.0 - 29.5		
3953.6	3952.0	3953.1	1398	0.007	1.00	IC	42.0 - 43.0		
3971.7	3969.2	3971.2	32091	0.168	1.00	IC	22.0 - 22.5	✓	
3986.4	3985.4	3986.3	2495	0.013	1.00	IC	42.5 - 43.0		
3986.4	3984.3	3986.3	1323	0.007	1.00	I	33.5 - 34.5		
3993.5	3991.7	3993.7	1803	0.009	1.00	IC	22.0 - 22.5	✓	*
4009.8	4007.2	4009.2	2433	0.013	1.00	IC	22.0 - 22.5		*
4020.0	4017.3	4019.3	38274	0.200	1.00	I	25.5 - 26.5		
4020.1	4017.3	4019.3	35923	0.188	1.00	I	27.0 - 27.5		
4029.5	4027.3	4029.2	9414	0.049	1.00	IC	22.5 - 23	✓	
4042.6	4041.3	4041.3	1039	0.005	0.89	I	25.5 - 26.0		
4052.1	4049.4	4051.5	6471	0.034	1.00	IC	28.5 - 29.0		*
4053.5	4052.4	4052.4	1180	0.006	0.76	I	28.5 - 29.0		
4061.1	4059.3	4059.3	941	0.005	1.00	I	25.5 - 26.5		

Mass (Avg.)	Mass (Mono)	Apex Mass	Area	Relative Area	Score	Series	Time (min)	Shared Mass?	Adduct?
4114.3	4113.5	4114.4	1128	0.006	1.00	I	26.5 - 27.5		
4134.4	4132.4	4134.4	10944	0.057	1.00	IC	31.0 - 31.5		
4173.1	4170.5	4172.5	7911	0.041	1.00	IC	38.0 - 38.5		
4205.3	4203.0	4203.0	3858	0.020	1.00	IC	5.0 - 5.5	✓	
4207.3	4205.5	4207.1	755	0.004	1.00	IC	30.5 - 31.5	✓	
4223.7	4221.3	4223.2	740	0.004	0.89	I	24.0 - 24.5		
4226.1	4223.5	4226.5	1322	0.007	1.00	IC	32.5 - 33.5		
4241.9	4240.5	4241.5	647	0.003	0.94	I	31.0 - 32.0		
4303.0	4302.5	4302.5	249	0.001	1.00	I	50.0 - 50.5		
4303.4	4300.5	4303.6	4762	0.025	1.00	IC	50.0 - 50.5		
4339.2	4336.6	4339.6	3104	0.016	1.00	IC	23.5 - 24.0		
4464.2	4462.5	4464.5	325	0.002	1.00	I	21.5 - 22.0	✓	
4528.6	4528.0	4529.0	379	0.002	1.00	I	54.5 - 55.0		
4877.8	4876.9	4876.9	328	0.002	1.00	I	37.0 - 37.5		
4930.4	4928.4	4930.4	871	0.005	1.00	I	41.0 - 41.5	✓	
5100.0	5098.2	5099.0	1716	0.009	1.00	I	54.0 - 55.0		
5467.4	5465.3	5466.2	703	0.004	0.95	I	54.0 - 55.0		
6706.6	6705.0	6707.0	1097	0.006	1.00	I	44.5 - 45.5		
6756.3	6754.2	6755.4	102870	0.537	1.00	IC	54.0 - 55.0	✓	
6770.1	6777.7	6777.7	1513	0.008	0.85	I	54.0 - 55.0	✓	
6795.7	6793.8	6794.7	3504	0.018	0.89	I	54.5 - 55.0		*
6803.0	6801.7	6801.7	566	0.003	1.00	I	54.0 - 55.0		
6816.3	6813.6	6816.6	1760	0.009	1.00	IC	54.0 - 55.0		
6820.7	6819.8	6817.6	1108	0.006	1.00	IC	54.0 - 55.0		
6991.5	6989.1	6992.1	5665	0.030	1.00	IC	54.0 - 54.5		

Appendix B. LC-MS Data for *Mesobuthus tamulus* venom from Konkan region.

LC-MS was performed on *Mesob. tamulus* venom (Konkan region) and data analysed as described (2.2.3.4 and 2.2.3.5). Component masses and their elution windows were calculated using LC-MS peak reconstruction software (Applied biosystems) with a mass tolerance of 0.01%, signal-to-noise ratio of 10 and 2000-10000Da final mass range. Peak areas were standardised against that of a peptide standard and the masses corresponding to those in a standard-only sample removed. Masses differing by 1Da were assumed products of peptide oxidation or amidation and their relative areas pooled. Masses occurring in venoms from both regions (same isotopic and average mass +/- 0.02%, same retention time +/- 1min) were averaged and noted. Masses suspected of representing adducted peptides were noted.

Mass (Avg) Average mass of the neutral species.

Mass (Mono) Monoisotopic mass ($[M+H]^+$). Based upon the lowest detected peak in the isotope series.

Apex Mass Mass of isotope distribution at maximum intensity.

Area Integrated total intensity (counts sec⁻¹) over the m/z range of the contributing ions.

Relative area Area standardised against that of peptide standard.

Score Least squares correlation coefficient for fit of observed values to calculated masses.

Evidence Type of series used for mass determination. I = isotope series, C = charge series, IC = isotope series that is also part of a charge series.

Time Elution window of ions contributing to mass information. Time is shown to nearest 0.5 min from initiation of data collection.

Shared Mass ✓ indicates mass eluting at similar time is also detected in venom of *Mesob. tamulus* from Aurangabad region.

Adduct * indicates possible adduct mass. Data was examined for potential masses relating to +Na, +K, +Na+K, -CO₂, -NH₃, -H₂O, mono- and di-oxidation, in addition to +74, +104 (adducts previously observed in scorpion venom mass data (Pimenta et al., 2001)).

Mass (Avg.)	Mass (Mono)	Apex Mass	Area	Relative Area	Score	Series	Time (min)	Shared Mass?	Adduct?
2046.4	2045.4	2046.4	903	0.002	1.00	I	58.5 - 59.5		
2052.1	2051.4	2051.4	431	0.001	1.00	I	60.0 - 60.5		
2055.4	2054.4	2055.4	558	0.001	1.00	I	50.0 - 51.5		
2094.3	2093.4	2093.4	548	0.001	1.00	I	49.5 - 50.5		
2109.1	2108.3	2108.3	2967	0.006	1.00	I	5.0 - 5.5		
2147.9	2147.3	2148.3	517	0.001	1.00	I	5.0 - 5.5		
2150.9	2150.0	2151.1	4310	0.009	1.00	IC	48.0 - 49.0	✓	*
2163.5	2162.5	2163.5	2968	0.006	1.00	I	39.5 - 40.5	✓	
2172.8	2172.4	2172.4	253	0.001	1.00	I	48.0 - 49.0		
2180.0	2179.5	2180.5	327	0.001	1.00	I	41.0 - 42.0		
2199.0	2198.5	2199.5	465	0.001	1.00	I	41.5 - 42.5		
2230.9	2229.4	2230.5	3165	0.007	1.00	IC	49.0 - 50.0		
2236.0	2234.9	2234.9	1155	0.002	0.89	I	50.5 - 51.5		
2238.1	2237.6	2237.6	732	0.002	1.00	I	50.5 - 51.5		
2246.4	2245.4	2246.4	947	0.002	1.00	I	49.5 - 50.0		*
2251.0	2249.5	2250.5	9612	0.020	1.00	I	39.5 - 40.5		
2255.0	2254.5	2254.5	907	0.002	1.00	I	39.5 - 40.5		
2290.2	2289.6	2290.6	579	0.001	1.00	I	42.0 - 43.0		
2293.5	2292.6	2293.6	1019	0.002	1.00	I	42.0 - 43.0		
2296.7	2295.6	2296.5	3104	0.007	1.00	I	41.5 - 42.5		
2301.7	2300.6	2301.6	2167	0.005	1.00	I	44.5 - 42.0		
2338.0	2337.6	2337.6	2018	0.004	1.00	I	42.0 - 43.0		
2374.6	2373.5	2374.5	4899	0.010	1.00	IC	48.5 - 49.5	✓	
2380.7	2379.5	2381.5	752	0.002	1.00	I	48.5 - 49.5		
2407.7	2406.6	2407.6	1325	0.003	1.00	I	42.0 - 43.0		
2436.7	2435.7	2437.2	2500	0.005	1.00	I	41.5 - 42.0	✓	
2447.0	2445.6	2446.7	3084	0.006	1.00	I	42.0 - 42.5		
2479.2	2477.6	2478.6	1975	0.004	1.00	I	42.0 - 42.5		*
2495.9	2494.6	2495.7	1813	0.004	1.00	I	42.0 - 42.5		
2521.2	2519.8	2520.8	5775	0.012	1.00	I	53.5 - 54.0	✓	*
2521.4	2520.8	2520.8	2929	0.006	0.89	I	53.4 - 54.0		
2536.1	2534.7	2535.7	11440	0.024	1.00	IC	42.0 - 43.0		
2555.2	2554.6	2555.6	324	0.001	1.00	I	42.0 - 42.5		*
2557.7	2556.6	2558.7	821	0.002	1.00	I	42.0 - 42.5		*
2577.9	2576.8	2577.8	4338	0.009	1.00	I	45.5 - 46.0	✓	
2585.6	2584.5	2584.5	951	0.002	1.00	I	42.0 - 42.5		
2586.5	2585.5	2585.5	336	0.001	1.00	I	47.5 - 48.0		
2592.9	2591.7	2592.7	2509	0.005	1.00	I	42.0 - 42.5	✓	
2613.9	2613.5	2613.5	1712	0.004	1.00	I	47.5 - 48.0		
2621.1	2619.8	2620.8	1544	0.003	1.00	I	39.5 - 40.0		
2628.4	2627.8	2628.8	2138	0.004	1.00	I	45.0 - 45.5		
2643.0	2641.7	2642.8	406	0.001	1.00	I	55.5 - 56.0		*
2645.0	2643.5	2645.0	335	0.001	1.00	I	51.5 - 52.0	✓	*
2717.0	2715.4	2716.1	508	0.001	1.00	I	50.5 - 60.0	✓	
2727.4	2725.6	2727.1	98630	0.207	1.00	IC	47.5 - 48.0	✓	
2751.8	2749.8	2750.8	6399	0.013	1.00	IC	47.5 - 48.0	✓	
2757.7	2756.6	2758.6	508	0.001	1.00	I	51.5 - 52.0	✓	

Mass (Avg.)	Mass (Mono)	Apex Mass	Area	Relative Area	Score	Series	Time (min)	Shared Mass?	Adduct?
2765.1	2763.5	2765.5	5052	0.011	1.00	IC	47.5 – 48.0		*
2771.1	2770.5	2771.5	317	0.001	1.00	I	47.5 – 48.0		
2771.1	2769.5	2771.5	485	0.001	1.00	I	47.5 – 48.0		
2792.3	2790.6	2791.6	819	0.002	1.00	I	51.5 – 52.0		
2793.1	2791.4	2792.4	2514	0.005	1.00	IC	24.5 – 25.0		*
2802.5	2801.8	2801.8	983	0.002	0.99	I	24.5 – 25.0		
2816.8	2815.7	2816.6	548	0.001	1.00	I	49.5 – 50.0		
2827.6	2826.7	2827.6	738	0.002	1.00	I	49.5 – 50.0		
2834.2	2832.7	2833.7	762	0.002	1.00	I	51.5 – 52.0		
2845.6	2843.6	2844.6	81856	0.171	1.00	IC	49.0 – 50.0		
2868.6	2865.6	2866.6	6243	0.013	1.00	IC	49.5 – 50.0		
2877.2	2875.7	2876.7	818	0.002	1.00	I	51.5 – 52.0		*
2883.5	2881.6	2883.6	5550	0.012	1.00	IC	49.5 – 50.0		*
2887.8	2886.6	2887.7	713	0.001	1.00	I	51.5 – 52.0		
2889.1	2887.6	2888.6	2389	0.005	1.00	I	49.5 – 50.0		*
2905.7	2903.7	2904.7	103973	0.218	1.00	IC	51.5 – 52.0		*
2917.5	2916.5	2917.5	362	0.001	1.00	I	24.5 – 25.0		
2928.7	2927.6	2928.6	7564	0.016	1.00	IC	51.5 – 52.0		
2931.2	2930.4	2931.5	324	0.001	1.00	I	24.5 – 25.0		
2931.5	2929.4	2931.5	11099	0.023	1.00	IC	26.0 – 27.0		
2933.9	2932.5	2934.5	1046	0.002	1.00	I	24.5 – 25.0		
2943.5	2941.6	2943.6	6538	0.014	1.00	IC	51.5 – 52.0		*
2949.5	2947.5	2948.5	649363	1.360	1.00	IC	24.5 – 25.0	✓	
2949.8	2948.6	2948.6	766	0.002	1.00	I	51.5 – 52.0		*
2963.1	2962.4	2963.4	311	0.001	1.00	I	24.5 – 25.0		*
2963.7	2961.7	2963.7	5152	0.011	1.00	IC	56.5 – 57.0		*
2967.1	2964.5	2969.4	6230	0.013	1.00	IC	24.5 – 25.0		
2967.2	2965.4	2966.4	3503	0.007	1.00	IC	49.0 – 50.0		
2969.9	2968.4	2970.4	5640	0.012	1.00	I	24.5 – 25.0		
2972.1	2969.4	2971.4	7755	0.016	1.00	IC	27.0 - 27.5		
2972.8	2970.4	2971.4	71537	0.150	1.00	IC	24.5 – 25.0		
2979.0	2978.4	2979.4	825	0.002	1.00	I	24.5 – 25.0		
2982.9	2980.4	2982.5	4270	0.009	1.00	IC	24.5 – 25.0		
2987.3	2985.4	2987.4	6762	0.014	1.00	IC	27.0 - 27.5		
2987.5	2985.4	2987.4	85057	0.178	1.00	IC	24.5 – 25.0		*
2988.9	2986.7	2988.7	168685	0.353	1.00	IC	5.0 – 5.5	✓	*
2990.1	2989.4	2989.4	22563	0.047	1.00	I	49.0 - 49.5		
2993.4	2991.4	2992.4	14690	0.031	1.00	IC	24.0 – 25.0		*
3003.6	3001.4	3003.4	7323	0.015	1.00	IC	24.5 – 25.0		*
3005.0	3005.4	3005.4	3831	0.008	1.00	IC	24.5 – 25.0		
3005.3	3003.8	3004.6	1364	0.003	1.00	IC	5.0 – 5.5		*
3009.9	3007.4	3008.4	15012	0.031	1.00	IC	24.5 – 25.0		*
3010.0	3008.6	3009.6	4535	0.010	1.00	IC	5.0 – 5.5		*
3015.2	3013.4	3014.4	6307	0.013	1.00	IC	24.5 – 25.0		*
3018.3	3017.4	3017.4	369	0.001	1.00	I	24.5 – 25.0		
3021.2	3019.6	3021.1	5501	0.012	1.00	I	5.0 – 5.5	✓	*
3025.2	3023.4	3024.4	13512	0.028	1.00	IC	24.0 – 25.0		*
3026.7	3025.6	3025.6	830	0.002	0.00	I	5.0 – 5.5		*

Mass (Avg.)	Mass (Mono)	Apex Mass	Area	Relative Area	Score	Series	Time (min)	Shared Mass?	Adduct?
3031.4	3029.4	3030.4	3565	0.007	1.00	I	24.0 - 25.0		
3036.9	3035.4	3037.4	1767	0.004	1.00	I	24.5 - 25.0		
3037.2	3036.7	3037.6	162	0.000	1.00	I	5.0 - 5.5		*
3039.2	3038.7	3039.6	146	0.000	1.00	I	5.0 - 5.5		
3042.7	3040.6	3041.6	1163	0.002	1.00	I	24.0 - 25.0		*
3047.6	3046.5	3046.5	2877	0.006	1.00	IC	24.5 - 25.0		*
3053.1	3051.4	3053.4	1910	0.004	1.00	I	24.0 - 25.0		*
3062.6	3061.4	3061.4	810	0.002	1.00	I	24.5 - 25.0		
3067.6	3066.9	3066.9	18630	0.039	0.99	I	41.0 - 42.0		
3069.5	3067.4	3070.5	5460	0.011	1.00	IC	24.5 - 25.0		*
3080.8	3080.4	3080.4	272	0.001	1.00	I	24.5 - 25.0		
3086.0	3084.3	3086.4	937	0.002	0.93	I	24.5 - 25.0		
3091.6	3089.3	3091.4	1877	0.004	1.00	I	24.0 - 25.0		*
3107.7	3105.4	3107.4	2025	0.004	1.00	IC	24.5 - 25.0		*
3110.6	3108.7	3110.7	3864	0.008	1.00	IC	34.0 - 35.0	✓	
3114.5	3112.4	3115.5	1240	0.003	1.00	I	24.5 - 25.0		
3156.3	3155.8	3156.8	401	0.001	1.00	I	5.0 - 5.5		
3168.5	3166.7	3168.2	566	0.001	1.00	I	29.5 - 30.0	✓	
3173.0	3171.9	3172.9	17674	0.037	1.00	IC	5.0 - 5.5		
3174.3	3173.9	3173.9	36626	0.077	1.00	IC	5.0 - 5.5		
3174.7	3172.9	3173.9	98413	0.206	1.00	IC	5.0 - 5.5		*
3176.7	3175.8	3175.8	11801	0.025	0.94	I	5.0 - 5.5		
3191.8	3189.7	3191.7	68603	0.144	1.00	IC	5.0 - 5.5	✓	
3207.8	3205.9	3207.8	7753	0.016	1.00	IC	5.0 - 5.5		*
3210.3	3207.8	3207.8	2110	0.004	1.00	IC	5.0 - 5.5		
3213.2	3211.8	3211.8	847	0.002	1.00	IC	5.0 - 5.5		
3215.4	3213.6	3215.6	1603	0.003	1.00	IC	5.0 - 5.5		
3222.4	3221.8	3222.8	340	0.001	1.00	I	5.0 - 5.5		
3225.6	3223.8	3225.7	924	0.002	1.00	IC	5.0 - 5.5		
3229.6	3227.6	3228.6	1899	0.004	1.00	IC	5.0 - 5.5		*
3272.0	3270.9	3271.9	1200	0.003	1.00	IC	5.0 - 5.5		
3281.7	3279.7	3280.7	3453	0.007	1.00	IC	47.0 - 47.5		*
3309.0	3306.8	3308.8	48355	0.101	1.00	IC	38.0 - 38.5	✓	
3331.1	3328.9	3330.9	3400	0.007	1.00	IC	31.5 - 32.0		*
3331.4	3328.7	3330.7	3200	0.007	1.00	IC	38.0 - 38.5		*
3332.0	3330.7	3331.7	2994	0.006	1.00	IC	38.0 - 38.5		
3336.0	3334.9	3336.7	1173	0.002	0.99	I	50.5 - 51.5		
3346.8	3345.8	3346.8	1179	0.002	1.00	I	27.0 - 28.0		
3346.8	3345.7	3345.7	2162	0.005	1.00	IC	38.0 - 38.5	✓	
3346.9	3345.4	3346.1	5356	0.011	1.00	IC	38.0 - 38.5	✓	
3347.2	3344.9	3346.9	33243	0.070	1.00	IC	29.0 - 29.5	✓	*
3352.8	3351.7	3353.7	485	0.001	1.00	I	37.5 - 38.5	✓	
3352.9	3350.8	3351.8	10038	0.021	1.00	IC	50.5 - 51.5		
3363.5	3362.3	3362.3	1916	0.004	1.00	I	50.5 - 51.5		
3368.7	3367.8	3368.8	471	0.001	1.00	I	28.5 - 29.5		*
3369.4	3367.7	3369.8	1438	0.003	1.00	I	50.5 - 51.5		
3380.8	3380.3	3381.3	481	0.001	1.00	I	50.5 - 51.5		
3389.9	3388.1	3389.6	10225	0.021	1.00	IC	62.0 - 63.0	✓	*

Mass (Avg.)	Mass (Mono)	Apex Mass	Area	Relative Area	Score	Series	Time (min)	Shared Mass?	Adduct?
3392.7	3390.7	3392.7	2707	0.006	1.00	I	52.0 – 53.0	✓	
3411.2	3408.8	3410.8	90343	0.189	1.00	IC	48.0 – 49.0	✓	
3411.8	3410.3	3411.8	1999	0.004	1.00	I	50.0 – 50.5	✓	
3413.4	3412.7	3413.7	800	0.002	1.00	IC	62.0 – 63.0		
3424.8	3422.9	3424.9	1706	0.004	1.00	IC	22.5 – 23.5		*
3428.2	3427.7	3428.7	1026	0.002	1.00	I	62.0 – 63.0		
3432.1	3431.1	3432.1	784	0.002	1.00	I	24.0 – 25.0		
3432.3	3430.1	3432.1	7641	0.016	1.00	IC	22.5 – 23.5		
3433.4	3430.7	3432.7	8789	0.018	1.00	IC	48.0 – 49.0		*
3436.3	3435.1	3436.0	1247	0.003	1.00	I	24.0 – 25.0		
3449.7	3448.4	3449.4	26295	0.055	1.00	I	48.0 – 49.0	✓	
3452.5	3451.9	3451.9	1118	0.002	0.27	I	5.0 – 5.5	✓	
3454.6	3452.7	3454.7	1414	0.003	1.00	I	48.0 – 49.0		
3466.2	3463.9	3465.9	10356	0.022	1.00	IC	24.5 – 25.0		
3471.7	3469.7	3471.7	1114	0.002	1.00	IC	48.0 – 49.0		*
3476.6	3475.7	3476.7	377	0.001	1.00	I	48.0 – 49.0		
3477.4	3476.9	3477.9	262	0.001	1.00	I	5.0 – 5.5		
3478.3	3476.4	3477.9	21813	0.046	1.00	IC	40.0 – 40.5	✓	
3497.3	3494.8	3496.8	37933	0.079	1.00	IC	5.0 – 5.5		
3500.6	3498.6	3500.1	12287	0.026	1.00	IC	25.5 – 26.5	✓	
3502.8	3501.7	3502.9	438	0.001	1.00	I	24.5 – 25.0		
3507.3	3504.9	3506.9	95430	0.200	1.00	IC	28.0 – 28.5		*
3509.3	3507.9	3510.0	1948	0.004	1.00	I	5.0 – 5.5		*
3511.3	3509.1	3511.6	15761	0.033	1.00	IC	5.0 – 5.5	✓	
3517.5	3514.9	3516.9	2250	0.005	1.00	IC	36.5 – 37.5	✓	
3519.2	3517.0	3519.0	14948	0.031	1.00	IC	28.5 – 29.0	✓	
3527.6	3526.5	3527.6	4647	0.010	1.00	I	40.5 – 41.0		
3529.5	3527.0	3529.0	47969	0.100	1.00	IC	34.5 – 35.5		*
3530.2	3529.8	3530.8	4084	0.009	1.00	IC	28.0 – 28.5		
3534.0	3531.9	3533.8	778	0.002	1.00	IC	5.0 – 5.5		
3535.4	3532.9	3534.9	5452	0.011	1.00	IC	40.0 – 40.5	✓	*
3545.1	3542.8	3544.8	4348	0.009	1.00	IC	28.0 – 28.5		*
3545.4	3542.9	3545.0	13135	0.028	1.00	IC	29.5 – 30.0		*
3546.9	3545.6	3547.5	1040	0.002	1.00	I	5.0 – 5.5	✓	
3560.4	3558.1	3560.1	5112	0.011	1.00	IC	5.0 – 5.5	✓	
3567.5	3565.9	3569.0	1634	0.003	1.00	IC	35.0 – 35.5		
3588.3	3586.5	3588.0	875	0.002	1.00	I	41.0 – 42.0	✓	
3593.3	3591.5	3593.0	1953	0.004	0.89	I	5.0 – 5.5	✓	
3672.5	3670.6	3672.1	1598	0.003	1.00	I	22.5 – 23.0	✓	
3684.9	3682.5	3684.5	41066	0.086	1.00	IC	26.0 – 27.0	✓	
3685.5	3683.1	3685.1	3141	0.007	1.00	I	24.0 – 25.0	✓	
3689.6	3688.0	3689.0	1397	0.003	1.00	I	37.0 – 38.0		
3709.7	3707.1	3709.1	32410	0.068	1.00	IC	38.0 – 28.5		
3711.7	3710.1	3712.1	492	0.001	1.00	I	41.5 – 42.0		*
3722.4	3720.5	3722.0	1148	0.002	1.00	IC	48.5 – 50.0	✓	
3723.4	3721.5	3723.5	1556	0.003	1.00	IC	26.0 – 26.5	✓	
3725.6	3723.2	3725.2	8505	0.018	1.00	IC	42.0 – 42.5		*
3741.8	3739.1	3741.1	28422	0.060	1.00	IC	41.5 – 42.0		*

Mass (Avg.)	Mass (Mono)	Apex Mass	Area	Relative Area	Score	Series	Time (min)	Shared Mass?	Adduct?
3743.5	3741.9	3742.9	6777	0.014	1.00	IC	28.5 - 29.0		*
3770.6	3770.0	3770.9	1348	0.003	1.00	IC	51.0 - 52.0		
3785.0	3782.8	3784.9	3523	0.007	1.00	IC	41.5 - 42.0	✓	
3797.7	3795.0	3797.5	52149	0.109	1.00	IC	29.0 - 29.5	✓	
3819.6	3816.9	3818.9	2139	0.004	1.00	I	29.0 - 29.5	✓	*
3821.8	3821.0	3820.5	520	0.001	1.00	I	29.0 - 29.5	✓	
3825.8	3823.2	3825.1	1881	0.004	1.00	I	5.0 - 5.5		
3825.8	3824.1	3825.1	1179	0.002	0.81	I	5.0 - 5.5		
3835.3	3833.0	3834.5	2619	0.005	1.00	IC	29.0 - 29.5	✓	*
3838.0	3836.1	3838.2	360	0.001	1.00	I	5.0 - 5.5		
3840.5	3838.1	3840.1	7205	0.015	1.00	IC	24.0 - 24.5	✓	
3845.8	3844.1	3845.1	15442	0.032	1.00	IC	24.5 - 25.0		
3851.6	3849.2	3851.2	4661	0.010	1.00	IC	37.0 - 38.0		
3852.2	3850.1	3852.2	1754	0.004	1.00	IC	39.5 - 40.0		
3860.5	3859.0	3859.9	2632	0.006	1.00	IC	41.5 - 42.0		
3869.7	3867.1	3869.1	3702	0.008	1.00	IC	57.5 - 58.0		
3886.7	3884.0	3886.0	32413	0.068	1.00	IC	27.5 - 28.5		
3887.9	3885.1	3887.1	23889	0.050	1.00	IC	53.5 - 54.0		
3897.0	3894.2	3896.2	37126	0.078	1.00	IC	5.0 - 5.5		
3902.5	3900.0	3902.0	21787	0.046	1.00	IC	27.0 - 28.0		*
3908.3	3907.0	3908.0	1369	0.003	1.00	I	27.5 - 28.5		
3910.6	3908.7	3910.3	751	0.002	1.00	I	41.5 - 42.0	✓	
3911.8	3911.0	3911.0	352	0.001	1.00	I	53.5 - 54.0		
3912.5	3911.1	3912.2	1564	0.003	1.00	I	5.0 - 5.5	✓	
3913.0	3910.2	3912.2	4251	0.009	1.00	IC	5.0 - 5.5	✓	*
3913.7	3913.0	3914.0	11365	0.024	1.00	IC	38.0 - 38.5		
3913.8	3911.0	3913.0	29437	0.062	1.00	IC	38.0 - 38.5		
3914.6	3912.0	3914.0	1740	0.004	1.00	I	32.5 - 33.5	✓	
3915.1	3912.8	3914.8	824	0.002	0.80	I	33.0 - 33.5		
3917.7	3916.1	3918.1	1243	0.003	1.00	I	36.5 - 37.0		
3925.3	3924.1	3925.1	486	0.001	1.00	I	53.5 - 54.0		
3935.5	3934.1	3934.9	432	0.001	0.99	I	38.0 - 38.5		
3936.9	3934.2	3936.2	12397	0.026	1.00	I	24 - 25		
3951.8	3951.0	3951.0	424	0.001	1.00	I	38.0 - 38.5		*
3971.7	3969.2	3971.2	20654	0.043	1.00	IC	23.5 - 24.5	✓	
3973.9	3971.4	3973.3	5676	0.012	1.00	IC	39.0 - 40.0		*
3974.6	3972.2	3974.2	4537	0.010	1.00	IC	26.5 - 27.0		*
3989.8	3988.4	3989.3	912	0.002	1.00	I	39.0 - 40.0		
3993.5	3992.7	3993.7	566	0.001	1.00	I	23.5 - 24.5	✓	
4004.9	4003.2	4004.2	1939	0.004	1.00	I	25.0 - 26.0		
4005.9	4003.3	4005.3	7430	0.016	1.00	IC	34.5 - 35.5		*
4029.5	4027.3	4029.2	4348	0.009	1.00	IC	24.0 - 25.0	✓	
4037.8	4035.1	4038.2	5354	0.011	1.00	IC	24.0 - 24.5		
4055.9	4053.1	4055.1	234241	0.491	1.00	IC	24.5 - 25.0		
4078.3	4075.1	4078.1	8872	0.019	1.00	IC	24.5 - 25.0		
4088.9	4087.1	4090.1	1746	0.004	1.00	IC	24.5 - 25.0		*
4093.8	4091.1	4093.1	6153	0.013	1.00	IC	24.5 - 25.0		*
4107.1	4106.2	4108.1	497	0.001	1.00	I	24.5 - 25.0		

Mass (Avg.)	Mass (Mono)	Apex Mass	Area	Relative Area	Score	Series	Time (min)	Shared Mass?	Adduct?
4159.8	4157.5	4159.6	7007	0.015	1.00	IC	5.0 - 5.5		*
4161.2	4160.4	4160.4	449	0.001	1.00	I	23.0 - 24.0		
4176.0	4173.4	4175.4	4019	0.008	1.00	IC	34.5 - 35.5		
4176.1	4175.0	4176.1	759	0.002	1.00	I	24.5 - 25.0		
4205.3	4203.0	4204.0	23812	0.050	1.00	IC	5.0 - 5.5	✓	
4207.3	4204.5	4207.6	13650	0.029	1.00	IC	35.0 - 36.0	✓	
4217.3	4215.6	4215.6	7641	0.016	1.00	IC	5.0 - 5.5		
4258.5	4257.6	4258.5	511	0.001	1.00	I	41.0 - 42.0		
4294.3	4292.6	4292.6	4345	0.009	1.00	IC	5.0 - 5.5		
4298.9	4295.5	4298.6	4335	0.009	1.00	IC	5.0 - 5.5		
4300.5	4297.5	4299.5	94288	0.198	1.00	IC	41.5 - 42.5		
4322.5	4320.5	4322.5	1204	0.003	1.00	I	41.5 - 42.5		
4338.3	4337.5	4337.5	1098	0.002	1.00	I	41.5 - 42.5		
4364.1	4362.4	4364.5	1609	0.003	1.00	IC	23.0 - 23.5	✓	
4455.2	4454.5	4454.5	1011	0.002	1.00	I	50.5 - 51.5		
4627.3	4626.6	4626.6	1242	0.003	1.00	I	41.5 - 42.0		
4634.5	4633.2	4634.0	1697	0.004	0.94	I	41.0 - 42.0		
4713.2	4711.6	4713.7	514	0.001	1.00	I	22.5 - 23.5		
4746.9	4744.9	4745.9	661	0.001	0.94	I	24.0 - 25.0		
4930.4	4928.4	4930.4	12989	0.027	1.00	I	42.0 - 42.5	✓	
4952.1	4950.2	4952.2	1184	0.002	1.00	I	42.0 - 42.5		
4968.1	4966.3	4967.3	2555	0.005	1.00	I	42.0 - 42.5		*
5308.8	5307.7	5308.8	592	0.001	1.00	I	24.5 - 25.0		
5394.0	5393.3	5393.3	1021	0.002	1.00	I	52.5 - 53.5		
5406.7	5405.2	5406.1	1477	0.003	0.95	I	52.5 - 53.5		
5637.1	5636.0	5636.9	428	0.001	1.00	I	42.0 - 42.5		
5758.2	5757.2	5758.2	3614	0.008	0.90	I	52.5 - 53.0		
5768.9	5767.4	5769.3	782	0.002	1.00	I	41.5 - 42.0		
5899.2	5896.8	5898.8	878	0.002	1.00	I	24.5 - 25.0		
5921.9	5917.9	5920.8	5220	0.011	1.00	I	24.5 - 25.0		
5935.0	5933.8	5935.8	1056	0.002	1.00	I	24.5 - 25.0		
5954.4	5953.8	5954.7	307	0.001	1.00	I	24.5 - 25.0		
5958.4	5955.8	5958.8	1703	0.004	1.00	I	24.5 - 25.0		
5965.0	5961.8	5964.8	2089	0.004	1.00	I	24.5 - 25.0		
5996.3	5994.8	5996.7	544	0.001	1.00	I	24.5 - 25.0		
6001.3	5998.8	6002.8	787	0.002	0.94	I	24.5 - 25.0		
6006.7	6004.7	6004.7	792	0.002	0.79	I	24.5 - 25.0		
6660.5	6657.7	6659.7	442169	0.926	1.00	IC	50.5 - 51.5		
6682.9	6679.7	6681.5	35146	0.074	1.00	IC	50.5 - 51.5		*
6685.5	6683.7	6683.7	4913	0.010	0.85	I	50.5 - 51.5		
6698.1	6694.6	6697.6	43183	0.090	1.00	IC	50.5 - 51.5		
6712.5	6710.5	6712.6	2743	0.006	1.00	I	50.5 - 51.5		
6717.9	6717.8	6717.8	12296	0.026	1.00	IC	52.5 - 53.0		
6718.0	6715.7	6717.7	30442	0.064	1.00	IC	52.5 - 53.5		
6718.4	6714.8	6717.8	23778	0.050	1.00	IC	52.5 - 53.5		
6722.3	6720.7	6718.6	9203	0.019	1.00	IC	50.5 - 51.5		
6736.1	6734.5	6735.6	1421	0.003	0.99	I	50.5 - 51.5		
6740.1	6738.6	6739.7	1265	0.003	1.00	I	52.5 - 53.5		

Mass (Avg.)	Mass (Mono)	Apex Mass	Area	Relative Area	Score	Series	Time (min)	Shared Mass?	Adduct?
6741.0	6740.5	6740.5	516	0.001	0.99	I	52.5 - 53.5		
6756.3	6754.2	6755.4	4591	0.010	1.00	IC	52.5 - 53.5	✓	*
6766.9	6765.6	6765.6	819	0.002	1.00	I	50.5 - 51.5		
6780.1	6777.7	6778.7	6163	0.013	1.00	IC	50.5 - 51.5	✓	
6940.6	6937.8	6939.8	31422	0.066	1.00	IC	39.0 - 39.5		
7143.8	7142.0	7142.0	39557	0.083	1.00	I	41.5 - 42.5		
7157.5	7155.1	7157.2	76442	0.160	1.00	IC	41.0 - 42.0		
7415.8	7414.4	7414.4	14946	0.031	1.00	IC	41.0 - 42.0		

Appendix C. LC-MS Data for *Leiurus quinquestriatus hebraeus* venom.

LC-MS was performed on *Lqh* venom and data analysed as described (2.2.3.4 and 2.2.3.5). Component masses and their elution windows were calculated using LC-MS peak reconstruction software (Applied biosystems) with a mass tolerance of 0.01%, signal-to-noise ratio of 10 and 2000-10000Da final mass range. Peak areas were standardised against that of a peptide standard and the masses corresponding to those in a standard-only sample removed. Masses differing by 1Da were assumed products of peptide oxidation or amidation and their relative areas pooled. Masses suspected of representing adducted peptides were noted.

Mass (Avg) Average mass of the neutral species.

Mass (Mono) Monoisotopic mass ($[M+H]^+$). Based upon the lowest detected peak in the isotope series.

Apex Mass Mass of isotope distribution at maximum intensity.

Area Integrated total intensity (counts sec^{-1}) over the m/z range of the contributing ions.

Relative area Area standardised against that of peptide standard.

Score Least squares correlation coefficient for fit of observed values to calculated masses.

Evidence Type of series used for mass determination. I = isotope series, C = charge series, IC = isotope series that is also part of a charge series.

Time Elution window of ions contributing to mass information. Time is shown to nearest 0.5 min from initiation of data collection.

Adduct * indicates possible adduct mass. Data was examined for potential masses relating to +Na, +K, +Na+K, -CO₂, -NH₃, -H₂O, mono- and di-oxidation, in addition to +74, +104 (adducts previously observed in scorpion venom mass data (Pimenta et al., 2001)).

Mass (Avg.)	Mass (Mono.)	Apex Mass	Area	Relative Area	Score	Evidence	Time (min)	Adduct?
2003.4	2002.5	2002.5	326	0.001	1.00	I	6.0 - 6.5	
2008.2	2007.8	2007.8	2607	0.008	1.00	I	4.5 - 5.5	
2008.3	2007.2	2008.2	992	0.003	1.00	IC	35.5 - 36.0	
2014.0	2013.4	2014.4	329	0.001	1.00	I	34.0 - 35.0	
2019.6	2018.5	2019.5	2396	0.007	1.00	I	27.5 - 28.5	
2024.6	2024.2	2024.2	856	0.003	1.00	I	35.5 - 36.0	
2026.2	2025.7	2026.7	610	0.002	1.00	I	4.5 - 5.5	
2030.8	2030.0	2030.0	1440	0.004	1.00	I	27.5 - 28.5	
2046.4	2045.4	2046.4	1895	0.006	1.00	I	58.5 - 59.0	
2049.0	2048.3	2049.4	309	0.001	1.00	I	4.5 - 5.5	
2052.2	2051.3	2052.4	845	0.003	1.00	I	60.0 - 60.5	*
2055.6	2054.4	2055.4	1837	0.005	1.00	I	50.5 - 51.0	
2057.3	2056.7	2057.7	2877	0.009	1.00	I	42.0 - 42.5	
2060.9	2059.8	2059.8	810	0.002	1.00	I	4.5 - 5.5	
2068.2	2067.4	2068.3	995	0.003	1.00	I	58.5 - 59.0	*
2071.0	2070.4	2071.4	560	0.002	1.00	IC	50.5 - 51.0	*
2074.2	2073.3	2074.3	634	0.002	1.00	I	60.0 - 60.5	*
2084.2	2083.3	2083.3	641	0.002	1.00	I	58.5 - 59.0	*
2090.1	2089.3	2090.3	348	0.001	1.00	I	60.0 - 60.5	*
2094.3	2093.4	2094.4	955	0.003	1.00	I	49.5 - 50.0	
2098.5	2097.5	2098.4	913	0.003	0.90	I	37.0 - 38.0	
2114.0	2113.4	2114.5	468	0.001	1.00	IC	37.0 - 38.0	
2124.4	2122.8	2123.8	911	0.003	1.00	I	4.5 - 5.5	
2139.3	2137.9	2137.9	1293	0.004	1.00	I	4.5 - 5.5	
2140.0	2139.3	2139.3	778	0.002	0.89	I	4.5 - 5.5	
2141.5	2140.4	2141.4	694	0.002	1.00	I	33.0 - 33.5	
2145.0	2144.5	2145.5	535	0.002	1.00	I	42.0 - 42.5	*
2148.5	2147.3	2148.3	32427	0.097	1.00	IC	4.5 - 5.5	*
2150.5	2149.4	2150.4	16687	0.050	1.00	IC	48.0 - 48.5	*
2156.6	2155.2	2155.2	1131	0.003	0.29	I	4.5 - 5.5	
2159.3	2158.8	2158.8	697	0.002	0.97	I	4.5 - 5.5	
2161.2	2160.3	2161.2	1370	0.004	1.00	IC	4.5 - 5.5	
2163.0	2162.5	2163.5	3614	0.011	1.00	I	36.5 - 37.0	
2165.5	2164.6	2165.6	613	0.002	1.00	I	44.0 - 44.5	
2168.4	2167.8	2167.8	8525	0.025	1.00	IC	4.5 - 5.5	
2172.6	2171.4	2172.4	1725	0.005	1.00	I	48.0 - 48.5	*
2173.0	2172.5	2172.5	199	0.001	1.00	I	6.0 - 6.5	
2176.7	2175.3	2176.2	1398	0.004	1.00	I	4.5 - 5.5	
2180.2	2179.3	2179.3	565	0.002	1.00	I	4.5 - 5.5	
2180.4	2179.5	2180.5	644	0.002	1.00	I	38.0 - 38.5	
2180.9	2180.3	2181.3	192	0.001	1.00	I	4.5 - 5.5	
2183.9	2182.5	2183.5	693	0.002	1.00	I	36.5 - 37.0	
2186.3	2185.8	2186.8	295	0.001	1.00	I	4.5 - 5.5	
2199.7	2198.5	2199.5	1312	0.004	1.00	I	40.5 - 41.0	*
2208.0	2207.5	2208.5	418	0.001	1.00	I	46.0 - 46.5	
2210.7	2209.5	2210.5	1483	0.004	1.00	I	29.5 - 30.5	*
2213.9	2212.5	2213.5	779	0.002	1.00	I	37.0 - 37.5	

Mass (Avg.)	Mass (Mono.)	Apex Mass	Area	Relative Area	Score	Evidence	Time (min)	Adduct?
2214.6	2213.5	2214.5	1660	0.005	1.00	I	42.0 - 42.5	
2216.0	2214.9	2215.9	298	0.001	0.89	I	4.5 - 5.5	
2217.4	2216.5	2217.5	818	0.002	1.00	I	48.5 - 49.0	
2229.5	2228.3	2229.4	477	0.001	1.00	I	4.5 - 5.5	
2230.9	2229.5	2230.5	3515	0.010	1.00	I	49.0 - 49.5	
2232.5	2231.5	2232.5	2546	0.008	1.00	IC	42.0 - 42.5	*
2237.4	2236.5	2237.5	426	0.001	1.00	I	38.0 - 38.5	*
2238.3	2237.5	2238.4	599	0.002	1.00	I	34.0 - 34.5	
2246.5	2245.5	2246.5	2780	0.008	1.00	IC	49.0 - 49.5	*
2249.6	2248.6	2249.6	635	0.002	1.00	I	42.5 - 43.5	*
2250.7	2249.5	2250.5	3525	0.010	1.00	I	36.5 - 37.0	
2252.5	2251.6	2252.6	29583	0.088	0.89	I	48.0 - 49.0	
2254.2	2253.3	2254.3	915	0.003	1.00	I	52.0 - 52.5	*
2254.7	2253.5	2254.6	1883	0.006	1.00	I	36.5 - 37.0	*
2255.5	2254.9	2254.9	647	0.002	0.99	I	4.5 - 5.5	
2259.9	2258.4	2259.5	1097	0.003	1.00	I	48.0 - 48.5	*
2261.2	2260.9	2260.9	373	0.001	1.00	I	48.0 - 49.0	
2263.4	2263.0	2263.9	325	0.001	0.99	I	48.0 - 49.0	
2275.4	2274.4	2275.5	513	0.002	1.00	I	48.0 - 48.5	*
2276.2	2275.3	2276.3	360	0.001	1.00	I	41.5 - 42.0	*
2293.8	2292.6	2293.6	1586	0.005	1.00	I	52.0 - 52.5	
2296.8	2295.6	2296.6	2723	0.008	1.00	I	41.5 - 42.0	
2308.7	2307.5	2308.5	2923	0.009	1.00	IC	50.5 - 51.5	
2318.2	2317.3	2318.4	586	0.002	1.00	I	35.5 - 36.0	
2326.5	2325.5	2326.5	729	0.002	1.00	I	44.5 - 45.0	*
2331.0	2330.5	2330.5	570	0.002	1.00	I	50.5 - 51.5	
2344.1	2342.6	2343.6	400	0.001	1.00	I	6.0 - 6.5	*
2344.7	2343.3	2344.3	3407	0.010	1.00	IC	4.5 - 5.5	
2350.8	2349.6	2350.6	1876	0.006	1.00	I	43.0 - 44.0	
2367.0	2365.6	2366.6	5028	0.015	1.00	I	41.5 - 42.0	
2374.9	2373.5	2374.5	4535	0.014	1.00	IC	48.5 - 49.0	
2379.6	2378.6	2379.6	447	0.001	1.00	I	51.0 - 51.5	*
2380.6	2379.6	2380.6	697	0.002	1.00	I	48.5 - 49.0	
2394.4	2393.7	2393.7	2349	0.007	1.00	I	43.0 - 43.5	
2396.5	2395.6	2395.6	480	0.001	1.00	I	48.5 - 49.0	*
2424.6	2423.6	2424.6	566	0.002	1.00	I	31.5 - 32.0	*
2437.0	2435.6	2436.7	3431	0.010	1.00	I	38.5 - 39.5	
2447.1	2445.7	2446.7	8081	0.024	1.00	IC	42.0 - 42.5	
2447.5	2445.8	2446.7	887	0.003	1.00	I	39.5 - 40.5	
2447.6	2446.6	2447.7	708	0.002	1.00	I	46.0 - 46.5	
2455.7	2454.6	2455.6	1306	0.004	1.00	I	44.0 - 45.0	
2472.9	2471.6	2472.6	1763	0.005	1.00	I	40.5 - 41.0	
2520.8	2519.8	2520.7	619	0.002	1.00	I	51.5 - 52.0	
2521.0	2519.8	2520.7	1346	0.004	1.00	I	49.5 - 50.5	
2521.4	2519.8	2520.8	8887	0.026	1.00	IC	53.5 - 54.0	*
2524.0	2522.6	2524.7	770	0.002	1.00	I	42.0 - 42.5	
2524.8	2523.6	2524.6	572	0.002	1.00	I	39.5 - 40.5	
2525.3	2524.6	2524.6	1477	0.004	1.00	I	42.0 - 42.5	

Mass (Avg.)	Mass (Mono.)	Apex Mass	Area	Relative Area	Score	Evidence	Time (min)	Adduct?
2526.0	2525.6	2525.6	429	0.001	1.00	I	39.5 - 40.5	
2527.7	2526.7	2526.7	2179	0.006	1.00	I	42.0 - 42.5	
2535.7	2534.7	2535.7	1231	0.004	1.00	I	45.0 - 46.0	
2536.5	2535.7	2535.7	288	0.001	1.00	I	6.0 - 6.5	
2557.8	2556.8	2557.7	255	0.001	1.00	I	2.0 - 3.0	*
2559.0	2557.7	2558.8	869	0.003	1.00	I	53.5 - 54.0	*
2561.4	2560.6	2561.7	204	0.001	0.98	I	2.0 - 3.0	
2564.6	2562.7	2563.7	595	0.002	1.00	I	2.0 - 3.0	
2573.2	2571.0	2571.9	1348	0.004	1.00	I	4.5 - 5.5	
2573.7	2572.7	2573.7	617	0.002	1.00	I	40.5 - 41.5	*
2574.4	2574.0	2574.0	587	0.002	1.00	I	4.5 - 5.5	
2576.2	2574.7	2575.7	455	0.001	1.00	I	2.0 - 3.0	
2577.8	2576.7	2577.8	1896	0.006	1.00	I	45.5 - 46.0	
2577.8	2576.8	2577.8	3054	0.009	1.00	I	46.5 - 47.0	
2577.8	2576.8	2577.8	3945	0.012	1.00	I	47.5 - 48.0	
2590.0	2589.6	2589.6	164	0.000	1.00	I	2.0 - 3.0	
2593.1	2591.8	2592.8	2148	0.006	1.00	I	42.0 - 42.5	
2593.5	2592.9	2592.9	592	0.002	1.00	I	37.5 - 38.0	
2600.2	2598.8	2599.8	641	0.002	1.00	I	47.5 - 48.0	*
2608.3	2606.7	2607.7	399	0.001	1.00	I	2.0 - 3.0	*
2615.8	2614.8	2615.8	551	0.002	1.00	I	47.5 - 48.0	*
2616.6	2615.7	2615.7	322	0.001	1.00	I	2.0 - 3.0	
2621.1	2619.8	2620.9	3102	0.009	1.00	IC	36.0 - 36.5	
2624.1	2622.6	2623.7	347	0.001	0.89	I	2.0 - 3.0	*
2628.1	2626.8	2627.8	2275	0.007	1.00	I	44.5 - 45.0	*
2636.5	2634.6	2635.7	572	0.002	1.00	I	2.0 - 3.0	
2643.1	2641.8	2642.8	1371	0.004	1.00	I	55.0 - 56.0	*
2656.7	2654.8	2655.7	500	0.001	1.00	I	2.0 - 3.0	
2665.2	2664.7	2665.7	185	0.001	1.00	I	2.0 - 3.0	*
2692.6	2691.7	2691.7	366	0.001	1.00	I	2.0 - 3.0	
2697.6	2696.6	2697.7	228	0.001	1.00	I	2.0 - 3.0	
2702.1	2701.7	2701.7	180	0.001	1.00	I	2.0 - 3.0	
2717.2	2715.8	2716.8	1703	0.005	1.00	I	66.0 - 66.5	*
2728.5	2727.6	2727.6	319	0.001	1.00	I	2.0 - 3.0	
2731.1	2730.4	2730.4	885	0.003	1.00	I	4.5 - 5.5	
2737.3	2736.6	2737.7	129	0.000	0.99	I	2.0 - 3.0	
2747.1	2745.5	2746.4	2217	0.007	1.00	IC	4.5 - 5.5	
2799.6	2798.3	2800.5	598	0.002	0.99	I	4.5 - 5.5	
2800.4	2799.4	2800.5	755	0.002	0.89	I	4.5 - 5.5	
2806.4	2804.5	2805.6	3260	0.010	1.00	I	4.5 - 5.5	
2810.5	2809.6	2809.6	1336	0.004	1.00	I	4.5 - 5.5	
2813.9	2813.6	2813.6	154	0.000	0.99	I	4.5 - 5.5	
2818.3	2816.6	2817.6	1235	0.004	1.00	I	4.5 - 5.5	
2819.3	2818.6	2818.6	519	0.002	0.88	I	4.5 - 5.5	
2824.5	2823.6	2823.6	299	0.001	1.00	I	2.0 - 3.0	
2827.2	2826.5	2827.5	226	0.001	1.00	I	4.5 - 5.5	
2829.6	2828.5	2829.6	868	0.003	1.00	I	4.5 - 5.5	
2844.5	2843.6	2844.5	3639	0.011	1.00	IC	4.5 - 5.5	

Mass (Avg.)	Mass (Mono.)	Apex Mass	Area	Relative Area	Score	Evidence	Time (min)	Adduct?
2846.5	2844.5	2845.6	10621	0.032	1.00	IC	4.5 - 5.5	*
2846.7	2845.6	2846.5	7829	0.023	1.00	IC	4.5 - 5.5	
2900.2	2898.6	2901.7	408	0.001	0.87	I	4.5 - 5.5	
2902.0	2900.6	2901.7	755	0.002	1.00	I	4.5 - 5.5	
2906.6	2905.6	2906.6	496	0.001	1.00	I	4.5 - 5.5	*
2913.1	2912.6	2912.6	141	0.000	0.99	I	4.5 - 5.5	
2917.5	2915.6	2916.7	7246	0.022	1.00	IC	4.5 - 5.5	
2919.0	2918.6	2918.6	1233	0.004	1.00	I	4.5 - 5.5	
2924.7	2922.6	2923.6	87790	0.261	1.00	IC	4.5 - 5.5	
2926.7	2925.6	2925.6	1983	0.006	0.72	I	4.5 - 5.5	
2932.7	2930.6	2931.7	2684	0.008	1.00	IC	4.5 - 5.5	
2935.1	2933.7	2933.7	991	0.003	1.00	IC	4.5 - 5.5	
2940.5	2939.5	2940.6	360	0.001	0.88	I	4.5 - 5.5	
2945.3	2943.7	2945.7	9832	0.029	1.00	IC	4.5 - 5.5	
2948.5	2946.6	2947.6	29385	0.087	1.00	IC	4.5 - 5.5	*
2950.6	2949.6	2949.6	5780	0.017	1.00	IC	4.5 - 5.5	*
2957.8	2956.6	2958.6	1890	0.006	1.00	IC	4.5 - 5.5	
2958.7	2957.6	2959.6	2987	0.009	1.00	IC	4.5 - 5.5	*
2962.7	2960.7	2962.7	793181	2.362	1.00	IC	4.5 - 5.5	*
2966.2	2964.6	2965.6	71244	0.212	1.00	IC	23.0 - 24.0	
2973.6	2972.6	2973.6	579	0.002	1.00	I	4.5 - 5.5	*
2979.3	2977.6	2978.6	51858	0.154	1.00	IC	4.5 - 5.5	
2985.1	2982.6	2984.6	25083	0.075	1.00	IC	4.5 - 5.5	
2985.7	2985.6	2985.6	4002	0.012	1.00	IC	4.5 - 5.5	
2986.0	2984.6	2984.6	5452	0.016	1.00	IC	4.5 - 5.5	
2990.5	2988.6	2989.7	2921	0.009	1.00	I	4.5 - 5.5	
2995.9	2994.6	2995.7	27436	0.082	1.00	IC	4.5 - 5.5	*
2998.7	2997.7	2998.6	8293	0.025	1.00	IC	4.5 - 5.5	
3001.1	2999.6	3000.6	50870	0.151	1.00	IC	4.5 - 5.5	*
3006.6	3004.6	3005.6	9497	0.028	1.00	IC	4.5 - 5.5	*
3009.5	3009.7	3010.6	1929	0.006	1.00	IC	4.5 - 5.5	
3012.6	3010.7	3012.7	8293	0.025	1.00	IC	4.5 - 5.5	*
3015.7	3013.7	3014.6	5558	0.017	1.00	IC	4.5 - 5.5	
3016.8	3017.7	3017.7	2028	0.006	1.00	IC	4.5 - 5.5	*
3016.8	3015.6	3015.6	2253	0.007	1.00	IC	4.5 - 5.5	
3022.9	3021.6	3022.6	5596	0.017	1.00	IC	4.5 - 5.5	*
3024.4	3022.6	3022.6	1213	0.004	1.00	IC	4.5 - 5.5	*
3027.9	3026.6	3027.6	2348	0.007	1.00	IC	4.5 - 5.5	
3028.2	3026.6	3027.7	4595	0.014	1.00	IC	4.5 - 5.5	*
3033.0	3030.6	3033.6	2763	0.008	1.00	IC	4.5 - 5.5	
3036.2	3035.6	3036.6	752	0.002	1.00	IC	4.5 - 5.5	
3039.0	3037.6	3038.5	4752	0.014	1.00	IC	4.5 - 5.5	*
3042.2	3040.7	3040.6	1409	0.004	1.00	IC	4.5 - 5.5	
3045.1	3043.6	3044.5	1296	0.004	1.00	IC	4.5 - 5.5	*
3046.5	3045.7	3045.7	307	0.001	1.00	I	4.5 - 5.5	
3051.3	3049.7	3050.6	1798	0.005	1.00	IC	4.5 - 5.5	
3053.0	3051.6	3051.6	416	0.001	0.30	I	4.5 - 5.5	*
3061.5	3059.7	3061.7	1627	0.005	1.00	IC	4.5 - 5.5	

Mass (Avg.)	Mass (Mono.)	Apex Mass	Area	Relative Area	Score	Evidence	Time (min)	Adduct?
3069.2	3067.7	3069.7	781	0.002	1.00	I	4.5 - 5.5	*
3075.9	3074.6	3075.6	1229	0.004	1.00	IC	4.5 - 5.5	
3077.8	3077.7	3078.7	1711	0.005	1.00	IC	4.5 - 5.5	
3081.6	3080.6	3081.7	3818	0.011	1.00	IC	4.5 - 5.5	
3097.4	3095.6	3095.6	664	0.002	1.00	IC	4.5 - 5.5	
3136.7	3135.8	3136.8	260	0.001	1.00	I	4.5 - 5.5	
3165.4	3163.7	3164.8	342	0.001	1.00	I	4.5 - 5.5	*
3166.3	3165.8	3166.8	166	0.000	1.00	I	4.5 - 5.5	
3173.3	3169.7	3174.6	1057	0.003	1.00	IC	4.5 - 5.5	
3181.3	3180.7	3181.7	6694	0.020	1.00	I	4.5 - 5.5	
3183.0	3180.8	3182.7	225139	0.670	1.00	IC	4.5 - 5.5	
3193.8	3192.8	3192.8	9162	0.027	1.00	IC	4.5 - 5.5	
3199.5	3197.7	3199.7	3065	0.009	1.00	IC	4.5 - 5.5	
3205.4	3202.7	3203.7	3734	0.011	1.00	IC	4.5 - 5.5	
3207.0	3204.8	3206.7	21954	0.065	1.00	IC	23.0 - 24.0	
3210.6	3209.7	3209.7	318	0.001	0.88	I	4.5 - 5.5	*
3216.8	3213.8	3214.9	6280	0.019	1.00	IC	4.5 - 5.5	
3217.0	3215.5	3217.5	859	0.003	1.00	I	49.0 - 50.0	
3220.5	3218.7	3220.7	5936	0.018	1.00	IC	4.5 - 5.5	
3222.1	3221.7	3221.7	916	0.003	1.00	I	4.5 - 5.5	
3224.8	3223.7	3223.7	408	0.001	0.88	I	4.5 - 5.5	
3227.3	3226.8	3226.8	956	0.003	1.00	IC	4.5 - 5.5	
3231.5	3230.7	3230.7	593	0.002	1.00	I	4.5 - 5.5	
3235.0	3232.7	3234.7	1142	0.003	1.00	IC	4.5 - 5.5	
3281.8	3279.8	3281.7	468	0.001	1.00	I	4.5 - 5.5	
3282.6	3281.7	3281.7	272	0.001	1.00	I	4.5 - 5.5	
3354.9	3353.8	3355.8	1560	0.005	1.00	I	56.0 - 57.0	
3359.8	3357.9	3359.8	6030	0.018	1.00	IC	31.0 - 31.5	
3370.3	3368.4	3370.3	655	0.002	0.81	I	4.5 - 5.5	
3370.9	3370.4	3371.4	390	0.001	1.00	I	4.5 - 5.5	
3420.7	3419.0	3420.0	21523	0.064	1.00	IC	4.5 - 5.5	
3421.4	3420.0	3420.0	2435	0.007	0.00	I	4.5 - 5.5	
3422.4	3422.0	3422.0	2537	0.008	1.00	I	4.5 - 5.5	
3423.5	3421.1	3423.1	33941	0.101	1.00	IC	28.0 - 29.0	
3445.0	3443.0	3444.1	1033	0.003	1.00	I	4.5 - 5.5	
3505.5	3503.0	3505.0	20968	0.062	1.00	IC	40.5 - 41.0	
3506.5	3504.0	3506.0	6811	0.020	1.00	IC	36.5 - 37.0	
3534.3	3533.0	3534.0	410	0.001	1.00	I	37.0 - 37.5	
3541.1	3538.9	3540.9	2374	0.007	1.00	I	26.5 - 37.5	
3542.4	3540.0	3542.0	6322	0.019	1.00	IC	35.5 - 36.0	
3543.0	3542.0	3543.0	1407	0.004	1.00	IC	40.5 - 41.0	
3558.5	3556.0	3558.0	97759	0.291	1.00	IC	34.5 - 35.5	*
3574.2	3571.9	3574.0	3954	0.012	1.00	IC	34.5 - 35.5	*
3578.1	3577.0	3578.1	1022	0.003	1.00	I	40.5 - 41.0	
3578.5	3576.0	3578.0	38456	0.115	1.00	IC	38.0 - 38.5	
3580.8	3577.9	3578.9	7361	0.022	1.00	IC	34.5 - 35.5	
3596.1	3593.9	3595.9	6210	0.018	1.00	IC	34.5 - 35.5	*
3600.3	3599.0	3600.0	1354	0.004	1.00	I	37.5 - 38.5	

Mass (Avg.)	Mass (Mono.)	Apex Mass	Area	Relative Area	Score	Evidence	Time (min)	Adduct?
3602.1	3599.9	3601.9	1547	0.005	1.00	I	34.5 - 35.5	
3616.0	3614.0	3616.0	1069	0.003	1.00	I	37.5 - 38.5	
3627.0	3626.0	3627.0	547	0.002	1.00	I	24.5 - 25.5	
3645.4	3643.0	3645.0	228896	0.682	1.00	IC	24.5 - 25.5	
3646.5	3643.9	3645.9	97876	0.291	1.00	IC	28.0 - 29.0	
3661.8	3660.9	3660.9	768	0.002	1.00	I	24.5 - 25.5	
3668.1	3665.0	3666.9	11438	0.034	1.00	IC	24.5 - 25.5	
3668.3	3665.8	3667.9	3601	0.011	1.00	IC	28.0 - 29.0	
3673.7	3672.2	3673.3	1096	0.003	1.00	I	27.0 - 28.0	
3675.4	3673.0	3674.9	15284	0.046	1.00	IC	25.0 - 26.0	
3676.5	3673.9	3675.9	74398	0.222	1.00	IC	28.0 - 29.0	*
3682.9	3680.9	3681.9	14096	0.042	1.00	IC	25.0 - 26.0	
3683.7	3681.8	3682.8	1362	0.004	1.00	I	28.0 - 29.0	
3684.7	3683.8	3683.8	1913	0.006	1.00	I	28.0 - 29.0	
3689.2	3686.9	3688.9	2485	0.007	1.00	I	24.5 - 25.5	
3691.7	3689.3	3691.2	18353	0.055	1.00	IC	28.0 - 29.0	
3691.9	3691.0	3692.0	642	0.002	1.00	I	25.0 - 26.0	
3697.9	3697.0	3697.9	844	0.003	1.00	IC	25.0 - 26.0	
3699.0	3696.8	3697.9	3726	0.011	1.00	IC	28.5 - 29.5	
3705.2	3702.9	3705.9	1726	0.005	1.00	IC	24.5 - 25.5	*
3709.3	3708.3	3709.2	451	0.001	1.00	I	30.5 - 31.5	
3711.0	3708.9	3711.9	1372	0.004	1.00	IC	25.0 - 26.0	
3714.5	3712.8	3713.9	5929	0.018	1.00	IC	28.5 - 29.5	
3720.1	3717.8	3719.8	1403	0.004	1.00	IC	28.5 - 29.0	*
3721.9	3719.9	3720.9	1160	0.003	1.00	IC	25.0 - 25.5	
3727.3	3725.9	3726.8	347	0.001	0.89	I	25.0 - 25.5	
3736.7	3735.8	3735.8	222	0.001	1.00	I	28.5 - 29.0	
3743.3	3741.9	3743.9	449	0.001	1.00	I	25.0 - 25.5	*
3752.8	3750.2	3752.3	20731	0.062	1.00	IC	25.5 - 26.5	
3765.8	3763.9	3764.9	512	0.002	1.00	I	25.0 - 25.5	
3766.8	3764.3	3766.3	182411	0.543	1.00	IC	26.5 - 27.0	
3775.1	3774.2	3774.2	510	0.002	1.00	I	25.5 - 26.5	
3788.8	3786.2	3788.2	18234	0.054	1.00	IC	26.5 - 27.0	*
3804.5	3802.3	3804.2	16745	0.050	1.00	IC	26.5 - 27.0	
3810.4	3808.2	3810.2	3553	0.011	0.96	I	26.5 - 27.0	
3831.7	3830.2	3831.2	1437	0.004	1.00	I	26.5 - 27.0	
3842.2	3841.2	3842.2	510	0.002	1.00	I	26.5 - 27.0	
3848.0	3846.2	3848.2	1258	0.004	1.00	IC	26.5 - 27.0	*
3859.6	3858.4	3858.4	1172	0.003	1.00	I	4.5 - 5.5	
3859.7	3857.5	3858.4	1966	0.006	1.00	I	4.5 - 5.5	
3861.8	3859.1	3861.0	13760	0.041	1.00	IC	28.5 - 29.0	
3864.9	3864.1	3864.1	742	0.002	1.00	I	26.0 - 26.5	
3865.9	3863.3	3865.4	12676	0.038	1.00	IC	27.5 - 28.0	
3868.2	3867.2	3868.2	699	0.002	1.00	I	48.0 - 49.0	
3873.8	3873.3	3874.3	405	0.001	1.00	I	48.0 - 49.0	
3894.6	3893.2	3894.3	862	0.003	1.00	I	31.0 - 31.5	
3897.1	3894.4	3897.5	1583	0.005	1.00	IC	4.5 - 5.5	
3897.2	3895.4	3897.4	2385	0.007	1.00	IC	4.5 - 5.5	

Mass (Avg.)	Mass (Mono.)	Apex Mass	Area	Relative Area	Score	Evidence	Time (min)	Adduct?
3914.9	3912.4	3914.4	30964	0.092	1.00	IC	4.5 - 5.5	
3916.0	3915.4	3915.4	9202	0.027	1.00	IC	4.5 - 5.5	
3921.9	3920.4	3921.3	1439	0.004	1.00	I	29.5 - 30.5	*
3932.7	3931.4	3932.4	799	0.002	1.00	I	4.5 - 5.5	
3934.7	3933.4	3934.4	2620	0.008	1.00	IC	4.5 - 5.5	
3936.1	3934.4	3935.4	5611	0.017	1.00	IC	4.5 - 5.5	
3948.7	3946.5	3947.4	688	0.002	1.00	I	4.5 - 5.5	
3951.3	3949.4	3950.4	734	0.002	1.00	I	4.5 - 5.5	
3958.4	3955.5	3958.5	4400	0.013	1.00	IC	4.5 - 5.5	
3959.5	3958.5	3958.5	1332	0.004	1.00	IC	4.5 - 5.5	
3969.8	3967.3	3969.3	1905	0.006	1.00	I	4.5 - 5.5	*
3977.6	3976.1	3977.1	732	0.002	1.00	I	26.5 - 37.5	
3995.7	3993.1	3995.1	391795	1.167	1.00	IC	27.5 - 28.5	
3996.9	3994.1	3997.1	107700	0.321	1.00	IC	30.5 - 31.0	
4015.3	4012.4	4014.5	14855	0.044	1.00	IC	4.5 - 5.5	
4018.1	4015.1	4017.0	18541	0.055	1.00	IC	27.5 - 28.5	
4019.4	4016.0	4018.0	7489	0.022	1.00	IC	30.5 - 31.0	
4028.4	4027.1	4028.1	1459	0.004	1.00	IC	27.5 - 28.5	
4033.7	4031.0	4033.1	22042	0.066	1.00	IC	27.5 - 28.5	*
4034.9	4032.0	4034.0	6627	0.020	1.00	IC	30.5 - 31.0	*
4038.5	4036.4	4038.4	1238	0.004	0.96	I	4.5 - 5.5	
4039.7	4037.0	4039.0	4719	0.014	1.00	I	27.5 - 28.5	
4040.2	4038.0	4041.0	2055	0.006	1.00	IC	30.5 - 31.0	
4042.9	4042.4	4043.4	397	0.001	1.00	I	4.5 - 5.5	
4048.0	4047.4	4048.5	375	0.001	1.00	I	4.5 - 5.5	
4053.2	4050.4	4053.4	4648	0.014	1.00	IC	4.5 - 5.5	*
4054.0	4051.1	4054.1	30978	0.092	1.00	IC	29.0 - 30.0	
4054.6	4053.4	4053.4	750	0.002	0.27	I	4.5 - 5.5	
4054.9	4052.0	4054.1	1390	0.004	0.94	I	32.0 - 33.0	
4055.8	4054.0	4055.0	3829	0.011	1.00	IC	27.5 - 28.5	
4061.0	4059.0	4061.0	1758	0.005	1.00	I	4.5 - 5.5	
4065.1	4062.3	4064.3	49558	0.148	1.00	IC	31.0 - 31.5	
4070.5	4068.4	4070.3	87546	0.261	1.00	IC	4.5 - 5.5	*
4073.4	4073.0	4073.0	308	0.001	1.00	I	27.5 - 28.5	
4076.1	4075.1	4076.1	373	0.001	1.00	I	29.0 - 30.0	
4077.2	4074.9	4078.0	1334	0.004	1.00	IC	27.5 - 28.5	
4084.5	4082.3	4086.4	288	0.001	0.72	I	4.5 - 5.5	
4085.0	4083.3	4084.3	2384	0.007	1.00	IC	4.5 - 5.5	
4085.8	4084.4	4087.4	400	0.001	0.89	I	4.5 - 5.5	
4090.5	4088.5	4089.5	13031	0.039	1.00	IC	4.5 - 5.5	
4091.7	4089.5	4091.5	22790	0.068	1.00	IC	4.5 - 5.5	*
4091.9	4091.1	4091.1	484	0.001	1.00	I	29.0 - 30.0	*
4094.6	4092.1	4094.1	4192	0.012	1.00	IC	27.5 - 28.5	
4102.9	4101.3	4102.3	2761	0.008	1.00	I	31.0 - 31.5	
4105.0	4104.4	4105.4	444	0.001	1.00	I	4.5 - 5.5	
4107.6	4105.4	4108.4	3338	0.010	1.00	IC	4.5 - 5.5	*
4114.5	4111.6	4114.6	26242	0.078	1.00	IC	4.5 - 5.5	
4115.5	4114.6	4114.6	4853	0.014	1.00	IC	4.5 - 5.5	

Mass (Avg.)	Mass (Mono.)	Apex Mass	Area	Relative Area	Score	Evidence	Time (min)	Adduct?
4116.2	4114.1	4117.1	3648	0.011	1.00	IC	27.5 - 28.5	
4123.6	4121.4	4124.5	735	0.002	1.00	I	4.5 - 5.5	*
4128.9	4127.5	4127.5	391	0.001	0.94	I	4.5 - 5.5	*
4138.1	4136.5	4138.5	18877	0.056	1.00	IC	28.0 - 29.0	
4149.5	4147.6	4148.6	3121	0.009	1.00	IC	4.5 - 5.5	
4166.1	4163.2	4165.3	87240	0.260	1.00	IC	30.0 - 30.5	
4192.0	4190.6	4192.6	1326	0.004	1.00	IC	4.5 - 5.5	
4207.0	4205.4	4207.3	594	0.002	1.00	I	24.5 - 25.5	*
4210.0	4207.5	4210.4	1392	0.004	1.00	I	4.5 - 5.5	
4248.1	4246.6	4248.6	570	0.002	0.93	I	4.5 - 5.5	
4248.7	4247.6	4248.7	1150	0.003	1.00	IC	4.5 - 5.5	
4268.2	4265.5	4267.5	5217	0.016	1.00	IC	4.5 - 5.5	
4278.9	4276.5	4277.4	1538	0.005	1.00	I	4.5 - 5.5	
4296.5	4293.5	4295.5	212286	0.632	1.00	IC	4.5 - 5.5	
4297.9	4296.5	4296.5	17885	0.053	0.00	I	4.5 - 5.5	
4306.4	4305.5	4305.5	343	0.001	1.00	I	34.0 - 35.0	
4309.8	4309.5	4310.5	1176	0.004	1.00	IC	4.5 - 5.5	
4312.5	4309.5	4312.5	12910	0.038	1.00	IC	4.5 - 5.5	*
4318.0	4315.5	4319.4	1795	0.005	1.00	IC	4.5 - 5.5	
4319.0	4318.4	4319.5	335	0.001	1.00	I	4.5 - 5.5	
4322.6	4321.5	4323.5	11555	0.034	1.00	IC	4.5 - 5.5	*
4329.6	4327.5	4329.5	7177	0.021	1.00	IC	4.5 - 5.5	
4333.8	4333.4	4332.5	3656	0.011	1.00	IC	4.5 - 5.5	
4336.6	4333.5	4335.5	48747	0.145	1.00	IC	4.5 - 5.5	
4345.3	4342.5	4343.5	1697	0.005	1.00	IC	4.5 - 5.5	
4346.5	4345.6	4344.6	1081	0.003	1.00	IC	4.5 - 5.5	
4350.3	4348.5	4350.5	478	0.001	0.76	I	4.5 - 5.5	
4352.7	4349.6	4352.5	2721	0.008	1.00	IC	4.5 - 5.5	*
4355.5	4352.5	4355.4	9367	0.028	1.00	IC	30.5 - 31.0	
4356.0	4354.4	4354.4	3716	0.011	1.00	IC	25.0 - 25.5	
4358.4	4355.5	4358.5	1142	0.003	1.00	IC	4.5 - 5.5	*
4358.9	4358.5	4358.5	237	0.001	0.99	I	4.5 - 5.5	
4366.1	4364.5	4365.6	392	0.001	0.72	I	4.5 - 5.5	*
4367.4	4363.5	4365.6	991	0.003	1.00	IC	4.5 - 5.5	
4372.3	4369.5	4372.4	1357	0.004	1.00	I	4.5 - 5.5	*
4412.4	4411.7	4412.7	4392	0.013	1.00	IC	4.5 - 5.5	
4412.8	4409.7	4412.7	10195	0.030	1.00	IC	4.5 - 5.5	
4414.5	4413.7	4413.7	2460	0.007	1.00	IC	4.5 - 5.5	
4470.2	4467.5	4469.5	2681	0.008	1.00	I	25.0 - 25.5	
4475.9	4472.6	4475.6	21645	0.064	1.00	IC	4.5 - 5.5	
4485.4	4482.5	4485.5	10333	0.031	1.00	IC	26.5 - 27.0	
4492.1	4490.6	4492.6	617	0.002	1.00	I	4.5 - 5.5	
4493.0	4492.6	4492.6	208	0.001	1.00	I	4.5 - 5.5	
4502.2	4500.6	4500.6	255	0.001	0.75	I	4.5 - 5.5	
4502.2	4499.7	4501.7	486	0.001	0.98	I	4.5 - 5.5	
4513.8	4511.7	4512.7	675	0.002	1.00	I	4.5 - 5.5	
4528.7	4527.7	4527.7	795	0.002	1.00	I	4.5 - 5.5	
4741.1	4738.8	4739.8	6470	0.019	1.00	IC	31.5 - 32.0	

Mass (Avg.)	Mass (Mono.)	Apex Mass	Area	Relative Area	Score	Evidence	Time (min)	Adduct?
4819.6	4818.0	4819.9	513	0.002	1.00	I	27.5 - 28.0	
4862.4	4861.8	4862.8	251	0.001	1.00	I	23.0 - 24.0	
4889.5	4887.9	4888.9	1147	0.003	1.00	I	24.5 - 25.5	
4895.5	4894.9	4896.0	299	0.001	0.99	I	4.5 - 5.5	
4931.0	4929.5	4929.5	19039	0.057	1.00	I	42.0 - 42.5	
4952.6	4950.4	4952.3	4885	0.015	1.00	IC	42.0 - 42.5	
4968.3	4966.5	4968.4	5609	0.017	1.00	I	42.0 - 42.5	
4974.1	4973.2	4973.2	1102	0.003	1.00	I	42.0 - 42.5	
4990.3	4988.4	4990.4	1698	0.005	0.97	I	42.0 - 42.5	*
5006.2	5005.3	5005.3	594	0.002	1.00	I	42.0 - 42.5	*
5219.8	5219.5	5219.5	2312	0.007	0.99	I	4.5 - 5.5	
5795.7	5794.8	5794.8	354	0.001	1.00	I	48.0 - 49.0	
5796.0	5794.5	5796.5	1118	0.003	1.00	I	42.0 - 42.5	
5810.4	5808.3	5810.4	934	0.003	0.78	I	48.0 - 49.0	
5887.7	5886.2	5886.2	470	0.001	0.84	I	4.5 - 5.5	
5947.0	5946.1	5947.2	333	0.001	1.00	I	4.5 - 5.5	
5948.7	5948.1	5949.1	229	0.001	1.00	I	4.5 - 5.5	
6145.6	6142.3	6145.3	1831	0.005	1.00	I	4.5 - 5.5	
6552.4	6550.8	6551.9	26640	0.079	1.00	IC	40.5 - 41.5	
6668.1	6664.7	6667.7	129297	0.385	1.00	IC	56.0 - 57.0	
6682.2	6680.6	6682.6	18575	0.055	0.94	I	57.5 - 58.0	
6691.0	6688.7	6689.6	10783	0.032	1.00	IC	56.0 - 57.0	
6705.8	6702.7	6705.6	12790	0.038	1.00	IC	56.0 - 57.0	
6744.1	6740.9	6742.9	157653	0.469	1.00	IC	47.0 - 47.5	
6758.0	6754.0	6756.9	573542	1.708	1.00	IC	48.0 - 49.0	
6769.5	6768.0	6769.0	1538	0.005	1.00	I	48.0 - 49.0	
6779.5	6776.8	6779.8	1952	0.006	0.90	I	48.0 - 49.0	
6788.7	6786.9	6790.0	704	0.002	1.00	I	48.0 - 49.0	
7259.9	7257.1	7259.1	777	0.002	0.92	I	4.5 - 5.5	
7464.9	7461.4	7464.4	53690	0.160	1.00	IC	49.5 - 50.0	
7992.8	7991.1	7991.1	2118	0.006	1.00	I	27.5 - 28.5	

Appendix D. Mass Profiling Data for *Mesob. tamulus* venom.

Mass data was obtained by MALDI-TOF and LC-ESI mass spectrometry for the 'main' size exclusion peak fractionated by ion exchange and reverse phase chromatography as described. LC-MS masses were calculated from component ions using commercial LC-MS mass reconstruction software (API). Within an ion exchange group (or the data corresponding to direct analysis of the 'main' size exclusion peak) MALDI-TOF data was assumed to represent a single mass if data was within 0.1% variation and was detected in continuous consecutive fractions, and as such were averaged. Mean MALDI-derived masses with >0.1% SD and those derived from <3 separate masses from <2 sample spots were discarded. Resulting LC-MS and MALDI-TOF data is shown in the table. Within a single group all possible adduct masses for addition of matrix, Na, K and Na+K, loss of CO₂, NH₃ and H₂O, mono- and di-oxidation, along with those corresponding to +74 and +104 were calculated, and any corresponding masses (+/- 0.1% for MALDI-TOF, +/- 0.01% for LC-MS) are shaded.

Mass (Avg.)	Average mass of the neutral species.
Mass (Mono.)	Monoisotopic mass ($[M+H]^+$). Based upon the lowest detected peak in the isotope series. (LC-MS only)
Apex Mass	Mass of isotope distribution at maximum intensity. (LC-MS only)
Score	Least squares correlation coefficient for fit of observed values to calculated masses. (LC-MS only)
Evidence	Type of series used for mass determination. I = isotope series, C = charge series, IC = isotope series that is also part of a charge series. (LC-MS only)
Time	Elution window of ions contributing to mass information. Time is shown to nearest 0.5 min from initiation of data collection. (LC-MS only)
MALDI Fraction	Fraction(s) from offline reverse phase HPLC in which mass was noted. (MALDI-TOF/ MS only).

Size exclusion 'main' peak

Mass (average)	Mass (mono.)	Apex Mass	Score	Evidence	Time	MALDI fraction
2001.5	2000.8	2001.8	1.00	I	0-5	
2005.5	2005.0	2006.0	1.00	I	35-40	
2016.5	2014.8	2015.9	1.00	I	0-5	
2017.4	2016.9	2017.9	1.00	I	0-5	
2021.6	2020.9	2021.9	1.00	I	0-5	
2033.5	2032.8	2033.8	1.00	I	0-5	
2053.5	2052.8	2053.8	1.00	I	0-5	
2067.8	2066.9	2067.9	1.00	I	0-5	
2085.7	2084.9	2085.9	1.00	I	0-5	
2088.4	2086.9	2087.9	1.00	I	0-5	
2121.4	2120.8	2121.8	1.00	I	0-5	
2133.9	2132.8	2133.9	1.00	I	0-5	
2139.5	2138.9	2139.9	1.00	I	0-5	
2152.4	2150.9	2151.9	1.00	I	0-5	
2157.6	2156.9	2157.8	1.00	I	0-5	
2189.5	2188.8	2189.8	1.00	I	0-5	
2203.5	2202.8	2203.8	1.00	I	0-5	
2257.5	2256.8	2257.9	1.00	I	0-5	
2274.1	2273.9	2273.9	1.00	I	0-5	
2287.6	2286.8	2287.9	1.00	I	0-5	
2288.6	2286.8	2287.8	1.00	I	0-5	
2292.7	2291.8	2291.8	1.00	I	0-5	
2304.6	2303.8	2303.8	1.00	I	0-5	
2340.4	2338.8	2339.8	1.00	I	0-5	
2361.4	2360.8	2361.8	1.00	I	0-5	
2389.5	2388.9	2389.8	1.00	I	0-5	
2408.5	2406.9	2407.8	1.00	I	0-5	
2419.5	2418.8	2419.8	1.00	I	0-5	
2424.4	2422.9	2423.8	1.00	I	0-5	
2476.2	2474.8	2475.8	1.00	I	0-5	
2492.2	2490.8	2491.8	1.00	I	0-5	
2497.4	2496.8	2497.8	1.00	I	0-5	
2508.2	2506.9	2507.8	1.00	I	0-5	
2514.1	2513.8	2513.8	1.00	I	0-5	
2524.4	2522.9	2523.8	1.00	I	0-5	
2544.4	2542.9	2543.8	1.00	I	0-5	
2544.7	2543.8	2543.8	1.00	I	0-5	
2560.2	2559.8	2559.8	1.00	I	0-5	

Mass (average)	Mass (mono.)	Apex Mass	Score	Evidence	Time	MALDI fraction
2560.3	2558.8	2559.8	1.00	I	0-5	
2576.4	2574.8	2575.8	1.00	I	0-5	
2584.1	2583.8	2583.8	1.00	I	0-5	
2592.6	2590.8	2591.8	1.00	I	0-5	
2612.7	2610.8	2611.8	1.00	I	0-5	
2622.2	2621.8	2621.8	1.00	I	0-5	
2628.3	2626.8	2627.8	1.00	I	0-5	
2644.6	2642.8	2643.8	1.00	I	0-5	
2660.4	2658.8	2659.8	1.00	I	0-5	
2678.6	2676.7	2679.8	1.00	I	0-5	
2688.2	2686.5	2687.5	1.00	IC	35-40	
2691.4	2690.8	2691.8	1.00	I	0-5	
2693.5	2692.7	2693.8	1.00	I	0-5	
2696.4	2694.7	2695.8	1.00	I	0-5	
2712.2	2710.8	2711.8	1.00	I	0-5	
2714.6	2712.6	2713.6	1.00	IC	35-40	
2716.7						SE main
2732.2	2730.7	2731.8	1.00	I	0-5	
2758.7	2757.8	2757.8	1.00	I	0-5	
2796.2	2794.8	2795.8	0.89	I	0-5	
2814.4	2812.8	2813.8	1.00	I	0-5	
2816.6						SE main
2818.2	2817.8	2817.8	1.00	I	0-5	
2822.7	2821.8	2821.8	1.00	I	0-5	
2830.2	2829.7	2829.7	0.99	I	0-5	
2836.6	2835.8	2835.8	1.00	I	0-5	
2848.0	2847.8	2847.8	1.00	IC	0-5	
2852.9	2851.8	2852.8	1.00	I	0-5	
2877.1	2875.8	2875.8	1.00	I	0-5	
2884.6	2882.9	2883.8	1.00	I	0-5	
2894.4	2892.7	2895.8	0.99	I	0-5	
2904.6	2903.8	2903.8	1.00	I	0-5	
2908.6	2907.8	2907.8	1.00	I	0-5	
2924.6	2923.8	2924.8	1.00	IC	0-5	
2936.6	2935.7	2935.7	1.00	I	0-5	
2941.8	2940.7	2941.7	1.00	IC	0-10	
2968.7	2967.8	2967.8	1.00	I	0-5	
2972.7	2971.8	2971.8	1.00	IC	0-5	
2988.8						SE main
2988.8	2986.7	2987.7	1.00	IC	0-10	
2996.8	2995.7	2997.7	1.00	I	0-5	

Mass (average)	Mass (mono.)	Apex Mass	Score	Evidence	Time	MALDI fraction
3056.8	3055.8	3056.7	1.00	I	0-5	
3059.8						SE main
3060.5	3058.7	3059.7	1.00	I	35-40	
3093.1	3092.8	3092.8	1.00	I	0-5	
3106.5	3105.7	3106.6	1.00	I	20-30	
3164.0	3162.7	3164.8	1.00	I	0-5	
3166.2	3164.6	3166.6	1.00	I	35-40	
3183.9	3181.9	3183.0	0.98	I	35-40	
3188.4	3186.7	3187.6	1.00	I	35-40	
3191.8	3189.7	3190.7	1.00	IC	0-10	
3192.7						SE main
3236.7	3235.7	3235.7	1.00	I	0-5	
3261.1	3259.7	3260.7	1.00	I	0-5	
3262.2	3261.8	3261.8	1.00	I	0-5	
3296.8	3295.9	3296.9	1.00	I	0-10	
3309.9						SE main
3332.6	3330.7	3332.8	1.00	I	0-5	
3391.9	3390.9	3391.9	1.00	I	0-10	
3392.0						SE main
3398.6	3397.8	3398.7	1.00	I	0-5	
3399.1	3398.7	3398.7	1.00	I	0-5	
3449.9						SE main
3450.5	3448.0	3450.0	1.00	IC	0-10	
3464.7	3463.8	3464.7	1.00	I	0-5	
3466.1	3465.1	3467.0	0.99	I	0-10	
3477.8						SE main
3482.1	3481.0	3483.0	1.00	I	0-10	
3500.9	3500.1	3500.1	1.00	I	20-25	
3519.3	3517.0	3519.0	1.00	IC	20-25	
3519.7	3518.1	3519.0	1.00	IC	0-10	
3560.4	3558.1	3560.1	1.00	IC	0-10	
3572.1	3570.9	3572.0	1.00	I	0-10	
3578.0	3576.0	3578.0	0.83	I	0-10	
3685.0						SE main
3709.7	3707.2	3709.2	1.00	IC	20-25	
3722.4	3719.9	3722.0	1.00	IC	35-40	
3740.8	3739.8	3740.7	1.00	I	0-5	
3760.3	3759.0	3759.9	1.00	I	35-40	
3775.8	3774.8	3775.7	1.00	I	0-5	
3782.7	3781.7	3782.7	1.00	I	0-5	
3788.7	3786.6	3787.7	0.87	I	0-5	

Mass (average)	Mass (mono.)	Apex Mass	Score	Evidence	Time	MALDI fraction
3797.8						SE main
3800.7	3799.7	3800.7	1.00	I	0-5	
3804.6	3803.7	3803.7	1.00	I	0-5	
3807.0	3806.7	3806.7	1.00	I	0-5	
3807.8	3805.3	3807.3	1.00	IC	0-10	
3819.1	3816.9	3818.9	1.00	I	20-25	
3824.7	3822.8	3824.7	1.00	I	0-5	
3835.6	3833.0	3835.0	1.00	IC	20-25	
3836.6	3835.7	3836.7	1.00	I	0-5	
3839.9						SE main
3842.9	3840.7	3842.8	0.80	I	0-5	
3853.9	3852.8	3854.7	0.99	I	0-5	
3860.9	3859.6	3860.7	1.00	I	0-5	
3866.7	3865.7	3866.8	1.00	I	0-5	
3872.2	3871.6	3872.6	1.00	I	0-5	
3874.8	3873.7	3875.7	1.00	I	0-5	
3879.1	3876.4	3878.4	1.00	IC	0-10	
3879.1	3876.7	3878.7	0.97	I	0-5	
3891.2	3890.7	3890.7	1.00	I	0-5	
3896.9	3895.6	3896.7	1.00	I	0-5	
3902.6	3901.6	3902.6	1.00	I	0-5	
3908.7	3906.7	3908.6	1.00	I	0-5	
3912.9						SE main
3913.0	3910.3	3912.3	1.00	IC	0-10	
3920.6	3919.7	3920.7	1.00	I	0-5	
3926.9	3924.8	3926.7	0.86	I	0-5	
3928.9	3927.6	3929.7	1.00	I	0-5	
3932.3	3930.6	3932.7	1.00	I	0-5	
3937.1	3935.7	3935.7	0.75	I	0-5	
3938.3	3936.7	3938.7	1.00	I	0-5	
3945.1						SE main
3948.1	3945.7	3947.7	0.97	I	0-5	
3957.6	3955.6	3956.7	1.00	I	0-5	
3972.9						SE main
3973.8	3971.1	3973.1	1.00	IC	35-40	
3974.4	3972.6	3974.7	0.74	I	0-5	
3980.3	3979.7	3980.7	1.00	I	0-5	
3983.3	3982.7	3983.7	0.99	I	0-5	
3987.6	3985.7	3986.7	1.00	I	0-5	
3993.3	3991.7	3993.7	0.79	I	0-5	
3996.2	3994.1	3996.1	1.00	IC	35-40	

Mass (average)	Mass (mono.)	Apex Mass	Score	Evidence	Time	MALDI fraction
3998.3	3997.7	3998.7	1.00	I	0-5	
4002.5	3999.6	4001.7	1.00	I	0-5	
4010.9	4009.7	4010.7	1.00	I	0-5	
4011.9	4010.1	4011.1	1.00	I	35-40	
4016.6	4015.7	4016.7	0.99	I	0-5	
4019.0						SE main
4025.7	4023.7	4025.7	1.00	I	0-5	
4029.0	4028.6	4028.6	0.99	I	0-5	
4034.7	4033.7	4034.7	1.00	I	0-5	
4041.0	4039.7	4040.7	1.00	I	0-5	
4058.7	4057.7	4058.6	1.00	I	0-5	
4076.7	4075.6	4076.7	1.00	I	0-5	
4078.8						SE main
4082.2	4081.7	4082.7	1.00	I	0-5	
4082.3	4081.7	4082.7	1.00	I	0-5	
4086.6	4084.6	4085.6	1.00	I	0-5	
4089.1	4088.7	4088.7	1.00	I	0-5	
4094.3	4092.7	4094.7	0.93	I	0-5	
4096.4	4095.5	4096.5	1.00	I	0-10	
4100.7	4099.7	4100.7	1.00	I	0-5	
4101.0						SE main
4106.2	4105.7	4106.6	1.00	I	0-5	
4109.2	4107.6	4109.7	1.00	I	0-5	
4118.9	4117.6	4118.7	1.00	I	0-5	
4124.3	4122.8	4124.7	0.99	I	0-5	
4130.3	4129.7	4130.7	1.00	I	0-5	
4131.8	4129.7	4130.7	0.95	I	0-5	
4136.6	4135.7	4136.6	0.99	I	0-5	
4142.8	4140.7	4142.7	0.82	I	0-5	
4147.8	4146.6	4148.6	1.00	I	0-5	
4148.5	4146.6	4148.5	0.94	I	0-10	
4152.4	4149.6	4151.7	0.96	I	0-5	
4157.3	4156.6	4157.6	1.00	I	0-5	
4160.7	4159.6	4160.7	1.00	I	0-5	
4167.0	4164.6	4166.6	0.97	I	0-5	
4172.2						SE main
4190.3	4189.8	4190.7	0.98	I	0-5	
4191.0	4189.8	4190.6	1.00	I	0-5	
4196.3	4194.7	4196.7	1.00	I	0-5	
4208.0						SE main
4213.5	4211.7	4211.7	1.00	I	0-5	

Mass (average)	Mass (mono.)	Apex Mass	Score	Evidence	Time	MALDI fraction
4216.2	4214.7	4214.7	0.79	I	0-5	
4226.2	4225.6	4226.7	0.99	I	0-5	
4230.2	4227.6	4229.7	0.84	I	0-5	
4237.2	4236.6	4237.6	1.00	I	0-5	
4249.2	4246.7	4247.7	1.00	I	0-5	
4263.7	4261.7	4262.6	1.00	I	0-5	
4266.9						SE main
4268.7	4267.5	4268.6	1.00	I	0-5	
4274.6	4273.7	4274.7	0.99	I	0-5	
4281.1	4279.6	4280.7	1.00	I	0-5	
4287.3	4285.7	4286.7	0.94	I	0-5	
4292.6	4291.6	4292.6	1.00	I	0-5	
4325.3	4324.7	4325.7	1.00	I	0-5	
4329.7	4327.7	4331.6	0.95	I	0-5	
4363.9						SE main
4365.5	4363.7	4367.7	0.94	I	0-5	
4381.0	4379.7	4379.7	1.00	I	0-5	
4395.5	4393.7	4394.7	0.94	I	0-5	
4401.3	4399.7	4400.6	0.95	I	0-5	
4412.3	4410.6	4412.6	0.76	I	0-5	
4419.0	4416.6	4418.7	0.96	I	0-5	
4424.3	4423.6	4424.7	1.00	I	0-5	
4428.7	4426.8	4427.7	0.92	I	0-5	
4433.3	4432.7	4433.7	1.00	I	0-5	
4437.5	4435.6	4436.7	0.93	I	0-5	
4449.1	4447.7	4448.6	1.00	I	0-5	
4467.0	4464.6	4467.6	0.81	I	0-5	
4483.1	4481.7	4481.7	1.00	I	0-5	
4521.6	4519.7	4523.7	0.74	I	0-5	
4522.6	4520.7	4523.6	1.00	I	0-5	
4550.6	4548.6	4550.6	1.00	I	0-5	
4551.1	4550.7	4550.7	1.00	I	0-5	
4556.7	4555.7	4555.7	1.00	I	0-5	
4569.3	4567.6	4568.7	0.94	I	0-5	
4588.1						SE main
4605.7	4603.7	4604.7	1.00	I	0-5	
4612.6	4611.6	4613.6	1.00	I	0-5	
4615.9	4613.6	4615.6	0.80	I	0-5	
4637.4	4635.7	4637.6	0.94	I	0-5	
4649.2	4648.7	4649.7	1.00	I	0-5	
4653.4	4651.7	4652.6	0.95	I	0-5	

Mass (average)	Mass (mono.)	Apex Mass	Score	Evidence	Time	MALDI fraction
4690.4	4687.7	4691.6	0.98	I	0-5	
4718.7	4717.7	4719.6	1.00	I	0-5	
4737.2	4735.7	4737.7	1.00	I	0-5	
4740.5	4739.6	4739.6	1.00	I	0-5	
5564.2						SE main
6623.9						SE main
6829.7						SE main
6846.7						SE main
6986.1						SE main
7036.8						SE main
7048.9						SE main
7124.6						SE main
7156.9						SE main
7224.6						SE main
7345.3						SE main
7502.1						SE main
7588.6						SE main
7823.5						SE main
8103.0						SE main
8210.1						SE main
10927.7						SE main
11122.7						SE main

Flow through from ion exchange column

Mass (average)	Mass (mono.)	Apex Mass	Score	Evidence	Time	MALDI fraction
2411.2						H13
2644.1						H15-I3
2670.9						I2-I3
2690.0						H15-I3
2714.3						H15-I3
2741.3						I2-I3
2774.4						I1-I3
2781.3						I6
2787.2						I2
2789.8	2788.6	2790.6	1.00	I	45-50	
2813.8						H6-H7
2814.8	2812.6	2813.6	1.00	IC	25-30	
2836.6	2835.6	2835.6	0.89	I	25-30	
2842.8						I2

Mass (average)	Mass (mono.)	Apex Mass	Score	Evidence	Time	MALDI fraction
2951.3						H7
2959.9	2958.9	2960.8	1.00	I	0-5	
2968.0						H5-H9
2969.2	2968.5	2968.5	1.00	I	30-35	
2969.7	2968.6	2969.6	1.00	I	20-25	
2971.5						G14
2990.4	2988.5	2989.5	1.00	I	30-35	
3030.7						G14
3060.5	3058.7	3060.7	0.90	I	30-35	
3062.2						H11-H12
3087.8	3085.7	3086.7	0.90	I	30-35	
3089.3						H11-H12
3097.8	3096.7	3097.7	1.00	I	30-35	
3104.6						H6-H7
3105.9	3103.6	3105.6	1.00	IC	20-25	
3111.8						H4-H5
3115.7						I2-I3
3127.6	3126.7	3127.6	0.99	I	20-25	
3165.7						H6-H7
3168.7						H1
3169.6	3168.7	3168.7	1.00	I	20-25	
3180.0						G15
3185.4						I2-I3
3191.9	3189.7	3191.7	1.00	IC	5-10	
3194.0						G8-G14
3196.8						H10-H11
3214.5						I2-I3
3224.3						G15-H1
3226.2						H7
3250.9						G14-G15
3269.0						H6
3278.7						H14
3285.0						H7
3296.1						H10
3308.8						H5-H7
3311.1						H10-H11
3321.2	3318.9	3320.9	1.00	IC	20-25	
3322.0						H1
3332.2						H6
3334.3						H9
3356.1						H5-H6
3374.5						H5-H6
3392.5						H8-H9
3397.7						H15-I2
3408.4						G11-G12
3411.3						H11-H14

Mass (average)	Mass (mono.)	Apex Mass	Score	Evidence	Time	MALDI fraction
3411.3	3409.8	3410.9	0.88	I	35-40	
3422.7						G14
3426.3						H5-H7
3431.5						G12
3459.7						H5
3460.0	3458.7	3459.8	0.87	I	20-25	
3496.1						H4
3506.8						H10
3519.0						H11
3519.5	3517.0	3519.0	1.00	IC	20-25	
3520.2						H3-H6
3521.2						I11
3521.7						H1-H2
3524.6						I3-I5
3541.8	3541.0	3541.0	1.00	I	20-25	
3549.4						H5-H7
3557.3	3554.9	3556.9	0.98	I	20-25	
3569.2						I1-I2
3626.9						H6-H8
3648.5						H15-I2
3649.0						I8
3679.3						I4
3691.0						I7
3698.3						I4
3698.3						H15
3700.4						I9
3722.4	3720.0	3722.0	1.00	IC	35-40	
3722.7						H11-H12
3755.4						H15-I1
3756.0						H9
3769.9						H13-H14
3770.5	3769.0	3770.0	1.00	IC	40-45	
3776.9						I3-I4
3787.6						I4-I5
3800.4						H15
3813.0						H1
3827.3						H7-H8
3830.5						G15
3847.2						G14
3853.8						H4-H6
3870.1						H10-H11
3885.9						G15
3900.9						I4-I5
3906.3						G14
3911.6						H10-H11
3913.7						H15-I3

Mass (average)	Mass (mono.)	Apex Mass	Score	Evidence	Time	MALDI fraction
3914.1						H4-H5
3914.8						H7
3916.6						I4
3920.7						I7
3924.5						H4-H8
3932.8						H10-H11
3959.0						H11
3972.3						I6
3973.5	3971.1	3973.1	1.00	IC	35-40	
3973.6	3971.1	3973.1	1.00	IC	35-40	
3973.6	3972.2	3973.1	1.00	IC	35-40	
3973.7						H11-I2
3985.4						H7-H9
4003.7						H10-H15
4009.8						G14-H1
4011.8						H6-H7
4016.1						H8
4020.8						H5
4048.7						H8-H11
4076.8						H7-H10
4077.7						H2-H4
4078.8	4077.1	4079.1	1.00	IC	20-25	
4081.0						I2-13
4101.3						I2
4108.8						H2-H5
4111.2						I11-I12
4111.7						H15
4133.8	4132.3	4133.3	1.00	I	20-25	
4135.5						H7-H8
4168.0						H2
4176.8						I2
4176.8						H10-H11
4203.0						H15
4223.9						H2-H3
4255.9						H2-H3
4308.1						H15
4319.2						H12-I2
4326.3						H7
4345.5						I2
4365.9						H14
4665.3						H11-H12
4825.2						H13-I3
4843.3						H11
4851.7						H15
5469.1						I10
5553.7						I9

Mass (average)	Mass (mono.)	Apex Mass	Score	Evidence	Time	MALDI fraction
5631.5						H10-H12
6181.5						H15
6624.0						H10
6712.0						H12-H13
6746.7						H15
6841.5						H9
6859.0						H5-H10
6878.5						I2
6879.5						H11
7028.8						H10
7055.7						I3-I5
7065.3						H10-H11
7139.2						I1-I2
7159.6						H14-I3
7255.3						H13-H14
7269.1						H15
7356.3						H14-H15
7403.4						H13-H15
7552.5						H10-H15
7596.0						H12-H14
7622.1						H13-H15
7850.7						H15-I2
7878.5						H10
8226.0						H14-H15

Group 1 from ion exchange column

Mass (average)	Mass (mono.)	Apex Mass	Score	Evidence	Time	MALDI fraction
2018.5						A14-A15
2085.4	2084.8	2085.8	1.0	I	1-5	
2087.4						B14-B15
2089.4	2088.8	2088.8	1.0	I	1-5	
2121.3	2120.7	2121.7	1.0	I	1-5	
2215.4	2214.7	2215.7	1.0	I	1-5	
2225.4	2224.7	2224.7	1.0	I	1-5	
2279.3	2278.7	2279.7	1.0	I	1-5	
2293.8	2292.7	2292.7	1.0	I	1-5	
2360.3	2358.7	2359.7	1.0	I	1-5	
2407.6	2406.7	2407.7	1.0	I	1-5	
2428.4	2426.7	2427.7	1.0	I	1-5	
2476.0	2474.7	2475.7	0.9	I	1-5	
2496.4	2494.7	2495.7	1.0	I	1-5	
2544.0	2542.7	2543.6	0.9	I	1-5	
2551.3	2550.7	2551.7	1.0	I	1-5	

Mass (average)	Mass (mono.)	Apex Mass	Score	Evidence	Time	MALDI fraction
2554.5	2553.7	2553.7	1.0	I	1-5	
2557.1						A10
2560.4	2558.7	2559.7	1.0	I	1-5	
2564.6	2563.7	2563.7	1.0	I	1-5	
2584.0						A11
2598.0	2596.6	2597.6	0.9	I	1-5	
2611.9	2610.7	2611.7	0.9	I	1-5	
2619.2	2618.6	2619.6	1.0	I	1-5	
2632.4	2630.7	2631.7	1.0	I	1-5	
2680.1	2678.7	2679.7	0.9	I	1-5	
2687.3	2686.7	2687.6	1.0	I	1-5	
2687.5						C1-C2
2696.4	2694.6	2695.7	1.0	I	1-5	
2700.6	2699.7	2699.7	1.0	I	1-5	
2710.6	2709.6	2709.6	1.0	I	1-5	
2715.6						C3-C6
2717.1	2715.4	2716.4	1.0	IC	45-50	
2718.1						C9-C10
2732.2	2730.6	2731.6	0.9	I	1-5	
2746.6	2745.7	2745.7	1.0	I	1-5	
2768.4	2766.7	2767.6	1.0	I	1-5	
2816.0	2814.7	2815.6	0.9	I	1-5	
2826.5	2825.6	2825.6	1.0	I	1-5	
2828.1	2826.4	2827.5	1.0	IC	25-30	
2832.5	2830.6	2831.7	1.0	I	1-5	
2836.4	2835.6	2835.6	1.0	I	1-5	
2854.0	2853.7	2853.7	1.0	I	1-5	
2868.5	2867.6	2867.6	1.0	I	1-5	
2884.1	2882.7	2883.6	0.9	I	1-5	
2889.6						B2-B3
2894.6	2893.6	2895.6	1.0	I	1-5	
2902.3						C3
2904.6	2903.6	2903.6	1.0	I	1-5	
2914.5	2913.6	2913.6	1.0	I	1-5	
2925.0	2923.7	2924.7	1.0	I	1-5	
2937.2	2936.7	2937.7	1.0	I	1-5	
2959.2	2958.6	2959.6	1.0	I	1-5	
2962.7	2960.6	2963.6	1.0	I	1-5	
2968.5	2966.5	2967.6	1.0	I	1-5	
2972.6	2971.6	2971.6	1.0	I	1-5	
2996.0	2994.6	2996.6	1.0	I	1-5	
3017.0						A13
3018.9	3017.6	3017.6	1.0	I	1-5	
3040.6	3039.6	3039.6	1.0	I	1-5	
3053.7						A12
3056.0	3054.5	3055.6	0.9	I	1-5	

Mass (average)	Mass (mono.)	Apex Mass	Score	Evidence	Time	MALDI fraction
3058.4	3057.6	3057.6	1.0	I	1-5	
3062.6	3061.6	3061.6	1.0	I	1-5	
3064.6	3063.6	3063.6	1.0	I	1-5	
3081.6						A15
3095.6						A13-A14
3098.6	3097.6	3099.6	1.0	I	1-5	
3105.2	3104.7	3105.6	1.0	I	1-5	
3108.0	3106.6	3107.6	1.0	I	1-5	
3112.0						A12-A13
3167.3	3165.6	3167.6	0.9	I	1-5	
3172.3						C1-C2
3174.4						B2
3176.6	3175.6	3175.6	1.0	I	1-5	
3182.2						C3-C4
3194.4	3193.6	3193.6	1.0	I	1-5	
3198.3	3197.6	3197.6	1.0	I	1-5	
3208.5	3207.6	3207.6	1.0	I	1-5	
3219.3						B9
3240.8	3239.6	3239.6	1.0	I	1-5	
3244.4	3243.6	3243.6	1.0	I	1-5	
3251.3	3249.6	3251.7	1.0	I	30-40	
3252.7						B14-B15
3261.5	3259.6	3261.6	0.7	I	1-5	
3266.4	3265.6	3265.6	1.0	I	1-5	
3272.9	3271.5	3271.5	1.0	I	1-5	
3276.5	3275.6	3275.6	1.0	I	1-5	
3295.6						B13-B14
3315.4						B14-C1
3317.7						B8
3323.1						B3-B4
3333.0	3331.6	3332.6	1.0	I	1-5	
3344.0	3342.6	3343.6	0.9	I	1-5	
3358.6						B5
3368.5	3367.6	3367.6	1.0	I	1-5	
3369.2	3368.1	3370.1	1.0	I	1-5	
3382.2						C7
3393.4						B3
3396.6						C6-C8
3397.9	3396.6	3397.6	1.0	I	1-5	
3400.8	3399.7	3399.7	0.9	I	25-30	
3401.7	3399.6	3401.6	1.0	I	1-5	
3403.9						B2
3404.8	3404.6	3404.6	1.0	I	1-5	
3409.3						B14-B15
3412.5	3411.0	3412.9	0.9	I	1-5	
3417.5						B6

Mass (average)	Mass (mono.)	Apex Mass	Score	Evidence	Time	MALDI fraction
3417.8	3415.6	3417.7	1.0	I	25-30	
3422.2						B5
3432.8						B9
3458.5	3456.5	3458.6	1.0	I	1-5	
3465.8	3463.5	3465.6	1.0	I	1-5	
3471.1	3469.6	3470.6	1.0	I	1-5	
3477.2						B11-B13
3480.4	3479.5	3479.5	1.0	I	1-5	
3483.8						A15-B2
3486.2						B9
3496.8						A14-B1
3501.3						C2
3508.6						B12-C1
3512.0	3510.6	3511.7	1.0	I	20-25	
3513.2						
3514.2	3512.1	3514.1	0.8	I	1-5	B2-B3
3516.8						A13
3519.0	3517.5	3519.5	1.0	I	1-5	
3536.6	3534.5	3536.6	1.0	I	1-5	
3541.1	3539.0	3540.9	0.8	I	1-5	
3544.1	3543.6	3543.6	1.0	I	1-5	
3547.6	3545.5	3547.5	1.0	I	1-5	
3552.5	3551.5	3551.5	1.0	I	1-5	
3562.0						B11-B13
3562.7	3561.5	3563.5	1.0	I	1-5	
3573.7						C2
3583.7	3582.3	3582.3	1.0	I	1-5	
3584.6	3583.6	3584.5	1.0	I	1-5	
3589.0						B15
3591.1	3590.5	3591.5	1.0	I	1-5	
3595.0						B3
3595.1						B14
3596.5	3594.7	3596.7	1.0	IC	20-25	
3596.9	3595.6	3596.7	1.0	I	20-25	
3602.4	3601.6	3601.6	1.0	I	1-5	
3606.3	3605.6	3605.6	1.0	I	1-5	
3608.8	3608.6	3608.6	1.0	I	1-5	
3609.2						C2
3616.0	3615.6	3615.6	1.0	I	1-5	
3629.8						B9-B10
3647.5	3645.6	3647.5	1.0	I	1-5	
3648.6	3648.1	3649.0	1.0	I	1-5	
3651.4	3650.5	3650.5	1.0	IC	1-5	
3662.2	3660.5	3662.6	1.0	I	1-5	
3665.7	3664.7	3666.7	1.0	I	25-30	
3669.8	3667.5	3669.5	1.0	I	1-5	

Mass (average)	Mass (mono.)	Apex Mass	Score	Evidence	Time	MALDI fraction
3674.8	3672.5	3674.5	1.0	I	1-5	
3676.3	3675.5	3675.5	1.0	I	1-5	
3704.0						B10
3713.8						B9
3740.6	3738.5	3740.6	1.0	I	1-5	
3765.0	3764.1	3764.9	1.0	I	1-5	
3775.8	3774.5	3776.5	1.0	I	1-5	
3780.7	3778.7	3779.8	1.0	I	25-30	
3788.4	3787.5	3788.5	1.0	I	1-5	
3794.9	3794.5	3794.5	1.0	I	1-5	
3797.7						B5-B10
3798.4	3796.7	3798.7	1.0	IC	25-30	
3801.6						C9-C15
3802.9	3801.5	3802.5	1.0	I	1-5	
3805.8	3804.6	3805.5	1.0	I	1-5	
3809.7	3807.5	3809.5	1.0	I	1-5	
3810.2						B8
3812.8	3812.5	3812.5	1.0	I	1-5	
3816.0	3814.5	3815.5	1.0	I	1-5	
3819.7	3817.6	3819.7	1.0	I	25-30	
3819.9	3819.5	3819.5	1.0	I	1-5	
3820.8						B14-B15
3831.9						C1
3834.9	3832.7	3834.7	1.0	IC	25-30	
3835.8	3834.7	3835.7	1.0	I	25-30	
3836.9	3835.7	3836.6	0.9	I	25-30	
3840.5	3837.8	3839.8	1.0	IC	20-25	
3840.6						B4-B6
3841.7	3839.8	3840.8	1.0	I	20-25	
3857.1	3855.5	3857.5	0.9	I	1-5	
3868.6	3867.5	3869.5	1.0	I	1-5	
3873.9	3871.5	3873.5	1.0	I	1-5	
3878.3	3876.7	3877.7	1.0	IC	20-25	
3879.3	3877.5	3878.5	1.0	I	1-5	
3884.1	3883.5	3884.5	1.0	I	1-5	
3902.2						C5
3909.3	3908.5	3908.5	1.0	I	1-5	
3932.1						B8-B10
3938.6	3936.5	3938.5	1.0	I	1-5	
3944.8	3942.5	3944.5	0.8	I	1-5	
3945.8						A7-A11
3953.1						B1-B2
3959.8						A10-A12
3978.3	3977.5	3977.5	1.0	I	1-5	
3982.2						B11
3987.5						B2

Mass (average)	Mass (mono.)	Apex Mass	Score	Evidence	Time	MALDI fraction
3989.1	3988.1	3989.0	1.0	I	1-5	
3992.5	3991.6	3992.5	1.0	I	1-5	
3994.6						B10
3998.1	3997.4	3998.5	1.0	I	1-5	
4001.0						B1
4001.4	3999.4	4001.5	0.9	I	1-5	
4004.8	4004.5	4004.5	1.0	I	1-5	
4009.7	4008.5	4009.5	1.0	I	1-5	
4014.5	4011.5	4013.5	1.0	I	1-5	
4021.5						B11
4030.3	4028.0	4030.0	1.0	I	20-25	
4030.6						A13-B1
4052.3						B10-B13
4059.4	4058.4	4059.4	1.0	I	1-5	
4070.2	4068.5	4070.5	1.0	I	1-5	
4077.7	4075.4	4077.5	1.0	I	1-5	
4083.0	4080.4	4082.5	1.0	I	1-5	
4088.1	4087.5	4088.5	1.0	I	1-5	
4094.4	4093.4	4094.5	1.0	I	1-5	
4100.3						A14-A15
4102.1						C1-C2
4113.0	4112.5	4112.5	1.0	I	1-5	
4113.0						B10
4130.8	4128.5	4130.5	0.8	I	1-5	
4142.0						B11-B13
4142.6	4140.5	4142.5	1.0	I	1-5	
4148.7	4146.4	4148.5	0.8	I	1-5	
4160.5	4159.5	4160.5	1.0	I	1-5	
4172.0						B12-C1
4172.2	4171.2	4172.2	1.0	I	35-40	
4191.2	4189.5	4190.5	0.9	I	1-5	
4195.7	4194.4	4196.5	1.0	I	1-5	
4197.2						B14
4200.0	4197.5	4199.5	0.9	I	1-5	
4205.9	4204.5	4205.5	0.9	I	1-5	
4213.7	4212.4	4214.4	1.0	I	1-5	
4218.5	4215.5	4217.4	1.0	I	1-5	
4228.6	4227.4	4229.4	1.0	I	1-5	
4232.2	4230.5	4232.4	1.0	I	1-5	B12
4233.3						
4258.6	4257.5	4259.4	1.0	I	1-5	
4263.0	4261.5	4263.4	1.0	I	1-5	
4269.3						C1
4274.9	4274.4	4274.4	1.0	I	1-5	
4281.9	4279.4	4281.5	1.0	I	1-5	
4287.1	4285.5	4286.4	1.0	I	1-5	

Mass (average)	Mass (mono.)	Apex Mass	Score	Evidence	Time	MALDI fraction
4296.9	4295.4	4295.4	1.0	I	1-5	
4313.5	4311.4	4313.5	0.8	I	1-5	
4318.5	4317.5	4319.4	1.0	I	1-5	
4332.7	4329.5	4331.4	1.0	I	1-5	
4346.6	4344.5	4346.4	1.0	I	1-5	
4352.6	4350.4	4352.5	1.0	I	1-5	
4355.3						B3
4355.6	4354.1	4356.1	1.0	I	20-25	
4365.3	4363.5	4364.4	0.9	I	1-5	
4375.2						B1
4395.3	4393.5	4394.4	0.9	I	1-5	
4401.7	4399.5	4400.4	1.0	I	1-5	
4407.1	4405.5	4407.4	0.8	I	1-5	
4412.3	4411.4	4411.4	1.0	I	1-5	
4419.1	4416.4	4418.4	1.0	I	1-5	
4424.6	4422.5	4424.5	1.0	I	1-5	
4430.0	4429.4	4430.4	1.0	I	1-5	
4434.3	4431.4	4436.4	1.0	I	1-5	
4463.4	4461.4	4463.4	1.0	I	1-5	
4468.9	4466.4	4469.4	1.0	I	1-5	
4474.3	4472.4	4475.4	0.9	I	1-5	
4480.8	4479.4	4481.4	1.0	I	1-5	
4485.6	4483.4	4485.4	1.0	I	1-5	
4491.1	4488.4	4490.4	1.0	I	1-5	
4498.2						B2
4499.6	4497.3	4499.4	0.8	I	1-5	
4506.4	4504.5	4505.4	1.0	I	1-5	
4515.5						B1
4518.8	4517.4	4517.4	1.0	I	1-5	
4521.9	4521.4	4522.3	1.0	I	1-5	
4539.0	4536.3	4538.4	1.0	I	1-5	
4545.8	4543.4	4547.4	0.9	I	1-5	
4550.9	4549.4	4550.4	1.0	I	1-5	
4556.9	4554.4	4556.4	1.0	I	1-5	
4566.4	4563.3	4565.4	0.9	I	1-5	
4580.8	4579.4	4580.4	1.0	I	1-5	
4590.8	4587.4	4589.4	0.9	I	1-5	
4600.3	4597.5	4601.4	0.9	I	1-5	
4616.4	4614.3	4616.4	1.0	I	1-5	
4621.1	4619.4	4622.4	1.0	I	1-5	
4626.4	4623.4	4625.4	1.0	I	1-5	
4636.0	4634.4	4637.4	1.0	I	1-5	
4641.0						C1
4641.2	4639.4	4640.4	0.9	I	1-5	
4672.6	4670.4	4673.4	1.0	I	1-5	
4677.9	4676.4	4679.4	0.9	I	1-5	

Mass (average)	Mass (mono.)	Apex Mass	Score	Evidence	Time	MALDI fraction
4683.5	4681.3	4685.4	1.0	I	1-5	
4689.6	4687.4	4691.4	1.0	I	1-5	
4694.8	4692.3	4694.4	1.0	I	1-5	
4699.9	4699.4	4700.4	1.0	I	1-5	
4704.4	4701.3	4706.4	0.8	I	1-5	
4718.3	4717.4	4717.4	1.0	I	1-5	
4740.8	4737.4	4739.4	0.9	I	1-5	
4775.8	4773.3	4775.4	0.9	I	1-5	
4789.3	4787.3	4787.3	1.0	I	1-5	
4802.4	4801.4	4803.3	1.0	I	1-5	
4808.2	4805.4	4808.4	0.8	I	1-5	
4815.8	4815.3	4815.3	1.0	I	1-5	
4820.4	4819.4	4820.4	1.0	I	1-5	
4825.1	4823.3	4825.4	0.7	I	1-5	
4830.5	4827.4	4829.4	1.0	I	1-5	
4841.2	4838.4	4841.4	1.0	I	1-5	
4856.7	4854.3	4856.4	0.8	I	1-5	
4869.0	4867.5	4869.3	0.8	I	1-5	
4876.0	4874.3	4877.4	1.0	I	1-5	
4887.9	4886.4	4889.3	1.0	I	1-5	
4893.5	4890.3	4893.4	1.0	I	1-5	
4899.1	4897.4	4898.3	1.0	I	1-5	
4904.3	4903.5	4904.3	1.0	I	1-5	
4915.6	4914.3	4915.4	0.9	I	1-5	
4920.3	4919.3	4919.3	1.0	I	1-5	
4930.9	4928.3	4931.3	0.9	I	1-5	
4937.0	4934.4	4937.3	1.0	I	1-5	
4946.0	4944.2	4946.3	1.0	I	1-5	
4951.3	4949.3	4952.3	1.0	I	1-5	
4956.2	4955.4	4955.4	1.0	I	1-5	
4961.7	4958.3	4961.4	1.0	I	1-5	
4967.0	4965.3	4967.4	1.0	I	1-5	
4977.8	4975.4	4979.4	1.0	I	1-5	
4996.6	4994.4	4997.3	1.0	I	1-5	
5002.2	5000.3	5000.3	0.9	I	1-5	
5006.8	5005.4	5005.4	1.0	I	1-5	
5011.9	5009.3	5011.4	1.0	I	1-5	
5020.0	5017.4	5021.3	0.9	I	1-5	
5024.4	5023.4	5024.4	1.0	I	1-5	
5029.7	5027.4	5029.4	1.0	I	1-5	
5034.7	5033.3	5033.3	1.0	I	1-5	
5045.3	5042.3	5045.3	1.0	I	1-5	
5059.5	5057.3	5059.3	0.8	I	1-5	
5079.9	5077.4	5079.3	1.0	I	1-5	
5092.3	5090.3	5093.3	1.0	I	1-5	
5097.0	5095.4	5097.3	1.0	I	1-5	

Mass (average)	Mass (mono.)	Apex Mass	Score	Evidence	Time	MALDI fraction
5102.2	5099.3	5102.3	1.0	I	1-5	
5109.3	5107.3	5111.3	1.0	I	1-5	
5129.3	5128.2	5129.3	1.0	I	1-5	
5134.6	5132.3	5135.4	0.8	I	1-5	
5148.8	5147.4	5147.4	1.0	I	1-5	
5157.8	5155.3	5159.3	1.0	I	1-5	
5165.7	5162.3	5165.3	1.0	I	1-5	
5173.8	5172.2	5172.2	1.0	I	1-5	
5191.6	5189.3	5191.3	0.8	I	1-5	
5200.9	5199.2	5201.3	0.7	I	1-5	
5215.1	5212.3	5216.3	1.0	I	1-5	
5227.3	5225.3	5227.4	1.0	I	1-5	
5233.4	5230.4	5233.4	1.0	I	1-10	
5238.7	5237.3	5237.3	1.0	I	1-5	
5249.4	5246.4	5249.3	1.0	I	1-5	
5264.9	5263.3	5265.3	1.0	I	1-5	
5285.2	5282.3	5285.3	1.0	I	1-5	
5295.1	5293.4	5295.2	0.9	I	1-5	
5301.4	5298.3	5301.3	1.0	I	1-5	
5338.9	5336.4	5339.3	1.0	I	1-5	
5347.4	5346.4	5347.3	1.0	I	1-5	
5352.3	5349.3	5351.2	1.0	I	1-5	
5361.2	5358.3	5363.3	0.9	I	1-5	
5369.5	5366.2	5369.3	1.0	I	1-5	
5383.5	5381.3	5381.3	0.7	I	1-5	
5390.3	5388.2	5390.3	1.0	I	1-5	
5397.1	5395.2	5399.4	0.9	I	1-5	
5402.7	5400.2	5402.2	1.0	I	1-5	
5409.1	5407.3	5409.3	0.9	I	1-5	
5420.0	5417.2	5420.3	1.0	I	1-5	
5431.0	5429.3	5431.4	0.7	I	1-5	
5436.5	5434.3	5437.3	1.0	I	1-5	
5443.4	5441.3	5441.3	0.8	I	1-5	
5451.8	5451.2	5452.3	1.0	I	1-5	
5454.7	5453.2	5455.2	1.0	I	1-5	
5460.9	5459.2	5461.4	1.0	I	1-5	
5475.7	5475.2	5475.2	1.0	I	1-5	
5488.9	5487.3	5487.3	0.9	I	1-5	
5498.4	5497.4	5498.3	1.0	I	1-5	
5501.2	5500.4	5501.3	1.0	I	1-5	
5505.3	5504.3	5505.2	1.0	I	1-5	
5509.7	5507.3	5509.2	1.0	I	1-5	
5523.1	5521.2	5523.1	1.0	I	1-5	
5527.3	5526.4	5527.4	1.0	I	1-5	
5533.1	5531.3	5534.3	0.8	I	1-5	
5537.3	5536.2	5537.3	1.0	I	1-5	

Mass (average)	Mass (mono.)	Apex Mass	Score	Evidence	Time	MALDI fraction
5556.2	5553.2	5555.2	0.8	I	1-5	
5573.7	5571.3	5573.3	1.0	I	1-5	
5579.3	5577.3	5577.3	0.9	I	1-5	
5589.6	5587.4	5589.3	0.8	I	1-5	
5612.8	5611.2	5611.2	0.9	I	1-5	
5625.8	5624.2	5627.3	1.0	I	1-5	
5634.5	5633.2	5633.2	0.9	I	1-5	
5641.7	5640.2	5641.2	1.0	I	1-5	
5778.6	5776.2	5777.3	1.0	I	1-5	
5783.9	5782.2	5783.3	0.9	I	1-5	
5829.7	5828.2	5829.2	1.0	I	1-5	
6760.6						C7
6797.8						C6-C8
6818.8						B10
6850.1						D3
6908.0						C5
6960.4						B9
7007.6						B15-C3
7015.5						B12-B13
7121.8						C5
7125.7						B10-B14
7158.0						C2
7196.0						B10
7319.5						B15
7604.8						B7
7643.7						B14-B15
7814.6						C5
7839.3						C1
7921.5						C1
8213.2						C1-C2
8357.7						B14

Group 2 from ion exchange column

Mass (average)	Mass (mono.)	Apex Mass	Score	Evidence	Time	MALDI fraction
2007.7	2006.8	2006.8	1.0	I	0-5	
2014.8						B5
2019.9	2018.8	2019.8	1.0	I	0-5	
2062.5	2061.8	2061.8	1.0	I	0-5	
2084.8						B12
2113.2	2112.8	2112.8	1.0	I	0-5	
2144.9	2143.8	2144.7	1.0	I	0-5	
2156.2	2154.8	2155.8	1.0	I	0-5	
2224.1	2222.8	2223.8	1.0	I	0-5	

Mass (average)	Mass (mono.)	Apex Mass	Score	Evidence	Time	MALDI fraction
2279.3	2278.8	2279.8	1.0	I	0-5	
2292.1	2290.8	2291.8	1.0	I	0-5	
2334.5	2333.8	2333.8	1.0	I	0-5	
2340.3						B11
2360.0	2358.8	2359.8	1.0	I	0-5	
2428.1	2426.8	2427.8	1.0	I	0-5	
2564.1	2562.8	2563.8	1.0	I	0-5	
2617.4						B14-B15
2618.2	2616.3	2618.3	1.0	IC	20-30	
2628.8	2627.3	2628.4	1.0	I	25-30	
2632.0	2630.8	2631.8	1.0	I	0-5	
2639.8						C9
2643.8						C10
2644.7						C1-C5
2646.7	2644.4	2645.4	1.0	IC	25-30	
2657.0	2656.3	2656.3	1.0	I	20-30	
2669.0	2667.3	2668.3	1.0	IC	25-30	
2672.1	2670.4	2671.4	1.0	I	20-30	
2683.8	2682.3	2683.3	1.0	IC	25-30	
2686.4						B14-C1
2689.0	2687.4	2688.4	1.0	IC	20-30	
2690.1	2688.4	2689.4	1.0	IC	20-30	
2690.9	2690.4	2690.4	1.0	IC	25-30	
2691.4	2689.4	2690.4	1.0	IC	25-30	
2699.5	2698.4	2700.4	1.0	I	25-30	
2700.0	2698.8	2699.8	1.0	I	0-5	
2708.3	2707.4	2708.4	1.0	IC	20-25	
2711.1	2709.4	2711.3	1.0	IC	20-30	
2711.8	2711.3	2712.3	1.0	I	20-30	
2713.1						C1-C5
2716.2						C9-C14
2716.6	2714.4	2715.4	1.0	IC	25-30	
2718.0	2716.4	2717.4	1.0	I	25-30	
2719.3	2718.4	2718.4	1.0	I	25-30	
2719.8	2718.3	2719.4	1.0	I	25-30	
2727.7	2726.4	2727.3	1.0	IC	20-30	
2727.8	2727.3	2727.3	1.0	I	20-30	
2731.4	2730.3	2732.3	1.0	I	20-30	
2734.5	2733.4	2734.5	1.0	I	20-25	
2735.9	2734.4	2735.4	1.0	I	25-30	
2738.9	2737.4	2739.4	1.0	I	25-30	
2738.9						C3-C4
2749.3	2748.3	2748.3	1.0	I	20-30	
2754.4	2753.4	2754.4	1.0	IC	25-30	
2756.8	2756.4	2756.4	1.0	I	25-30	
2764.9	2763.3	2764.3	1.0	I	20-30	

Mass (average)	Mass (mono.)	Apex Mass	Score	Evidence	Time	MALDI fraction
2767.3	2766.3	2766.3	0.9	I	20-30	
2828.8	2827.5	2827.5	1.0	I	20-30	
2836.0	2834.7	2835.7	1.0	I	0-5	
2858.0	2856.7	2857.8	0.9	I	0-5	
2902.6	2901.5	2902.6	1.0	IC	25-30	
2904.1	2902.7	2903.7	1.0	I	0-5	
2940.5	2939.5	2940.5	1.0	I	25-30	
2941.5	2940.5	2941.5	1.0	I	15-20	
2969.1	2968.2	2968.2	1.0	I	0-5	
2971.6	2970.7	2971.7	1.0	I	0-5	
2994.2	2992.8	2993.7	1.0	I	0-5	
3019.1						A13-A14
3036.3						A13
3038.4	3036.7	3037.7	0.9	I	0-5	
3052.7						A12-A13
3062.2	3060.7	3061.7	1.0	I	0-5	
3078.0	3076.6	3078.6	1.0	I	15-20	
3104.0						B2-B3
3105.1	3104.2	3104.2	1.0	I	0-5	
3107.9	3106.7	3107.7	1.0	I	0-5	
3118.7						C5
3129.7	3127.7	3128.7	1.0	I	0-5	
3182.6	3181.8	3182.8	1.0	I	20-25	
3184.7	3183.8	3184.8	1.0	IC	20-25	
3184.9	3182.8	3184.8	1.0	IC	20-25	
3198.6	3196.7	3197.7	1.0	I	0-5	
3205.3						A14
3222.2	3221.7	3222.7	1.0	I	20-25	
3222.8	3220.8	3221.7	1.0	I	20-25	
3223.9						A13
3236.7						A12
3242.9	3241.7	3243.7	1.0	I	15-25	
3266.1	3264.7	3265.7	1.0	I	0-5	
3318.7						B12
3319.2	3317.7	3317.7	1.0	I	15-20	
3325.7	3323.8	3325.8	1.0	I	15-20	
3332.4	3330.7	3332.7	1.0	I	0-5	
3343.1	3341.7	3341.7	1.0	I	0-5	
3377.1	3375.7	3375.7	1.0	I	0-5	
3377.4	3376.2	3376.2	1.0	I	0-5	
3383.6						C7
3402.1						C8
3402.6	3400.7	3401.7	1.0	I	0-5	
3402.9						B9-B10
3417.7	3415.7	3417.7	1.0	IC	15-25	
3418.7						A13-A14

Mass (average)	Mass (mono.)	Apex Mass	Score	Evidence	Time	MALDI fraction
3422.5						C2-C3
3432.5						B8
3448.3						A14
3454.0						B4-B5
3455.2						C4-C5
3456.9	3454.7	3456.8	1.0	I	15-25	
3465.5						A13
3470.1	3468.7	3469.7	1.0	I	0-5	
3478.0						A15-B1
3481.7						C8
3487.4						C9-C12
3494.1						A14-A15
3495.3						C15
3507.2						A13
3507.7						B2
3523.6						C4-C5
3536.3	3534.7	3536.7	1.0	I	0-5	
3563.9	3562.9	3563.9	1.0	I	15-20	
3572.3	3569.9	3572.0	1.0	I	20-25	
3576.0						B12-B14
3587.3	3585.9	3587.9	1.0	IC	20-25	
3603.3	3601.7	3601.7	1.0	I	0-5	
3607.0						B2-B4
3614.8	3613.0	3614.2	1.0	I	0-5	
3617.4	3614.8	3616.8	1.0	IC	15-20	
3620.6	3619.8	3619.8	1.0	I	15-20	
3635.3	3634.8	3634.8	1.0	I	15-20	
3635.3	3633.8	3634.8	1.0	I	15-20	
3638.5						B3
3641.7						B12-B14
3643.7						C2
3649.2	3647.6	3647.6	1.0	I	0-5	
3649.3	3648.1	3648.1	1.0	I	0-5	
3674.0	3672.7	3673.7	1.0	I	0-5	
3685.3						B10
3695.5						B13-B15
3711.9						C7-C8
3721.6						B12
3723.2	3720.9	3723.9	1.0	IC	15-20	
3723.5	3720.9	3722.9	1.0	IC	15-20	
3724.3	3722.9	3722.9	1.0	IC	15-20	
3734.3						C8-C9
3740.3	3738.7	3740.7	1.0	I	0-5	
3742.3						B13-B14
3751.3	3750.2	3750.2	1.0	I	0-5	
3761.8	3760.8	3760.8	1.0	I	15-20	

Mass (average)	Mass (mono.)	Apex Mass	Score	Evidence	Time	MALDI fraction
3782.7	3781.9	3781.9	1.0	I	15-25	
3800.4	3799.7	3799.7	1.0	I	0-5	
3801.6						C1-C2
3801.9						B8-B10
3807.4	3805.7	3805.7	1.0	I	0-5	
3824.6	3823.0	3824.0	1.0	IC	15-20	
3839.9	3838.9	3839.9	1.0	IC	15-20	
3840.2	3837.9	3840.9	1.0	IC	15-20	
3850.9						B4-B5
3854.3	3851.9	3853.9	1.0	IC	15-20	
3854.5	3851.9	3854.9	1.0	IC	15-20	
3858.2						B3-B4
3860.2	3857.9	3858.9	1.0	IC	15-25	
3875.4	3873.6	3873.6	1.0	I	0-5	
3892.3	3890.8	3892.8	1.0	I	15-20	
3907.5						C4-C5
3920.6	3919.6	3920.7	1.0	I	0-5	
3944.3	3942.6	3944.6	1.0	I	0-5	
3954.7						B1-B2
3954.8	3952.0	3954.0	1.0	IC	15-20	
3969.9						A14-A15
3972.9	3972.0	3972.0	1.0	I	15-20	
3979.3						B11
3982.7	3980.1	3982.1	1.0	IC	20-25	
3988.2	3985.6	3987.6	0.8	I	0-5	
3992.6	3991.6	3991.6	1.0	I	0-5	
3994.4						B11
4011.4	4009.6	4009.6	1.0	I	0-5	
4019.1						B5-B10
4021.4						C8-C15
4022.0						C4-C5
4022.3	4020.0	4021.0	1.0	IC	15-25	
4022.9	4020.9	4022.9	1.0	I	15-25	
4025.5						A14
4026.2	4025.0	4025.0	1.0	I	15-25	A14
4031.0	4028.0	4030.1	1.0	IC	15-20	
4031.6	4031.0	4031.0	1.0	IC	15-20	
4040.9	4038.1	4040.0	1.0	IC	15-25	
4041.3	4039.0	4041.0	1.0	I	15-25	
4042.0	4040.0	4042.0	1.0	I	15-25	
4042.6						B5
4047.7						B8-B11
4052.0	4050.9	4052.9	1.0	I	15-20	
4053.7	4052.2	4053.2	1.0	IC	20-25	
4058.6	4058.2	4058.2	1.0	I	0-5	
4070.3	4069.2	4070.2	1.0	I	15-20	

Mass (average)	Mass (mono.)	Apex Mass	Score	Evidence	Time	MALDI fraction
4079.4	4077.6	4077.6	1.0	I	0-5	
4116.6						B8-B10
4128.0						A14
4149.1	4146.6	4148.6	1.0	I	0-5	
4155.0						B12
4172.7						B12
4179.5						C1
4180.0						B15
4197.2	4195.6	4196.6	0.9	I	0-5	
4208.5	4207.6	4207.6	1.0	I	0-5	
4215.4	4213.6	4213.6	1.0	I	0-5	
4226.9	4226.1	4226.1	1.0	I	0-5	
4229.9	4228.6	4228.6	0.8	I	0-5	
4246.1						B12-B14
4264.5	4263.6	4263.6	1.0	I	0-5	
4276.5	4275.6	4275.6	1.0	I	0-5	
4283.3	4280.6	4281.6	1.0	I	0-5	
4294.7	4293.5	4294.4	1.0	I	0-5	
4295.9	4295.0	4295.0	1.0	I	0-5	
4338.0						B9
4338.0						B9
4344.4	4343.6	4343.6	1.0	I	0-5	
4363.0	4361.5	4362.6	1.0	I	0-5	
4365.4						B1-B2
4397.0	4395.6	4396.7	0.9	I	0-5	
4401.2	4399.6	4400.6	0.9	I	0-5	
4407.5						B3
4413.3	4411.6	4411.6	0.9	I	0-5	
4419.7	4417.6	4417.6	1.0	I	0-5	
4468.5	4467.6	4467.6	1.0	I	0-5	
4471.3						B9
4487.8	4485.6	4485.6	1.0	I	0-5	
4533.4	4532.1	4533.0	1.0	I	0-5	
4536.8	4535.6	4535.6	1.0	I	0-5	
4584.7						C2
4584.7						C2
4601.7						B13-B14
4605.4	4603.6	4604.6	1.0	I	0-5	
4616.4	4615.6	4615.6	1.0	I	0-5	
4623.7	4621.6	4621.6	1.0	I	0-5	
4672.5	4671.5	4671.5	1.0	I	0-5	
4682.1	4679.7	4680.6	1.0	IC	20-25	
4683.0						B10-B11
4684.5	4683.5	4683.5	1.0	I	0-5	
4691.1	4689.5	4689.5	1.0	I	0-5	
4695.6	4694.5	4694.5	1.0	I	0-5	

Mass (average)	Mass (mono.)	Apex Mass	Score	Evidence	Time	MALDI fraction
4716.5						B1-B2
4727.6						B9-B10
4740.8	4739.5	4739.5	1.0	I	0-5	
4751.0						B11
4752.9	4751.5	4751.5	1.0	I	0-5	
4760.8	4758.5	4758.5	1.0	I	0-5	
4796.6						C2
4800.3						C1
4820.5	4819.5	4819.5	1.0	I	0-5	
4827.1	4825.5	4825.5	1.0	I	0-5	
4833.3						B12
4861.4						B1
4876.9	4875.6	4875.6	0.9	I	0-5	
4895.2	4893.5	4893.5	1.0	I	0-5	
4944.8	4943.5	4943.5	1.0	I	0-5	
4956.9	4955.5	4955.5	1.0	I	0-5	
5024.5	5023.5	5024.5	1.0	I	0-5	
5031.2	5027.5	5029.5	0.9	I	0-5	
5080.9	5079.5	5080.6	1.0	I	0-5	
5092.5	5091.5	5093.5	1.0	I	0-5	
5099.2	5097.5	5097.5	1.0	I	0-5	
5133.6						B9-B10
5148.9	5147.5	5147.5	1.0	I	0-5	
5167.3	5165.5	5165.5	1.0	I	0-5	
5228.4	5227.5	5228.4	1.0	I	0-5	
5235.2	5231.5	5233.5	0.9	I	0-5	
5285.1	5283.5	5283.5	1.0	I	0-5	
5303.2	5301.5	5301.5	1.0	I	0-5	
5352.8	5351.5	5351.5	1.0	I	0-5	
5364.9	5363.4	5365.5	1.0	I	0-5	
5371.2	5367.4	5369.5	0.9	I	0-5	
5439.1	5435.4	5437.4	0.9	I	0-5	
5488.4	5487.4	5488.5	1.0	I	0-5	
5507.6	5505.5	5505.5	1.0	I	0-5	
5557.2	5555.4	5555.4	1.0	I	0-5	
5568.9	5567.4	5567.4	1.0	I	0-5	
5575.4	5573.4	5573.4	1.0	I	0-5	
5625.8	5623.5	5624.4	0.6	I	0-5	
5636.4	5635.4	5636.4	1.0	I	0-5	
5643.4	5639.4	5641.4	0.9	I	0-5	
5693.2	5691.5	5691.5	0.9	I	0-5	
5711.6	5709.4	5709.4	1.0	I	0-5	
5760.8	5759.4	5760.4	1.0	I	0-5	
5779.5	5776.4	5777.4	1.0	I	0-5	
5830.1	5828.4	5829.2	0.9	I	0-5	
5847.5	5845.4	5845.4	1.0	I	0-5	

Mass (average)	Mass (mono.)	Apex Mass	Score	Evidence	Time	MALDI fraction
5915.6	5913.4	5913.4	1.0	I	0-5	
5964.3	5963.4	5963.4	1.0	I	0-5	
6005.0	6003.4	6003.4	0.9	I	0-5	
6051.2	6049.3	6050.4	1.0	I	0-5	
6119.3	6117.3	6117.3	1.0	I	0-5	
6136.1	6134.3	6135.2	0.9	I	0-5	
6180.9	6180.4	6181.4	1.0	I	0-5	
6186.3	6183.3	6186.5	0.2	I	0-5	
6278.0	6275.4	6276.5	1.0	I	0-5	
6289.4	6288.0	6289.0	1.0	I	0-5	
6323.8	6321.3	6323.4	1.0	I	0-5	
6392.0	6389.3	6391.2	1.0	I	0-5	
6413.5	6411.3	6411.3	1.0	I	0-5	
6481.9	6479.4	6479.4	1.0	I	0-5	
6492.7	6491.3	6493.1	1.0	I	0-5	
6527.1	6525.3	6527.5	0.9	I	0-5	
6549.5	6547.3	6547.3	1.0	I	0-5	
6597.9	6597.3	6597.3	1.0	I	0-5	
6698.1	6696.8	6696.8	1.0	I	0-5	
6748.5	6747.0	6747.8	1.0	I	0-5	
6758.7						C7
6784.0						C7
6801.6						C7-C8
6821.5	6819.3	6820.3	1.0	I	0-5	
6845.4						C2-C4
6848.4						C12
6850.4	6848.2	6849.2	0.9	I	0-5	
6859.2						C1
6896.9						C5
6957.8	6955.3	6955.3	1.0	I	0-5	
6998.6						B8-B9
7022.3						C1
7025.8	7023.3	7023.3	1.0	I	0-5	
7049.7						C5
7093.9	7091.2	7091.2	1.0	I	0-5	
7128.0						B11
7166.3						C1
7199.7						C4-C5
7365.4	7363.4	7363.4	0.9	I	0-5	
7392.8						B13-C1
7426.0						B12
7520.9						B8-B9
7569.4	7567.2	7567.2	1.0	I	0-5	
7637.9	7635.2	7636.3	0.9	I	0-5	
7642.8	7642.3	7643.3	1.0	I	0-5	
7743.7						B9

Mass (average)	Mass (mono.)	Apex Mass	Score	Evidence	Time	MALDI fraction
7809.4						C4
7826.5						C1
7909.6	7907.4	7908.2	1.0	I	0-5	
8014.1						B9-B10
8030.6						B5
8045.0	8043.2	8044.3	1.0	I	0-5	
8045.6	8043.0	8046.9	1.0	I	15-25	
8113.0	8111.1	8113.1	1.0	I	0-5	
8317.2						C8
8317.9	8315.1	8316.2	1.0	I	0-5	

Group 3 from ion exchange column

Mass (average)	Mass (mono.)	Apex Mass	Score	Evidence	Time	MALDI fraction
2105.0						B11
2332.3						C1
2442.3						B15
2554.1						A10-A11
2647.6						C3
2700.6						C3
2701.4	2700.5	2700.5	0.88	I	25-30	
2710.3						C6
2716.1	2715.5	2716.5	1.00	IC	25-30	
2717.5						C3-C4
2717.8	2716.5	2717.5	1.00	IC	25-30	
2737.9						C3
2783.7	2782.6	2784.6	0.99	I	20-25	
2794.8	2793.5	2793.5	1.00	IC	20-25	
2795.1	2793.5	2794.4	0.92	I	20-25	
2811.5	2809.5	2810.4	1.00	IC	20-25	
2812.5	2811.5	2812.5	1.00	IC	20-25	
2813.0	2812.5	2813.5	1.00	I	20-25	
2909.5	2907.5	2909.5	1.00	IC	20-25	
2910.7	2908.5	2910.5	1.00	IC	20-25	
2922.8	2921.5	2921.5	1.00	I	20-25	
2927.0	2926.5	2926.5	1.00	I	20-25	
2927.0	2925.6	2926.5	1.00	I	20-25	
3018.3						A13-A15
3021.1	3021.7	3019.6	1.00	IC	20-25	
3021.6	3019.6	3021.6	1.00	IC	20-25	
3021.9	3019.7	3021.6	1.00	IC	20-25	
3038.9	3037.7	3039.7	1.00	IC	20-25	
3078.8	3078.6	3078.6	1.00	IC	20-25	
3079.7	3077.6	3078.6	1.00	IC	20-25	

Mass (average)	Mass (mono.)	Apex Mass	Score	Evidence	Time	MALDI fraction
3079.9	3077.6	3079.6	1.00	IC	20-25	
3081.6	3080.6	3080.6	1.00	I	20-25	
3092.9	3090.9	3092.9	1.00	I	20-25	
3094.3	3093.6	3094.6	1.00	IC	20-25	
3096.6	3095.6	3096.6	1.00	IC	20-25	
3097.2	3095.7	3096.6	1.00	IC	20-25	
3102.0	3101.6	3101.6	1.00	I	20-25	
3112.2	3111.7	3112.6	0.99	I	20-25	
3114.3	3112.7	3113.7	1.00	IC	20-25	
3114.7	3113.7	3114.7	0.89	I	20-25	
3119.9						B13
3138.3	3136.6	3137.7	0.93	I	20-25	
3150.0	3149.0	3150.0	1.00	I	20-25	
3205.5	3204.8	3205.8	1.00	I	20-25	
3207.9	3205.8	3207.8	1.00	IC	20-25	
3208.2	3205.8	3208.8	1.00	IC	20-25	
3209.7	3208.8	3208.8	0.29	I	20-25	
3216.3	3215.7	3216.7	1.00	I	20-25	
3218.7	3216.7	3217.7	1.00	I	20-25	
3219.3	3217.7	3217.7	0.73	I	20-25	
3222.6						B10
3225.2	3223.8	3224.8	1.00	IC	20-25	
3226.1	3224.8	3224.8	1.00	IC	20-25	
3226.2	3225.8	3225.8	1.00	I	20-25	
3228.3	3226.7	3228.8	1.00	IC	20-25	
3229.6	3228.7	3228.7	1.00	I	20-25	
3237.0	3234.7	3236.7	1.00	I	20-25	
3256.3						B14-B15
3260.2	3258.8	3259.8	1.00	I	25-30	
3266.9	3264.7	3266.6	1.00	IC	25-30	
3288.5	3287.7	3287.7	1.00	I	25-30	
3289.1	3288.6	3288.6	1.00	I	25-30	
3293.8	3292.8	3293.8	1.00	I	15-20	
3293.9	3291.8	3293.8	1.00	IC	15-20	
3295.5	3293.8	3295.8	1.00	I	20-25	
3295.6	3293.8	3294.8	1.00	IC	20-25	
3310.7	3309.9	3310.9	1.00	I	20-25	
3312.9	3310.8	3312.8	1.00	IC	20-25	
3313.5	3310.8	3312.8	1.00	IC	20-25	
3317.6	3315.8	3315.8	1.00	I	20-25	
3331.4	3330.8	3331.8	1.00	I	20-25	
3334.3						B15
3334.4	3333.9	3333.9	1.00	I	15-25	
3334.5	3332.9	3334.9	1.00	I	15-25	
3336.4	3334.9	3335.9	1.00	IC	20-25	
3349.2	3346.8	3348.8	1.00	I	20-25	

Mass (average)	Mass (mono.)	Apex Mass	Score	Evidence	Time	MALDI fraction
3350.2	3349.8	3349.8	1.00	I	20-25	
3351.5	3350.9	3350.9	1.00	I	10-20	
3352.0	3349.8	3351.8	1.00	IC	20-25	
3352.8	3350.7	3352.8	1.00	I	20-25	
3354.1	3350.9	3355.8	1.00	IC	20-25	
3355.1	3353.8	3353.8	1.00	IC	20-25	
3363.3						B13-B14
3365.0	3362.9	3363.9	1.00	IC	20-25	
3365.3	3362.9	3364.9	1.00	IC	20-25	
3365.3	3363.9	3364.8	1.00	I	20-25	
3365.3	3363.8	3364.8	1.00	I	20-25	
3367.3	3364.8	3366.8	1.00	IC	20-25	
3367.5	3366.8	3368.9	1.00	IC	20-25	
3369.9	3367.9	3368.9	1.00	I	20-25	
3372.0						B1
3375.4						C8
3375.5	3374.7	3374.7	1.00	I	20-25	
3383.5	3382.9	3383.9	1.00	I	20-25	
3386.4	3384.9	3386.8	1.00	I	20-25	
3391.9	3390.7	3391.8	1.00	I	20-25	
3402.1	3399.9	3400.9	1.00	IC	20-25	
3402.6	3400.9	3401.8	1.00	IC	20-25	
3403.1	3401.8	3401.8	1.00	IC	20-25	
3404.2	3403.8	3403.8	1.00	I	20-25	
3404.8						C7
3407.3						B9
3417.9	3416.9	3418.9	1.00	I	15-25	
3420.4	3417.9	3418.9	1.00	IC	20-25	
3420.5	3417.9	3419.8	1.00	IC	20-25	
3421.4	3418.9	3419.8	1.00	IC	20-25	
3429.7						B7-B9
3430.6	3428.8	3431.8	0.88	I	20-25	
3431.8	3429.8	3431.8	1.00	IC	20-25	
3432.2	3430.8	3432.8	1.00	IC	20-25	
3432.3	3431.8	3432.8	1.00	I	20-25	
3434.0	3432.9	3434.9	1.00	I	20-25	
3434.0						C3-C5
3440.3	3439.8	3439.8	1.00	I	20-25	
3440.5	3438.8	3440.8	1.00	IC	20-25	
3447.9						B3-B6
3448.5	3448.0	3448.9	1.00	I	20-25	
3449.9	3447.9	3449.9	1.00	IC	20-25	
3450.6						A13-A14
3451.4	3448.9	3449.9	1.00	IC	20-25	
3451.8						C6-C13
3452.1	3449.9	3450.9	1.00	I	20-25	

Mass (average)	Mass (mono.)	Apex Mass	Score	Evidence	Time	MALDI fraction
3452.4	3450.9	3451.8	1.00	IC	20-25	
3459.9	3459.0	3459.9	1.00	I	20-30	
3460.7						B1
3465.1						A12
3465.9	3463.9	3465.9	1.00	IC	15-20	
3466.0						C14
3466.4	3463.9	3465.9	1.00	IC	10-15	
3466.5	3463.9	3465.9	1.00	IC	10-15	
3466.8	3464.9	3466.9	1.00	IC	15-20	
3467.1	3465.9	3465.9	0.00	I	10-15	
3467.2	3464.9	3466.9	1.00	IC	15-20	
3467.4	3464.9	3466.9	1.00	IC	15-20	
3468.2	3466.9	3467.9	1.00	IC	20-25	
3468.7	3467.9	3468.9	0.60	I	15-20	
3468.8	3466.9	3467.9	1.00	IC	20-25	
3469.1	3466.9	3468.9	1.00	IC	20-25	
3469.3	3469.9	3469.9	1.00	IC	20-25	
3473.1	3470.8	3471.8	1.00	IC	20-25	
3475.8						A15
3476.3						B10-B12
3477.5	3476.8	3477.8	1.00	I	25-30	
3479.8	3477.8	3479.8	1.00	IC	25-30	
3480.0	3477.8	3478.8	1.00	IC	25-30	
3480.8						A11
3481.4						B9
3481.5						C15
3482.6	3481.8	3481.8	0.75	I	25-30	
3482.8	3481.9	3482.9	1.00	IC	20-25	
3484.6	3482.9	3484.9	1.00	IC	20-25	
3485.3	3483.9	3485.9	1.00	IC	20-25	
3488.2	3486.8	3487.8	1.00	I	10-15	
3488.2	3486.8	3487.8	1.00	IC	20-25	
3488.7	3487.9	3487.9	1.00	I	20-25	
3488.9	3487.7	3488.8	1.00	I	20-25	
3489.1	3486.8	3488.8	1.00	IC	15-20	
3493.4						B15-C3
3495.0	3492.8	3493.8	1.00	I	20-25	
3497.0	3495.9	3497.9	1.00	I	20-30	
3498.3	3497.9	3497.9	1.00	I	20-25	
3502.3	3502.8	3505.8	1.00	IC	20-25	
3502.5	3501.9	3502.9	1.00	IC	20-25	
3504.1	3501.9	3503.8	1.00	IC	15-20	
3504.4	3501.9	3503.8	1.00	IC	15-20	
3506.0	3503.9	3507.8	1.00	IC	20-25	
3506.5	3503.8	3505.8	1.00	IC	20-25	
3507.6	3506.8	3506.8	0.89	I	15-20	

Mass (average)	Mass (mono.)	Apex Mass	Score	Evidence	Time	MALDI fraction
3510.2	3508.8	3508.8	1.00	I	20-25	
3510.3	3507.9	3509.8	1.00	I	15-20	
3510.6	3508.9	3509.8	1.00	I	15-20	
3511.1	3508.8	3509.8	1.00	IC	20-25	
3515.6	3513.8	3514.8	1.00	I	20-25	
3517.3	3516.7	3517.8	1.00	IC	25-30	
3517.7	3515.8	3516.7	1.00	IC	25-30	
3522.4	3521.9	3521.9	1.00	I	20-25	
3522.4	3521.8	3522.9	1.00	IC	20-25	
3525.6	3523.9	3525.8	1.00	IC	20-25	
3528.2	3525.8	3528.8	1.00	IC	20-25	
3532.2	3530.8	3530.8	1.00	I	20-25	
3538.7	3536.8	3537.8	1.00	I	20-25	
3542.7	3540.8	3543.8	1.00	IC	20-25	
3544.9	3543.7	3545.8	1.00	I	20-25	
3546.2	3544.9	3544.9	1.00	I	20-25	
3548.8	3546.8	3547.8	1.00	I	20-25	
3553.0	3552.0	3552.9	1.00	I	20-25	
3553.1	3551.8	3551.8	1.00	I	20-25	
3557.0						B10-B11
3562.9	3562.1	3562.1	0.99	I	20-25	
3563.3						B1-B3
3564.2						C14-C15
3564.6	3562.0	3563.9	1.00	IC	20-25	
3564.7	3562.0	3564.0	1.00	IC	20-25	
3565.5	3564.9	3564.9	1.00	IC	20-25	
3567.3	3566.9	3566.9	1.00	I	20-25	
3567.7						B6
3578.3	3577.0	3579.0	1.00	IC	20-25	
3578.8						C13-C15
3579.1	3579.0	3580.0	1.00	IC	20-25	
3579.3						A15
3581.2						C3-C6
3581.7	3580.0	3582.0	1.00	IC	20-25	
3583.2	3581.9	3581.9	1.00	IC	20-25	
3585.9	3583.9	3583.9	1.00	I	20-25	
3590.9						B3-B4
3597.6	3597.0	3598.0	1.00	I	20-25	
3600.3	3599.0	3601.0	1.00	IC	20-25	
3602.4	3599.9	3601.9	1.00	IC	20-25	
3604.7	3602.9	3602.9	0.25	I	20-25	
3618.5	3615.9	3617.9	1.00	IC	20-25	
3621.8	3620.9	3620.9	1.00	I	20-25	
3629.3						B1-B2
3631.8	3629.8	3630.8	1.00	IC	20-25	
3635.9	3634.9	3636.9	1.00	I	20-25	

Mass (average)	Mass (mono.)	Apex Mass	Score	Evidence	Time	MALDI fraction
3639.5	3637.9	3640.9	1.00	I	20-25	
3642.7						B5-B6
3645.4	3643.9	3644.9	1.00	IC	20-25	
3650.2	3648.8	3648.8	1.00	I	20-25	
3650.5	3648.9	3651.9	1.00	I	20-25	
3680.3						B11
3685.8	3684.0	3685.1	1.00	I	20-25	
3685.9	3685.0	3685.0	1.00	I	20-25	
3685.9	3685.0	3685.0	1.00	I	20-25	
3686.1	3684.0	3685.1	1.00	IC	20-25	
3694.3						B4-B6
3695.2	3692.9	3694.9	1.00	IC	20-25	
3703.0	3702.0	3703.1	1.00	I	20-25	
3707.4						B6
3712.0	3710.1	3712.0	1.00	IC	20-25	
3714.7						C7
3740.3						B9
3798.5						B7-B10
3809.2						B9
3827.4	3826.9	3827.9	1.00	I	20-25	
3827.8	3825.9	3827.0	1.00	I	20-25	
3828.7						B4-B5
3829.3	3828.8	3828.8	1.00	I	20-25	
3860.2						B13-B14
3912.8	3911.9	3911.9	1.00	I	20-25	
3937.6	3937.1	3938.1	1.00	I	20-25	B5
3938.6	3936.2	3939.1	1.00	I	20-25	
3938.9						B5
3954.2	3952.1	3954.1	0.75	I	20-25	
3955.5	3953.1	3955.1	1.00	IC	20-25	
3956.5	3956.1	3956.1	1.00	I	20-25	
3970.0						A13-A15
3971.1						C5-C13
3972.9	3970.1	3972.1	1.00	IC	20-25	
3973.2	3970.0	3972.1	1.00	IC	20-25	
3973.8	3971.1	3974.0	1.00	IC	20-25	
3979.9	3978.3	3979.3	0.88	I	20-30	
3981.6	3979.3	3981.3	1.00	I	20-30	
3990.8	3988.1	3990.1	1.00	IC	20-25	
3991.0	3989.2	3991.1	1.00	IC	20-25	
3994.2						C11-C12
3995.7	3993.0	3995.0	1.00	IC	20-25	
3996.2	3995.1	3995.1	1.00	I	20-25	
4006.8	4007.1	4008.1	1.00	IC	20-25	
4007.1	4006.1	4007.2	1.00	I	20-25	
4007.3	4005.2	4007.2	1.00	IC	20-25	

Mass (average)	Mass (mono.)	Apex Mass	Score	Evidence	Time	MALDI fraction
4008.4						B5
4009.6	4009.0	4010.0	1.00	I	20-25	
4010.5	4008.1	4010.0	1.00	IC	20-25	
4016.9	4016.0	4016.0	1.00	I	20-25	
4017.6						B6-B10
4018.9						A7-A8
4019.4						B13
4022.5	4021.1	4021.1	1.00	IC	20-25	
4022.7	4020.1	4022.1	1.00	IC	20-25	
4024.3	4022.1	4022.1	0.00	I	20-25	
4041.6	4039.1	4040.1	1.00	IC	20-25	
4060.6	4059.1	4061.0	1.00	I	20-25	
4081.0	4078.3	4081.3	0.80	I	20-25	
4081.3						B8
4081.7	4079.4	4081.3	1.00	IC	20-25	
4083.7	4083.3	4083.3	1.00	I	20-25	
4097.9	4096.3	4098.4	1.00	I	20-25	
4132.6						B9-B10
4151.3						B12-B14
4153.9	4152.4	4154.4	1.00	I	20-25	
4156.2						B8
4156.5						B3
4164.6						B5
4204.4						B11-B13
4206.5	4205.4	4206.4	1.00	IC	20-25	
4209.5	4206.4	4209.4	1.00	IC	20-30	
4210.0	4208.4	4210.4	1.00	IC	20-30	
4228.8	4224.4	4226.4	1.00	IC	20-30	
4232.3	4231.3	4232.4	1.00	I	20-30	
4235.3						B14-B15
4236.1	4234.4	4236.4	1.00	IC	20-30	
4245.4	4243.3	4246.3	0.88	I	20-30	
4245.7						B13
4246.7	4244.4	4247.4	1.00	IC	20-30	
4247.7	4245.3	4247.3	1.00	I	20-30	
4268.1	4267.2	4267.2	1.00	I	20-25	
4279.4						B12
4323.1	4321.3	4323.3	1.00	I	20-25	
4323.2	4321.3	4324.3	0.76	I	20-25	
4345.3	4344.4	4345.3	1.00	I	20-30	
4396.6						B14
4463.4	4462.2	4463.3	1.00	I	20-25	
4463.8	4463.4	4463.4	0.99	I	20-25	
4466.1	4465.3	4465.3	1.00	I	20-25	
4543.7	4541.5	4545.6	1.00	I	20-25	
4544.1	4542.6	4544.6	1.00	I	20-25	

Mass (average)	Mass (mono.)	Apex Mass	Score	Evidence	Time	MALDI fraction
4548.8						B12
4637.6						B12-B13
4808.8	4807.7	4808.7	1.00	I	25-30	
4809.2	4808.7	4809.6	1.00	I	25-30	
4880.4	4878.7	4879.7	1.00	IC	25-30	
4880.4	4877.8	4879.7	1.00	IC	25-30	
4881.1	4879.7	4879.7	1.00	I	25-30	
4882.2	4881.8	4881.8	1.00	IC	25-30	
4884.0						B15
4898.3						B14
4951.1	4949.6	4950.7	1.00	I	20-25	
5522.2	5521.3	5522.2	0.99	I	20-25	
6658.4						B13-B14
6680.8						B14-B15
6777.0						C8
6803.1						C7-C8
6865.5						C3-C5
6885.3						B13
6909.1						B11
6910.0						C6
6910.0						C6
6919.6	6918.1	6919.2	1.00	I	20-30	
6925.2						B10
6988.1	6987.2	6988.2	1.00	IC	25-30	
6988.4	6986.3	6986.3	1.00	IC	25-30	
6988.4	6984.2	6988.3	1.00	IC	25-30	
6988.8						C1-C3
6992.4						B15
7006.0	7004.3	7006.2	1.00	IC	20-30	
7006.6	7004.3	7006.2	1.00	IC	20-30	
7007.8	7007.3	7007.3	1.00	I	20-30	
7026.8	7024.1	7026.2	1.00	I	20-30	
7116.7						B11
7125.4	7123.2	7124.2	1.00	I	20-25	
7125.5	7123.2	7125.2	1.00	IC	20-25	
7129.8						B10
7142.6	7141.2	7141.2	1.00	IC	20-30	
7143.3	7140.3	7142.4	1.00	IC	20-30	
7143.9						B2
7163.8						C1-C4
7179.0						C6
7227.0						B2
7393.2						B13
7393.2						B13
7429.3						B14
7447.1						B15

Mass (average)	Mass (mono.)	Apex Mass	Score	Evidence	Time	MALDI fraction
7449.8	7448.1	7449.2	1.00	I	20-25	
7449.9	7448.3	7450.3	1.00	IC	20-25	
7467.9	7466.2	7467.3	1.00	I	20-25	
7490.6						B9-B10
7561.0						A15
8327.1						C2

Group 4 from ion exchange column

Mass (average)	Mass (mono.)	Apex Mass	Score	Evidence	Time	MALDI fraction
2051.6	2051.1	2051.1	1.00	I	25-35	
2753.9						B14
2773.4	2772.4	2772.4	1.00	I	40-50	
2889.5	2888.4	2889.4	1.00	I	5-10	
2890.3	2888.5	2889.4	1.00	I	10-15	
2890.9	2889.4	2890.4	1.00	I	5-10	
2940.4						C14-C15
2940.9						B2-B3
2941.1	2939.5	2940.5	1.00	IC	20-25	
2987.0						C8-C13
2988.5	2986.5	2988.5	1.00	IC	5-15	
2988.6	2986.5	2987.5	1.00	IC	5-15	
2988.6						C4-C5
2989.5	2987.5	2989.5	1.00	IC	5-15	
2990.6	2988.5	2990.5	1.00	IC	10-15	
2991.9						A11-A15
3000.8						C9-C10
3006.5	3005.6	3006.6	1.00	I	10-20	
3010.5	3008.5	3009.5	1.00	IC	5-15	
3012.2	3010.4	3011.4	1.00	IC	5-15	
3012.7	3011.5	3011.5	1.00	I	10-15	
3017.4						A12
3017.6						C9
3026.3	3024.4	3026.4	1.00	IC	5-15	
3027.5	3025.4	3026.4	1.00	IC	5-15	
3028.2	3026.4	3028.4	1.00	I	10-15	
3033.4	3031.4	3032.4	1.00	I	10-15	
3043.9	3042.7	3043.7	1.00	I	35-40	
3044.2	3043.7	3043.7	1.00	I	35-40	
3045.7	3043.7	3045.7	1.00	IC	35-40	
3045.9						C1

Mass (average)	Mass (mono.)	Apex Mass	Score	Evidence	Time	MALDI fraction
3049.3	3047.4	3049.4	1.00	I	10-15	
3060.6						C3
3105.8	3104.8	3104.8	1.00	I	25-35	
3112.5	3111.6	3112.6	1.00	I	20-25	
3141.6	3140.6	3141.6	1.00	I	25-30	
3150.5	3148.8	3149.8	1.00	IC	25-30	
3152.3						B8-B11
3155.1	3154.6	3154.6	1.00	I	25-30	
3155.1	3154.7	3154.7	1.00	I	25-30	
3177.4						B8
3297.9						C12
3297.9						C12
3298.0						A15
3298.0						A15
3306.3	3304.7	3306.7	1.00	I	25-30	B11-B13
3309.4						B11-B13
3339.4	3337.6	3339.6	1.00	IC	30-35	
3347.0						B14
3374.0						A15
3404.4	3402.7	3404.7	1.00	IC	20-25	
3405.4						B1-B2
3406.0	3404.6	3405.6	1.00	I	25-30	
3450.2	3447.8	3449.8	1.00	IC	20-25	
3450.9						C14
3456.5						A14-B5
3458.3	3455.9	3457.9	1.00	IC	20-25	
3464.0						B11
3464.2	3461.8	3463.8	1.00	IC	10-15	
3465.8						C11
3467.3						A13-A15
3469.0						C13-C14
3478.7						B9-B10
3480.0						C4
3480.3						C10-C12
3501.9	3500.8	3501.8	1.00	IC	25-30	
3501.9						B5-B6
3502.6	3500.8	3501.8	1.00	I	20-30	
3503.2	3502.8	3502.8	1.00	IC	25-30	
3508.0						B14
3516.1						B3
3521.3	3519.7	3521.7	1.00	I	5-10	

Mass (average)	Mass (mono.)	Apex Mass	Score	Evidence	Time	MALDI fraction
3521.3	3520.8	3521.7	1.00	I	5-10	
3542.8						C15
3552.9	3550.8	3552.8	1.00	IC	25-30	
3553.4						B9-B10
3554.3	3551.8	3553.8	1.00	IC	25-35	
3556.4	3555.8	3555.8	1.00	IC	30-35	
3560.8	3558.8	3560.8	1.00	IC	20-25	
3578.5						A15-C1
3581.2						B15
3583.0						C5
3587.1						C2-C4
3590.1						B1-B2
3592.2	3590.8	3591.8	1.00	IC	25-35	
3596.8						C3
3638.2	3636.8	3637.8	1.00	I	20-25	
3684.4	3682.9	3685.8	1.00	I	25-30	
3685.5						B6-B8
3688.2	3686.7	3687.7	0.94	I	25-30	
3708.3						C15
3708.6						B3-B5
3708.9	3708.0	3708.0	1.00	I	25-30	
3710.3	3708.0	3710.0	1.00	IC	25-30	
3711.0	3708.9	3711.0	1.00	IC	25-30	
3711.4	3709.0	3711.0	1.00	IC	25-30	
3712.4	3710.9	3711.9	1.00	I	25-30	
3715.7						C5
3750.4						B14
3910.8						A14
3911.0						B14
3913.3						C11
3913.7	3911.0	3913.0	1.00	IC	10-15	
3914.7	3913.0	3915.0	1.00	IC	15-20	
3928.3						B7
3940.7						A14-A15
3941.9						C11-C12
3986.7						B5-B6
3988.1	3987.0	3989.0	1.00	I	25-30	
4003.2						A13
4018.0						B11
4022.9						B5
4082.0						B8-B9

Mass (average)	Mass (mono.)	Apex Mass	Score	Evidence	Time	MALDI fraction
4103.2	4102.2	4104.2	1.00	I	25-35	
4104.7						B8
4112.3						B7-B8
4156.9						B3
4224.1						B10
4245.9						B9
4283.2						B11
4303.3						B10
4307.3						B7
4390.0						B3
4464.4	4462.1	4464.1	1.00	IC	20-25	
4466.9						B1-B2
4481.3						A15
4493.7	4492.2	4494.2	1.00	I	20-25	
4501.2						B11
4565.3	4564.3	4565.4	1.00	I	20-30	
4637.5						B7-B8
4658.0						A15-B1
4666.5						C13
4671.9						B3
4675.9						B11
4679.7						C15
4863.7						B13
4881.6						B11-B12
6304.5						B11
6614.6						B12-B13
6659.1						B11
6677.2						B14
6867.4						C2-C5
6931.4						B8-B9
7017.9						B14
7160.8						B15-C1
7176.3						C2
7191.1						C1
7208.6						C3-C5
7331.0						C2
7428.6						B12
7497.0						B14-B15
7822.6						B14
8290.3						B14

Group 5 from ion exchange column

Mass (average)	Mass (mono.)	Apex Mass	Score	Evidence	Time	MALDI fraction
2020.3	2018.9	2019.9	1.00	IC	0-5	
2022.3	2021.4	2021.4	1.00	I	0-5	
2031.2	2030.6	2031.6	1.00	I	0-5	
2034.4	2033.9	2034.8	0.99	I	0-5	
2041.1	2040.3	2041.2	1.00	I	0-5	
2043.3						B5
2043.5	2042.9	2043.8	1.00	I	0-5	
2049.7	2048.4	2049.4	1.00	I	0-5	
2052.8	2052.3	2052.3	1.00	I	0-5	
2059.3	2058.9	2058.9	1.00	I	0-5	
2073.8	2073.1	2074.2	0.99	I	0-5	
2079.5	2078.9	2079.9	1.00	I	0-5	
2088.4	2087.9	2088.9	1.00	I	0-5	
2100.6	2099.9	2099.9	1.00	IC	0-5	
2102.8	2101.5	2102.6	0.88	I	0-5	
2109.5	2109.1	2109.1	1.00	I	0-5	
2111.8	2111.3	2112.2	0.99	I	0-5	
2117.3	2116.4	2117.3	1.00	I	0-5	
2128.5	2127.9	2128.8	1.00	I	0-5	
2134.4	2133.0	2134.1	1.00	I	0-5	
2138.6						B6-B7
2142.4	2141.7	2142.8	1.00	I	0-5	
2144.2	2143.2	2144.2	1.00	I	0-5	
2145.3						A15-B1
2147.9	2146.4	2147.3	1.00	I	0-5	
2150.9	2149.8	2150.9	1.00	I	0-5	
2155.9	2154.9	2155.9	1.00	IC	0-5	
2160.3	2159.8	2159.8	1.00	I	0-5	
2171.1	2170.0	2171.0	0.87	I	0-5	
2180.2						B7
2180.5	2179.9	2180.9	1.00	I	0-5	
2185.7	2184.9	2184.9	1.00	I	0-5	
2188.3	2187.8	2187.8	1.00	I	0-5	
2200.3	2199.5	2199.5	1.00	I	0-5	
2210.7	2209.6	2210.6	1.00	I	0-5	
2215.5	2214.8	2215.9	1.00	I	0-5	
2224.2	2222.9	2223.9	1.00	I	0-5	
2229.3	2228.9	2228.9	1.00	I	0-5	
2232.9	2232.1	2232.1	1.00	I	0-5	

Mass (average)	Mass (mono.)	Apex Mass	Score	Evidence	Time	MALDI fraction
2236.5	2235.9	2235.9	1.00	I	0-5	
2250.6	2249.8	2249.8	1.00	I	0-5	
2292.5	2290.9	2291.9	1.00	I	0-5	
2335.4	2334.4	2334.4	1.00	I	0-5	
2336.6						B5-B6
2336.7						D1-D2
2360.2	2358.9	2359.9	1.00	I	0-5	
2372.5	2371.9	2371.9	1.00	I	0-5	
2395.6						C5
2402.7	2402.3	2402.3	1.00	I	0-5	
2428.4	2426.9	2427.9	0.97	I	0-5	
2432.5						A10-A11
2438.2						C8
2464.9	2463.7	2464.7	1.00	I	35-45	
2488.1	2486.8	2487.9	0.88	I	0-5	
2496.2	2494.9	2495.9	1.00	I	0-5	
2508.6	2507.8	2507.8	1.00	I	0-5	
2564.3	2562.9	2563.8	1.00	I	0-5	
2576.5	2575.8	2575.8	1.00	I	0-5	
2623.9	2622.8	2623.8	0.90	I	0-5	
2644.6	2643.8	2643.8	1.00	I	0-5	
2693.5	2692.8	2693.9	1.00	I	0-5	
2696.9	2694.8	2695.8	1.00	I	0-5	
2704.1	2702.7	2703.8	0.87	I	0-5	
2710.5						B15-C3
2710.6						C7-C9
2710.9						A10
2711.9	2710.8	2711.8	1.00	I	0-5	
2715.1	2713.6	2714.6	1.00	IC	40-45	
2716.3	2714.6	2715.6	1.00	IC	45-50	
2716.7	2714.6	2715.6	1.00	IC	40-45	
2717.5	2715.6	2716.6	1.00	IC	45-50	
2734.2	2732.6	2734.6	1.00	I	35-45	
2762.1	2761.8	2761.8	1.00	I	0-5	
2769.0	2767.8	2767.8	1.00	I	0-5	
2780.6	2779.8	2779.8	1.00	I	0-5	
2790.3	2788.9	2789.9	1.00	I	0-5	
2799.0	2797.8	2797.8	1.00	I	0-5	
2825.4						A10
2829.5	2828.8	2829.8	1.00	I	0-5	
2833.0	2830.8	2831.8	1.00	I	0-5	

Mass (average)	Mass (mono.)	Apex Mass	Score	Evidence	Time	MALDI fraction
2839.8	2838.8	2839.8	1.00	I	0-5	
2847.9	2846.9	2847.8	1.00	I	0-5	
2858.3	2856.8	2857.8	1.00	I	0-5	
2863.4	2862.8	2863.8	1.00	I	0-5	
2867.1	2865.8	2865.8	0.94	I	0-5	
2874.8	2873.8	2873.8	1.00	I	0-5	
2895.2						B15-C1
2896.2	2894.8	2895.8	0.89	I	0-5	
2901.5	2900.8	2900.8	1.00	IC	40-45	
2904.3	2902.8	2903.8	1.00	I	0-5	
2916.9	2915.8	2915.8	1.00	I	0-5	
2923.7						B5-B6
2923.9						D1-D3
2925.2	2923.7	2924.7	1.00	IC	20-25	
2925.9						A10
2938.6						C8-D1
2939.6						B2-B3
2940.0						B10
2941.8	2939.6	2941.7	1.00	IC	15-20	
2962.9	2961.8	2961.8	1.00	I	0-5	
2963.6	2962.6	2963.6	1.00	I	15-20	
2969.2	2966.9	2967.8	1.00	I	0-5	
2969.6						C14
2969.8						B2
2983.5	2982.9	2983.8	1.00	I	0-5	
2986.3						C8-C13
2986.4						A12-B1
2995.1	2992.9	2993.8	1.00	IC	0-5	
3003.3	3001.8	3001.8	1.00	I	0-5	
3012.2	3010.8	3011.8	0.89	I	0-5	
3029.2						A10
3043.5	3042.9	3043.8	0.99	I	0-5	
3052.7	3051.8	3051.8	1.00	I	0-5	
3062.2	3060.8	3061.8	1.00	I	0-5	
3088.5						D1-D4
3090.9						B9-B10
3092.9	3092.0	3093.0	1.00	I	25-35	
3094.5	3093.0	3094.0	1.00	IC	25-30	
3105.2	3103.3	3104.3	0.79	I	0-5	
3105.3	3102.8	3103.8	1.00	I	0-5	
3111.4	3110.7	3111.8	1.00	I	0-5	

Mass (average)	Mass (mono.)	Apex Mass	Score	Evidence	Time	MALDI fraction
3120.1	3119.8	3119.8	1.00	I	0-5	
3129.8	3127.9	3128.9	1.00	I	0-5	
3163.4	3162.8	3163.8	1.00	I	0-5	
3165.9	3164.7	3165.8	1.00	I	0-5	
3179.2	3177.8	3179.8	1.00	I	0-5	
3198.2	3196.8	3197.8	1.00	IC	0-5	
3202.9	3201.8	3203.8	1.00	I	0-5	
3212.0	3210.8	3212.8	1.00	I	0-5	
3232.1	3231.8	3231.8	1.00	I	0-5	
3234.2	3233.8	3233.8	0.98	I	0-5	
3237.4	3235.8	3237.8	1.00	I	0-5	
3263.1	3261.8	3261.8	1.00	I	0-5	
3267.9	3266.8	3266.8	1.00	IC	0-5	
3280.8	3279.8	3281.8	1.00	I	0-5	
3301.3	3299.8	3301.7	0.77	I	0-5	
3306.0	3304.9	3306.9	1.00	IC	25-30	
3313.8	3312.8	3313.8	1.00	I	0-5	
3316.5						B10-B12
3328.8						C7-C9
3332.4	3330.8	3332.8	1.00	I	0-5	
3336.3						B13-B15
3372.9	3371.8	3373.8	1.00	I	0-5	
3376.8	3374.3	3376.3	0.81	I	0-5	
3383.3	3381.8	3383.8	1.00	I	0-5	
3394.0	3391.9	3393.9	1.00	I	25-30	
3394.4	3392.9	3394.9	1.00	I	25-35	
3402.5	3400.8	3401.8	1.00	I	0-5	
3407.0	3405.8	3407.8	1.00	I	0-5	
3417.3						B8
3419.1	3417.8	3418.9	1.00	IC	25-30	
3430.5						B3-B5
3431.7						D1-D2
3432.0	3430.1	3431.2	1.00	IC	20-25	
3436.2	3434.7	3435.8	0.88	I	0-5	
3455.5						B5
3461.4	3459.8	3459.8	1.00	IC	0-5	
3467.4	3464.8	3465.8	1.00	IC	0-5	
3471.0	3470.8	3470.8	1.00	IC	0-5	
3473.3	3472.7	3473.7	1.00	I	0-5	
3478.7	3476.4	3478.4	0.83	I	0-5	
3481.9	3481.8	3480.8	1.00	IC	0-5	

Mass (average)	Mass (mono.)	Apex Mass	Score	Evidence	Time	MALDI fraction
3496.0						B6
3508.9	3507.8	3509.7	1.00	I	0-5	
3513.1	3510.8	3511.8	1.00	I	0-5	
3519.0	3518.0	3518.0	1.00	I	5-10	
3520.1	3519.0	3520.0	1.00	IC	5-15	
3522.1	3520.0	3521.0	1.00	IC	5-10	
3530.3	3528.8	3530.8	1.00	I	0-5	
3536.4	3534.8	3536.8	1.00	I	0-5	
3551.9	3547.8	3553.7	1.00	IC	0-5	
3572.0						A15-B3
3573.0						C8-C13
3586.9	3585.0	3587.0	1.00	IC	20-25	
3588.5						C2-C4
3603.6	3600.9	3601.8	1.00	IC	0-5	
3607.3	3605.0	3607.0	1.00	IC	25-30	
3609.1	3608.0	3608.0	1.00	I	25-30	
3611.6						B7-B8
3615.3	3613.2	3614.4	1.00	I	0-5	
3636.3						D1-D2
3637.4						B5-B7
3637.5	3635.0	3637.0	1.00	IC	30-35	
3638.4	3636.0	3638.0	1.00	IC	20-25	
3641.0						B10
3649.6	3646.8	3647.8	1.00	IC	0-5	
3665.0	3662.8	3663.8	1.00	I	0-5	
3671.1	3668.8	3669.8	1.00	I	0-5	
3675.6	3674.8	3674.8	0.88	I	0-5	
3675.8						A10-A12
3676.1						C7-C8
3677.8	3677.1	3678.1	1.00	I	5-10	
3680.3	3678.0	3679.0	1.00	IC	5-10	
3686.7	3685.7	3685.7	1.00	I	0-5	
3693.8						B6
3696.8	3695.8	3697.7	1.00	I	0-5	
3702.1						D1-D3
3705.7						B3-B7
3707.0	3705.8	3707.7	0.99	I	0-5	
3710.2	3709.8	3709.8	1.00	I	0-5	
3731.1	3729.7	3730.6	1.00	I	0-5	
3740.2						B5
3740.6	3738.8	3740.8	0.80	I	0-5	

Mass (average)	Mass (mono.)	Apex Mass	Score	Evidence	Time	MALDI fraction
3744.3						D2
3746.7	3745.8	3746.7	1.00	I	0-5	
3753.3	3751.8	3753.8	1.00	I	0-5	
3759.6	3757.0	3759.0	1.00	IC	25-30	
3774.4	3773.1	3775.1	1.00	I	20-25	
3777.1	3775.7	3775.7	1.00	I	0-5	
3778.0						B8-B9
3793.3	3792.8	3793.8	1.00	I	0-5	
3801.0	3800.0	3800.0	1.00	IC	10-15	
3801.8						D1-D2
3802.9	3802.0	3803.0	1.00	IC	20-25	
3807.5	3804.7	3805.8	1.00	I	0-5	
3821.3						A12
3823.6	3819.8	3821.8	1.00	IC	0-5	
3826.4	3825.2	3826.3	0.87	I	0-5	
3843.7	3841.8	3842.9	0.60	I	0-5	
3851.0						B5
3856.8	3855.8	3857.8	1.00	I	0-5	
3857.6						D1-D4
3858.6						B6-B8
3868.9	3867.7	3867.7	1.00	I	0-5	
3874.7	3871.7	3873.8	1.00	IC	0-5	
3879.0	3877.7	3877.7	1.00	I	0-5	
3891.4	3889.7	3889.7	1.00	IC	0-5	
3908.0						B5-B6
3908.3						C13
3909.2						A12-A15
3909.2						B15
3909.6						D1-D2
3911.1						C7-C11
3913.0	3911.2	3912.2	1.00	IC	5-10	
3915.2	3913.2	3915.2	1.00	IC	5-10	
3927.3						B8
3945.5	3942.7	3944.8	0.88	I	0-5	
3951.8	3951.2	3952.3	0.99	I	0-5	
3957.1	3955.6	3957.7	1.00	IC	0-5	
3962.1	3959.7	3962.8	1.00	IC	0-5	
3972.2	3969.5	3971.5	1.00	IC	20-25	
3978.8	3977.6	3979.7	0.99	I	0-5	
3983.8						B6
3985.6	3984.5	3986.5	1.00	I	0-5	

Mass (average)	Mass (mono.)	Apex Mass	Score	Evidence	Time	MALDI fraction
3994.2	3991.8	3992.8	1.00	IC	0-5	
4004.8	4003.7	4003.7	1.00	I	0-5	
4011.5	4008.7	4009.7	1.00	I	0-5	
4018.5						B5-B6
4020.4						D1-D2
4022.7	4019.7	4021.7	0.81	I	0-5	
4027.3	4023.8	4025.7	1.00	IC	0-5	
4030.7	4029.2	4030.3	1.00	I	0-5	
4039.4	4037.7	4037.7	0.94	I	0-5	
4047.9	4045.7	4047.5	0.84	I	0-5	
4050.2	4049.2	4050.3	1.00	I	0-5	
4056.5	4054.8	4057.8	1.00	I	0-5	
4058.9	4054.3	4059.8	1.00	IC	0-5	
4072.7	4070.8	4071.7	1.00	I	0-5	
4079.5	4076.7	4077.7	1.00	I	0-5	
4087.4						B5-B6
4091.0	4090.2	4090.2	1.00	I	0-5	
4096.3	4093.7	4094.7	1.00	IC	0-5	
4098.8						D1-D4
4131.7	4129.7	4131.8	1.00	I	0-5	
4134.7	4133.2	4134.2	1.00	I	0-5	
4149.7	4147.2	4150.2	0.81	I	0-5	
4162.4	4159.8	4161.8	1.00	IC	0-5	
4174.8						B10
4178.8	4177.4	4178.5	1.00	I	30-35	
4179.8	4178.4	4179.5	1.00	I	35-40	
4183.4	4181.8	4182.7	0.73	I	0-5	
4189.3	4188.8	4189.8	1.00	I	0-5	
4192.6	4190.7	4190.8	1.00	IC	0-5	
4201.0	4198.8	4198.8	0.28	I	0-5	
4209.1	4207.7	4207.7	1.00	IC	0-5	
4215.3	4212.6	4213.7	1.00	IC	0-5	
4230.8	4227.7	4229.7	1.00	I	0-5	
4240.6						B10
4262.7	4261.8	4263.7	1.00	IC	0-5	
4263.3						D1-D4
4265.4						B6-B9
4268.0	4266.6	4267.5	1.00	IC	20-30	
4271.1						B7
4276.6	4274.7	4275.7	1.00	I	0-5	
4283.6	4280.7	4281.7	1.00	I	0-5	

Mass (average)	Mass (mono.)	Apex Mass	Score	Evidence	Time	MALDI fraction
4286.0	4284.6	4285.6	1.00	IC	35-40	
4286.6						A15-B1
4287.4	4286.5	4286.5	1.00	I	35-40	
4288.9						C8-C13
4298.6	4296.7	4297.8	0.71	I	0-5	
4329.3	4328.7	4328.7	1.00	IC	0-5	
4331.9						B6-B8
4335.4	4332.7	4334.8	1.00	IC	0-5	
4339.2	4337.6	4338.6	1.00	IC	20-25	
4339.3						D1-D4
4340.1	4338.6	4339.5	1.00	I	20-30	
4346.7	4344.8	4347.7	0.90	I	0-5	
4355.4						B7
4364.3						B3
4366.1	4363.8	4365.7	1.00	IC	0-5	
4395.4	4393.8	4396.8	1.00	I	0-5	
4401.5	4398.7	4400.7	1.00	I	0-5	
4404.0						D1-D2
4412.5	4409.7	4412.7	0.85	I	0-5	
4419.8	4416.7	4417.7	1.00	IC	0-5	
4434.0	4431.8	4433.7	1.00	IC	0-5	
4438.2	4436.7	4437.8	1.00	I	0-5	
4449.1	4447.8	4448.7	1.00	I	0-5	
4456.0	4454.2	4455.3	0.92	I	0-5	
4461.2	4460.7	4460.7	0.98	I	0-5	
4464.8	4462.9	4463.7	1.00	I	0-5	
4468.3	4467.6	4467.6	1.00	IC	0-5	
4480.6	4478.7	4479.7	1.00	I	0-5	
4487.5	4484.7	4485.7	1.00	I	0-5	
4503.3	4500.7	4503.6	0.74	I	0-5	
4537.4	4535.7	4535.7	1.00	I	0-5	
4542.1	4540.8	4541.7	1.00	I	0-5	
4549.1	4547.7	4547.7	1.00	I	0-5	
4552.1	4551.7	4551.7	1.00	I	0-5	
4557.7	4556.5	4557.4	0.99	I	0-5	
4560.7	4559.0	4561.1	0.93	I	0-5	
4570.4	4567.8	4569.7	1.00	I	0-5	
4597.8	4596.6	4597.7	0.99	I	0-5	
4598.3						B14-B15
4604.9	4602.7	4604.7	1.00	IC	0-5	
4616.2	4613.7	4616.7	1.00	IC	0-5	

Mass (average)	Mass (mono.)	Apex Mass	Score	Evidence	Time	MALDI fraction
4623.2	4619.7	4621.7	1.00	I	0-5	
4638.6	4635.7	4637.7	1.00	I	0-5	
4667.4						B6
4672.5	4669.8	4671.7	1.00	I	0-5	
4678.4						D1-D3
4682.4						B4-B5
4684.4	4681.7	4683.7	1.00	I	0-5	
4691.0	4687.7	4689.7	1.00	I	0-5	
4696.1	4694.7	4694.7	1.00	I	0-5	
4713.0	4711.9	4712.7	1.00	I	0-5	
4728.7	4727.7	4727.7	1.00	I	0-5	
4735.2	4733.7	4736.7	1.00	I	0-5	
4740.6	4737.6	4739.7	0.84	I	0-5	
4752.8	4749.6	4751.7	0.83	I	0-5	
4759.2	4755.6	4757.7	1.00	I	0-5	
4773.7	4770.5	4773.7	1.00	I	0-5	
4779.3	4777.7	4778.7	0.94	I	0-5	
4820.5	4817.7	4820.7	1.00	I	0-5	
4826.9	4823.7	4825.7	1.00	I	0-5	
4842.2	4839.7	4841.7	1.00	I	0-5	
4846.8	4845.6	4846.6	0.89	I	0-5	
4876.1	4873.8	4875.7	1.00	IC	0-5	
4879.9						B12
4888.2	4884.7	4887.7	0.88	I	0-5	
4895.0	4891.7	4893.7	1.00	I	0-5	
4900.4	4898.7	4899.7	1.00	I	20-25	
4910.1	4907.7	4910.7	1.00	I	0-5	
4924.7	4923.6	4925.7	0.99	I	0-5	
4938.7	4937.6	4937.6	1.00	I	0-5	
4944.3	4940.6	4943.7	0.91	I	0-5	
4956.9	4954.8	4955.6	1.00	I	0-5	
4963.2	4959.7	4961.7	1.00	I	0-5	
4977.5	4974.6	4977.6	1.00	I	0-5	
4995.4	4993.7	4994.6	0.94	I	0-5	
5008.3	5006.7	5009.6	1.00	I	0-5	
5013.7	5010.6	5013.5	0.96	I	0-5	
5023.9	5020.7	5024.7	0.91	I	0-5	
5031.2	5027.6	5029.7	1.00	I	0-5	
5039.1	5037.7	5039.7	1.00	I	0-5	
5045.9	5042.6	5045.7	1.00	I	0-5	
5071.5						D1

Mass (average)	Mass (mono.)	Apex Mass	Score	Evidence	Time	MALDI fraction
5080.6	5077.7	5079.7	1.00	I	0-5	
5092.3	5089.7	5091.7	1.00	I	0-5	
5099.0	5095.7	5097.6	1.00	I	0-5	
5104.1	5102.7	5102.7	1.00	I	0-5	
5113.2	5112.6	5113.7	0.99	I	0-5	
5133.6	5131.7	5131.7	1.00	I	0-5	
5142.1	5141.6	5141.6	1.00	I	0-5	
5148.4	5144.7	5147.7	0.93	I	0-5	
5161.1	5159.6	5161.6	1.00	I	0-5	
5167.2	5163.6	5165.7	1.00	I	0-5	
5181.5	5178.7	5181.6	1.00	I	0-5	
5186.6	5185.7	5185.7	0.99	I	0-5	
5197.1	5196.5	5196.5	1.00	I	0-5	
5217.3	5215.7	5216.7	0.75	I	0-5	
5224.1	5223.5	5223.5	0.98	I	0-5	
5228.5	5225.6	5228.7	1.00	I	0-5	
5235.2	5231.6	5233.7	1.00	I	0-5	
5244.6	5243.7	5243.7	0.99	I	0-5	
5249.8	5246.6	5249.6	1.00	I	0-5	
5255.7	5253.6	5255.6	0.81	I	0-5	
5259.0	5258.7	5258.7	0.98	I	0-5	
5278.8	5276.6	5279.6	1.00	I	0-5	
5284.9	5282.6	5283.6	1.00	I	0-5	
5289.6	5288.7	5288.7	1.00	I	0-5	
5292.1	5291.7	5291.7	0.99	I	0-5	
5296.4	5293.6	5295.6	1.00	I	0-5	
5303.0	5299.7	5301.6	1.00	I	0-5	
5316.9						C12-C13
5319.6	5316.7	5319.5	0.97	I	0-5	
5347.2	5345.7	5345.7	1.00	I	0-5	
5352.8	5349.5	5351.6	1.00	I	0-5	
5360.5	5359.4	5359.4	0.99	I	0-5	
5364.4	5362.7	5365.6	1.00	I	0-5	
5370.8	5366.6	5369.6	0.93	I	0-5	
5380.2	5378.6	5381.6	1.00	I	0-5	
5385.9	5382.6	5385.5	1.00	I	0-5	
5392.0	5390.7	5390.7	1.00	I	0-5	
5397.8	5395.8	5396.7	1.00	I	0-5	
5403.7	5402.7	5403.6	0.99	I	0-5	
5414.7	5412.7	5413.7	1.00	I	0-5	
5433.2	5431.7	5432.7	1.00	I	0-5	

Mass (average)	Mass (mono.)	Apex Mass	Score	Evidence	Time	MALDI fraction
5439.2	5435.7	5437.6	1.00	I	0-5	
5447.4	5445.5	5446.4	1.00	I	0-5	
5454.2	5451.8	5454.5	1.00	I	0-5	
5463.6	5461.7	5462.6	1.00	I	0-5	
5465.0						D1-D2
5479.2	5478.7	5478.7	1.00	I	0-5	
5483.6	5480.6	5483.6	0.96	I	0-5	
5489.9	5487.6	5488.6	1.00	I	0-5	
5495.0	5493.5	5495.5	1.00	I	0-5	
5500.3	5497.5	5500.6	1.00	I	0-5	
5507.4	5503.7	5506.6	1.00	I	0-5	
5518.9	5516.8	5519.7	1.00	I	0-5	
5555.5	5552.6	5555.6	0.91	I	0-5	
5569.1	5567.6	5569.5	1.00	I	0-5	
5575.2	5571.5	5573.6	1.00	I	0-5	
5583.7	5581.7	5581.7	1.00	I	0-5	
5590.1	5587.7	5589.7	0.98	I	0-5	
5607.2	5605.7	5605.7	1.00	I	0-5	
5613.7	5611.7	5615.6	1.00	I	0-5	
5626.0	5622.5	5625.6	0.99	I	0-5	
5631.9	5631.5	5631.5	1.00	I	0-5	
5636.0	5633.5	5636.6	1.00	I	0-5	
5643.4	5639.6	5641.6	1.00	I	0-5	
5652.7	5651.7	5651.7	1.00	I	0-5	
5658.1	5654.6	5658.6	1.00	I	0-5	
5685.9	5684.8	5686.8	1.00	I	0-5	
5693.9	5691.6	5693.6	1.00	I	0-5	
5704.8	5702.7	5705.6	1.00	I	0-5	
5711.4	5707.7	5710.7	1.00	I	0-5	
5718.6	5717.7	5717.7	1.00	I	0-5	
5724.1	5723.6	5723.6	0.99	I	0-5	
5760.3	5758.7	5761.5	1.00	I	0-5	
5772.5	5770.8	5773.8	1.00	I	0-5	
5778.6	5774.6	5777.6	0.86	I	0-5	
5795.9	5793.7	5795.6	1.00	I	0-5	
5820.0	5817.5	5818.7	1.00	I	0-5	
5829.9	5826.6	5829.5	0.76	I	0-5	
5832.8	5830.7	5830.7	0.34	I	0-5	
5846.9	5843.6	5846.6	0.89	I	0-5	
5853.0	5852.6	5853.4	0.95	I	0-5	
5855.5	5854.5	5855.7	0.99	I	0-5	

Mass (average)	Mass (mono.)	Apex Mass	Score	Evidence	Time	MALDI fraction
5859.3	5858.6	5859.8	0.98	I	0-5	
5862.8	5860.6	5861.6	1.00	I	0-5	
5897.0	5895.6	5895.6	1.00	I	0-5	
5902.2	5899.7	5900.8	1.00	I	0-5	
5907.8	5905.7	5909.7	1.00	I	0-5	
5915.9	5913.6	5914.6	1.00	I	0-5	
6001.1	5998.7	5998.7	1.00	I	0-5	
6013.1	6011.6	6012.6	1.00	I	0-5	
6023.0	6020.6	6023.7	0.91	I	0-5	
6050.9	6047.6	6050.6	0.89	I	0-5	
6100.3	6099.8	6099.8	1.00	I	0-5	
6107.7	6105.6	6106.7	1.00	I	0-5	
6114.5	6113.5	6115.5	1.00	I	0-5	
6122.2	6117.6	6123.6	1.00	IC	0-5	
6125.1	6124.6	6124.6	1.00	I	0-5	
6167.5	6165.7	6168.8	1.00	I	0-5	
6174.1	6172.1	6173.1	0.75	I	0-5	
6188.2	6185.5	6186.4	0.92	I	0-5	
6199.6	6197.6	6199.5	0.86	I	0-5	
6238.2	6236.5	6237.4	1.00	I	0-5	
6255.3	6253.7	6253.7	0.95	I	0-5	
6278.2	6275.6	6275.6	0.92	I	0-5	
6324.6	6322.7	6322.7	1.00	I	0-5	
6360.0	6358.6	6358.6	1.00	I	0-5	
6377.1	6374.5	6376.6	0.76	I	0-5	
6393.9	6393.5	6393.5	0.99	I	0-5	
6413.8	6411.6	6411.6	1.00	I	0-5	
6481.9	6479.6	6479.6	0.94	I	0-5	
6490.5	6489.4	6489.4	1.00	I	0-5	
6495.7	6493.6	6495.6	1.00	I	0-5	
6526.6	6523.5	6526.4	1.00	I	0-5	
6531.5	6530.5	6530.5	1.00	I	0-5	
6552.3	6549.5	6551.5	0.99	I	0-5	
6627.2						B10-B12
6635.8						D3-D4
6656.8						C7-C13
6673.1						B13-B14
6675.2						D1
6678.6	6677.5	6678.6	1.00	I	0-5	
6691.8						B15
6718.2	6716.3	6716.3	1.00	I	0-5	

Mass (average)	Mass (mono.)	Apex Mass	Score	Evidence	Time	MALDI fraction
6736.3	6735.6	6735.6	1.00	I	0-5	
6759.7	6758.5	6758.5	1.00	IC	0-5	
6795.3						C4
6810.6	6809.2	6809.2	1.00	I	0-5	
6821.8	6819.6	6819.6	1.00	I	0-5	
6830.1	6828.6	6831.6	1.00	I	0-5	
6837.2	6835.5	6835.5	0.94	I	0-5	
6850.7	6848.5	6850.6	0.93	I	0-5	
6929.2						B4-B5
6945.6						D1-D2
6995.1						B15
7086.1	7083.5	7087.5	0.83	I	0-5	
7103.6	7101.3	7106.4	0.59	I	0-5	
7170.5						C2-C3
7183.8						C5-C6
7198.7						C4
7229.7						C7
7234.0	7231.5	7231.5	0.56	I	0-5	
7290.5	7289.4	7291.5	1.00	I	0-5	
7366.2	7363.5	7364.6	1.00	I	0-5	
7379.0	7377.4	7380.5	1.00	I	0-5	
7416.2						B10
7495.0						B13-B15
7561.7	7559.4	7563.4	1.00	I	0-5	
7569.8	7567.5	7567.5	1.00	I	0-5	
7637.9	7635.5	7636.6	0.90	I	0-5	
7653.7						B15
7665.0						B10
7665.3	7663.4	7667.5	0.94	I	0-5	
7689.5	7687.5	7687.5	0.94	I	0-5	
7748.6	7747.4	7747.4	0.87	I	0-5	
7766.0	7764.4	7765.4	1.00	I	0-5	
7815.2						B15
7839.3						A13
7840.8	7836.5	7841.5	0.81	I	0-5	
8025.6	8024.4	8026.4	1.00	I	0-5	
8106.5	8105.5	8107.4	1.00	I	0-5	
8129.4	8128.6	8128.6	1.00	I	0-5	
8368.4	8366.5	8367.4	1.00	I	0-5	
8453.8	8451.4	8452.5	1.00	I	0-5	
8515.4						C3-C4

Group 6 from ion exchange column

Mass (average)	Mass (mono.)	Apex Mass	Score	Evidence	Time	MALDI fraction
2009.5	2008.8	2010.0	0.99	I	0-5	
2012.0	2011.6	2011.6	1.00	I	0-5	
2020.6	2018.9	2019.9	1.00	IC	0-5	
2029.0	2028.1	2028.1	1.00	I	0-5	
2063.1	2062.0	2062.9	1.00	I	0-5	
2079.4						B3
2085.5	2084.9	2084.9	1.00	I	0-5	
2089.6	2088.9	2089.9	1.00	I	0-5	
2101.5	2100.9	2101.9	1.00	I	0-5	
2117.5	2116.2	2117.3	1.00	I	0-5	
2131.0	2129.9	2129.9	1.00	I	0-5	
2156.4	2154.9	2155.9	1.00	I	0-5	
2168.6	2167.9	2167.9	1.00	I	0-5	
2192.4	2190.9	2191.9	0.88	I	0-5	
2204.4	2202.9	2203.9	0.89	I	0-5	
2216.2						B7-B9
2225.5	2224.9	2224.9	1.00	I	0-5	
2236.6	2235.9	2235.9	1.00	I	0-5	
2266.5	2265.4	2266.4	1.00	I	0-5	
2283.4	2282.9	2282.9	1.00	I	0-5	
2286.2						B14
2292.4	2290.9	2291.9	1.00	I	0-5	
2296.8	2295.9	2295.9	1.00	I	0-5	
2304.4	2302.9	2303.9	1.00	I	0-5	
2340.3	2338.9	2339.9	0.89	I	0-5	
2360.4	2358.9	2359.9	1.00	I	0-5	
2366.2						C4-C5
2372.4	2370.9	2371.9	1.00	I	0-5	
2374.8						B8-B9
2428.6	2426.9	2427.9	1.00	I	0-5	
2453.6	2452.9	2453.9	1.00	I	0-5	
2508.6	2507.9	2507.9	1.00	I	0-5	
2519.5	2518.8	2519.9	1.00	I	0-5	
2529.9	2528.9	2529.9	1.00	I	0-5	
2558.0	2556.9	2557.9	1.00	I	0-5	
2564.5	2562.9	2563.9	1.00	I	0-5	
2577.5	2576.9	2577.9	0.99	I	0-5	
2596.7	2594.9	2595.9	1.00	I	0-5	
2604.7	2603.9	2603.9	1.00	I	0-5	

Mass (average)	Mass (mono.)	Apex Mass	Score	Evidence	Time	MALDI fraction
2612.6	2610.9	2611.9	1.00	I	0-5	
2624.3	2622.9	2623.9	0.89	I	0-5	
2632.6	2631.9	2631.9	1.00	I	0-5	
2642.8						C2
2644.6	2642.9	2643.9	1.00	I	0-5	
2649.2	2647.9	2647.9	1.00	IC	0-5	
2664.7	2662.9	2663.9	1.00	I	0-5	
2690.6	2688.8	2689.8	1.00	I	0-5	
2696.7	2694.8	2695.9	1.00	I	0-5	
2699.2	2698.4	2698.4	0.99	I	0-5	
2700.8	2699.9	2699.9	1.00	I	0-5	
2704.7	2703.9	2703.9	1.00	I	0-5	
2710.4						C1-C2
2711.5						C7-C8
2712.4	2710.8	2711.9	1.00	I	0-5	
2740.7	2739.9	2739.9	1.00	I	0-5	
2748.6	2746.9	2747.9	1.00	I	0-5	
2768.7	2767.9	2767.9	1.00	I	0-5	
2780.8	2778.8	2779.9	1.00	I	0-5	
2790.7	2789.8	2789.8	1.00	I	0-5	
2800.5	2798.9	2799.9	1.00	I	0-5	
2816.2	2815.0	2815.8	0.90	I	0-5	
2829.5	2828.8	2829.8	1.00	I	0-5	
2833.4	2831.3	2832.4	0.88	I	0-5	
2836.9	2835.8	2835.8	1.00	I	0-5	
2840.1	2839.9	2839.9	1.00	I	0-5	
2847.8	2847.8	2847.8	1.00	IC	0-5	
2854.5	2852.8	2853.9	1.00	I	0-5	
2858.6	2857.9	2857.9	1.00	I	0-5	
2862.2	2861.9	2861.9	1.00	I	0-5	
2873.5	2872.9	2873.9	1.00	I	0-5	
2876.4	2874.9	2875.8	1.00	I	0-5	
2884.3	2882.9	2883.9	0.89	I	0-5	
2894.8	2893.8	2893.8	1.00	I	0-5	
2906.5	2904.9	2905.8	1.00	I	0-5	
2920.6	2918.9	2919.8	1.00	I	0-5	
2926.7	2925.8	2925.8	1.00	I	0-5	
2937.4	2936.8	2937.8	1.00	I	0-5	
2952.3	2950.9	2951.8	1.00	I	0-5	
2962.6	2961.8	2961.8	1.00	I	0-5	
2965.5	2964.8	2965.8	1.00	I	0-5	

Mass (average)	Mass (mono.)	Apex Mass	Score	Evidence	Time	MALDI fraction
2968.9	2967.3	2968.4	0.87	I	0-5	
2972.8	2971.8	2971.8	1.00	I	0-5	
2976.1	2975.8	2975.8	1.00	I	0-5	
2984.1	2983.8	2983.8	1.00	I	0-5	
2988.1						A12-A13
2990.7	2988.9	2989.9	1.00	I	0-5	
2994.9	2993.9	2993.9	1.00	I	0-5	
2999.5	2998.8	2999.8	1.00	I	0-5	
3006.5	3004.8	3005.8	1.00	I	0-5	
3012.3	3011.0	3011.8	0.99	I	0-5	
3020.3	3018.9	3019.8	0.90	I	0-5	
3030.2	3029.8	3029.8	1.00	I	0-5	
3051.7	3050.9	3051.9	1.00	I	0-5	
3058.7	3056.9	3057.9	1.00	IC	0-5	
3063.1	3061.9	3061.9	1.00	I	0-5	
3071.6	3070.4	3070.4	0.99	I	0-5	
3091.5						B14-C1
3099.4	3098.8	3099.8	1.00	I	0-5	
3101.4	3100.8	3101.8	1.00	I	0-5	
3104.9	3103.3	3104.4	0.87	I	0-5	
3108.9	3107.8	3107.8	1.00	I	0-5	
3156.2	3154.8	3155.8	0.89	I	0-5	
3165.5	3163.8	3165.8	0.76	I	0-5	
3194.7	3192.9	3193.9	1.00	I	0-5	
3199.1	3197.9	3197.9	1.00	I	0-5	
3212.6	3210.8	3212.9	1.00	I	0-5	
3240.7	3239.8	3239.8	1.00	I	0-5	
3244.9	3243.8	3243.8	1.00	I	0-5	
3257.6	3255.9	3257.9	0.94	I	0-5	
3262.7	3260.8	3261.9	1.00	I	0-5	
3267.1	3265.8	3265.8	1.00	I	0-5	
3279.4	3277.9	3277.9	1.00	IC	0-5	
3283.6	3281.8	3283.8	1.00	I	0-5	
3286.1	3283.9	3285.9	1.00	IC	20-30	
3287.3	3285.8	3286.8	1.00	IC	25-30	
3295.0						D2-D3
3297.0	3294.9	3296.9	1.00	IC	10-15	
3298.1						A15-B1
3298.1	3295.9	3297.9	1.00	IC	15-20	
3303.1	3301.9	3303.8	1.00	I	25-30	
3315.8	3313.9	3314.9	1.00	IC	20-30	

Mass (average)	Mass (mono.)	Apex Mass	Score	Evidence	Time	MALDI fraction
3316.8	3315.8	3316.9	1.00	I	25-30	
3319.3						B8-C1
3319.7	3317.8	3319.8	1.00	I	15-20	
3327.2	3325.8	3326.8	1.00	I	0-5	
3332.6	3330.9	3332.9	1.00	I	0-5	
3335.7	3333.8	3335.8	1.00	I	15-20	
3344.0						C2
3345.3	3343.9	3344.9	1.00	I	0-5	
3345.3						B9
3348.2	3346.0	3348.0	1.00	IC	15-20	
3353.3						B12
3354.9	3353.9	3355.0	1.00	I	25-30	
3376.9	3374.7	3375.8	1.00	I	0-5	
3378.1						C7-C8
3383.3	3381.8	3383.8	1.00	I	0-5	
3392.6	3391.8	3392.9	1.00	I	0-5	
3398.7	3396.8	3397.9	1.00	I	0-5	
3402.5	3401.9	3401.9	1.00	I	0-5	
3405.0	3404.9	3404.9	1.00	I	0-5	
3411.8	3407.8	3409.8	1.00	IC	0-5	
3418.5	3417.8	3416.9	1.00	IC	0-5	
3433.2	3431.9	3433.0	1.00	I	20-25	
3433.9						B4
3434.2	3432.9	3434.0	1.00	IC	20-30	
3460.5	3457.9	3459.8	0.83	I	0-5	
3461.3						B3
3466.7	3464.8	3465.8	1.00	I	0-5	
3471.1	3469.8	3469.8	1.00	I	0-5	
3476.5						B10-B11
3482.6	3481.8	3482.9	1.00	I	0-5	
3495.9	3493.9	3495.9	1.00	IC	20-25	
3501.3						B15
3504.7	3503.3	3505.2	1.00	I	0-5	
3506.7	3505.8	3505.8	1.00	I	0-5	
3512.9	3510.6	3511.8	0.95	I	0-5	
3518.0						C10
3518.5						C14-C15
3519.6						A11-A13
3520.0	3519.0	3520.0	1.00	I	10-15	
3521.2	3519.0	3520.1	1.00	IC	5-10	
3521.2	3519.0	3521.0	0.98	I	10-15	

Mass (average)	Mass (mono.)	Apex Mass	Score	Evidence	Time	MALDI fraction
3522.2	3520.0	3521.0	1.00	IC	5-10	
3526.6						B1-B4
3530.8	3528.8	3530.8	1.00	I	0-5	
3534.5						B5-B6
3536.7	3534.8	3536.9	0.80	I	0-5	
3543.8	3543.0	3543.0	1.00	I	20-30	
3544.3						C4-C5
3547.3	3543.8	3545.8	1.00	IC	0-5	
3550.6						A15
3555.7	3553.8	3555.8	1.00	I	0-5	
3557.0						C7-D3
3559.9						B1-B4
3561.1	3560.1	3561.1	1.00	IC	10-15	
3567.6						C3
3567.8	3565.8	3567.8	0.94	I	0-5	
3589.9	3589.1	3589.1	1.00	I	20-30	
3597.9	3595.8	3596.8	1.00	IC	0-5	
3602.9	3600.8	3601.9	1.00	IC	0-5	
3606.5	3605.8	3605.8	1.00	I	0-5	
3609.0	3608.9	3608.9	1.00	I	0-5	
3615.6	3614.8	3614.8	1.00	I	0-5	
3620.4	3618.8	3620.8	1.00	I	0-5	
3642.8	3641.8	3641.8	0.99	I	0-5	
3653.4	3651.8	3653.8	0.94	I	0-5	
3664.3	3661.8	3665.8	1.00	I	0-5	
3671.2	3668.8	3669.8	1.00	I	0-5	
3676.1	3674.8	3674.8	0.97	I	0-5	
3685.3	3683.1	3685.1	1.00	IC	20-25	
3686.9	3685.1	3687.1	1.00	IC	20-25	
3692.2						B5-B6
3701.5						C8-D3
3703.3	3701.2	3703.2	1.00	IC	20-30	
3711.0						B9
3711.1	3710.2	3711.2	1.00	IC	25-30	
3714.6	3713.2	3714.1	1.00	IC	20-25	
3715.7						B5
3720.3	3719.2	3719.2	0.72	I	0-5	
3723.2						B7-B8
3724.5						B4
3734.9	3732.8	3734.8	1.00	I	0-5	
3740.7	3738.8	3740.9	1.00	IC	0-5	

Mass (average)	Mass (mono.)	Apex Mass	Score	Evidence	Time	MALDI fraction
3752.8	3750.9	3750.9	1.00	IC	0-5	
3755.1	3754.2	3754.2	1.00	I	20-25	
3761.1	3759.2	3761.1	0.94	I	0-5	
3765.2						B7
3776.2	3773.8	3776.8	1.00	IC	0-5	
3779.8						B7-B9
3782.8	3781.8	3782.9	1.00	I	0-5	
3788.2	3786.8	3788.8	1.00	I	0-5	
3791.6	3789.8	3791.8	1.00	I	0-5	
3800.8	3799.8	3800.8	1.00	I	0-5	
3806.7	3804.8	3805.8	1.00	I	0-5	
3811.4	3809.8	3809.8	1.00	I	0-5	
3818.1	3816.8	3818.8	1.00	I	0-5	
3821.0	3819.8	3821.8	1.00	IC	0-5	
3825.5	3824.8	3824.8	1.00	I	0-5	
3830.0						B11
3834.0						B7
3844.4	3843.8	3845.0	0.97	I	0-5	
3847.9	3845.8	3847.8	0.94	I	0-5	
3853.1						A13-A14
3854.1						D1-D2
3856.9	3855.8	3857.8	1.00	I	0-5	
3861.1	3859.8	3860.8	1.00	I	0-5	
3868.9	3867.8	3869.8	1.00	I	0-5	
3874.5	3871.8	3873.8	1.00	I	0-5	
3875.5						B4-B7
3879.4	3877.8	3877.8	1.00	I	0-5	
3884.6	3883.8	3884.8	1.00	I	0-5	
3890.7	3888.8	3890.8	1.00	I	0-5	
3903.9						B6
3911.2						D1-D2
3911.6	3909.8	3911.8	1.00	I	0-5	
3911.7						A14-A15
3925.2	3923.8	3923.8	1.00	I	0-5	
3939.0	3936.8	3939.8	1.00	IC	0-5	
3944.8	3942.8	3944.8	0.79	I	0-5	
3956.3	3955.7	3956.8	1.00	IC	0-5	
3961.2	3959.8	3959.8	1.00	IC	0-5	
3963.9	3962.8	3962.8	1.00	IC	0-5	
3980.1	3978.8	3980.8	1.00	I	0-5	
3982.5						B4

Mass (average)	Mass (mono.)	Apex Mass	Score	Evidence	Time	MALDI fraction
3987.0	3985.9	3986.9	1.00	I	0-5	
3993.6	3991.8	3992.8	1.00	IC	0-5	
3998.3						B11-B12
4000.9	3999.7	4001.8	1.00	I	0-5	
4004.9	4003.8	4004.8	1.00	I	0-5	
4010.4	4007.8	4009.8	1.00	I	0-5	
4011.0						B12
4015.5	4013.8	4013.8	1.00	I	0-5	
4020.9	4019.8	4019.8	1.00	I	0-5	
4026.9	4023.8	4025.8	1.00	I	0-5	
4059.5	4057.8	4061.8	1.00	IC	0-5	
4064.5	4062.7	4064.8	0.93	I	0-5	
4072.7	4069.8	4073.8	0.84	I	0-5	
4078.5	4075.8	4077.8	1.00	I	0-5	
4083.4	4081.8	4081.8	1.00	I	0-5	
4088.4	4087.8	4088.8	1.00	I	0-5	
4091.1	4089.8	4091.8	1.00	I	0-5	
4094.2	4092.7	4094.8	1.00	IC	0-5	
4114.2	4113.8	4113.8	0.99	I	0-5	
4129.0	4125.8	4127.8	1.00	I	0-5	
4134.2	4132.7	4133.8	1.00	I	0-5	
4140.9	4137.7	4139.8	0.83	I	0-5	
4144.3	4143.8	4143.8	1.00	I	0-5	
4148.4						B3
4148.9	4146.7	4148.8	0.79	I	0-5	
4150.3	4147.6	4149.6	1.00	IC	20-25	
4154.8						C3
4161.8	4158.7	4160.8	1.00	I	0-5	
4166.2	4164.6	4165.6	1.00	IC	20-25	
4173.3						B4
4176.5	4173.8	4175.8	0.73	I	0-5	
4182.6	4181.8	4181.8	1.00	I	0-5	
4191.2	4189.8	4190.8	1.00	I	0-5	
4196.7	4194.7	4196.8	1.00	I	0-5	
4202.7						A15
4203.7						D1-D3
4208.8	4206.7	4207.8	1.00	I	0-5	
4214.4	4211.8	4213.8	1.00	I	0-5	
4219.3	4217.8	4217.8	1.00	I	0-5	
4225.2	4224.7	4225.7	1.00	I	0-5	
4225.7						B11

Mass (average)	Mass (mono.)	Apex Mass	Score	Evidence	Time	MALDI fraction
4228.9						A15
4230.4	4227.8	4229.8	1.00	I	0-5	
4235.5	4233.8	4235.8	1.00	I	0-5	
4247.0						B8-B10
4263.1	4260.8	4263.8	1.00	I	0-5	
4268.7	4266.7	4268.8	1.00	I	0-5	
4276.7	4274.8	4277.7	1.00	I	0-5	
4282.5	4279.8	4281.8	1.00	I	0-5	
4287.8	4285.8	4285.8	1.00	IC	0-5	
4298.8	4296.7	4298.8	1.00	I	0-5	
4317.6						B12
4318.9	4317.7	4319.7	1.00	I	0-5	
4322.6	4320.8	4322.8	0.74	I	0-5	
4328.2	4326.7	4329.8	0.86	I	0-5	
4335.5	4332.8	4334.8	1.00	I	0-5	
4346.9	4344.8	4346.8	1.00	I	0-5	
4365.8	4362.6	4367.7	1.00	I	0-5	
4370.4	4369.8	4370.8	1.00	I	0-5	
4375.1	4372.7	4373.8	0.90	I	0-5	
4382.7						B14
4386.1	4383.7	4385.8	1.00	I	0-5	
4401.9	4398.8	4400.8	1.00	I	0-5	
4412.3	4409.7	4412.8	1.00	I	0-5	
4418.4	4415.8	4417.8	1.00	I	0-5	
4423.4	4421.8	4421.8	1.00	I	0-5	
4425.4						B6-B9
4434.8	4431.7	4433.8	1.00	I	0-5	
4435.3						B10
4468.8	4465.8	4467.8	1.00	I	0-5	
4473.2	4472.7	4472.7	0.99	I	0-5	
4480.1	4477.8	4479.7	1.00	I	0-5	
4486.5	4483.8	4485.8	1.00	I	0-5	
4491.5	4489.8	4489.8	1.00	I	0-5	
4494.8						B7
4503.5	4500.7	4502.8	1.00	I	0-5	
4509.0	4507.8	4507.8	0.79	I	0-5	
4523.5	4521.7	4523.7	1.00	I	0-5	
4531.2	4527.7	4531.8	0.21	I	0-5	
4539.6	4536.7	4538.8	1.00	I	0-5	
4549.2	4545.7	4547.7	0.86	I	0-5	
4557.5	4554.7	4556.8	0.84	I	0-5	

Mass (average)	Mass (mono.)	Apex Mass	Score	Evidence	Time	MALDI fraction
4564.5	4562.7	4562.7	1.00	I	0-5	
4567.3						B13-B15
4570.0	4567.8	4568.7	1.00	I	0-5	
4576.0	4573.8	4574.7	0.98	I	0-5	
4584.6	4581.6	4583.8	1.00	I	0-5	
4585.9						B9-B10
4593.7	4590.8	4592.7	1.00	I	0-5	
4609.6						B13
4611.6	4610.7	4610.7	1.00	I	0-5	
4616.5	4613.7	4616.8	0.84	I	0-5	
4622.9	4619.7	4621.8	1.00	I	0-5	
4628.3	4626.7	4626.7	1.00	I	0-5	
4633.0	4631.7	4631.7	1.00	I	0-5	
4638.7	4635.7	4637.8	1.00	I	0-5	
4642.8						B7
4673.0	4670.7	4673.7	1.00	I	0-5	
4676.6						B6-B7
4684.7	4682.8	4685.7	1.00	I	0-5	
4686.3						B11
4691.1	4687.8	4689.7	1.00	I	0-5	
4696.2	4694.8	4694.8	1.00	I	0-5	
4703.0	4701.8	4703.7	1.00	I	0-5	
4706.9	4704.7	4707.6	1.00	I	0-5	
4713.2	4711.9	4711.9	0.80	I	0-5	
4725.6						B8
4726.6	4723.9	4727.7	1.00	I	0-5	
4741.4	4737.7	4739.7	1.00	I	0-5	
4749.8						B8-B10
4753.1	4751.7	4751.7	1.00	I	0-5	
4759.3	4755.8	4757.8	1.00	I	0-5	
4773.8	4770.6	4772.7	1.00	I	0-5	
4779.9						B8
4780.0	4777.7	4781.7	1.00	I	0-5	
4793.6	4790.7	4793.7	0.91	I	0-5	
4800.2	4799.7	4799.7	1.00	I	0-5	
4803.9	4801.8	4805.8	1.00	I	0-5	
4809.5	4806.7	4808.8	1.00	I	0-5	
4815.5	4814.7	4814.7	1.00	I	0-5	
4820.4	4817.7	4820.7	1.00	I	0-5	
4826.4	4823.7	4825.8	1.00	I	0-5	
4831.6	4829.7	4829.7	1.00	I	0-5	

Mass (average)	Mass (mono.)	Apex Mass	Score	Evidence	Time	MALDI fraction
4841.8	4838.7	4841.8	1.00	I	0-5	
4850.7						B4
4856.7	4855.8	4856.7	0.99	I	0-5	
4871.7	4870.8	4871.7	0.99	I	0-5	
4876.7	4873.8	4877.7	1.00	I	0-5	
4883.2	4880.8	4883.7	1.00	I	0-5	
4888.7	4886.7	4889.7	1.00	I	0-5	
4894.5	4891.7	4893.7	1.00	I	0-5	
4899.6	4897.7	4897.7	1.00	I	0-5	
4911.2	4908.7	4910.7	0.96	I	0-5	
4916.7						B12-B14
4919.5	4917.8	4917.8	0.73	I	0-5	
4930.8	4929.7	4931.7	1.00	I	0-5	
4934.7	4932.6	4934.7	1.00	I	0-5	
4944.9	4941.7	4943.8	1.00	I	0-5	
4952.0	4949.7	4952.7	1.00	I	0-5	
4958.8	4956.8	4958.7	1.00	I	0-5	
4966.7	4964.7	4964.7	1.00	I	0-5	
4978.1	4975.8	4977.7	1.00	I	0-5	
4983.1	4981.8	4982.7	1.00	I	0-5	
4987.1	4985.7	4985.7	1.00	I	0-5	
4999.9	4997.7	5000.8	1.00	I	0-5	
5013.9	5010.6	5012.7	1.00	I	0-5	
5018.2	5017.8	5017.8	0.99	I	0-5	
5024.4	5021.7	5024.7	1.00	I	0-5	
5030.9	5027.7	5029.7	1.00	I	0-5	
5036.3	5034.7	5034.7	1.00	I	0-5	
5040.5	5039.7	5039.7	1.00	I	0-5	
5045.9	5042.6	5045.7	1.00	I	0-5	
5050.2	5049.7	5049.7	0.99	I	0-5	
5052.5	5051.7	5051.7	1.00	I	0-5	
5080.8	5077.8	5079.7	1.00	I	0-5	
5086.3	5084.7	5087.7	1.00	I	0-5	
5091.9	5088.8	5091.7	1.00	I	0-5	
5099.0	5095.7	5097.7	1.00	I	0-5	
5104.2	5102.7	5102.7	1.00	I	0-5	
5108.6	5107.7	5107.7	1.00	I	0-5	
5113.4	5112.7	5113.8	0.99	I	0-5	
5127.4	5125.7	5127.6	0.77	I	0-5	
5136.1	5133.6	5135.7	1.00	I	0-5	
5143.8	5142.6	5144.7	0.99	I	0-5	

Mass (average)	Mass (mono.)	Apex Mass	Score	Evidence	Time	MALDI fraction
5149.0	5145.6	5147.7	1.00	I	0-5	
5156.1	5154.5	5156.6	1.00	I	0-5	
5161.2	5159.7	5159.7	1.00	I	0-5	
5167.3	5163.6	5165.7	1.00	I	0-5	
5181.6	5178.7	5180.7	1.00	I	0-5	
5186.3	5185.7	5186.7	1.00	I	0-5	
5190.2	5187.6	5189.7	0.93	I	0-5	
5204.3	5202.8	5204.6	1.00	I	0-5	
5209.7	5207.7	5207.7	1.00	I	0-5	
5217.2	5213.7	5216.7	1.00	I	0-5	
5228.3	5225.7	5228.7	1.00	I	0-5	
5234.9	5231.7	5233.7	1.00	I	0-5	
5249.9	5246.6	5249.7	1.00	I	0-5	
5277.3						C5
5277.7	5276.7	5276.7	1.00	I	0-5	
5280.1	5279.7	5279.7	0.95	I	0-5	
5284.7	5281.7	5284.7	1.00	I	0-5	
5291.9	5289.7	5291.8	0.80	I	0-5	
5296.6	5294.7	5297.7	1.00	I	0-5	
5303.0	5299.7	5301.7	1.00	I	0-5	
5307.9	5306.7	5306.7	1.00	I	0-5	
5316.1	5313.6	5317.7	0.87	I	0-5	
5323.8						C10
5329.2	5328.7	5328.7	1.00	I	0-5	
5337.9	5335.8	5335.8	0.84	I	0-5	
5346.4	5344.8	5345.8	1.00	I	0-5	
5353.9	5352.6	5353.6	0.88	I	0-5	
5358.6	5356.8	5357.7	1.00	I	0-5	
5364.8	5362.8	5363.7	1.00	I	0-5	
5371.0	5367.7	5369.7	1.00	I	0-5	
5386.2	5383.7	5384.7	0.98	I	0-5	
5409.9	5408.5	5409.6	0.86	I	0-5	
5414.6	5413.6	5414.7	1.00	I	0-5	
5418.8	5417.7	5419.8	1.00	I	0-5	
5423.2	5420.7	5420.7	1.00	I	0-5	
5428.5	5427.6	5427.6	1.00	I	0-5	
5432.7	5431.7	5433.6	1.00	I	0-5	
5438.1	5434.7	5437.7	1.00	I	0-5	
5445.3	5442.7	5444.7	1.00	I	0-5	
5453.7	5450.7	5453.6	1.00	I	0-5	
5469.2	5467.7	5470.8	1.00	I	0-5	

Mass (average)	Mass (mono.)	Apex Mass	Score	Evidence	Time	MALDI fraction
5483.2	5481.8	5483.7	1.00	I	0-5	
5489.0	5486.7	5487.7	1.00	I	0-5	
5494.7	5493.6	5495.7	1.00	I	0-5	
5500.6	5498.6	5499.6	1.00	I	0-5	
5506.9	5503.7	5505.7	1.00	I	0-5	
5516.2	5515.7	5515.7	1.00	I	0-5	
5518.8	5517.7	5519.7	1.00	I	0-5	
5524.1	5521.6	5523.6	0.94	I	0-5	
5535.6	5532.7	5535.7	0.85	I	0-5	
5557.0	5555.7	5555.7	1.00	I	0-5	
5562.7	5560.9	5561.7	1.00	I	0-5	
5568.8	5567.7	5569.8	1.00	I	0-5	
5574.7	5570.7	5573.7	0.86	I	0-5	
5580.7	5579.7	5579.7	0.86	I	0-5	
5589.0	5586.5	5587.6	1.00	I	0-5	
5632.1	5631.6	5631.6	0.98	I	0-5	
5637.1	5634.7	5636.7	0.97	I	0-5	
5644.9	5642.7	5642.7	0.91	I	0-5	
5650.7	5649.6	5650.5	0.91	I	0-5	
5658.1	5656.6	5657.6	1.00	I	0-5	
5674.6	5672.8	5675.7	1.00	I	0-5	
5680.4	5678.7	5678.7	1.00	I	0-5	
5692.3	5690.7	5692.9	1.00	I	0-5	
5696.2	5694.6	5694.6	0.71	I	0-5	
5699.2	5698.7	5699.7	1.00	I	0-5	
5703.6	5700.6	5702.7	0.95	I	0-5	
5711.6	5708.7	5709.6	1.00	I	0-5	
5716.0	5715.6	5715.6	0.98	I	0-5	
5727.5	5725.7	5726.7	0.73	I	0-5	
5737.4	5733.7	5735.7	1.00	IC	0-5	
5763.3	5761.9	5761.9	1.00	I	0-5	
5773.3	5772.7	5772.7	0.99	I	0-5	
5776.0						B14
5782.5	5780.8	5780.8	0.93	I	0-5	
5794.0	5791.9	5792.8	1.00	I	0-5	
5847.7	5844.5	5846.7	1.00	I	0-5	
5861.9	5859.9	5860.8	0.99	I	0-5	
5868.9	5866.7	5867.6	0.94	I	0-5	
5881.8	5879.6	5881.5	0.85	I	0-5	
5915.1	5912.7	5913.7	1.00	I	0-5	
5920.1	5918.8	5919.6	0.99	I	0-5	

Mass (average)	Mass (mono.)	Apex Mass	Score	Evidence	Time	MALDI fraction
5929.9	5928.6	5929.6	0.91	I	0-5	
5936.6	5934.9	5934.9	1.00	I	0-5	
5964.5	5961.8	5963.8	0.75	I	0-5	
5971.1	5969.7	5970.6	1.00	I	0-5	
5978.0	5975.7	5979.9	1.00	I	0-5	
6024.7	6023.8	6024.7	0.99	I	0-5	
6034.4	6031.4	6033.5	0.90	I	0-5	
6045.7	6043.8	6045.6	1.00	I	0-5	
6051.3	6049.7	6049.7	0.95	I	0-5	
6065.1	6064.6	6065.6	1.00	I	0-5	
6119.8	6117.7	6119.7	0.96	I	0-5	
6134.0	6131.5	6135.6	1.00	I	0-5	
6148.3	6145.9	6147.0	1.00	I	0-5	
6227.5	6225.3	6227.1	0.84	I	0-5	
6239.9	6238.2	6238.2	0.92	I	0-5	
6281.8	6277.6	6279.7	1.00	IC	0-5	
6291.2	6288.7	6291.6	1.00	IC	0-5	
6338.0	6335.5	6338.4	0.91	I	0-5	
6408.7						C6
6553.1	6550.6	6552.8	0.68	I	0-5	
6596.0	6593.6	6593.6	0.98	I	0-5	
6635.9						B12-C1
6657.0	6654.5	6655.6	0.91	I	0-5	
6677.9						C2
6691.1						C6
6707.0						B13-B14
6736.6						B8
6758.3	6756.7	6759.7	0.78	I	0-5	
6767.7						C7-C8
6918.8						B3-B4
7004.9						B14-B15
7087.5						C4-C5
7098.5	7096.7	7096.7	0.35	I	0-5	
7101.2	7098.5	7098.5	0.37	I	0-5	
7116.4						C5
7118.5						B2
7134.3						C3
7174.7	7173.1	7173.1	0.26	I	0-5	
7184.5						C2-C5
7280.3	7278.4	7278.4	1.00	I	0-5	
7297.9	7295.7	7297.7	1.00	I	0-5	

Mass (average)	Mass (mono.)	Apex Mass	Score	Evidence	Time	MALDI fraction
7355.6						B7-B8
7390.0						B5-B6
7394.2						C2
7500.3	7497.5	7500.5	0.90	I	0-5	
7536.2						C1
7559.2						B8-B9
7583.2	7580.6	7583.5	0.82	I	0-5	
7628.6	7627.6	7627.6	1.00	I	0-5	
7667.9						B11
7773.3	7770.5	7771.6	1.00	I	0-5	
7778.0	7777.6	7777.6	0.99	I	0-5	
7809.9	7807.4	7811.5	0.81	I	0-5	
7918.1						C5-C6
7993.6						C6-C7
8072.0						B15

Group 7 from ion exchange column

Mass (average)	Mass (mono.)	Apex Mass	Score	Evidence	Time	MALDI fraction
2008.7	2006.8	2007.8	1.00	IC	0-5	
2011.5	2010.8	2010.8	1.00	IC	0-5	
2018.9	2018.5	2018.5	1.00	I	0-5	
2021.9	2020.8	2020.8	1.00	I	0-5	
2034.7	2033.8	2033.8	1.00	I	0-5	
2036.6	2036.1	2037.1	1.00	I	0-5	
2041.5	2041.1	2041.1	1.00	I	0-5	
2045.5	2044.1	2045.1	1.00	I	0-5	
2046.6	2045.8	2045.8	1.00	I	0-5	
2049.3	2048.8	2049.8	1.00	I	0-5	
2053.5	2052.8	2053.8	1.00	I	0-5	
2058.6	2058.1	2059.1	1.00	I	0-5	
2075.1	2074.7	2075.7	1.00	IC	0-5	
2085.5	2084.8	2085.8	1.00	IC	0-5	
2089.4	2088.8	2088.8	1.00	I	0-5	
2097.6	2097.8	2097.8	1.00	IC	0-5	
2101.5	2100.8	2101.8	1.00	I	0-5	
2112.7	2112.2	2113.2	1.00	I	15-25	
2137.8	2136.7	2137.8	1.00	I	0-5	
2142.9						B12-B14

Mass (average)	Mass (mono.)	Apex Mass	Score	Evidence	Time	MALDI fraction
2143.4	2142.8	2143.7	1.00	I	0-5	
2147.3	2146.8	2147.8	1.00	I	0-5	
2157.9	2156.8	2156.8	1.00	I	0-5	
2163.5	2162.8	2163.8	1.00	I	0-5	
2166.0	2165.8	2165.8	1.00	I	0-5	
2190.1	2188.7	2189.7	1.00	I	0-5	
2198.6	2197.7	2197.7	1.00	I	0-5	
2204.4	2202.8	2203.7	1.00	I	0-5	
2225.4	2224.8	2224.8	1.00	I	0-5	
2234.0	2233.8	2233.8	1.00	I	0-5	
2236.8	2235.8	2235.8	1.00	I	0-5	
2241.5	2240.8	2241.7	1.00	I	0-5	
2265.8						B5
2272.3	2270.8	2271.8	1.00	I	0-5	
2279.4	2278.7	2279.7	1.00	I	0-5	
2283.3	2282.8	2283.8	1.00	I	0-5	
2292.4	2290.8	2291.8	1.00	I	0-5	
2296.6	2295.7	2295.7	1.00	I	0-5	
2326.1	2324.8	2325.7	1.00	I	0-5	
2332.4	2330.8	2331.7	1.00	I	0-5	
2340.3	2338.8	2339.8	1.00	I	0-5	
2351.4	2350.8	2351.7	1.00	I	0-5	
2372.5	2370.8	2371.7	1.00	I	0-5	
2395.5	2394.8	2395.7	1.00	I	0-5	
2408.1	2406.8	2407.7	1.00	I	0-5	
2414.6	2413.7	2413.7	1.00	I	0-5	
2419.3	2418.8	2419.7	1.00	I	0-5	
2428.4	2426.8	2427.7	1.00	I	0-5	
2432.0	2431.7	2431.7	1.00	I	0-5	
2441.4	2440.7	2441.7	1.00	I	0-5	
2462.1	2460.7	2461.7	1.00	I	0-5	
2467.3						B5
2468.5	2467.7	2467.7	1.00	I	0-5	
2476.3	2474.8	2475.7	1.00	I	0-5	
2482.6	2481.7	2481.7	1.00	I	0-5	
2487.4	2486.7	2487.7	1.00	I	0-5	
2500.1	2498.7	2499.7	0.89	I	0-5	
2506.6	2505.7	2505.7	1.00	I	0-5	
2523.5	2522.8	2523.7	1.00	I	0-5	
2528.7	2527.7	2527.7	1.00	I	0-5	
2551.3	2550.7	2551.7	1.00	I	0-5	

Mass (average)	Mass (mono.)	Apex Mass	Score	Evidence	Time	MALDI fraction
2554.5	2552.7	2553.7	1.00	I	0-5	
2564.4	2562.7	2563.7	1.00	I	0-5	
2568.6	2567.7	2567.7	1.00	I	0-5	
2574.0	2573.7	2573.7	1.00	I	0-5	
2598.4	2596.7	2597.7	1.00	I	0-5	
2604.5	2603.7	2603.7	1.00	I	0-5	
2612.1	2610.7	2611.7	1.00	I	0-5	
2616.7	2614.7	2615.7	0.89	I	0-5	
2632.6	2631.7	2631.7	1.00	I	0-5	
2636.6	2635.7	2635.7	0.76	I	0-5	
2644.5	2642.7	2643.7	1.00	I	0-5	
2650.2	2648.7	2649.7	1.00	I	0-5	
2654.4	2653.7	2654.7	1.00	I	0-5	
2659.5	2658.7	2659.7	1.00	I	0-5	
2664.4	2663.7	2663.7	1.00	I	0-5	
2678.7	2677.7	2677.7	1.00	I	0-5	
2690.6	2688.7	2689.7	1.00	I	0-5	
2696.5	2694.7	2695.7	1.00	I	0-5	
2700.7	2699.7	2699.7	1.00	I	0-5	
2704.6	2703.7	2703.7	1.00	I	0-5	
2712.1	2710.7	2711.7	0.89	I	0-5	
2713.9						C1-C2
2732.7	2731.7	2731.7	1.00	I	0-5	
2740.5	2739.7	2739.7	1.00	I	0-5	
2746.8	2745.7	2745.7	1.00	I	0-5	
2755.4	2754.7	2755.7	1.00	I	0-5	
2758.6	2757.7	2757.7	1.00	I	0-5	
2768.6	2767.7	2767.7	1.00	I	0-5	
2784.4	2782.7	2783.7	1.00	I	0-5	
2790.9	2789.7	2789.7	1.00	IC	0-5	
2800.5	2799.7	2799.7	1.00	I	0-5	
2826.5	2824.7	2825.7	1.00	I	0-5	
2832.5	2830.6	2831.7	1.00	I	0-5	
2836.7	2835.7	2835.7	1.00	I	0-5	
2847.8	2846.7	2847.7	1.00	IC	0-5	
2854.3	2852.6	2853.7	1.00	I	0-5	
2858.5	2857.7	2857.7	1.00	I	0-5	
2868.8	2867.7	2867.7	1.00	I	0-5	
2882.6	2881.7	2881.7	1.00	I	0-5	
2888.7	2886.7	2887.7	0.89	I	0-5	
2894.6	2893.7	2893.7	1.00	I	0-5	

Mass (average)	Mass (mono.)	Apex Mass	Score	Evidence	Time	MALDI fraction
2904.6	2903.7	2903.7	1.00	I	0-5	
2916.6	2914.7	2915.6	1.00	I	0-5	
2927.3	2926.7	2927.7	1.00	I	0-5	
2930.3	2928.6	2929.7	0.88	I	0-5	
2937.2	2936.7	2937.7	1.00	I	0-5	
2952.0	2950.8	2951.7	0.91	I	0-5	
2962.5	2961.7	2961.7	1.00	I	0-5	
2968.6	2966.7	2967.7	1.00	I	0-5	
2972.8	2971.7	2971.7	1.00	IC	0-5	
2979.2	2977.6	2978.7	1.00	I	0-5	
2986.5						A12
2990.5	2988.7	2989.7	1.00	I	0-5	
2994.9	2993.7	2993.7	1.00	I	0-5	
3004.8	3003.7	3003.7	1.00	I	0-5	
3012.0	3010.7	3011.6	0.89	I	0-5	
3018.6	3017.7	3017.7	1.00	I	0-5	
3032.1	3030.7	3031.6	0.89	I	0-5	
3039.2	3038.7	3038.7	1.00	I	0-5	
3051.2	3049.6	3050.7	1.00	I	0-5	
3058.4	3056.7	3057.7	1.00	I	0-5	
3063.4	3061.7	3061.7	1.00	IC	0-5	
3071.5						A12
3071.6	3071.7	3071.7	1.00	IC	0-5	
3095.9	3095.6	3095.6	1.00	IC	0-5	
3106.4	3104.7	3105.7	1.00	I	0-5	
3120.1	3118.7	3119.6	0.89	I	0-5	
3140.4	3139.6	3139.6	1.00	I	0-5	
3146.3	3144.6	3147.7	0.87	I	0-5	
3156.0	3154.7	3155.6	0.90	I	0-5	
3163.9	3161.7	3162.6	1.00	IC	10-15	
3164.7	3163.4	3165.4	1.00	I	20-25	
3173.2						A12-B1
3176.8	3174.7	3176.7	1.00	IC	5-15	
3183.3	3182.6	3182.6	1.00	I	0-5	
3188.5	3187.7	3188.7	1.00	I	0-5	
3194.5	3192.7	3193.7	1.00	I	0-5	
3198.4	3197.7	3197.7	1.00	I	0-5	
3201.1	3200.7	3200.7	1.00	I	0-5	
3231.9	3230.6	3231.6	0.87	I	0-5	
3235.5	3234.7	3235.6	1.00	I	0-5	
3237.5						B10

Mass (average)	Mass (mono.)	Apex Mass	Score	Evidence	Time	MALDI fraction
3241.3	3239.6	3239.6	1.00	IC	0-5	
3246.8						A14
3254.3	3253.6	3254.6	1.00	I	0-5	
3255.6						A12-B1
3257.4	3255.6	3257.7	0.94	I	0-5	
3262.4	3260.6	3261.7	1.00	I	0-5	
3267.1	3265.7	3265.7	1.00	I	0-5	
3272.2	3271.6	3272.6	1.00	I	0-5	
3278.4	3277.6	3277.6	1.00	I	0-5	
3297.6	3296.6	3297.6	1.00	I	0-5	
3298.7						A11-A12
3327.4	3325.6	3327.6	0.94	I	0-5	
3332.6	3330.6	3332.7	1.00	I	0-5	
3368.0	3366.6	3368.6	1.00	I	0-5	
3373.6						B10
3375.9	3373.7	3375.6	1.00	IC	0-5	
3380.7	3379.7	3380.7	1.00	I	0-5	
3387.3	3386.6	3386.6	1.00	I	0-5	
3392.4	3391.6	3392.6	1.00	I	0-5	
3398.5	3396.7	3397.7	1.00	I	0-5	
3400.5	3398.8	3400.8	1.00	IC	20-25	
3401.8	3399.8	3400.8	1.00	IC	20-25	
3402.4	3401.6	3401.6	1.00	I	0-5	
3404.8	3404.6	3404.6	1.00	I	0-5	
3412.5	3411.6	3411.6	1.00	I	0-5	
3418.7	3416.8	3418.8	1.00	I	15-25	
3423.9	3423.6	3423.6	1.00	I	0-5	
3426.1	3425.6	3425.6	0.99	I	0-5	
3433.2	3431.9	3431.9	0.94	I	15-25	
3437.8	3436.8	3438.7	1.00	I	15-25	
3438.6						B10-B11
3447.7	3445.7	3447.7	0.76	I	0-5	
3450.2	3449.6	3449.6	1.00	I	0-5	
3458.3	3457.7	3458.6	1.00	I	0-5	
3461.4	3459.6	3461.6	1.00	I	0-5	
3464.8						A14
3466.4	3464.6	3465.6	1.00	I	0-5	
3471.1	3469.6	3469.6	1.00	I	0-5	
3476.5	3475.6	3476.6	1.00	I	0-5	
3479.0						B8-B11
3482.3	3480.6	3482.6	1.00	I	0-5	

Mass (average)	Mass (mono.)	Apex Mass	Score	Evidence	Time	MALDI fraction
3491.3						B7-B9
3492.9	3491.1	3492.1	1.00	IC	20-25	
3502.2						B9-B11
3503.1	3501.6	3503.6	1.00	I	0-5	
3512.1	3509.6	3511.6	0.80	I	0-5	
3519.3						B8-B11
3521.8	3519.6	3521.6	0.81	I	0-5	
3522.3						A12
3528.7						B3
3530.2						C3
3539.8	3537.6	3539.6	0.84	I	0-5	
3543.3						B1
3548.8	3547.6	3548.6	1.00	I	0-5	
3552.9						B9-B11
3555.0	3553.6	3555.6	1.00	I	0-5	
3555.9						B2-B3
3561.8	3560.9	3560.9	1.00	I	15-25	
3571.1	3569.6	3569.6	1.00	I	0-5	
3584.5						B2-B3
3584.7	3583.6	3584.6	1.00	I	0-5	
3590.5	3588.6	3590.6	1.00	I	0-5	
3596.5	3595.6	3596.6	1.00	I	0-5	
3601.9	3600.9	3600.9	1.00	IC	15-25	
3606.3	3605.6	3605.6	1.00	I	0-5	
3617.5	3615.6	3617.6	0.82	I	0-5	
3627.3						B9-B11
3648.1	3645.6	3647.6	0.79	I	0-5	
3652.5	3650.9	3652.9	1.00	IC	15-25	
3658.2	3656.1	3658.1	1.00	IC	15-20	
3665.4	3663.6	3665.6	0.95	I	0-5	
3668.3	3666.9	3669.0	1.00	I	15-25	
3670.5	3668.5	3669.6	1.00	I	0-5	
3673.3	3670.9	3672.9	1.00	IC	15-25	
3674.9						B2-B3
3675.0	3673.6	3673.6	1.00	I	0-5	
3679.4	3677.6	3679.6	0.76	I	0-5	
3681.3						C2-C6
3682.9						B2-B5
3684.5	3683.9	3684.9	1.00	I	15-25	
3685.7						C8-C15
3686.6	3685.9	3686.9	1.00	IC	15-25	

Mass (average)	Mass (mono.)	Apex Mass	Score	Evidence	Time	MALDI fraction
3690.1	3687.9	3690.0	1.00	IC	15-25	
3691.3	3690.0	3690.0	1.00	I	20-25	
3692.7	3690.9	3690.9	1.00	IC	15-25	
3693.1	3692.6	3692.6	1.00	I	0-5	
3694.0						C8-C9
3695.5						C6-C7
3697.7	3695.9	3695.9	1.00	IC	15-25	
3699.8						B6-B7
3701.5	3700.9	3701.9	1.00	IC	15-25	
3702.7						C4
3704.3	3702.9	3704.9	1.00	IC	15-25	
3705.3						B2-B4
3706.5	3705.9	3706.9	1.00	I	15-25	
3710.0	3708.0	3709.9	1.00	IC	15-25	
3716.2	3714.8	3715.8	1.00	I	15-25	
3726.6	3724.9	3727.9	1.00	IC	15-25	
3731.7	3729.8	3731.8	1.00	I	15-25	
3743.6	3741.6	3743.6	0.85	I	0-5	
3747.7	3745.9	3747.9	1.00	IC	15-25	
3753.7	3751.6	3751.6	1.00	IC	0-5	
3768.1						C1
3770.2	3769.5	3770.5	1.00	I	0-5	
3773.9	3771.6	3773.6	1.00	I	0-5	
3776.8	3776.6	3776.6	1.00	I	0-5	
3782.2	3779.6	3779.6	1.00	IC	0-5	
3788.5	3786.6	3788.6	1.00	IC	0-5	
3793.1	3792.5	3793.6	1.00	I	0-5	
3801.2	3800.6	3800.6	1.00	I	0-5	
3806.5	3804.6	3805.6	1.00	I	0-5	
3808.3	3808.0	3809.1	1.00	IC	15-25	
3810.3	3809.6	3809.6	1.00	I	0-5	
3811.8	3811.1	3811.1	1.00	IC	15-25	
3817.1	3815.6	3815.6	1.00	I	0-5	
3822.1						B2
3822.9	3822.6	3824.5	1.00	IC	15-25	
3824.5	3822.0	3824.1	1.00	I	0-5	
3829.0	3828.6	3828.6	1.00	I	15-25	
3846.7						B7-B8
3848.2	3846.1	3848.1	1.00	IC	15-25	
3856.9	3854.1	3856.1	1.00	IC	0-5	
3864.5	3861.5	3863.5	0.85	I	0-5	

Mass (average)	Mass (mono.)	Apex Mass	Score	Evidence	Time	MALDI fraction
3866.2	3864.1	3866.1	1.00	IC	15-25	
3869.2						C3-C4
3869.5	3867.6	3869.6	1.00	I	0-5	
3872.6	3871.0	3872.0	1.00	I	15-25	
3873.7	3872.1	3873.1	0.74	I	15-25	
3879.2	3877.5	3877.5	1.00	I	0-5	
3879.7						C6-C8
3881.0						B5-B6
3881.0	3878.2	3880.2	1.00	IC	15-25	
3884.5	3883.5	3884.5	1.00	IC	0-5	
3890.4	3888.6	3890.5	1.00	I	0-5	
3892.6	3892.1	3893.1	1.00	I	15-25	
3898.9	3896.2	3899.2	1.00	IC	15-25	
3902.1	3901.2	3901.2	1.00	IC	15-25	
3911.6						A14
3912.8	3912.2	3913.1	1.00	I	15-25	
3914.8	3914.2	3915.2	1.00	I	15-25	
3917.5	3915.2	3917.2	1.00	IC	15-25	
3920.9	3921.1	3921.1	1.00	IC	15-25	
3930.0						B7
3932.3	3931.1	3933.1	1.00	I	15-25	
3936.9	3934.2	3936.1	1.00	IC	15-25	
3939.2	3938.6	3938.6	1.00	I	0-5	
3943.2						B3-B4
3946.9	3944.2	3947.2	1.00	IC	15-25	
3951.3						B6-B7
3954.1	3952.2	3954.2	1.00	I	15-25	
3960.0	3958.2	3960.2	1.00	IC	15-25	
3960.7						C14-C15
3965.8	3963.3	3965.2	1.00	IC	15-25	
3972.1						B7
3972.4	3969.5	3971.5	0.84	I	0-5	
3974.2	3973.2	3975.1	1.00	I	15-25	
3979.1	3977.2	3978.2	1.00	IC	15-25	
3982.1	3981.2	3981.2	1.00	I	15-25	
3983.7						B8-B11
3984.3	3982.2	3982.2	0.64	I	15-25	
3986.8	3985.6	3986.6	1.00	I	0-5	
3993.7	3992.2	3992.2	0.73	I	15-25	
3996.7	3995.2	3996.2	1.00	I	15-25	
4003.2	4002.2	4002.2	1.00	I	15-25	

Mass (average)	Mass (mono.)	Apex Mass	Score	Evidence	Time	MALDI fraction
4006.9	4005.5	4007.5	1.00	I	0-5	
4010.3	4008.6	4009.6	1.00	IC	0-5	
4014.3	4013.6	4013.6	1.00	I	0-5	
4019.3						B3
4021.8	4020.5	4022.5	1.00	I	0-5	
4024.7	4023.6	4025.5	1.00	I	0-5	
4028.3	4026.5	4028.5	0.94	I	0-5	
4032.1	4031.5	4031.5	1.00	I	0-5	
4045.3	4043.6	4045.6	0.76	I	0-5	
4045.6						A14-A15
4047.8						B7-B11
4059.2	4058.1	4058.1	1.00	I	0-5	
4061.2	4059.6	4061.5	1.00	IC	0-5	
4065.0	4064.5	4064.5	1.00	I	0-5	
4069.0	4068.5	4069.5	1.00	I	0-5	
4072.9	4071.5	4073.5	1.00	I	0-5	
4077.3						B3
4078.5	4075.5	4077.6	1.00	IC	0-5	
4083.3	4081.5	4081.5	1.00	I	0-5	
4086.8						B1
4088.1	4087.5	4088.5	1.00	I	0-5	
4089.2						B11-B15
4092.3	4089.5	4091.5	1.00	I	0-5	
4095.9	4095.5	4095.5	0.99	I	0-5	
4097.7	4095.3	4097.3	1.00	IC	15-25	
4099.4						B10-B11
4106.6	4104.7	4106.5	1.00	I	0-5	
4108.0						B3-B4
4110.3						B10
4111.9	4111.3	4112.2	1.00	I	15-25	
4112.1						A14
4113.1	4111.3	4113.3	1.00	IC	15-25	
4114.6	4112.3	4114.3	1.00	IC	15-25	
4123.1						C3-C4
4123.7	4122.5	4124.5	1.00	I	0-5	
4128.9	4125.6	4127.5	1.00	I	0-5	
4132.3	4131.3	4132.3	1.00	I	15-25	
4137.8						C2-C3
4142.6	4140.6	4142.5	1.00	I	0-5	
4143.5						B3
4149.3	4148.6	4148.6	1.00	I	0-5	

Mass (average)	Mass (mono.)	Apex Mass	Score	Evidence	Time	MALDI fraction
4150.2	4147.4	4149.3	1.00	IC	15-25	
4156.0						B11-B12
4157.4						B3
4158.9	4155.5	4157.5	0.88	I	0-5	
4163.2	4162.6	4163.5	1.00	I	0-5	
4167.3	4164.5	4166.5	0.96	I	0-5	
4176.0						B15
4181.0						B10-B11
4182.7	4179.5	4181.5	1.00	I	0-5	
4189.7						B12-B14
4189.8	4188.5	4190.5	1.00	I	0-5	
4192.7	4191.5	4193.5	1.00	I	0-5	
4196.6	4194.5	4196.5	1.00	I	0-5	
4197.3						C3
4201.0						A15
4201.5						B13
4202.5						B1
4207.7	4206.4	4208.6	1.00	I	0-5	
4210.8	4209.5	4211.5	1.00	I	0-5	
4214.5	4212.5	4213.5	1.00	I	0-5	
4218.3						C11
4219.2	4217.5	4217.5	1.00	I	0-5	
4225.6	4223.3	4225.4	1.00	I	15-25	
4225.7	4223.4	4225.3	1.00	IC	15-25	
4229.2	4228.5	4229.5	1.00	I	0-5	
4233.4	4230.5	4232.5	1.00	I	0-5	
4259.9	4258.6	4259.5	1.00	I	0-5	
4264.8	4262.5	4265.5	1.00	I	0-5	
4268.8	4268.5	4268.5	0.99	I	0-5	
4273.1						B11-B12
4276.3	4273.4	4277.5	0.82	I	0-5	
4282.2	4279.5	4281.5	1.00	I	0-5	
4287.3						A15-B1
4287.3	4285.5	4285.5	1.00	I	0-5	
4288.4						B12
4292.0	4291.5	4292.5	1.00	I	0-5	
4294.7	4293.5	4295.5	1.00	I	0-5	
4297.8	4296.5	4298.5	1.00	IC	0-5	
4305.3						B11-B14
4309.7	4308.6	4310.5	1.00	I	0-5	
4314.2	4311.5	4313.5	0.85	I	0-5	

Mass (average)	Mass (mono.)	Apex Mass	Score	Evidence	Time	MALDI fraction
4319.2	4317.5	4319.5	1.00	I	0-5	
4319.8						B12-B14
4328.3	4326.5	4328.5	1.00	I	0-5	
4337.4						B12-B14
4337.5	4335.5	4337.5	1.00	I	0-5	
4346.6	4344.5	4346.5	1.00	I	0-5	
4353.3	4352.5	4352.5	1.00	I	0-5	
4362.9	4359.4	4361.5	0.87	I	0-5	
4368.9	4366.5	4367.5	1.00	I	0-5	
4380.1	4377.4	4379.5	1.00	I	0-5	
4386.8	4383.5	4385.5	1.00	I	0-5	
4394.7	4392.4	4395.5	0.86	I	0-5	
4401.3	4398.4	4400.5	1.00	I	0-5	
4412.5	4410.4	4412.5	1.00	I	0-5	
4418.1	4415.5	4417.5	1.00	I	0-5	
4423.2	4421.5	4421.5	1.00	I	0-5	
4423.3						B7-B11
4434.3	4431.6	4433.5	1.00	I	0-5	
4439.9	4438.6	4439.5	0.99	I	0-5	
4448.8	4447.5	4448.5	1.00	I	0-5	
4463.5	4462.6	4463.5	1.00	I	0-5	
4468.5	4465.6	4469.5	1.00	I	0-5	
4476.3	4473.5	4475.5	0.87	I	0-5	
4480.8	4479.5	4481.5	1.00	I	0-5	
4486.2	4483.5	4485.5	1.00	I	0-5	
4491.4	4489.5	4489.5	1.00	I	0-5	
4500.3	4497.4	4499.5	1.00	I	0-5	
4520.6						B5-B7
4523.3	4521.5	4523.5	1.00	I	0-5	
4536.7	4533.5	4535.5	1.00	I	0-5	
4542.8						B6
4544.8	4542.4	4544.5	0.90	I	0-5	
4551.2	4549.4	4551.5	0.75	I	0-5	
4557.4	4554.4	4559.5	0.84	I	0-5	
4569.4	4566.4	4568.5	1.00	I	0-5	
4570.7						B14
4575.7	4573.4	4574.5	1.00	I	0-5	
4580.0	4579.4	4580.5	1.00	I	0-5	
4584.0	4581.4	4583.5	1.00	I	0-5	
4599.1	4597.5	4599.5	0.79	I	0-5	
4604.3	4601.5	4604.5	1.00	I	0-5	

Mass (average)	Mass (mono.)	Apex Mass	Score	Evidence	Time	MALDI fraction
4615.3						B13
4615.9	4613.5	4615.5	1.00	I	0-5	
4622.1	4619.5	4621.5	1.00	I	0-5	
4627.2	4625.5	4625.5	1.00	I	0-5	
4636.5	4633.5	4637.5	1.00	I	0-5	
4652.6	4650.4	4652.5	1.00	I	0-5	
4667.5	4666.5	4667.5	0.99	I	0-5	
4672.5	4669.5	4671.4	1.00	I	0-5	
4684.3	4681.5	4685.4	0.87	I	0-5	
4690.2	4687.5	4689.5	1.00	I	0-5	
4695.3	4693.5	4693.5	1.00	I	0-5	
4705.9	4703.4	4706.5	1.00	I	0-5	
4726.4	4723.4	4727.5	1.00	I	0-5	
4734.1	4731.3	4735.5	0.12	I	0-5	
4740.7	4737.4	4739.5	1.00	I	0-5	
4753.6	4752.4	4754.4	1.00	I	0-5	
4759.0	4755.4	4757.5	0.96	I	0-5	
4763.7	4763.5	4763.5	0.99	I	0-5	
4773.3	4770.3	4772.5	1.00	I	0-5	
4779.6	4777.4	4778.4	0.93	I	0-5	
4784.1	4783.6	4784.4	0.97	I	0-5	
4788.4	4785.5	4787.4	1.00	I	0-5	
4795.1	4792.6	4796.5	1.00	I	0-5	
4801.5	4799.4	4802.5	1.00	I	0-5	
4808.3	4805.5	4808.5	1.00	I	0-5	
4820.5	4818.4	4820.5	1.00	I	0-5	
4826.0	4823.5	4825.5	1.00	I	0-5	
4831.2	4829.5	4829.5	1.00	I	0-5	
4841.4	4838.5	4841.4	1.00	I	0-5	
4856.6	4854.4	4856.4	1.00	I	0-5	
4869.0	4867.5	4868.4	1.00	I	0-5	
4876.5	4873.3	4875.5	1.00	I	0-5	
4894.2	4891.5	4893.4	1.00	I	0-5	
4898.7	4897.5	4897.5	1.00	I	0-5	
4907.2	4904.5	4907.4	1.00	I	0-5	
4930.8	4928.4	4931.4	1.00	I	0-5	
4931.4						B7
4939.0						B5
4944.6	4941.4	4943.5	1.00	I	0-5	
4950.4	4949.4	4949.4	1.00	I	0-5	
4955.0	4952.4	4955.4	1.00	I	0-5	

Mass (average)	Mass (mono.)	Apex Mass	Score	Evidence	Time	MALDI fraction
4962.7	4959.4	4961.4	1.00	I	0-5	
4967.5						B6-B7
4968.4	4966.4	4967.4	1.00	I	0-5	
4975.8	4973.4	4973.4	1.00	I	0-5	
4985.4	4983.4	4985.4	1.00	I	0-5	
4999.1	4996.5	4999.4	1.00	I	0-5	
5005.9	5003.4	5006.4	1.00	I	0-5	
5012.3	5009.4	5012.4	1.00	I	0-5	
5030.1	5027.4	5029.5	1.00	I	0-5	
5034.8	5033.4	5033.4	1.00	I	0-5	
5045.3	5043.4	5044.4	1.00	I	0-5	
5051.6	5048.4	5051.4	0.89	I	0-5	
5057.5	5055.6	5057.4	0.99	I	0-5	
5074.9	5072.4	5075.5	1.00	I	0-5	
5081.3	5078.5	5081.4	1.00	I	0-5	
5092.0	5089.5	5091.4	1.00	I	0-5	
5098.2	5095.4	5097.4	1.00	I	0-5	
5103.4	5101.5	5101.5	1.00	I	0-5	
5111.2	5108.4	5111.4	1.00	I	0-5	
5129.2	5126.5	5129.4	1.00	I	0-5	
5133.8	5133.4	5133.4	1.00	I	0-5	
5142.8	5141.4	5141.4	1.00	I	0-5	
5148.6	5145.4	5147.4	1.00	I	0-5	
5160.9	5159.4	5159.4	1.00	I	0-5	
5166.6	5163.4	5165.4	0.96	I	0-5	
5171.2	5170.4	5171.4	1.00	I	0-5	
5179.8	5177.4	5177.4	1.00	I	0-5	
5184.9	5183.4	5183.4	1.00	I	0-5	
5187.8	5187.4	5187.4	0.96	I	0-5	
5192.4	5190.3	5192.4	1.00	I	0-5	
5197.5	5196.6	5198.4	0.99	I	0-5	
5203.4	5200.5	5203.5	1.00	I	0-5	
5207.8	5207.4	5207.4	0.99	I	0-5	
5211.9	5210.4	5213.4	1.00	I	0-5	
5217.5	5214.4	5216.4	1.00	I	0-5	
5234.5	5231.4	5233.4	1.00	I	0-5	
5239.8	5238.4	5239.4	1.00	I	0-5	
5249.3	5246.4	5249.4	1.00	I	0-5	
5255.7	5253.4	5255.4	1.00	I	0-5	
5264.6	5262.3	5265.4	0.87	I	0-5	
5278.9	5277.4	5279.5	1.00	I	0-5	

Mass (average)	Mass (mono.)	Apex Mass	Score	Evidence	Time	MALDI fraction
5284.5	5281.5	5283.4	1.00	I	0-5	
5290.5	5289.4	5291.4	1.00	I	0-5	
5294.7	5292.4	5295.3	0.97	I	0-5	
5301.8	5298.4	5301.4	1.00	I	0-5	
5307.4	5305.5	5305.5	1.00	I	0-5	
5312.3	5311.4	5311.4	0.99	I	0-5	
5317.2	5314.5	5318.4	1.00	I	0-5	
5327.5	5326.5	5328.4	0.99	I	0-5	
5338.3	5335.4	5339.4	1.00	I	0-5	
5342.8	5342.4	5342.4	0.98	I	0-5	
5351.9	5348.4	5351.4	0.93	I	0-5	
5357.5	5355.4	5357.4	0.81	I	0-5	
5364.4	5362.5	5365.4	1.00	I	0-5	
5370.7	5367.3	5369.4	1.00	I	0-5	
5378.2	5376.4	5376.4	1.00	I	0-5	
5387.7	5385.3	5385.3	1.00	I	0-5	
5397.5	5395.5	5397.4	1.00	I	0-5	
5401.9	5400.2	5402.3	0.75	I	0-5	
5407.4	5405.4	5408.4	1.00	I	0-5	
5413.5	5411.4	5414.4	0.96	I	0-5	
5421.4	5418.4	5421.3	1.00	I	0-5	
5427.8	5427.3	5427.3	1.00	I	0-5	
5431.5	5429.4	5433.4	1.00	I	0-5	
5437.6	5434.3	5437.4	1.00	I	0-5	
5444.0	5441.4	5441.4	1.00	I	0-5	
5453.3	5450.4	5453.4	0.86	I	0-5	
5459.6	5457.5	5459.4	0.94	I	0-5	
5464.4	5463.4	5465.4	1.00	I	0-5	
5483.4	5481.3	5483.4	1.00	I	0-5	
5489.6	5486.4	5487.4	1.00	I	0-5	
5499.9	5498.3	5501.4	1.00	I	0-5	
5505.7	5502.3	5505.4	1.00	I	0-5	
5511.4	5509.3	5509.3	1.00	I	0-5	
5516.9	5515.5	5515.5	0.80	I	0-5	
5524.2	5522.4	5523.3	1.00	I	0-5	
5535.3	5533.4	5533.4	1.00	I	0-5	
5542.8	5541.4	5543.4	1.00	I	0-5	
5547.4	5546.4	5548.4	0.99	I	0-5	
5550.3	5549.4	5551.2	0.98	I	0-5	
5556.9	5553.3	5555.4	0.87	I	0-5	
5563.4	5562.2	5563.1	0.88	I	0-5	

Mass (average)	Mass (mono.)	Apex Mass	Score	Evidence	Time	MALDI fraction
5567.9	5566.3	5567.3	1.00	I	0-5	
5574.0	5570.3	5573.4	0.92	I	0-5	
5583.9	5582.4	5583.5	1.00	I	0-5	
5588.3	5586.3	5588.3	1.00	I	0-5	
5595.1	5593.4	5595.3	0.94	I	0-5	
5601.2	5599.5	5601.3	0.94	I	0-5	
5606.3	5604.3	5606.4	1.00	I	0-5	
5611.8	5609.3	5612.4	1.00	I	0-5	
5617.3	5615.3	5619.2	1.00	I	0-5	
5624.4	5621.4	5625.3	0.98	I	0-5	
5636.7	5635.3	5635.3	1.00	I	0-5	
5642.8	5639.3	5642.3	1.00	I	0-5	
5648.3	5647.3	5647.3	1.00	I	0-5	
5651.0	5650.5	5651.5	1.00	I	0-5	
5656.3	5654.3	5657.4	1.00	I	0-5	
5661.9	5660.4	5663.3	1.00	I	0-5	
5682.9	5682.5	5682.5	1.00	I	0-5	
5686.9	5685.3	5687.4	1.00	I	0-5	
5692.8	5689.1	5691.3	1.00	I	0-5	
5704.1	5702.3	5703.3	0.90	I	0-5	
5710.4	5708.4	5709.3	1.00	I	0-5	
5714.7	5713.3	5713.3	0.93	I	0-5	
5739.4	5737.2	5740.3	1.00	I	0-5	
5746.7	5745.3	5745.3	1.00	I	0-5	
5749.8	5749.3	5749.3	0.99	I	0-5	
5754.1	5751.3	5753.4	0.83	I	0-5	
5760.8	5759.4	5759.4	1.00	I	0-5	
5767.7	5765.3	5765.3	0.89	I	0-5	
5772.3	5771.3	5772.4	0.99	I	0-5	
5778.0	5774.2	5777.4	0.91	I	0-5	
5782.8						B13-B14
5787.9	5787.4	5788.3	0.99	I	0-5	
5792.1	5789.3	5791.2	1.00	I	0-5	
5809.9	5809.3	5810.3	1.00	I	0-5	
5813.5	5811.3	5813.3	0.96	I	0-5	
5820.9	5819.4	5821.4	1.00	I	0-5	
5834.8	5834.3	5835.2	1.00	I	0-5	
5838.9	5837.3	5839.4	1.00	I	0-5	
5842.4	5841.2	5843.3	1.00	I	0-5	
5847.3	5844.3	5845.4	1.00	I	0-5	
5852.8	5851.3	5851.3	0.73	I	0-5	

Mass (average)	Mass (mono.)	Apex Mass	Score	Evidence	Time	MALDI fraction
5860.3	5858.2	5859.1	0.89	I	0-5	
5873.5	5871.3	5873.2	0.94	I	0-5	
5887.8	5886.3	5886.3	1.00	I	0-5	
5892.7	5891.4	5891.4	0.99	I	0-5	
5901.5	5899.5	5903.4	1.00	I	0-5	
5909.9	5908.5	5909.3	1.00	I	0-5	
5914.8	5912.2	5917.3	0.96	I	0-5	
5926.9	5925.2	5926.4	0.99	I	0-5	
5966.8	5965.4	5965.4	1.00	I	0-5	
5974.2	5972.3	5972.3	0.88	I	0-5	
5982.1	5979.3	5982.3	1.00	I	0-5	
5994.1	5991.2	5994.1	0.85	I	0-5	
6024.7	6023.1	6026.1	1.00	I	0-5	
6043.8	6043.3	6044.3	1.00	I	0-5	
6048.0	6045.3	6049.3	1.00	I	0-5	
6055.3	6053.3	6057.4	0.88	I	0-5	
6064.0	6062.2	6064.2	0.95	I	0-5	
6072.2	6070.4	6071.4	0.89	I	0-5	
6096.2	6093.2	6095.3	1.00	I	0-5	
6115.3	6113.2	6117.3	1.00	I	0-5	
6131.7	6130.3	6130.3	0.86	I	0-5	
6167.4	6165.2	6168.3	1.00	I	0-5	
6172.8	6170.3	6173.3	0.65	I	0-5	
6186.8	6183.4	6185.3	0.88	I	0-5	
6191.6	6190.3	6191.3	0.94	I	0-5	
6203.0	6201.2	6201.2	0.96	I	0-5	
6236.9	6233.9	6238.1	0.97	I	0-5	
6242.3	6241.0	6241.0	0.99	I	0-5	
6250.7	6248.3	6249.4	1.00	I	0-5	
6254.8	6254.3	6254.3	0.99	I	0-5	
6270.4	6268.4	6269.4	1.00	I	0-5	
6327.7	6325.5	6326.4	0.95	I	0-5	
6339.8	6338.4	6338.4	1.00	I	0-5	
6390.6	6387.2	6390.1	0.76	I	0-5	
6583.0	6580.4	6583.3	0.92	I	0-5	
6652.8						B12-B13
6674.3						B12-B13
6721.0	6719.2	6719.2	1.00	I	0-5	
7032.8	7031.2	7031.2	0.94	I	0-10	
7064.2	7063.3	7063.3	1.00	I	0-5	
7096.9	7095.2	7095.2	1.00	I	0-5	

Mass (average)	Mass (mono.)	Apex Mass	Score	Evidence	Time	MALDI fraction
7191.5	7190.0	7191.1	0.99	I	0-5	
7365.5						B5
7387.8						B5
7547.9						C1
7624.9	7624.2	7625.3	0.99	I	0-5	
7629.9	7627.1	7631.2	1.00	I	0-5	
8028.3	8027.0	8027.9	1.00	I	0-5	
8144.0						B13

Group 8 from ion exchange column

Mass (average)	Mass (mono.)	Apex Mass	Score	Evidence	Time	MALDI fraction
2005.5	2005.1	2005.1	1.00	I	15-20	
2007.6	2006.8	2007.8	1.00	I	5-10	
2016.6	2015.8	2015.8	1.00	I	5-10	
2027.3	2026.8	2026.8	1.00	I	5-10	
2046.3	2045.8	2045.8	1.00	I	5-10	
2055.6	2054.8	2055.7	1.00	I	5-10	
2065.8	2064.8	2065.8	1.00	I	5-10	
2075.4	2074.8	2075.8	1.00	I	5-10	
2085.4	2084.8	2085.8	1.00	I	5-10	
2109.2	2108.8	2108.8	1.00	I	15-20	
2143.5	2142.8	2143.8	1.00	I	5-10	
2169.5						B3
2181.3	2180.9	2181.8	0.98	I	5-10	
2183.4	2182.8	2183.7	1.00	I	5-10	
2191.7	2190.7	2191.7	1.00	I	5-10	
2201.7	2200.7	2201.7	1.00	I	5-10	
2279.6	2278.8	2279.8	1.00	I	5-10	
2326.1	2325.7	2325.7	1.00	I	5-10	
2415.6	2414.8	2415.7	1.00	I	5-10	
2462.0	2461.6	2461.6	1.00	I	5-10	
2551.6	2550.7	2551.7	1.00	I	5-10	
2687.6	2686.7	2687.7	1.00	I	5-10	
3176.7	3175.8	3176.8	1.00	I	15-20	
3193.9						A11-A13
3202.3						B1
3314.0	3313.6	3313.6	1.00	I	5-10	
3366.2						B10

Mass (average)	Mass (mono.)	Apex Mass	Score	Evidence	Time	MALDI fraction
3369.8						A12-A13
3380.7	3379.8	3380.8	1.00	IC	15-25	
3381.0	3379.8	3380.8	1.00	IC	15-25	
3382.2	3381.8	3381.8	1.00	I	15-25	
3396.9	3395.8	3396.8	1.00	IC	15-25	
3483.0						A13
3608.4	3607.1	3609.1	1.00	I	15-20	
3609.2	3607.1	3609.1	1.00	IC	15-20	
3615.3						B10-B12
3634.7						B10-B13
3636.6	3636.1	3636.1	1.00	I	15-20	
3637.4	3636.1	3637.1	1.00	IC	15-20	
3673.0	3671.0	3672.0	1.00	IC	15-20	
3705.9						B5-B6
3724.0	3722.2	3724.2	1.00	IC	15-20	
3724.4	3722.2	3724.2	1.00	IC	15-20	
3725.5	3725.1	3725.1	1.00	I	15-20	
3725.8	3725.2	3725.2	0.89	I	15-20	
3737.3	3736.2	3738.2	1.00	I	15-20	
3740.7	3740.2	3741.2	1.00	I	15-20	
3741.8	3739.2	3741.2	1.00	IC	15-20	
3742.7	3741.1	3743.2	1.00	IC	15-20	
3744.3	3743.1	3743.1	0.76	I	15-20	
3745.5	3744.1	3744.1	1.00	I	15-20	
3755.3						B10
3756.1	3755.2	3756.2	1.00	I	15-20	
3756.5	3754.1	3755.2	1.00	IC	15-20	
3761.6	3761.1	3762.1	1.00	I	15-20	
3762.1	3760.1	3761.1	1.00	I	15-20	
3781.0	3780.2	3780.2	1.00	I	15-20	
3808.6	3806.1	3808.1	1.00	IC	15-20	
3821.9	3821.1	3822.1	1.00	I	15-20	
3825.3	3823.1	3825.1	1.00	IC	15-20	
3829.9	3829.0	3829.0	1.00	I	15-20	
3838.2						B1-B4
3840.7	3839.1	3841.1	1.00	I	15-20	
3863.1	3862.1	3863.1	1.00	I	15-20	
3878.8	3877.2	3878.2	1.00	IC	15-20	
3880.5						B6
3892.3	3891.2	3892.2	1.00	IC	15-20	
3895.9	3894.2	3895.2	1.00	IC	15-20	

Mass (average)	Mass (mono.)	Apex Mass	Score	Evidence	Time	MALDI fraction
3947.1						B5-B8
3947.4	3944.3	3946.3	1.00	IC	15-20	
3958.0						B8-B14
3959.6						A7-A9
3960.6	3958.3	3961.3	1.00	IC	15-20	
3963.4						B11-B12
3965.8	3963.3	3965.3	1.00	IC	15-20	
3970.8	3969.2	3969.2	1.00	IC	15-20	
3974.0	3972.2	3975.2	1.00	IC	15-20	
3975.8	3975.2	3976.2	1.00	I	15-20	
3978.7	3976.3	3979.2	1.00	IC	15-20	
3981.7	3981.2	3981.2	1.00	I	15-20	
3982.3						B9-B10
3983.0	3981.3	3981.3	1.00	IC	15-20	
3985.1	3983.2	3985.2	1.00	IC	15-20	
3988.1	3987.1	3987.1	1.00	I	15-20	
3989.0						A14-B1
3992.5	3992.2	3992.2	1.00	IC	15-20	
3993.9	3993.3	3994.3	1.00	I	15-20	
3996.9	3994.3	3997.3	1.00	IC	15-20	
3998.7	3998.2	3999.2	1.00	I	15-20	
4002.4	4001.2	4003.2	1.00	IC	15-20	
4005.1	4004.2	4004.2	1.00	I	15-20	
4011.2	4009.4	4009.4	1.00	I	15-20	
4012.5						B1
4013.7	4013.2	4014.2	1.00	I	15-20	
4016.7	4014.2	4017.2	1.00	IC	15-20	
4020.2						B6
4021.0	4019.2	4019.2	1.00	I	15-20	
4041.1	4040.2	4040.2	1.00	I	15-20	
4058.6						A14-A15
4061.1	4060.2	4061.2	1.00	I	15-20	
4082.5	4081.1	4082.2	1.00	I	15-20	
4098.2	4097.2	4099.2	1.00	I	15-20	
4110.3						B4-B5
4155.4						B12-B13
4163.0						A15-B1
4205.6	4204.5	4206.4	1.00	IC	15-20	
4207.0	4206.5	4207.4	1.00	I	15-20	
4207.5	4206.4	4208.4	1.00	I	15-20	
4216.5						B1

Mass (average)	Mass (mono.)	Apex Mass	Score	Evidence	Time	MALDI fraction
4218.8	4217.5	4219.5	1.00	IC	15-20	
4219.0	4216.5	4219.5	1.00	IC	15-20	
4230.8						B1
4287.8						B3
4298.9	4297.4	4299.4	1.00	I	15-20	
4300.8	4299.5	4300.5	1.00	IC	15-20	
4302.4	4300.5	4301.5	0.98	I	15-20	
4329.5						B3
4342.0						B4
4938.7						B5
7901.3						B7
7922.2						B8